

VOLATILE ARSENIC IN AQUATIC ENVIRONMENTS

Der Fakultät für Geowissenschaften, Geotechnik und Bergbau
der Technischen Universität Bergakademie Freiberg

eingereichte

DISSERTATION

zur Erlangung des akademischen Grades

doctor rerum naturalium

Dr. rer. nat.

vorgelegt

von Dipl. Geol. Britta Planer-Friedrich

geboren am 15.09.1975 in Gunzenhausen

Freiberg, den 27.08.2004

ABSTRACT

To understand the behavior of metals and metalloids in the environment, speciation is one of the most important requirements because occurrence, sorption, mobility, potential assimilation, and toxicity depend significantly on the individual species. The release of As to groundwater in Bangladesh by reduction of As(V) to As(III) is a well-known example for the complexity and possible consequences of species conversions. Yet, inorganic As(III) and As(V) are not the only important As species. Trivalent and pentavalent organic (methylated) species act as connecting links for the transfer between hydrosphere and biosphere. The most reduced forms of organic and inorganic As species are volatile and, thus, enable transport from the hydrosphere to the atmosphere. They are also the most toxic As species known. Their accidental release has been documented as early as in the mid of the 19th century. Species-selective determination methods, however, have not been introduced until the early 1970s with the invention of the hydride generation technique. Arsenic biomethylation pathways in different organisms have been investigated, but reports about the occurrence of dissolved methylated and especially volatile As species in aquatic environments are still rare. Quantification has seldom been achieved and several compounds such as volatile sulfur- or chloroarsines have not even been qualitatively identified in nature, yet.

A major requirement for identifying volatile As compounds in the environment is a simple standardized sampling procedure that guarantees long-term stability of the sample. In the present research work a robust method for in-situ sampling of volatile metallics from aqueous environments was developed. Efficient gas-water separation is achieved with a PTFE membrane (porosity 0.1 μm) inside a PTFE collector cell that can be placed at the sediment-water interface or in the aqueous body itself. Vacuum up to -500 mbar can be applied to force the gases to a trapping system of either liquid or solid sorbents. As liquid sorbent a 1:100 diluted NaOCl solution in a PTFE bottle is used. PTFE rings in the oxidizing bottle increase the reaction surface and thus trapping efficiency that was $84\% \pm 6.6$ for As in the laboratory. The build-up of a high pressure from the intense gas evolution during hydride generation might be responsible for the loss of some volatile As, especially at the beginning of the reaction. Quantitative evaluation of volatile metallics concentrations is achieved by referring the trapped mass in the oxidizing solution [μg] to the replaced vacuum volume [m^3].

Besides this fast screening method on total volatile metallics concentrations, two species-selective sampling techniques were investigated for As. Solid phase micro extraction (SPME) fibers enabled the detection of more volatile As species in lower concentrations than solid sorbent tubes. For SPME fibers, selective sorption was observed dependent on the volatile As species. Volatile chloro-arsines $(\text{CH}_3)\text{AsCl}_2$ and $(\text{CH}_3)_2\text{AsCl}$ with larger molecular weights were sorbed on polydimethylsiloxane fibers whereas polydimethylsiloxane fibers with Carboxen and divinylbenzene coating proved best for MMA, DMA, and TMA. The fibers with only Carboxen coating showed by far the largest peak areas of all fibers for DMA, TMA, and $(\text{CH}_3)_2\text{AsCl}$. The most effective sorption material in sorption tubes was also Carboxen but only TMA and traces of $(\text{CH}_3)_2\text{AsCl}$ were detected. Probably the selected Carboxen type (CAR 564) is not the optimum fit yet. The volatile

As species were stable on the SPME fibers for at least 3 days when wrapped in aluminum foil and stored at 4°C in the refrigerator. Quantification could not be achieved mainly because of unknown sorption affinities of the individual arsines, non-availability of calibration standards, and potential competitive sorption with other, unknown gases.

As an example for an aqueous environment predestined for the release of volatile metallics Yellowstone National Park was investigated. It is located over the largest continental hot spot world wide and contains more than 10,000 geothermal features. After the first detection of volatile As during a reconnaissance study in 2002, 5 study areas (Nymph Lake, Hazle Lake, Ragged Hills, Gibbon Geyser Basin, and Lower Geyser Basin) were sampled for their water and gas chemistry. Sulfate-dominated waters with low pH and As concentrations between 20 and 2,000 µg/L were differentiated from chloride-dominated waters with near neutral pH and As concentrations between 1,050 and 11,000 µg/L. The precipitation of As minerals was thermodynamically calculated for Hazle Lake (orpiment supersaturation) and actually observed for a low temperature hot spring at Ragged Hills (precipitation of an amorphous Fe, S, and As rich material).

Volatile As was found in all samples besides volatile Al, B, Ba, Cu, Fe, K, Li, Si, Sr, Zn, and S. By species-selective sampling on SPME fibers, four volatile As species were detected: $(\text{CH}_3)_3\text{As}$, $(\text{CH}_3)\text{AsCl}_2$, $(\text{CH}_3)_2\text{AsCl}$, and $(\text{CH}_3)_2\text{AsSCH}_3$. The latter three were all found for the first time in a natural environment. Modeling of the gaseous As species proved impossible because of a lack of thermodynamic constants for the species detected. The volatile inorganic As, As-S, As-F, and As-Cl species for which thermodynamic data were available showed negligible partial pressures of $<10^{-11}$ Vol%. Total concentrations in the trapping solution from passive, diffusion based sampling were converted to concentrations in gas phase using Fick's first law. Medium concentrations were 18 mg/m³ for sulfate-dominated waters and 50 mg/m³ for the chloride-dominated ones. Concentrations from active gas sampling by pumping were lower (20-100 µg/m³) but are supposed to be subject to significant dilution by withdrawing ambient air from over-pumping. The detected concentrations are significantly increased compared to the acute toxicity limit for 1 hour exposure (160 µg/m³) with respect to AsH₃. However AsH₃ is probably not the predominant volatile species. Even though concentrations decrease rapidly with increasing distance from a geothermal feature animals grazing and warming up at hot springs might be exposed to significant amounts of volatile metallics, particularly As.

Further research on volatile metallics in aquatic environments should focus on quantification of individual volatile species, on their chemical or microbial origin, their distribution, and their toxicity potential.

ZUSAMMENFASSUNG

Um das Verhalten von Metallen und Metalloiden in der Umwelt zu verstehen, ist die Speziierung eine der wichtigsten Anforderungen, da Vorkommen, Mobilität, mögliche Assimilation und Toxizität entscheidend von den jeweiligen Spezies abhängen. Die Freisetzung von As ins Grundwasser in Bangladesh durch Reduktion von As(V) zu As(III) ist ein gut bekanntes Beispiel für die Komplexität und möglichen Konsequenzen von Speziesumwandlungen. Doch anorganisches As(III) und As(V) sind nicht die einzigen wichtigen As Spezies. Dreiwertige und fünfwertige organische (methylierte) Spezies stellen das Bindeglied für den Transfer zwischen Hydro- und Biosphäre dar. Die reduziertesten Formen von organischem und anorganischem As sind flüchtig und ermöglichen somit einen Transport von der Hydro- in die Atmosphäre. Sie sind auch die As Spezies mit der höchsten bekannten Toxizität. Ihre unbeabsichtigte Freisetzung wurde bereits im 19. Jahrhundert dokumentiert. Speziesselektive Bestimmungsmethoden wurden jedoch erst in den frühen 1970ern mit der Erfindung der Hydridgenerierungstechnik eingeführt. Biomethylierungspfade von Arsen in verschiedenen Organismen wurden untersucht, aber Berichte über das Vorkommen von gelösten methylierten und vor allem flüchtigen As Spezies in der Hydrosphäre sind immer noch rar. Eine Quantifizierung wurde selten erreicht und verschiedene Verbindungen, wie z.B. volatile Schwefel- und Chlorarsine, wurden bisher nicht einmal qualitativ in der Natur nachgewiesen.

Eine wesentliche Anforderung für den Nachweis von flüchtigen As Verbindungen in der Umwelt ist ein einfaches standardisiertes Verfahren, das eine Langzeitstabilität der Probe garantiert. In der vorliegenden Forschungsarbeit wurde eine robuste Methode für die in-situ Probenahme volatiler Metall(oid)e in wässrigen Medien entwickelt. Eine effiziente Gas-Wasser Trennung wird erreicht über eine PTFE Membran (Porosität = $0.1 \mu\text{m}$) in einer PTFE Sammelzelle, die an der Grenzschicht Wasser-Sediment oder im Wasserkörper selbst eingebaut werden kann. Ein Vakuum bis zu -500 mbar kann angelegt werden, um die Gase in eine Sorptionslösung oder auf einen Feststoffsorbent zu überführen. Als Sorptionslösung wird eine 1:100 verdünnte NaOCl Lösung in einer PTFE Flasche verwendet. PTFE Ringe in der Oxidationsflasche erhöhen die Reaktionsfläche und somit die Sorptionseffizienz, die im Labor für As bei $84\% \pm 6.6$ lag. Der große Druckaufbau infolge intensiver Gasentwicklung während der Hydridgenerierung ist vermutlich verantwortlich für einen Teil des Verlusts an volatilem As, vor allem zu Beginn der Reaktion. Eine quantitative Bestimmung der Konzentrationen an flüchtigen Metall(oid)en wird erreicht, indem man die Masse an sorbierter Substanz in der Oxidationslösung [μg] auf das verdrängte Vakuumvolumen [m^3] bezieht.

Neben dieser schnellen Screening-Methode für Gesamtkonzentrationen an volatilen Metall(oid)en, wurden zwei speziesselektive Probenahmetechniken für As untersucht. Mit Festphasenmikroextraktion (soild phase micro extraction SPME) - Fasern waren mehr volatile As Spezies in geringeren Konzentrationen nachweisbar als mit Festphasen-Sorptionsröhrchen. Für SPME Fasern wurde eine selektive Sorption in Abhängigkeit von der jeweiligen volatilen As Spezies beobachtet. Während die volatilen Chloroarsine $(\text{CH}_3)\text{AsCl}_2$ und $(\text{CH}_3)_2\text{AsCl}$ mit dem höheren Molekulargewicht auf Polydimethylsiloxan-Fasern sorbiert wurden, erwiesen sich die Polydimethylsiloxan-Fasern mit Carboxen und Divinyl-Beschichtung am geeignetsten für MMA, DMA, und TMA. Die nur mit Carboxen beschichteten Fasern zeigten bei weitem die größten Peakflächen aller Fasern für DMA,

TMA, und $(\text{CH}_3)_2\text{AsCl}$. Das effektivste Sorptionsmaterial in Sorptionsröhrchen war ebenfalls Carboxen, aber nur TMA und Spuren von $(\text{CH}_3)_2\text{AsCl}$ wurden nachgewiesen. Wahrscheinlich war der gewählte Carboxen-Typ (CAR 564) noch nicht optimal. Eingewickelt in Aluminium-Folie und bei 4°C im Kühlschrank gelagert waren die volatilen As Spezies auf den SPME Fasern mindestens 3 Tage stabil. Eine Quantifizierung konnte nicht erreicht werden, vor allem wegen unbekannter Sorptionsaffinitäten der einzelnen Arsine auf den SPME Fasern, fehlender Kalibrierstandards und möglicher Konkurrenzreaktionen mit anderen, unbekanntem Gasen um Sorptionsplätze.

Als Beispiel für ein aquatisches System, das prädestiniert für die Freisetzung von volatilen Metall(oid)en ist, wurde der Yellowstone National Park untersucht. Er befindet sich über dem größten kontinentalen Hot Spot weltweit und umfaßt mehr als 10.000 geothermale Strukturen. Nach dem ersten Nachweis von volatilem As während eines Erkundungstrips 2002 wurden 5 Untersuchungsgebiete (Nymph Lake, Hazle Lake, Ragged Hills, Gibbon Geyser Basin und Lower Geyser Basin) bezüglich ihrer Wasser- und Gaschemie beprobt. Sulfat dominierte Wässer mit niedrigem pH und As Konzentrationen zwischen 20 und $2.000 \mu\text{g/L}$ konnten unterschieden werden von Chlorid dominierten Wässern von nahezu neutralem pH-Wert und As Konzentrationen zwischen 1.050 und $11.000 \mu\text{g/L}$. Die Ausfällung von As Mineralen wurde thermodynamisch berechnet für Hazle Lake (Orpiment-Übersättigung) und tatsächlich beobachtet für eine Niedrig-Temperatur Quelle in Ragged Hills (Ausfällung von amorphem Fe-, S- und As-reichen Material).

Volatiles As wurde in allen Proben neben volatilem Al, B, Ba, Cu, Fe, K, Li, Si, Sr, Zn und S gefunden. Über die speziesselektive Probenahme mittels SPME Fasern wurden vier volatile As Spezies nachgewiesen: $(\text{CH}_3)_3\text{As}$, $(\text{CH}_3)\text{AsCl}_2$, $(\text{CH}_3)_2\text{AsCl}$ und $(\text{CH}_3)_2\text{AsSCH}_3$. Die letzten drei wurden alle zum ersten Mal in natürlicher Umgebung gefunden. Die Modellierung volatiler As Spezies erwies sich als unmöglich aufgrund fehlender thermodynamischer Konstanten für die gefundenen Spezies. Die volatilen anorganischen As, As-S, As-F und As-Cl Spezies, für die thermodynamischen Konstanten vorhanden waren, zeigten vernachlässigbare Partialdrücke von $<10^{-11}$ Vol%. Die Gesamtkonzentrationen in der Sorptionslösung aus der passiven, diffusiven Probenahme wurden über das 1. Fick'sche Gesetz umgerechnet in Konzentrationen in der Gasphase. Mittlere Konzentrationen waren 18 mg/m^3 in den Sulfat dominierten Wässern und 50 mg/m^3 in den Chlorid dominierten. Die Konzentrationen aus der Gasprobenahme durch Pumpen waren geringer ($20\text{-}100 \mu\text{g/m}^3$), unterliegen aber vermutlich erheblicher Verdünnung durch mitangesaugte Umgebungsluft. Die nachgewiesenen Konzentrationen sind deutlich erhöht im Vergleich zum Grenzwert akuter Toxizität für AsH_3 bei einstündiger Exposition ($160 \mu\text{g/m}^3$). Allerdings ist AsH_3 vermutlich nicht die prädominante volatile As Spezies. Obwohl die Konzentrationen mit zunehmender Entfernung von den Geothermalstrukturen rasch abnehmen, könnten Tiere, die an den heißen Quellen grasen oder sich wärmen einer erheblichen Menge an volatilen Metall(oid)en, insbesondere As, ausgesetzt sein.

Weitere Forschung über volatile Metall(oid)e in aquatischen Systemen sollte sich auf die Quantifizierung einzelner volatiler Spezies, ihren chemischen oder mikrobiellen Ursprung, ihre Verteilung und ihr Toxizitätspotential konzentrieren.

ACKNOWLEDGEMENT

Three years of study on a subject yet untouched by scientists of our department and quite „chemical“ for a geologist did make up for a very interesting and instructive time. I would like to thank Prof. Dr. Jörg Matschullat from my home university Technische Universität Bergakademie Freiberg, Interdisciplinary Environmental Research Center, for his supervisorship, his support on papers and posters during this time and proof-reading of my thesis. Some lessons were hard to learn especially in the beginning spending hours in the laboratory without any apparent success. Sincere thanks for some decisive hints and the chemical discussions to Prof. Dr. Gerhard Roewer (Department of Inorganic Chemistry, Technische Universität Bergakademie Freiberg).

My second supervisor, Dr. Darrell Kirk Nordstrom (U.S. Geological Survey Boulder / USA), did not only enable first access to Yellowstone National Park and all important contacts on a spontaneous email from an unknown German PhD student but also provided laboratory facilities and endured me and my master students during several stays in Yellowstone and Boulder. Special thanks for his proof-reading of this thesis and his never-ending efforts on improving my English.

The whole PhD project would never have been realized without the financial support of the German National Academic Foundation who did not only provide a 3-years-scholarship plus 2 travel grants to USA but were refreshingly non-bureaucratic towards my plans of interrupting my scholarship for half a year to organize an international conference and accept a DAAD short term lectureship in Mexico. Special thanks here to Dr. Max Brocker, Dr. Angelika Wittek and Dr. Matthias Frenz, as well as to their contact persons here in Freiberg, Prof. Dr. Gert Grabbert and Prof. Dr. Karl Lohmann. Thanks also to the PhD program of the Technische Universität Bergakademie Freiberg and its coordinators Dr. Corina Dunger and Edda Paul for supporting 2 Yellowstone field trips. The Leisler-Kiep Travel Grant awarded by Dr. Walther Leisler-Kiep in November 2003 helped to continue research in USA even after all other funds were exhausted.

Development of a new equipment is always difficult but it would have been impossible without the creativity of Michael Sekul and his crew at the workshop of the Technische Universität Bergakademie Freiberg constructing PTFE collector cells, oxidizing bottles, thermal desorption units, etc. from draft sketches. Their splendid performance and never-ending patience helped to improve the equipment up to the last detail. For laboratory assistance on the (sometimes tricky) GF-AAS I would like to thank Dipl. Chem. Peter Volke, for introduction to the GC-MS and assistance at various column changes Dipl. Chem. (FH) Hans-Joachim Peter. Thanks also to Prof. Dr. Matthias Otto, Dr. Silke Lehmann, and Dipl. Ing. (FH) Gisela Sachse from the Department of Analytical Chemistry for access to their GC-MS.

For providing free sample material for my initial research studies I would like to thank Dr. Michael Marquardt at Varian (Chromosorb 105, 106), Eric Butrym at Scientific Instrument Services (Carbosieve), Dr. Petra Münch at Sigma Aldrich (Carboxen, Carbotrap), Dr. Susanne Faulhaber at Sigma Aldrich (CAR/DVB fiber), and Maike Pieper at Infiltec (PTFE membrane sample).

An especially instructive part of my own work was supervising master students in various study areas and I'd like to acknowledge the good cooperation with Manja Seidel, Silke Mannigel, Anja Landgraf, Katja Zimmermann, Cornelius Goldhahn, Sandra Göhler, Ulrich Knauthe, and Juliane Becker.

Several research groups in Germany and abroad have provided equipment or valuable scientific advices during my research. For scientific cooperation and discussions about volatile As mass spectra I would like to thank Prof. Dr. Alfred V. Hirner and Jan Kösters (Department for Environmental Analytics and Applied Geochemistry, University Essen / Germany). For supervising the master thesis on volatile As in a constructed wetland thanks to Prof. Dr. Hendrik Emons and Zita Sebesvari (at that time Research Center Jülich / Germany). Dr. Yong Cai and Sheena Szuri (Department of Chemistry, Florida International University Miami / USA) offered great hospitality and assistance when investigating the Florida Everglades. Prof. Dr. Johnnie Moore (University of Montana Missoula / USA) was the first to suggest volatile As studies at Yellowstone besides the original study area Milltown Reservoir in Missoula and provided his laboratory facilities. His assistant Dr. Heiko Langner was not only a valuable support for all my analyses but he and his family also offered me a warm and vivid home for 6 weeks.

Special thanks goes to Dr. Henry Heasler, Christie Hendrix, Shannon Savage, and Steve Miller (National Park Service, Yellowstone Nationalpark, Wyoming) for their support with Park bureaucracy, logistics and field work especially during our trip in September 2003. The spontaneous great cooperation with Dr. Earl Mattson and Dr. Mitchell Plummer (Idaho National Engineering and Environmental Laboratory Idaho Falls / USA) during the same trip is gratefully acknowledged. Further thanks goes to Prof. Dr. Tim McDermott and Dr. Corinne Lehr (Montana State University Bozeman / USA) for organizing GC-MS access at their university and especially to Dr. John Garbarino, Dr. Mark Sandstrom and Kevin Fehlberg (United States Geological Survey, Federal Center Denver / USA) for numerous GC-MS analyses in a fascinating laboratory environment.

My acknowledgements to the colleagues Dr. James W. Ball and Blaine R. McCleskey (United States Geological Survey Boulder / USA) do not only include assistance in the field and especially during laboratory work, but extend to the pleasure it is working within their research group. Finally, Yellowstone field work would have never been as enjoyable as it was without Manja Seidel, Beate Böhme and Juliane Becker accompanying me in June/July and September/October 2003, without Betty DeWeese's warm hospitality (Yellowstone River Motel), and of course without survey, organizational, and scientific help from Steve Dill (Federal Highway, Northwestern Division).

Sincere thanks to my parents and my sister Kerstin for their interest and patience in sharing the ups and downs during my research work. For his scientific support, for believing in me, and for keeping my ambitions high by always putting new tasks ahead I would like to thank Broder.



For the benefit and enjoyment of the people...

LIST OF CONTENTS

Introduction	1
1 Methylated and volatile metallics.....	5
2 Arsenic.....	11
2.1 Geogenic occurrences	11
2.2 Anthropogenic use	12
2.3 General toxicity.....	13
2.4 Global balances	14
2.5 Species	15
2.5.1 Dissolved inorganic arsenic	17
2.5.1.1 Inorganic As(V)	17
2.5.1.2 Inorganic As(III)	18
2.5.2 Dissolved organic arsenic species.....	22
2.5.2.1 Mono- and dimethylated As(V) acids.....	26
2.5.2.2 Tri- and tetramethylated As(V) acids.....	28
2.5.2.3 Mono- and dimethylated As(III) acids.....	29
2.5.2.4 Arsenosugars, arsenocholine, arsenobetaine.....	31
2.5.2.5 Organic arsenic sulfur compounds.....	32
2.5.2.6 Organic arsenic halogen compounds	33
2.5.3 Volatile arsenic species.....	35
2.5.3.1 Inorganic AsH ₃	35
2.5.3.2 Monomethylarsine	36
2.5.3.3 Dimethylarsine.....	36
2.5.3.4 Trimethylarsine.....	37
2.5.3.5 Organic Sulfur Arsines.....	38
2.5.3.6 Inorganic and organic halogen arsines.....	38
2.6 Analytical speciation techniques.....	39
2.6.1 Arsenic separation.....	39
2.6.1.1 Hydride generation.....	39
2.6.1.2 HPLC	43
2.6.1.3 Gas chromatography	44
2.6.1.4 Capillary zone electrophoresis	44
2.6.2 Arsenic detection.....	45
2.6.3 Arsenic quantification.....	46
2.7 Field sampling.....	47
2.7.1 Water sample stability and preservation	47
2.7.2 On-site species separation for water samples.....	49

2.7.3 Gas sampling without pre-concentration.....	50
2.7.4 Gas sampling with pre-concentration.....	51
2.7.4.1 Liquid sorbents.....	51
2.7.4.2 Solid sorbents.....	51
2.7.4.3 Cryotrapping.....	55
2.7.5 Techniques for collecting volatile metallics.....	56
2.7.5.1 Collection of volatile metallics from a gas phase.....	56
2.7.5.2 Collection of volatile metallics dissolved in an aqueous phase.....	57
2.8 Summary of chapter 2.....	58
3 Development of a field method.....	59
3.1 Development of an in-situ gas-collector cell.....	59
3.2 Gas generation and trapping.....	61
3.2.1 Optimization of arsine generation.....	62
3.2.2 Optimization of screening on total concentrations (liquid sorbents).....	65
3.2.3 Species-selective sampling (solid sorbents).....	70
3.2.3.1 Sorption tubes.....	70
3.2.3.2 Solid-phase micro-extraction (SPME).....	73
3.3 Summary of chapter 3.....	77
4 Yellowstone National Park.....	79
4.1 Introduction.....	79
4.1.1 Geology of the Park.....	80
4.1.1.1 Pre-Quaternary Geology.....	80
4.1.1.2 Quaternary Volcanism.....	81
4.1.1.3 Quaternary Glaciation.....	83
4.1.1.4 Hotspot development after the last volcanic cycle.....	84
4.1.1.5 Hydrogeochemistry of geothermal features.....	86
4.1.2 Study areas.....	89
4.1.2.1 Nymph Lake area.....	91
4.1.2.2 Hazle Lake area.....	93
4.1.2.3 Norris Geyser Basin.....	94
4.1.2.4 Gibbon Geyser Basin.....	98
4.1.2.5 Lower Geyser Basin.....	99
4.2 Methodology.....	100
4.2.1 Field methods.....	100
4.2.1.1 Reconnaissance trip 2002.....	100
4.2.1.2 Sampling trips 2003.....	102
4.2.2 Laboratory.....	106
4.2.3 Data processing.....	107

4.2.3.1 Water data check.....	107
4.2.3.2 Gas concentration conversion.....	110
4.2.3.3 Gas chromatography interpretation.....	115
4.2.3.4 Statistics.....	115
4.2.3.5 Speciation modeling.....	115
4.3 Results.....	116
4.3.1 Cluster analysis.....	116
4.3.1.1 Clustering of the water samples.....	116
4.3.1.2 Clustering of the gas samples.....	119
4.3.2 Description of water and gas chemistry.....	120
4.3.2.1 Type I steam-heated waters.....	120
4.3.2.2 Type II deep thermal waters.....	130
4.3.3 Modeling As species and mineral phases.....	138
4.3.4 Volatile As speciation.....	141
4.3.5 Modeling volatile As speciation.....	145
4.3.6 Quantification of volatile metallics.....	146
4.4 Summary of chapter 4.....	151
5 Recommendations.....	153
6 References.....	155
7 Appendix.....	173

LIST OF ABBREVIATIONS

a	activity
AAS	atomic absorption spectrometry
AES	atomic emission spectrometry
AFS	atomic fluorescence spectrometry
AMD	acid mine drainage
AMP	adenosine monophosphate
amu	atomic mass unit
Apoptosis	normal series of events in a cell that lead to its death (and then replacement), apoptosis can also be induced by external influences, cancer cells avoid apoptosis
Ars	arsenic resistance
ArsR	protein that encodes a repressor protein
ArsA	protein that transports an energizing subunit, produces As(III)-specific ATPase
ArsB	protein that translocates the As(III) via a transmembrane efflux channel driven by the ATP hydrolysis produced by ArsA
ArsC	arsenate reductase; protein that converts As(V) in the cell to As(III) which is pumped out of the cell via the ArsA/ArsB anion pump
ArsD	regulatory protein
As(V)	inorganic pentavalent arsenic (H_3AsO_4^0 , H_2AsO_4^- , HAsO_4^{2-} , AsO_4^{3-})
As(III)	inorganic trivalent arsenic (H_3AsO_3^0 , H_2AsO_3^- , HAsO_3^{2-} , AsO_3^{3-})
ATP	adenosine triphosphate
ATPase	protein complex responsible for converting electrical potential energy into ATP
b.p.	boiling point
cAMP	cyclic ester of AMP
CAR	Carboxen
cytotoxicity	toxicity to cells
CW	Carbowax TM
CZE	capillary zone electrophoresis
DMA	gaseous dimethylarsine, $(\text{CH}_3)_2\text{AsH}$
DMAA	organic dimethylated arsenic acid, without distinction between tri-or pentavalent species
DMA ^V A	organic pentavalent dimethylated arsenic acid [$(\text{CH}_3)_2\text{AsO}(\text{OH})$, $(\text{CH}_3)_2\text{AsO}_2^-$]
DMA ^{III} A	organic trivalent dimethylated arsenic acid [$(\text{CH}_3)_2\text{As}(\text{OH})$, $(\text{CH}_3)_2\text{AsO}^-$]
DNA	deoxyribonucleic acid
DTT	dithiothreitol, $\text{C}_4\text{H}_{10}\text{O}_2\text{S}_2$
DVB	divinylbenzene
EDTA	ethylenediaminetetraacetic acid
ESI	electrospray ionization
ET-AAS	electrothermal AAS
fd	film thickness (GC column)
FI-HG	flow injection HG
GC	gas chromatography
GF-AAS	graphite furnace AAS
GFP	green fluorescent protein
$(\text{GS})_2\text{AsSe}$	seleno-bis(S-glutathionyl) arsinium ion
GSH	glutathione
HG	hydride generation
HG-AAS	hydride generation AAS
HPLC	high performance liquid chromatography

HRTEM	high resolution transmission electron microscope
ICP	inductively coupled plasma
ID	inner diameter (GC column)
L	length (GC column)
mesh size	largest diameter of sorption material grains, e.g., 60 mesh = grains that passed through 0.25 mm mesh size, 80 mesh = 0.18 mm, 100 mesh = 0.15 mm, 200 mesh = 0.07 mm
Michaelis constant	measure for the enzyme-substrate affinity, the higher the Michaelis constant, the weaker the affinity
MMA	gaseous monomethylarsine, $(\text{CH}_3)\text{AsH}_2$
MMAA	organic monomethylated arsenic acid, without distinction between tri- or pentavalent species
MMA ^V A	organic pentavalent monomethylated arsenic acid $[(\text{CH}_3)\text{AsO}(\text{OH})_2^0, (\text{CH}_3)_2\text{AsO}_2(\text{OH})^-, (\text{CH}_3)\text{AsO}_3^{2-}]$
MMA ^{III} A	organic trivalent monomethylated arsenic acid $[(\text{CH}_3)\text{As}(\text{OH})_2, (\text{CH}_3)_2\text{AsO}(\text{OH})^-, (\text{CH}_3)_2\text{AsO}_2^{2-}]$
m.p.	melting point
MS	mass spectrometry
MS/MS	tandem mass spectrometry
Operon	functional unit of the DNA which synthesizes a special protein
PA	polyacrylat
PDMS	polydimethylsiloxane
PE	polyethylene
PFA	perfluoroalkoxy, teflon, m.p. 310°C, tensile strength 110 kg/cm ² at 250°C
Pit	non-specific and fast phosphate inorganic transport system, active at high phosphate concentration
Pst	energy requiring, specific phosphate inducible transport system, works in times of phosphate depletion
PTFE	polytetrafluorethylene, teflon, m.p. 327°C, tensile strength 85 kg/cm ² at 250°C
REE	rare earth elements (La, Ce, Pr, Nd, Sm, Eu, Gd, Tb, Dy, Ho, Er, Tm, Yb, Lu)
Repressor protein	the product of a regulatory gene that blocks the function of another gene
RSH	thiols, monovalent -SH radicals attached to a carbon atom, mercaptan
RS-SR	disulfide
SAHC	S-adenosylhomocysteine
SAM	S-adenosylmethionine
SEM	scanning electron microscope
SPE	solid-phase extraction
SPME	solid-phase micro extraction
TETRA	tetramethyl arsonium ion $(\text{CH}_3)_4\text{As}^+$
Thiols	monovalent -SH radicals attached to a carbon atom, mercaptan
TMA	gaseous trimethylarsine, $(\text{CH}_3)_3\text{As}$
TMAO	trimethylarsineoxide, $(\text{CH}_3)_3\text{AsO}$
TPR	templated resin
transferase	enzyme that realizes the transport of groups from their donor to their acceptor

INTRODUCTION

On January 22, 2001, the U.S. Environmental Protection Agency (EPA) lowered the enforceable maximum contamination level for As from 0.05 mg/L to 0.01 mg/L finally following the provisional guideline advised in the World Health Organization guidelines for drinking-water quality (World Health Organization 1993) and enforceable drinking-water standards in other countries (e.g., TrinkwV 1990). The revision was preceded by various discussions on the level to be proposed including 0.003 mg/L as minimum feasible level and 0.005 mg/L as proposed on June 22, 2000. Numerous disputes and contradictions caused a further delay of the effective date until February 22, 2002 to conduct additional health effect, risk, cost, and benefit reviews. Public water systems must comply with the 0.01 mg/L standard beginning January 23, 2006 (Environmental Protection Agency 2001).

This uproar in the As community is a result of new knowledge about As toxicity and its global occurrence in increased concentrations both naturally and man-made. Since the late 1980s, naturally high As concentrations in West Bengal and Bangladesh have become known as the cause of „the worst mass poisoning of a population in history“ (Smith et al. 2000). Groundwater wells drilled to supply the population with clean drinking-water without microbial contamination penetrated peat layers in the sedimentary basin which caused reduction of iron oxyhydroxides and release of their sorbed arsenic load to solution (Ravenscroft et al. 2001). Examples of generally more localized, man-made As contaminations include sites of mining activities, metal processing, high-temperature combustion, and electronic and chemical industries (pesticides, growth stimulants, pharmaceuticals, glass ware, galvanizing, tanning).

High total As concentrations are, however, not the only concern: Occurrence, sorption, mobility, potential assimilation, and toxicity depend significantly on the individual As species. Dissolved tri- and pentavalent inorganic and organic (methylated) as well as volatile As species can be distinguished. A thorough review on As speciation literature revealed that within the last three decades, since species-selective determination methods were introduced, significant progress has been made on inorganic As speciation and on in vivo and in vitro studies of organic As species. Hydrogeochemical studies on the occurrence of dissolved methylated and especially volatile As species in aquatic environments, however, are still rare. The qualitative and quantitative detection of methylated and volatile compounds is important because they act as connecting links for the transfer between hydrosphere - biosphere and hydrosphere - atmosphere, respectively. Furthermore, trivalent methylated and volatile As are the most toxic As compounds known.

Considering the sampling of volatile As, one major problem is extracting gases from an aqueous phase. The other problem is the stabilization of volatile As after collection because it is easily hydrolyzed and oxidized. To solve these problems was one of the primary goals of the present research work. A robust technique for in-situ separation of gaseous compounds from the aquatic phase by a PTFE membrane in a specially designed PTFE collector cell was developed. The cell can be placed at the sediment-water interface or in the aqueous body and gases are withdrawn from

the aqueous phase by vacuum up to -500 mbar and trapped in either liquid or solid sorbent. Trapping the gases in a liquid sorbent will not only allow screening of the main target element volatile As but of all other volatile metals and metalloids present at the sampling site, summarized in the following as volatile metallics.

After the initial development of the method, various study sites were chosen for a first screening on the occurrence of volatile As in solution. Study sites comprised wetlands at two abandoned uranium tailings in Lengenfeld and Schneckenstein / Germany, the US superfund site Milltown, Montana / USA, mine water irrigated rice fields in Luojiqiao town / China, a constructed wetland in Jülich / Germany, a smouldering heap of As-rich coal in Oelsnitz / Germany, the Florida Everglades / USA, and Yellowstone National Park / USA.

The screening of the different aquatic environments mainly served for optimizing the developed sampling and trapping method for field application and for selecting one model area for further detailed studies on correlation of aqueous and gaseous As chemistry and volatile As speciation. Only the results from Yellowstone National Park are presented here. A brief introduction to the other study sites is given in Appendix 1. Yellowstone National Park was selected as final study area because of the high dissolved (up to 11 mg/L) and volatile As concentrations detected here under a wide range of hydrogeochemical conditions (pH from 1.9 to 8.7, temperature from 20 to 92°C, redox potential from -260 mV to 720 mV, and anion predominance from chloride and sulfate to hydrogencarbonate). The sampling campaigns were conducted in June/July and September/October 2003. The results are a central part of this research project besides the As review and the development of the field sampling technique for volatile metallics.

The thesis starts with a brief introduction to methylated and volatile metallics in general, their chemical characteristics, occurrence in the environment and typical concentration ranges (chapter 1). The second chapter provides a thorough review of the main target element As. Many reviews exist about As and central aspects are often global balances, toxicity, or, especially since the last 10 years, microbiology. The major focus of this review is the presentation of data available for the individual species especially the methylated and volatile species that are often not considered. Natural occurrences, chemical properties, toxicity, and abiotic and microbially catalyzed species conversion are described (section 2.5). Analytical speciation techniques with As separation, detection and quantification are summarized in section 2.6. Field sampling methods are discussed in section 2.7. For aqueous As species, this section includes water sample stability and preservation as well as possibilities of on-site species separation. For gaseous As species, sampling methods without pre-concentration are described compared to pre-concentration on solid sorbents, in liquid sorbents and in cryotrap.

Even though volatile As species at Yellowstone were mainly sampled directly from the gas phase, not by separation from the aquatic phase, the equipment for achieving the gas-water separation in aquatic environments is described in chapter 3. The outline of the field method development further includes the results of trapping efficiencies of various liquid sorbents (GF-AAS analysis) and tests

on species-selective determinations by solid sorbents and solid phase micro extraction fibers with GC-MS analysis.

After an introduction to geology, hydrogeology and hydrogeochemistry of the main study area Yellowstone National Park, chapter 4 gives the details of field and laboratory methodology and data processing (section 4.2). Results are discussed in clusters of similar water and gas chemistry and speciation modeling is provided (section 4.3.1 to 4.3.3). For volatile As, speciation by GC-MS is described (section 4.3.4) and an attempt of hydrogeochemical modeling is presented (section 4.3.5). In the last section (4.3.6), an evaluation of the quantification of volatile metallics is given. One page summaries at the end of the chapters 2, 3, and 4 provide the most important information of each chapter.

A digital MS Access database included on a CD together with this thesis contains all presented information from pictures and descriptions of the study sites, raw analytical data, to data for quality control, and interpreted results.

1 METHYLATED AND VOLATILE METALLICS

Within the last 40 years, lessons learned from numerous accidents and an increasing public interest in environmental problems have led to intensive studies about the fate of metallics in the environment. Interdisciplinary work between geoscientists, chemists, toxicologists and physicians has shown that it is not sufficient to know total metallics concentrations for an understanding of the complex chemistry of metallics from geogenic and anthropogenic sources in natural systems, nor are total metallics concentrations sufficient for making predictions and giving advice for remediation measures. Speciation has become one of the most pressing subjects in research, since occurrence, mobility, sorption, potential assimilation, and toxicity vary significantly between different species of the same element.

Considerable attention has been paid to the detection of inorganic metal and metalloid species, yet the occurrence of organometallics in the environment is still widely unknown. The transition process from inorganic to organometallics is called alkylation, i.e. the replacement of an OH-group by an alkyl-group. In natural processes, the alkyl group mostly is a methyl (CH_3^-) group, more seldom an ethyl (C_2H_5^-), phenyl (C_6H_5^-) or butyl (C_4H_9^-) group. Methylation is enzymatically catalyzed and occurs in a wide range of conditions from anoxic-methanic to oxic - not only in microorganisms, but also in algae, plants, animals, and humans. Few animals are known that are not capable of biomethylation, e.g., several monkeys, chimpanzees, and the guinea pig (Healy et al. 1997; Wildfang et al. 1997). High total concentrations of organometallics are not a prerequisite. Methylation occurs at low concentrations. Purely abiotic methylation is possible, e.g., in the presence of methyl iodide, but is rarely observed. Transalkylation, i.e. the transfer of an alkyl group, can occur. Jewett et al. (1975) state the following sequence for transmethylation: $\text{Pb} > \text{Sn} > \text{Hg} > \text{As}$. Thus, Sn can transfer a methyl group to Hg according to the reaction $\text{Sn}(\text{CH}_3)_3^+ + \text{Hg}^{2+} \leftrightarrow \text{Sn}(\text{CH}_3)_2^{2+} + \text{Hg}(\text{CH}_3)^+$, while Hg can not transfer the methyl group to Sn.

Organometallics are among the most mobile environmental compounds, soluble in polar and non-polar media, accumulating in fatty tissue, capable of passing biological membranes, and most of them readily volatile due to their high vapor pressures. Compared to their inorganic predecessors some of them are less toxic, others are more toxic. Volatile organometallics have, comparable to inorganic volatiles (hydrides), an extremely high biotoxicity potential. All compounds with a boiling point $<150^\circ\text{C}$ and a vapor pressure $>10^3\text{Pa}$ (Clemens and Lewis 1988) are defined as "volatile". The first methylated compounds detected in the beginning of the 19th century were the volatile ones. In 1824, "bismuth breath" was described as a garlic odor in the breath of mine workers who were exposed to bismuth carbonate. The same phenomenon is reported from patients treated with bismuth carbonate for stomach disorders. Later, this volatile compound was identified to be $(\text{CH}_3)_2\text{Te}$ from Te, an impurity in bismuth carbonates that is biotransformed in humans (Bentley and Chasteen 2002b). After several incidents of arsenic poisoning in Germany and Great Britain, Gmelin (1839) noted that a garlic smell was present in the rooms, where the poisoning had occurred. This compound was identified as $(\text{CH}_3)_3\text{As}$, volatilized from wallpapers painted with As pigments (Challenger et al. 1933). Hofmeister (1894) reported strong garlic odor in the expired

breath of a dog after subcutaneous administration of 0.06 g sodium tellurate; another early hint on biomethylation of inorganic Te to $(\text{CH}_3)_2\text{Te}$.

Methylated mercury achieved worldwide attention. In 1956, fishermen of the small town of Minamata, Japan began to show symptoms of a neurological disorder. About 3 years later, the causes were traced back to methylmercury poisoning. A local company, Chisso Corporation, used Hg in the process of manufacturing acetaldehyde and dumped their processing wastes into the Minamata Bay. From 1932 to 1968, an estimated 27 tons of inorganic Hg were dumped into the bay. Some of the Hg was biomethylated to methylmercury chloride, accumulated in fish, and finally, since fish and shellfish were the main sources of food for the local residents, in humans (Takizawa 1979). Because of the "Minamata" disease Hg became the model for the formation of organometallics and many papers report its presence in the environment.

A more recent example is the methylation of Sb that became a news topic in the mid 1990s. Richardson (1994) claimed that the sudden infant death syndrome (SIDS) might be related to methylation and volatilization of toxic gases from flame retardants in mattresses and covers. The flame retardants contained Sb and increased Sb concentrations in the liver of SIDS victims were thought to result from trimethylstibine inhalation. Later investigations, however, found no causal relationship between SIDS and levels of trimethylstibine (Jenkins et al. 2000).

Both Hg and Sb biomethylation leads to increasing toxicity for humans. However, biomethylation may also act as a detoxification mechanism for humans. One example is Se. Frankenberger and Karlson (1989) suggested methylation and subsequent volatilization as a passive rehabilitation measure for the Kesterson Reservoir US Superfund Site, California. By the beginning of the 1980s, sediment significantly enriched in Se that was transported by the San Luis drain had accumulated in the reservoir. Evaporation further increased Se concentrations in the sediment. Bioaccumulation in flora and fauna led to toxic levels of Se among the high-end consumers of the food chain, causing deaths and deformities, especially in bird species.

To date, methylated volatile and non-volatile compounds have been found in many environments such as sea water, estuaries, geothermal areas, waste heaps, sewage and digester gases, or urban air (Table 1). Higher alkylated species (e.g., tetraethyllead, butyltin, phenylmercury, ethyldimethylarsine, triethylarsine) are usually attributed to anthropogenic sources (Feldmann and Hirner 1995; Hirner et al. 1998). Evidence for naturally occurring ethylmercury in soils and sediments from the Everglades in Florida was presented by Cai et al. (1997). Transition metals rarely form volatile species, even though carbonyl-compounds are known for Ni from anthropogenic sources like cigarette smoke, carbon monoxide containing industrial hydrogen or nitrogen gas or automobile exhaust. Feldmann and Cullen (1997) detected 0.2-0.3 $\mu\text{g}/\text{m}^3$ volatile $\text{Mo}(\text{CO})_6$ and 0.005-0.01 $\mu\text{g}/\text{m}^3$ volatile $\text{W}(\text{CO})_6$ in waste deposit gases. Considerably more alkylated compounds have been created in experiments with incubated microbial cultures over soil, sediment, and water, as well as from biological samples. Moreover innumerable organometallics have been synthesized chemically

in the laboratory. Several reviews exist about organometallics in the environment (Craig 1986; Crompton 1998; Hirner and Emons 2004; Thayer 1995).

Table 1 Environmental occurrence of volatile and dissolved inorganic and organometallics

Atom	Species	Occurrence
As	AsH ₃ (g)	waste heap gas ¹ ; digester gas ² ; hot spring gas, British Columbia ³
	(CH ₃)AsH ₂ (g)	waste heap gas ¹ ; digester gas ² ; hot spring gas, British Columbia ³ ; geothermal water, New Zealand 0.08-1.9 µg/kg ³ ; soil from domestic waste heap 205-8540 ng/kg ⁴ ; soil below gas station 1780-6720 ng/kg ⁴ ; soil below coal mining industry 200-1350 ng/kg ⁴ ; river and harbor sediment 0.6-21.7 ng/kg ⁵
	(CH ₃) ₂ AsH (g)	waste heap gas ¹ ; digester gas ² ; hot spring gas, British Columbia ³ ; geothermal water, New Zealand 0.02-8.9 µg/kg ³ ; soil from domestic waste heap 215-2320 ng/kg ⁴ ; soil below gas station 1030-6620 ng/kg ⁴ ; coal mining 260-720 ng/kg ⁴ ; river and harbor sediment 0.8-7.3 ng/kg ⁵
	(CH ₃) ₃ As (g)	waste heap gas ¹ ; digester gas ² ; hot spring gas, British Columbia ³ ; geothermal water, New Zealand 0.18-0.25 µg/kg ³ ; soil from domestic waste heap 55-1020 ng/kg ⁴ ; soil below gas station 50-250 ng/kg ⁴ ; soil below coal mining industry 14-215 ng/kg ⁴ ; river and harbor sediment 0.6-11.4 ng/kg ⁵
	(CH ₃) ₂ As(C ₂ H ₅) (g)	river and harbor sediment 7.2 ng/kg ⁵
	(CH ₃)As(C ₂ H ₅) ₂ (g)	river and harbor sediment 3.8 ng/kg ⁵
	As(C ₂ H ₅) ₃ (g)	river and harbor sediment 1.2 ng/kg ⁵
	As (g) (no speciation)	0.1-1.8 ng/mL gas at a cattle dipping vat site, Florida ²⁵
Bi	BiH ₃ (g)	landfill and sewage gas (up to 25 µg/m ³) ⁶
	(CH ₃)BiH ₂ (g)	river and harbor sediment 0.1 ng/kg ⁵
	(CH ₃) ₃ Bi (g)	digester gas ² ; landfill, sewage gas (25 µg/m ³) ²⁶ ; domestic waste heap soil 40 ng/kg ⁴
Cd	(CH ₃) ₂ Cd (g)	waste heap gas ¹ ; digester gas ²
Ge	(CH ₃)GeH ₃ (g)	geotherm. water, New Zealand 0.02-0.06 µg/kg ³ ; coal mining ind. soil 12-50 ng/kg ⁴
	(CH ₃) ₂ GeH ₂ (g)	geotherm. water, New Zealand 0.02-0.03 µg/kg ³ ; domest. waste heap soil 350 ng/kg ⁴
	(CH ₃) ₃ GeH (g)	geotherm. water, New Zealand 0.04-0.17 µg/kg ³ ; domest. waste heap soil 430 ng/kg ⁴
Hg	(CH ₃)Hg ⁺ (aq)	geothermal water, New Zealand 0.1-15.3 µg/kg ³ ; peatland pore water in Experimental Lake Area, Ontario, Canada (up to 6 ng/L, average 0.25-0.65 ng/L) ⁷ ; Everglades sediment (< 0.1-5 ng/g dry weight = < 0.2-2% of total Hg) ⁸ ; Everglades 20% of total Hg ⁹ ; high altitude lakes, Western US (0.01-0.73 ng/L = 0.02-12.3 % of total Hg) ¹⁰ ; estuaries (78-393 fmol/L Gironde, 77-445 fmol/L Rhine, 44-1147 fmol/L Scheldt) ¹¹
	(CH ₃) ₂ Hg (g)	digester gas ² ; sewage gas ¹² ; urban air ¹³ ; river and harbor sediment 2.8 ng/kg ⁵ ; Gironde estuary 0-12 fmol/L ¹¹
Pb	(CH ₃) ₄ Pb (g)	digester gas ² ; urban air, Bordeaux (0.09-95.2 ng/m ³) ¹⁴ ; estuaries (0-4.4 fmol/L Gironde, 0-1.2 fmol/L Rhine, 0-8.9 Scheldt) ¹¹
	(CH ₃) ₃ (C ₂ H ₅)Pb (g)	digester gas ² ; estuaries (0-0.7 fmol/L Gironde, 0-0.7 fmol/L Rhine, 0-2.1 Scheldt) ¹¹
	(CH ₃) ₂ (C ₂ H ₅) ₂ Pb (g)	digester gas ² ; estuaries (0-0.5 fmol/L Gironde, 0-90.5 fmol/L Rhine, 0-3.0 Scheldt) ¹¹
	(CH ₃)(C ₂ H ₅) ₃ Pb (g)	digester gas ² ; estuaries (0-1.7 fmol/L Gironde, 0-3.6 Scheldt)
	(C ₂ H ₅) ₄ Pb (g)	digester gas ² ; estuaries (0-3.0 fmol/L Gironde, 0-0.9 fmol/L Rhine, 0-7.6 Scheldt)
Sb	SbH ₃ (g)	landfill and sewage gas (thermophilic step 6.7-14.7 µg/m ³) ⁶
	(CH ₃)SbH ₂ (g)	geothermal water, New Zealand 0.007-0.07 µg/kg ³ ; soil from domestic waste heap 120-430 ng/kg ⁴ ; soil below gas station 260-300 ng/kg ⁴ ; soil below coal mining industry 110-195 ng/kg ⁴ ; river and harbor sediment 0.2-9.8 ng/kg ⁵
	CH ₃ SbO(OH) ₂ (aq)	Florida Ochlockonee river 92 ppt, ~Bay 2.3 ppb ¹⁵ ; river and seawater (1-12 ng/L) ¹⁶
	(CH ₃) ₂ SbH (g)	geothermal water, New Zealand 0.01-0.08 µg/kg ³ ; soil from domestic waste heap 90-350 ng/kg ⁴ ; soil below gas station 60-120 ng/kg ⁴ ; soil below coal mining industry 6-25 ng/kg ⁴ ; river and harbor sediment 0.1-1.2 ng/kg ⁵
	(CH ₃) ₂ SbO(OH) (aq)	Ochlockonee Bay 110 ppt, Gulf of Mexico 588 ppt ¹⁵ ; river, seawater (1-12 ng/L) ¹⁶

Atom	Species	Occurrence
	Sb(C ₂ H ₅) ₃	river and harbor sediment 0.1 ng/kg ⁵
Se	(CH ₃)SeH	Mediterranean Sea 0.3-0.8 pmol/m ³ in air; 60-158 pmol/m ³ in ocean water ¹⁷
	(CH ₃) ₂ Se	waste heap gas ¹ ; urban air, Bordeaux (0.7-8.7 ng/m ³) ¹⁴ ; hot spring gas, British Columbia ³ ; air over Gironde estuary ¹⁷ ; Mediterranean Sea 0.3-1.2 pmol/m ³ in air, 60-636 pmol/m ³ in ocean water ¹⁷ ; sewage sludge ¹⁸ ; soil from domestic waste heap 140 ng/kg ⁴ ; soil below coal mining industry 25-45 ng/kg ⁴ ; estuaries (294-1107 fmoL/L Gironde, 284-8784 fmoL/L Rhine, 191-12793 fmoL/L Scheldt) ¹¹ ; river and harbor sediment 1.0 ng/kg ⁵
	(CH ₃) ₂ Se ₂	waste heap gas ¹ ; Mediterranean Sea 0.3-0.6 pmol/m ³ in air 71-259 pmol/m ³ in ocean water ¹⁷ ; estuaries (25-90 fmoL/L Gironde, 0-289 fmoL/L Rhine, 0-1625 fmoL/L Scheldt) ¹¹ ; river and harbor sediment 2.1 ng/kg ⁵
	Se (g) (no speciation)	ponds in Kesterson Reservoir over barley and salt grass
Si	(CH ₃)SiOH (g)	waste deposit gas 3.4-17.5 mg/m ³ ; waste composting gas 0.3-3.5 mg/m ³ ²⁰
Sn	SnH ₄ (g)	waste heap gas ¹ ; harbor and estuarine sediment ²¹
	CH ₃ SnH ₃ (g)	soil from domestic waste heap 40-18.000 ng/kg ⁴ ; soil below gas station 40-80 ng/kg ⁴ ; soil below coal mining industry 2440 ng/kg ⁴ ; river, harbor sediment 0.4-12.3 ng/kg ⁵
	(CH ₃) ₂ SnH ₂ (g)	soil from domestic waste heap 20-3350 ng/kg ⁴ ; soil below gas station 25-55 ng/kg ⁴ ; river and harbor sediment 0.3-2.9 ng/kg ⁵
	(CH ₃) ₃ SnH (g)	soil from domestic waste heap 15-3100 ng/kg ⁴ ; soil below gas station 3-15 ng/kg ⁴ ; soil below coal mining industry 3-9 ng/kg ⁴ ; river, harbor sediment 0.1-0.5 ng/kg ³
	(CH ₃) ₄ Sn (g)	waste heap gas ¹ ; digester gas ² ; landfill gas, Vancouver ²² ; soil below gas station 9-35 ng/kg ⁴ ; estuaries (0-4.3 fmoL/kg Gironde, 0-2.5 fmoL/L Rhine, 1-30.8 fmoL/L Scheldt) ¹¹ ; harbor and estuarine sediment ²³
	(CH ₃) ₃ (C ₄ H ₉)Sn (g)	estuaries (0-0.5 fmoL/L Gironde, 0-1.2 fmoL/L Rhine, 0-5.5 Scheldt) ¹¹
	(CH ₃) ₂ (C ₄ H ₉) ₂ Sn (g)	estuaries (0-3.8 fmoL/L Gironde, 0-3.6 fmoL/L Rhine, 7.4-331.4 Scheldt) ¹¹
	(CH ₃)(C ₄ H ₉) ₃ Sn (g)	estuaries (0-72.8 fmoL/L Gironde, 0-55.1 fmoL/L Rhine, 0-1457.5 Scheldt) ¹¹
	Sn(C ₄ H ₉)H ₃ (g)	river and harbor sediment 0.4-9.6 ng/kg ⁵
	Sn(C ₄ H ₉)(CH ₃)H ₂ (g)	river and harbor sediment 0.1 ng/kg ⁵
	Sn(C ₄ H ₉)(CH ₃) ₂ H (g)	river and harbor sediment 4.5 ng/kg ⁵
	Sn(C ₄ H ₉) ₂ H ₂ (g)	river and harbor sediment 8.6 ng/kg ⁵
Te	(CH ₃) ₂ Te (g)	waste heap gas ¹ ; thermophilic digester gas ² ; river and harbor sediment 0.2 ng/kg ⁵
Tl	(CH ₃) ₂ Tl ⁺ (aq)	Atlantic Ocean <0.4 – 3.2 ng/L (3-48% of total Tl) ²⁴

* list is exemplary and does not claim to be complete, only compounds detected in the environment, no laboratory experiments are included; (g) = gaseous species in ambient air or gas, and dissolved species volatilized from water or sediment, (aq) = aqueous species in water or sediment;

reference numbers cited: ¹ Feldmann 1995, ² Feldmann and Kleinmann 1997, ³ Hirner et al. 1998, ⁴ Hirner et al. 2000, ⁵ Krupp et al. 1996, ⁶ Feldmann and Hirner 1995, ⁷ Branfireun et al. 1996, ⁸ Gilmour et al. 1998, ⁹ Cai et al. 1999, ¹⁰ Krabbenhoft et al. 2002, ¹¹ Amouroux et al. 1998, ¹² Bzezinska et al. 1983, ¹³ Schroeder 1982, ¹⁴ Pécheyran et al. 1998, ¹⁵ Andrae et al. 1981, ¹⁶ Andrae and Froehlich 1984, ¹⁷ Amouroux and Donard 1996, ¹⁸ Reamer and Zoller 1980, ¹⁹ Biggar and Jayaweera 1993, ²⁰ Grümping et al. 1998, ²¹ Donard and Weber 1988, ²² Maillefer et al. 2003, ²³ Jantzen 1992, ²⁴ Schedlbauer and Heumann 1999, ²⁵ Thomas and Rhue 1997, ²⁶ Feldmann et al. 1999a

Strictly speaking, all alkylated compounds are thermodynamically unstable with respect to oxidation, UV irradiation, thermal influence, hydrolysis, reaction with radicals, and demethylation. Because their reaction kinetics are usually slow, they can be detected under natural conditions. Mean dissociation energies can be taken to estimate the stability of organometallics, because the weak bond between the metal or metalloid and the C atom is easily replaced by much stronger bonds between C-O or C-X (X = halogens). The increasing polarity between metal and C atom as well as the presence of other ligands, like humic or fulvic acids, can further destabilize the compounds. Figure 1 shows estimates for the stability of (CH₃)_nM species.

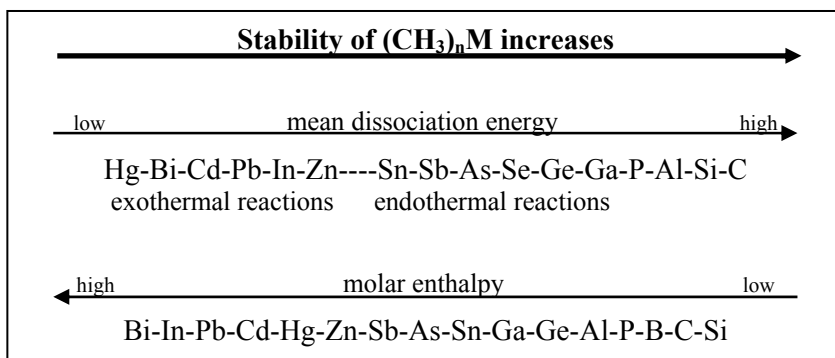


Figure 1 Estimations for the stability of $(\text{CH}_3)_n\text{M}$ species; stability increases with increasing mean dissociation energy, and with decreasing molar enthalpy (M = metal or metalloid; modified after Feldmann 1995)

Trimethylbismuth and tetramethyllead decompose spontaneously in the gaseous phase, whereas dissociation reactions for all compounds with higher mean dissociation energies than Sn-C compounds are endothermic and consequently more stable (Figure 1). Higher alkylated species are generally considered less stable than methylated species. If low-energy orbitals are available, H atoms from the organic substitute can be transferred to the metal or metalloid, leading to the formation of an alkene (Davidson et al. 1976).

One of the most investigated elements, especially with regard to its organic speciation, is the metalloid arsenic. Natural occurrences, anthropogenic use, toxicity and a global As balance will be presented in the following sections, before the more common inorganic and organic As species will be discussed. The As biomethylation pathway will be described in detail with relevant chemicals and enzymes, and differences in mobility and toxicity of the respective species will be given.

2 ARSENIC

For an introduction to the element arsenic (As), first discovered in 1250 by the German scholastic Albertus Magnus, several detailed reviews exist, e.g., Cullen and Reimer (1989); Fowler (1983); Korte and Fernando (1991); Mandal and Suzuki (2002); Matschullat (2000); Merkel and Sperling (1998); Nriagu (1994a); Nriagu (1994b); Rde (1996); and Smedley and Kinniburgh (2002).

2.1 Geogenic occurrences

The semi-metal or metalloid As ranks 44th in abundance in the earth's crust with average concentrations of 2.0 ppm in the upper crust and 1.3 ppm in the lower crust (Wedepohl 1995). It is mainly associated with magmatic or sedimentary rocks, especially iron ores (Table 2, detailed review also in Smedley and Kinniburgh 2002).

Table 2 Arsenic concentrations in different rock types (Woolson 1983)

Rock	Minimum [mg/kg]	Maximum [mg/kg]	Mean [mg/kg]
Andesite, Dacite	0.5	5.8	2.0
Basalts, Gabbros	0.06	113	2.0
Ultrabasites	0.3	16	3.0
Granite	0.2	13.8	1.5
Carbonate	0.1	20	1.7
Sandstone	0.6	120	2.0
Coal	0	2000	13
Shale, Clay	0.3	490	14.5
Phosphorite	0.4	188	22.6
Sedimentary iron ores	1	2900	400

Average concentrations in soils vary significantly, depending on the parent rock and inhomogeneities. Values cited are between 0.1 for sandy soils and 40 mg/kg for clayey soils or soils rich in organic matter. The world-wide average is about 5-6 mg/kg (Woolson 1983). Extreme concentrations were found over Dartmoor granites in Great Britain with 250 mg/kg, quartzites in Brisbane, Australia, with 100-200 mg/kg, and gold mines in Zimbabwe with 2000 mg/kg (Peterson et al. 1981).

About 245 As minerals are known (Onishi 1969). Besides the four elemental As modifications there are 27 arsenides (e.g., loellingite FeAs_2 , rammelsbergite NiAs_2), 13 sulfides (e.g., arsenopyrite $\text{Fe}(\text{As},\text{S})_2$, cobaltite CoAsS , gersdorffite NiAsS , enargite Cu_3AsS_4 , realgar As_4S_4 , orpiment As_4S_6), 65 sulfo-salts, 2 oxides, 11 arsenites, 116 arsenates (e.g., mimetesite $\text{Pb}_5[\text{Cl}[\text{AsO}_4]_3$, scorodite $\text{FeAsO}_4 \cdot 2\text{H}_2\text{O}$), and 7 silicates.

High-pH groundwaters in closed basins in arid to semi-arid areas and strongly reducing groundwaters in organic-rich sediments with slow flushing rates tend to have higher As concentrations (> 1 $\mu\text{g/L}$) As concentrations. This pH and redox dependence is explained in the chemistry of dissolved, inorganic As (section 2.5.1). Areas known for high As concentrations in groundwater are parts of Argentina, Chile, China, Hungary, Mexico, Western USA, and with about 40 million people exposed to high-As groundwater, Bangladesh, Vietnam, and West Bengal. On a more localized scale, high As concentrations are also encountered in mineralized, and mined areas as well as in geothermal areas (Table 3). Smedley and Kinniburgh (2002) and Mandal and Suzuki (2002) provide a

review of typical As concentrations in natural waters, as well as in different countries world-wide. Also Nordstrom (2002) lists global As contaminations in groundwater.

Table 3 Examples for increased As concentrations in some aquatic systems worldwide

Country, geological setting	As [$\mu\text{g/L}$]	reference
Groundwater, geogenic As source		
Argentina (loess, rhyolitic volcanic ash, thermal springs, oxidizing, neutral to high pH, often saline)	<1 to 5,300	Sancha and Castro (2001); Smedley et al. (2002)
Bangladesh (alluvial, deltaic sediments, strongly reducing, slow groundwater flow rates)	<1 to 2,5000	British Geological Survey Department of Public Health Engineering (2001)
Chile, Antofagasta (Quaternary volcanic sediments, oxidizing, arid, high salinity)	100-1000	Sancha and Castro (2001)
China, Xinjiang (alluvial sediments, reducing)	40-750	Wang and Huang (1994)
Germany (Keuper sandstone)	<10 to 150	Heinrichs and Udluft (1999)
Hungary (alluvial sediments, organics, reducing, some groundwaters high in humic acid)	<2-176	Gurzau and Gurzau (2001)
Mexico, Lagunera (volcanic sediments, oxidizing, neutral to high pH)	8-620	Del Razo et al. (1990)
Taiwan (sediments, including black shales, strongly reducing, some groundwaters containing humic acid)	10 to 1,820	Kuo (1968); Tseng et al. (1968)
USA, Southern Carson Desert, Nevada (holocene aeolian, alluvial, lacustrine sediments, reducing, high salinity)	up to 2,600	Welch and Lico (1998)
Vietnam, Red River delta (alluvial, deltaic sediments, reducing, high Fe, Mn, NH_4)	1-3050	Berg et al. (2001)
West Bengal (alluvial, deltaic sediments)	< 10 to 3,200	Sun et al. (2001)
Geothermal*		
New Zealand, Waimangu, Waitapu, Tokaanu	11-6,700	Hirner et al. (1998)
Philippines, Mt Apo	3,100-6,200	Webster (1999)
USA, Imperial Valley, California	up to 15,000	Welch et al. (1988)
USA, Lassen Volcanic NP, California	up to 27,000	Thompson et al. (1985)
USA, Steamboat Springs, Nevada	up to 2,700	Welch et al. (1988)
USA, Yellowstone NP, Wyoming	<1-5,800	Ball et al. (1998a, 1998b, 2001, 2002); Stauffer and Thompson (1984)
Mining areas		
Brazil, gold mining, Morro Velho	7,300	Williams (2001)
Canada, British Columbia	<0.2 – 556	Azcue et al. (1994)
Mexico, Zimapan (mine tailings, but also naturally occurring arsenopyrite, scorodite, tennantite)	< 14 – 1,000	Armienta et al. (1997, 2001)
Thailand, Ron Phibun	5,114	Williams (2001)
USA, Fairbanks, Alaska (gold mine tailings, schist, alluvium)	up to 10,000	Welch et al. (1988)
Zimbabwe, Globe and Phoenix	7,400	Williams (2001)
Zimbabwe, Iron Duke	72,000	Williams (2001)

* more examples in Webster & Nordstrom (2003)

2.2 Anthropogenic use

Arsenic-bearing minerals were already mined by the early Chinese, Indian, Greek, and Egyptian civilizations (Azcue and Nriagu 1994), and arsenic found wide-spread applications. As long ago as 55 B.C., Nero poisoned Britannicus to secure his Roman throne and inorganic As_2O_3 became very popular as a poison especially in the Middle Ages. Famous poisoners were the Borgias, Pope Alexander VI and his son Cesare Borgia. The popularity of the "inheritance powder" came to an abrupt end when in 1836 the development of Marsh's assay created a possibility to prove arsenic in the bodies. The first poisoner to be convicted was Marie Lafarge in 1842 for the murder of her husband

(Gorby 1994). Later on, As found a widespread application in agriculture. Inorganic As_2O_3 was used as pesticide, Pb- and Ca-arsenates as insecticides, and organic arsenicals as herbicides. In 1974, the application (not the production!) of As pesticides was banned in Germany (Bundesminister für Ernährung, Landwirtschaft und Forsten 1974) and the USA. Dimethylarsenic acid achieved notoriety as defoliant (“agent blue”) during the war in Vietnam (Léonard 1991). Poison on the one hand, remedy on the other, As was also used as a prominent medicine to treat rheumatism, malaria, sleeping sickness, and syphilis until the introduction of Penicillin in 1909 (Gorby 1994). More recent applications range from metal processing to chemical industries.

In 1989, As production was 53,000 t As_2O_3 (Ishiguro 1992). By 1993, it had decreased to 30,453 t (Matschullat 2000) and thereafter it stayed more or less constant with approximately 35,500 t in 2001, and 35,000 t in 2002 and 2003 (Brooks 2004). However, As is still released to the environment from numerous sources, e.g., high-temperature combustion (oil, coal, waste, cement), compost and dung (growth stimulant e.g., for poultry), glass ware production (decoloring agent), electronic industries (GaAs or InAs as semiconductor material), ore production and processing, metal treatment (lead and copper alloys, admixture in bronze production), galvanizing industry, tanning industry (depilation agent), ammunition factories, chemical industry (dyes and colors, wood preservatives, pesticides, pyrotechniques, drying agent for cotton, oil, and solvent recycling), and pharmaceutical and cosmetic industry (Ishiguro 1992; Léonard 1991).

2.3 General toxicity

Arsenic is still the most common source of acute inorganic metal poisoning and is second only to lead in chronic ingestion. Symptoms of acute As poisoning are restlessness, throat discomfort, nausea, chest pain, vomiting, diarrhea, convulsions, collapse, and cardiac failure, sometimes even leading to coma or death. Chronical effects include bronchitis, myocardial infarction, arterial thickening, peripheral neuropathy, hyperkeratosis, hyperpigmentation, the so-called “black foot” disease (necrosis, mainly on palms and soles, first identified in Taiwan), skin (Col et al. 1999; Tsuruta et al. 1998), lung, bladder (Hopenhayn-Rich et al. 1996a), liver and kidney cancer, as well as teratogenic effects (inorganic As can cross the placenta), mutagenic changes, and genotoxicity (Carson et al. 1986; Florea et al. 2004; Mandal and Suzuki 2002). It is, however, often hard to eliminate other pathological factors, like malnutrition, or concurrent exposures. A detailed recent review about As toxicology is provided in Chou et al. (2000).

Main sources of arsenic uptake are food, inhalation, ingestion of dust or soil, and drinking-water. Average daily intake rates are between 12 and 50 μg . In areas where fish and shellfish, known to yield relatively high levels of arsenic, are the main diet, intake may be up to several 100 $\mu\text{g}/\text{day}$ (Bentley and Chasteen 2002a). Much higher doses were consumed by people from Styria, Austria in the 19th century, for “plumpness to the figure, cleanness and softness to the skin, beauty and freshness to the complexion, as well as to improve breathing” (Wanklyn 1901). These so-called “arsenic-eaters” began with less than 30 mg doses 2 or 3 times a week and increased the dosage to

about 130 mg. In some cases, the practice continued for 40 years without apparent detrimental effects. In one recorded case, a woodcutter was observed by a physician to eat about 300 mg of pure As_2O_3 for two days in a row without apparent health effects, whereas in many cases 65 mg of As_2O_3 is already fatal (Roscoe and Schorlemmer 1911).

Dermal sorption is still controversial. In experiments with rhesus monkeys, Wester et al. (1993) found a low degree of As sorption with only 2-6% of the arsenic applied finally absorbed by the skin. Arsenic uptake in plants occurs in the oxidized form as arsenate in competition with phosphate for the same uptake carriers in the root plasmalemma. Mycorrhizal fungi are likely to play an important role in that assimilation because they enhance phosphate acquisition for the host plants (Meharg and Hartley-Whitaker 2002).

Once incorporated, As undergoes a complex pathway of chemically and enzymatically induced reactions, partly resulting in metabolites that are even more toxic than the educts. Arsenic toxicity strongly depends on the respective As species. The most toxic form of As are gaseous As compounds, followed by dissolved organic trivalent, inorganic trivalent, inorganic pentavalent, and organic pentavalent As compounds, and last but not least elemental arsenic and arsenosugars. Each species' toxicity, species conversions and human detoxification mechanisms will be discussed in detail in section 2.5.

2.4 Global balances

Trying to quantify the geogenic and anthropogenic As fluxes and its sources and sinks, is extremely difficult, because many of the published quantitative data are questionable. Two major problems are sampling or analytical errors and generalizations from only locally representative results to global budgets or even a lack of precise information on the reservoirs for which fluxes are to be balanced. Several approaches exist, e.g., Lantzy and MacKenzie (1979), MacKenzie et al. (1979), Walsh et al. (1979), and Chilvers and Peterson (1987). Figure 2 shows a scheme of the As fluxes, reservoir sizes, and average background concentrations according to one of the most recent detailed studies (Matschullat 2000).

One of the most critical points in all global As budget models is quantifying the emissions from the lithosphere and the hydrosphere to the atmosphere. Based upon an assumed high release of As by volatilization, especially from the ocean, MacKenzie et al. (1979) estimated the gaseous emissions to be 300,000 t/a. As Cullen and Reimer (1989) point out, those results are probably incorrect, since they were based upon assumptions of As concentrations in rain water that were too high. Chilvers and Peterson (1987) estimate 160 to 26,200 t/a for low temperature volatilization from soils and 22,000 t/a for volcanic emissions (terrestrial and submarine). The calculated ratio of anthropogenic to natural emissions according to them is 40:60. Matschullat (2000), however, states that especially the volcanic emissions are probably underestimated.

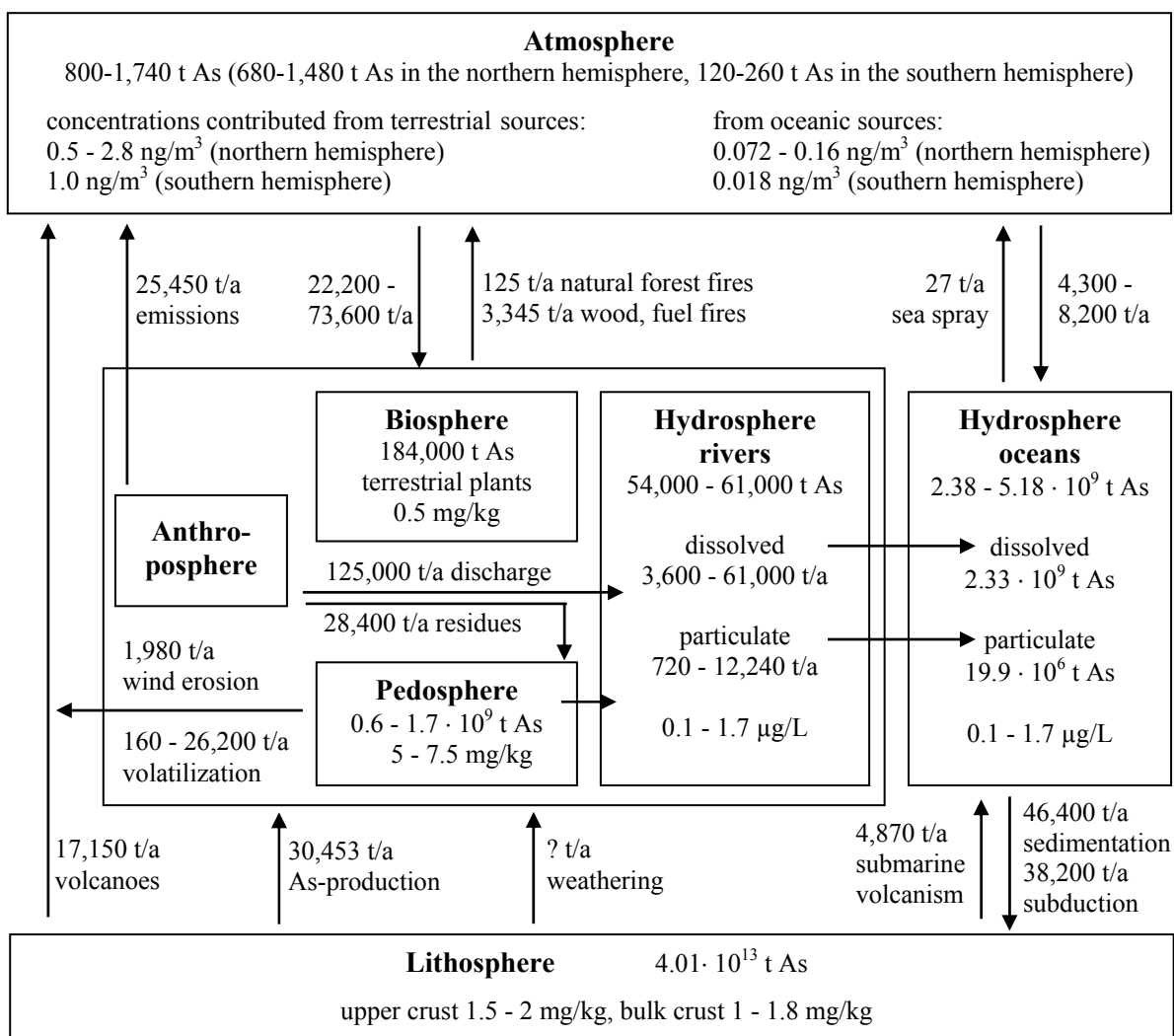


Figure 2 Global As cycle with fluxes and reservoir sizes for atmosphere, biosphere, pedosphere, hydrosphere, anthrosphere and lithosphere (modified after Matschullat 2000)

2.5 Species

In aqueous solutions As forms no single cations, but reacts readily with C, O, S, halogens or H. Predominant oxidation states are 3+ and 5+. Coordinate numbers are mainly 3 (AsF₃) and 5 (AsF₅), but also 4 (As(CH₃)₄⁺) or 6 (AsF₆⁻). Although As-C, As-O, As-S or As-halogen bonds are polarized (As^{δ+} - X^{δ-}), As-H bonds are not because the electronegativities of As and H are equal (EN = 2.20, Mortimer 1987). In most papers, however, As in a As-H bond is referred to as the more electronegative element (oxidation state 3-), in others as the more electropositive (oxidation state 3+, Cullen and Reimer 1989).

Beginning with the first positive identification of As by Marsh (1836), there was no shortage of analytical procedures for determinations of total As. However it was not until 1973 that As speciation became an issue, when Braman and Foreback (1973) introduced the first hydride generation technique, capable of separating different inorganic and methylarsenic compounds even in small

concentrations. Even though mobility, degradability, and toxicity vary significantly between the different species, there is still a lack of standard procedures for As speciation, especially for the methylated or volatile As species.

The As species outlined in Figure 3 will be described in more detail in the following sections. After a description of chemical properties, behavior in aqueous solutions, toxicity and transformation of the predominant dissolved inorganic species As(V) and As(III) (section 2.5.1), methylation of inorganic to organic As compounds and their respective properties, occurrence, and toxicity will be explained (section 2.5.2). Section 2.5.3 is dedicated to As compounds with a boiling point < 150°C, the so-called volatile arsenicals or arsines which form as intermediates and end products of the As biotransformation pathway or in a purely chemical reaction. Further details for the chemical generation of hydrides are provided in section 2.6.1.1.

	inorg.	organic compounds			
		1 CH ₃	2 CH ₃	3 CH ₃	4 CH ₃
As-Cl (III) volatile	AsCl ₃	CH ₃ AsCl ₂	(CH ₃) ₂ AsCl		
As-S (III) volatile		CH ₃ As(SR) ₂	(CH ₃) ₂ As(SR)		
As (III) volatile	AsH ₃	CH ₃ AsH ₂	(CH ₃) ₂ AsH	(CH ₃) ₃ As	
As (III) dissolved	H ₃ AsO ₃	CH ₃ As(OH) ₂	(CH ₃) ₂ As(OH)		
As-S (III) dissolved		CH ₃ As(SR) ₂ (OH)	(CH ₃) ₂ As(SR) ₂ (OH)	(CH ₃) ₃ As(SR) ₂	
As (V) dissolved	H ₃ AsO ₄	CH ₃ AsO(OH) ₂	(CH ₃) ₂ AsO(OH)	(CH ₃) ₃ AsO	(CH ₃) ₄ As ⁺
			(CH ₃) ₂ AsOCH ₂ COOH	(CH ₃) ₃ As ⁺ CH ₂ COO ⁻	
arsenosugars (link to lipophils)			(CH ₃) ₂ AsOCH ₂ CH ₂ OH	(CH ₃) ₃ As ⁺ CH ₂ CH ₂ OH	

Figure 3 Selective scheme of the more common inorganic and organic As compounds, As-S-compounds (formed in the presence of H₂S or thiols), and As-Cl-compounds (formed in the presence of Cl), gray line = main reaction pathway for As biomethylation as explained in section 2.5.2; shaded = volatile species

2.5.1 Dissolved inorganic arsenic

2.5.1.1 Inorganic As(V)

The oxidized form of dissolved As is As(V). Figure 4 shows the As(V) species as a function of pH. In natural groundwaters with a near neutral pH, the negatively charged complexes H_2AsO_4^- and HAsO_4^{2-} predominate. Significant amounts of the uncharged complex H_3AsO_4^0 occur in strong acid solutions (pH < 2) only. Solution properties of H_3AsO_4^0 closely resemble those of phosphoric acid H_3PO_4^0 . The pK values for individual As species vary sometimes significantly between different references. Therefore, the most commonly cited pK values are listed in a table next to the predominance diagram. A review on thermodynamic data for inorganic As is given in Nordstrom (2000) and Nordstrom and Archer (2003).

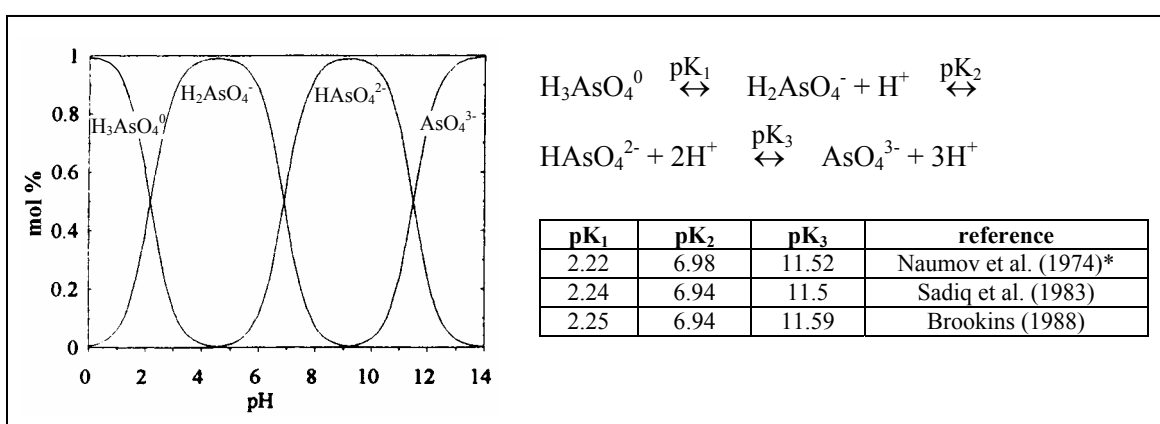


Figure 4 pH-dependent dissociation of As(V) species ($a(\text{As}) = 1.33 \cdot 10^{-7}$ mol/L; * data used for the diagram)

In surface water, arsenate shows a significant correlation with biological activity. Depletion in the aqueous solution during phytoplankton bloom due to uptake alternates with an increase in dissolved arsenate in the absence of biological activity, e.g., during winter (Anderson and Bruland 1991; Cabon and Cabon 2000; Howard et al. 1995; Sanders 1985; Sohrin et al. 1997). In oxidizing groundwaters As(V) is the predominant species, e.g., in Holocene aquifers in Argentina (Smedley et al. 2002), in aquifers of Quaternary volcanogenic sediments in Chile (Thornton and Farago 1997), Mexico (Del Razo et al. 1990), or in alluvial aquifers in the Basin and Range province, USA (Robertson 1989).

Sorption on Fe-, Mn-, Al-oxides and hydroxides, clay minerals and organic matter (Chiu and Hering 2000; Gulens et al. 1979) as well as substitution of arsenate for SO_4^{2-} in jarosite are probably the most important processes for As(V) removal from aqueous solutions (Savage et al. 2000; Figure 5). Smedley and Kinniburgh (2002) present a review of several solid-solution partition coefficients for a range of oxides and clays. At higher pH (pH > 8.5) sorption is inhibited or even desorption occurs. Consequently, groundwaters in semiarid or arid basins with high pH are often enriched in As. Reductive dissolution of Fe and Mn oxides leads to As release under reducing aquifer conditions (Smedley and Kinniburgh 2002). High concentrations of phosphate, bicarbonate, silicate, or organic matter can also decrease As sorption due to competition for the same binding sites.

Alkaline earth metal-arsenates, or rather their hydrates, may form limiting mineral phases (e.g., Ca-As-hydrate; Bothe and Brown 1999). However, due to inconsistencies in the experimental setup, the initial pH, the acids used for pH adjustment, the ionic strengths, the As concentrations, the consideration of formation of additional mineral phases, etc., existing thermodynamical solubility products, as presented e.g., in Wagemann 1978, are often dubious. A typical example is barium arsenate ($\text{Ba}_3(\text{AsO}_4)_2 = 3 \text{Ba}^{2+} + 2 \text{AsO}_4^{3-}$). Current databases still list $\text{Ba}_3(\text{AsO}_4)_2$ as a highly stable phase ($\log K = -50.110$; Chukhlantsev 1956), even though Robins (1985; $\log K = -16.58$) and Essington (1988; $\log K = -21.62$) got much higher solubility products from their experiments and proved that Chukhlantsev erroneously interpreted the precipitating mineral phase $\text{BaHAsO}_4 \cdot \text{H}_2\text{O}$ as $\text{Ba}_3(\text{AsO}_4)_2$.

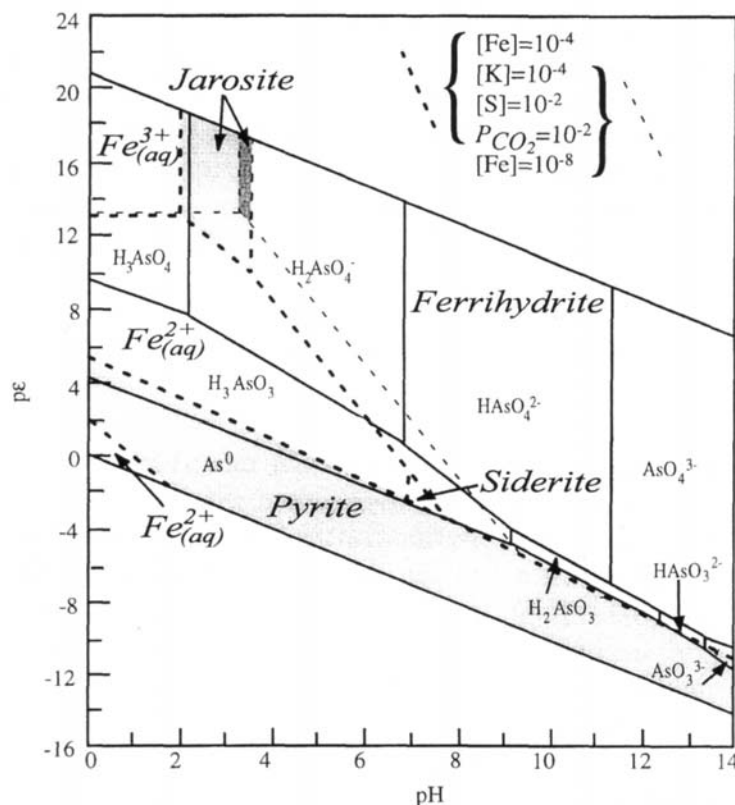


Figure 5 Predominance diagram for As(III) and As(V) species, superimposed the predominance diagram for the Fe-S-K-CO₂-system at 25°C, 1 bar, shaded fields = limiting mineral phases (modified after Savage et al. 2000)

2.5.1.2 Inorganic As(III)

Reduction of As(V) to As(III) and oxidation of As(III) to As(V) can be both enzymatically and abiotically catalyzed. For certain prokaryotes and eukaryotes As(V) can serve as respiratory oxidant (Ehrlich 2002). Energy is conserved if the reduction of As(V) to As(III) is coupled with the oxidation of organic matter (e.g. lactate) because the As(V)/As(III) oxidation/reduction potential is +135 mV (Oremland and Stolz 2003). Examples of dissimilatory arsenate-reducing prokaryotes (DARPs) are *Pseudomonas fluorescens* (Myers et al. 1973), *Anabaena oscillaroides* (Freeman 1985), *Desulfotomaculum auripigmentum* (Newman et al. 1997), *Desulfitobacterium GBFH* (Niggemyer et al. 2001), the Proteobacterium *Sulfurospirillum barnesii* SES-3, and *Sulfurospirillum arsenophilum* MIT-13 (Ahmann et al. 1997). The latter has just been recently classified as belong-

ing to the genus *Sulfurspirillum* (Stolz et al. 1999). Yeast (wine yeast; Crecelius 1977a) as well as aquatic organisms like coral species (Pilson 1974) and the freshwater phytoplankton *Chlorella* (Blasco et al. 1972), can catalyze the reduction from As(V) to As(III).

In contrast to the DARPs several other bacteria, cyanobacteria, archaea, and eukarya (review in Mukhopadhyay et al. 2002) reduce As(V) to As(III) only as a mechanism of As detoxification and resistance not for respiration. The most well studied detoxification mechanism is the so-called “ars operon” (Oremland and Stolz 2003). The operon is a functional unit of the DNA that causes resistance to trivalent and pentavalent arsenicals. *ArsR* encodes a repressor protein that further produces 4 proteins in gram-negative bacteria: *ArsA*, *ArsB*, *ArsC*, *ArsD*. *ArsA*, the transport energizing subunit, produces an As(III)-specific ATPase, i.e. a protein complex responsible for converting electrical potential energy into ATP (adenosin triphosphate), the so-called “molecular motor”. *ArsB* translocates the As(III) via a transmembrane efflux channel driven by the ATP hydrolysis produced by *ArsA*. *ArsC*, the so-called arsenate reductase (Aposhian 1997; Wildfang et al. 1998) converts As(V) in the cell to As(III) which is pumped out of the cell via the *ArsA/ArsB* anion pump, and *ArsD* is a further regulatory protein. In gram-positive bacteria *ArsA* and *ArsD* are absent (reviewed in Roberto et al. 2002).

Dissimilatory iron-reducing bacteria (DIRB) and sulfate-reducing bacteria (SRB) can not only reduce As enzymatically, but also by producing inorganic compounds (e.g., for SRB: glutathione GSH or other thiols that are monovalent -SH radicals attached to a carbon atom RSH) that in turn reduce As(V) to As(III) abiotically (Harrington et al. 1998; Spliethoff et al. 1995). However, the purely chemical conversion rates are low. Although Cherry et al. (1979) suggested significant As(V) reduction in the presence of reduced sulfur (H_2S or S_2O_3), especially at low pH, Harrington et al. (1998) showed that dissolved sulfide concentrations of more than 100 $\mu M/L$ would be necessary to reduce only 10% of a 10 mM/L As(V) solution over a 30-day-period, while biotic reduction was observed to be 2 to 4-fold higher.

“Spontaneous” oxidation back to As(V) was first detected in cattle-dipping fluids in 1909 (Brünnich 1909). A correlation between oxidation and bacterial growth was proven in 1918 by isolation of the bacterium *Bacillus arsenoxydans*, probably an *Achromobacter* (Green 1918). This bacterium, however, was eventually lost. In 1943, new species of arsenite-oxidizing bacteria were characterized from the genus of *Pseudomonas*, *Xanthomonas*, and *Achromobacter* (Turner 1949). Those bacteria grow under aerobic conditions in a pH range of 6.1-9.4. Some of them, e.g., *Pseudomonas acidovorans-arsenoxydans* YE56, can also survive under anaerobic conditions and use nitrate to oxidize various carbon compounds, but can not oxidize arsenite under these conditions (Phillips and Taylor 1976).

Arsenite oxidizers can be both heterotrophic or chemolithoautotrophic. Heterotrophic oxidation catalyzed by a periplasmic enzyme (Mo-containing hydroxylase) is primarily a detoxification mechanism to convert As(III) to As(V) that is less likely to enter the cell (Ehrlich 2002). Chemolithoautotrophic oxidizer couple the oxidation of As(III) to the reduction of O_2 or NO_3 . The energy

gained is converted to fix CO₂ in organic cellular material and achieve growth (Oremland and Stolz 2003). The *α-Proteobacterium NT-26* is the most rapidly growing chemolithoautotrophic arsenite oxidizer known, with a doubling time of 7.6 hours in a minimal medium of arsenite, oxygen, and carbon-dioxide-bicarbonate (Santini et al. 2000). In general, however, microbial detoxification is the more common As(III) oxidation mechanism compared to chemoautotrophism (Nordstrom 2003).

Inorganic As(III) oxidation is generally slow but can be increased by heat (Tingle 1911), ultrasonic irradiation (Witekowa and Farbotko 1972), the presence of particulate matter (Oscarson et al. 1981), metal catalysts such as MnO₂, and strong oxidizing agents such as Fe(III) (Cherry et al. 1979) especially when catalyzed by light (Johnson and Pilson 1975; McCleskey et al. 2004; Nordstrom 2003; Reay and Asher 1977). Illumination with 90 W/m² is sufficient for photochemical oxidation of 90% of a 500 µg/L As(III) solution in 2-3 h, in the presence of 0.06-5 mg/L Fe(II,III), or even more effective, 50 µM citrate as photocatalysts (Hug et al. 2001).

Oxidation rates are described by Scudlark and Johnson (1982) to be 0.3 nmol/L/day for a 0.45 ppb standard in a purely chemical reaction, 1.5 nmol/L/day considering the presence of bacteria (*Pseudomonas arsenoxydans*). Wilkie and Hering (1998) describe rapid As(III) oxidation (half-life 0.3 h) in the geothermal waters of Hot Creek, California, in the presence of a group of (unidentified) bacteria attached to submerged macrophytes; no oxidation occurred in samples after sterile filtration. *Agrobacterium albertimagni* (strain AOL15), later identified by Salmassi et al. (2002) as an As(III) oxidizing bacteria, might have been the unidentified bacteria in the study of Wilkie and Hering (1998). Nordstrom (2003) report a microbial oxidation rate of 3 mg/L/min at 40-60°C and pH 2.6 for a cooling hot spring flow at Yellowstone National Park. Gihring et al. (2001) identified the bacterium *Thermus aquaticus* in the hot springs of Yellowstone to oxidize As(III) at a rate of about 0.5 mg/L/min. Laboratory experiments indicate similar oxidation rates for *Thermus aquaticus* and *Thermus thermophilus* of about 0.14 mg/L/min after slow oxidation during the first 16 hours. Abiotic oxidation was about 100-fold less (Gihring et al. 2001). Data from McCleskey et al. (2004) indicate an even lower abiotic oxidation rate of 10⁻⁵ µmol/L/h. That is about 5 orders of magnitude lower than the biotic oxidation rate. Hambsch et al. (1995) found no As(III) oxidation in sterile samples over 14 days at all. They also suggest that there is a temperature threshold for biotic conversion, with no detected As(III) oxidation over a period of 14 days below 4°C.

Figure 6 shows the As(III) species dependence on pH. In aqueous solutions with a pH < 9 the uncharged H₃AsO₃⁰ complex predominates. It is 4 to 10 times more soluble and mobile than As(V) (Cullen and Reimer 1989). Gulens et al. (1979) found that under oxidizing conditions at a slightly acid pH (5.6), As(III) moved 5-6 times faster through a sand column than As(V). At neutral pH, As(V) movement increased, but was still slower than that of As(III). Under reducing conditions at pH 8.3, As(III) and As(V) passed the column rapidly. While H₃AsO₄⁰ solution properties closely resemble those of H₃PO₄⁰, H₃AsO₃⁰ rather resembles boric acid H₃BO₃. Unlike H₃PO₃ that has P-O and P-H bonds, H₃AsO₃⁰ has no As-H bonds.

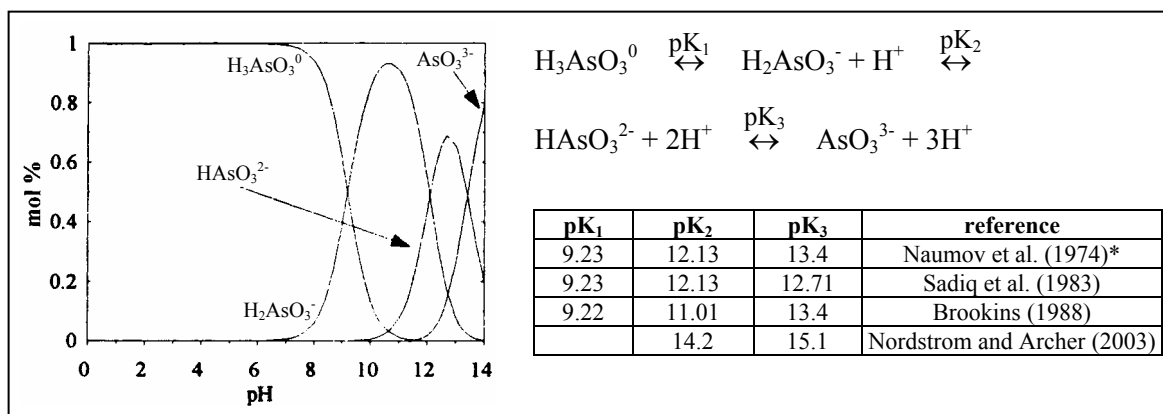


Figure 6 pH-dependent dissociation of As(III) species ($a(\text{As}) = 1.33 \cdot 10^{-7}$ mol/L; * data used for the diagram)

In contrast to predictions derived from pe-pH diagrams about the clear predominance of As(V) in natural waters (Andreae 1979 calculated ratios of 10^{15} - 10^{26} $\text{As}^{\text{V}} / \text{As}^{\text{III}}$ for seawater), significant amounts of As(III) may be found, especially due to biologically mediated redox reactions (ratios 0.1- 250; Cullen and Reimer 1989). Several reports confirm the predominance of As(III) in early spring with the beginning of algal bloom, before significant methylation (section 2.5.2.1) in late summer and autumn takes place and leads to a predominance of methylated As (Anderson and Bruland 1991; Cabon and Cabon 2000; Howard et al. 1995; Sanders 1985; Sohrin et al. 1997). Korte and Fernando (1991) were among the first to point out that As(III) in groundwater is likely to be more predominant than previously assumed. Inadequate sampling techniques with oxidation of As(III) to As(V) during storage might be the reason for the reported clear predominance of As(V) in most older reports (McCleskey et al. 2004; section 2.7.1). The British Geological Survey Department of Public Health Engineering (2001) found that 50-60% of all As in the Holocene alluvial aquifers in Bangladesh is As(III). Arsenite predominates in sedimentary aquifers including black shales in Taiwan (Chen et al. 1994) and makes up 60-90% of the total As in Holocene alluvial and lacustrine aquifers in Inner Mongolia (Smedley et al. 2001). For aquifers in Holocene basin fill sediments in the San Joaquin Valley, California As(III) was found to increase with increasing well depth (Fujii and Swain 1995).

In the presence of sulfides under reducing conditions the formation of arsenic sulfides (orpiment As_2S_3 , realgar AsS , arsenopyrite) may limit the aqueous As(III) concentrations (Cherry et al. 1979; Savage et al. 2000; Figure 5).

Compared to As(V), As(III) was found to be about 18-50 times more toxic by Petrick et al. (2000) and 25-60 times more toxic by Morrison et al. (1989). Investigations on macrophages, one of the principal and most sensitive immune effector cells, showed a 100-fold lower toxicity for As(V) than for As(III) (Sakurai et al. 1998). Arsenite reacts with sulfurhydryl groups of amino acids such as cysteine and thereby inactivates a wide range of enzymes in intermediate metabolism (Squibb and Fowler 1983).

Oxidation of arsenite to arsenate is generally considered a protective mechanism against enzyme deactivation. Landner (1989), however, reports that under low phosphorous conditions arsenate is at least ten times more toxic than arsenite for algae cultures. Arsenate replaces phosphate, indistinguishable for biota, disturbing central regulatory processes in the biological system concerning genetic (DNA), hormonal (cAMP), energetic (ATP) or enzymatic (substrates and protein phosphorylation) codes (Squibb and Fowler 1983). Only under conditions of high phosphorous concentrations, the toxicity of arsenate is insignificant compared to arsenite. Cullen and Reimer (1989) proposed that with high phosphate concentrations cells switch to a more selective transport system for phosphate, reducing arsenate accumulation. Probably this is not really a switch in transport systems but rather a competition resulting in the uptake of the predominant compound. Considering switches in the transport systems, low phosphate concentrations are more likely to trigger phosphate specific uptake. While at high phosphate concentrations the non-specific and fast phosphate inorganic transport system (Pit) is active, the energy-requiring, specific phosphate inducible system (Pst) works during phosphate depletion. It is about 100 times more specific for phosphate than for arsenate (Petänen et al. 2001).

Complexation with other ions is rarely observed for inorganic As. At fluoride concentrations > 1.5 mg/L, $\text{HAS}^{\text{III}}\text{O}_3\text{F}^-$ and $\text{As}^{\text{III}}\text{O}_3\text{F}^{2-}$ might form (Creelius et al. 1986). Lowenthal et al. (1977) report that in seawater Ca- and Mg-As(V) complexes can predominate but Nordstrom (2000) emphasizes the uncertainty of information about the significance of aqueous metal As(V) complexes because of a lack of measured thermodynamic equilibrium constants. Assuming divalent metal P(V) complexes as analogues association constants for divalent metal As(V) complexes were estimated. Using these for a water sample from Bangladesh showed that free As(V) concentrations decreased by about 50% when divalent As(V) complexes were considered (Nordstrom 2000). Under reducing conditions, at neutral to alkaline pH, soluble thioarsenites, commonly referred to as $\text{As}^{\text{III}}\text{S}_3^{3-}$, become important (Cullen and Reimer 1989). The hypothesis by Kim et al. (2000) of stable As carbonate complexes ($\text{As}^{\text{III}}(\text{CO}_3)_2^-$, $\text{As}^{\text{III}}(\text{CO}_3)(\text{OH})_2^-$, $\text{As}^{\text{III}}\text{CO}_3^+$) formed during a leaching experiment with As sulfides in NaHCO_3 solution, was disproved by Wilkin et al. (2003). They found a predominance of mononuclear thioarsenites at sulfide concentrations $> 10^{-4.3}\text{M}$ at neutral pH.

2.5.2 Dissolved organic arsenic species

Both inorganic trivalent and pentavalent As compounds can be methylated. The process is not purely chemical but requires the involvement of a living organism and, presumably, the intervention of As within the metabolic pathways of the cells. Cullen and Reimer (1989) as well as Bentley and Chasteen (2002b) provide excellent reviews about the As biomethylation pathway. Abiotic As methylation is possible, e.g., in the presence of methyl iodide, but is rarely observed.

Early studies on organisms that methylated As focused on *in vitro* experiments using crude extracts of fungi and bacteria. Among the most prominent fungi for methylation of inorganic arsenicals are *Apiotrichum humicola*, formerly named *Candida humicola* (Cox and Alexander 1973; Cullen et al.

1995), and *Scopulariopsis brevicaulis* (Challenger et al. 1933, 1954). The aerobic fungus *Scopulariopsis brevicaulis* also metabolizes Se and Te (Challenger 1951), as well as Sb (Jenkins et al. 1998). Andrewes et al. (2000) found that in the presence of Sb(III), As methylation from As(III) by *Scopulariopsis brevicaulis* is inhibited significantly, even though in the absence of Sb, As is much more readily biomethylated than Sb in the absence of As (1.2-5.3% of the added As biomethylated compared to 0.0006-0.008% of the added Sb). On the other hand, $(\text{CH}_3)_3\text{Sb}$ production increased with increasing dissolved As(III) concentrations. Several fungi also have a more selective methylation mechanism. *Gliocladium roseum* and *Penicillium notatum* e.g., do not methylate inorganic As, but readily metabolize alkylarsenicals (Cox and Alexander 1973).

Although Challenger (1945) doubted that bacteria can methylate As, McBride and Wolfe (1971) were the first to prove the production of (probably) $(\text{CH}_3)_2\text{AsH}$ by a Methanobacterium strain *MoH* (Archaeobacter group). Wickenheiser et al. (1998) also confirmed the production of volatile inorganic and organic As from *Methanobacterium formicicum*. A number of nonmethanogenic bacteria have also been identified as methylarsine producers, e.g., *Pseudomonas* and *Flavobacterium* (Shariatpanahi et al. 1981, 1983), *Escheria coli* (Shariatpanahi et al. 1981), *Proteus*, *Achromobacter*, *Aeromonas*, *Enterobacter* (Shariatpanahi et al. 1983), as well as several bacteria not normally associated with arsenic metabolism, e.g., *Veillonella alcalescens*, *Streptococcus sanguis*, and *Fusobacterium nucleatum* (Pickett et al. 1988). A detailed review of the microbiological methylation of As is provided in Cullen and Reimer (1989).

Temperature seems to be one decisive factor in the methylation process. Howard et al. (1982, 1984) described a temperature threshold, stating that no methylation occurs below 9-12°C. The methylation reaction pathway as indicated already in Figure 3 is a sequence of alternating reduction steps (including the replacement of OH^- -groups by CH_3^- -groups) and oxidizing steps. The principle was already proposed by Challenger (1945), however, detailed information about the compounds and enzymes involved (Figure 7) was only gathered in more recent research studies on laboratory animals or humans.

As described above (section 2.5.1.2), inorganic As(V) is first reduced either non-enzymatically by glutathione (GSH) or other thiols (RSH) or enzymatically by ArsC, arsenate reductase (Aposhian 1997; Wildfang et al. 1998), to inorganic As(III), then methylated to Monomethylarsonic acid ($\text{MMA}^{\text{V}}\text{A}$, $(\text{CH}_3)\text{As}^{\text{V}}\text{O}(\text{OH})_2$). Concerning the nature of the methyl donor, Challenger (1945) proposed another already methylated compound such as a betaine, a methionine, or a choline derivative. Experiments with $^{14}\text{CH}_3$ labeled derivatives revealed that only methionine transferred its methyl group to As(III) and was detected in the final volatile product $(\text{CH}_3)_3\text{As}$. Cantoni (1953) identified the methionine derivative as S-adenosylmethionine (SAM). Yet, it was another 40 years later that Cullen et al. (1995) actually proved the direct uptake of deuterium labeled methionine also by non-volatile As metabolites in growing cultures of *Apiotrichum humicola*.

Thus, $\text{MMA}^{\text{V}}\text{A}$ is metabolized by the conversion from SAM to SAHC (S-adenosylhomocysteine) in the presence of the enzyme arsenite methyltransferase (Wildfang et al. 1998; Zakharyan et al.

1999). For further methylation, $\text{MMA}^{\text{V}}\text{A}$ has to be reduced to Monomethylarsonous acid ($\text{MMA}^{\text{III}}\text{A}$, $(\text{CH}_3)\text{As}^{\text{III}}(\text{OH})_2$) by RSH and the enzyme MMA^{V} reductase (Zakharyan and Aposhian 1999). $\text{MMA}^{\text{III}}\text{A}$ is then methylated to dimethylarsinic acid ($\text{DMA}^{\text{V}}\text{A}$, $(\text{CH}_3)_2\text{As}^{\text{V}}\text{O}(\text{OH})$) via the conversion from SAM to SAHC and in the presence of MMA^{III} methyltransferase (Zakharyan et al. 1999).

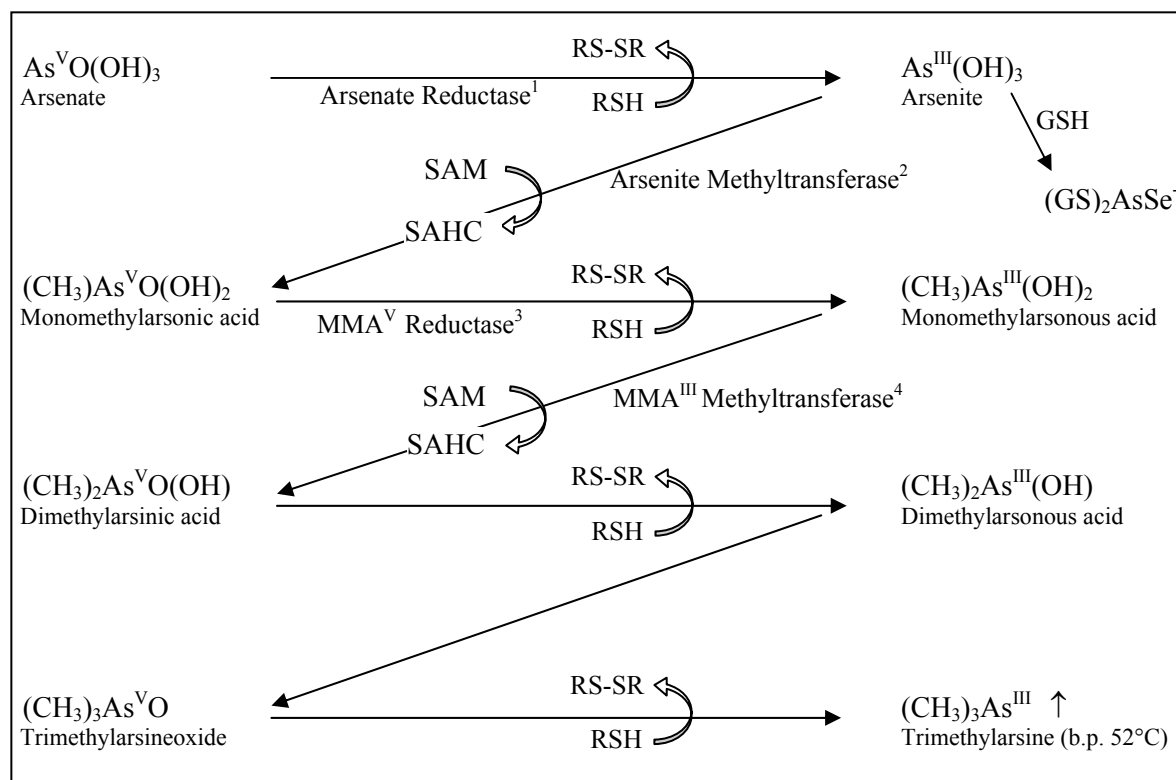


Figure 7 Model for the As methylation pathway; GSH = glutathione, RSH = other thiols, RS-SR = disulfide that is recycled to RSH by RSH reductase, SAM = S-adenosylmethionine, SAHC = S-adenosylhomocysteine, b.p. = boiling point, $(\text{GS})_2\text{AsSe}^-$ = seleno-bis(S-glutathionyl) arsinium ion (references: general scheme already proposed by Cullen and Reimer 1989, enzymes purified by ¹ Aposhian 1997; Wildfang et al. 1998; ² Wildfang et al. 1998; Zakharyan et al. 1999; ³ Zakharyan and Aposhian 1999; ⁴ Zakharyan et al. 1999)

Compared to arsenite methyltransferase (Michaelis constant $K_m = 5.5 \cdot 10^{-6}$ M in rabbit liver) and MMA^{III} methyltransferase ($9.2 \cdot 10^{-6}$ M), the enzyme MMA^{V} reductase ($2.16 \cdot 10^{-3}$ M) shows the weakest enzyme-substrate affinity, and is thus the rate-limiting enzyme (Zakharyan and Aposhian 1999). This rate-limiting process can explain why not only the end products, but also intermediates in the As biomethylation pathway can be found in different studies, e.g., $\text{MMA}^{\text{III}}\text{A}$ (section 2.5.2.3). According to Zakharyan and Aposhian (1999) it is also possible to reduce MMA^{V} in the absence of the enzyme only with GSH, however this non-enzymatic chemical reduction yielded 11 times lower reaction rates. On the other hand, the MMA^{V} reductase enzyme absolutely required the presence of GSH. Neither L-cysteine, nor DTT (dithiothreitol) proved to be sufficient as alternative reductants. L-cysteine, however, yielded greater activities for As(III) and MMA^{III} methyltransferase in *in vitro* experiments with hamster liver (Wildfang et al. 1998) and dithiols were found to be more effective for MMA^{III} methyltransferase from hamster liver (Zakharyan et al. 1999).

Aposhian et al. (1999) report from *in vitro* experiments that methylation by methylcobalamin (methylvitamin B12) only requires a reducing environment but no enzymatic reactions. This report might indicate a different metabolic pathway for anaerobic microorganisms, a controversial subject as presented in detail in Bentley and Chasteen (2002b). Rosen (2002) reviews differences in specific proteins resulting from separate evolutionary pathways between prokaryotes and eukaryotes. The overall scheme of As biomethylation, however, seems to be valid as explained above.

The majority of research groups postulates $\text{DMA}^{\text{V}}\text{A}$ to be the ultimate metabolite in humans (Buchet et al. 1981; Hopenhayn-Rich et al. 1996b; Le et al. 2000a), while it is further methylated to trimethylarsineoxide ($\text{TMA}^{\text{V}}\text{O}$, $(\text{CH}_3)_3\text{As}^{\text{V}}\text{O}$) by the fungus *Apiotrichum humicola* (Cullen et al. 1995), and hamsters and rats (Yamauchi and Yamamura 1984a; Yoshida et al. 1997). Styblo et al. (1999b) did not detect metabolism of DMA compounds for rat hepatocytes. The $\text{TMA}^{\text{V}}\text{O}$ concentrations of several ng/L in all urine samples investigated by Sur (1999) questioned $\text{DMA}^{\text{V}}\text{A}$ as the ultimate metabolite and supported the hypothesis of further methylation beyond $\text{DMA}^{\text{V}}\text{A}$. Marafante et al. (1987) made a similar observation, 48 hours after application of 0.1 mg DMAA about 4% of the applied dose was excreted as $\text{TMA}^{\text{V}}\text{O}$.

Trimethylarsine (TMA, $(\text{CH}_3)_3\text{As}^{\text{III}}$) is the theoretical volatile end product in the outlined reaction pathway. During investigations of intra-oral air from 6 test persons, however, neither TMA, nor mono- (MMA), nor dimethylarsine (DMA) were detected in human breath as volatile intermediates in the As biomethylation pathway (Feldmann et al. 1996).

One factor that might inhibit the methylation process is the formation of the seleno-bis(S-glutathionyl) arsinium ion $(\text{GS})_2\text{AsSe}^-$ (Figure 7). Aposhian et al. (1999) and Gailer et al. (2000) propose that $(\text{GS})_2\text{AsSe}^-$ is rapidly formed from arsenite in the presence of GSH, before any methylation occurs, and is easily excreted. That can explain the known antagonism between As and Se which was first reported in the late 1930s (Moxon 1938). When co-administered Se and As mutually inhibit the individual methylation pathways. Lethal doses for co-administration of Se and As are higher than for administration of either of the elements alone.

Aposhian et al. (1999) report a lower limit for methylation that could also explain the known delay in excretion of methylated As compounds after As exposure (Vather 1999). According to studies on rabbit livers, arsenite firmly binds to proteins (20 times better than arsenate). It seems that methylation does not take place before the protein binding sites are occupied and additional arsenite accumulates. Concerning an upper limit for methylation, there seems to be some evidence that methylation decreases with very high concentrations of inorganic As, indicating an inhibition of the methylation process by an excess of As(III) and a saturation of the enzymic conversion from MMAA to DMAA (threshold hypothesis by Petit and Beck 1990). Hopenhayn-Rich et al. (1993) conclude from epidemiological and experimental human studies cited in the literature that those data do not support the methylation threshold hypothesis, because there was always about 20-25% non-methylated inorganic As present in the urine regardless of the absorbed dose of inorganic As. In contrast, results from Farago and Kavanagh (1999) show 79-96% DMAA in the urine of popula-

tions at low exposure levels compared to 60% at high exposure levels, supporting the threshold hypothesis. Also an increase of MMAA compared to DMAA can be taken as evidence for a disturbance or saturation of the methylation process, as shown by Styblo et al. (1999a, 1999b) for human and rat hepatocytes. They also found a decrease of total methylation at higher As concentrations, suggesting the inhibition of methylation according to the threshold hypothesis. An example for methylation inhibition in environmental samples might be Mono Lake that has inorganic As concentrations of up to 17 mg/L, but no methylated As species (Anderson and Bruland 1991).

Like all organometallics, organic As compounds are thermodynamically unstable. However, their decomposition kinetics is so slow that they may have a transient existence under a variety of environmental conditions. For microbial demethylation from DMAA to As(V) by an estuarine microbial culture, Sanders (1979) reports a rate of 1 ng/L/day. Chemical demethylation is very slow. However, oxidation, reduction, hydrolysis, and reactions with sulfur compounds can significantly alter distribution, volatility, and mobility of biologically produced compounds.

2.5.2.1 Mono- and dimethylated As(V) acids

As explained above, MMA^VA [(CH₃)As^VO(OH)₂] and predominantly DMA^VA [(CH₃)₂As^VO(OH)] are the main metabolites in the As biomethylation pathway, except for those animals who lack the As methyltransferase enzymes such as the guinea pig (Healy et al. 1997), gorilla, orangutan, and chimpanzee (Wildfang et al. 1997). Several studies indicate an average of 10-30% inorganic As, 10-20% MMAA and 60-70% DMAA in human urine after exposure to inorganic As (Vather 1999). Compared to inorganic As, MMA^VA and DMA^VA are much more easily excreted because they are less reactive with tissue constituents. Following oral intake of methylated As compounds, about 75% of the ingested dose is excreted after 4 days, compared to only 45% of a similar dose of inorganic As (Buchet et al. 1981). Vather (1999) reviews variations in the human metabolism of As and shows differences between different population groups (the percentage of MMAA in urine was detected to be below average with only 2-4 % in Andean natives, for people from Taiwan above average with 27%) and individuals, also depending on age (children seem to have a lower methylation capacity and a higher As retention potential; Del Razo et al. 1999), gender (women showed 3% more DMAA, but less MMAA in urine compared to men, pregnant women up to 90% DMAA), exposure level (see threshold hypothesis discussed above), and nutritional status (lack of vitamins and methyl donors may inhibit As metabolism). However, detailed studies are still rare and it is often hard to exclude cross reactions and factors influencing each other.

According to a review on As species in plants (Meharg and Hartley-Whitaker 2002), rice, apple, tomato (in a laboratory experiment with a deficiency of nitrogen and phosphorous), wild strawberry, bilberry, raspberry (only DMAA), Norway spruce, white alder, sedge, and cedar were found to contain significant amounts of MMAA and DMAA (no distinction between penta- and trivalent species). However, it is not yet clear, whether plants actually methylate As themselves or the As is methylated by microbes in the rhizosphere and then taken up by the plant.

Extracellular MMAA and DMAA (without distinction between penta- and trivalent species) were already determined together with arsenate and arsenite in 1973 in some fresh and seawater samples by Braman and Foreback (1973). While the average amount of methylated compounds (predominantly DMAA), is 10-20% of the total As, it could also become up to 70% depending on bioactivity and temperature. These results compare well with several later studies, e.g., Sanders (1985), who determined up to 60% methylated compounds during the summer bloom in an estuary (Chesapeake Bay). The concentrations of MMAA in this study were equal to or even exceeded those of DMAA. For the estuarine Southampton Waters, United Kingdom, where phytoplankton concentrations are about 10 times less than those in Chesapeake Bay, DMAA made up about 25% of total As, MMAA about 12% (Howard et al. 1995). Andreae (1978) and Froehlich et al. (1985) determined the proportion of methylated compounds in freshwater samples to average 10% of total As, with MMAA concentrations being only 1/10 of those of DMAA. Anderson and Bruland (1991) reported between 1 and 59% methylated As in Californian lakes during late summer and fall with a clear predominance of DMAA. Sohrin et al. (1997) detected up to 64% DMA^VA in Lake Biwa, Japan, in summer, MMA^VA was an order of magnitude less. Cabon and Cabon (2000) found 20% DMAA and 3% MMAA during the phytoplankton bloom at the French Atlantic. Methylated As concentrations of less than 10% total As (DMAA > MMAA) determined in subarctic lakes in Canada are below the average values described above and seem to support the temperature dependence of methylation mentioned in section 2.5.2. Interestingly, all these methylarsenicals were found in oxic waters, in contrast to the publication of Wood (1974), and the still generally widespread opinion that methylarsenicals would only be found under strictly anoxic conditions. The possibility that such reducing conditions occur in microenvironments is certainly not discounted.

Lower concentrations of methylated compounds (0.01-1% of the total As) were found in geothermal waters (Hirner et al. 1998). From 6 samples, 5 showed a predominance of MMAA. Only in one sample (the one with the lowest temperature, 20°C) DMAA concentrations exceeded MMAA by about one order of magnitude. The compounds MMAA and DMAA were also detected in German harbor and river sediments by Krupp et al. (1996) and in deposited domestic waste and contaminated soil in the vicinity of a gas station and a coal processing industry (Hirner et al. 2000). Bednar et al. (2004) reported concentrations of up to 100 µg As/L for MMAA, and 10 µg As/L for DMAA in the stagnant surface water of a cotton-producing area in Arkansas that might have been impacted by the use of monosodium methylarsonate as cotton herbicide. No methylated compounds were found in the groundwater.

Figure 8 shows the predominant MMA^VA species as a function of pH. Similar to inorganic As(V), the negatively charged complex $\text{CH}_3\text{AsO}_2(\text{OH})^-$ predominates under near neutral conditions, and the uncharged complex only in acid solutions (pH < 3.6).

Figure 9 shows the predominant DMA^VA species as a function of pH. According to Doak and Freedman (1970) as well as Baes and Mesmer (1976), only two species exist for DMA^VA, and the predominant one (pH < 6.2) is the uncharged $(\text{CH}_3)_2\text{AsO}(\text{OH})$.

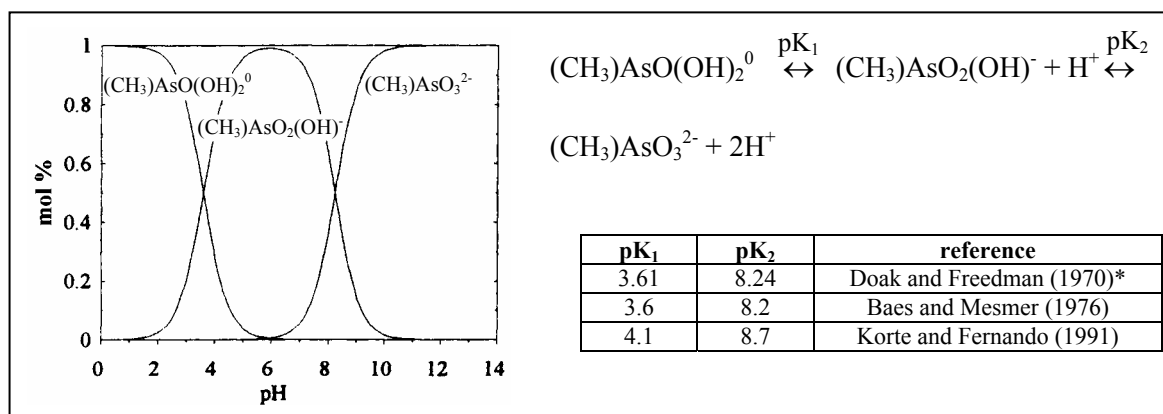


Figure 8 pH-dependent dissociation of MMAA species ($a(\text{As}) = 1.33 \cdot 10^{-7}$ mol/L; * data used for the diagram)

In contrast to the highly mobile inorganic As(III) uncharged complex, the uncharged DMA^VA complex shows some non-specific sorption both on cation and anion exchangers. This non-specific sorption could be caused by hydrophobic interactions with the exchanger matrix that the hydrophilic inorganic As(III) does not exhibit. Korte and Fernando (1991) and Hansen et al. (1992) suggested a protonated DMA^VA species $(\text{CH}_3)_2\text{AsO}(\text{OH})\text{-H}^+$ that appears below pH 4 and becomes predominant at pH < 1.6, and pH 1.2 respectively.

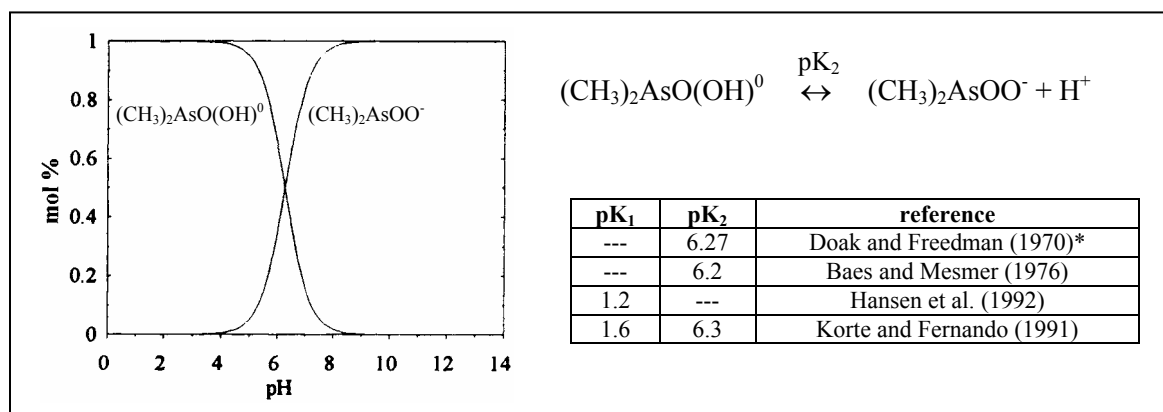


Figure 9 pH-dependent dissociation of DMAA species ($a(\text{As}) = 1.33 \cdot 10^{-7}$ mol/L; * data used for the diagram)

MMA^VA and DMA^VA are the only dissolved methylated As species positively identified extracellular in environmental samples so far.

2.5.2.2 Tri- and tetramethylated As(V) acids

Less frequent than MMA^VA and DMA^VA is TMA^VO $[(\text{CH}_3)_3\text{As}^{\text{V}}\text{O}]$. The pK value for the reaction $(\text{CH}_3)_3\text{As}^{\text{V}}\text{O} \leftrightarrow (\text{CH}_3)_3\text{As}^+\text{OH} + \text{H}^+$ is 3.6 (Hansen et al. 1992). The rare occurrence of TMA^VO might be due to facile reduction to the volatile $(\text{CH}_3)_3\text{As}$ by aerobic and anaerobic organisms, as well as in the presence of thiols (RSH). TMA^VO has so far mainly been found intracellular in a number of fish species. While Cullen and Dodd (1989) describe TMA^VO as a minor component, maybe even the breakdown product of some yet unknown precursor only, Kaise et al. (1997) found it to be predominant in fish with 55-78% of total As. Also marsh snails contained significant

amounts of TMA^VO. In their review on As species in plants, Meharg and Hartley-Whitaker (2002) list cocksfoot grass, Norway spruce, European Larch, wild strawberry, and raspberry as plants containing TMA^VO.

Kaise et al. (1997) also claim to have found 2 µg/L TMAO (6.8% of total As) extracellular in the Hayakawa river at hot springs in Hakone, Japan. Hirner et al. (1998) report 0.18 and 0.25 µg/L TMAO for two samples of geothermal waters from New Zealand. However, both studies used hydride generation under the oversimplified assumption that only TMAO can produce the volatile TMA (section 2.6.1.1). Similarly questionable is the detection of TMAO as TMA in pore water of subarctic lake sediments in Canada (Bright et al. 1996), in German harbor and river sediments by Krupp et al. (1996), and in deposited domestic waste and contaminated soil in the vicinity of a gas station and a coal processing industry (Hirner et al. 2000). No evidence is found so far for the existence of TMAO in normal freshwater environments.

The tetramethyl arsonium ion (CH₃)₄As⁺ (TETRA) has only been found in tissues of clams (*Meretrix lusori*; Shiomi et al. 1987), a crab, a sea cucumber (Shibata et al. 1992), and other gastropods (Francesconi et al. 1988), never extracellular in natural waters. Koch et al. (1999) report trace amounts of TETRA in the monkey flower *Mimulus sp.*, thought to be synthesized by this plant. Wild strawberry, broad buckler fern, and cocksfoot grass are other examples of plants with TETRA occurrences (Meharg and Hartley-Whitaker 2002). Geiszinger et al. (2002) report for the first time a predominance of TETRA (up to 85% of the arsenate accumulated from seawater) in marine annelids (*Polychaetes Nereis diversicolor* and *Nereis virens*). The biosynthesis of TETRA is unclear because the end product of As biomethylation according to Figure 3 is (CH₃)₃As. Tetramethyl arsonium could result from decarboxylation of arsenobetaine (section 2.5.2.4), however Geiszinger et al. (2002) found no evidence of such a transformation in their study.

2.5.2.3 Mono- and dimethylated As(III) acids

The existence of the trivalent organic acids MMA^{III}A [(CH₃)As(OH)₂] and DMA^{III}A [(CH₃)₂As(OH)] was neglected or doubted in many former reviews (e.g., Farago and Kavanagh 1999; Korte and Fernando 1991; Vather 1999). Cullen and Reimer (1989) mentioned them as possible theoretical intermediates in the biotransformation pathway, but also stated that they were "unknown". Aposhian et al. (2000), Le et al. (2000a, 2000b), Sampayo-Reyes et al. (2000), Wildfang et al. (1998), and Zakharyan and Aposhian (1999) proved their existence as metabolites in mammals exposed to increased concentrations of inorganic As. In all these reports MMA^{III}A clearly predominated over DMA^{III}A. Aposhian et al. (2000) determined the share of MMA^{III}A in urine of humans exposed to inorganic As in drinking-water to be 7-11% of the total As and 35-44% of the total MMAA (MMA^{III}A + MMA^VA). It seems that a certain amount (in the millimolar range) of MMA^VA reductase, the rate-limiting enzyme for the biotransformation, is needed for a significant conversion from MMA^VA to MMA^{III}A. More recent reports also emphasize the probability of erroneous interpretation of all MMAA just as MMA^VA in earlier studies without actually measuring MMA^{III}A and the consequent need of re-interpretation of some of these data.

Extracellular occurrence of trivalent methylated compounds is reported for Lake Biwa, Japan, by Hasegawa et al. (1994) with 0.3-3.0 nM MMA^{III}A and 0.2-11 nM DMA^{III}A, and by Sohrin et al. (1997) with < 20 ng/L MMA^{III}A and DMA^{III}A. Gong et al. (2001) showed that the few reports on detection of trivalent methylated species, especially DMA^{III}A, are probably caused by inadequate sampling techniques. When stored at room temperature, MMA^{III}A was completely oxidized within one week and DMA^{III}A in 17 hours. With storage at -20°C only 10% MMA^{III}A was oxidized over a period of 5 months, while DMA^{III}A was found to be very unstable showing complete oxidation within 15 days. Stability in urine is even less, with 98% MMA^{III}A oxidized after 30 days and 100 % DMA^{III}A after 90 min at room temperature.

Several papers state that As methylation in contrast to Hg methylation is always a detoxification mechanism, with methylated As compounds being several 100 times less toxic than inorganic As compounds (e.g., Korte and Fernando 1991; Morrison et al. 1989; Vather 1999; Yamauchi and Fowler 1994). The pentavalent organic As compounds might in fact be less toxic than the inorganic arsenicals. Sakurai et al. (1998) report for macrophages a 1000-fold lower toxicity for DMA^VA compared to As(III) and no toxicity at all was detected for MMA^VA or TMA^{VO}. Whereas Mass et al. (2001) could not determine any DNA nicking or degrading up to MMA^VA concentrations of 3 M and DMA^VA concentrations of 300 mM, Yamanaka et al. (1997) reported for laboratory animals that DMA^VA might be able to damage DNA and promote tumors. In their overview about genotoxicity of organoarsenic compounds Florea et al. (2004) show that DMA^VA so far has proven to be responsible for cell growth inhibition, decrease of cell viability, apoptosis (cell death), sister chromatid exchanges, carcinogenicity, and mutagenicity.

Even though the pentavalent organic arsenicals might be less toxic under certain aspects, already Horiguchi (1970) claimed that the intermediates in the As biomethylation pathway, MMA^{III}A and DMA^{III}A, are more toxic to mammals than inorganic arsenite. Petrick et al. (2000) confirmed for human hepatocytes that MMA^{III}A is up to 26 times more toxic than arsenite and in fact the most toxic compound in the biotransformation pathway. Investigations of rat and human cells by Styblo et al. (2000) revealed a 4-20 times higher cytotoxicity for MMA^{III}A compared to As(III), whereas the cytotoxicity of DMA^{III}A was comparable to that of As(III). Comparable to that, for rat hepatocytes MMA^{III}A was about 25 times more toxic than As(III) or DMA^{III}A (Styblo et al. 1997). Interesting is the study of Sakurai et al. (1998) who report an increase of macrophage cell toxicity for DMAA when GSH is added. Because GSH is the major reductant in the As biomethylation pathway (Figure 7) this result supports the conclusion that DMA^VA was further reduced to the more toxic DMA^{III}A. Although this hypothesis was also discussed by the authors it was not investigated further.

The higher toxicity of the trivalent organic As species is related to their high affinity for specific cellular proteins and their potential as inhibitors for enzymes which generate cellular energy in the citric acid cycle (Styblo et al. 1997). The MMA^{III}A has an additional toxic potential in that it is retained in cells and, in contrast to DMA^{III}A, not released into the medium. According to Lin et al. (1999), MMA^{III}A is over 100 times more potent than inorganic As(III) as an inhibitor for thiore-

doxin reductase, a selenoprotein for the reduction of disulfides and therefore critical for the maintenance of the intracellular redox state. Disturbances to the reduction of thioredoxin, a modulator of cell proliferation and DNA synthesis, might result in tumor growth. Mass et al. (2001) found that $\text{MMA}^{\text{III}}\text{A}$ and $\text{DMA}^{\text{III}}\text{A}$ were able to nick DNA *in vitro* without the need of exogenously added enzymatic or chemical activation at concentrations of 30 mM, and 150 μM respectively. Full DNA degradation occurred at 60 mM $\text{MMA}^{\text{III}}\text{A}$, and 10 mM $\text{DMA}^{\text{III}}\text{A}$ respectively. In single-cell gel assays in human lymphocytes, $\text{MMA}^{\text{III}}\text{A}$ was 77 times, $\text{DMA}^{\text{III}}\text{A}$ 386 times more potent than inorganic As(III) in damaging the DNA.

Little is known about the toxicity of TETRA. According to Penrose (1974) it is harmless. Maeda (1994) specified that it is excreted renally without undergoing any metabolism. In contrast to this, Shiomi (1994) states that it is considerably lethal to marine organisms, being more toxic than MMAA and DMAA.

2.5.2.4 Arsenosugars, arsenocholine, arsenobetaine

Dimethylarsinoyl ribosides, better known under their trivial name arsenosugars X - XIII (Figure 10), were found as intermediates of the As cycling in marine ecosystems, mainly in algae (Edmonds and Francesconi 1981; Shibata et al. 1992) and seaweeds (Edmonds et al. 1982; McSheehy et al. 2000). Arsenosugar XIII was the major metabolite of the marine diatom *Chaetoceros concavicornis* (Edmonds et al. 1997). Shibata et al. (1992) also found arsenosugar XI and, more seldom, arsenosugar X in bivalves, and gastropodes. Samples from freshwater or terrestrial environments are rare. Lai et al. (1997) found the terrestrial soil / freshwater cyanobacterium *Nosto sp.* to contain up to 32% arsenosugar X. Koch et al. (1999) reported for the Meager Creek hot springs in British Columbia the occurrence of the arsenosugars X and XI in microbial mats (maybe including cyanobacteria) and green algae as well as of arsenosugar X in moss and arsenosugar XI in lichens.

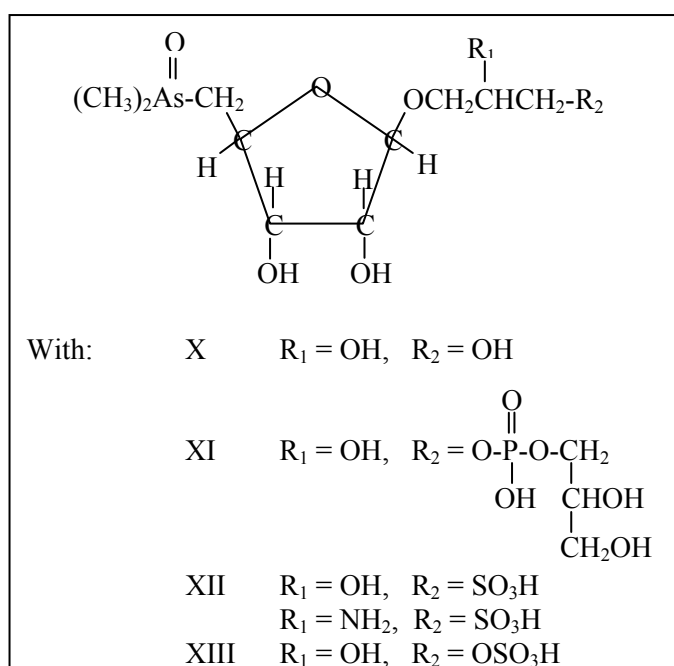


Figure 10 Structure for arsenosugars and abbreviations for the different structures (numbering arsenosugar X to XIII according to Shibata et al. 1992)

Arsenosugars are stable at neutral pH and react with acids or bases to DMA^VA. Consequently, DMA^VA increases in human urine following arsenosugar ingestion (Le and Ma 1998). Arsenosugars, especially arsenosugar XI, are probably the link between hydrophilic and lipophilic As compounds. Those sugar derivatives are anaerobically degraded to dimethyloxarsylethanol (CH₃)₂AsOCH₂CH₂OH that is the intermediate for arsenocholine (AC, (CH₃)₃As⁺CH₂CH₂OH) (Figure 11). The existence of AC was claimed in shrimps by Norin et al. (1983) and in one gastropod by Shiomi et al. (1987).

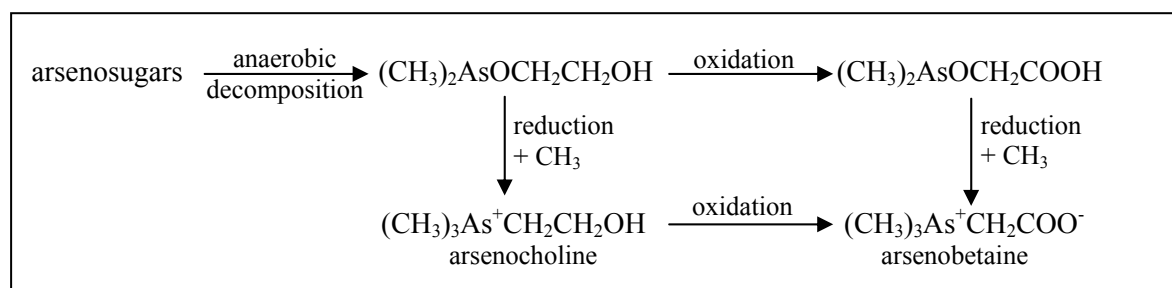
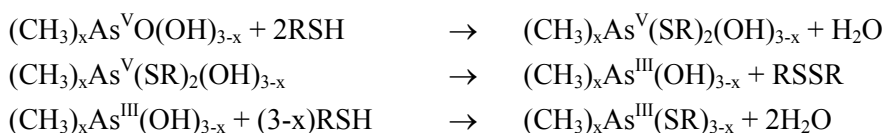


Figure 11 Interactions of the organic As species arsenosugar, arsenocholine, and arsenobetaine

The (CH₃)₂AsOCH₂CH₂OH is easily converted by further oxidation to (CH₃)₂AsOCH₂COOH, the intermediate for arsenobetaine (AB, (CH₃)₃As⁺CH₂COO⁻) (Figure 11). The pK value for the reaction (CH₃)₃As⁺CH₂CO(OH)⁰ ↔ (CH₃)₃As⁺CH₂COO⁻ + H⁺ is 2.18 (Hansen et al. 1992). AB was first isolated in 1977 (Edmonds et al. 1977). It is the predominant As species in marine organisms that generally show organoarsenical concentrations significantly above average background (≈ 2 ppb; Penrose 1974; Shibata et al. 1992). This predominance is commonly related to accumulation of compounds that have been synthesized from arsenate at lower trophic levels (Ünlü and Fowler 1979), even though investigations from Klumpp and Peterson (1981) show that organoarsenicals in snails do not come from the lower trophic level (algae), but are manufactured directly from arsenate. AB is very stable and excreted from human bodies without metabolism (Crecelius 1977b; Ma and Le 1998). Only under extreme temperatures (150-180°C) it decomposes into TMA^VO and TMA (Devesa et al. 2001). Neither MMAA, DMAA, TMAO, TETRA, nor AC showed these decompositions with temperature. AB is essentially nontoxic (Cullen and Reimer 1989; Francesconi and Edmonds 1997).

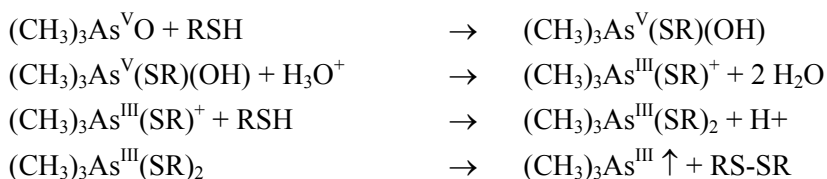
2.5.2.5 Organic arsenic sulfur compounds

The As biomethylation pathway is further complicated by the ability of As compounds to react with thiols (Bentley and Chasteen 2002b; Delnomdedieu et al. 1994). Complexation of inorganic As(III) with GSH produces arsenotriglutathione As^{III}(GS)₃ which is easily excreted at the beginning of the As biomethylation pathway, comparable to (GS)₂AsSe⁻ (section 2.5.2). It is interesting to remark that As^{III}(GS)₃ inhibits the GSH reductase enzyme that recycles GS-SG to GSH. It could thus be a potent inhibitor for any further As methylation. For organic As-S-compounds the following sequence is likely (Bentley and Chasteen 2002b; Cullen et al. 1984):



for $x = 1$ (monomethyl), and $x = 2$ (dimethyl compounds)

Reduction of trimethylarsine oxide to trimethylarsine was possible with a variety of thiol reagents (cysteine, dimercaptopropanol, lipoic acid, mercaptoacetic acid, and mercaptoethanol). The following reactions were postulated by Bentley and Chasteen 2002b:



In anoxic environments, with $\text{pH} < 7$, and in the presence of H_2S or thiols (RSH) methylated As-S-compounds could also form naturally. During periods of high bioproductivity, thiol concentrations can reach values comparable to those of inorganic S-compounds and the presence of such As-thiol-compounds would lead to an underestimation of the extent of biomethylation (Cullen and Reimer 1989). Like the $(\text{CH}_3\text{As}^{\text{III}}\text{O})_x$ compounds, the $(\text{CH}_3\text{As}^{\text{III}}\text{S})_x$ compounds are more toxic than inorganic As(III). $\text{CH}_3\text{As}(\text{SR})_2$, is two orders of magnitude more potent as an inhibitor of glutathione reductase, the key enzyme in the detoxification pathway to $\text{DMA}^{\text{V}}\text{A}$, than As(III) (Styblo et al. 2000). Between $(\text{CH}_3\text{As}^{\text{III}}\text{O})_x$ and $(\text{CH}_3\text{As}^{\text{III}}\text{S})_x$, Cullen et al. (1989) state that for the fungus *Apiotrichum humicola* $(\text{CH}_3\text{As}^{\text{III}}\text{S})_x$ is more toxic, whereas Styblo et al. (2000) found that $(\text{CH}_3)_2\text{As}(\text{SR})$ is less toxic to human cells than $(\text{CH}_3)_2\text{As}(\text{OH})$. The existence of thioorganoarsenate as a mammalian metabolite was recently proven by Hansen et al. (2004). A 2-dimethylarsinothiol acetic acid was characterized in the urine of Orkney Island wild sheep that consume about 30 mg As as arsenosugars daily from their major food source, seaweed.

Bright et al. (1996) deduct the existence of $(\text{CH}_3)_x\text{As}^{\text{III}}(\text{SR})_{3-x}$ from the formation of volatile methyl compounds at pH 6 during hydride generation on pore water samples from subarctic lake sediments in Canada. Whereas $\text{MMA}^{\text{V}}\text{A}$, $\text{DMA}^{\text{V}}\text{A}$, and $\text{TMA}^{\text{V}}\text{O}$ are not volatilized above pH 1 (section 2.6.1.1), monomethyl-, dimethyl-, and trimethylarsinothiols were proven to do so. Because trimethylated arsenicals were not considered in this study, it is not really clear whether the original substances could also have been $\text{MMA}^{\text{III}}\text{A}$ and $\text{DMA}^{\text{III}}\text{A}$ that volatilize at a higher pH ($\text{pH} > 5$). This study provides the only “evidence” for the existence of $(\text{CH}_3)_x\text{As}^{\text{III}}(\text{SR})_{3-x}$ in aqueous samples.

2.5.2.6 Organic arsenic halogen compounds

De Bettencourt et al. (1994) appear to be the first to propose the possible existence of dissolved dimethyl halogenated As species, $(\text{CH}_3)_2\text{OAsCl}$ (or $(\text{CH}_3)_2\text{OHAsF}$), in natural water samples from the Tagus estuary in Portugal. They made up 19-25 % of the total As species. The results were deduced from mass spectra after DCI (desorption chemical ionization)-MS/MS analysis (Figure

12). However, the compound detected proved refractory to normal hydride generation techniques by not forming volatile As species, a fact that is hardly explicable from the chemical structure of a dimethyl chloro or a trimethyl fluoro As compound. Alternatively, the authors interpreted the detected compound as halo-arsenobetaine, or halo-arsenocholine.

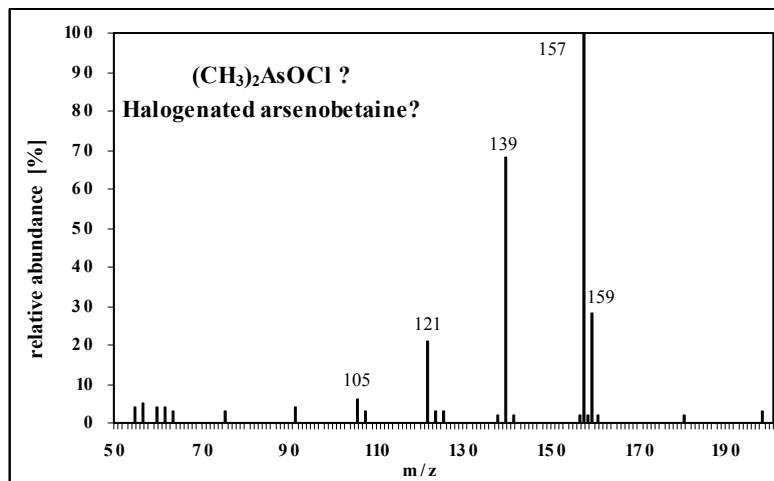


Figure 12 DCI mass spectrum for an As species assumed to be $(\text{CH}_3)_2\text{OAsCl}$, $(\text{CH}_3)_3\text{OHAsF}$, or a halogenated arsenobetaine (de Bettencourt et al. 1994; % = relative abundance by taking predominant mass = 100)

Hasegawa et al. (2002) investigated the conversion of inorganic and methylarsenic(III) hydroxides into the corresponding halides in aqueous HCl solutions and determined stability constants and partition coefficients (Figure 13).

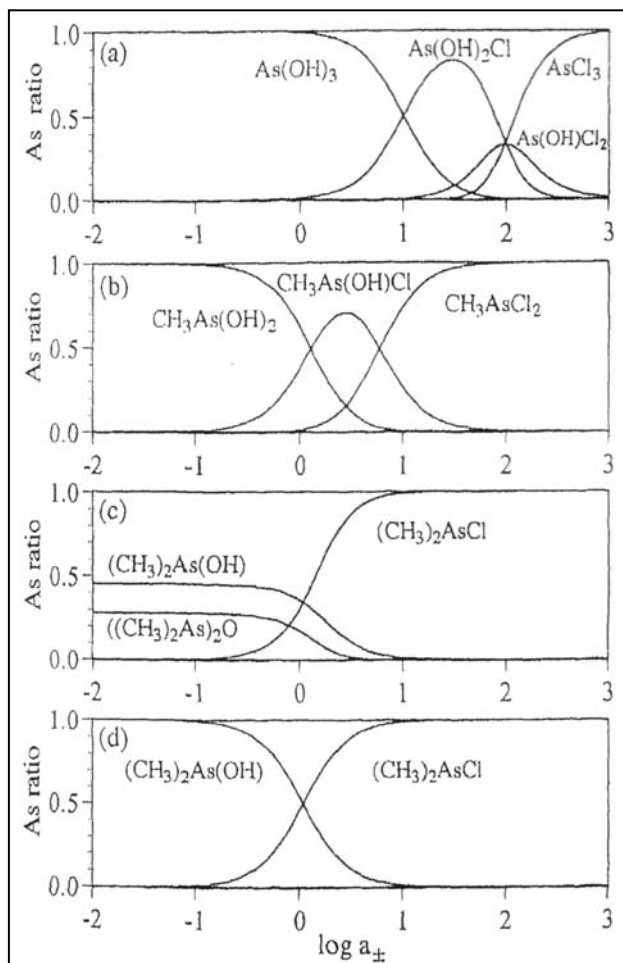


Figure 13 Dissociation in HCl solution according to Hasegawa et al. (2002) of (a) inorganic As(III) $<1 \cdot 10^{-3}$ mol/L, (b) MMA^{III}A $<1 \cdot 10^{-3}$ mol/L, (c) DMA^{III}A $1.0 \cdot 10^{-4}$ mol/L, $((\text{CH}_3)_2\text{As})_2\text{O}$ is a dimethyl As dimer, the so-called cacodyloxyde that forms at low total DMA^{III}A concentrations; (d) DMAA $1.0 \cdot 10^{-8}$ mol/L; AsCl_3 , $(\text{CH}_3)\text{AsCl}_2$, and $(\text{CH}_3)_2\text{AsCl}$ are volatile species and will be discussed in section 2.5.3.6

The stepwise substitution of hydroxide ions by chloride ions can be described as $(\text{CH}_3)_n\text{As}(\text{OH})_{i+1}\text{Cl}_{j-1} + \text{H}^+ + \text{Cl}^- \leftrightarrow (\text{CH}_3)_n\text{As}(\text{OH})_i\text{Cl}_j + \text{H}_2\text{O}$ ($n + i + j = 3$). The stability constants increase from As(III) to MMA^{III}A to DMA^{III}A. Methyl groups are classified as weak electron donors. Attached to the As atom they increase the electron density on the central As atom and reduce the ionic interaction of As-OH bonds. Thus, a higher number of methyl groups facilitates the replacement of hydroxide ions by chloride ions bound to the As, and organic As-Cl species occur at lower HCl concentrations (higher pH) than inorganic As-Cl species (Figure 13).

2.5.3 Volatile arsenic species

Volatile arsenicals, so-called As hydrides, are As compounds with a boiling point below 150°C. They can be formed either as intermediates or end products of the As biotransformation pathway as indicated in Figure 3 or in a purely chemical reaction. This chemical hydride generation is commonly used in analytical techniques; details will be discussed in section 2.6.1.1.

The first indication about the existence of volatile As is cited in Gmelin (1839). After several incidents of arsenic poisoning in Germany and Great Britain, Gmelin noted that a garlic smell was present in the rooms, in which arsenic poisoning occurred. Following this clue, Fleck (1872) showed experimentally that molds growing on the wallpapers that were painted with As pigments (copper aceto-arsenites, called Scheel's green, and Schweinfurt or emerald green, used from 1806 until the 1960s), were able to produce a volatile, toxic and garlic smelling arsenic compound. Fleck proposed the produced gaseous compound to be arsine (AsH_3) but he was not able to identify it. Finally, Gosio was able to isolate various cultures that produced this gas and it was named Gosio gas in his honor (Gosio 1893, 1901). Biginelli (1900a, 1900b) purged the Gosio gas produced by the molds through acidified HgCl_2 solution and identified the resulting precipitate, incorrectly, as diethylarsine ($(\text{C}_2\text{H}_5)_2\text{AsH}$). About 30 years later Challenger et al. (1933) reviewed Biginelli's work and positively identified the produced gas as trimethylarsine. The mold, earlier named by Gosio *Penicillium brevicaulis* was later identified as *Scopulariopsis brevicaulis* (Challenger 1945).

2.5.3.1 Inorganic AsH_3

Although *Scopulariopsis brevicaulis* is one of the most prominent fungi in the methylation process of inorganic to organic (volatile) As, it does not produce AsH_3 . According to Cheng and Focht (1979), *Pseudomonas* and *Alcaligenes* (*Achromobacter*) produce AsH_3 both from arsenite and arsenate under anaerobic conditions. Michalke et al. (2000) incubated sewage sludge anaerobically and detected 0.76 ng/L AsH_3 . The highest concentrations of all volatile As compounds were found in pure cultures of the archaea *Methanobacterium formicicum*, whereas the *Methanobacterium thermoautotrophicum* produced AsH_3 only. According to the studies of Michalke et al. (2000) sulfate-reducing bacteria are not able to form AsH_3 .

With a boiling point of -55°C (Lido 2003), AsH_3 is the most volatile of the As gases. It is unstable under atmospheric conditions and is readily oxidized by oxygen (50 μg are totally oxidized in air

within 120 hours; Pantsar-Kallio and Korpela 2000). The Henry constant for solubility in water at 298.15 K is 0.0089 mol/kg/bar (Wilhelm et al. 1977).

AsH₃ is the most toxic inorganic form of As, causing immediate hemolysis. Fewer than 250 cases of arsine gas poisoning have been reported in the past 65 years, half of which were fatal (Gorby 1994). Immediate death occurs at 150 µg/m³. Extensive hemolysis ending in death follows 30 minutes of exposure to 25 to 50 µg/m³ and less than 30 minutes after 100 µg/m³ (Ellenhorn 1997). The Office of Environmental Health Hazard Assessment (1999) describes acute toxicity after 1 hour exposition to 160 µg/m³. The odor threshold is 0.5 ppm or 1.6 mg/m³ at 25°C (New Jersey Hazardous Substances Fact Sheets 1993).

Feldmann et al. (1994) investigated gases from a domestic waste heap in Asslar (Germany) by LTGC-ICP-MS. They identified AsH₃ via boiling point retention time correlation and semi-quantitatively measured total concentrations of volatile As (AsH₃, DMA and TMA) to be between 16.2 and 48.5 µg/m³ relative to a liquid standard. Similar investigation on the gases from a thermophilic and mesophilic digester showed concentrations of 6.4-25.3 µg/m³ total volatile As for the mesophilic and 16.1-30.4 µg/m³ for the thermophilic digestion (Feldmann and Kleinmann 1997). Arsine, however, was herein identified in traces only. Hirner et al. (1998) detected AsH₃ in 2 samples of geothermal gases in the Meager Creek area, British Columbia, by LTGC-ICP-MS but did not quantify it.

Another inorganic volatile As compound, just recently structurally analyzed by Kösters et al. (2003) is diarsine (As₂H₄) with a boiling point of 100°C. It has not been reported in environmental samples so far.

2.5.3.2 Monomethylarsine

Monomethylarsine (MMA, (CH₃)AsH₂) has a boiling point of +2°C (Lido 2003). Like AsH₃ it can be produced by *Methanobacterium formicicum* (Michalke et al. 2000), as well as by *Achromobacter sp.*, *Aeromonas sp.*, *Alcaligenes sp.*, *Flavobacterium sp.*, *Pseudomonas sp.*, and *Nocardia sp.* (Shariatpanahi et al. 1983). Concentrations detected above anaerobically incubated sewage sludge are comparable to AsH₃ (0.68 ng/L, Michalke et al. 2000). MMA was not detected in the domestic waste heap gases by Feldmann et al. (1994), but in digester gases (Feldmann and Kleinmann 1997), and in 2 samples together with AsH₃ in geothermal gases of British Columbia by Hirner et al. (1998). Another monomethylated volatile As compound with two As atoms, is monomethyl diarsine (CH₃)As₂H₃ (Kösters et al. 2003). It has not yet been identified in natural samples.

2.5.3.3 Dimethylarsine

Dimethylarsine (DMA, (CH₃)₂AsH) has a boiling point of +36°C (Lido 2003). Like AsH₃ and MMA, it can be produced by *Methanobacterium formicicum* (Michalke et al. 2000) or by *Escheria coli*, *Flavobacterium sp.*, *Proteus sp.*, *Pseudomonas sp.* (Shariatpanahi et al. 1981), *Achromobacter*

sp., *Aeromonas sp.*, *Alcaligenes sp.*, and *Nocardia sp.* (Shariatpanahi et al. 1983). Concentrations detected above anaerobically incubated sewage sludge are comparable to AsH₃ and MMA (0.51 ng/L). DMA was detected in domestic waste heap gases by Feldmann et al. (1994), and in digester gases (Feldmann and Kleinmann 1997) but not in geothermal gases of British Columbia by Hirner et al. (1998).

2.5.3.4 Trimethylarsine

The completely methylated volatile As species, trimethylarsine (TMA, (CH₃)₃As) with a boiling point of +52°C (Lido 2003) is the most stable volatile As compound. It is also the most toxic form, except AsH₃ because arsines gain toxicity with each added methyl group. Like the other volatile As compounds it can be produced by *Methanobacterium formicicum* (Michalke et al. 2000; Wickenheiser et al. 1998) as well as by *Pseudomonas sp.* and *Nocardia sp.* (Shariatpanahi et al. 1981). Wickenheiser et al. (1998) pointed out that the predecessor for TMA production by *Methanobacterium formicicum* is DMA^VA rather than TMA^VO. Trimethylarsine was the predominant species (3.3 ng/L) above anaerobically incubated sewage sludge. According to these experiments, it is the only volatile As species formed by sulfate-reducing bacteria and the peptolytic bacteria *Clostridium collagenovorans*, *Desulfovibrio gigas* and *Desulfovibrio vulgaris*. According to Pickett et al. (1988), the most active anaerobic bacterium to volatilize trimethylarsine oxide to trimethylarsine from samples of river water, sea sediments, sewage sludge was *Staphylococcus aureus* (208 nmol/min/g cells), the most active aerobic bacterium a marine pseudomonad (585 nmol/min/g cells).

Typical for all volatile As compounds is their distinct garlic-like smell. For TMA, the odor threshold is reported to be 2 ng/kg in a dilute aqueous solution (Yamauchi and Yamamura 1984b). Challenger (1945) described this garlic-like odor from the breath of animals after being injected with DMAA. As mentioned before, TMA is the theoretical volatile end product of the As biomethylation pathway but has never been found in human breath (Feldmann et al. 1996).

The occurrence of all volatile arsenicals in natural systems is limited due to their reactivity towards oxygen which decreases with an increasing degree of methylation. For TMA, the most stable compound, Parris and Brinckman (1976) report a second-order rate constant for gas-phase oxidation by O₂ of 10⁻⁶ M⁻¹s⁻¹. Compared to (CH₃)₃Sb with an oxidation rate of 9 orders of magnitude higher (2·10³ M⁻¹s⁻¹, assumed half-life: 50 ms, Jenkins et al. 1998; Haas and Feldmann 2000 found a half-life of > 24 h!), TMA appears to be relatively stable and could travel considerable distances without undergoing any chemical changes. Experiments by Panssar-Kallio and Korpela (2000) confirm that TMA is relatively stable in air. Within 9 days only 30% of 10 µg TMA were oxidized to TMAO. This slow rate of oxidation explains why in most environmental samples TMA is the predominant or only detectable arsine. Mukai et al. (1986) found a significant predominance of TMA, with ratios of 0.15 -0.34 for DMA to TMA when sampling airborne particulate matter at two sites (a polluted and a rural area) in Japan. As expected, the samples showed seasonal variations with higher concentrations in summer and lower concentrations in winter, in accordance with tempera-

ture changes. TMA was also detected in domestic waste heap gases by Feldmann et al. (1994), and as predominant volatile As species in gases from thermophilic and mesophilic digestion (Feldmann and Kleinmann 1997) as well as in geothermal gases of British Columbia by Hirner et al. (1998).

2.5.3.5 Organic Sulfur Arsines

Little is known about methylated sulfur arsines. Cullen and Reimer (1989) state that the rate of arsine evolution from $(\text{CH}_3)_2\text{AsSR}$ is lower than from $(\text{CH}_3)_2\text{AsO}(\text{OH})$, and that the arsines produced are $(\text{CH}_3)_3\text{As}$ and $(\text{CH}_3)_2\text{AsH}$, no volatile S-As compounds. One volatile As-S compound (dimethylarsenomercaptane, $(\text{CH}_3)_2\text{AsS}(\text{CH}_3)$), has already been synthesized in the laboratory by Ashe and Ludwig (1986) and by Kösters et al. (2003). So far, this compound has never received any attention in environmental studies, and has not yet been identified in natural samples.

2.5.3.6 Inorganic and organic halogen arsines

Tesfalidet and Irgum (1988) showed that it is possible to volatilize inorganic As(III) chemically as inorganic trichloroarsine (AsCl_3) by acidifying dissolved ultrapure As_2O_3 with an excess amount of HCl (Figure 13) and purging it, even without adding any reducing agent (commonly NaBH_4). The aim of this study was to decrease interferences from metal ions that often occur during hydride generation analysis following the reduction with NaBH_4 (section 2.6.1.1). Trichloroarsine (also named arsenic butter or fuming liquid arsenic) has a boiling point of 130°C . According to Arcand (1957), volatile AsCl_3 is the only As species present in significant quantity in 12 M HCl. Trichloroarsine and dissolved $\text{As}(\text{OH})\text{Cl}_2$ are the predominant species in 9 M HCl, while in 5.9 M HCl, AsCl_3 , $\text{As}(\text{OH})\text{Cl}_2$, $\text{As}(\text{OH})_2\text{Cl}$, $\text{As}(\text{OH})_2^+$, and H_3AsO_3 all exist in significant quantities.

Mester and Sturgeon (2001) studied the formation of volatile chloroarsines during hydride generation and detected the organic volatiles monomethylchloroarsine $(\text{CH}_3)\text{AsCl}_2$ (b.p. 133°C) and dimethylchloroarsine $(\text{CH}_3)_2\text{AsCl}$ (b.p. unknown) besides the inorganic AsCl_3 . They confirmed that inorganic AsCl_3 can form in the absence of a reducing agent. The volatilization of mono- and dimethylchloroarsines, however, required a strong reducing agent. Hydride and halide generation processes are similar and coexistent, with the share of halides increasing with increasing HCl concentrations in solution. Contact of arsine with HCl vapor also resulted in the formation of AsCl_3 . Finally, Mester and Sturgeon (2002) found volatile arsines in a model atmosphere above seawater and sediment. The authors assumed that because the sediment was previously γ -irradiated, biomethylation and biohydride generation can be excluded and the volatile species have to be halides. The halides seem to form abiotically, with an increasing release with increasing temperature. Killelea and Aldstadt (2002) report the detection of dimethyl chloroarsine in the gas phase over a collected freshwater sediment core obtained from central Green Bay, Lake Michigan near a former herbicide factory. No studies were found of chloroarsine occurrence in the environment.

2.6 Analytical speciation techniques

As mentioned before, since 1836 when Marsh for the first time positively identified As, there was no shortage of analytical procedures for the determination of total As. The volatile trimethylarsine $(\text{CH}_3)_3\text{As}$ was detected already in 1933. Due to its volatilization from a bacterial culture it could be detected on a silver nitrate filter paper reducing the AgNO_3 to elemental Ag. Further speciation was not achieved until 1973 when Braman and Foreback (1973) introduced the first hydride generation technique that was capable of separating different inorganic and methylarsenic compounds even in small concentrations. An excellent overview of As speciation analytics is provided in Gong et al. (2002).

2.6.1 Arsenic separation

2.6.1.1 Hydride generation

Hydride generation (HG) is based on the reduction of dissolved species, typically with sodium borohydride (NaBH_4), to volatile species (hydrides) in an acid medium. Dissolved pentavalent As species are initially reduced to trivalent As species, before the arsines are produced according to the following two reactions:



Borane, generated during these reductions, hydrolyses into the intermediate BH_3OH^- in a first reaction step and boric acid and gaseous hydrogen in a second reaction. The overall reaction is:



The advantage of HG for analysis is isolating the analyte from the matrix in the aqueous phase by transferring it to the gas phase (headspace). This process eliminates interferences and enhances sensitivities 10 to 100-fold (Howard 1997).

Typical concentrations for the reductant NaBH_4 are 0.01-2%. Higher concentrations lead to increased back pressure in reaction vials due to the formation of excess hydrogen. Oxidation rates of NaBH_4 in acid solutions are $6 \cdot 10^5$ L/mol/s for the first reaction step and $1 \cdot 10^7$ L/mol/s for the second, compared to much lower reaction rates in alkaline solutions with $2.9 \cdot 10^{-4}$ L/mol/s and $4.7 \cdot 10^{-2}$ L/mol/s (Gardiner and Collat 1965). Thus, for long-term stability during storage, NaBH_4 is prepared in NaOH. For rapid NaBH_4 oxidation with metals reduction during HG, an acid medium is used. The NaOH concentration for storage has to be optimized according to the amount of acid used during HG (Yin et al. 1996). Less commonly, $\text{NaB}(\text{C}_2\text{H}_5)_4$ is used as a reducing agent, even though it has the advantage that the produced ethylates are more stable than hydrides generated with NaBH_4 (Craig 1989). Feldmann et al. (2004) state that $\text{NaB}(\text{C}_2\text{H}_5)_4$ as well as the also commonly used Grignards reagents (e.g., $\text{C}_5\text{H}_{11}\text{MgBr}$) do not yield quantitative As derivatization.

The efficiency of arsine generation from individual As species is strongly dependent on pH. It seems that for the reaction to proceed rapidly, the species have to be present fully protonated, as

uncharged complexes (Howard 1997; Pantsar-Kallio and Korpela 2000). Negatively charged complexes would repel the electrons necessary for the reduction of the central As atom. Diagrams of arsine generation as a function of pH vary between different reports because of different acids used and different acid to reductant ratios (Bermejo-Barrera et al. 1998; Pantsar-Kallio and Korpela 2000; Rude 1996; Shraim et al. 1999). Figure 14 summarizes the data according to Howard (1997).

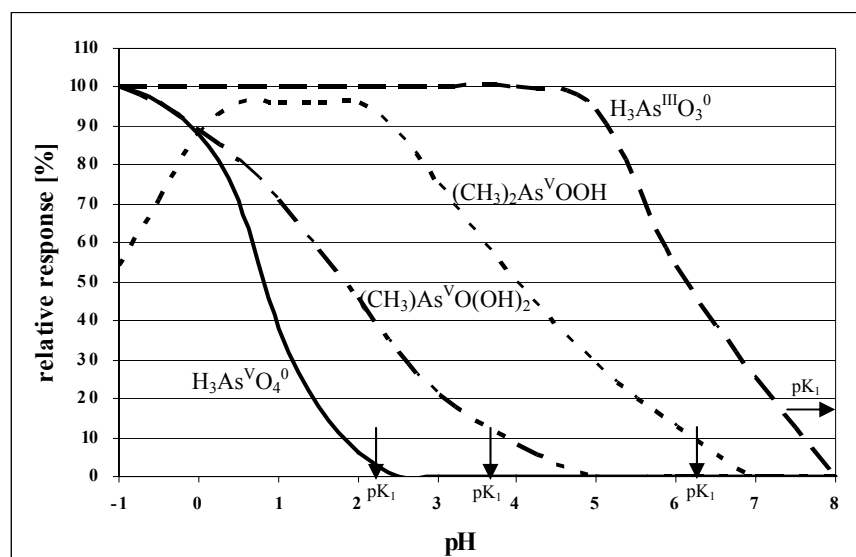


Figure 14 pH dependence of arsine hydride generation from solutions containing As(V), MMAA, DMAA, and As(III) respectively; vertical arrows indicate the pK_1 values for each acid (As(V) = 2.2, MMAA = 3.2, DMAA = 6.2, As(III) = 9.2 (modified from Howard 1997))

Arsenite predominates as $H_3AsO_3^0$ up to a pH of 9.2 and reacts with the reducing agent just at slightly acid conditions. Arsine generation from $MMA^V A$ must be carried out at a pH < 4, As(V) even below pH 2. The most effective arsine generation in both cases is below pH 1. $DMA^V A$ shows a clear peak in relative response at a pH between 0.5-2. The decrease at more acid conditions might be owed to the formation of the cationic $DMA^V A$ species $(CH_3)_2AsO(OH)-H^+$ mentioned in section 2.5.2.1. Upon additional H^+ -input during acidification an H_2O molecule easily splits from this species. A general decrease in response for all four As species can also be observed at excess HCl concentrations (not shown in Figure 14), since the surplus H^+ rapidly consumes the reductant that does not volatilize the As species anymore (Luna et al. 2000). According to experiments from Sur (1999) (not shown in Figure 14) $TMA^V O$ shows a decreasing signal intensity with increasing HCl concentration. Trivalent methylated arsines and methylated sulfur arsines (not shown in Figure 14) can be generated like As (III) at a pH of about 6 (Bright et al. 1996; Hasegawa et al. 1994).

Trying to illuminate the observed variations in arsine-generation efficiency, Pergantis et al. (1997) used deuterium-labeled reagents for HG, and investigated the products with mass spectrometry. They found that AsH_3 , generated from As(III) or As(V), was deuterated when using deuterium labeled $NaBH_4$ ($NaBD_4$), however, not when using deuterium labeled HCl (DCl). MMA showed deuterium signature both when using $NaBD_4$ or DCl. After an initial predominance of $(CH_3)AsD_2$, the concentration of non-deuterated $(CH_3)AsH_2$ increased with time. This time-series trend indicated that arsines once generated may further react with acids present in the reaction mixture, thus allowing for deuterium-hydrogen exchange. The relative rates of deuterium-hydrogen exchange depend on the basicity of the arsines. Arsine with the lowest basicity shows no exchange reactions,

whereas the most basic arsine, DMA, easily protonates according to the following reaction: $(\text{CH}_3)_2\text{AsH} + \text{H}^+ \leftrightarrow (\text{CH}_3)_2\text{AsH}_2^+$. The water-soluble dimethylarsonium $(\text{CH}_3)_2\text{AsH}_2^+$ is unstable and oxidizes rapidly to $(\text{CH}_3)_2\text{AsO}(\text{OH})\text{-H}^+$. The hydrogen isotope signature in DMA equals that of the acid, i.e. it is $(\text{CH}_3)_2\text{AsD}$ when using DCl, and $(\text{CH}_3)_2\text{AsH}$ when using HCl. According to Pergantis et al. (1997) deuterium-hydrogen exchange was only detected in the aqueous phase, not in the gas phase with HCl vapor.

The presence of other metals may suppress hydride generation (Creed et al. 1996), probably by decomposing NaBH_4 before it has reacted with the analyte (Agterdenbos and Bax 1986). Total As recoveries are generally less affected by metal interferences than As(III) recoveries. Data from McCleskey et al. (2003) show that only Sb(III) and Sb(V) interfere with total As determination when the molar ratios of $\text{Sb(III)/As}_{\text{total}}$ exceed 4 and $\text{Sb(V)/As}_{\text{total}}$ exceed 2. Poor As(III) recoveries because of hindered arsine generation or oxidation of As(III) were found when the following ratios were exceeded: $\text{Cd/As(III)} > 800$, $\text{Cr(VI)/As(III)} > 2$, $\text{Cu(II)/As(III)} > 120$, $\text{Fe(III)/As(III)} > 70$, $\text{Sb(III)/As(III)} > 3$, $\text{Sb(V)/As(III)} > 12$, and $\text{Se(IV)/As(III)} > 1$. High Fe(II) concentrations ($\text{Fe(II):Fe(III)} > 2$) inhibited the As(III) oxidation by the oxidizing agent Fe(III). Poor As(III) recoveries in the presence of Fe(II):Fe(III) ratios > 2 occurred only at Fe(III) concentrations of more than 10 mg/L. The elements Fe(II), Al, Cr(III), Co, Pb, Mn, Ni, and Se(VI) did not lead to significant decreases in arsine generation (McCleskey et al. 2003). In a 2 $\mu\text{g/L}$ As(V) solution, Yin et al. (1996) observed significant interferences only from a 150-fold excess of Se(IV) and Bi(III), slight signal depressions from Fe(III) (10 mg/L) and Ni (10 mg/L), but none from Pb(II), Ag(I), Al(III), Ga(II). In contrast to McCleskey et al. (2001, 2003), they found no interference from Cu(II) up to 10 mg/L. In experiments conducted by Jamoussi et al. (1996) 1 mg/L Au(III) and Pd(II), 2 mg/L Ni (II), 25 mg/L Cu(II), and 50 mg/L Co(II) severely suppressed the As signal (recovery $< 80\%$). Little interference was found for Pb(II) with a recovery of more than 90% for 100 mg/L Pb(II).

Interfering metal cations can be removed by a cation exchange resin without alteration of the original $\text{As(III)/As}_{\text{total}}$ ratio (McCleskey et al. 2003). Pre-reduction of As with cysteine also yields a greater resistance to interferences from metal ions by forming stable ligand-metal complexes with the metal ions as well as more uniform sensitivities for the four main As species (Howard 1997; Jamoussi et al. 1996; Yin et al. 1996). The latter is probably caused by the lower acid concentrations when working with pre-reduction, generating less hydrogen which is advantageous for the atomization of As (Yin et al. 1996). Similarly, Yano et al. (2000) found much better recoveries for As(V) using potassium iodide and microwave treatment for pre-reduction, working at lower HCl and NaBH_4 concentrations.

For total As determination by HG, the pH dependent difference in signal response of the different As species poses a problem, since a compromise for the pH has to be found for all species or pre-reduction steps have to be performed. On the other hand, these differences can be used to achieve simple As speciation by stepwise HG at pH 6, yielding trivalent As species, and consequently at pH 1, for the sum of tri- and pentavalent As species. Pentavalent species are then calculated from the difference. Further speciation between inorganic, mono-, di- and trimethylated As is mostly done

by subsequent cryogenic trapping and sequential release to a detector according to boiling point differences (section 2.6.2).

However, by laborious optimization of acid, reductant, and pre-reductant concentrations as well as reagents contact time, it is possible to develop a selective reduction scheme for the identification of As(III), As(V), MMAA, and DMAA. Bermejo-Barrera et al. (1998) used a citric acid / sodium hydroxide buffer at pH 5 and 0.2% NaBH₄ to volatilize As(III) alone, 0.14 M acetic acid and 0.2% NaBH₄ for As(III) + DMAA, 4 M HCl + 2% NaBH₄ for As(III) + As(V), and 0.02 M thioglycolic acid + 1 % NaBH₄ for HG of all As species together. Shraim et al. (1999) used 0.01 M HCl, 2% NaBH₄, 5% L-cysteine and a contact time <10 min for total As, 1 M HCl, 0.3-0.6% NaBH₄, 4% L-cysteine, < 5 min for DMAA, 4-6 M HCl, 0.05% NaBH₄, no L-cysteine for As(III), 4 M HCl, 0.03% NaBH₄, 0.4% L-cysteine, 30 min for MMA determination. As mentioned before, reports about efficiency of HG from individual As species differ, being highly sensitive towards type and amount of reagents. Shraim et al. (1999) also discuss some of these contradictions. The successful separation of As(III) + As(V) at 4 M HCl by Bermejo-Barrera et al. (1998) is based upon their experiments; no MMA was volatilized at any HCl concentration. This finding contradicts to many other reports (e.g., Howard 1997; Shraim et al. 1999). Furthermore, Shraim's separation of DMAA is based on their findings that DMAA shows the highest signal response at low pH and low NaBH₄ which was not confirmed by Howard (1997). Determination of inorganic and organic As species by hydride generation is possible but still far from being a standardized routine application.

The HG techniques have some further restrictions. First, in contrast to the inorganic and organic As species described above, several organoarsenicals are not reducible with borohydride, e.g., arsenobetaine, arsenocholine, or arsenosugars. Those refractory or "hidden" arsenicals have to be pre-treated e.g., by alkaline digestion (de Bettencourt and Andreae 1991), microwave-assisted oxidation (Le et al. 1993; Santosa 2001; Sur 1999), UV photooxidation with K₂S₂O₈ (Howard and Hunt 1993; Sur 1999; van Elteren and Slejkovec 1997) or a combination of all three (Cabon and Cabon 2000; Yano et al. 2000) to become convertible to arsines. While the hybrid ion arsenobetaine is more resistant to oxidation than the cationic arsenocholine species, it is vice versa for alkaline digestion (Sur 1999).

The HG techniques include the simplified assumption that AsH₃ only forms from inorganic As, MMA only from monomethylated species, DMA only from dimethylated species, TMA only from TMA^VO. Transmethylation reactions during volatilization and later on in the gas phase are hereby neglected. Already Talmi and Bostick (1975) found that the reduction of MMAA resulted in the partial production of AsH₃, DMA, and TMA in addition to the expected MMA. Hydride generation on DMAA produced small amounts of MMA. According to experiments from Pantsar-Kallio and Korpela (2000), AsH₃ and MMA are not converted into other gaseous species during preparation or storage. For DMAA they found that at pH 1 to 2, about 90% of DMAA are volatilized as DMA, a small fraction, however, as TMA and MMA. This fraction increases with decreasing pH. At pH lower than -0.3 all DMA^VA is converted to TMA.

Furthermore, HG of $\text{MMA}^{\text{V}}\text{A}$ and $\text{DMA}^{\text{V}}\text{A}$ may not only yield the simple methylated arsines, but also more complex forms as methylated chloroarsines in the presence of excess Cl in solution or in the gas phase (section 2.5.2.6). Van Elteren et al. (1994) e.g., report that in their experiments only 85% of the originally present DMAA was converted to DMA. The remaining 15% showed a higher affinity to the gas chromatographic column, indicating a compound with a higher boiling point. The compound was unknown to the authors and could have been a dimethylated chloroarsine. Haas and Feldmann (2000) found a similar phenomenon of formation of various hydrides from one precursor during HG for Sb. They detected SbH_3 , $(\text{CH}_3)\text{SbH}_2$, $(\text{CH}_3)_2\text{SbH}$, $(\text{CH}_3)_3\text{Sb}$ only from $(\text{CH}_3)_3\text{SbCl}_2$ as precursor due to rearrangement and demethylation reactions. Bergmann and Glindemann (1997) also detected other volatile As species besides the expected AsH_3 after HG of an As(V) solution. The concentrations of these additional arsines increased with increasing concentration of dissolved As(V). The authors explain this trend by the formation of oligomers from the monohydrides or the formation of methylated arsines from contaminations in the reducing agent NaBH_4 . Re-dissolution of the generated hydrides might further increase losses and uncertainties. Using flow injection HG (FI-HG) instead of batch-wise operation, first developed and applied by Aström (1982) and Yamamoto et al. (1985), will decrease re-dissolution and interactions in the headspace. However, there might still be significant errors in simply concluding from the volatile species detected during HG to the dissolved species (Feldmann et al. 2004).

Much more reliable than HG alone is a combination of HG with a preceding separation step, like chromatographic separation by high performance liquid chromatography (HPLC). For chromatography the sample is introduced unaltered, differences in boiling points yield different retention times and an easy species separation. Subsequent HG is used for improved detection limits.

2.6.1.2 HPLC

For As speciation via separation by high performance liquid chromatography (HPLC), the technique of ion pair, ion exchange and size exclusion chromatography are used. The most commonly used pairing cation is tetrabutyl ammonium (elution order $\text{As(III)} > \text{DMA}^{\text{V}}\text{A} > \text{MMA}^{\text{V}}\text{A} > \text{As(V)}$ in a pH between 5 and 7). Arsenite and arsenobetaine co-elute in this pH range. To separate both species, anionic-pairing conditions and a higher mobile-phase pH ($\text{pH} > 9$) have to be used so that As(III) is slightly retarded and while the hybrid ion arsenobetaine passes through the column (Thomas and Sniatecki 1995). Using a reversed-phase column and a mobile phase of 5 mM tetrabutyl ammonium hydroxide (TEAH), 3 mM malonic acid, and 5% methanol at pH 5.8, $\text{MMA}^{\text{III}}\text{A}$ and $\text{DMA}^{\text{III}}\text{A}$ were also determined by Le et al. (2000a, 2000b). Le and Ma (1997) used a reversed-phase column and a mixed ion-pair mobile phase of 10 mM hexanesulfonate and 1 mM TEAH to separate As(III), As(V), $\text{MMA}^{\text{V}}\text{A}$, $\text{DMA}^{\text{V}}\text{A}$, arsenobetaine, arsenocholine, and TETRA. Londeborough et al. (1999) separated optimally those species plus $\text{TMA}^{\text{V}}\text{O}$ with a 0.05 mM benzenedisulfonic acid as eluent modifier. They encountered, however, problems resolving As(III) and MMAA as well as identifying $\text{TMA}^{\text{V}}\text{O}$, TETRA, and arsenocholine in natural samples because of matrix effects.

Different research groups developed methods for the separation of the four main As species (As(III), As(V), MMA^VA, DMA^VA) by gradient elution on anion exchangers, mainly styrol-divinylbenzole copolymers. For the mobile phase, Stummeyer et al. (1996) and Bednar et al. (2004) used 2.5 mM to 50 mM, and 38 mM to 75 mM phosphate buffers respectively, Lindemann et al. (1999) used 2 mM ammonium hydrogen carbonate, and 2.2 to 45 mM tartaric acid at a pH of 8.2, whereas Bissen and Frimmel (2000) used 2 mM and 50 mM NaOH. Using a boric acid buffer (10 mmol and 50 mmol Na₂B₄O₇·10H₂O in 20 and 30 mmol NaCl) at pH 9 instead of the weaker phosphorous buffer, Sur (1999) could additionally separate TMA^VO, however with the drawback of relatively long analysis times. By gradient elution with nitric acid (2.5 mM and 50 mM) Bednar et al. (2004) were able to resolve roxarsone (3-nitro-4-hydroxyphenylarsonic acid) besides the four main As species. Cation exchange chromatography was successfully used to separate arsenobetaine, arsenocholine, TMA^VO, and TETRA (Ackely et al. 1999). Feldmann et al. (2004) also achieved separation of arsenosugars and their metabolites via cation exchange.

In the ion exclusion mode, a carboxylated methacrylate resin separates As(V), MMA^VA, DMA^VA, As(III), and arsenobetaine. However, differentiation of TMAO and arsenocholine was not achieved (Taniguchi et al. 1999). McSheehy et al. (2000) used size exclusion to separate arsenosugars from other As species.

2.6.1.3 Gas chromatography

Separation of volatile species or originally dissolved species after HG can be achieved by gas chromatography, often combined with cryofocusing, i.e. the pre-concentration of the analyte in a cooled trap (section 2.7.4.3). Different hydride species can be separated by sequential release due to boiling point differences. Various columns have been used for separation, e.g., Chromosorb coated with 10% methyl silicon SP-2100 (Amouroux et al. 1998; Feldmann et al. 1994; Grüter et al. 2000; Hirner et al. 2000), a DB624 column with 6% cyanopropylphenyl and 94% dimethylpolysiloxane (medium polarity, Prohaska et al. 1999), or a SPB-5 with 5% phenyl and 95% dimethylpolysiloxane (low polarity, Mester and Sturgeon 2001).

2.6.1.4 Capillary zone electrophoresis

Another way of separation is capillary zone electrophoresis (CZE), used by Schlegel et al. (1996) for the separation of As(V), As(III), DMAA, As^VF₆, p-aminobenzenearsonate, and phenylarsonate, as well as by Greschonig et al. (1998) for As(III), As(V), DMAA, diphenylarsinic acid, methanearsonic acid, phenyl- and p-aminophenyl arsonic acid, phenylarsineoxide and phenarsazinic acid and by Michalke and Schramel (1997) for As(III), As(V), DMA^VA, MMA^VA, arsenobetaine and arsenocholine. Problems occurred in some studies with As(V). At alkaline pH it could not be analyzed, because its electrophoretic mobility was higher than the velocity of the electroosmotic flow, at acidic pH analysis time was long. In general, CZE proved to have a worse sensitivity compared to HPLC with a poor resolution especially in complex matrices (Gong et al. 2002). To

improve the limits of detection in CZE, pre-concentration by stacking larger sample volumes and removal of the sample matrix were performed, normally at negative polarity or by adding a modifier, or, as proposed by Vanifatova et al. (1999), by using a polymer-coated capillary to decrease the zeta potential at the capillary walls which diminishes the electroosmotic flow.

2.6.2 Arsenic detection

Arsenic detection after HG can be done e.g., by coupled AAS (atomic absorption spectrometry), AFS (atomic fluorescence spectrometry that shows a very high sensitivity in the absence of light scattering and background interference from the sample matrix after HG), ICP-AES (inductively coupled plasma atomic emission spectrometry), or ICP-MS (inductively coupled plasma mass spectrometry). Bermejo-Barrera et al. (1998) describe electrothermal AAS (ET-AAS) with in situ pre-concentration of arsines on coated graphite tubes as superior to conventional HG-AAS. Testing Ir-, W-, Zr-coatings, they found the best analytical performance with detection limits of around 50 ng/L for Zr coatings.

Another possibility that is used both for volatile species as well as for originally dissolved species after HG, is cryofocusing (section 2.7.4.3) and subsequent injection into AAS (Cabon and Cabon 2000; Howard 1997; Van Elteren et al. 1994) or GC (LT-GC, low temperature GC). The advantage is that different hydride species can be detected by sequential release from the cold trap based on boiling point differences. Unknown compounds can be detected by boiling point – retention time relationships (Feldmann et al. 1994; Grüter et al. 2000), or, in the case of GC, by additional detectors, e.g., ICP-MS (Amouroux et al. 1998; Feldmann et al. 1996; Feldmann 1997; Hirner et al. 2000; Prohaska et al. 1999). Especially for As, however, there is the problem of validating ICP-MS signals caused by interferences of ^{35}Cl and ^{40}Ar with the mono-isotopic ^{75}As (Pécheyrans et al. 2000). In the absence of known standards, structural information and species identification can only be gained using GC-MS (Cullen et al. 1995; Feldmann and Kleinmann 1997; Kaise et al. 1997; Maillefer et al. 2003; Panssar-Kallio and Korpela 2000). Electrospray ionization (ESI) MS, possibly combined with tandem mass spectrometry (ESI-MS/MS), is also well suited for As speciation, especially of arsenosugars (Gallagher et al. 2001a; McSheehy et al. 2000; Pergantis et al. 2000; Shimizu et al. 1999).

HPLC or CZE can further be coupled with

- UV- or conductivity detection
- HG-AAS (Carrero et al. 2001; Howard and Hunt 1993; Shraim et al. 2000; Sur 1999)
- HG-AFS (Le and Ma 1998; Le et al. 2000a; Ma and Le 1998; van Elteren and Slejkovec 1997)
- HG-ICP-AES (Gettar et al. 2000; Rauret et al. 1991)
- HG-ICP-MS (Prohaska et al. 1999)
- IPC-AES (Chausseau et al. 2000; Ebdon et al. 1987; Weeger et al. 1999) or
- ICP-MS (Guerin et al. 2000; Lindemann et al. 1999; Londesborough et al. 1999; Saeki et al. 2000).

Gómez et al. (1997) propose anion cartridge pre-concentrators for improvement of the detection limits of HPLC-HG-AAS (0.1 - 0.6 µg/L). Often, the post column reaction loop in a HPLC-HG-AAS setup is heated to increase signal intensity, especially for the methylated arsenicals. Stummeyer et al. (1996) found a 20% and 40% increase in signal intensity for MMA and DMA respectively, by heating the reaction loop to 100°C compared to reduction at room temperature. Detection limit was 0.5 µg/L.

Detection limits of HPLC-HG-AFS are in the sub-microgram per liter range, comparable to those achieved with HPLC-ICP-MS using pneumatic nebulization. Le et al. (2000a) successfully separated As(III), As(V), MMA^{III}A, MMA^VA, DMA^{III}A, DMA^VA by HPLC-HG-AFS with detection limits of 0.5-2 µg/L without further sample pre-treatment. The ICP techniques are especially interesting for multi-element studies. Coupling HPLC and ICP-AES is straightforward because the flow rates in both cases are similar, typically about 1 mL/min. However, ICP-AES is mostly used for samples with higher As concentrations because it has poor sensitivity. For higher sensitivity either a HG step is established between HPLC and ICP-AES or ICP-MS is used with about 100 to 1000 times higher sensitivities compared to ICP-AES, provided corrections for Cl-Ar interferences are made.

Less common techniques include a gold ultramicroelectrode array proposed by Feeney and Kounaves (2000) that responds with high sensitivity to As(III) using square-wave anodic stripping voltammetry, or biosensors, such as the biosensing microbe *Pseudomonas fluorescens* OS8 (Petänen et al. 2001) or the GFP (green fluorescent protein) reporter gene biosensor that is fused to the ars operon protein ArsR for arsenite repression (section 2.5.1.2) and produces GFP in response to As(III) (Roberto et al. 2002).

2.6.3 Arsenic quantification

While the quantification of dissolved As species is relatively simple via aqueous standard solutions, the quantification of the gaseous As species is more difficult since few commercial standard gas mixtures and no reference material exist. High pressure standards of AsH₃, MMA, DMA, and TMA were synthesized e.g., by Bergmann and Glindemann (1997). The pure As substances were evaporated in evacuated high-pressure stainless steel gas cylinders and stored in a He-atmosphere.

Calibration is often performed externally with gaseous standards produced by HG and transferred offline to a GC (Prohaska et al. 1999). Feldmann (1995, 1997) alternatively developed an online calibration method for GC-ICP-MS. The dry aerosol of the gas sample from the GC output is mixed in a T-piece or in a high-solid torch with an aqueous standard solution containing Rh as continuous internal standard to monitor the plasma stability and identify irregular transient signals caused by the presence of CH₄ or CO₂. The aqueous standard is introduced as a wet aerosol by nebulization. Nebulized water is also added to the dry aerosol from the GC outlet in order to obtain the same response for volatile and aqueous species during their simultaneous introduction into the plasma. Otherwise the different water content in the plasma would cause significant differences in

electron density, ion energy, and ionization temperature. While the external calibration with HG requires multi-species standards (AsH_3 , MMA, DMA, etc.), the Feldmann method is based on the species independent calibration with only one As-specific response curve. An error of $\pm 35\%$ can be expected for the determination of the mass of the internal Rh standard.

2.7 Field sampling

2.7.1 Water sample stability and preservation

Several papers on the stability of As species over time show that generally rapid oxidation of As(III) to As(V) occurs in natural water samples without preservation. Hall et al. (1999) report a complete reduction of As(V) to As(III) within a few days storage at room temperature for samples of Ottawa river water and deionized water. Such a reduction can occur during storage when the water sample contains dissolved organic carbon as food source for microorganisms and turns anoxic because it is sealed. In the case of Hall et al. (1999) the microorganisms most likely came from organic resins used in the deionization cartridges. Seyler and Martin (1989) found no changes in the As(III) concentrations at all after 10 days storage at 4°C and a pH of 7. McCleskey et al. (2004) detected such an unchanged As redox species distribution only in distilled, deionized, and otherwise uncontaminated water (16 days at pH 3.7 under light and dark conditions). For the organic arsenicals Larsen et al. (1993) report that $\text{DMA}^{\text{V}}\text{A}$, $\text{MMA}^{\text{V}}\text{A}$, and arsenobetaine are relatively stable. Jokai et al. (1998) stored solutions with 0.01-10 ng/mL MMAA and DMAA over 5-6 months at room temperature without any significant losses. Trivalent methylated compounds, especially $\text{DMA}^{\text{III}}\text{A}$, however, oxidize rapidly (Gong et al. 2001; section 2.5.2.3).

As discussed in section 2.5.1.2, oxidation of As(III) to As(V) or reduction of As(V) to As(III) are mainly microbial processes but inorganic reduction can occur in the presence of strong reducing agents such as H_2S and S_2O_3 , inorganic oxidation in the presence of metal catalysts such as MnO_2 or strong oxidizing agents such as Fe(III) especially when catalyzed by light. Species preservation methods therefore must include filtration of colloids and microorganisms, addition of a reagent to prevent dissolved Fe and Mn oxidation and precipitation, and cool and dark storage (McCleskey et al. 2004). Creating an inert N_2 atmosphere shows no improvement for species preservation (McCleskey et al. 2004).

Filtration shall be done with $0.1\ \mu\text{m}$ (McCleskey et al. 2004). For storage, Palacios et al. (1997) recommend freezing as the best way. However, freezing promotes the formation of iron hydroxides leading to oxidation, sorption, and co-precipitation of As. Lindemann et al. (2000) and Daus et al. (2002) found the worst storage results at -20°C , the best at 3°C , similar to McCleskey et al. (2004) at 4°C . Various reagents have been tested for stabilization. Filtration alone without adding any stabilizing agent does not inhibit algal growth (McCleskey et al. 2004). McCleskey et al. (2004) recommend acidification with HCl to pH 2 as stabilization. Dark storage is crucial because highly reactive dichlororadicals can form under the influence of light and lead to rapid oxidation. Nitric

acid can undergo photochemical reaction and should thus not be used for redox species preservation (Fanning 2000). Sulfuric acid works for the preservation of As redox species (Bednar et al. 2002) but it is difficult to purify and forms precipitates with many other metals such as BaSO_4 . Daus et al. (2002) used 0.01 mol/L phosphoric acid because they found that using the strong acid HCl or the weak nitrilotriacetic acid as preservatives led to an overestimation of As(V) by dissolving colloidal soluble adsorbates containing arsenate and by promoting ferric ion formation. McCleskey et al. (2004) point out that Daus et al. (2002) did not exclude light from their experiments and that thus As(III) oxidation is to be expected. The use of phosphoric acid has the disadvantage that it may encourage microbial growth and may lead to supersaturation with respect to metal phosphates and sorption or co-precipitation of As or other redox sensitive elements. Edwards et al. (1998) used ascorbic acid and HCl to preserve the As(III) and As(V) concentrations for 28 days in spiked synthetic water, however in natural samples 25% of the As(III) was converted to As(V) within 8 days despite of the preservation measures. Using an optimized method of filtration with 0.1 μm , acidification with HCl to pH 2, and storage at 4°C in opaque bottles the As(III) to As(V) ratio was found to be stable for more than 15 months in surface and groundwaters (McCleskey and Nordstrom 2002; McCleskey et al. 2003, 2004).

An excess of Fe(II) was used successfully by Borho and Wilderer (1997) to inhibit As(III) oxidation in Fe(III) rich samples. McCleskey et al. (2004) showed that addition of Fe(II) and SO_4^{2-} slows down the As(III) oxidation by Fe(III) in light experiments and stops it for 71 days in dark experiments. The Fe(II) competes with As(III) for dichloro- and hydroxyl radicals, SO_4^{2-} complexes with Fe(III) and the FeSO_4^+ complex sorbs photons, thus binding free radicals.

If detection is to be performed by ICP-MS McCleskey et al. (2004) and Bednar et al. (2002, 2004) recommend ethylenediaminetetraacetic acid (EDTA) as preservative because of the molecular interference of ^{35}Cl from HCl and ^{40}Ar from the carrier gas on the monoisotopic ^{75}As . The EDTA chelates Fe and thus prevents photochemical oxidation and precipitation. Gallagher et al. (2001b) also report that As(III) concentrations were stable for 16 days after addition of EDTA. The disadvantage is that relatively high concentrations of EDTA, partly exceeding its solubility, are needed in Fe rich waters. Manganese, a similarly efficient catalyst for As(III) oxidation, is not chelated at all. A further disadvantage is that metals sequestered by EDTA can not be removed by cation exchange as described in section 2.6.1.1 (McCleskey et al. 2003) and might interfere with arsine generation.

For human urine Feldmann et al. (1999b) report a significant reduction of As(V) to As(III) as well as a demethylation of MMAA and DMAA to As(III) with strong acidification (0.1 mol/L HCl). They found no improvement of species recovery with other preservatives tested (sodium azide, benzyltrimethylammonium chloride, benzoic acid, cetylpyridinium chloride, methanol) and state that samples can best be kept without any additives at 4°C or -20°C for 2 months. The problems of storage at -20°C were discussed above.

2.7.2 On-site species separation for water samples

To exclude potential losses during storage and transport, several on-site species separation techniques have been developed. Van Elteren et al. (1994) propose on-site sequential coprecipitation of As(III) with carbamate and As(V) with molybdate. The precipitates are filtered under vacuum on a 0.45 μm filter and dissolved with HCl, HNO₃ or H₂SO₄ upon return to the laboratory. Hasegawa et al. (1994) developed another method that was successfully applied by Sohrin et al. (1997) for the separation of six As species. All As(III) species (i.e. As(III), MMA^{III}A, DMA^{III}A) are extracted on site with diethylammonium diethyldithiocarbamate (DDDC) into carbon tetrachloride. In the laboratory this aliquot is back-extracted into 0.1 M NaOH, including several clean-up steps to remove the remaining DDDC, and analyzed by HG-AAS. The sum of As(III) and As(V) species are analyzed from a different aliquot filtered with 0.45 μm upon collection and acidified to pH 2. Finally, the As(V) species (As(V), MMA^VA, DMA^VA) are obtained as the difference between total As and As(III). One problem with this method is that trivalent As-S-compounds can not be identified or distinguished from MMA^{III}A, DMA^{III}A which are extracted as dithioldicarbamate complexes. Another drawback is the relatively complicated and time consuming back-extraction in the laboratory.

Ion exchange on solid phases (SPE = solid-phase extraction) has been used as a rather simple, inexpensive, and sensitive method for As(III) and As(V) on-site separation (Ficklin 1983; Kim 2001). The species separation is based on the different dissociation constants of As(III) and As(V) as shown in Figure 4 and Figure 6. The method was further improved by Le et al. (2000c) and Yalcin and Le (2001) for the additional separation of the methylated arsenicals. A filtered water sample is passed through a resin-based strong cation exchanger, on which DMAA is sorbed, followed by a silica-based strong anion exchanger that retains MMAA and As(V). Arsenite as uncharged complex passes through both exchange cartridges and remains in the solution. The sample has to be filtered to avoid precipitation of Fe, Mn, or Al-hydroxides at the head of the cartridge that would provide additional sorption sites (Bednar et al. 2004). The sequence of cation exchanger mounted on top of the anion exchanger is important because DMAA that predominates as uncharged complex at pH > 1.6 (Figure 9) shows non-specific sorption both on the cation and anion exchanger, whereas MMAA and As(V), as negatively charged complexes, pass through the cation exchange cartridge and sorb on the anion exchanger only. Concomitant anions, like sulfate, carbonate, or chloride can compete with As species for exchange sites if present in high concentrations, such as sulfate in an acid mine drainage (AMD) with concentrations in the g/L range (Bednar et al. 2004).

In the laboratory, the cation exchange cartridge is eluted with 1 M HCl to mobilize the sorbed DMAA fraction. The anion exchange cartridge is first rinsed with 60 mM acetic acid at a pH of approximately 4 to mobilize MMAA with a pK₁ value of 3.6 (Figure 8). At this pH, As(V) is still retained as negatively charged complex. It only desorbs after treatment with 1 M HCl at a pH of approximately 1 (pK₁ = 2.2; Figure 4). Each eluent fraction is analyzed separately by HG-AAS with a detection limit of 0.05 $\mu\text{g/L}$. Sealed and stored in the refrigerator at 4°C, the As species were found to be stable for up to 4 weeks on the ion exchangers. Instead of pre-conditioning the exchanger cartridges with 50% methanol and deionized water (Le et al. 2000c), Bednar et al. (2004)

suggest converting the resin from the chloride form to the acetate form by washing it with 1.7 M acetic acid to achieve higher buffering capacity and a better long-term stability (recovery after 47 days of storage 99% for the acetate form compared to 85% for the chloride form).

2.7.3 Gas sampling without pre-concentration

Gas containers, or gas bags are used to take whole air gas samples without pre-concentration. Schweigkofler and Niessner (1999) used evacuated stainless steel gas containers with electro-polished internal surfaces for chemical inertness described in the EPA canister method TO-14 (Falter et al. 1999) for storing volatile organic carbons (VOC). The recovery for the non-polar compounds was more than 85% and significant losses occurred for polar compounds only, e.g., propanethiol, and butanethiol. No applications for volatile metallics were found in the literature.

Gas bags of Teflon or Tedlar have the advantage of an easier handling compared to gas canisters. A variety of gas volumes (1-100 L) can be taken, whereas canister volume is limited to a few liters unless the sampled air is pressurized. Applications of gas bags are described by Feldmann et al. (1996), Feldmann and Cullen (1997), and Hirner et al. (1998). Haas and Feldmann (2000) investigated the stability of volatile As, Sb, and Sn in Tedlar bags. Surprisingly, the most stable compound was AsH₃ with a recovery rate of 75% after 8 weeks storage at 20°C and an estimated half-life of 3-4 months. The recovery rate of TMA on the other hand was only 75% after 24 hours of storage and 15% after 5 weeks.

Commonly, losses in gas bags occur due to sorption effects. Andino and Butler (1991) found that water vapor sorbs on the Tedlar walls and subsequent partitioning of VOCs into the absorbed water can occur. Wang et al. (1996) found for the VOCs trichloroethylene, dichloroethane, and toluene that commercial Tedlar bags showed significant sorption at the stainless steel hose valves or septa. They exclude losses due to leakage because the decrease was exponential and typical for a finite number of available sorption sites. Also surface to volume ratios have an effect on sorption losses, with larger volumes showing less sorption losses.

Haas and Feldmann (2000), however, concluded that for their experiments with concentrations between 0.3 to 10 ng/L sorption or condensation on the walls of the bag were a minor problem, especially when working with higher concentrations. Significant losses are attributed to immobilization of the volatile arsines due to oxidation and demethylation. The differences in stability found between AsH₃ and TMA are explained by the different dissociation energies for As-H (352 kJ/mol for AsH₃) and As-C (averaged dissociation energy 262 kJ/mol for TMA) bonds. These findings contrast with experiments from Pansar-Kallio and Korpela (2000) and Parris and Brinckman (1976) that TMA is more stable than AsH₃ (section 2.5.3.1, 2.5.3.4). The dissociation energy for As-H cited in Haas and Feldmann (2000; original from Thayer 1995) seems too high, compared to 229 kJ/mol in Elsenbroich and Salzer (1992). Independent of these unresolved differences, Tedlar bags can be successfully applied for gas sampling, if analysis is completed after a maximum of 8 hours storage, where all arsines could be recovered to approximately 100%.

Simple storage of gas samples, without any pre-concentration steps has several advantages. In contrast to trapping techniques described below there is no potential danger of analyte loss due to breakthrough. The whole gas composition can be determined, whereas trapping techniques are mostly optimized for selected compounds. Last but not least, multiple analyses can be performed from one sample.

2.7.4 Gas sampling with pre-concentration

The major challenge for sampling volatile metallics are their low concentrations, and possible interferences with other gas components (typically CO_2 , CH_4 , H_2S). Selective trapping with pre-concentration is therefore the preferred choice. Trapping gas samples over a certain period of time, so-called integrative sampling, leads to a pre-concentration of the volatile metallics, and smoothes out short term temporal noise. Liquid and solid sorbents are used as trapping media.

2.7.4.1 Liquid sorbents

Commonly used liquid sorbents for volatile metallics are oxidizing reagents, e.g., NaOCl , H_2O_2 , $\text{Na}_2\text{S}_2\text{O}_8$, or Na_2O_2 (Klusman 1991). $\text{Ca}(\text{OCl})_2$ is more reactive than NaOCl , and more soluble in water. However, because of its instability as solid substance and in solution $\text{Ca}(\text{OCl})_2$ is generally less suited for analysis than NaOCl . For As also the solubility of $\text{Ca}_3(\text{AsO}_4)_2$ or $\text{CaHAsO}_4 \cdot \text{H}_2\text{O}$ is a limiting factor (section 2.5.1.1; Bothe and Brown 1999). The maximum amount of As soluble in a 50 mL 1M $\text{Ca}(\text{OCl})_2$ solution is 12.2 mg As at 25°C. For sulfur containing gases, only 0.12 mg sulfate could be collected without precipitating calcium sulfate, and probably decreasing As concentrations by co-precipitation or sorption (Klusman 1991).

The use of liquid sorbents is well suited as a fast screening method, since a large variety of volatile metallics can be trapped efficiently, stabilized up to several weeks, and analyzed by multi-element analysis. However, the oxidation results in a complete destruction of species information, the individual arsines will all be detected as the sum of volatile As. In contrast to liquid sorbents, the solid sorbent methods described in the following section are species-conserving.

2.7.4.2 Solid sorbents

Two types of species-conserving solid sorbents are presented in the following: glass tubes filled with sorptive material comparable to small (max. 10 cm length) chromatographic columns (sorption tubes), and microfibers coated with sorptive material, the so-called SPME (solid-phase micro extraction) technique. In both cases, the sorption of volatile metallics on the sorbent is followed by thermal desorption and capillary gas chromatographic analysis.

Synthetic porous polymers (Tenax, Porapak, Chromosorb), carbon molecular sieves (Carbosieve, Carboxen) or non-porous graphitized carbon (Carbotrap) are commonly used as sorptive materials with a large surface area for quantitative sorption of volatile compounds (Table 4). Especially

Tenax finds widespread application for environmental sampling due to its wide range of possible sorbents, relative hydrophobicity, reproducible behavior during thermal desorption, and low chromatographic background noise.

Table 4 Different sorption materials for sorption tubes and their properties (Supelco catalogue information; elemental composition according to Knobloch and Engewald 1995)

sorption material	type	description	max. temp. [°C]	specific area [m ² /g]	sampling range	breakthrough volume [H ₂ O 30°C, mL/g]	Elemental composition [%]				
							C	H	N	S	O
Tenax TA	porous polymer	2,6-diphenyl-p-phenylene ether	300	35	C6-C14	32	88.5	5.0	---	---	6.3
Chromosorb 105	porous polymer	polyaromatic, for compounds with a boiling point ca. 200°C	225	650	C5-C12	---	---	---	---	---	---
Chromosorb 106	porous polymer	cross-linked polystyrene, low boiling compounds, gases, C2-C5 alcohols	250	750	C2-C5	---	---	---	---	---	---
Carbosieve S III	carbon molecular sieve	small molecules, hydrophilic	400	820	C2-C5	111	96.8	0.5	<1	---	---
Carboxen 564	carbon molecular sieve	C2-C5 volatile organic carbons	400	426	C2-C5	---	82.1	0.6	<1	6.3	---
Carbotrap	graphitized carbon black	C4-C5 to polychlorinated biphenyls, larger molecules	350	100	C5-C9	0	99.6	---	0.2	---	---

Jenkins et al. (1998) used Tenax TA to trap (CH₃)₃Sb and encountered oxidation on the sorption material under aerobic conditions. The oxidation product was less volatile, tightly bound to the sorptive, and not released during thermal desorption, but only after extraction with nitric acid. Transferring the analyte to the sorption material under anaerobic conditions enabled reversible sorption. Grüter et al. (2000) detected the same irreversible sorption of Sb and losses of over 50% with different tin and arsenic species during sorption studies on Tenax at room temperature (18 °C). Other potential problems using Tenax sorption tubes are degradation by exposure to oxidants like NO_x, O₃, H₂O₂, and OH radicals (Kleno et al. 2002; Pellizzari and Krost 1984) and alteration by irradiation with sunlight (Calogirou et al. 1996; Peters et al. 1994), producing significant concentrations of degradation products such as benzaldehydes, acetophenones, and aliphatic aldehydes.

Cao and Hewitt (1994) found that such build-up of degradation products is even worse for Carbotrap with the formation of benzene, and toluene, and to an even greater extent for Chromosorb 106 and thus it is not suitable for trapping volatile compounds at low concentrations. Nevertheless, Whitfield et al. (1983) used Chromosorb 105 for collecting TMA. Thomas and Rhue (1997) used Supelco ORBO-32 sorption tubes containing 0.65 g activated coconut charcoal for arsine trapping, but the analysis was not done conserving species by thermal desorption. It was done by solvent desorption with HNO₃. Thus, despite the advantages of sorbent tubes concerning low costs, easy

handling, pre-concentration, and preservation of species information, no really successful applications for volatile metals or metalloids are known.

The solid-phase micro-extraction (SPME) technique was first described by Arthur and Pawliszyn (1990). The commercial SPME design is similar to a GC injector syringe with a fused silica fiber of approximately 1 cm length coated with different stationary phases. Table 5 gives an overview of stationary phases available to date (07/2004), their properties, and application range. Liquid phase coatings, such as polydimethylsiloxane (PDMS) show sorption characteristics with extraction capacity proportional to the coating volume. Solid coatings, such as Carboxen (CAR) or divinylbenzene (DVB), extract analytes by sorption with the extraction capacity proportional to the coating's total surface area. The fiber's cylindrical surface geometry is well defined and less complex than the surface in sorption tubes, facilitating more efficient extraction and desorption.

Table 5 Available SPME fibers and their properties (available date as of 07/2004; op. temp. = recommended operating temperature, cond. temp. = conditioning temperature, cond. time = conditioning time; non-bonded phases are stable with some water-miscible organic solvents, but slight swelling might occur, bonded-phases are stable with all organic solvents, slight swelling may occur when used with some non-polar solvents; PDMS = polydimethylsiloxane, DVB = divinylbenzene, CAR = Carboxen, PA = polyacrylate, CW = Carbowax, TPR = templated resin; Supelco catalogue information)

stationary phase	film thickness	description	pH	max. temp. [°C]	op. temp. [°C]	cond. temp. [°C]	cond. time [h]	application range
PDMS	100 µm (GC/HPLC)	Non-bonded	2-10	280	200-280	250	0.5	low molecular weights (M = 60-275), volatiles
PDMS	30 µm (GC/HPLC)	Non-bonded	2-11	280	200-280	250	0.5	higher molecular weights (M = 80-500), non-polar, semivolatile
PDMS	7 µm (GC/HPLC)	Bonded	2-11	340	220-320	320	1	high molecular weights, non-polar M = 125-600
PDMS/DVB	65 µm (GC) 60 µm (HPLC)	Bonded	2-11	270	200-270	250	0.5	smaller molecules, volatile polar analytes (alcohols, amines, nitroaromates), M = 50-300
PA	85 µm (GC)	Bonded	2-11	320	220-310	300	2	polar semivolatile analytes (M = 80-300) from polar samples
CAR/PDMS	75 µm (GC) 85 µm (GC)	Bonded	2-11	320	250-310	300	1-2	smaller molecules, traces of highly volatiles, M = 30-225
CW/DVB	65 µm (GC) 70 µm (GC)	Bonded	2-9	260	200-250	220	0.5	smaller molecules, alcohols, polar compounds, M = 40-275
CW/TPR	50 µm (HPLC)	Bonded	---	---	---	---	---	surface active substances
PDMS/CAR/DVB	50/30 µm (GC)	Bonded	2-11	270	230-270	270	1	smaller molecules, screening of a large range of molecular masses (C3-C20), M = 40-275

Sorption tubes quantitatively sorb the analytes from the gas stream, but the SPME technique is based on the adjustment of a dynamic equilibrium between the concentration in the aqueous sample, in the gaseous headspace, and on the fiber according to Fick's second law (Zhang and Pawliszyn 1993):

$$\frac{\partial c_i(x, t)}{\partial t} = D_i \frac{\partial^2 c_i(x, t)}{\partial x^2}$$

$c_i(x, t)$ analyte concentration at time t and position x in the aqueous sample ($i = \text{aq}$), in the gaseous headspace ($i = \text{g}$) or on the fiber ($i = \text{f}$)

D_i diffusion coefficient in the gaseous headspace ($i = \text{g}$) and on the fiber ($i = \text{f}$; only diffusion along the fiber is considered, radial diffusion is assumed to be infinitely fast)

The two techniques “immersed SPME” (Arthur and Pawliszyn 1990) and “headspace SPME” (Zhang and Pawliszyn 1993) are used for sampling aqueous and gaseous environments, respectively. With the headspace SPME technique, equilibrium is generally reached more quickly (for As in 30-60 s on average) because diffusion rates are approximately 4 orders of magnitude higher in gas compared to water. Also, there are no matrix effects and the fiber is protected from swelling or degradation that might occur upon exposure to acid or highly mineralized solutions during immersed SPME.

Using a fiber with a liquid coating, the amount of analyte absorbed on the SPME fiber in the 3-phase system aqueous solution - gaseous headspace - fiber coating can be predicted from the following equation (Zhang and Pawliszyn 1993):

$$n_s = \frac{C_{\text{aq}}^0 \cdot V_f \cdot V_{\text{aq}} \cdot K_{\text{gaq}} \cdot K_{\text{fg}}}{K_{\text{fg}} \cdot K_{\text{gaq}} \cdot V_f + K_{\text{gaq}} \cdot V_g + V_{\text{aq}}}$$

n_s amount of analyte absorbed by the fiber coating

C_{aq}^0 initial concentration of analyte in aqueous sample solution

V_f volume of fiber coating

V_{aq} volume of aqueous sample solution

V_g volume of gaseous headspace

K_{gaq} partition coefficient of analyte between aqueous solution and headspace

K_{fg} partition coefficient of analyte between headspace and fiber coating

Special narrow-bore liners ($\text{id} = 0.8 \text{ mm}$, compared to 2-3 mm normally) are used for GC injection, guaranteeing a high laminar flow of the mobile phase along the fiber with sharp peaks and no repeated sorption and desorption effects.

Mester et al. (2000) investigated the suitability of a 100 μm PDMS and a 75 μm PDMS/CAR fiber for the sorption of volatile As, Se, Sb, and Sn. They found that both higher extraction efficiency and faster desorption were achieved with PDMS/CAR compared to PDMS fibers. The slower desorption from PDMS is attributed to decomposition of the volatile compounds and consequent enhanced interaction with the polymer coating. The same research group successfully applied PDMS/CAR fibers for sampling chloroarsines (Mester and Sturgeon 2001, 2002). According to experiments by Sur (1999), AsH_3 shows only a low affinity to SPME fibers due to its low boiling point. Trimethylarsine could be successfully trapped on a PDMS/CAR/DVB fiber. However, fraying of this ternary fiber was encountered. Thus, the more stable PDMS/CAR fiber was chosen even

though signal intensities were only 78% of those on PDMS/CAR/DVB. The polar PA (Polyacrylat) and a bare PDMS fiber showed almost no trapping efficiency with 1 and 2%, respectively, of the signal intensity for PDMS/CAR/DVB.

The SPME technique has several advantages. Besides low costs, easy handling, and fast sample processing, it also has few interferences. With headspace SPME technique, matrix effects are eliminated and contamination potential and analyte losses are minimized. Using HG (section 2.6.1.1) with SPME trapping instead of continuous HG, interferences from excess hydrogen are eliminated because hydrogen is not efficiently trapped by the fiber at room temperature. One major disadvantage of the SPME technique is the fragile nature of the thin fibers, especially for applications in the field. A further development beyond SPME application is the so-called stir bar sorptive extraction (SBSE) that consists of magnetic stir bars sealed in glass and coated with 50-300 μL PDMS (Baltussen et al. 1999). Compared to $<0.5 \mu\text{L}$ PDMS normally used for SPME fibers, this method increases sampling capacity and, consequently, sensitivity 100 to 1000-fold. It might thus be very attractive for sampling volatile metallics of low concentrations, but no applications in this field have been found so far in literature.

2.7.4.3 Cryotrapping

Another method of gas trapping combined with analyte pre-concentration is cryotrapping. The gas samples are purged through a column packed with a porous polymer material (e.g., Chromosorb (10% SP-2100, 60/80 mesh) and cooled in liquid nitrogen or acetone to about -80°C (Feldmann et al. 1994, Feldmann and Kleinmann 1997). The temperature of -80°C , instead of the commonly used -196°C , prevents trapping of CH_4 and CO_2 which could block the cryotrap by condensation thus limiting sampling volume and negatively affecting the plasma stability when using ICP-MS. Alternatively, Feldmann et al. (2001) and Maillefer et al. (2003) used NaOH pellets for CO_2 , H_2S , and H_2O removal prior to trapping the target compounds on the Chromosorb column. Although this worked well for As, unstable or slightly acidic compounds such as SbH_3 could react with NaOH. Cartridges filled with drying sorbents like CaSO_4 (Maillefer et al. 2003), K_2CO_3 , CaCl_2 or $\text{Mg}(\text{ClO}_4)_2$ (Feldmann 1995) can also be used for H_2O removal. After trapping, Feldmann et al. (1994), Feldmann and Kleinmann (1997), and Maillefer et al. (2003) closed the column with Swagelock stoppers, stored it in liquid nitrogen, and directly implemented it into the capillary column of a GC.

The major advantage of cryotrapping is its very low selectivity, enabling the pre-concentration of highly volatile compounds. The disadvantages are possible matrix effects from other gas components such as CO_2 , CH_4 , H_2S and possible losses due to the condensation of water and co-condensation of semivolatile compounds. Also the cryotrapping requires a costly setup, carrying a pump, liquid nitrogen, and a power supply to the field. The liquid nitrogen presents a possible hazard during transport. The vicinity of a laboratory is required for rapid analyses after sampling.

2.7.5 Techniques for collecting volatile metallics

In the previous sections several methods for trapping and stabilizing the volatile metallics with their advantages and disadvantages were presented. The initial task, however, is, to collect the volatile metallics in natural environments. Although sampling from the gas phase is relatively simple, it is much more complicated when volatile metallics dissolved in an aqueous phase are sampled and a gas-water separation has to be achieved.

2.7.5.1 Collection of volatile metallics from a gas phase

Well defined point sources such as gas wells on waste heaps, mine gas wells, and fumes in digester plants, can be sampled simply by connecting tubes to the gas outlet. Diffusive gas outlets can be sampled by different kinds of simple gas chambers. Feldmann and Cullen (1997) collected landfill gas which was visibly bubbling through a rain water puddle under a Plexiglas cylinder floating on a Styrofoam ring over the puddle. Hirner et al. (1998) used the same device for sampling geothermal gases bubbling through hot springs and pools. Maillefer et al. (2003) used an inverted plastic dish of 20 cm diameter, and 10 cm height for gas collection from underneath a compost pile. For sampling volatile Se from soils and plants, Biggar and Jayaweera (1993) used an acrylic volatilization chamber that was inserted approximately 10 cm into the soil and isolated a soil column with its plants. Similarly, Thomas and Rhue (1997) constructed a Plexiglas box with an internal air pump to trap surface soil gas flux of As from contaminated cattle dipping solutions.

Klusman (1991) developed and patented (US patent No. 4,993,874) an in-situ method for passive collection and immediate stabilization of volatile metals or metalloids. It was especially designed for As, Sb, and S, in soil gas or in the atmosphere above the ground as indicators for the exploration of subsurface mineral, geothermal and petroleum anomalies. Collectors with an oxidizing liquid inside are buried underneath a plastic shielding cone in the soil at a shallow depth. Apertures in the threaded plug in the top portion of the collector allow entry of ambient gases that are dissolved and oxidized in the trapping solution. Clean, high-quality glass wool is used to increase the surface area of the oxidizing liquid. After a certain period of time, the collectors are retrieved, sealed, and transported back to the laboratory. According to a written communication with Ron Klusman in June 2001, the efficiency of the apparatus was low based on laboratory calibration done with H₂S to produce S(VI) in H₂O₂ as oxidizing liquid. The actual volume sampled is not known, since it depends on several parameters, like porosity, permeability, percentage of water filled porosity, gas solubility, oxygen exchange, and other parameters hard to determine. Results could only be interpreted quantitatively by comparing a large number of collectors used in a survey with the same climate. Natural barometric gradients over sampling time were used as a “passive pump” for soil gas flow into the collectors. Applying a vacuum would have improved collection efficiency significantly but it entrained soil dust, contaminating the collector. One application for the patented method was an investigation on volatile As in soils at Ron Phibun, Thailand (Wongsanoon et al. 1997). Further work on this equipment was suspended.

2.7.5.2 Collection of volatile metallics dissolved in an aqueous phase

For sampling volatile metallics dissolved in an aqueous phase, little suitable equipment is available. A common technique for sampling gases dissolved in water is to take the water sample with a submersible pump and analyze its gas content in the laboratory. Degassing prior to analysis has to be avoided by gas-tight sampling equipment and sample storage. In the laboratory the gas can either be extracted quantitatively from the water by vacuum application, or purging with an inert gas or obtained by setting up a dynamic equilibrium between the water sample and a gas phase above (headspace technique). The amount of analyte in the headspace depends on its Henry constant.

Amouroux et al. (1998) used a method, they called “in-situ purging” to sample volatile metallics (Se, Sn, Hg, Pb) dissolved in natural waters. The water sample is taken by a PTFE (Polytetrafluorethylene) coated sampler that can be opened in a certain sampling depth, and transferred through a silicon tubing into a gas-tight 1 L pyrex bottle without headspace. Within 30 minutes after sample collection, the sample is purged through a moisture trap maintained at -20°C by a mixture of acetone and ice to remove water vapor, then finally condensed into the cryogenic trap immersed in liquid nitrogen at -196°C . Hirner et al. (1998) similarly took geothermal water samples in sealed teflon tubes, and purged them with helium in the laboratory for dissolved volatile compounds. These purging methods, however, have some serious disadvantages. First, they are non-integrative determinations with the drawback of short-term temporal noise as described above. To achieve low detection limits, relatively large amounts of water have to be taken. Exact depth-dependent sampling is difficult and presents a major disturbance for the sampled water body. The sensitive gas equilibrium might further be disturbed during storage and while purging the sample. Especially for studies focusing on the diffusive degassing at the sediment - water interface in-situ methods are required. However, such methods are still rare.

So-called passive diffusion samplers eliminate the problem of non-integrative sampling and possible disturbances of the gas equilibrium. After installation they are left several days to weeks outside while the air in the sampler equilibrates with the gaseous compounds in the surrounding aqueous phase. Church et al. (2002) developed passive vapor-diffusion samplers (empty glass vials enclosed in two layers of polyethylene membrane tubing) to detect volatile organic compounds in discharge areas of contaminated groundwater. However, the passive diffusion samplers include no pre-concentration or on-site stabilization and are hardly suitable for the generally low concentrations of volatile metallics. Furthermore, equilibration times of up to 3 weeks (Church et al. 2002) are not practical for fast screening. According to Klusman (1991), the patented method described above for in-situ collection and stabilization of volatile metallics can also be used for gas collection from the sediment-water interface at the bottom of a shallow water body. The shielding cone is then weighted to hold it to the bottom and used like a diving bell. A nylon mesh screen that is secured to the covering cone supports the collector. For deeper water application, the author recommends to add air or inert gas as the assembly is lowered to compensate for compression during descent. The whole application, however, is rather impractical with a high potential for flooding the collector. No applications of this method were found in literature.

2.8 Summary of chapter 2

Section 2.5 has given a detailed overview over some of the most predominant As species in aquatic environments, illuminating their significant differences in occurrence, mobility, stability and toxicity, as well as the potential of chemical and biologically mediated species conversions. As early as in the mid of the 19th century, focus has already been drawn to accidental releases of volatile As (section 2.5.3). Species-selective determination methods, however, have not been introduced until the early 1970s with the invention of the hydride generation technique (section 2.6.1.1). Within the last 10 years, considerable effort has been paid to scrutinizing the As biomethylation pathways in different organisms (section 2.5.2). However, comprehensive studies on the occurrence of dissolved methylated and especially volatile As species in natural aquatic environments are still rare. Quantification has seldom been achieved, and several, especially volatile compounds, like sulfur (section 2.5.2.5) or chloroarsines (section 2.5.2.6), have not been even qualitatively identified in natural systems, yet.

The problem with identifying volatile As compounds in the environment is partly attributed to a lack in standardized sampling procedures. A wide variety of tests and methods was presented (section 2.6), however most of them are not available commercially as standard equipment, but custom-made coupled methods that are specifically developed by different research groups mostly from the field of analytical chemistry. Different opinions exist about the stability of dissolved and volatile As species, and various on-site trapping methods have been proposed (section 2.7). Some of them, however, are only applicable if analysis can be guaranteed within a few hours of sampling. Few suggestions exist for sampling remote areas. A fast and efficient method for in-situ sampling of volatile As species from the aqueous phase is still lacking (section 2.7.5.2).

The present thesis therefore focused on the development of a robust technique for sampling volatile metallics in aquatic systems (section 3) as well as on investigating from a hydrogeochemical point of view geothermal features at Yellowstone National Park, as an example for an aqueous environment predestined for the release of volatile metallics (section 4).

3 DEVELOPMENT OF A FIELD METHOD

To sample volatile metallics from diffusive sources in aquatic environments two different methods were applied; field practicability was the major criterion. For a first screening on total concentrations of volatile metallics, a method was developed with an in-situ gas-water separation using a gas-collector cell with a porous PTFE (Polytetrafluorethylene) membrane (section 3.1), trapping the volatile metallics in a liquid sorbent (background section 2.7.4.1; Planer-Friedrich et al. 2002). The advantage of this screening method is its low cost, easy handling, applicability in the field, efficiency in separating gas samples from aqueous environments, long-time stability of the dissolved gas samples, and the possibility for quantitative interpretation (section 3.2.2). The disadvantage is that species information is lost due to hydrolysis and oxidation of the volatile metallics. Therefore, the suitability of sorption tubes and SPME technique (background section 2.7.4.2) followed by GC-MS analysis was investigated in the laboratory to be used in areas where significant total concentrations of volatile metallics were found during screening (section 3.2.3).

3.1 Development of an in-situ gas-collector cell

For efficient gas-water separation, a gas-collector cell was designed that can be placed inside a water body or at the sediment-water interface. It is connected to the trapping unit with liquid or solid sorbents to be described in section 3.2. The material used for the gas-collector cell is PTFE (Polytetrafluorethylene, $[-F_2C-CF_2-]_n$). It was discovered by Roy Plunkett at DuPont in 1938 and is commonly known by the DuPont brand name Teflon[®]. Besides its chemical inertness and low adhesion, it is one of the most hydrophobic materials with a surface tension of 18 dynes/cm, compared to 73 dynes/cm for water making it ideal for efficient gas-water separation.

Three different prototypes were designed and constructed in a workshop of the Technische Universität Bergakademie Freiberg (Figure 15 - Figure 17). For the first prototype (Figure 15 right, and Figure 16 right) the collector cell was drilled from teflon bars with different porosities (5 μm and 10 μm , porous PTFE from Bohlender). Two different side thicknesses, 3 mm and 6 mm, were chosen. The cells are closed by a non-porous teflon cap with a screw connection for a 2 mm teflon capillary leading collected gases from inside the gas-collector cell to the trapping unit. The cap is attached to the porous cell below by two stainless steel rings, kept together by 4 screws. A greased O-ring inside seals the connection gas-tight. The second prototype (Figure 15 left, and Figure 16 left) consists of a porous teflon tube of 10 μm porosity, 6.4 mm thickness, an outer diameter of 52.4 mm, and an inner diameter of 39.6 mm (PTFE from Reichelt Chemietechnik). On top and bottom the tube fits in small joints of non-porous teflon plates (PTFE from Reichelt Chemietechnik). The plate on top contains a screw connection for a 2 mm teflon capillary to lead the collected gases to the trapping unit. Three 6.5 cm long titanium screws keep the upper and lower lid together. Threads are drilled in the titanium plates supporting the teflon lids.

The gas-collector cells were kept small (5 and 6 cm high, 3 and 5 cm wide) to allow for an accurate depth-orientated sampling. Inserting these gas-collector cells in the aqueous medium, only gas dif-

fusion takes place through the porous teflon surfaces. Water does not penetrate due to the hydrophobic properties of teflon. Applying vacuum to the gas-collector cells increases sampling efficiency. At a vacuum exceeding -50 mbar, even though all connections were still waterproof, the bubbling point of the porous teflon was reached and water breakthrough occurred. The different designs with porosities of 5 and 10 μm , and wall thicknesses of 3 and 6 mm did not show significant differences in water breakthrough points.

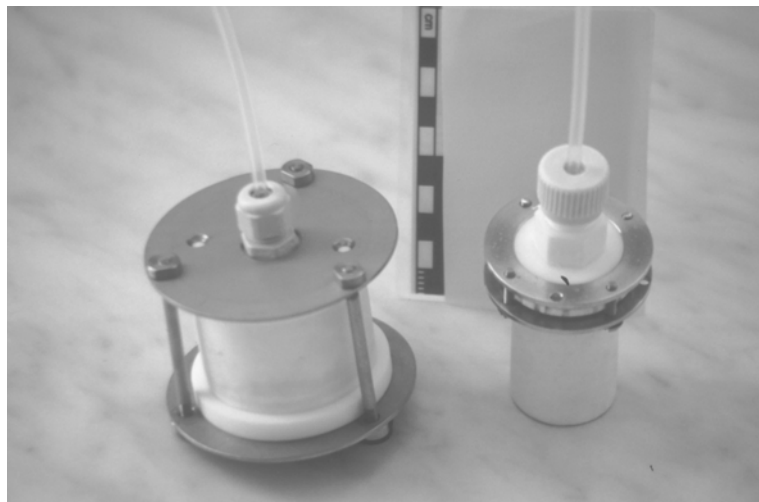


Figure 15 Gas-collector cells prototype 1 (right) and 2 (left), for collecting gases from diffusive sources in aqueous environments applying no or low (-50 mbar) vacuum; teflon capillaries lead the collected gases from inside the gas-collector cell to the trapping unit



Figure 16 Gas-collector cells prototype 1 (right) and 2 (left); material: porous PTFE with a porosity of 5 and 10 μm and a side thickness of the 3 and 6 mm

A third prototype was developed to apply higher vacuum for increased sampling efficiency (Figure 17). In contrast to the first two designs, gas transport does not take place through pores over the entire body of a hollow porous teflon tube, but through a teflon membrane (PTFE from Infiltec, porosity 0.1 μm), placed in a filter of solid teflon. The outer side is protected towards the sampling medium by a porous teflon disk (PTFE from Bohlender, porosity 10 μm , thickness 5 mm) and towards the inner side by a solid teflon disk (PTFE from Bohlender, thickness 6 mm) to withstand vacuum-induced deformation. To allow gas passage, the solid teflon disk contains numerous 1 mm holes, similar to a sieve. This gas-collector cell withstands vacuum up to -500 mbar (Infiltec even cites applications with > 2 bar pressure) without breakthrough of water. Figure 18 shows a setup of the described equipment including gas-collector cell, liquid sorbent and vacuum container. Vacuum

is applied only once and the sampling set is left out in the field until the vacuum is completely diminished. Concentrations of the volatile metallics in the gas phase [ng/m^3] can then be calculated from the mass of volatile metallics trapped in the liquid sorbent [μg] and the replaced vacuum volume [m^3]. Connecting a battery-powered pump would be an option for continuous low flow gas sampling.

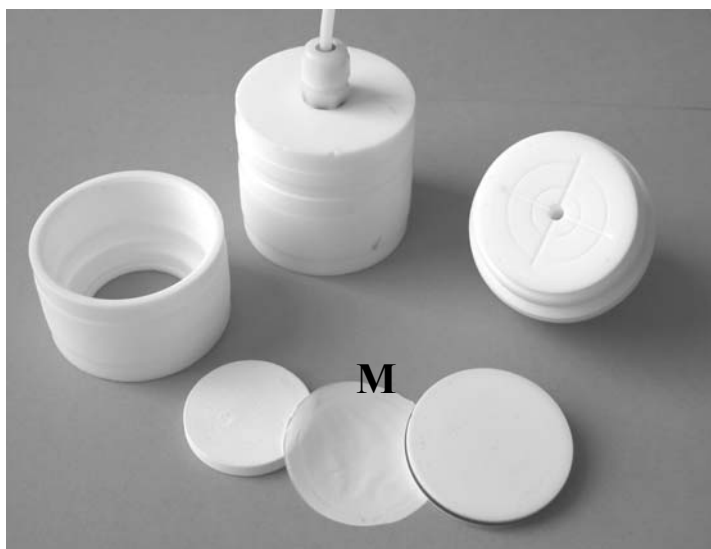


Figure 17 Gas-collector cells prototype 3 for collecting gases from diffusive sources in aqueous environments applying vacuum up to -500 mbar; material: PTFE membrane (M) with a porosity of $1 \mu\text{m}$, placed in a filter of solid PTFE, protected to the sampling media below by a porous PTFE disk (porosity $10 \mu\text{m}$, thickness 5 mm , left of the membrane) and above by a solid PTFE disk with numerous 1 mm holes for gas transport to withstand deformation because of vacuum application (to the right of the membrane)

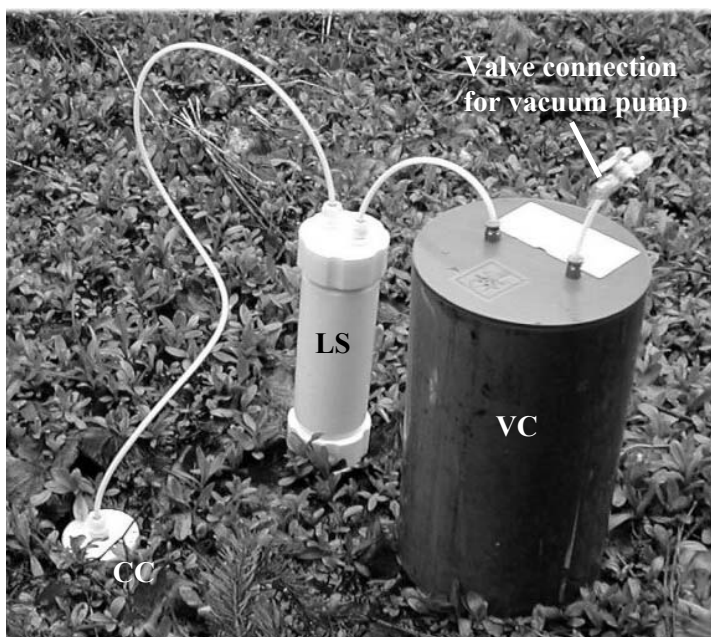


Figure 18 Field setup of the sampling and trapping equipment showing the gas-collector cell (CC) installed close to the surface of the water saturated sediment, the trapping and stabilizing unit (liquid sorbent, LS), and a vacuum container (VC)

3.2 Gas generation and trapping

Volatile metallics were produced by HG (section 2.6.1.1) in the laboratory, to test the efficiency of the trapping unit connected behind the gas-collector cell. Figure 19 shows the laboratory setup. A high-grade stainless-steel reaction vessel (250 mm high, 100 mm diameter) was constructed as an abiotic reactor symbolizing the natural aqueous environment, where volatile metallics are produced. PTFE coating of the steel proved to be necessary to avoid sorption effects and precipitation

because of pH-changes during HG. The reaction vessel is filled to about half its height with sample solution (475 mL). Chemical reagents for abiotic hydride generation are added with a syringe and a capillary connected to the bottom of the reaction vessel.

A porous ceramic disk (6 cm diameter, 0.6 cm height) was initially used on the inside bottom of the reaction vessel for finer distribution of the added chemical reagents. Cleaning the disk in 1 N HCl after 24 experiments with a total supply of 18.3 mg As, yielded a total of 0.75 mg As, equivalent to an accumulative sorption of 4%. Because hydride generation starts at a pH of about 1.2, some of the As sorbed on the ceramic disk is probably released at the beginning of each new experiment and precipitated again with increasing pH. Complete desorption during each experiment on the other hand can be excluded because the last experiment before cleaning the ceramic disk yielded 0.073 mg total As only compared to 0.75 mg detected in the cleaning solution. More likely, it is a dynamic equilibrium, where the 0.75 mg As sorbed may already present the maximum sorption capacity of the ceramic disk. However, to be on the safe side, the disc was dismissed in the following experiments and the reagents were added to the reaction vessel directly through a hole in the bottom. The gas-collector cell is placed inside the reaction vessel. Gases created in the reaction vessel pass the teflon membrane of the gas-collector cell and finally leave the vessel to the trapping unit by a teflon capillary.

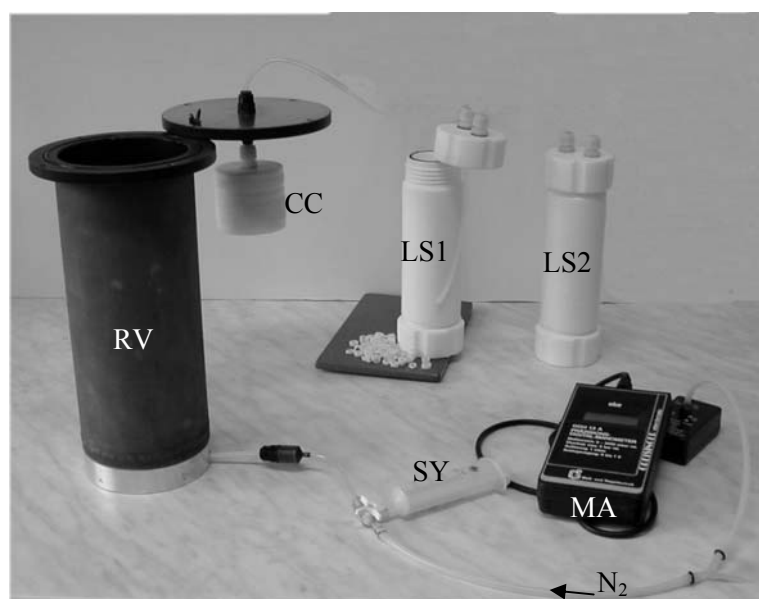


Figure 19 Laboratory setup for generation of volatile metal hydrides in a PTFE coated reaction vessel (RV), consequent sampling with the developed collector cell (CC) and transfer to the liquid sorbent (LS); syringe (SY) is used to add reducing agent and acid for hydride generation, N₂ provides reducing environment during the whole experiment, pressure is monitored by a digital manometer (MA).

3.2.1 Optimization of arsine generation

Dimethylated arsines created from dimethyl arsenic sodium salt trihydrate ($C_2H_6AsNaO_2 \cdot 3H_2O$; FLUKA p.a. $\geq 98\%$) were used to optimize the method. The optimized conditions found application for additional experiments with inorganic arsine AsH_3 (created from $As^V HNa_2O_4 \cdot 7H_2O$, FLUKA, p.a. $\geq 98\%$) and proved the method's efficiency. Trapping other volatile metal hydrides should perform in the same way. Because optimum generation of other volatile metal hydrides requires addi-

tional time-consuming adjustments, explicit confirmation of these conditions was dispensed. NaBH_4 (p.a. $\geq 96\%$, MERCK) in NaOH was used as a reducing agent.

Small-scale derivatization experiments yielded the best relative response for arsine generation from DMAA in a pH range between 0.4 and 1.5, with an optimum at pH 1.3 (Figure 20) in general accordance with other literature discussed in section 2.6.1.1. Even though HG is a standard method, common volumes are significantly less than 1 mL. For the experiments presented here, the goal was to test sampling efficiency in an aqueous environment using the developed collector cell, requiring water volumes of approximately 0.5 L in the reaction vessel. Problems were encountered with simply upscaling the amount of chemicals needed for HG. Few reports were found in literature dealing with HG from large sample volumes. Luna et al. (2000) reported no signals for Ag, Cu, Au and Zn in hydride generation when relatively large volume (> 1 mL) batch reactions were attempted. The authors presented no reasons or solutions for this drawback.

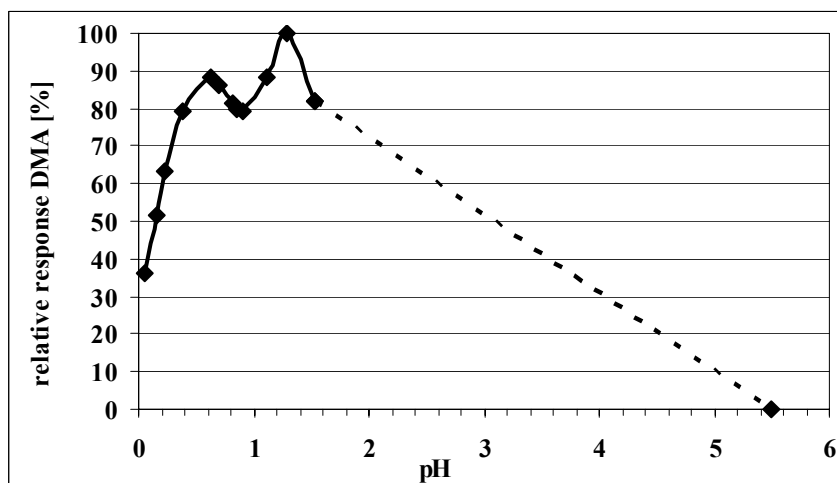


Figure 20 Experiments for DMA HG from 10 mL deionized water containing 20 $\mu\text{g/L}$ As as $\text{C}_2\text{H}_6\text{AsNaO}_2 \cdot 3\text{H}_2\text{O}$. Reduction was performed for pH of 0.05 to 5.5 by adding variable amounts (0 to 2.5 mL) of 30% HCl and 2.4 mL 3% NaBH_4 in 1% NaOH

To check the efficiency of hydride generation in the reaction vessel under various conditions, samples were taken from the original standard solution prior to the experiment (samples “C” = control) and from the solution in the reaction vessel after the experiment (samples “R” = remaining). The percentage of volatilized As was calculated according to the following equation:

$$100\% - \frac{c_R \cdot V_R}{c_C \cdot V_C} \cdot 100 = \% \text{ volatilized}$$

c = concentration

V = volume of initial solution in reaction vessel (C), and solution after reaction in reaction vessel (R)

All samples were analyzed for total As by GF-AAS (graphite furnace AAS EA4, Zeiss, Germany) using platform technique and the conditions given in Table 6, section 3.2.2.

Using FI-HG, a constant purging gas stream transfers the created volatile compounds directly to the detection unit. The PTFE membrane of the collector cell slows down the gaseous flow, leading to longer residence times of volatile compounds in the reaction vessel. Because the reducing agent NaBH_4 is prepared in NaOH for stability reasons, the pH increases significantly during the creation of the volatile compounds. Not all As is completely reduced to dimethylarsine and degassed from

solution. The remainder is re-transformed to dissolved $\text{Na}(\text{CH}_3)_2\text{As}^{\text{V}}\text{OO}$ once the solution is alkaline again.

During the first experiments (Appendix 2: experiments No.1-23), a vacuum pump was used for gas flow control. Because HG increases the pressure inside the reaction vessel, the injection times for the reducing agent and the experiment's total time were adjusted to keep the differential pressure at about 60 mbar, resulting in extremely variable HG rates. The shorter the total reaction times, the lower was the percentage of As volatilized. The experiments 2, 4, and 8 (Appendix 2) yielded volatilization rates of 45, 41, and 63% only with total reaction times of 320, 185, and 435 min, respectively, compared to volatilization rates of 70-76% for total reaction times > 500 min (Appendix 2: 1, 3, 5-7, 9). Increasing NaBH_4 concentrations, and decreasing HCl concentrations (Appendix 2: 10-23) increased average volatilization rates to 72-89%; the highest NaBH_4 concentrations yielded 95-96% As volatilization (Appendix 2: 11, 12), the lowest HCl concentration 98% (Appendix 2: 18).

Because oxidation of the generated arsines was thought to be the major cause for low volatilization rates, a continuous N_2 flow was applied to maintain reducing conditions during the further experiments (Appendix 2: 24-105). After initial experiments with N_2 pressures of 800 to 200 mbar, N_2 pressure was adjusted as low as possible (approximately 30 mbar differential pressure) to keep the pressure inside the reaction vessel below the gas transfer rate limited by the permeability of the PTFE membrane. The N_2 flow was interrupted only during the few seconds of reactant injection.

Finally, a two-step strategy of reduction, re-acidification and second reduction proved to yield complete and reproducible volatilization (Figure 21; Appendix 2: 29, 41-105). The primarily acidified DMAA standard solution with a pH of approximately 1.2 in the reaction vessel was first purged with N_2 for 10 minutes to create reducing conditions. Flow from the bottom to the top allowed for complete oxygen removal. The reducing agent NaBH_4 was used in a concentration of 15% in 5% NaOH. As Shraim et al. (1999) already detected, concentrations >1% NaBH_4 result in turbid solutions. The non-dissolved particles settle down and the solution becomes clear with time. However, when mixed with acid solution during HG, the particles re-dissolve producing a non-homogeneous reaction mixture with localized cells of NaBH_4 concentrations. To reduce this instability, the solution was filtered before usage.

The reducing agent was added discontinuously over 20 minutes in steps of approximately 2 mL every 2 minutes. This stepwise addition of small amounts of reducing agent was chosen because an intense arsine generation at the beginning significantly increased the pressure in the vessel due to the limiting permeability of the PTFE membrane, partly leading to backflow through the bottom capillary. The reaction vessel was purged with N_2 for another 5 minutes after the first reduction step; pH was at about 12. The solution was acidified again (pH 1 to 2) by adding 40 mL of 1 N HCl over 20 minutes. All As, not yet degassed and re-dissolved in solution, was transferred again to $(\text{CH}_3)_2\text{AsO}(\text{OH})$ and reduced in a second step with 20 mL 15% NaBH_4 in 5% NaOH inserted over

15 minutes. A final N₂ flow for 20 minutes ensured that all volatile compounds were volatilized from the reaction vessel via the PTFE membrane. The whole experiment took 90 minutes.

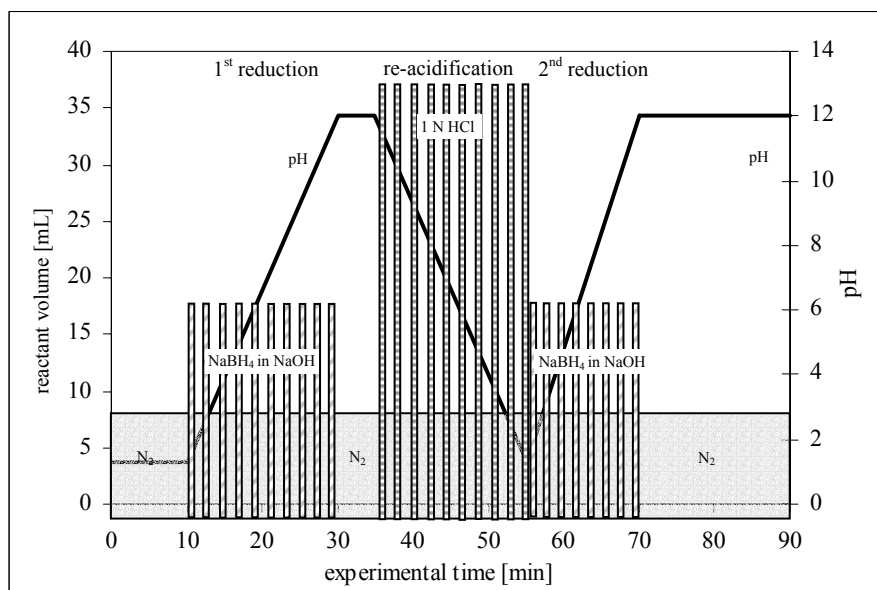


Figure 21 Two-step strategy of reduction, re-acidification and second reduction for complete and reproducible HG of volatile arsines from 475 mL of a dimethyl arsenic sodium salt trihydrate solution at a continuous N₂ flow of 30 mbar; single bars indicate stepwise injection of reactants (HCl, NaBH₄)

With the described two-step approach of two times acidification and reduction, As concentrations after reaction were close to or below the detection limit of 1.5 µg As/L. Volatilization rates generally were >95%. Further experiments to decrease the amount of chemical reagents (Appendix 2 E 31-33) or shorten the reaction time (Appendix 2 E 34-37) led to incomplete transfer from the aqueous to the gaseous phase (85-90% volatilization). Not acidifying the solution initially (Appendix 2 E 84) yielded volatilization rates as low as 41%. No difference was found in volatilization efficiency between the collector cell prototypes 1 and 2 with gas flow through porous (5 and 10 µm) Teflon bodies (Appendix 2 E 48-51) and prototype 3 with gas flow through the Teflon membrane (porosity 0.1 µm).

3.2.2 Optimization of screening on total concentrations (liquid sorbents)

Four different reaction vessels, and three different oxidizing agents were tested for their suitability of trapping total volatile As. The amounts of liquid sorbent were kept small to achieve an optimum enrichment of the naturally low concentrations of volatile metallics. The reaction vessels were columns of small diameter and at least 12 cm height to guarantee sufficient reaction time while the gas is bubbling through the oxidizing solution. Small glass and teflon bodies, so-called Raschig rings, were used to further increase reaction surface and reaction time.

Trapping efficiency in liquid sorbent is calculated according to the following equation:

$$\frac{c_O \cdot V_O}{c_C \cdot V_C - c_R \cdot V_R} \cdot 100 = \% \text{ trapped of the volatilized fraction}$$

c = concentration

V = volume of initial solution in reaction vessel (C), and solution after reaction in reaction vessel (R), and oxidation solution (O)

Laboratory experiments began with a commercial glass wash bottle (250 mL volume, 14 cm height) as oxidizing trap. However, the lid did not prove to be completely gas-tight under the high pressure created during hydride generation. Volatile As was observed by garlic-like odor. The oxidizing agent, hydrogen peroxide (H_2O_2 , perhydrole p.a. 30% MERCK), was not suitable for rapid oxidation, yielding trapping rates of 3-17% only (Appendix 3 E 1-23). No significant improvement was found for different H_2O_2 strengths (5% to 30% in the final solution) or making basic the oxidizing solution with 0.1 and 1 N NaOH. The low trapping efficiency was even worse than that reported by Wongsanoon et al. (1997) who deducted trapping efficiency for volatile metallics in 30% H_2O_2 from tests with hydrogen sulfide to be about 50%.

Using a stainless steel cylinder (40 cm high, 4.5 cm diameter) as an alternative oxidizing trap, instead of the glass wash bottle, H_2O_2 showed slightly higher trapping rates of 10, and 22% (Appendix 3: 24, 25). A 1.5 M sodiumperoxodisulfate ($\text{Na}_2\text{S}_2\text{O}_8$, p.a. $\geq 99\%$ FLUKA) solution as oxidizing agent (Appendix 3: 26) caused problems due to high matrix effects during the following analysis by GF-AAS. Further experiments with $\text{Na}_2\text{S}_2\text{O}_8$ were dismissed. Sodium hypochlorite (NaOCl , 6-14% Cl active, Riedel-de-Haen) turned out to be effective for rapid and complete oxidation. However, a special temperature-time-program had to be developed to analyze the complex matrix of the NaOCl -samples by GF-AAS (Table 6).

Table 6 AAS conditions for analyzing the original standard solution before the experiment (samples "C" = control), the solution in the reaction vessel (samples "R" = remaining) and the oxidizing solution (samples "O")

STEP	TEMP [°C]	RAMP [°C/s]	HOLD [s]	TIME [s]	RUN
Drying	120	10	0	10.1	
Drying	150	3	30	40.0	
Dry ashing	1350 C	135 C	30 C	38.9 C	
	1400 R	140 R	40 R	48.9 R	
	1500 O	150 O	60 O	69.0 O	
Atomization	2400	FP (full power)	4	4.7	C 0.2 R 0.2 O
Cleaning	2600	1000	3	3.2	

Note: 15 μL sample solution + 8 μL modifier ($\text{Pd}(\text{NO}_3)_2$; MERCK $c(\text{Pd}) = 10 \text{ g/L Pd}(\text{NO}_3)_2$ in ca. 15% HNO_3 ; dilution 1:10); wave length 193.7 nm, gap width 60 mm, standards for C-samples (initial solution before HG) in 0.1N HCl matrix, standards for R-samples (solution after HG) in 8 mL 1 N HCl and 19 mL 1 N NaOH matrix to 50 mL, standards for O-samples (oxidizing solution) in 11.1mL NaOCl and 11.1 mL HCl matrix to 50 mL

Non-specific sorption peaks appeared during analysis because of the high salt concentrations in these samples. The method development aimed at a complete separation of those peaks from the As signal by varying dry ashing conditions. High dry ashing temperatures and a total duration of about 70 s were used for this step. To avoid As losses during this thermal treatment an increased modifier concentration, 8 μL of a 1 g Pd/L stock solution ($\text{Pd}(\text{NO}_3)_2$), was added to 15 μL sample solution. Experiments with NH_4NO_3 to improve the separation of non-specific and specific signals showed no success. Furthermore 1 mL 1N HCl and 2.5 mL H_2O were added to 1 mL of oxidizing sample ("O"-sample) due to problems with the high alkalinity and the applied high As concentrations.

Overall trapping efficiencies for NaOCl were between 53% and 86% in the stainless steel cylinder (Appendix 3 E 27-36, 38). Acidifying pure NaOCl from pH 11.8 to pH 4.0 (1:1 NaOCl : 1N HCl; Appendix 3: 37) brought trapping efficiency down to 1%, probably due to degassing of reactive Cl during acidification of the oxidizing agent (strong Cl odor). Strongly alkaline oxidizing solutions (pH 12.3, 1:1 NaOCl : 1N NaOH; Appendix 3: 39) also yielded a lower than average trapping efficiency with 57%. The 90 min two-step approach optimized for arsine generation also proved the best results for trapping (79, 86%; Appendix 3: 38, 29), whereas single-step reduction yielded always lower trapping rates (53-67%; Appendix 3: 27, 28, 30, 31). This result suggests that during the initial reduction and arsine generation combined with high pressure and rapid gas flow, the oxidation capacity of the trapping solution was exceeded. Stepwise injection and longer reaction times gradually transferred the arsines, leading to a better sampling capacity. This problem is mainly a laboratory artifact. During gradual biotic generation of volatile metallics in nature, sorption capacities will not be exceeded in that way.

Glass beads in the NaOCl solution increased sampling efficiency from 53% (Appendix 3: 30) to 58% (Appendix 3: 28), and from 75% (Appendix 3: 32) to 86% (Appendix 3: 29). However, glass beads showed about 2% accumulative As sorption (12 μg from about 530 μg total As from 14 experiments). A control experiment with an As-free solution yielded 28 $\mu\text{g/L}$ As in the stainless steel cylinder oxidizing trap filled with glass beads (Appendix 3: 40). This blank value proved desorption both from the stainless steel cylinder and the glass beads.

Therefore, a commercial teflon wash bottle (250 mL, height 13.5 cm, teflon = perfluoroalkoxy PFA from BOLA) replaced the stainless steel cylinder, and PTFE rings replaced the glass beads. The PFA bottle did not show sorption effects but the relatively soft material was not really suitable for field application nor for withstanding the built-up of high pressures during hydride generation in the laboratory. Volatile As losses at connections and threads were detected by garlic-like odor. Trapping rates were less than with the stainless steel cylinder (23-62%; Appendix 3: 41, 43-55). PTFE rings used instead of the glass beads showed an interesting phenomenon. The teflon rings were cut from teflon tubes with 6 mm or 2 mm inner diameter and 8 mm or 4 mm outer diameter (T6x8, respectively T2x4) and about 2-3 mm thickness. Using only T6x8 significantly increased trapping efficiency (77%; Appendix 3: 42) compared to experiments without Raschig rings (42, 45%; Appendix 3: 45, 41). When T2x4 were used, however, trapping efficiencies were low (Appendix 3: 43, 44, 46-55). This result could indicate that inside the smaller teflon rings isolated gas bubbles form which can not interact with the oxidizing medium and also reduce further gas transport through the rings, thus decreasing reaction time inside the oxidizing solution. For the T6x8 rings the inner cavities are large enough to allow unimpeded gas flow. For all subsequent experiments, rings with an inner diameter of 4 mm (T4x6) were found to be a good compromise between optimum surface reaction and unimpeded gas flow.

As final oxidizing vessels, sturdy and inert PTFE bottles (20 cm high, 4 cm diameter) were designed and constructed in a workshop at the Technische Universität Bergakademie Freiberg. With a

teflon capillary, collected gases are conducted through the top lid directly inside to the bottom of the bottle without any further connections, thus excluding losses.

Different dilutions of the NaOCl solution were tested from undiluted to 1:500 NaOCl : deionized H₂O, and a pure deionized water control solution (Figure 22). Dilution ratios of 1 : 100 (0.06-0.14% active Cl) proved sufficient to obtain overall recovery rates of $84\% \pm 6.6$ ($86\% \pm 7.8$ for HG from DMA only (Appendix 3: 64, 71, 77-83), and $82\% \pm 2.9$ for HG from As(V) only (Appendix 3: 82 a-f). This result was confirmed for a concentration range from 6-150 $\mu\text{g As/L}$ in solution before HG (Figure 23).

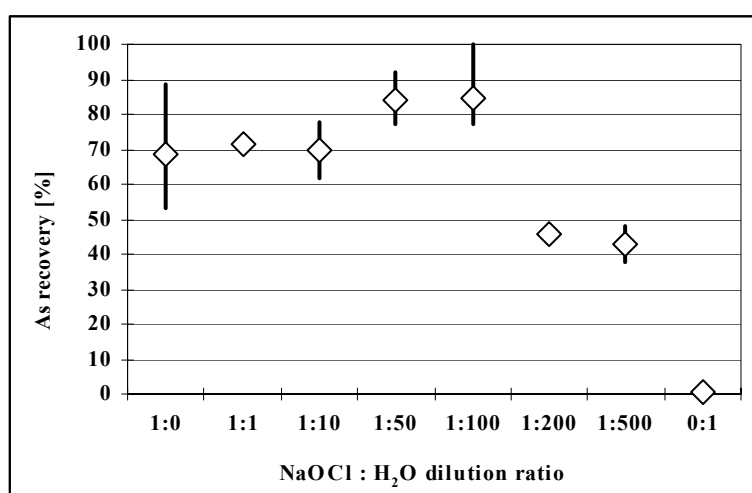


Figure 22 As recovery after volatilization from DMAA and As(V) solutions and trapping in NaOCl in different dilution ratios from 1:0 (pure NaOCl) to 0:1 (deionized water, control) (bars indicate minimum and maximum values, diamonds indicate mean values)

Dilution 1:0	68 % \pm 12.2	(Appendix 3: 56, 58, 59, 60, 61, 65, 68)
Dilution 1:1	71 %	(Appendix 3: 69)
Dilution 1:10	70 % \pm 8.2	(Appendix 3: 62, 70)
Dilution 1:50	84 % \pm 5.5	(Appendix 3: 63, 66, 74, 76)
Dilution 1:100	84 % \pm 6.6	(Appendix 3: 64, 71, 77-83, 82a-f)
Dilution 1:200	45 %	(Appendix 3: 73)
Dilution 1:500	43 % \pm 5.1	(Appendix 3: 74, 75)
Dilution 0:1	<1%	(Appendix 3: 67)

Concentrations in a second oxidizing solution (LS 2; Figure 19), mounted behind the first one (LS 1), were close to or below detection limit. Lower recovery rates for the more concentrated oxidizing solutions (1:0, 1:1, 1:10), as opposed to the 1:100 solutions, are probably not related to insufficient trapping but to problems with GF-AAS analysis because of high matrix effects. Dilutions of 1:200 and 1:500 led to incomplete trapping, the second oxidizing solution (pure NaOCl) mounted behind the first one showed higher As concentrations (up to 25%). A blind test with deionized water as LS1 showed As concentrations of less than 1% in LS1 and 86% in LS2 (pure NaOCl) (Appendix 3: 67).

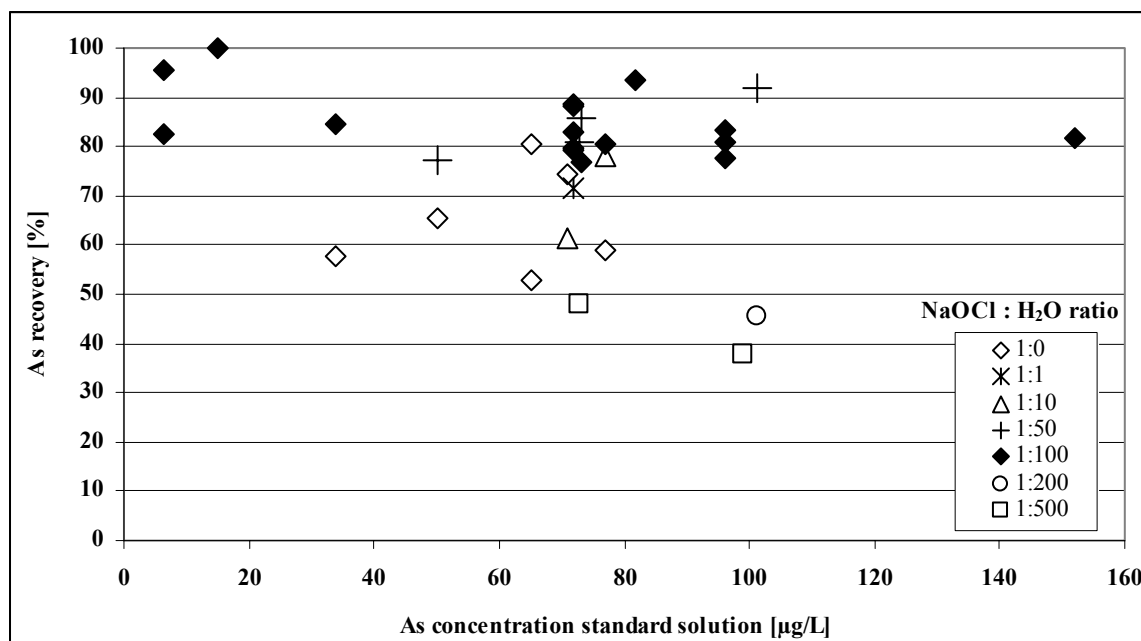


Figure 23 Volatile As recoveries from solutions of different DMAA and As(V) concentrations; symbols indicate varying dilutions of the NaOCl oxidizing solution (Appendix 3: 56, 58-66, 68-83, 82a-f)

The long-term stability of the 1:100 diluted solutions is shown in Table 7. Maximum losses during 6 weeks storage in a refrigerator were 12% in glass bottles and 13% in PE bottles compared to results obtained 1-2 days after the experiment. Mean losses were 5% in glass, and 8% in PE bottles. Even though the losses in glass bottles were slightly lower than in PE bottles, PE bottles are recommended for further analysis in order to avoid sorption effects of other metallics on the glass walls, due to the high pH (pH = 11.1 - 11.3).

Table 7 Long-term stability of the 1:100 diluted solution comparing the analysis 1-2 days after the experiment to the analysis after 6 weeks of storage in a refrigerator; mean losses were 5% in glass and 8% in PE bottles

As concentrations [µg/L]				As losses after 6 weeks [%]	
in glass bottles 1-2 days after the experiment	in PE bottles 1-2 days after the experiment	in glass bottles 6 weeks after experiment	in PE bottles 6 weeks after experiment	in glass bottles	in PE bottles
284	278	251	255	12	8
136	132	135	129	0	2
373	373	382	394	-3	-6
22	21	20	19	8	10
70	72	69	63	1	13

3.2.3 Species-selective sampling (solid sorbents)

The gas-collecting procedure for species-selective determinations is the same as described in section 3.1. The laboratory setup shown in Figure 19 with the optimized HG conditions discussed in section 3.2.1 was applied. The liquid sorbent traps (LS1, LS2 in Figure 19) are replaced by solid sorbents (sorption tubes, SPME fibers) as described in section 2.7.4.2. In some experiments, a liquid sorbent was mounted behind the solid sorbent to estimate the amount of volatile As breakthrough.

3.2.3.1 Sorption tubes

Sorption tubes were custom made from about 9 cm long glass tubes. The tubes' outer diameter was set to 8 mm by the dimensions of the desorption port of the GC-MS used (Bruker mobile GC-MS EM 640). The inner diameter was 5 mm. Before packing the desorption tubes, they were acid cleaned, rinsed with deionized water and heated at 100°C overnight. About 26 mg of silanized glass wool (Glass Wool Silane Treated; Supelco) were inserted as a plug in the lower end of the tube that was tapered before. Five different types of sorption material were used: Tenax TA (60/80 and 80/100 mesh; SKC), Chromosorb 105 and Chromosorb 106 (60/80 mesh; Varian), Carbotrap (ORBO 100, 20/40 mesh; Sigma-Aldrich), Carbosieve S III (60/80 mesh; Scientific Instrument Services), and Carboxen 564 (ORBO 92, 20/45 mesh; Sigma-Aldrich) (Table 4). A total amount of 150 to 250 mg sorption material resulted in packing heights between 1.5 cm and 3.5 cm. Larger bed sizes were avoided because they will trap more water and contribute more background noise to the chromatogram.

Single-bed resins (Appendix 4 No.17-20), double-bed resins (Appendix 4 No.1-9, 14-16) and triple-bed resins (Appendix 4 No.10-13) were designed. Multi-bed resins have the advantage that they can trap a wide variety of volatile compounds. They are packed so that the material that sorbs the smallest and most volatile analytes, forms the top layer of the multi-bed resin. Larger molecules are trapped on the bottom and do not block or irreversibly sorb on the finer sorption material. The direction of gas flow during desorption is reverse to that of sorption during sampling, guaranteeing that larger, less volatile molecules never pass through the finer material on top of the resin. Different packing materials in multi-bed resins were separated by 13 mg silanized glass wool. About 15 mg silanized glass wool were used as plug for the upper end of the resin together with a steel spring to keep the sorption material in place. Two tubes were filled with silanized glass wool only to test blind values in the absence of sorption material (Appendix 4 No. 28, 29).

The upper end of the glass tube was tapered after packing and the desorption tubes were conditioned at 50°C over their final operating temperature for 4 hours in a continuous N₂ flow (N₂ 6.0 = N₂ >99.9999 Vol%). So as not to load the chromatographic column with contaminants from this cleaning step, a desorption apparatus with continuous gas flow was designed and constructed by a workshop at the Technische Universität Bergakademie Freiberg (Figure 24). One GC run after the

conditioning step confirmed low blank levels. Besides the homemade sorption tubes, some commercial ones from SKC were selected (Appendix 4 No.21-27, 30-32) and conditioned the same way.

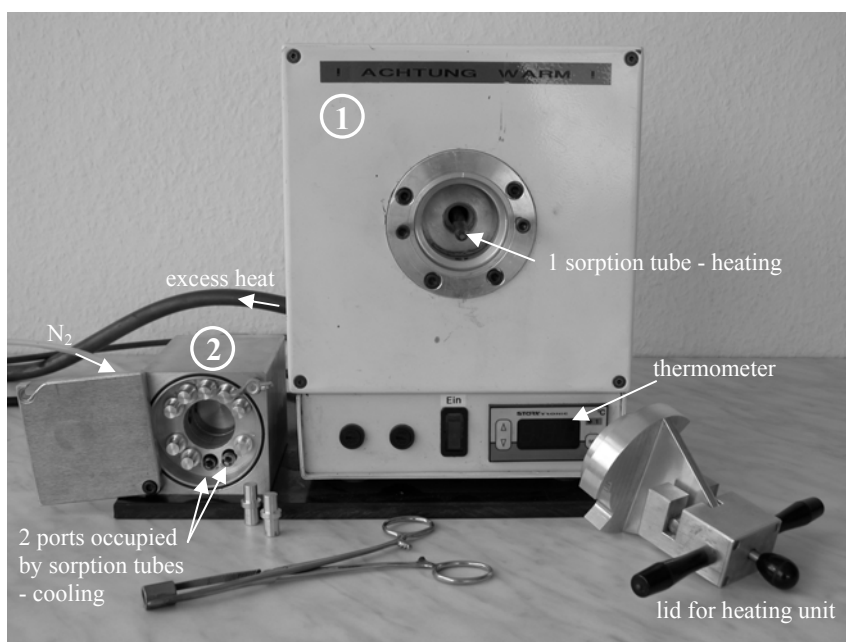


Figure 24 Desorption apparatus for conditioning and cleaning sorption tubes; continuous gas flow (N_2) can be applied both to the heating unit (1) that provides space for desorbing 1 sorption tube, and the cooling unit (2) with space for 10 sorption tubes to be cooled down under oxygen exclusion after heat desorption

Three different columns were used in the Bruker mobile GC-MS EM 640:

- DB-624 (6% cyanopropylphenyl-94% dimethylpolysiloxane) with a medium polarity, commonly used for volatile organics, column length (L) = 30 m, inner diameter (ID) = 0.25 mm, film thickness (fd) = 1.4 μm
- DB-5 (5% phenyl-95% dimethylpolysiloxane) non-polar, L = 12 m, ID = 0.32 mm, fd = 1 μm
- MDN-12 (exact composition patented, no information) low polarity, L = 30 m, ID = 0.25 mm, fd = 0.25 μm

With the DB-624 column no volatile arsine compounds could be detected in the chromatograms using sorption tubes with Tenax, Carbosieve, Carboxen, and Carbotrap beds (Appendix 5: 85-105). Oxidizing traps were mounted behind the sorption tubes to determine the breakthrough of arsine through the sorption tubes. A significant As breakthrough was found for the commercial Tenax TA tubes, single-bed resins of Carbosieve, and Carbotrap, as well as for the Tenax-Carbotrap double-bed resin. From the original As in solution 84% (Appendix 6: 85), 41% and 36% (Appendix 6: 92, 100), 53% (Appendix 6: 93), and 82% (Appendix 6: 89) passed the sorption tube and were trapped in the oxidizing solution. Increasing the total sorption surface by mounting two Tenax TA resins behind each other did not improve sorption capacities. Arsenic recovery rates in the oxidizing solution behind the sorption tube remained high with 82, and 92% respectively (Appendix 6: 104, 105). For all the other experiments with double and triple-bed resins no As breakthrough was detected in the oxidizing solutions. To test the response without sorption material, two tubes were filled with silanized glass wool only. The results yielded 88% As recovery in the oxidizing solution behind the sorption tubes (Appendix 6: 103). After the experiment, the sorption tubes were destroyed and the

glass wool was eluted with 1 N HCl. Arsenic concentrations below detection limits proved that the silanized glass wool was inert and no arsine was trapped on it.

Both the non-polar MDN-12 and the DB-5 columns proved to be suitable for arsine separation. The optimized GC-MS conditions are shown in Table 8. Desorption of the sorption tubes had to be conducted at 300°C. A temperature of 250°C was sufficient for desorption of arsines from the SPME fibers (Table 9) but insufficient for arsine desorption from sorption tubes (Appendix 5: 129).

Table 8 Optimized GC-MS conditions for analysis of volatile As on sorption tubes (Bruker mobile GC-MS EM 640)

Column	DB 5
Polarity	non-polar
Length	12 m
Diameter	0.32 mm
Film thickness	1 µm
Desorption temperature	300°C
Desorption time	3 min
Injection	20s
Split	split valve 1 turn
Gas flow over the column	ca. 1 mL/min
Temperature-time-program	40/3/10, 300/10
Total time	39 min
Purge	39 min
Carrier Gas	N ₂ 6.0
Carrier gas pressure	0.15 bar
MZ	70-180
Scan rate	8.2 ms/u
Scav. Time	0 min
Acq. Start	0 min

As mentioned in section 2.6.1.1, HG does not always yield the volatile equivalent of the aqueous species (e.g., DMA from DMAA) only. In the experiments presented in this section and in section 3.2.3.2, five different arsine species were detected after HG from the acidified solution of dimethyl arsenic sodium salt trihydrate: MMA, DMA, TMA, methylchloroarsine (CH₃)AsCl₂ and dimethylchloroarsine (CH₃)₂AsCl (mass spectra in Appendix 8-3, Appendix 8-5, Appendix 8-6, Appendix 8-9, Appendix 8-10). The only sorption material that was found suitable for sufficient sorption and desorption of arsines was the molecular carbon sieve Carboxen 564 (Appendix 5: 0A-0E, 129, 131, 136). The major As species detected was TMA. Dimethylchloroarsine was found in traces only in two samples (Appendix 5: 0A, 129). In contrast to SPME fibers (section 3.2.3.2), neither DMA nor MMA or (CH₃)AsCl₂ were detected on sorption tubes. Compared to Carboxen 564, the second molecular carbon sieve Carbosieve S III (Appendix 5: 134) yielded significantly lower TMA peak areas (2-3 orders of magnitude), and the porous polymer Chromosorb 106 only half of that of Carbosieve SIII (Appendix 5: 132). The porous polymer materials Tenax TA (Appendix 5: 52, 53, 130), Chromosorb 105 (Appendix 5: 133), and the graphitized carbon black Carbotrap (Appendix 5: 135) showed no sorption / desorption at all.

Initially, sorption tubes were thought to be both cheaper and more practical in the field compared to the sensitive SPME fibers that tend to break easily. The fact that only TMA could be trapped on the Carboxen sorption tubes compared to DMA, TMA, and (CH₃)₂AsCl on Carboxen coated SPME

fibers (section 3.2.3.2), might indicate the higher sensitivity of SPME fibers. However, because the exact composition of the Carboxen coating on SPME fibers is patented, no information could be obtained about it. Carboxen 564 that was used for the sorption tubes in this study might not be the best choice. Carboxen 1000 with a surface area of 1200 m²/g, advertised to trap very volatile gases even without cryotrapping, Carboxen 1001 with a surface area of 500 m²/g for C1 and C2 hydrocarbons, or alternatively Carboxen 1003 with a surface area of 1000 m²/g might yield better sorption and desorption characteristics. Further improvement of the method during this study was not pursued because for the field application in USA no GC-MS with a desorption port for sorption tubes was available, and the SPME technique was chosen for field applications.

3.2.3.2 Solid-phase micro-extraction (SPME)

Three different types of SPME fibers were purchased from Supelco: PDMS 100, PDMS/CAR, PDMS/CAR/DVB (Table 5). Conditioning was done according to the manufacturer's instructions listed in Table 5. Headspace SPME technique (section 2.7.4.2) was used and the fibers were exposed 15-20 minutes with the Supelco SPME holder for manual use (Figure 25). Total volumes to headspace volumes were 300 mL to 100 mL and 26 mL to 16 mL respectively (Appendix 7). The optimized GC-MS program is shown in Table 9.

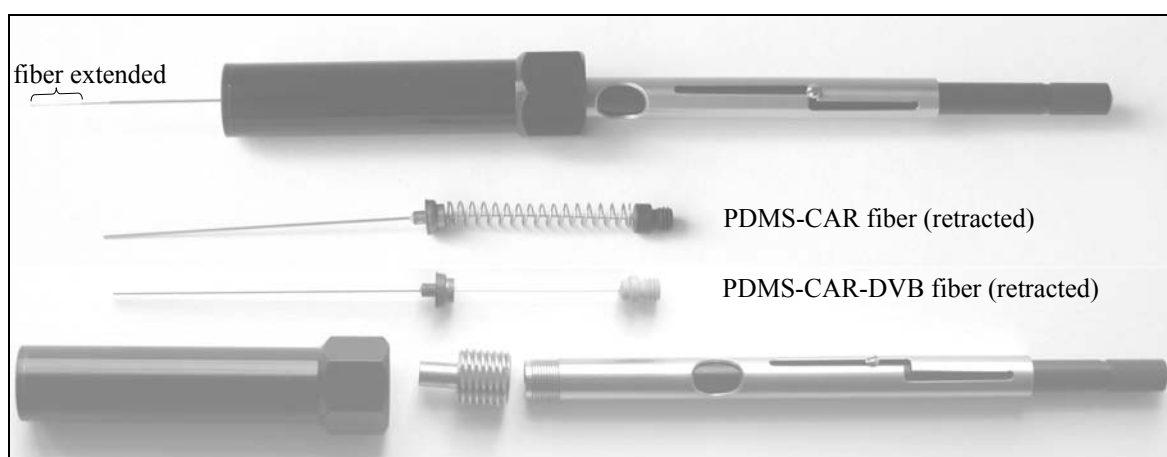


Figure 25 Supelco SPME holder for manual use (top with fiber extended); PDMS-CAR fiber with spring for manual sampling, PDMS-CAR-DVB without spring for automatic sampling

The five arsine species MMA, DMA, TMA, (CH₃)AsCl₂, and (CH₃)₂AsCl generated from the dimethyl arsenate solution showed a very different sorption behavior on the three fiber types (Figure 26). The pure PDMS fiber provided a very good separation of (CH₃)AsCl₂ and (CH₃)₂AsCl (Appendix 7: 116). The arsine compounds with a lower molecular weight (MMA, DMA, TMA), however, were not sorbed at all. The separation of DMA, TMA, and (CH₃)₂AsCl was possible by PDMS-CAR fibers (Appendix 7: 114, 117). The peak areas of (CH₃)₂AsCl were hereby about 2 orders of magnitude larger than those by sorption from PDMS. However, a plateau in the chromatogram from 1.5 to 6.5 minutes masked the DMA and TMA peaks partly and a possible methyl-dichloroarsine (CH₃)AsCl₂ peak completely. Very small amounts of MMA were detected on PDMS-CAR-DVB fibers only, together with DMA and TMA (Appendix 7: 115, 118). DMA and TMA

showed a much better separation on PDMS-CAR-DVB compared to PDMS-CAR. No chloroarsines were sorbed on PDMS-CAR-DVB.

Table 9 Optimized GC-MS conditions for analysis of volatile As on SPME fibers (Bruker mobile GC-MS EM 640; in brackets conditions for GC-MS HP 5890 Series II from the Department of Analytical Chemistry Technische Universität Bergakademie Freiberg; the HP 5 ms column is a low bleed column)

Column	DB 5 (HP 5 ms)
Polarity	non-polar
Length	12 m (30 m)
Diameter	0.32 mm (0.25 mm)
Film thickness	1 μm (0.25 μm)
Desorption temperature	250°C
Injection	20s
Split	splitless 3 min, then 1:20
Gas flow over the column	ca. 1 mL/min
Temperature-time-program	40/3/10, 250/10
Total time	34 min
Purge	34 min
Carrier Gas	N ₂ 6.0 (He 5.0)
Carrier gas pressure	0.15 bar
MZ	70-180 (70-250)
Scan rate	8.2 ms/u (2.1 / s)
Scav. Time	0 min
Acq. Start	0 min

The detection limits of the mobile GC-MS EM 640 proved insufficient for the detection of arsine species on PDMS 100 and PDMS-CAR-DVB fibers (Appendix 7: 119, 128). On PDMS-CAR, the predominant arsine species (CH₃)₂AsCl could always be detected (Appendix 7: 120-127). Also for TMA a slight peak was observed, however, mostly the separation from the baseline was too insignificant to allow for a peak area calculation. Only when a brand-new PDMS-CAR fiber was used, a clear TMA peak was detected, and the (CH₃)₂AsCl peak was about 2.5 times larger than for the PDMS-CAR fiber already used before (Appendix 7: 127a; Figure 27).

This new fiber also showed much larger peaks at the end of the chromatogram than the old fiber. Those additional peaks probably are hexamethylcyclotrisiloxane [amu 96-133-(207)], octamethylcyclotetrasiloxane [amu 73-133-(191-207-281)], and decamethylcyclopentasiloxane [amu 73-(267-355)]. Because of the selected mass range from 70-180 some of the mass fragments of these compounds were not scanned (numbers in brackets), but the remaining masses and a significant correlation between their boiling points and retention times make the identification highly likely. Those siloxanes are a typical indication for bleeding of the sorption material, probably a slow degradation of the fiber coating. A decrease in these compounds shows an increase in degradation, and obviously a decrease in sorption efficiency for arsines. This effect of larger arsine and siloxane peaks was already less pronounced for the second run with the new fiber, compared to the fiber already used about 15 times (Appendix 7: 127b).

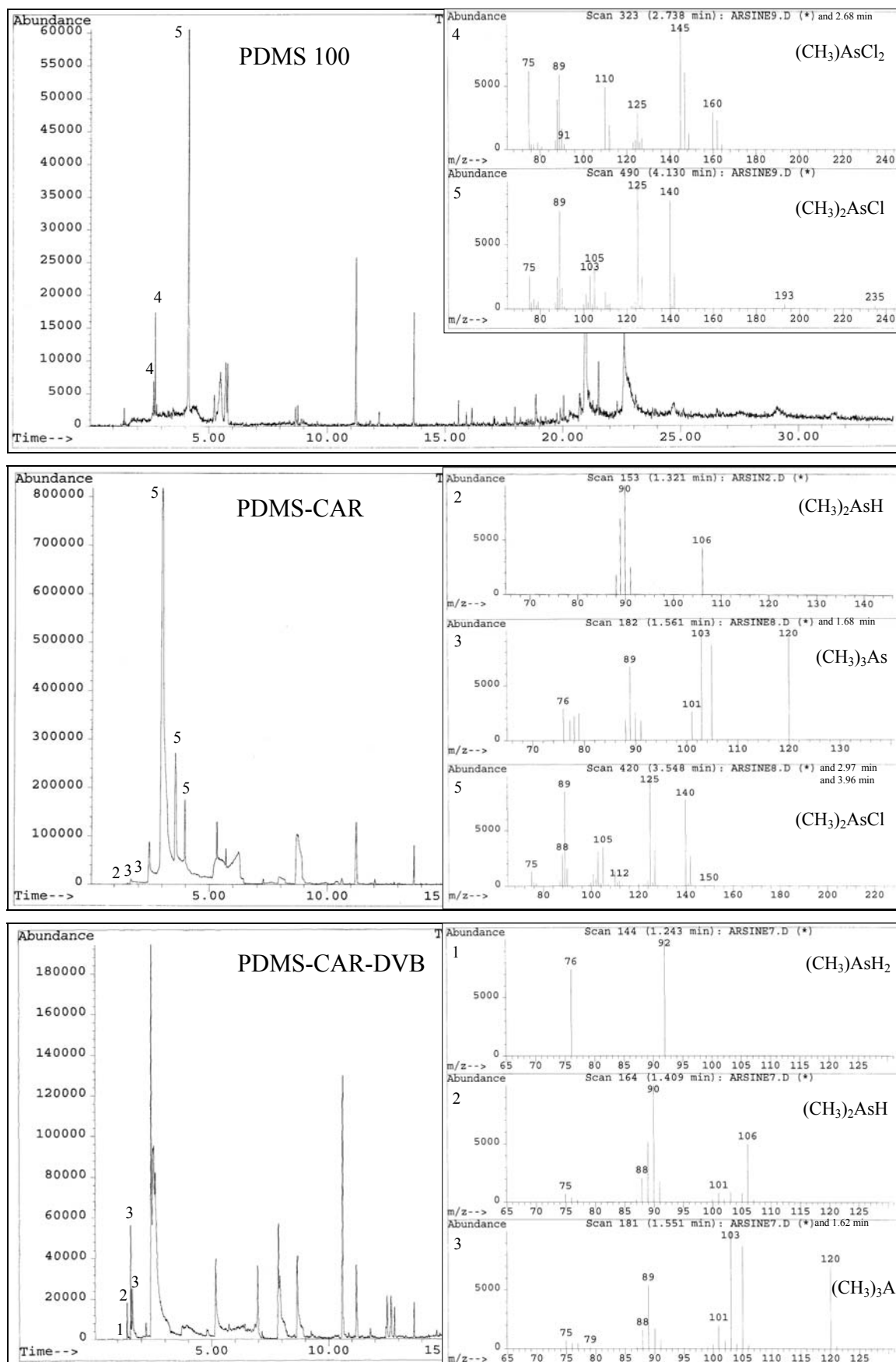


Figure 26 As species sorbed on different SPME fibers (experimental conditions and peak areas in Appendix 7: 116-118, analysis with GC-MS HP 5890 Series II; conditions in Table 9; mass spectra also in Appendix 8)

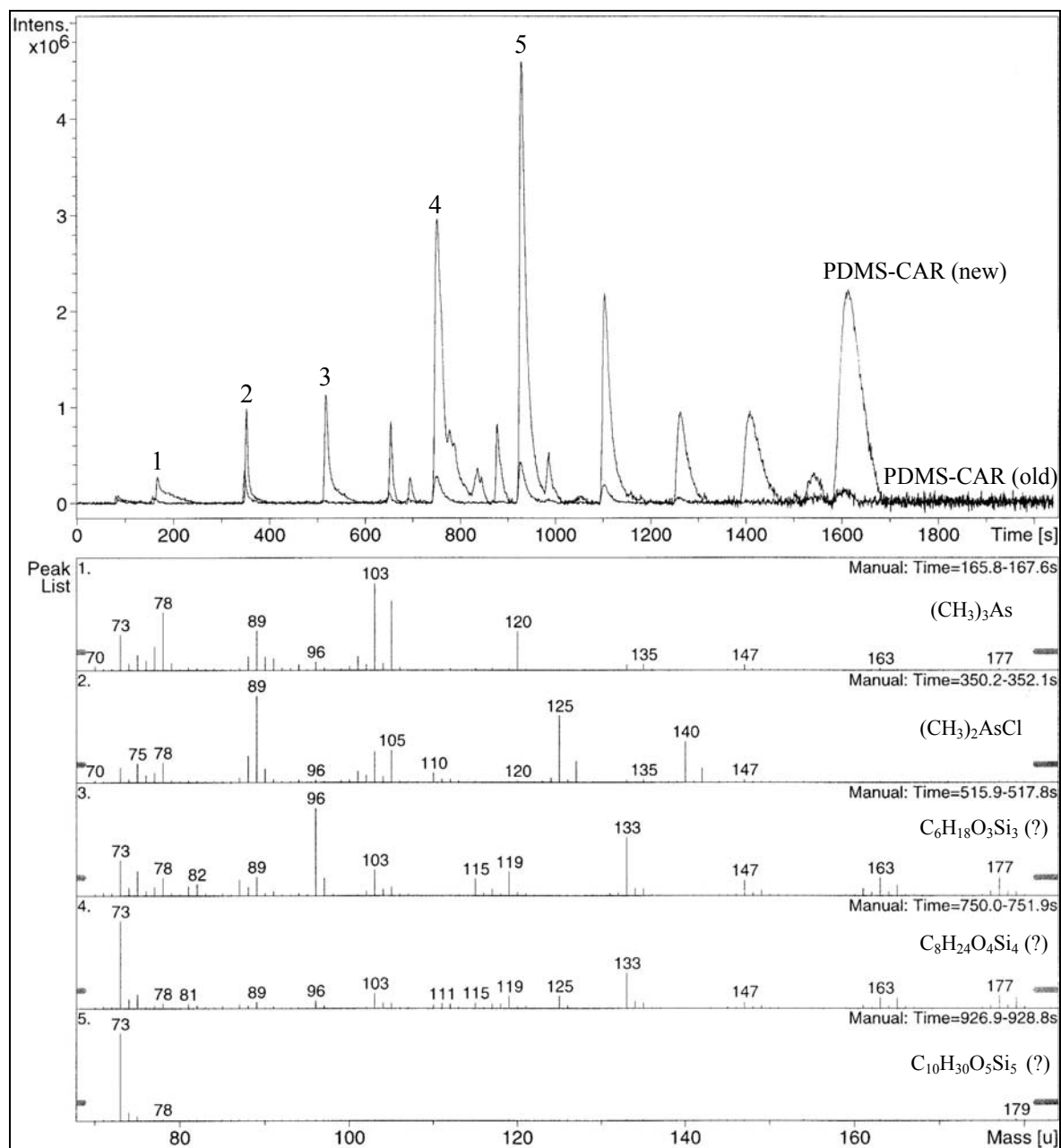


Figure 27 Comparison between chromatograms from an older PDMS-CAR SPME fiber (used about 15 times; lower line in the chromatogram) and a brandnew PDMS-CAR fiber (upper line in the chromatogram), both the arsine target peaks and additional peaks probably from siloxanes are larger on the new fiber

Storing the PDMS-CAR fibers retracted in their metal shaft and wrapped in aluminum foil at 4°C in the refrigerator yielded similar peak areas as for analysis immediately after the experiment (Appendix 7: 127b), suggesting that the arsines are stable on the fiber for at least 3 days. However, for an exact quantitative interpretation of storage losses and aging effects, the mobile Bruker GC-MS EM 640 is not suitable. For sampling in the field the quantification is further complicated by competitive sorption of other gases and unknown sorption affinities of the different arsines. Arsine can probably not be sorbed at all without using cryotrapping techniques. Thus, species-selective sampling by SPME was done qualitatively, not quantitatively.

3.3 Summary of chapter 3

The previous sections describe the development of a robust method for in-situ sampling of volatile metallics from aqueous environments. Efficient gas-water separation is achieved with a PTFE membrane (porosity 0.1 μm) inside a specially designed PTFE collector cell that can be placed at the sediment-water interface or in the aqueous body itself. Vacuum up to -500 mbar can be applied to force the gases to a trapping system of either liquid or solid sorbents. As liquid sorbent a 1:100 diluted NaOCl solution in a PTFE bottle is used. PTFE rings in the oxidizing bottle increase the reaction surface, and thus trapping efficiency. For As, laboratory trapping efficiencies of $84\% \pm 6.6$ were achieved. The build-up of a high pressure from the intense gas evolution during HG might be responsible for the loss of some volatile As, especially at the beginning of the reaction. In the field, continuous low-pressure arsine evolution will most likely result in even better trapping efficiencies. Quantitative evaluation of volatile metallics concentrations is achieved by referring the trapped mass in the oxidizing solution [μg] to the replaced vacuum volume [m^3].

Besides this fast screening method on total volatile metallics concentrations, two species-selective sampling procedures were investigated for As. Solid phase micro extraction (SPME) fibers enabled the detection of more volatile As species in lower concentrations than solid sorbent tubes. For SPME fibers, selective sorption was observed dependent on the volatile As species. The chloroarsines with the larger molecular weights $(\text{CH}_3)\text{AsCl}_2$ and $(\text{CH}_3)_2\text{AsCl}$ were sorbed on PDMS 100 fibers whereas PDMS-CAR-DVB fibers proved best for MMA, DMA, and TMA. The PDMS-CAR fibers showed by far the largest peak areas of all fibers for DMA, TMA, and $(\text{CH}_3)_2\text{AsCl}$. The most effective sorption material in sorption tubes was also Carboxen but only TMA and traces of $(\text{CH}_3)_2\text{AsCl}$ were detected. Probably the selected Carboxen type (CAR 564) does not present the optimum fit yet. Volatile As proved to be stable on the SPME fibers for at least 3 days, when wrapped in aluminum foil and stored at 4°C in the refrigerator. Quantitative evaluation could not be achieved because of insufficient detection limits of the GC-MS, unknown sorption affinities of the individual arsines on the various SPME fibers, non-availability of calibration standards, and potential competitive sorption with other, unknown gases. For the field investigations in this project, presented in the following chapter 4, species-selective sampling is only used for qualitative information.

4 YELLOWSTONE NATIONAL PARK

4.1 Introduction

Yellowstone National Park is located in the northwestern corner of Wyoming, USA. It was founded in 1872 as the world's first national park over an area of 8995 km². It is famous for its more than 10,000 geothermal features, including 200 geysers which equals 70% of the world's active geysers, numerous hot springs, fumaroles, and mud pots. The world's largest geyser, Steamboat Geyser, with a maximum eruption height of more than 115 m, as well as the world's third largest hot spring, Grand Prismatic Spring, with a diameter of approximately 110 m, are found here. The major watershed, the Continental Divide, cuts through the southwestern part of the Park. Rivers north of it discharge via the Madison River (confluence of Gibbon River and Firehole River), Gallatin River, and Yellowstone River to the Missouri and finally to the Gulf of Mexico. To the south the discharge follows mainly the Snake River and Falls River to the Pacific Ocean (Figure 28).

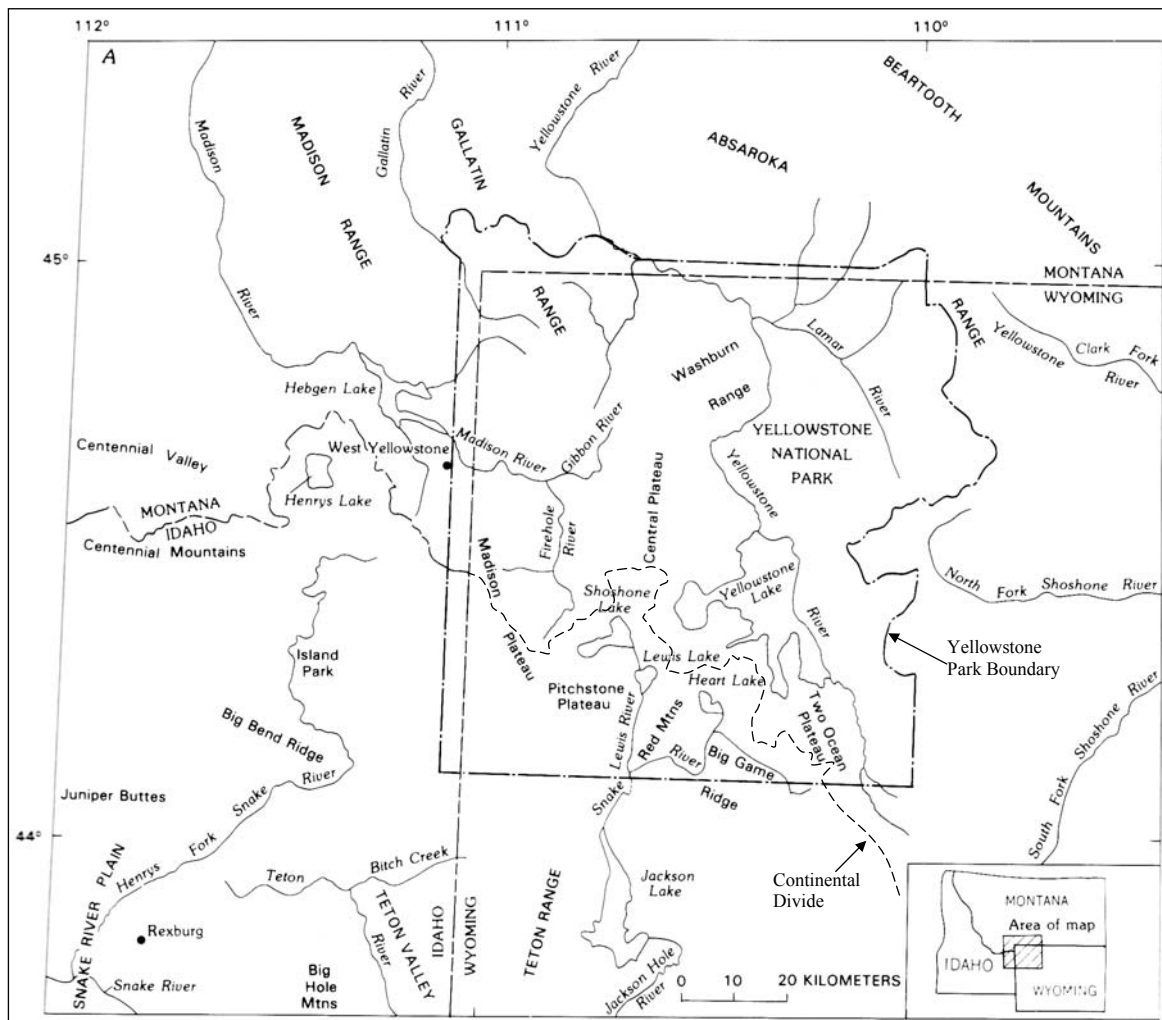


Figure 28 Yellowstone National Park (dot-dashed line is the park boundary) with topographic features, rivers, and lakes, and an approximation of the Continental Divide (dashed line) (modified from White et al. 1988)

4.1.1 Geology of the Park

4.1.1.1 Pre-Quaternary Geology

An overview of Yellowstone's geology is given in Smith and Siegel (2000) and a detailed technical review for the Pliocene and Quaternary can be found in Christiansen (2001). The oldest rocks found in the Park are 2.8 billion year-old granites and gneisses in the Gallatin Range at the north-central edge of the park (Figure 29). In some locations, they are intruded by 1.5 billion year-old diabase dikes. Up through the Laramide orogeny, Yellowstone showed a similar development as the rest of the Rocky Mountain area with marine conditions through Paleozoic and early Mesozoic and the formation of broad anticlinal and overthrust structures in the early Mesozoic as part of the Basin and Range Province. Paleozoic-Mesozoic deposits outcrop only at the southern- and northern-most margins of the Park. The following phase of extension during early Tertiary initiated intensive volcanism in the Eocene. The andesitic lava flows, basalt flows, ashes and mudflows of this Absaroka Volcanic Supergroup build up the mountain ridges in the eastern part of the Park (Mount Washburn). Intrusions of igneous rocks were minor in the Tertiary and formed isolated domes east of Yellowstone Lake and in the northwestern part of the Park only (e.g., Bunsen Peak).

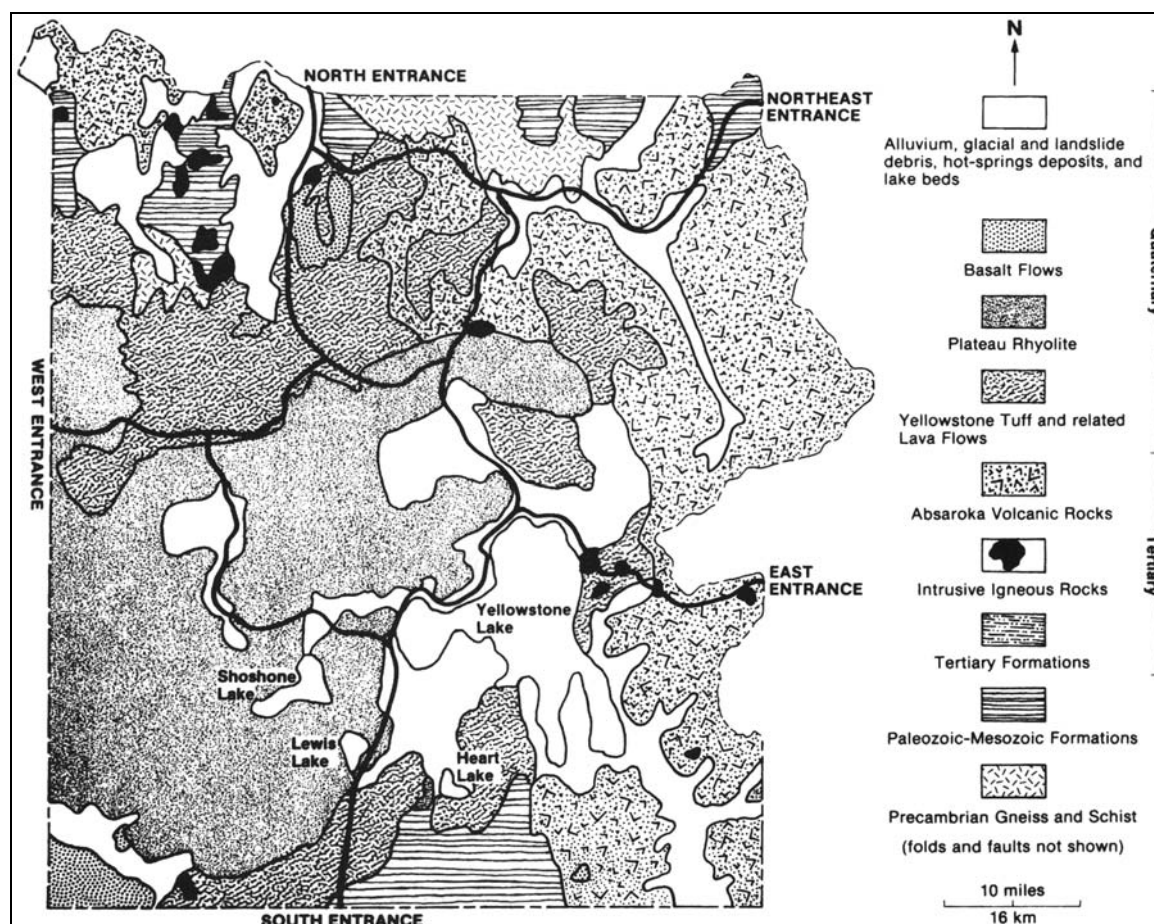


Figure 29 Simplified geological map of Yellowstone National Park (Kiver and Harris 1999)

4.1.1.2 Quaternary Volcanism

During late Tertiary to Quaternary, Yellowstone encountered three major volcanic cycles, each of which resulted in the formation of a caldera (Figure 30). Each explosive, pyroclastic-dominated activity was preceded and succeeded by large eruptions of rhyolitic lava. The oldest eruption occurred about 2.0 million years ago. It deposited 2,500 km³ of rhyolitic tuff, the so-called Huckleberry Ridge Tuff, with maximum thicknesses of 150 to 750 m. A second, smaller cycle began about 1.3 million years ago and ended with the deposition of about 280 km³ of Mesa Falls Tuff, up to 150 m thick. The latest eruption happened 630,000 years ago. The 1,000 km³ Lava Creek Tuff covers about 60% of the Park's surface with maximum thicknesses of 500 m. The caldera of this third volcanic cycle measures 45 km to 75 km in diameter. Compared to the 1980 eruption of Mount St. Helens, the three Yellowstone eruptions were 25000, 280, and 1000 times larger (Smith and Siegel 2000).

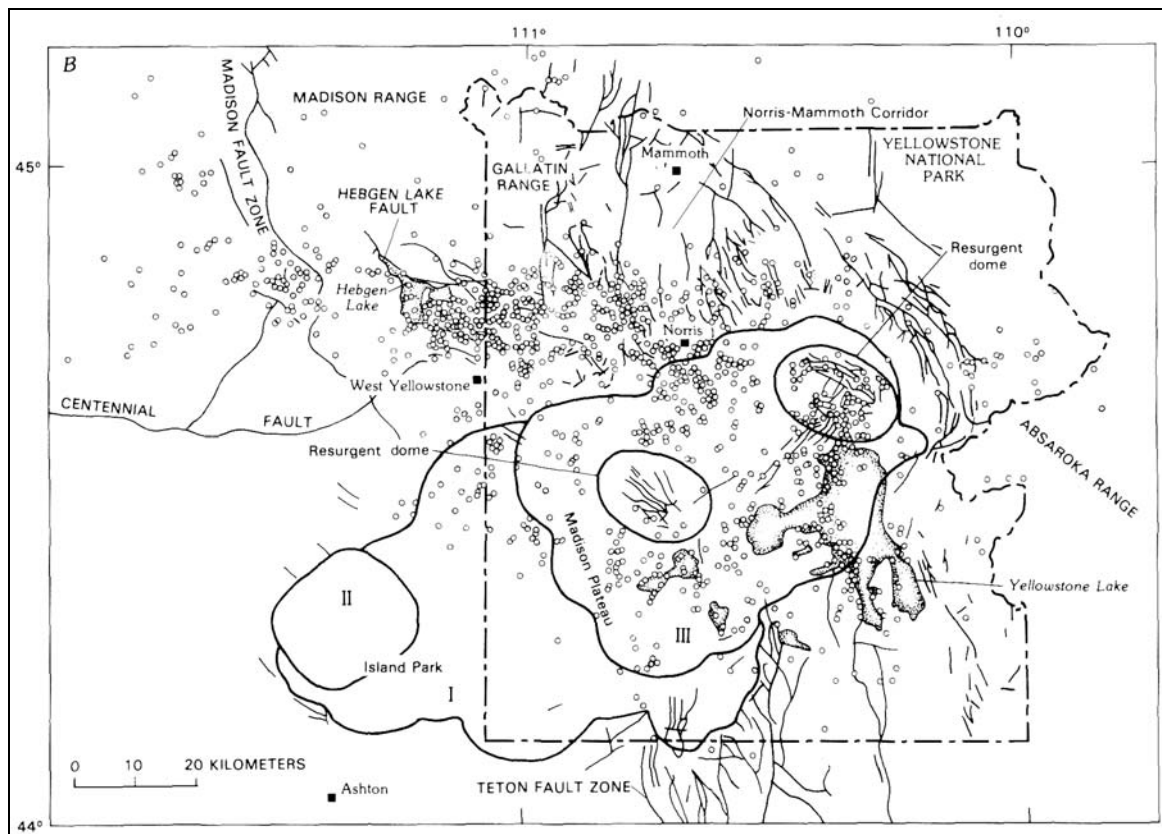


Figure 30 Major fracture zones and faults in and around Yellowstone National Park; I, II, and III indicate the three Yellowstone calderas formed 2, 1.3, and 0.6 Ma ago; circles picture epicenters of earthquakes with Richter magnitudes between 1 and 6 (White et al. 1988)

The source of this Late Tertiary to Quaternary volcanism is the Yellowstone hotspot, the largest hotspot under a continent worldwide (Pierce and Morgan 1990, 1992; Smith and Braile 1994). The origin of this hotspot is still controversial. Murphy et al. (1998) suggested that the hotspot first appeared already more than 55 million years ago beneath the Pacific Ocean. Duncan (1982) and Pyle et al. (1997) attribute a 55 million year-old captured island chain in the coast range of Oregon and Washington to the Yellowstone hotspot. The controversy of such theories and how they relate

to the global understanding of plate movement directions, rates and major orogenic events is discussed in Pierce et al. (2000). Assuming a first appearance of the hotspot 55 million years ago off the west coast, it is doubtful that there is a gap of approximately 40 million years without any surface manifestations of the hotspot's track. The first clear indication of the hotspot is an old caldera (McDermitt caldera) formed 16.5 million years ago in northern Nevada near its border to Oregon and Idaho along the Nevada-Oregon rift zone (Figure 31; Zoback and Thompson 1978). Because the North American plate drifts southwest over the Yellowstone hotspot, the eruptions formed a chain of progressively younger calderas stretching along a parabolic hotspot track from Nevada 800 km northeast up Idaho's Snake River Plain to Yellowstone.

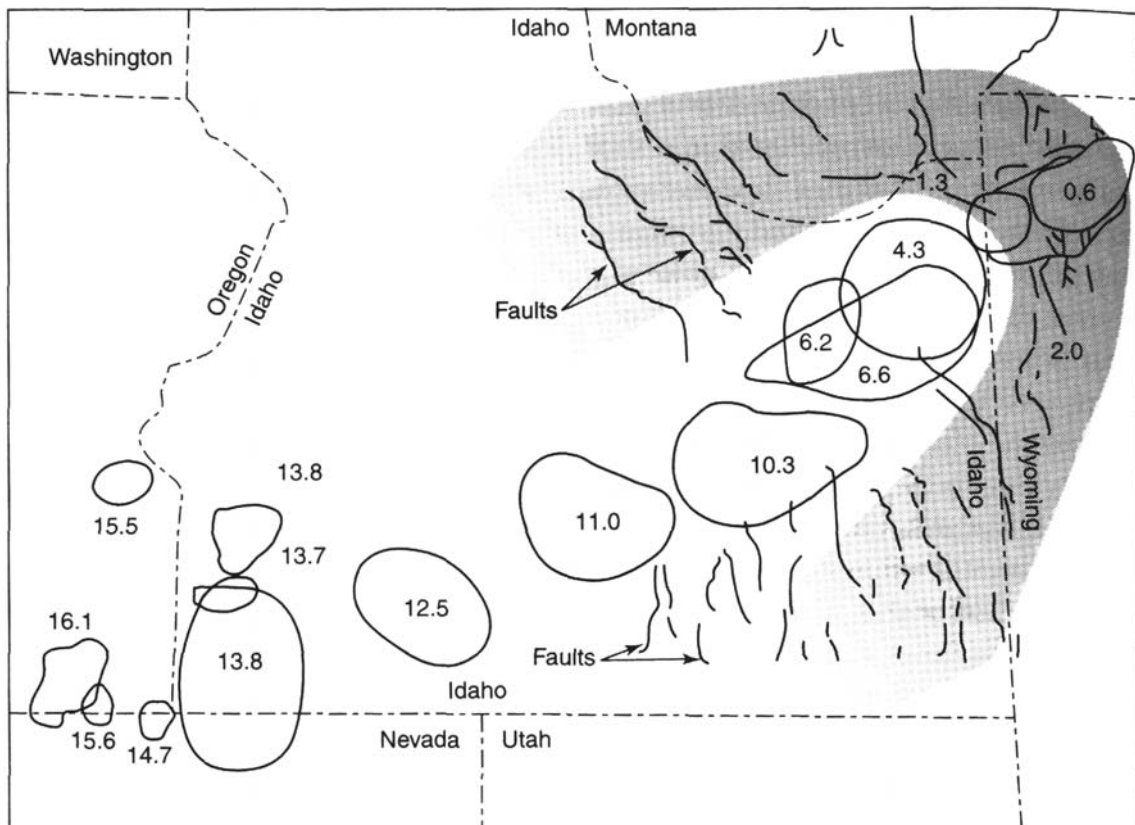


Figure 31 Path of the hotspot that triggered about 100 caldera eruptions from 7 major volcanic centers (McDermitt volcanic field 16.1-15.6 Ma, Owyhee volcanic center 14.7-13.8 Ma, Bruneau-Jarbidge volcanic center 12.5 Ma, Twin Falls volcanic center 11 Ma, Picabo volcanic center 10.3 Ma, Heise volcanic center 6.6- 4.3 Ma, Yellowstone volcanic center 2, 1.3, 0.6 Ma) (Kiver and Harris 1999)

The calculated average speed of the hotspot track during the last 16.5 million years was 4.5 cm annually. Until 8 million years ago, the average speed was 6.1 cm per year but then it slowed down to 3.3 cm per year. The direction of the track changed from east-northeast to northeast. Smith and Siegel (2000) explain this change in track direction as a slowdown and a change of the direction of the plate movement. In contrast, Pierce et al. (2000) state that the anomalously high average migration rates during the first 8 million years are three times faster than the predicted plate movements. Pierce et al. (2000) propose that 16 million years ago the hotspot's actual feeding tail was located 260 km east of the McDermitt caldera in a straight, continuous line with the younger calderas (no

change of plate movement direction assumed). At that time, the hotspot was located underneath the northeastward-tilting subduction zone of the oceanic lithosphere of the Juan de Fuca slab underneath the North American plate. The buoyantly rising plume head intersected with the overlying Juan de Fuca slab and was thus deflected west-southwestward, protruding to the surface at the position of today's McDermitt caldera. Because of an increasing inclination of the Juan de Fuca slab and the continuous southwestward plate movement, the subduction zone was shifted southwestwards away from the hotspot. Since about 10 million years ago, the plume head rises straight up to the surface from the feeding tail without any deflexions. This termination of southwestward deflexion can explain the apparently higher migration rates of the hotspot track to the northeast.

In the wake of the hotspot, the Snake River Plain sank as much as 600 m and was flooded by a series of basalt lava flows that today cover the rhyolites from the explosive eruptions and smoothed the topography of the old calderas. In Yellowstone, at least 30 subsequent smaller lava flows filled the youngest caldera from the third major volcanic cycle. The most recent lava flow, the Pitchstone Plateau flow in the southwestern part of the Park, dates back about 70,000 years (Smith and Siegel 2000).

Several recent reports argue against the theory of a Yellowstone deep mantle plume. In contrast to hotspots underneath oceanic plates, the Yellowstone hotspot probably does not root at the mantle-core boundary, but begins as a melting anomaly in the upper mantle at about 200 km beneath the surface (Christiansen et al. 2002; Humphreys et al. 2000). Seismic data show a low-wave-speed layer in this depth, extending no deeper than 200-250 km (Christiansen et al. 2002; Iyer et al. 1981). An extending region over a melting anomaly would not only explain the propagation of the Yellowstone hotspot to the northeast, but also another melting anomaly to the northwest, the Newberry anomaly.

4.1.1.3 Quaternary Glaciation

In addition to the filling by younger lava flows, the topography of the Yellowstone calderas was smoothed by glaciation. The Yellowstone plateau with average altitudes of about 2000 to 2500 m was covered by ice up to 1200 m thick during at least two major ice stages: Bull Lake stage from 160,000 to 130,000 years ago, and Pinedale stage from 50,000 to 14,000 years ago (Pierce 1979). These glacial events overlap with the volcanic events during Quaternary.

During glaciation the potentiometric surfaces for groundwater in the underlying rocks were raised hundreds of meters above the ground surface, raising the boiling point curves (Bargar and Fournier 1988). Excess thermal energy became stored in rocks at shallow depths. When the glaciers receded, this excess energy was released enhancing the geothermal circulation. Rapid draining of local lakes lowered the hydrostatic head to such an extent that pore water flashed to steam and produced several large hydrothermal explosion features, like e.g., Pocket Basin in Lower Geyser Basin or Roaring Mountain (Muffler et al. 1971).

4.1.1.4 Hotspot development after the last volcanic cycle

The hotspot under Yellowstone's youngest caldera consists of a column of hot rock with about 10-30% molten rocks, and extends upward to about 80 km beneath the surface. Basalt blobs are sheared off the top of the hotspot by the movement of the lithospheric plates. As these blobs rise in the crust, they melt silica-rich rock, to create a large sponge-like chamber of partly molten rhyolite. This magma chamber extends from about 8 to 13 km beneath the surface. In the northeastern part of the Park it might be as shallow as 5 km beneath the surface (Smith and Siegel 2000).

After the last volcanic cycle, two main conduits remained connected to the magma chamber above the Yellowstone hotspot. At the surface, they are expressed as two resurgent domes with a south-east-northwest striking (Figure 30). The 630,000 year-old Sour Creek dome has an extension of 10 x 16 km and rises 400 m above the surrounding countryside north of Yellowstone Lake. About 32 km southwest of Sour Creek, north of the Upper Geyser Basin, the 150,000 year-old Mallard Lake dome rises 300 m above its surroundings with a size of 11 x 8 km. Both domes are interconnected by the 153,000 year-old Elephant Back fault zone (Obradovich 1992) that outcrops for about 6 miles in between the two domes reaching altitudes of more than 2600 m (Smith and Siegel 2000).

Ever since the last volcanic cycle, Yellowstone caldera has been subject to uplift and subsidence. For the last 12,000 years this movement is expressed in deformations on postglacial terraces around Yellowstone Lake (Locke and Meyer 1994; Pierce et al. 2002) and changes in the gradient of the Yellowstone river (Pierce et al. 1997). Pelton and Smith (1982) documented an uplift of 14 ± 1 mm/year of the caldera floor in the 20th century by comparing leveling surveys from 1923 and 1975-1977. Further investigations by leveling and differential GPS measurements along a traverse from Lake Butte to Canyon Junction (and from 1989 further on to Mount Washburn) documented an uplift of the northeastern caldera floor (center at Le Hardy Rapids) from 1976 to 1984 with an average rate of 22 ± 1 mm/year. From 1984 to 1985, a phase without measurable deformation followed. Subsidence started in 1985 and proceeded through 1995 with an overall rate of -19 ± 1 mm/year. The rate was higher (-39 ± 5 mm/year) in the years 1993 to 1995 only (Dzurisin and Yamashita 1987; Dzurisin et al. 1990, 1994, 1999). From 1995 to 1998, a leveling survey by Dzurisin et al. (1999) showed a renewed uplift of 8 ± 1 mm/year.

Since 1992, high resolution synthetic aperture radar (SAR) images obtained from European Space Agency satellites ERS-1 and ERS-2 were used to measure year-to-year deformation over the whole surface of the caldera instead of movement on isolated points only (Dzurisin et al. 1999; Wicks et al. 1998). The resultant interferograms enable a much more detailed location of deformation sources. Dzurisin et al. (1999) and Wicks et al. (1998) observed that deformation centers changed on a scale of 1 to 2 years between the two resurgent domes. The center of subsidence shifted from Sour Creek dome during August 1992 to June 1993 to Mallard Lake dome during June 1993 to August 1995. Between August 1995 and September 1996, while the Mallard Lake dome continued to subside slightly, the region near the Sour Creek dome began to inflate. From September 1996 to June 1997, uplift proceeded at Mallard Lake dome. By June 1997, uplift extended across most of the caldera. Its center had risen by approximately 40 mm since August 1995 (Dzurisin et al. 1999).

The initiation of the renewed uplift from Sour Creek dome to Mallard Lake dome may indicate that the driving pressure source lies under Sour Creek dome or that Sour Creek dome has a preferential connection to the magma chamber below. A second conduit probably interconnects the two domes. Wicks et al. (1998) suggest a third conduit where fluids flow out of the caldera, initiating subsidence of the whole area. This third conduit is believed to extend to the northwestern corner of the park, feeding the geothermal features of Norris Geyser basin, and maybe connected to the Norris-Mammoth corridor (Figure 30). The Norris-Mammoth corridor is a complex subsidence structure of faults, volcanic vents, and thermal activity that extends north from Norris at least up to Mammoth, probably even further up to Corvin Springs. This structure was inferred from electromagnetic (Stanley et al. 1991), seismic, and gravity data (Lehmann et al. 1982). The hypothesis of this structural conduit is supported by the location of the two largest earthquake swarms ever recorded in the park since 1972 west of Madison junction, just outside of the northwest caldera rim. They initiated or accompanied the changes from uplift to subsidence in 1985 and to renewed uplift in 1995. The 1985 earthquake swarm started in October and persisted through 1986 with 28 earthquakes of a magnitude > 3.5 , the strongest being 4.9. The 1995 earthquake swarm began in late June and continued through mid-July with more than 560 earthquakes. The largest earthquake had a magnitude of 3.1 (Dzurisin et al. 1999). Most recent research reveals an inflation area of 30 x 40 km at the center of the proposed outlet (Wicks et al. 2002, 2003). From 1996 to 2002, a maximum uplift of 125 mm was detected over this Norris Uplift Anomaly.

The primary cause of uplift and subsidence in the two main resurgent domes may be explained by two end-member models (Dzurisin et al. 1990; Fournier 1989). Initiation of an uplift may be caused by the injection of basalt near the base of the cooling rhyolitic magma chamber. In the upper part of the magma chamber, rhyolite crystallizes and releases magmatic fluids in the shallow hydrothermal system. Subsidence starts, when the basalt supply rate is less than the subsidence caused by crystallization and loss of fluids. The thermal energy discharged by the advecting thermal waters could be supplied by the latent heat of crystallization of about 0.2 km³ rhyolitic magma per year that would lead to a volumetric contraction of about 0.014 km³. That contraction is close to the observed rate of subsidence from 1985 to 1995. The second model assumes that uplift is primarily caused by pressurization through magmatic fluids released during crystallization and trapped at lithostatic pressure beneath an impermeable self-sealed zone of mineral deposition. Subsidence occurs during episodic hydrofracturing. The short intervals of change in subsidence and uplift between the two resurgent domes (1-2 years) favor the second hypothesis with a low-viscosity fluid (gas plus brine) over a more viscous one (magma). Assuming that the magmatic fluids released from the crystallization of 0.2 km³ rhyolitic magma per year contain about 2 wt% water, and are trapped at lithostatic pressure at a depth of 4-5 km that results in a net volume increase of about 0.026 km³/year that can easily account for the observed inflation from 1923 to 1984 (Fournier 1989).

4.1.1.5 Hydrogeochemistry of geothermal features

Surface geothermal activity expressed in hot springs, geysers, fumaroles and mud pots indicates the final stage of the third caldera cycle. It started about 15,800 years ago after the Pinedale glaciation (Fournier et al. 1976). Most surficial geothermal features occur along the caldera's ring fracture zone and along the Norris-Mammoth corridor (Figure 32) in flat-bottomed valleys between lava flows with permeable stream and glacier sediments that allow water to percolate into the ground.

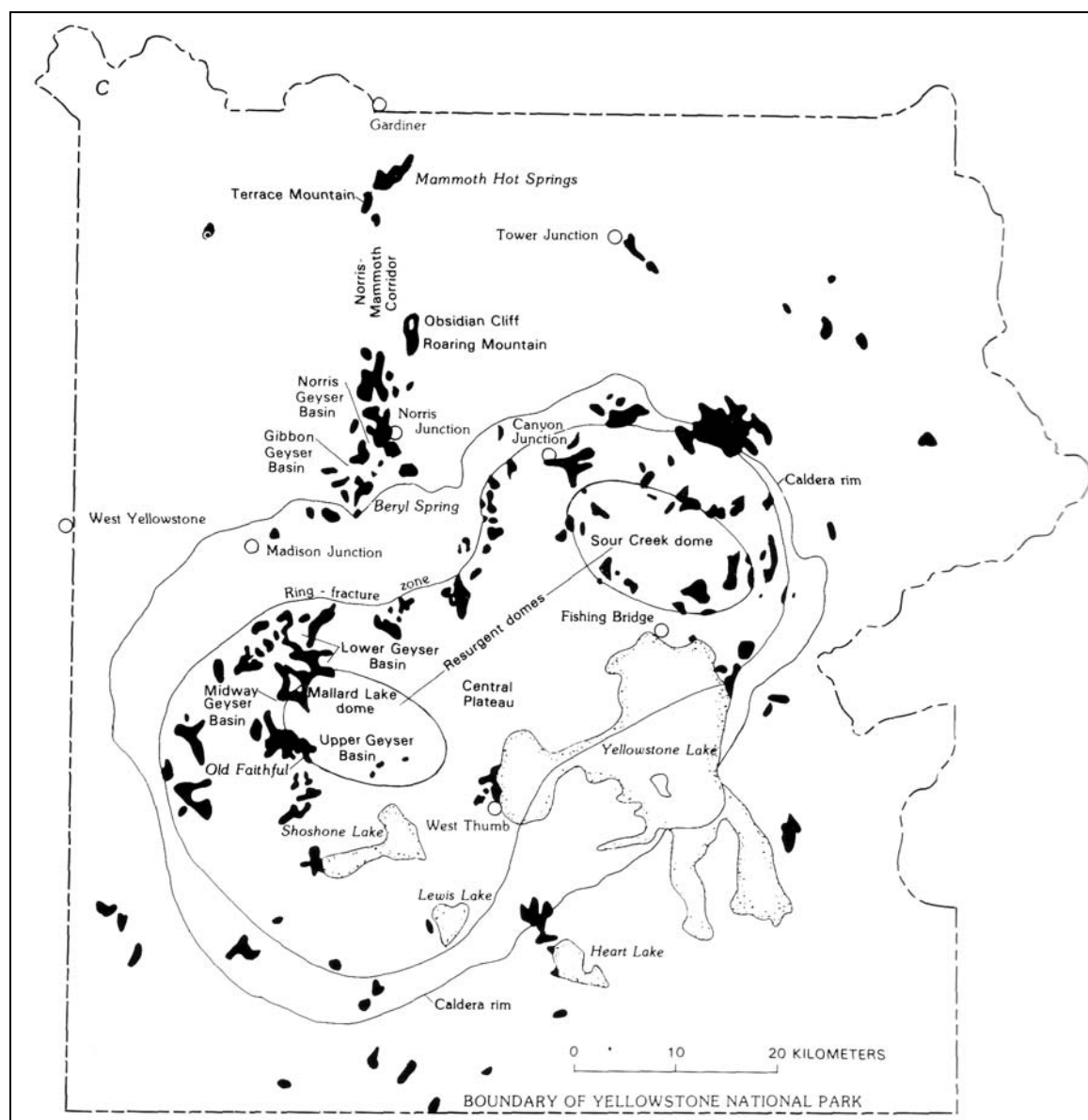


Figure 32 Yellowstone NP with the youngest caldera rim and ring-fracture zone, and the resurgent domes Mallard Lake (southwest), and Sour Creek (northeast); black areas indicate active and fossil geothermal systems (White et al. 1988)

Mainly over the last 40 years, the hydrogeochemistry of the geothermal features has been investigated intensively (Allen and Day 1935; Ball et al. 1998a, 1998b, 2001, 2002; Fournier 1989; Fournier et al. 1992, 1994a, 2002; Rowe et al. 1973; Thompson et al. 1975; Thompson and Yadav

1979; Thompson and DeMonge 1996; Truesdell and Fournier 1976; Truesdell et al. 1977; Stauffer et al. 1980). Several geochemical models were derived.

In the north and northwest where interlayered permeable rhyolite flows from the third and second caldera cycle form possible fluid reservoirs and water recharges from the Gallatin Range, there is a concentration of larger geothermal areas with geyser and hot springs discharging mostly high Cl and SiO₂ waters at a near-neutral pH (Truesdell et al. 1977). The eastern part of the Park, where impermeable ash flow tuffs predominate, is dominated by geothermal features with little or no discharge, such as mud pots and fumaroles (White et al. 1971). Stable isotope studies revealed that more than 95%, maybe even as much as 99.6-99.9% of the geothermal water circulating in the Yellowstone caldera is meteoric water, mixed with only little magmatic fluids (Craig et al. 1956; Fournier 1989). Infiltrating water is heated to about 350°C (inferred from enthalpy-chloride relations and Si-geothermometer) over the magmatic heat source in 4-5 km depth. This “parent water” contains about 400 mg/L Cl, high Na concentrations, high gas concentrations (mainly CO₂, and H₂S), and low concentrations of SO₄²⁻ and HCO₃⁻ (Fournier et al. 1986; Fournier 1989).

As geothermal fluids ascend adiabatically from the magma chamber, water and steam separate as pressure decreases at shallower depths, and at fractures or fissures. Two major water types form:

- Steam, rich in CO₂, and H₂S, rises and condenses or mixes with shallow groundwater. The H₂S is oxidized abiotically to elemental sulfur and sulfur is oxidized biotically to sulfuric acid. This water type (**type I**) is characterized by low pH, and high concentrations of S(VI) and high P_{CO₂}. Thiosulfate concentrations are low due to the instability of S₂O₃²⁻ in acid waters (Xu and Schoonen 1995; Xu et al. 1998). Increased concentrations of Al (on average several mg/L up to a maximum of 100 mg/L; Ball et al. 2002) and rare earth elements (20-1130 nmol/kg Σ REE; Lewis et al. 1997) are found from reactions with surrounding rhyolite.
- The residual liquid phase, depleted of the gaseous compounds separated with the steam, forms water **type II**. This water type has a near-neutral pH, and lower concentrations of S(VI) and lower P_{CO₂} compared to type I waters. The elements Si and Cl are enriched, often showing higher concentrations than the 400 mg Cl/L in the parent water. Rare earth element concentrations in type II waters with a near-neutral pH are mostly at or below detection limits (Lewis et al. 1997).

Both type I and type II waters can be diluted near or at the surface by meteoric waters. Mixing ratios can be determined using ²H and ¹⁸O isotopes (Ball and Nordstrom 2001; Kharaka et al. 1991, 2002; Truesdell et al. 1977). From mixing with meteoric waters, the Cl/S(VI) ratio of type II waters decreases. In these waters of slightly acidic to near-neutral pH, and enriched in S(VI) (Cl/S(VI) ratio 10-25), S₂O₃²⁻ may exceed dissolved H₂S concentrations. As a result of subsurface H₂S oxidation, elemental sulfur hydrolysis, or interaction with sulfate-bearing minerals, S₂O₃²⁻ concentrations of 9 to 95 μmol/L are found (Xu et al. 1998). The ³He/⁴He ratios of the geothermal waters are typically increased compared to atmospheric values, indicating a mantle source. Especially high values occur in water that discharges directly from deep reservoirs, lower values in waters depleted in mantle gas (Kennedy et al. 1985; Kharaka et al. 1991, 2000, 2002).

Arsenic is a typical element that occurs at high concentrations in geothermal fluids (Webster and Nordstrom 2003). At depth, most reservoir fluids are undersaturated with regard to As minerals. High As concentrations in geothermal features most likely result from leaching of the surrounding rocks during the ascent of the fluids as shown by Ellis and Mahon (1964) and Ewers and Keays (1977) using rock-leaching experiments. Vapor-liquid distribution factors for As ($K_m = m_{As(vapor)} [mol/kg] / m_{As(liquid)} [mol/kg]$) measured in different hot springs of modern geothermal fields typically are in the range of 0.001 to 0.01 at temperatures of 150 to 300°C (Ballantyne and Moore 1988). Experimental studies by Pokrovski et al. (2002) revealed that the small fraction of As that is separated into the steam (= type I waters at Yellowstone) is mainly $As(OH)_3(g)$. In the presence of $HCl(g)$ and at temperatures $<200^\circ C$, $AsCl_3(g)$ might predominate. Gaseous As sulfides were found to be negligible in the presence of H_2S . Type II waters contain higher As concentrations compared to type I, since the majority of As remains in the liquid phase during phase separation (Stauffer and Thompson 1984). This behavior is similar to Cl and the reason for the positive correlation of As and Cl in geothermal fluids, first observed by Ritchie (1961). In Yellowstone, many hot springs are enriched in As relative to Cl. This enrichment is either caused by high CO_2 concentrations increasing arsenite hydrolysis and solubility from host rocks (Stauffer and Thompson 1984) or by accumulation of As in precipitates near the surface (Nordstrom et al. 2001). A review on the source, transport, and fate of geothermal As is provided in Webster and Nordstrom (2003).

In Yellowstone, As was first detected by Gooch and Whitfield (1888). Concentrations range from 0.1 to 9 mg/L (Ball et al. 1998a, 1998b, 2001, 2002; Nordstrom et al. 2001; Stauffer and Thompson 1984). The As(III)/As(V) ratios are extremely variable with a distinct bimodal distribution of As being either fully reduced in hot springs or fully oxidized in drainages (Nordstrom et al. 2001). Upon discharge from the hot spring, As(III) oxidizes rapidly to As(V) (Stauffer et al. 1980; Stauffer and Thompson 1984). Langner et al. (2001) determined a half-life of 0.58 minutes for the microbially mediated oxidation at a hot spring in One Hundred Springs Plain, Norris Geyser Basin ("Dragon Spring", pH 3.1, temperature 58-62°C). Assignment of specific microbial populations to the As(III) oxidation and detection of their oxidation mechanisms - chemolithoautotrophic metabolism or extracellular oxidative detoxification - is under research. Often, a distinct zoning of yellow, brown and green microbial mats with increasing distance from a hot spring discharge is observed. Jackson et al. (2001) determined for "Dragon Spring" that 90% of the bacteria in yellow and brown microbial mats are *Hydrogenobacter acidophilus* (H_2 or S^0 oxidizing bacteria) and *Desulfurella sp.* (S^0 reducer). A strain of the arsenite-oxidizing *Hydrogenobaculum* was later isolated from the same spring by Donahoe-Christiansen et al. (2004). Archaeobacter were found in the brown mats only, *Cyanidium caldarium* was identified in the green mats (Langner et al. 2001). Investigating Twin Butte Vista hot spring in the Lower Geyser Basin (pH 8.8, temperature 65-82°C), Gihring et al. (2001) found that *Thermus aquaticus* oxidizes As(III) rapidly. Laboratory experiments confirmed that *Thermus* species are not able to grow with As as the only energy source, and no catabolic energy is derived from As(III) oxidation. Thus, As(III) oxidation is likely a detoxification mechanism for this species.

No investigations have ever been conducted in Yellowstone on methylated or volatile As compounds before the current project. In general, only few studies exist about organic and volatile As speciation in geothermal gases or waters. Crecelius et al. (1976) detected volatile As compounds in non-condensable gases in several hot-water fields in California. Total concentrations reached up to 79 ng/kg. No As speciation was performed. Hirner et al. (1998) detected AsH₃, MMA, DMA, and TMA in geothermal gases over hot springs in British Columbia. However, no quantification was achieved. In geothermal waters in New Zealand, methylated As made up 0.02-8.9 µg/L and an unidentified, probably organic As compound up to 30 µg/L (Hirner et al. 1998; see also Table 1).

4.1.2 Study areas

Five study sites were selected for hydrogeochemical sampling with focus on dissolved and volatile As speciation. From the north to the south, those areas are:

- Nymph Lake area with Frying Pan Spring
- Hazle Lake area
- Ragged Hills area in the Norris Geyser Basin
- Geyser Springs group in the Gibbon Geyser Basin
- Pocket Basin in the Lower Geyser Basin

Only Pocket Basin lies within the Yellowstone caldera. The areas 1-4 are located to the north of the caldera, along the Norris-Mammoth corridor (section 4.1.1.4; Figure 33).

White et al. (1988) present a model for the hydrogeochemistry of hot springs along the Norris-Mammoth corridor (Figure 34). A magma chamber is hypothesized to be centered near the vent of the 180,000 years old Obsidian Cliff flow. From there, geothermal fluids are flowing to the north and to the south.

To the north, extensive cooling and dilution by meteoric water occurs. The waters dissolve carbonate from pre-Tertiary sediments that is finally precipitated upon discharge at Mammoth hot springs. Kharaka et al. (1991) propose an alternative model with a separate magmatic body for the Mammoth hot springs area. This model is supported by high ³He/⁴He ratios in the geothermal waters at Norris and Mammoth and low ³He/⁴He ratios in all the major geothermal areas in between. The high ³He/⁴He ratios indicate a direct release from a deep reservoir. Additional evidence for a magmatic body in the Mammoth area comes from magnetotelluric and other geophysical surveys, indicating a partially molten area south of Bunsen Peak at a depth of 6 km (Stanley et al. 1991).

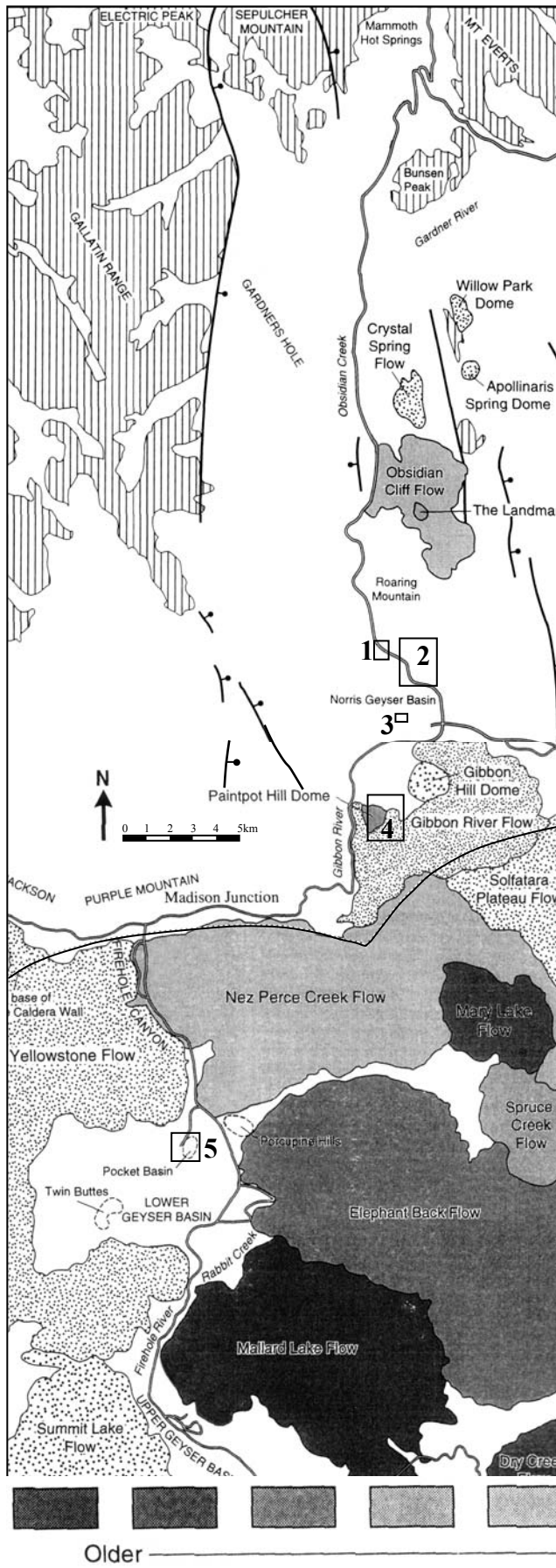
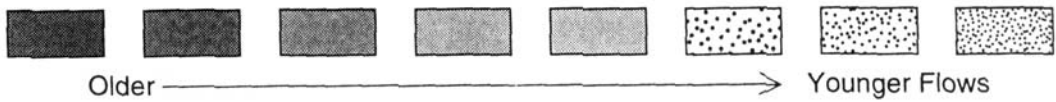


Figure 33 Geological map for the study sites; outside the caldera, along the Norris-Mammoth corridor: 1 = Nymph Lake (incl. Frying Pan Springs about 300 m south; Figure 35), 2 = Hazle Lake (Figure 36), 3 = Ragged Hills (Norris Geyser Basin; Figure 39), 4 = Geyser Springs group (Gibbon Geyser Basin; Figure 40); inside the caldera: 5 = Pocket Basin (Lower Geyser Basin; Figure 41); shaded areas show named Quaternary rhyolitic lava flows and domes, shading indicates age according to legend (modified after Fournier et al. 1994b)



In the model of White et al. (1988), the hot Cl^- and SiO_2 -rich waters of neutral pH flowing to the south, undergo subsurface boiling with a steam-water separation. At temperatures about 370°C , the steam rises and forms acid-altered areas by near-surface oxidation of steam-enriched H_2S . According to high resolution aeromagnetic mapping by Finn and Morgan (2002), there are many more yet unrecognized areas of hydrothermal alteration in the shallow subsurface along the Norris-Mammoth corridor. The residual water phase, enriched in chloride, discharges further to the south in the Norris Geyser Basin at temperatures around 270°C (section 4.1.2.3). The occurrence of acid alteration areas north of Norris is hard to combine with the detected low $^3\text{He}/^4\text{He}$ ratios in all the major geothermal areas between Mammoth and Norris (Kharaka et al. 2000). An early steam separation from a magmatic source in the Obsidian Cliff area explains the low pH, but it should yield higher $^3\text{He}/^4\text{He}$ ratios. More recent data summarized by Fournier (2004) indicate that either an injection of magma or an injection of hydrothermal fluid (or both) from the caldera magma has moved along faults to the Norris Basin and to Mammoth.

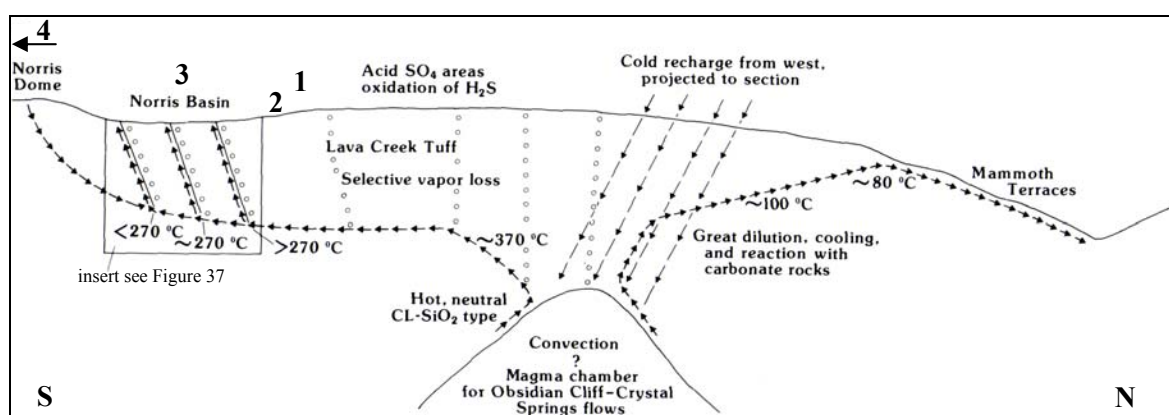


Figure 34 Model to explain hydrogeochemistry along the Norris-Mammoth corridor (White et al. 1988); from a central magma chamber underneath the area of Obsidian cliff geothermal fluids flow north to Mammoth (extensive cooling and dilution by meteoric water, dissolution of carbonate pre-Tertiary sediments) and south to Norris (steam-water separation; formation of acid-altered areas by near-surface oxidation of steam-enriched H_2S closer to the magma chamber, discharge of residual chloride enriched water in the Norris Geyser Basin); numbers indicate study areas (1 = Nymph Lake, 2 = Hazle Lake, 3 = Norris Geyser Basin, 4 = Gibbon Geyser Basin, south of Norris dome); Norris dome is the third resurgent dome (Norris Uplift Anomaly) mentioned in section 4.1.1.4

4.1.2.1 Nymph Lake area

Nymph Lake is located 3.5 km northwest of Norris. The lake stretches NE-SW with a maximum length of 500 m, and a maximum width of 150 m (Figure 35). Two geothermal areas with numerous fumaroles and hot springs ranging from centimeters to a few meters in size border the lake to the northeast and west. During the winter of 2002/2003, a new geothermal feature broke out, marking a line of fumarole vents in the lodgepole pine forest above the western geothermal area.

Nymph Lake has one major and two minor tributaries apart from the discharge of the geothermal areas. The northern tributary rises about 2 km northwest in the Twin Lakes. The northern lake of the Twin Lakes receives some drainage from Roaring Mountain. The second tributary on the north-eastern side of Nymph Lake is the 170 m long, 1-2 m wide, and 1-10 cm deep acid Nymph Creek

originating from multiple springs (pH approximately 2.8, temperature 45°C to 62°C; Ball et al. 2002). Its distinct green color stems from the growth of 2-3 mm thick mats of the acidophilic alga *Cyanidium caldarium*. Although the alga's color is exactly the same as that of many prokaryotic blue-green algae, careful scrutiny of the cells showed that it belongs to the group of eukaryotic red algae (Ferris et al. 2003; Henson and Ferris 2003). About 50 m south of Nymph Creek, "Frying Pan Spring Creek" flows into Nymph Lake, draining the Frying Pan Spring area about 250 m southeast. Note that names in quotation marks used here and in the following are unofficial names, most of them adapted from the research group of Dr. Kirk Nordstrom, United States Geological Survey in Boulder, Colorado.

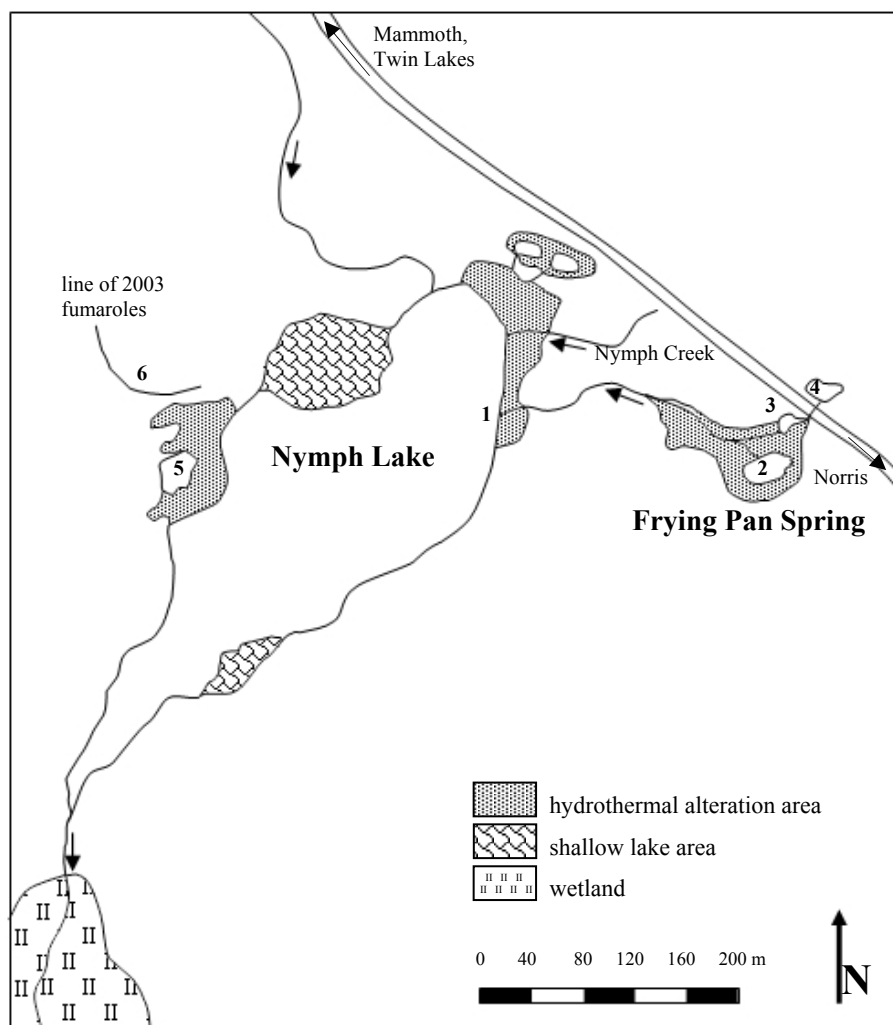


Figure 35
Nymph Lake area including Frying Pan Spring in the southeast; numbers 1-6 indicate sampling sites YNP NL01-YNP NL06

Because of the preponderance of gas discharge related to the model presented in Figure 34, the hot springs at Frying Pan Spring area show high concentrations of S(VI) (440 mg/L), $S_2O_3^{2-}$ (0.6 mg/L), and dissolved H_2S (1 mg/L; Ball et al. 1998b). Ferris et al. (2003) and Ball et al. (1998b) determined 0.07 to 0.2 mg/L and <0.001 to 0.12 mg/L H_2S respectively for the source water of Nymph Creek and attribute the higher concentrations downstream mainly to microbial reduction within the microbial mat. Goff and Janik (2002) determined 1.074 mol% dry gas H_2S at Frying Pan Spring, compared to 0.677 mol% at Beryl Spring, 0.387 mol% at Fountain Paint Pots, and 0.001-

0.298 mol% in the Mud Volcano area. Only fumaroles in the Lamar region showed higher values with 1.2-1.7 mol%. The concentration of H_2 (0.3305 mol%) is also 1-3 orders of magnitude higher than in other areas in the Park. Total dissolved As concentrations of 0.1-0.2 mg/L are significantly lower than in Norris Geyser Basin, Gibbon Geyser Basin or Lower Geyser Basin (Ball et al. 1998b).

4.1.2.2 Hazle Lake area

Hazle Lake area lies about 1 km southeast of Nymph Lake area, 250 m east of the road Norris-Mammoth (Figure 36). It consists of the lake itself with a length of approximately 600 m NNE-SSW and a maximum width of 200 m, and an adjacent wetland area with a length of 1 km, and a maximum width in the northeast of 700 m. In the northeast there is a 150 m by 400 m large zone of shallow water with significant thermal activity and precipitated alteration products. Gas discharges in shallow water can also be observed all along the lake's western side. Several geothermal areas, mainly on the northern and western side, discharge hot water into the lake.

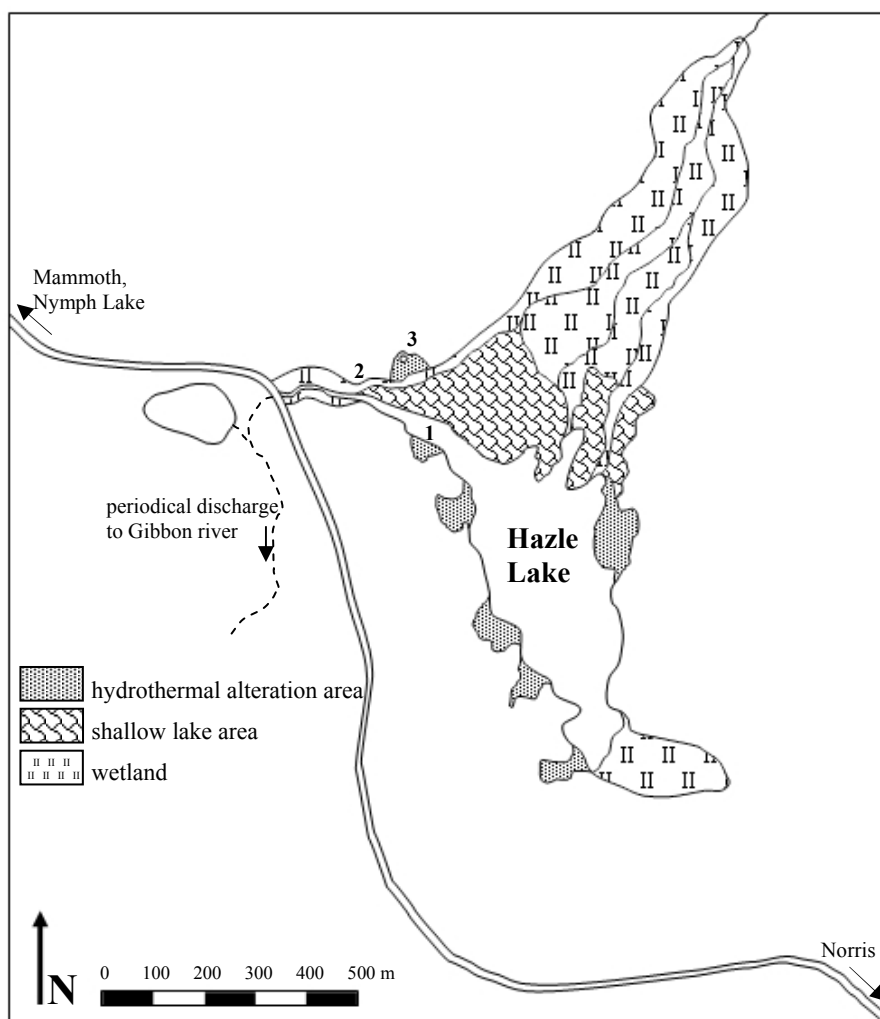


Figure 36
Hazle Lake area with periodic discharge to the south into the Gibbon river; numbers 1-3 indicate sampling sites YNPHL01-YNPHL03

Apart from the geothermal discharge, the lake is fed by one tributary rising about 1 km northeast of the Hazle Lake wetland area. The lake discharge flows at first to the west, then to the south and

joins Gibbon river. Inflow, outflow and lake level vary seasonally. Little research has been conducted at Hazle Lake so far. In 2000, U.S. Geological Survey researchers found significantly increased concentrations of inorganic and methyl-mercury (Table 10). A joint project between the U.S. Department of Energy's Idaho National Engineering and Environmental Laboratory, the U.S. Geological Survey and the University of Nevada-Reno in autumn 2003, revealed significant mercury emissions of 200-700 ng/m²/h all along the Norris-Mammoth corridor, with a maximum concentration of 2,400 ng/m²/h at Roaring Mountain (Department of Energy 2003).

Table 10 Unpublished data for Hg and Methyl-Hg from USGS researchers

Site	Date	Total Hg [ng/L]	Methyl-Hg [ng/L]
Hazle Lake Shore #1	9/24/2000	300	0.01
Hazle Lake Shore #2	9/24/2000	345	0.25
Hazle Lake Shore #3	9/24/2000	310	0.02
Hazle Lake inlet	9/24/2000	100	1.70
Hazle Lake outlet #1	9/24/2000	320	0.55
Hazle Lake outlet #2	9/24/2000	270	0.95
Hazle Lake outlet of wetland	9/24/2000	115	2.10

4.1.2.3 Norris Geyser Basin

Norris Geyser Basin, 4 km north of the northwest rim of the Yellowstone caldera, shows the greatest variety of geothermal features within the Park. It is located over the intersection of the Norris-Mammoth corridor and the eastward extension of the Hebgen Lake fault system. The Hebgen Lake earthquake on August, 17th 1959, with a magnitude of 7.5 was the strongest earthquake in recent times in the immediate vicinity of the Park (Marler 1964).

The hydrogeochemistry of the Norris Geyser Basin has been investigated and described among others by Ball et al. (2001, 2002) and Fournier et al. (1986, 1992, 1994a, 2002). As mentioned in section 4.1.2, Norris Geyser Basin receives the residual water phase from subsurface boiling of geothermal waters rising from the hypothesized Obsidian Cliff magma chamber (Figure 34). In an enlarged section of Figure 34, Figure 37 shows the hydrogeochemical model derived for Norris Geyser Basin from White et al. (1988). Near-neutral pH waters high in Cl and SiO₂, depleted in CO₂, H₂S, and other gases discharge along the central belt of springs and geysers without substantial dilution by cold water before boiling. Where near-surface mixing with meteoric waters increases S(VI) compared to Cl concentrations, 5-8 μmol/L S₂O₃²⁻ may be found (Xu et al. 1998). Acid waters occur in two belts along the northwestern and southeastern margin of the Norris Geyser Basin, and partly also in the central belt. White et al. (1988) propose that the acid waters result from surface acidification caused by oxidation of H₂S and relative enrichment due to evaporation. Oxidation of elemental sulfur is assumed at least for the eastern belt with a local circulation of water from the Norris dome. Reservoir temperatures underneath Norris Geyser Basin of 270°C to more than 300°C are higher than in other areas in the Park.

Norris Geyser Basin undergoes an annual basin-wide hydrothermal disturbance that occurs commonly in late summer (August / September). It is expressed in small hydrothermal explosions, a sudden increased discharge of thermal water and steam, an increased turbidity, and extreme fluctuation

tuations in temperature of many hot springs. Increased boiling also leads to enrichment in dissolved constituents in many hot springs. Observations by Fournier et al. (2002) during the seasonal disturbance in 1995 revealed that the disturbances only affected the hot springs from relatively deep reservoirs in the central belt. The chloride hot springs with near-neutral pH picked up an acid-sulfate component and became isotopically heavier for several days after the onset of the disturbance, indicating subsurface mixing. Initially acid waters and near-neutral pH waters from shallower reservoirs showed little response to the disturbance.

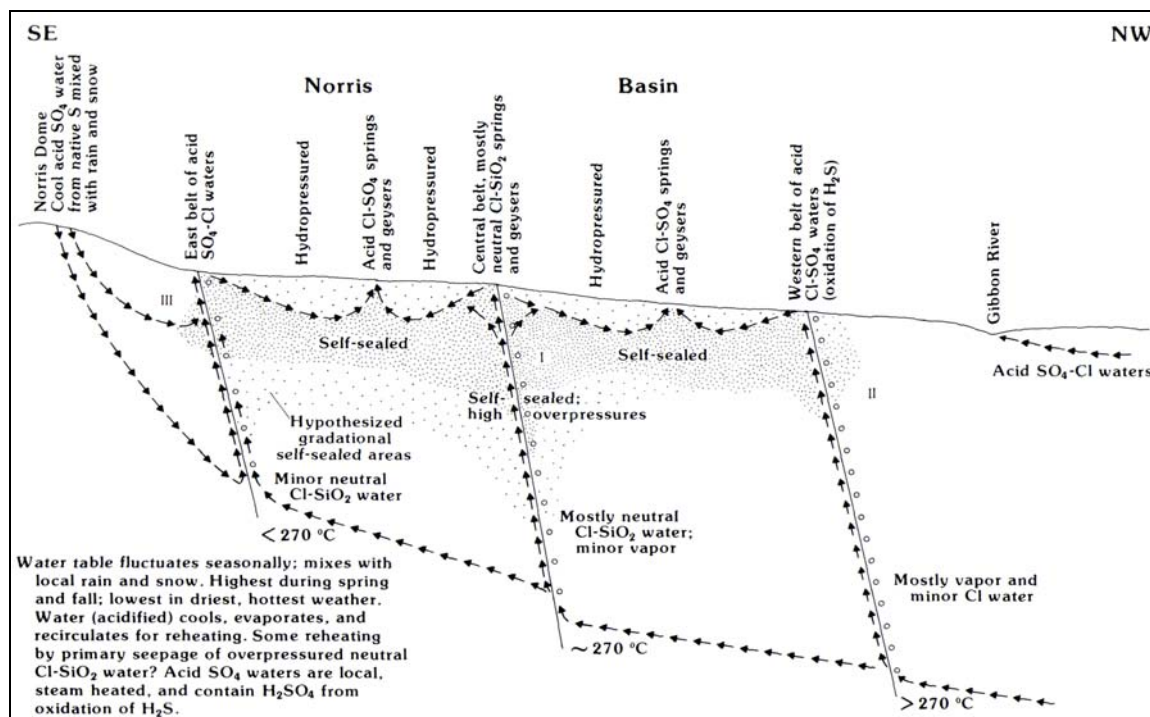


Figure 37 Schematic model of water types at Norris Geyser Basin (White et al. 1988)

According to models from different research groups, several factors trigger the seasonal disturbance. A seasonal scarcity in meteoric water results in minor dilution and consequently supersaturation of geothermal fluids especially with respect to silica minerals (White et al. 1988). High deposition rates lead to an increased rate of self-sealing. This self-sealed silica layer that can be identified in most of the research drill holes in the Park significantly decreases permeability (Dobson et al. 2003), increases the build-up of overpressure and finally leads to hydrofracturing followed by small hydrothermal explosions. Flow channels clogged by clay mineral deposition might produce similar effects. Deformation and fracturing induced by tectonic forces are additional, less frequent processes responsible for pressure changes within the hydrothermal system. Yet, the most important seasonal trigger is the fluctuation of the local potentiometric surface. A lower water table in summer leads to a decreasing pressure from the overlying cold water column. The boiling point within the hydrothermal system drops. In deeper, high-temperature reservoirs, excess heat released from previously heated rock causes evaporative boiling of ascending fluids. Eventually, the pressure at greater depths decreases, since the rate of water expulsion exceeds its supply from the deeper reservoirs. With the decline in pressure, water from shallow reservoirs, where temperatures

are less than the prevailing boiling temperature, can enter the discharge vents without hydrothermal explosions. There they mix with the waters from the deeper reservoirs, producing the change in chemistry of some hot springs described in the previous paragraph. The higher temperature gradients at Norris Geyser Basin with reservoir temperatures of 270°C to more than 300°C compared to lower-temperature gradients at shallower reservoirs as e.g., Lower Geyser Basin (200-125°C) might be the reason that the annual disturbance phenomena was only observed at Norris. It might also be a lack of the typical indicator, the distinct turbidity of hot springs at the beginning of the disturbance. This turbidity is owed to clay from acid altered rocks that are widely distributed at Norris but scarce at other Geyser Basins (Fournier et al. 2002).

Ragged Hills, the area investigated within the Norris Geyser Basin, is located about 1 km west of the Norris parking lot (Figure 38). It is one of the most recent and most dynamic geothermal areas in the Park with an anomalously high total heat flow.

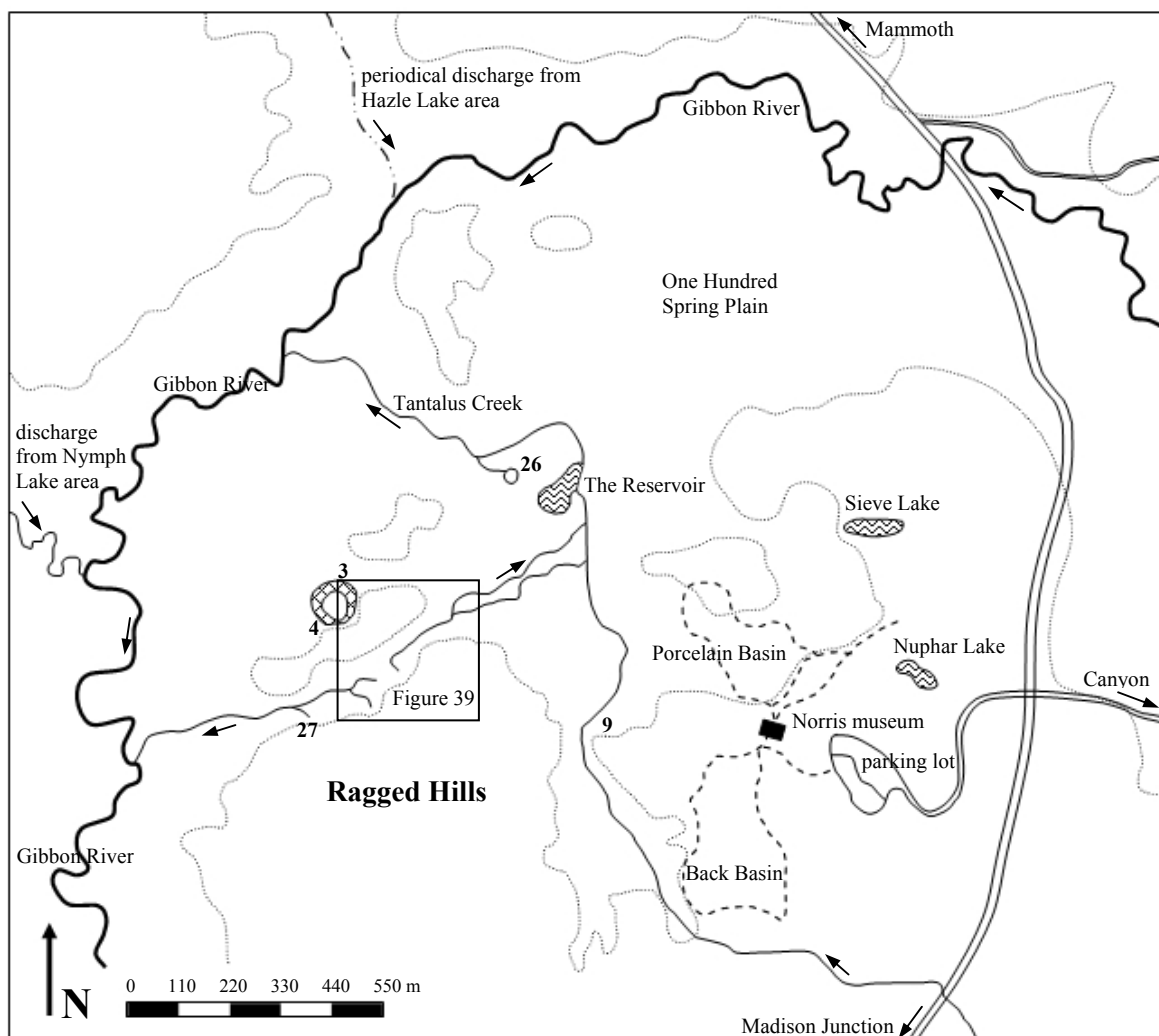


Figure 38 Overview Norris Geyser Basin with Ragged Hills area; numbers 3, 4, 9, 26, and 27 indicate sampling sites YNPRH03, 04 (“Verde Pool” located in a hydrothermal explosion crater), YNPRH09, YNPRH26 (“Dragon Spring”), YNPRH27 (“Steam Engine”); dotted lines = 7500 ft altitude; dashed lines = boardwalk through Back Basin and Porcelain Basin; inset The Gap (Figure 39)

The Ragged Hills are low hills of hydrothermally cemented older Pinedale kame deposits. Their crude stratification, chaotic bedding and cross stratification, lateral discontinuity of bedding and slump structures are typical for their formation beneath a glacier by melting of the ice due to hot spring activity. A detailed geological overview including a map of a scale of approximately 1:2,300 is provided by White et al. (1988).

In the northern part of the Ragged Hills area, about 1.2 km west of the Norris parking lot, and 400 m east of the Gibbon river, a crater-like structure with a rim of Lava Creek Tuff is interpreted as a hydrothermal explosion crater thought to have formed during the waning stage of the last glaciation (Muffler et al. 1971; White et al. 1988; Figure 38). Rapid draining of a local lake lowered the hydrostatic head to such an extent that pore water flashed to steam, producing an explosion. Today, the drainageless structure contains hot water of greenish-turquoise color, “Verde Pool”.

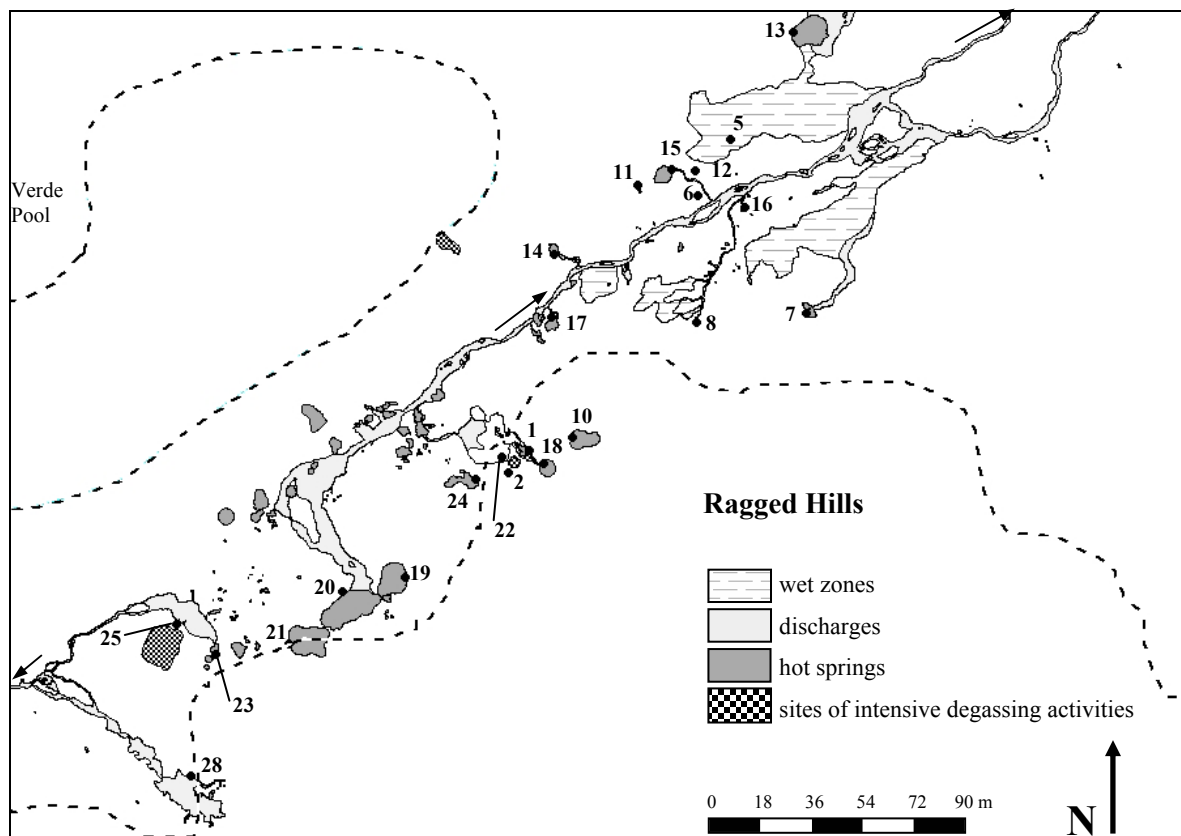


Figure 39 Ragged Hills, The Gap (insert of Figure 38; modified from Becker 2004); numbers 1, 2, 5-8, 10-25, and 28 indicate sampling sites YNPRH 01 (“Milky Way”), YNPRH02, YNPRH05-07, YNPRH08 (Crystal Springs), YNPRH10 (“Rainbow Growler”), YNPRH11-12, YNPRH13 (“Elk Geyser”), YNPRH14-16, YNPRH17 (“Dynamo”), YNPRH18 (“Kaolin Spring”), YNPRH19 (“Persnickety Geyser”), YNPRH20 (“Titanic Spring”), YNPRH21 (“Lifeboat Spring”), YNPRH22-25, YNPRH28 (“Milky Way II”); dashed lines = 7500 ft altitude

In a small area south of “Verde Pool” called The Gap an increase in temperatures was recognized from 1992 to 1995. Small seeps and springs appeared before intense hydrothermal activity began in 1995 with several eruptions (Figure 38, Figure 39). The western part of The Gap is drained directly towards Gibbon river. The drainage of the eastern part joins Tantalus Creek in the One Hundred Spring Plain before finally discharging to Gibbon river, approximately 1 km further north than the western drainage. In 1995, three springs erupted in an area of 20 by 50 m (Ball et al. 2002). Several later eruptions especially in 1999 led to a rapid growth of the thermal area that measured 270 m by 2150 m in the year 2000. The increased activity in 1999 correlates with a peak in the annual number of earthquakes (3,172 compared to less than 1,500 in the preceding four years). Ball et al. (2002) photo-documented significant changes and an increase in geothermal activity in The Gap from 1999 to 2001. “Persnickety Geyser” was a separate geyser in 1999 but now overlaps with “Titanic Spring”. The small land bridge between “Titanic Spring” and “Lifeboat Spring” subsided. During the winter 2002/2003 a discharge breakthrough formed from “Kaolin Spring” to “Milky Way”. The hydrogeochemistry of the waters in the whole Ragged Hills area covers a wide range from acid to near-neutral pH, from a predominance of S(VI) to Cl, and As concentrations of 0.2 to 9 mg/L (Ball et al. 2001, 2002).

4.1.2.4 Gibbon Geyser Basin

Geothermal activity in the Gibbon Geyser Basin is attributed to the Norris dome near the vent dome of the 90,000 year-old Gibbon river flow (White et al. 1988; Figure 34). Gibbon Geyser Basin comprises the geothermal areas of Gibbon Hill Geyser in the north, Sylvan Springs west of the road Norris-Madison Junction, and Artist Paint Pots and Geyser Springs group east of the road. Geyser Springs group that was investigated in this study lies 1.3 km east of the road Norris-Madison Junction, 0.6 km southeast of Artist Paint Pots, at the eastern side of the 2455 m (8054 ft) high Paintpot Hill (Figure 40). The whole geothermal area is approximately 600 m long, and at the maximum 150 m wide. The hot springs are distributed over four levels at altitudes of about 2286 m (7500 ft), 2298 m (7540 ft), 2310 m (7580 ft) and 2316 - 2347 m (7600 - 7700 ft). The most prominent feature is Avalanche Geyser at the southeastern most tip of the first level with an eruption interval of about 9-10 minutes and eruption durations of 2.5-3 minutes. The Geyser Springs group area is drained by Geyser creek that rises 1.8 km SSE from Avalanche Geyser, and discharges together with the discharge from Gibbon Hill Geyser group into the Gibbon river. Both acid, sulfate-rich and near-neutral pH, chloride-rich hot springs are present at the Geyser Springs group. Arsenic concentrations range from about 0.1-0.3 mg/L in the acid springs to 1.9-2.4 mg/L in the near-neutral pH springs (Ball et al. 1998a, 2001).

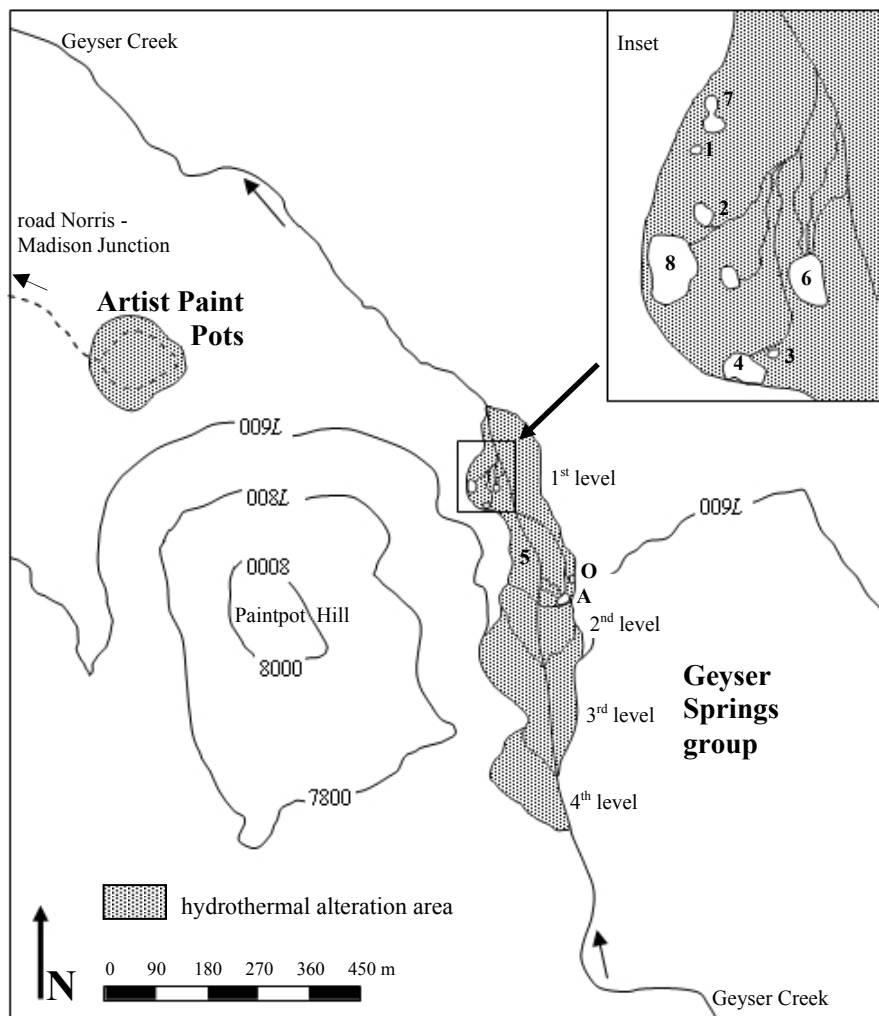


Figure 40
Geyser Springs group in the Gibbon Geyser Basin; numbers 1-8 indicate sampling sites YNPGG01 - YNPGG08; 7600, 7800 and 8000 are altitudes in feet; A = Avalanche Geyser; O = Oblique Geyser; 6 = "Bull's Eye"

4.1.2.5 Lower Geyser Basin

Pocket basin is located on the right (northwest) side of the Firehole river in the western part of the Lower Geyser Basin, about 1.5 km west of the road Madison - Old Faithful. It is, like "Verde Pool" in Norris Geyser Basin (section 4.1.2.3), interpreted as a hydrothermal explosion feature (Muffler et al. 1971). The shallow reservoir temperature underneath Lower Geyser Basin of 200-215°C is significantly cooler than in the Norris-Mammoth corridor. The geothermal waters of Lower Geyser Basin are typically alkaline, low in chloride, and high in bicarbonate as a result from dilution of the deep Cl-rich hydrothermal solutions with cold groundwater before subsurface boiling (Ball et al. 1998a, 1998b, 2001; Kennedy et al. 1987; Stauffer and Thompson 1984; Truesdell and Thompson 1982). In one hot spring within Pocket Basin, Azure Spring (Figure 41), significantly increased concentrations of $S_2O_3^{2-}$ (55 $\mu\text{mol/L}$) were found besides concentrations of 10.6 $\mu\text{mol/L}$ H_2S . The high thiosulfate concentrations might be explained either by oxidation of H_2S from thermal fluids that mix with oxygenated ground waters before they reach the surface or by hydrolysis of elemental sulfur and interaction with sulfate-bearing minerals that could stem from old solfatara deposits underlying the explosion crater (Xu et al. 1998). Total As concentrations are 1-2 mg/L (Ball et al. 1998a, 1998b, 2001; Kennedy et al. 1987; Stauffer and Thompson 1984).

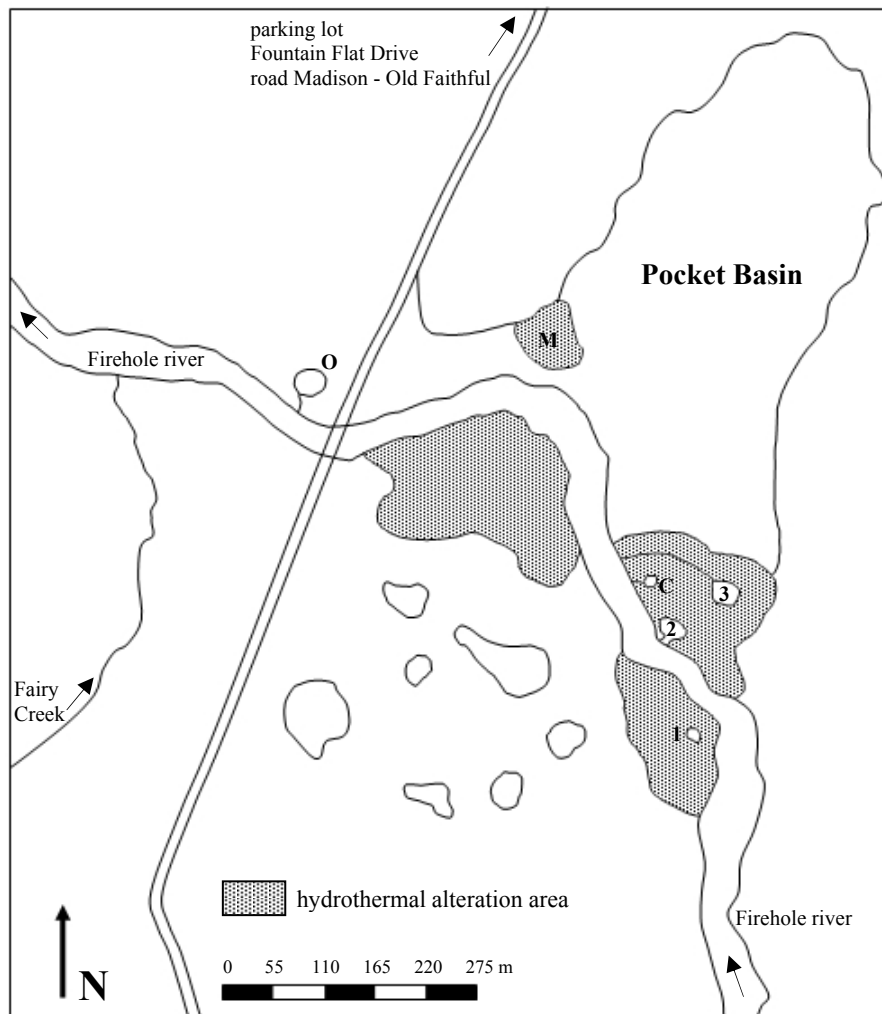


Figure 41
Pocket Basin at the
Firehole river (Lower
Geyser Basin); num-
bers 1-3 indicate sam-
pling sites YNPLG01 -
YNPGG03; 2 = “Bath”
hot spring, 3= Azure
Spring, O = Ojo Cali-
ente hot spring, M =
mud pot, C = “Cavern”
hot spring

4.2 Methodology

Site information, pictures, devices used, and data obtained and corrected, from the sampling of Yellowstone geothermal areas described in the following are presented in an Access database on the enclosed CD (detailed information and instructions see Appendix 9).

4.2.1 Field methods

4.2.1.1 Reconnaissance trip 2002

The field work at Yellowstone was conducted over three sampling campaigns. The first campaign from June, 26th, to July, 2nd, 2002 was a reconnaissance study where sampling focused on dissolved and volatile As species only. Ragged Hills (9 sites), Hazle Lake (3 sites), and Frying Pan Spring (2 site) were selected as the first study areas. Ragged Hills was chosen because it is the most active geothermal area in the Park with a wide range of hydrogeochemical conditions, and one of the highest known total As concentrations (section 4.1.2.3). The high Hg methylation capacity previously detected by USGS researchers (section 4.1.2.2; Table 10) made the Hazle Lake area an inter-

esting study site for As methylation and volatilization too. Frying Pan Spring was selected because of its location in the acid alteration area with lower As and high H_2S and $\text{S}_2\text{O}_3^{2-}$ concentrations (section 4.1.2.1). In addition to the three study areas, one mud pot and one hot spring 1.8 km northwest of the parking lot for Norris Geyser Basin were sampled in cooperation with the research group of Dr. Kirk Nordstrom, USGS, Boulder.

Speciation of dissolved As was achieved by the ion exchange technique of Le et al. (2000c), described in section 2.7.2. The ion exchangers were custom-made 5 mL disposable syringes, filled with 1500 mg of cation exchanger material (resin based DOWEX 50WX8 analytical grade, SERVA Electrophoresis, exchange capacity 1.9-2.0 meq/L), and anion exchanger material (silica based DOWEX 1X8 analytical grade, SERVA Electrophoresis, exchange capacity 1.1-1.2 meq/L). Silanized glass wool stoppers were used at the lower and upper end of the cartridges to prevent exchanger material loss. Le et al. (2003c) detected no breakthrough of As(V) when applying 250 mL of a 2 mg/L As(V) solution on 500 mg of a similar silica-based anion exchanger, i.e. the As sorption capacity was more than 500 μg . For the concentration of negatively charged As species expected ($< 0.02 \mu\text{g}$ in 20 mL) this capacity is sufficient even if competing reactions with other ions are considered. Before sampling, the ion exchangers were conditioned with 6 mL 50% methanol, then rinsed with 6 mL distilled H_2O and kept wet until use. Arsenic separation was performed on site immediately after taking a 20 mL water sample with a disposable syringe. The sample was filtered through a 200 nm cellulose acetate filter (Membrex) before passing the cation and anion exchanger. Flow velocity was approximately 0.5-1 mL/min. The filtrate was collected in a 50 mL PE bottle. All bottles used in the field were new, cleaned with HCl and rinsed with deionized water in the laboratory before use. The ion exchange cartridges were separated, wrapped in aluminum foil and stored in the refrigerator together with the PE bottles until elution at the most 4 weeks later. Own experiments and those of Le et al. (2000c) confirm that As on the exchangers can be quantitatively recovered after that time.

Volatile metalics were sampled with the optimized screening method described in section 3.2.2. For trapping, PTFE bottles containing 100 mL of a 1:100 diluted NaOCl solution were used. Raschig rings were added to increase reaction times. Sampling was performed both inside the hot springs via the PTFE collector cells described in section 3.1, and above the hot springs via inverted polyethylene (PE) household boxes as has been described for other projects before (section 2.7.5.1). For sampling volatile metalics dissolved in water, the collector cell inside the hot spring was attached to a 400 mL PTFE bottle via a PTFE capillary that directed the gases inside to the bottom of the bottle. A pump was connected by a valve to the second connection of the PTFE bottle. Approximately -350 mbar vacuum was applied to the whole system and the valve was closed, so that the vacuum could only be replaced by gas flow through the membrane of the collector cell. The vacuum container originally designed (Figure 17) had to be dismissed due to transport restrictions. The upper half of the 400 mL oxidizing bottle that was only half-filled with oxidizing solution, was used as vacuum space instead. The equipment was left in the field for 1-4 days for cumulative sampling. Whenever the vacuum was equalized (i.e. when a gas volume of approximately

200 mL · 0.35 = 70 mL had replaced the vacuum), vacuum was applied again. After sampling, the oxidizing bottle was detached from the collector cell, and the Raschig rings separated from the oxidizing solution by a sieve. The oxidizing solution was collected in 50 mL PE bottles, and stored in the refrigerator at 6°C until analysis.

The collector cell method turned out to be only successful in a few places with low temperatures, such as Hazle Lake. Especially in the hot springs at Ragged Hills, high temperatures deformed the teflon, widened the tight connections, and finally led to water breakthrough. For further sampling, the collector cells were dismissed and only gas samples were taken. The inverted polyethylene (PE) boxes used as gas hoods were approximately 30 cm long, 20 cm wide, and 10 cm high. Hot springs were only sampled where the water was shallow enough (few centimeters of water depth) to place the inverted PE boxes on the ground fixed by some stones. Surrounding water provided a gas-tight seal, so that gas could only leave the inverted PE box through the teflon tube outlet on top of the box connected to the oxidizing bottle. The outlet of the oxidizing bottle was left open. A T-shaped, open valve was used to protect the oxidizing solution from contamination by dust and rain (see also Figure 42). No active pumping was applied to this gas sampling setup and no gas flow was detected at the outlet of any oxidizing unit. Obviously, the pressure built up underneath the gas hood was insufficient to overcome the backpressure of the approximately 20 cm high column of oxidizing solution. Thus, trapping of volatiles was based only on equilibration of concentration gradients between the gas phase under the gas hood, and the oxidizing solution by diffusion. No species-selective sampling was done.

During the reconnaissance trip, volatile As was detected in all study areas. It was the first discovery of volatile As in the Park.

4.2.1.2 Sampling trips 2003

Based on the positive results from 2002, two hydrogeochemical sampling campaigns were carried out from June 5 to July 16 and from September 2 to October 12, 2003. In the water samples, temperature, pH, conductivity, redox potential, dissolved oxygen, Fe(II)/Fe(tot), S(-II), SiO₂, As species (As(III) / As(V) / MMAA / DMAA), major anions, and cations, trace elements, TIC, and TOC were determined. Gas samples were analyzed for volatile HCl, H₂S, and volatile metallics as the sum of all species oxidized in NaOCl, and species-selective for As. Besides re-sampling Ragged Hills and Hazle Lake, studies were extended from Frying Pan Spring to the Nymph Lake area, including the recently appeared fumaroles on the north side of the lake, and to two new study areas. Geyser Spring Group in the Gibbon Geyser Basin, located on the south side of Norris dome, shows a wide variety of hydrogeochemical conditions and As concentrations from 0.1-2.4 mg/L like Norris Geyser Basin. However, it does not seem as dynamic as Ragged Hills at the moment, and no seasonal variations in geothermal activity have been detected there yet (section 4.1.2.4). Pocket Basin in Lower Geyser Basin was the only study area that was located within the Yellowstone caldera and showed high As concentrations in alkaline waters (section 4.1.2.5). A total of 6 sites in the Nymph Lake / Frying Pan Spring area, 3 sites at Hazle Lake, 28 sites at Ragged Hills, 8 sites at

Geyser Spring Group, and 3 sites in the Pocket Basin were sampled one to three times during the two campaigns in 2003. Appendix 10 gives an overview of the parameters investigated at each site. Details on sample preparation, devices and methods used, as well as necessary corrections done are explained in Appendix 9 and together with the respective data in the digital database.

Sampling sites were located by a handheld GPS (Garmin-12). In the Ragged Hills area a differential GPS (Pathfinder Pro XR Trimble) with a higher precision was used during a GIS-project on high resolution mapping of the geothermal features (Becker 2004). Water temperature, conductivity, pH, redox potential and dissolved oxygen were determined on site with a WTW (Wissenschaftlich-Technische Werkstätten GmbH Weilheim) MultiLine P4 device by immersing probes directly into the source. Water temperature was measured both with the SenTix 97/T pH electrode and the TetraCon 325 conductivity cell. Generally, mean values of the two readings were taken. Both the redox Pt 4805/S7 probe and the Cellox 325 probe quit working at temperatures $>50^{\circ}\text{C}$ and measurements were dismissed for most samples with higher temperatures. Occasionally redox potential and dissolved oxygen were measured in a container after cooling down to $<50^{\circ}\text{C}$. However, because no flow-through cell and pump were available, these values are questionable. The redox potential measured against a Ag/AgCl electrode was corrected for standard hydrogen potential and temperature according to the following equation based on information provided by the manufacturer (WTW): $E_{\text{H}}(\text{corrected}) = E_{\text{H}}(\text{measured}) + (-0.7443 \cdot \text{temperature } [^{\circ}\text{C}] + 224.98)$.

Total Fe, Fe(II), SiO_2 , and S(-II) were determined on site by field photometry. A 20 mL disposable PE syringe rinsed 5 times with sample water was used to withdraw 10-25 mL sample directly from the sampling site. The sample was immediately filtered through a 200 nm cellulose acetate filter (Membrex) and analyzed with a HACH photometer DR/890 applying the FerroVer, 1,10-phenanthroline, silicomolybdate, and methylene blue method for total Fe, Fe(II), SiO_2 , and S(-II) respectively. The Fe(III) concentration was afterwards calculated as the difference between total Fe and Fe(II).

Commercial cation and anion exchangers were used for dissolved As speciation during the 2003 sampling campaigns. The strong resin-based cation exchanger with a particle size of 45-150 μm , and an exchange capacity of 1.9 meq/mL was obtained from Alltech, the silica based anion exchanger with a particle size of 50 μm , and a total capacity of 0.14 meq/g from Supelco. The 4 mL cartridges contained 500 mg exchanger material between 1 mm thick, porous disks. The disks proved advantageous compared to the glass wool plugs in the homemade exchangers used in 2002. They provided more uniform packing heights and caused no distortion of the exchanger material when applying the sample. As for on-site photometry, 20 mL sample were withdrawn from the sampling site by a disposable PE syringe and filtered through a 200 nm cellulose acetate filter (Membrex) before passing the ion exchangers with a flow rate of approximately 0.5-1 mL/min. The As(III) was collected in a 50 mL PE bottle. The ion-exchange cartridges were separated, wrapped in aluminum foil and stored in the refrigerator at 6°C together with the PE bottles until elution in the laboratory at most 4 weeks later.

All bottles used for sampling were soaked with 10% HNO₃ and rinsed with deionized water in the laboratory prior to sampling. Samples were taken unfiltered for IC (200 mL PE bottle), unfiltered for TOC/TIC (100 mL glass bottle), and filtered through a 200 nm cellulose acetate filter (Membrax) and stabilized with 1 mL HNO₃ suprapur (50 mL PE bottle) for ICP-MS, ICP-AES, and HG-AAS and GF-AAS. The bottles for IC and TOC/TIC were rinsed 5 times with unfiltered sample water, the bottles for ICP-MS, ICP-AES, HG-AAS, and GF-AAS with filtered sample water before filling them completely. Filtration was done immediately after withdrawing the sample from the sampling site with a disposable 20 mL PE syringe. At selected sites, Hg samples were taken. For inorganic Hg the water sample was filtered through a 200 nm filter into a glass bottle and 5 mL HNO₃ were added directly in the field. The methylated Hg samples were filtered through a 200 nm filter into a PE bottle, and 10 mL 50% HCl were added to 500 mL sample upon return from the field the same day.

After the experiences from the 2002 reconnaissance trip, volatile As was sampled with gas hoods only, and trapped in 100 mL of 1:100 diluted NaOCl. The gas hoods used were inverted PE boxes of different sizes (33 x 24 x 8 cm, 30 x 20 x 10 cm, diameter 30 cm x 13 cm). The equipment was left outside for 52 to 262 hours for cumulative sampling. Oxidizing solutions were then refilled in 50 mL PE bottles, and stored in the refrigerator at 6°C until analysis. Furthermore, PTFE bottles with 100 mL of a 0.1 N NaOH solution were used to oxidize and dissolve volatile HCl. The NaOH concentration was lower than cited in Giggenbach (1975) or Fahlquist and Janik (1992) who use 4 N NaOH. However, those experiments were done by purging a bubbling gas stream through the trapping solution, resulting in short reaction times. As mentioned before, the gas sampling described here was based on diffusion without apparent gas flow and with longer reaction times. Lower NaOH concentrations are advantageous since they show less matrix effects during analysis. After cumulative sampling, the NaOH solutions were also stored in 50 mL PE bottles in the refrigerator at 6°C until analysis.

Mainly during the third sampling campaign, different setups of gas hoods and oxidizing bottles were tested to determine:

- the decrease in concentration of volatile metallics above a sampling site by comparing the concentrations directly above the sampling site taken from within a gas hood to concentrations in ambient air approximately 25 cm above the sampling site taken without any funnel device (setup 1 and 3, Figure 42)
- the effectiveness of gas diffusion and dissolution in setups with the tube immersed in the oxidizing solution compared to setups where the tube is left in the headspace above (setup 1 and 2, Figure 42)
- the potential of contamination when preparing and re-filling the oxidizing solution in the field (field blank; setup 4, Figure 42)

Three samples of setup 1 (YNPNL02-1G; YNPNL03-3G; YNPRH11-4G), one sample of setup 2 (YNPRH23-4G), and one sample of setup 3 (YNPRH11-4G) were not considered for further inter-

pretation, since the rubber sealing of their oxidizing bottle was displaced and contamination of the sample could not be excluded.

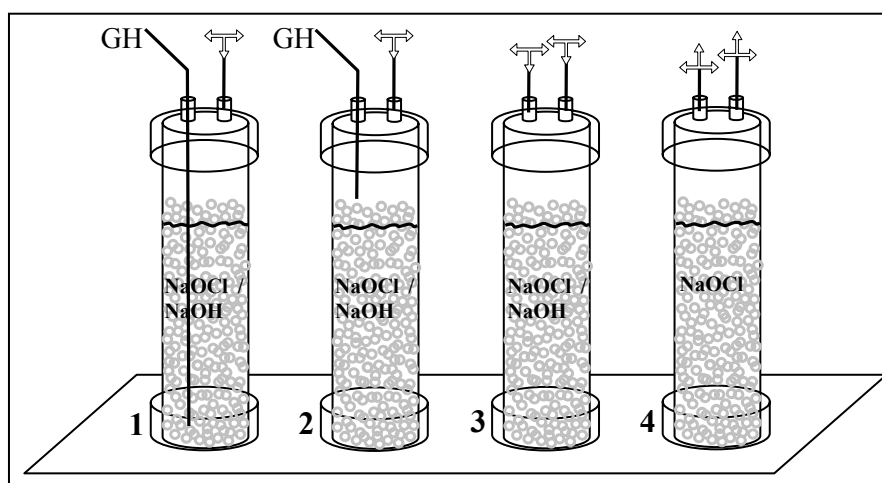


Figure 42 Different setups for diffusive sampling (setup 1-3); setup 4 was used to check accidental contamination effects

- 1 = Standard setup: tube from the gas hood (GH) is immersed in the oxidizing solution, outlet (on the right) of the PTFE bottle is protected with an open T-shaped valve from contamination from outside [samples: 51 NaOCl, 37 NaOH]
 2 = Headspace: PTFE bottle is connected to a gas hood (GH), but tube ends in the headspace above the oxidizing solution; outlet: open T-valve [samples: 4 NaOCl, 2 NaOH]
 3 = no gas hood, oxidizing bottle left with 2 open T-valves adjacent to the sampling site [samples: 19 NaOCl, 10 NaOH]
 4 = no gas hood, oxidizing bottle left with 2 closed T-valves adjacent to the sampling site (field blank) [sample: 1 NaOCl]

In addition, flat PE boxes (10 x 10 x 3 cm and \varnothing 7 cm x 3cm) filled with 100 mL 1:100 diluted NaOCl were placed adjacent to sampling sites at Hazle Lake (YNPHL01, 03), Frying Pan Spring (YNPNL02, 03, 04), and Ragged Hills (YNPRH01, YNPRH10). A PE lid was fixed on top of the “diffusion bowls” (DB) to prevent dust and particles from entering the oxidizing solution. Tiny rubber stoppers taped on the rim between PE lid and bowl left a 1 mm slit open for gas diffusion. The DBs were thought to be advantageous compared to the oxidizing bottles due to their larger reaction surface, however, significant evaporation losses were encountered for the oxidizing solution inside and samples could only be obtained from 21 of 43 setups (for details see digital database, and Appendix 9).

At four sites (YNPGG04, YNPHL01, YNPRH01, and YNPRH06), gas samples were obtained through gas hoods by active gas pumping with a Dräger hand pump (volume per stroke 0.1 L). Total volumes of 5 to 20 L were sampled in a period of 1 to 4.5 hours. An additional PTFE bottle was used as H₂O trap before the oxidizing solution. The amount of condensed water from the hot gases was 150 to 300 mL.

For species-selective sampling of volatile As, solid sorbents and SPME fibers as described in section 3.2.3 were used. The solid sorbents were custom-made single bed tubes of 250 mg Carboxen 564 mounted behind commercial SKC Tenax TA double layer tubes (Appendix 4). The Tenax TA tubes served as a pre-separation step to trap larger molecules in the gas samples, so that the Carboxen was supposed to be exclusively loaded with substance of higher volatility especially the target element As. Because no GC-MS with desorption port was available in the vicinity of the

study area, the tubes were wrapped in aluminum foil, and stored in a refrigerator at 6°C until they were sent to Germany by express mail. The analyses were performed 9 to 15 days later.

Because of their different performance in trapping individual As species, three different SPME fiber types (PDMS 100, PDMS-CAR, PDMS-CAR-DVB) were used. For the field application, a 2 mL plastic syringe was used as fiber holder (Figure 43). The fiber is protected inside the syringe's needle. The syringe plunger is used to press the spring together and expose the fiber inside the needle. The third way of the T-shaped valve works as an open gas outlet. A PE tube attached over the needle to the T-shaped valve connects the fiber holder to the gas hood (GH)

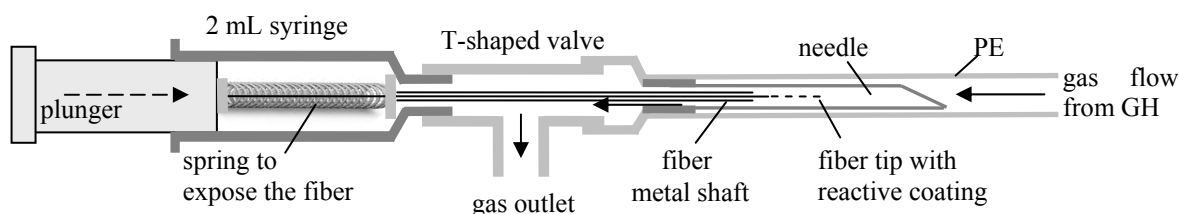


Figure 43 Custom-made SPME fiber holder for field application (fiber is protected inside the syringe needle; syringe plunger is used to expose the fiber; third way of T-shaped valve functions as gas outlet)

4.2.2 Laboratory

Ion exchangers for As speciation were eluted in the laboratory at the Technische Universität Bergakademie Freiberg. A volume of 10 mL of 60 mM acetic acid was used to desorb MMAA from the anion exchanger. Using 10 mL provided an enrichment factor of 2 compared to the 20 mL sample applied to the exchangers in the field resulting in a higher accuracy and lower detection limits. The As(V) left on the exchanger was eluted with 1N HCl applied in 10 mL steps until As concentrations in the eluent dropped below detection limit. Similarly, DMAA was desorbed from the cation exchanger in 10 mL steps with 1 N HCl. The acetic acid, HCl eluents, and the water sample with the As(III) fraction were analyzed by a Zeiss AAS EA4 spectrometer using graphite furnace with platform technique. Calibration was done with matrix-matched standards. Total As was analyzed separately from a filtered and HNO₃-acidified sample. Detection limits, quantification limits, and upper calibration ranges for this and all following determinations are given in the digital database as well as results from double and triple determinations and verification of reference material for quality control.

The TOC and TIC were determined in Freiberg with a LiquiTOC (Elementar Analysensysteme GmbH). Concentrations of Cl, S(VI), F, Br, and N(V) were determined by IC (Dionex model 2010i ion chromatograph with AG4A guard and AS4A separator columns and an anion micromembrane suppressor-II column; eluent: 0.018 M NaHCO₃ + 0.017 M Na₂CO₃) at the U.S. Geological Survey laboratories in Boulder, Colorado. Some samples were re-analyzed at the Technische Universität Bergakademie Freiberg with a Merck Hitachi D 6000 (conductivity detector; eluent: anions: 415 mg/L phthalic acid + 278 mg/L tri(hydroxymethyl)-aminomethane; cations: 167 mg/L pyridine-2,6,dicarbonicacid + 750 mg/L 2,3 dihydroxyamberacid).

The ICP-AES (Leeman Labs Direct Reading Echelle, dual view, sequential, multi-element, inductively coupled plasma spectrometer, Hildebrand grid nebulizer, glass Scott spray chamber) at the USGS laboratory was used to measure As, Al, B, Ba, Be, Ca, Cd, Co, Cr, Cu, Fe, K, Li, Mg, Mn, Mo, Na, Ni, Pb, Si, Se, Sr, V, and Zn. Information about scan mode (axial or radial), and wavelength for each element as well as about control material is given in the digital database. Selected samples were sent to Activation Laboratories, Canada (accredited by ISO 17025), for ICP-MS analysis on Li, Be, Na, Mg, Al, Si, K, Ca, Sc, Ti, V, Cr, Mn, Fe, Co, Ni, Cu, Zn, Ga, Ge, As, Se, Br, Rb, Sr, Y, Zr, Nb, Mo, Ru, Pd, Ag, Cd, In, Sn, Sb, Te, I, Cs, Ba, La, Ce, Pr, Nd, Sm, Eu, Gd, Tb, Dy, Ho, Er, Tm, Yb, Lu, Hf, Ta, W, Re, Os, Pt, Au, Hg, Tl, Pb, Bi, Th, and U (code 7, natural waters). Mercury was analyzed by cold-vapor atomic-fluorescence spectrophotometry (CVAFS) with a PS Analytical, model Galahad, at the USGS in Boulder, Colorado (Dr. Howard E. Taylor).

The NaOCl gas samples were analyzed by IC in Freiberg for dissolved S(VI). The ICP-AES in Boulder was used to analyze the NaOCl samples for the elements mentioned before. The HG-AAS in Boulder (Perkin-Elmer Analyst 300 with a FIAS-100 flow injection analysis system hydride generator) was applied to determine As concentrations. Pre-reduction was initially done with 1.2 mL 10% HCl, and 0.5 mL KI in ascorbic acid on 0.5 mL sample (diluted to a total of 5 mL with deionized H₂O). Because the June / July samples showed a greater variance between multiple determination, reducing agents were doubled for the September / October samples and the samples were allowed to pre-reduce for 1 hour before analysis to achieve a reproducible, complete reduction. Selected gas samples were sent for ICP-MS analysis to Actlabs. For NaOCl samples from diffusion bowls only the main target element As (HG-AAS) was determined due to the low amount of sample volume. Chloride in the NaOH samples was titrated in Freiberg by the mercury thiocyanate method. In adaptation of the standard procedure, the 0.1 N NaOH samples were first neutralized to pH 7 with 40 μ L HClO₄ per 5 mL sample. The samples were diluted with 20 mL H₂O before the mercury thiocyanate reaction.

Solid sorbents were analyzed in Freiberg with the Bruker mobile GC-MS EM 640 and the optimized conditions listed in Table 8. The SPME fibers were analyzed at the United States Federal Center in Denver, Colorado with a Varian 3400 in June/July 2003, and a Varian CP 3800 in October 2003. Both times the column was a HP5ms (L=30 m, ID=0.25 mm, fd=0.25 μ m). Optimized conditions for SPME analysis can be found in Table 9. Additionally, in September and October 2003 analyses were conducted with a HP 5890 GC-MS with a DB 5 column (L=30m, ID=0.32mm, fd=0.25 μ m) at the Department of Chemistry, Montana State University, Bozeman.

4.2.3 Data processing

4.2.3.1 Water data check

All water analyses were checked for accuracy by calculating the charge imbalance with the hydro-geochemical modeling program PHREEQC 2.8.03 (Parkhurst and Appelo 1999) and the database

WATEQ4F (V.2.4 with revised data from Nordstrom and Archer 2003) using the following equation:

$$\text{percent error} = \frac{100 * (\Sigma \text{cations}[\text{meq/L}] - \Sigma \text{anions}[\text{meq/L}])}{(\Sigma \text{cations}[\text{meq/L}] + \Sigma \text{anions}[\text{meq/L}])}$$

Negative analytical errors indicate a deficiency of cations or a surplus of anions, positive values a surplus of cations or a deficiency of anions. If errors compensate each other, e.g., in an overestimation of both a cation and an anion, they remain undetected with this check. An additional independent accuracy check was therefore applied using the difference between measured and calculated conductivity as proposed by Rossum (1975) and utilized in WATEQ4F (Ball and Nordstrom 1991; Table 11).

Table 11 Statements from accuracy checks of water analyses based on the calculation of the charge balance and a comparison of measured and calculated conductivity

	negative charge balance	positive charge balance
measured conductivity > calculated conductivity	deficiency of cations	deficiency of anions
measured conductivity < calculated conductivity	surplus of anions	surplus of cations

The conductivity is calculated from the equivalent conductance of the individual cation and anions in infinitely dilute solutions and their valence states according to the Kohlrausch Law:

$$G = \Lambda_0 \cdot C - (K_1 \cdot \Lambda_0 + K_2) \cdot C^{1.5}$$

G = conductivity of the solution

C = concentration of the solution

Λ_0 = equivalent conductance

K_1 and K_2 are constants associated with the relaxation of the ion-cloud effect and the electrophoretic effect relative to ion mobility. They are calculated from temperature, viscosity, and dielectric constant of water, and depend on the equivalent conductance and valence of each ion. For 25°C, a viscosity of 0.008949 poise, and a dielectric constant of 78.55 conductivity is calculated as:

$$G = G_{0+} + G_{0-} - \left[\frac{\Lambda_0 \cdot Z_+ \cdot Z_-}{115.2 \cdot (Z_+ + Z_-)} \cdot \left(\frac{2Q}{1 + \sqrt{Q}} \right) + 0.668 \right] \cdot [(Z_+ + Z_-)C]^{1.5}$$

with $\Lambda_0 \cdot C = G_{0+} + G_{0-}$ and $G_{0-} = \Sigma c_- \cdot \zeta_-$ and $G_{0+} = \Sigma c_+ \cdot \zeta_+$; ζ = equivalent conductance

$$Z_- = \frac{\Sigma c_- \cdot z_-^2}{\Sigma c_- \cdot z_-} \quad Z_+ = \frac{\Sigma c_+ \cdot z_+^2}{\Sigma c_+ \cdot z_+}$$

$$\lambda_- = \frac{G_{0-}}{\Sigma c_-} \quad \lambda_+ = \frac{G_{0+}}{\Sigma c_+} \quad \Lambda_0 = \lambda_+ + \lambda_-$$

$$Q = \frac{\Lambda_0 \cdot Z_+ \cdot Z_-}{(Z_+ + Z_-) \cdot (\lambda_- Z_+ + \lambda_+ Z_-)}$$

Extrapolated values for equivalent conductance of H^+ , OH^- , HCO_3^- , CO_3^{2-} , HSO_4^- , SO_4^{2-} , NO_3^- , Cl^- , F^- , Br^- , Na^+ , K^+ , Li^+ , Ca^{2+} , Mg^{2+} , Ba^{2+} , Fe^{2+} , Fe^{3+} , Al^{3+} , and Sr^{2+} in the standard state of infinitely

dilute solutions at 25°C were taken from Rossum (1975), completed by those listed in Coury (1999). Concentrations of each species were determined by speciation modeling with PHREEQC 2.8.03 (database WATEQ4F). For modeling, values below detection limit were replaced by 0.3 · detection limit, missing values were dismissed. Concentrations of H⁺ and OH⁻ were always considered because of the wide range of pH from 1.8 to 8.6 covered by the individual samples. Within the pH range of 5 to 8, neither H⁺ nor OH⁻ will contribute significantly to conductivity. From a total of 60 water samples, 34 samples showed analytical errors less than 2%, 15 samples 2-5%, and 11 samples >5%. The maximum analytical error was 8.3% (detailed results in the digital database).

Based on the results from the data check, all raw data were revised again, some re-analyzed. From double determinations in different dilutions or on different equipment the value with the better fit for the analytical error and a lower range of analysis of measured to calculated conductivity was selected. One of the parameters that was especially carefully checked was pH. In acid waters H⁺ is the predominant cation, and slight changes in the pH can already alter the ion balance significantly. Field pH was generally considered to be the most accurate. In addition, the pH of all samples was measured again in the laboratory. For samples, where the analytical error was more than 2% with the field pH, the laboratory pH was used if it resulted in a better charge balance. If speciation modeling showed a better charge balance with pH adaptations of ± 0.1 pH units, the modeled pH was accepted. Results of the revised pH and adaptations of other raw data are documented and justified in the digital database.

Values from As speciation were checked in comparison with total As determination by GF-AAS in Freiberg and ICP-AES in Boulder. The range of analysis (ROA) from GF-AAS and ICP-AES is 4.4% on average. If concentrations below 100 µg/L are not considered, ROA is 2.5% on average, with a maximum of 7% and a minimum of 0.06%. For concentrations less than 100 µg/L, GF-AAS is the more accurate method. The range of analysis of As calculated from the sum of the four species compared to As from ICP-AES (>100 µg As/L) was 3.1% on average with a maximum of 9%, compared to As from GF-AAS 2.6% on average with a maximum of 11%. Only in one case (YNNL01), the As concentration determined by speciation was obviously too low (107 µg/L compared to 160 µg/L by GF-AAS, and 164 µg/L by ICP-AES). In all other cases, the values were accepted as being in good agreement, considering that analytical errors of 4 single determinations influence the As concentration calculated from the sum of species.

The As speciation technique was originally developed for waters with near neutral to slightly acid pH only (section 2.7.2). It is influenced by the extreme pH some samples have. Below pH 4, part of the As(V) fraction occurs as non-charged complex (Figure 4). This non-charged complex passes the ion-exchanger and is thus (erroneously) determined in the As(III) fraction. For the lowest pH measured (1.94), the non-charged complex presents 60% of the As(V) fraction. Thus, the As(V) concentration might be too low by a factor of 2.5. Since the samples with low pH show As(V) concentrations in the range of a few µg/L only, compared to several 100 µg/L in the As(III) fraction, the error is minimal. For MMAA, the non-charged complex becomes predominant already at a pH below 3.6 (Figure 8). It should thus be expected that a significant amount of MMAA is not sorbed

on the anion exchanger. However, eluted MMAA fractions of 2-19% of all As species with an average of 8% are high compared to concentrations from literature (section 2.5.2.1). Assuming even higher concentrations seems implausible. These reflections could suggest that MMAA was completely bound to the exchanger. Considering that MMAA predominates as non-charged complex at pH below 3.6, an effective binding would require an additional interaction of MMAA with the matrix of the anion exchanger, not only sorption on the functional groups. These hydrophobic interactions are known for DMAA (section 2.5.2.1), but seem less likely for a compound with only one methyl group. Another explanation for the high As concentrations in the MMAA fraction is a co-elution of MMAA and As(V) compounds that are only weakly bound at low pH. Especially for sites where DMAA concentrations are low, the “MMAA” fraction is not much higher than the assumed percentage of non-charged As(V). To be consistent, the terms As(III), As(V), MMAA, and DMAA fraction were used throughout the report according to the method described in section 2.7.2. For interpretation, it has to be considered that only DMAA is positively identified because its sorption is independent of charge. The “As(III) fraction” may contain some non-charged As(V) and MMAA compounds, and thus is more correctly referred to as the fraction of non-charged As species at the individual pH. The “MMAA” fraction is the fraction of weakly bound, negatively charged As. It might contain some As(V) compounds. The “As(V)” fraction consists of the strongly bound, negatively charged As species that presents only a minor part at low pH.

The concentrations of Fe species were compared as determined by on-site photometry and ICP-AES. The overall ROA is 5.8% for Fe concentrations > 0.2 mg/L. On-site determinations were taken for all further modeling, because they contain species information on Fe(II)/Fe(III). Comparison between SiO₂ from on-site photometry and ICP-AES showed a ROA of 8.2% with a systematic error of photometric values being lower than ICP-AES values in 55 of 60 cases. Interference from S(-II) or Fe might be responsible for this reduction. Thus, ICP-AES values were taken for further modeling.

4.2.3.2 Gas concentration conversion

Volatile compounds were trapped in NaOCl and determined as their respective dissolved, oxidized species by GF-AAS or ICP-AES as described in the sections 4.2.1 and 4.2.2. For a quantitative interpretation of volatile compounds degassed from each sampling site, the dissolved concentrations in µg/L had to be converted into gaseous concentrations in µg/m³. Different approaches had to be used for the sites of passive gas sampling with different setups of gas hoods – oxidizing bottles (Figure 42), diffusion bowls, and active gas sampling with pumping.

Passive gas sampling

Passive gas sampling is mainly based on diffusion. The net diffusion rate for a volatile compound depends on its diffusion coefficient, the concentration gradient and the diffusion length according to Fick’s first law:

$$J = -D \cdot \frac{\Delta c}{\Delta x}$$

- J net diffusion rate = mass per time and diffusion area: $J = \frac{m}{t \cdot A}$
- m mass [μg] = concentration of dissolved, oxidized compound [$\mu\text{g/L}$] · volume of trapping solution [100 mL]; analytical precision of mass is about $\pm 5\%$ for Cd, Cr, Co, Pb, Sb, and Se, and $\pm 1\text{-}2\%$ for all other elements, including As
- t exposure time (for the 2003 sampling between 52 to 262 hours) [s]
- A diffusion area; flow cross-section of tube connecting sampling site and trapping solution; tube diameter = 2 mm ($r = 0.1$ cm); $A = r^2 \cdot \pi = 0.0314$ cm² [cm²]
- D diffusion coefficient [cm²/s]
- Δc concentration gradient between sampling site and trapping solution [$\mu\text{g/cm}^3$]
- Δx diffusion length; length of the tube connecting sampling site and trapping solution [cm]

Assuming a 100 % effective dissolution and oxidation, the concentration of the volatile compound in the trapping solution and at the gas-solution interface is 0 during the whole sampling time. Thus, the concentration gradient Δc equals the concentration c at the sampling site in $\mu\text{g/cm}^3$:

$$c = \frac{m \cdot \Delta x}{t \cdot A \cdot D}$$

The diffusion coefficient varies for individual gases and with temperature. If no values are available from literature, as in the case of all volatile As species, the Fuller, Schettler and Giddings (FSG) equation can be used for a semi-empirical estimation of the diffusion coefficient based on molecular volumes (Fuller et al. 1966; Tucker and Nelken 1990):

$$D = 0.001 \frac{T^{1.75} \cdot M_r^{0.5}}{P \cdot (V_A^{1/3} + V_B^{1/3})^2}$$

- D diffusion coefficient [cm²/s]
- T absolute temperature [K] above sampling site, estimated as the average of water temperature at the sampling site and average ambient air temperature (15°C); for the small fumaroles, where no water temperature was measured, an average temperature of 45°C was assumed
- Mr $M_r = \frac{M_A + M_B}{M_A \cdot M_B}$
- M_A = molecular weight of air (approximately 28.97 g/mol)
- M_B = molecular weight of compound of interest [g/mol]
- P pressure [bar]
- V_A molar volume of air (approximately 20.1 cm³/mol)
- V_B molar volume of the compound of interest [cm³/mol] = molecular weight [g/mol]: vapor density [g/cm³]

Typical values for diffusion coefficients of inorganic and organic gases in air are between 0.1 to 0.2 cm²/s. To achieve a higher accuracy, information about the exact composition of the gas including the percentage of each species for each element (e.g., AsH₃, MMA, DMA, TMA, etc.) would be needed. A sensitivity analysis was done for volatile As, assuming an uncertainty of $\pm 10^\circ\text{C}$ for the

temperature estimation above the sampling site, and the two extreme cases that all volatile As is present as the lightest volatile As species AsH_3 ($M_B = 77.945 \text{ g/mol}$; $V_B = 77.945 \text{ g/mol} : 2.70 \text{ g/cm}^3$ [Sax 1986] = $28.87 \text{ cm}^3/\text{mol}$) or as the heaviest volatile As species AsCl_3 ($M_B = 181.28 \text{ g/mol}$; $V_B = 181.28 \text{ g/mol} : 6.25 \text{ g/cm}^3$ [Clayton and Clayton 1981] = $29 \text{ cm}^3/\text{mol}$). Calculated diffusion coefficients ranged from $0.115 \text{ cm}^2/\text{s}$ to $0.172 \text{ cm}^2/\text{s}$ with a mean of $0.147 \pm 0.015 \text{ cm}^2/\text{s}$. This maximum deviation of 10% shows that neither temperature nor species are very sensitive parameters. Thus, a mean value from the four calculations was taken for each sampling site. The diffusion coefficients calculated for As were also accepted as an approximation for the other volatile compounds determined by ICP-AES. For all volatile Cl determined from the NaOH trapping solution, volatile HCl was assumed to be the only gaseous species ($M_B = 36.461 \text{ g/mol}$; $V_B = 36.461 \text{ g/mol} : 1.268 \text{ g/cm}^3$ (Merck 1983) = $28.75 \text{ cm}^3/\text{mol}$). Considering a temperature inaccuracy of $\pm 10^\circ\text{C}$, diffusion coefficients were between 0.145 and $0.196 \text{ cm}^2/\text{s}$ with a mean of $0.176 \pm 0.010 \text{ cm}^2/\text{s}$. A mean value from the calculation with the two temperature extremes was taken for each sampling site. Calculations are documented in the digital database (Appendix 9).

For the different sampling geometries, i.e. the different gas hood – oxidizing bottle setups, and diffusion bowls, calculations were performed as explained in the following. Because all oxidizing bottles had an inlet and an outlet on top for the gases to enter, the total net diffusion rate is the sum of the diffusion through inlet and outlet:

$$J = -D_1 \cdot \frac{\Delta c_1}{\Delta x_1} + (-D_2 \cdot \frac{\Delta c_2}{\Delta x_2}) \quad \text{where } D_1 = D_2$$

Calculation varies for the 4 different setups chosen (Figure 42):

- **Setup 4:** An oxidizing bottle was left at the sampling site with inlet and outlet being closed by valves to check on contamination of the samples in the field during preparation and filling of the oxidizing bottles or diffusion through caps or tube connections. This field blank showed values comparable to the laboratory blanks of a 1:100 diluted NaOCl solution, indicating that there was no contamination, and no diffusion with the valves closed.
- **Setup 3:** The oxidizing bottle in this setup was not connected to a gas hood and both valves were left open. This setup gives information about volatile gas concentrations in approximately 25 cm above ground. It was assumed that a stable layer of air with increased gas concentrations may form under calm wind conditions over the geothermal features. Diffusion coefficients, diffusion lengths and concentration gradients for this setup are identical for inlet and outlet. The net diffusion rate is:

$$J = -D \cdot \frac{\Delta c_1}{\Delta x_1} + (-D \cdot \frac{\Delta c_2}{\Delta x_2}) = 2 \cdot (-D \cdot \frac{\Delta c}{\Delta x}) \quad \text{and} \quad c = \frac{m \cdot \Delta x}{2 \cdot t \cdot A \cdot D}$$

with $\Delta x = 5 \pm 2 \text{ cm}$; $A = 0.0314 \text{ cm}^2$, and D as discussed above

- **Setup 1 and 2:** While setup 3 only gives information about concentrations in the ambient air about 25 cm above the sampling site, setup 1 and 2 integrate concentrations from ambient air in 25 cm above the sampling site (via the short tube) and concentrations from directly above

the sampling site (via the long tube connected to the gas hood). The following equation can not be solved due to the two unknown concentrations Δc_1 and Δc_2 :

$$J = -D \cdot \frac{\Delta c_1}{\Delta x_1} + (-D \cdot \frac{\Delta c_2}{\Delta x_2}) \quad \text{and} \quad \frac{\Delta c_1}{\Delta x_1} + \frac{\Delta c_2}{\Delta x_2} = \frac{m}{t \cdot A \cdot D}$$

with $\Delta x_1 = 5 \pm 2$ cm; $\Delta x_2 = 60 \pm 20$ cm; $A = 0.0314$ cm²

The concentration gradients Δc_1 and Δc_2 are most likely not identical. The general assumption is that concentrations underneath a gas hood should be higher than concentrations 25 cm above the sampling site that are subject to diffusion, turbulent convection (eddy flux), dilution, hydrolysis, and oxidation. However due to the longer diffusion length from gas hood to oxidizing bottle (60 cm) compared to diffusion length from the open air (5 cm) the net diffusion rate might be significant from both sides. The problem could have been solved by closing the outlet with a valve, so that only diffusion from the gas hood has to be accounted for. This setup was not realized, because initially it was assumed that some gas flow might occur apart from the net diffusion that would lead to a build-up of pressure inside the oxidizing bottle. In the end, no gas flow was detected at any sampling site during any sampling campaign, and there was nothing to change about the setup design anymore at that time.

An approximation that can be made, however, is the calculation of an upper value for both compartments from two end-member models. In the first model it is assumed that there is no concentration gradient between oxidizing solution and gas hood ($\Delta c_2 = 0$). The total amount of volatile compounds then results from diffusion between ambient air and oxidizing solution (maximum for c_1). In the other end-member model there is no concentration gradient between ambient air and oxidizing solution ($\Delta c_1 = 0$) and all volatile compounds enter through the gas hood (maximum for c_2).

$$\frac{\Delta c_1}{\Delta x_1} + \frac{0}{\Delta x_2} = \frac{m}{t \cdot A \cdot D} \quad c_1 = \frac{m \cdot \Delta x_1}{t \cdot A \cdot D}$$

hence $\frac{0}{\Delta x_1} + \frac{\Delta c_2}{\Delta x_2} = \frac{m}{t \cdot A \cdot D} \quad \text{and} \quad c_2 = \frac{m \cdot \Delta x_2}{t \cdot A \cdot D}$

For the 19 sites (13 NaOCl, 6 NaOH samples), where the setups 1 and 3 were run parallel, the concentration in 25 cm determined by setup 3 was also taken as representative for setup 1. In this case, the net gas flow by the short diffusion path was known (Δc_1), and the diffusion by the gas hood (Δc_2) could be calculated as:

$$\frac{\Delta c_1}{\Delta x_1} + \frac{\Delta c_2}{\Delta x_2} = \frac{m}{t \cdot A \cdot D} \quad \text{and} \quad \Delta c_2 = \Delta x_2 \cdot \left(\frac{m}{t \cdot A \cdot D} - \frac{\Delta c_1}{\Delta x_1} \right)$$

The results gave information about possible enrichment effects underneath the gas hood compared to ambient air 25 cm above the sampling site. At 5 sites (3 NaOCl, 2 NaOH), setup 2 was run together with setup 1 and 3, enabling a direct comparison between gas diffusion and dissolution directly in the oxidizing solution or with the headspace above.

For the **diffusion bowls** the calculation is

$$c = \frac{m \cdot \Delta x}{t \cdot A \cdot D}$$

- A diffusion area is the entrance area for the gases into the bowl defined by the circumference of the bowl and the height of the open slit: $4 \cdot 10 \text{ cm} \cdot 0.1 \text{ cm} = 4 \text{ cm}^2$ for the squared DBs (No. 1-40), $2 \cdot (7 \text{ cm} / 2) \cdot 3.14 \cdot 0.1 \text{ cm} = 2.198 \text{ cm}^2$ for the round DBs (No. 41-43)
- Δx diffusion length is the height from the gas entrance on the top of the bowl to the oxidizing solution; 100 mL oxidizing solution result in 1 cm filling height in the squared DBs, and 2.5 cm in the round DBs; total height 3 cm \rightarrow 2 cm and 0.5 cm from entrance to oxidizing solution for the squared and the round DBs respectively

Active gas sampling

Easier to convert are the gas concentrations from the active gas pumping done at the four sampling sites YNPGG04, YNPHL01, YNPRH01, and YNPRH06 (section 4.2.1.2):

$$c = \frac{m}{V}$$

- c concentration at sampling site [$\mu\text{g}/\text{m}^3$]
- m mass = concentration of dissolved, oxidized compound in $\mu\text{g}/\text{L} \cdot$ volume of trapping solution (100 mL) [μg]
- V sampled gas volume during pumping [m^3]

The uncertainty is significantly lower compared to the calculations based on gas diffusion discussed above. It only depends on the accuracy of analytical determination (about $\pm 5\%$ for Cd, Cr, Co, Pb, Sb, and Se, and $\pm 1\text{-}2\%$ for all other elements including As) and the uncertainty per stroke of the Dräger hand pump ($\pm 5\%$). The sampled gas volume is well defined and no problems with sampling geometry occurred. Two disadvantages are the longer field working times and the more expensive equipment requirements. Whereas setting up 10 passive diffusive samplers and recovering them after a passive sampling time of several days requires a total of about 2 hours, active gas sampling took between 1 to 4.5 hours per site depending on the gas flow from the ground. Dilution might occur during active gas sampling, if the pump rate exceeds the gas flow from the ground and additional ambient air is drawn in. Furthermore, the passive sampling over several days yields an integrated signal, whereas the active sampling for 1-4.5 hours is a “snapshot”. For several sites, passive sampling can be done more or less within the same sampling period whereas active pumping has to be done one by one on several consecutive days. The difference might be essential because temporal variations of gas composition are likely to occur, especially for microbially catalyzed volatilization of metallics. Pumps with a very low pump rate, supplied by a solar panel left in the field for several days, could also yield an integrative signal. However, this setup is not only more expensive for a screening study with numerous sampling sites but also more sensitive to disturbances (breakdown of electrical equipment, wildlife impact) and more difficult to camouflage from tourists and wildlife (National Park Service requirement). Thus passive gas sampling was the general method of choice, completed by active gas sampling at selected sites.

4.2.3.3 Gas chromatography interpretation

Chromatogram interpretation for solid sorbents was done with the Bruker Data Analysis Software 1.0i. For the interpretation of all SPME data, the public domain mass spectral data reduction computer program "Wsearch 32" (Version 01.01.2003) was used. Varian files in the new format (".sms"; from analysis in Denver) had to be converted to old format (".ms") via the "Batchsms" code, Version 1.0 from Varian CSB. Hewlett Packard Pascal file (".d"; from analysis in Bozeman) could be read directly by the Wsearch 32 software. Peaks were integrated manually. The chromatogram for each analysis and peak integration and mass spectra of volatile As species are presented in a tabular and graphic form in the digital database. The main objective was a qualitative interpretation with the detection of different As species. Quantitative interpretation was dismissed because of the problems discussed in section 3.2.3.2. Thus, no standard calibration was done. Integrated peak areas are given in the digital database for a semi-quantitative comparison. Occasional poor peak resolution from the background or double peaks are shown in the respective figures and considered for final data interpretation.

4.2.3.4 Statistics

Final data interpretation described in section 4.3 is discussed in groups classified by hierarchical cluster analysis via the statistical program SPSS for Windows, version 11.0. The best fit of different methods (between groups linkage, within groups linkage, nearest and furthest neighbor, centroid and median clustering, Ward's method) with the interval measure squared Euclidian distances was chosen. For the water samples the following parameters were considered: $\{H^+\}$ (10^{-pH}), temperature, conductivity, F, Cl, Br, N(V), S(VI), As species (As(III), As(V), MMAA, DMAA), Al, B, Ba, Be, Ca, Cd, Co, Cr, Cu, K, Li, Mg, Mn, Mo, Na, Ni, Pb, Sr, V, Zn, SiO₂, S(-II), Fe(II), Fe(III), TIC, and TOC. The volatile elements included for gas sample clustering are As (from GF-AAS), Al, B, Ba, Cu, Fe, K, Li, Si, Sr, Zn, S. All variables were standardized to a range of 0 to 1 and re-scaled before cluster analysis. Values below detection limit were replaced by $0.3 \cdot$ detection limit. The significance of each cluster analysis for all variables was checked with the non-parametric Kruskal-Wallis test. The grouping variable was the cluster number according to the different cluster methods. The significance of differences between two groups was tested by the Mann-Whitney Test for two independent samples. Bivariate correlation analysis for water and gas samples was done with the nonparametric Spearman correlation coefficient and a two-tailed test of significance.

4.2.3.5 Speciation modeling

Speciation modeling was done with PHREEQC 2.8.03 (Parkhurst and Appelo 1999) using the database WATEQ4F (V.2.4 with revised data from Nordstrom and Archer 2003). Parameters and species considered were pH, Temp, pe, F, Cl, Br, N(V), S(VI), As(III), As(V), Al, B, Ba, Ca, Cd, Cu, K, Li, Mg, Mn, Na, Ni, Pb, Se, Sr, Zn, Si, S(-II), Fe(II), Fe(III), and C(IV). No thermodynamic data could be found for the organic As species MMAA and DMAA. For modeling they were added according to their most probable redox state +5 to inorganic As(V) to get a better adaptation for the

As redox equilibrium. The concentration of thus-modeled As(V) complexes was referred to the actual concentration of inorganic As(V) determined by species-selective sampling as described in the sections 2.7.2 and 4.2.1.2. Thermodynamic data for gaseous As species were obtained from Spycher and Reed (1989) and Pokrovski et al. (2002) (Appendix 26).

4.3 Results

4.3.1 Cluster analysis

Cluster analysis was conducted for both water and gas samples. It is discussed briefly in the following before the clusters obtained are used for the description of water and gas chemistry in the 5 study areas in section 4.3.2.

4.3.1.1 Clustering of the water samples

By cluster analysis 60 water samples from 5 study areas were divided in 14 subgroups. A logical subdivision in two major groups with 7 subgroups each was found with the cluster methods of Ward's (Appendix 11) and the Average Linkage within Groups method (Appendix 12). Compared to those two methods, other clustering methods tested (section 4.2.3.4) were inferior and yielded many subgroups with only 1 or 2 single water samples without an overall context. Based on the dendrogram derived by Ward's automatic cluster method and close examination of hydrogeochemical data, a few samples were manually re-assigned to different subgroups (Appendix 11). In the Kruskal-Wallis test, the derived optimized cluster analysis showed significant overall differences between the subgroups for all variables on a significance level of 0.1%, except for Co (0.6%), Cd (0.7%), Pb (2.1%), and N(V) (4.2%). No significant overall difference was found for Cu (Appendix 13). The results are discussed based on the cluster membership of the optimized cluster analysis of water samples.

The two major groups found during cluster analysis are sulfate-dominated waters with a low pH outside the caldera, mainly along the Norris-Mammoth corridor (33 samples) compared to chloride-dominated waters with near-neutral pH closer to the caldera's margin at Norris Geyser Basin and Gibbon Geyser Basin and, inside the caldera, at Lower Geyser Basin (27 samples, Figure 44).

Significant differences between the two groups also exist for temperature, Na, Cl, Br, F, B, and Li that show a direct positive correlation to pH as well as for S(VI), Mg, Al, Mn, and Fe that show an inverse correlation to pH (Appendix 14). These two different groups correspond to the type I and type II waters discussed in section 4.1.1.5. The ternary diagram Cl-SO₄-HCO₃ in Figure 45 shows their origin from heated steam (type I) or deep thermal sources (type II).

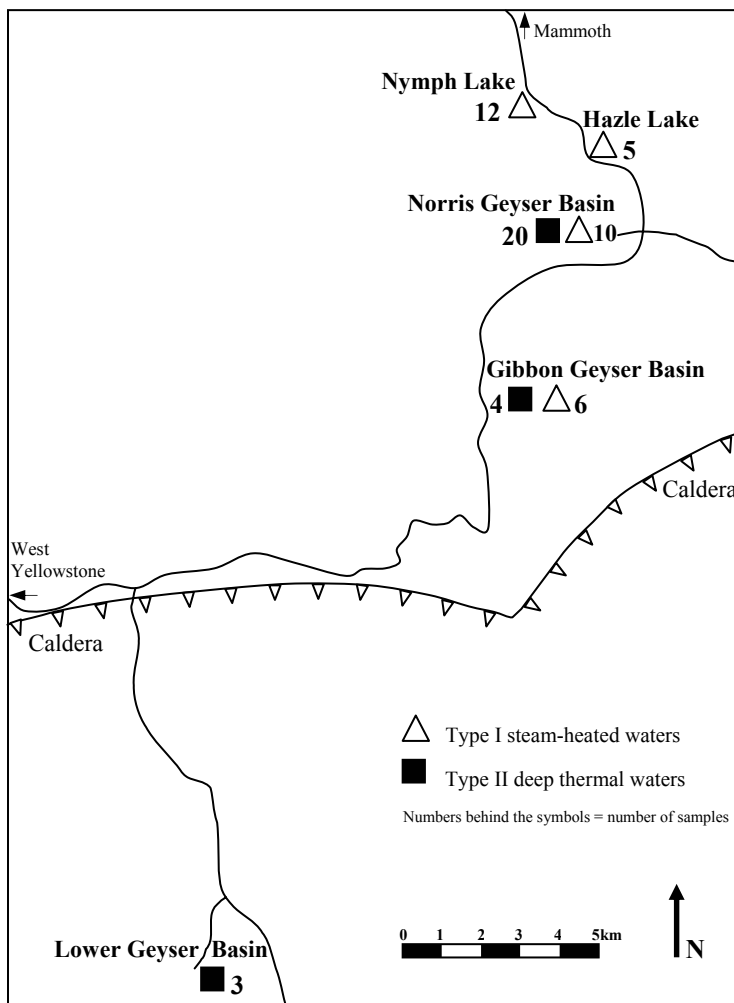


Figure 44 Distribution of type I steam-heated waters mainly along the Norris-Mammoth corridor to the north (33 samples, white triangles) and type II deep thermal waters closer to the caldera rim at Norris Geyser Basin (Ragged Hills) and Gibbon Geyser Basin as well as inside the caldera at Lower Geyser Basin (27 samples, black squares)

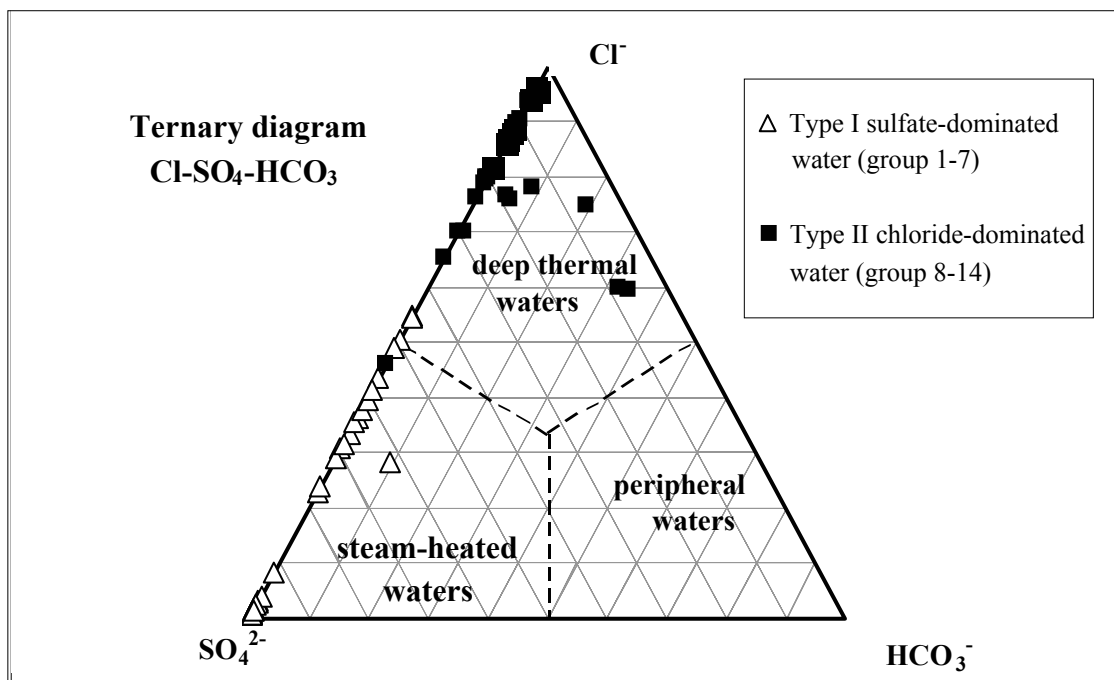


Figure 45 Ternary diagram Cl-SO₄-HCO₃ showing the origin of type I waters from heated steam and type II waters from deep thermal sources (after the classification scheme of Giggenbach and Goguel 1989)

In a ternary diagram based on Na/K and K/Mg geothermometers (Giggenbach 1988) type I waters are classified as “immature waters”, while type II waters are in “partial” to “full equilibrium” with respect to the mineral system albite-potassium feldspar-muscovite-clinocllore-silica (Figure 46). Saturation indices for these mineral phases were calculated by hydrogeochemical modeling to check the general validity of the simplified concept (Appendix 15). Quartz is supersaturated in all samples, SiO₂(a) in most, while Mg-clinocllore is undersaturated in all samples but one (YNPLG02-2W). Except for one sample (YNPHL02-1W), saturation and supersaturation of albite, potassium feldspar, and muscovite occurred as predicted only in samples characterized as being in “full equilibrium”. There are, however, also 6 sites classified as being in “full equilibrium” where albite, potassium feldspar, and muscovite are undersaturated. Thus, the simplified clustering was accepted as a first approximation to find water samples that show saturation or supersaturation with regard to the feldspar-mica system even though the classification of “full equilibrium” might be false in terms of thermodynamics for some of the samples. For the samples in full equilibrium, reservoir temperatures were calculated from the Si-, the Na-K-, the K-Mg-, and Na-K-Ca-geothermometers (Appendix 16).

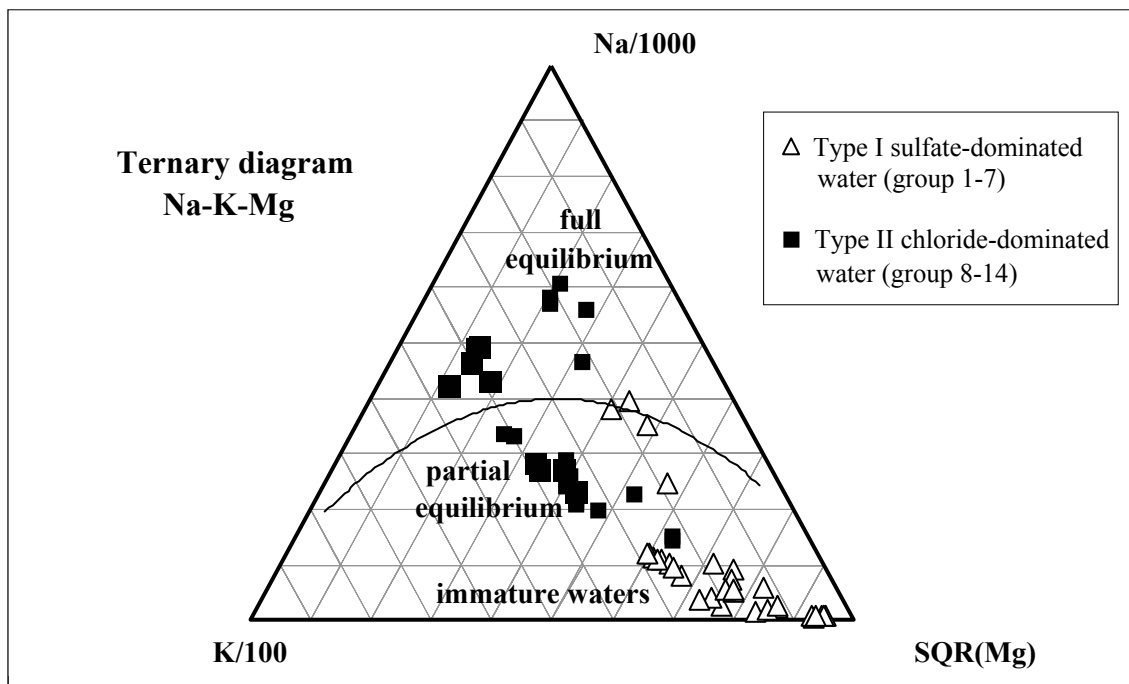


Figure 46 Ternary diagram Na-K-Mg showing type I sulfate-dominated, mostly immature waters, and type II chloride-dominated waters in partial or full equilibrium with the mineral system albite-potassium feldspar-muscovite-clinocllore-silica (equilibrium line calculated for 75 to 350°C in intervals of 25°C according to the equation for Na/K geothermometer by Arnórsson et al. 1998, cited in Arnórsson 2000 and for K/Mg geothermometer by Giggenbach 1988)

The positive correlation between As and Cl discussed in general in section 4.1.1.5 was confirmed for the 60 water samples by bivariate correlation analysis on a significance level of 1% (Appendix 14). Concentrations of As are generally higher in type II than in type I waters (Figure 47). While As occurs almost exclusively as As(III) in type II waters, an average of 30% As(V), MMAA, and

DMAA can be found in type I waters. The significant difference between the two main types for the variables mentioned in this paragraph was confirmed by a Mann-Whitney test (Appendix 17).

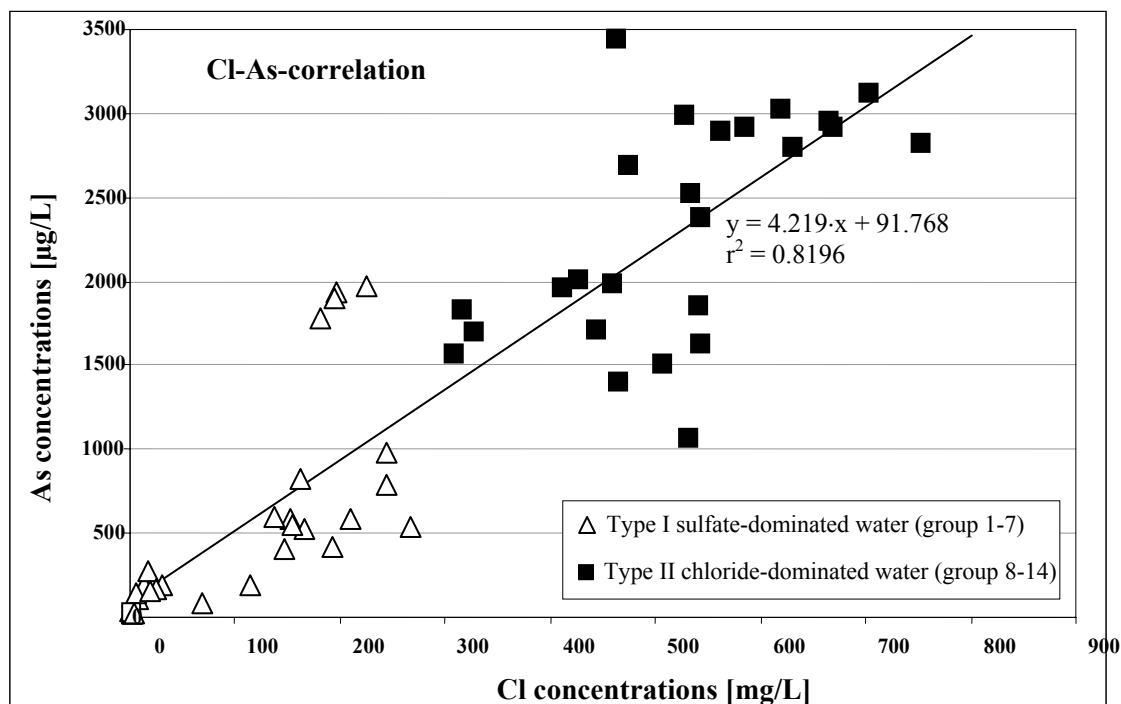


Figure 47 Positive correlation and significant trend of As and Cl concentrations due to similar behavior during steam-water separation; steam-heated type I waters show lower concentrations of As and Cl compared to deep thermal type II waters*

*The two samples of subgroup 9 (YNPRH05-1W, 3W with Cl: 399 and 385 mg/L, As: 6940 and 11085 µg/L) were excluded from the graph and the calculation of the regression equation

The 7 subgroups each for type I and type II will be discussed in section 4.3.2.1 and section 4.3.2.2 respectively.

4.3.1.2 Clustering of the gas samples

For clustering the gas samples, the 55 NaOCl samples taken by gas hoods directly above hot springs (setup 1 and 2 in Figure 42) were considered. Significant concentrations of volatile metallics were found in the NaOCl trapping solution for As (from GF-AAS), Al, B, Ba, Cu, Fe, K, Li, Si, Sr, and Zn from ICP-AES, and S from IC determination as well as in the NaOH trapping solution for Cl. Background values of the NaOCl and NaOH trapping solution were considered (see digital database, Appendix 9).

The gas samples could not be subdivided in the same 14 subgroups as described for the water samples in section 4.3.1.1. A Kruskal-Wallis test showed that the differences between the assumed water subgroups are not significant for none of the detected volatile elements (section 4.2.3.4). For 38 of the 55 gas samples water chemistry data was available for the same sampling time. The com-

bined data of gas and water analyses were used to conduct a hierarchical cluster analysis by Ward's method (Appendix 18). A logical subdivision in 6 subgroups was found and confirmed to yield significant differences between the subgroups for volatile As, Al, Fe, Li and all water parameters except for N(V), Ca, Cu, Sr, S(-II), and TIC on a significance level of 5% (Appendix 19). The 17 gas samples for which no contemporaneous water samples existed were assigned to the 6 subgroups based on knowledge of the sampling locations and the gas data. Considering the 55 gas samples only, and no water data, the 6 subgroups show significant differences for volatile As, Al, B, Ba, Fe, K, Li, and S on a significance level of 5% (Appendix 20).

A significance level of 5% was considered acceptable for the cluster analysis of the gas samples compared to a significance level of 0.1% for the water samples (section 4.3.1.1). The significance level of 5% takes into account that volatile metallics are subject to changes in even more parameters than the water chemistry and generalizations are harder to make. The assignment of a sampling site to a certain subgroup based on its gas chemistry might be more sensitive to seasonal changes than based on its water chemistry. While 3 of the 6 gas subgroups contain exclusively gas samples over type I waters and 2 exclusively gas samples over type II waters, there is one subgroup with 3 samples both over type I and type II waters. This subgroup shows the highest volatile As concentrations and supports the hypothesis that temporal changes can yield a completely different gas chemistry for one sampling site compared to the overall chemistry of its corresponding water phase.

In the following, the water and gas chemistry for the sites sampled will be discussed in two sections corresponding to the two main types of steam-heated (section 4.3.2.1) and deep thermal waters (section 4.3.2.2). Within the description of the individual study areas reference will be taken to the affiliation of sampling sites to individual subgroups found by water or gas cluster analysis.

4.3.2 Description of water and gas chemistry

4.3.2.1 Type I steam-heated waters

All of the type I waters are from outside the caldera, about half of them from sampling areas north of the Norris Geyser Basin along the Norris-Mammoth corridor. Seven subgroups can be distinguished within the type I waters that are, except for a few samples, all steam-heated, immature waters (Figure 48; Figure 49). The assignment of individual water samples to the 7 subgroups is given in Appendix 21. Figure 50 to Figure 53 show the main differences in the mean values of pH, conductivity, temperature, S(VI), Cl, dissolved total As and As species concentrations for the 7 water subgroups. Compared to type II waters As concentrations are low. They correlate with the low Cl concentrations (Figure 50). High S(VI) concentrations lead to low pH (Figure 51; Figure 53).

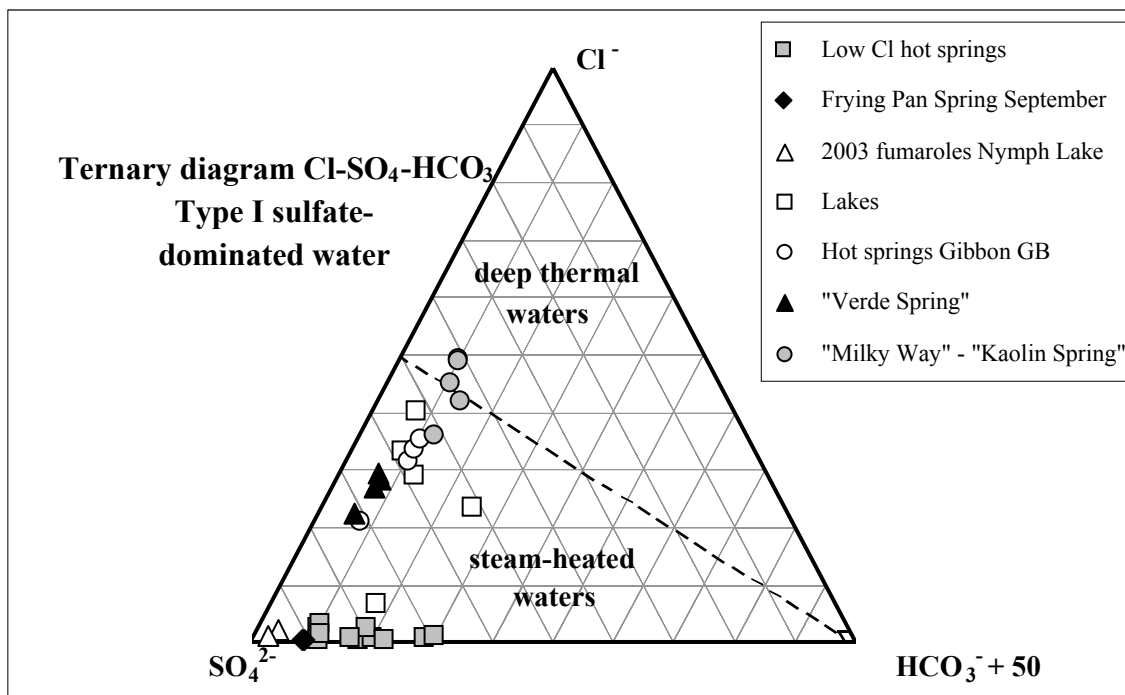


Figure 48 Ternary diagram Cl-SO₄-HCO₃ showing the origin of the 7 subgroups of type I steam-heated waters (modified after the classification scheme of Giggenbach and Goguel 1989, HCO₃⁻ + 50 instead of HCO₃⁻; for subgroup affiliation see Appendix 21)

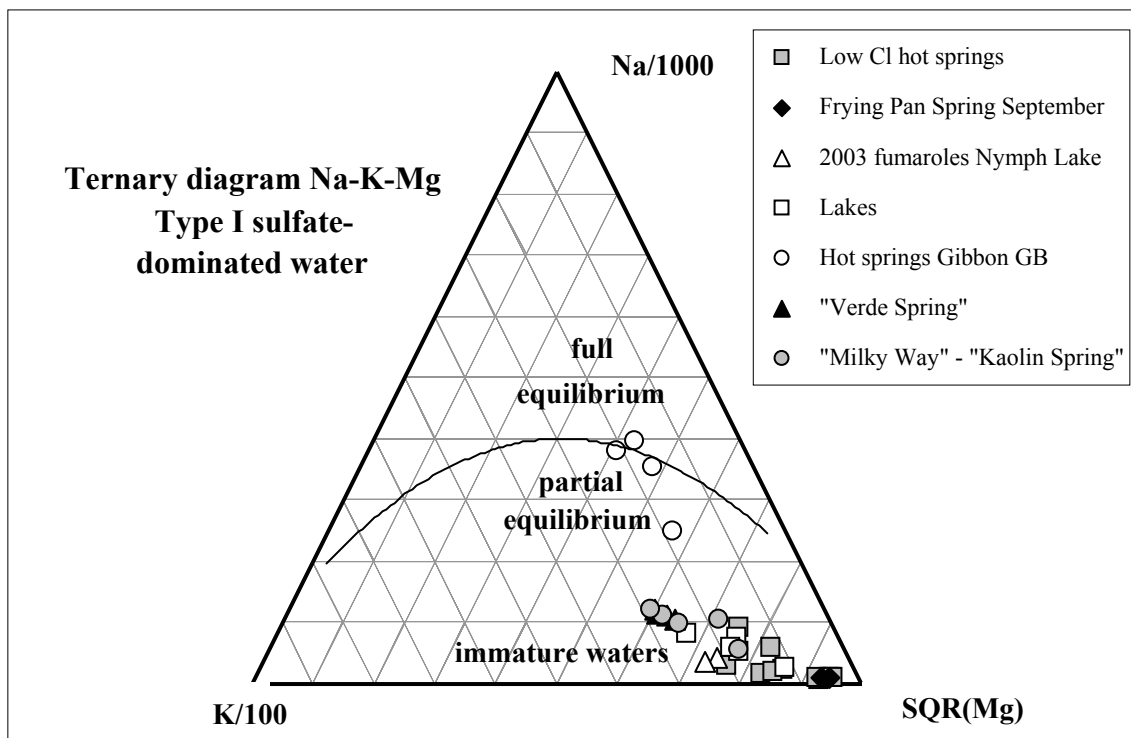


Figure 49 Ternary diagram Na-K-Mg showing the subgroups of type I sulfate-dominated waters that are mostly immature with respect to the mineral system albite-potassium feldspar-muscovite-clinocllore-silica (equilibrium line calculated for 75 to 350 °C in intervals of 25°C according to the equation for Na/K geothermometer by Arnórsson et al. 1998, cited in Arnórsson 2000 and for K/Mg geothermometer by Giggenbach 1988; for subgroup affiliation see Appendix 21)

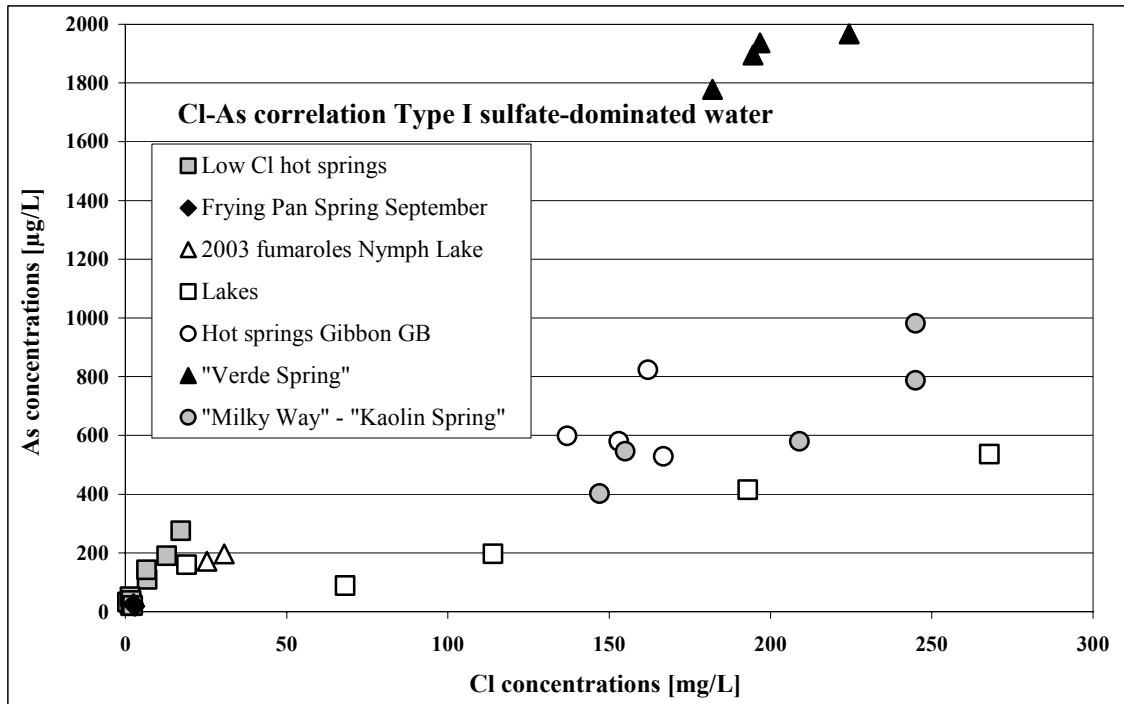


Figure 50 Positive correlation of As and Cl in steam-heated type I waters (subgroup affiliation: Appendix 21)

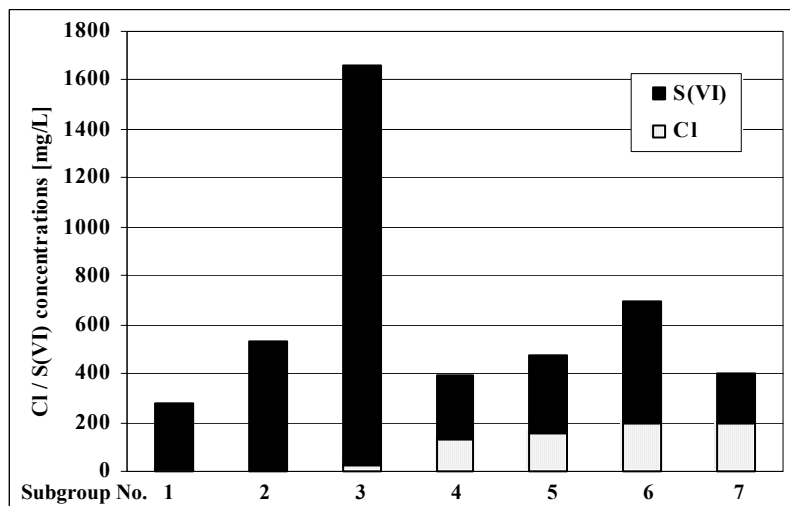
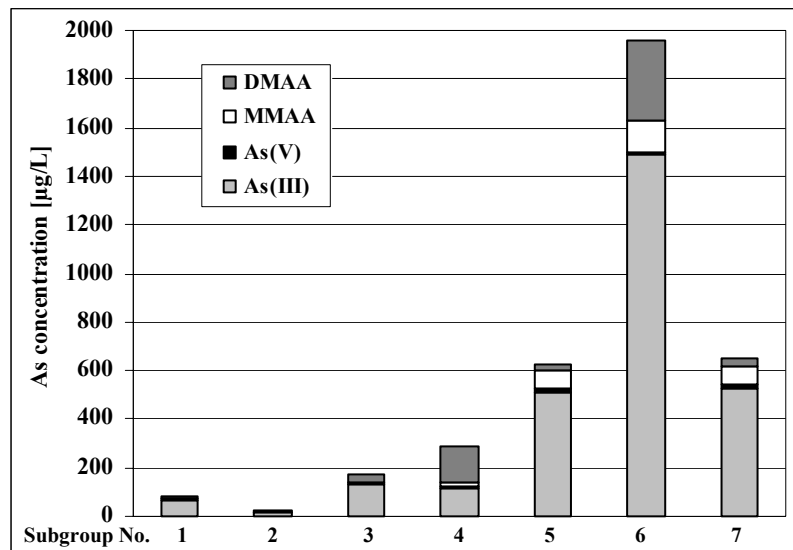


Figure 51 Differences in S(VI) and Cl concentrations for the 7 subgroups of steam-heated type I waters with a clear predominance of S(VI)

Figure 52 Differences in dissolved As species for the 7 subgroups of type I waters; DMAA predominates only in subgroup 4 Lake samples



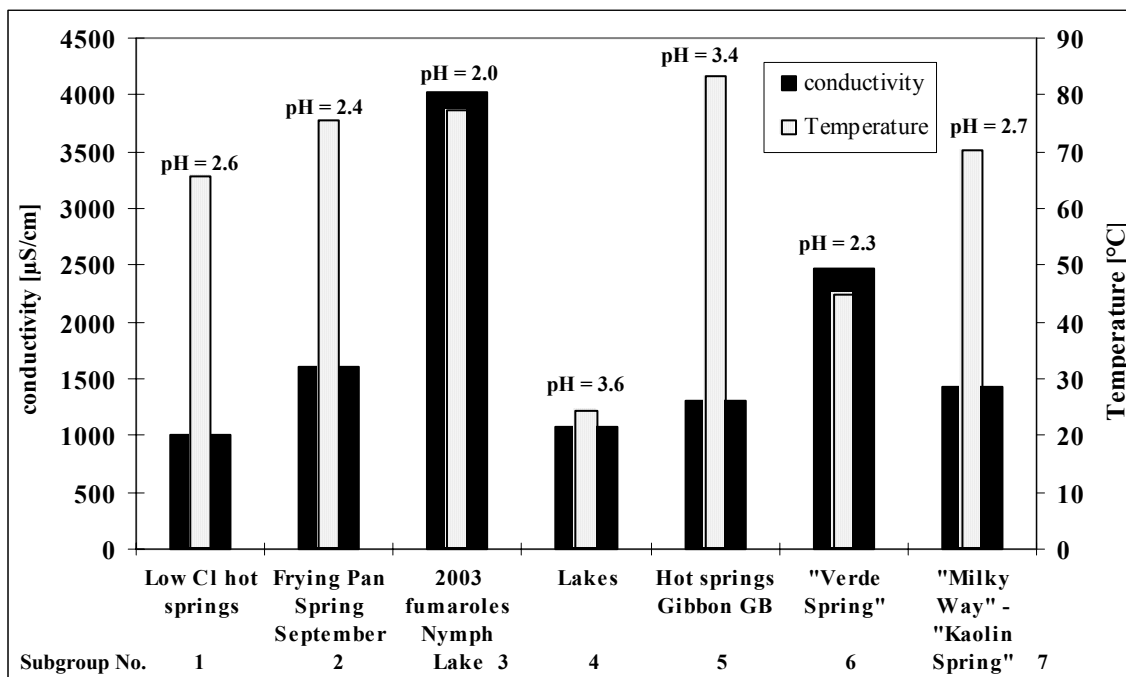


Figure 53 Differences in temperature, conductivity, and pH for the 7 subgroups of type I waters

Considering their gas chemistry, the samples of the 7 water subgroups can be subdivided into 4 gas subgroups. Figure 54 shows the differences of their mean volatile As, SiO₂, and S concentrations. For the assignment of individual gas samples to the gas subgroups see Appendix 21.

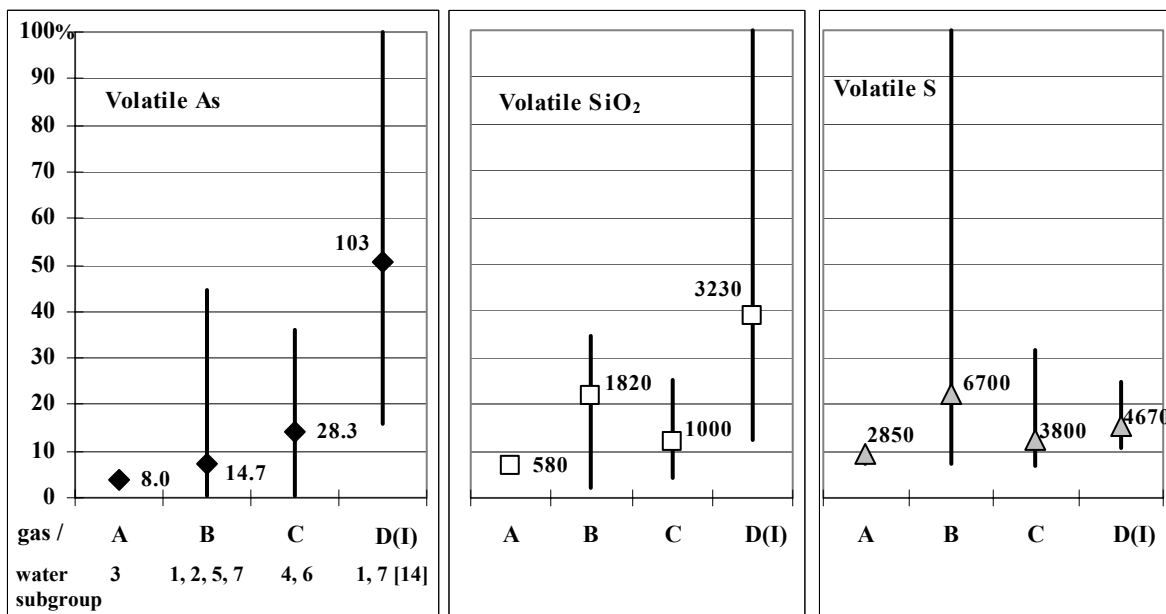


Figure 54 Volatile As, SiO₂, and S concentrations for the 3 gas subgroups A, B, C of type I waters; subgroup D also contains one sample of type II water that was not considered in the figure above: D(I); values are standardized to a range of 0 to 100 % (= highest concentration for each volatile species); mean value marked by symbol and number for mean concentration in mg/m³; bars represent maximum and minimum concentrations

Nymph Lake / Frying Pan Spring

The area at the northern side of Nymph Lake with the new fumaroles appearing during the winter of 2002/2003 (section 4.1.2.1; Figure 35; Figure 55) shows the highest conductivities (3860 and 4190 $\mu\text{S}/\text{cm}$), the highest S(VI) concentrations (1.3 and 1.9 g/L) and the lowest pH (2.0 and 1.9) of all samples (Figure 51; Figure 53). Judging by the cluster analyses of both gas and water data (Appendix 11; Appendix 12; Appendix 18) these two samples (YNPNL05 and 06) have the least similarity with any other site sampled. Concentrations of dissolved Al (48 and 70 mg/L), B (2.7 and 3.8 mg/L), Fe (30 and 34 mg/L), SiO_2 (304 and 374 mg/L), Pb (8 $\mu\text{g}/\text{L}$), Zn (0.051 and 0.058 mg/L) as well as total Hg (600 ng/L) and methylated Hg (0.55 ng/L) are significantly increased compared to the other samples within the subgroup. For the June sample, rare earth elements were analyzed. Almost all rare earth elements showed higher concentrations than for the other sites sampled, especially U (1.8 $\mu\text{g}/\text{L}$), Th (15 $\mu\text{g}/\text{L}$), Ce (40 $\mu\text{g}/\text{L}$), and La (20 $\mu\text{g}/\text{L}$). From June to July, pH decreased whereas temperature, conductivity and S(VI) concentrations increased. In contrast to the high concentrations of dissolved species, almost all volatile species at YNPNL05 and 06 (gas subgroup A; Figure 54) show concentrations lower than at all other sampling sites. Volatile As concentrations range from 7.0 to 8.9 mg/m^3 (quantification is discussed in detail in section 4.3.6). Volatile B concentrations are below detection limit, Li (2.8 mg/m^3), Sr (2.3 mg/m^3), SiO_2 (580 mg/m^3) and S concentrations (2.8 mg/m^3) are among the lowest concentrations sampled at all

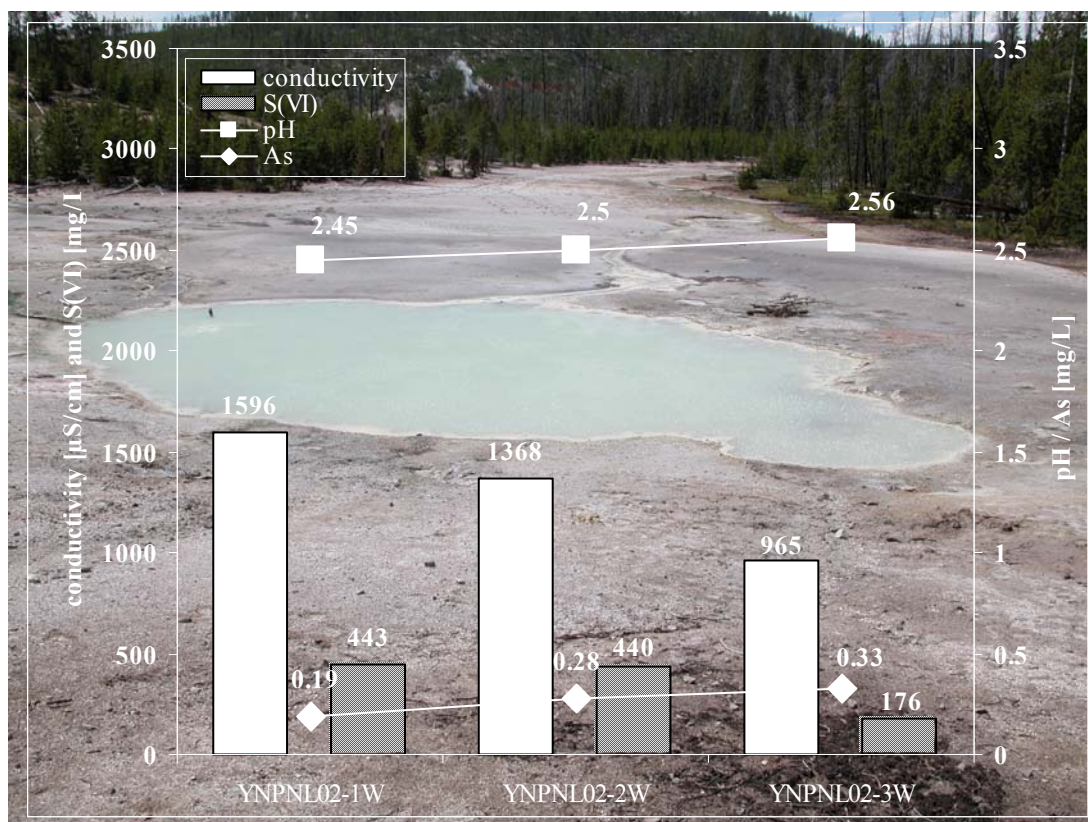


Figure 55 Sampling sites at Nymph Lake: 1 = Lake sample; 2, 3, 4 (Frying Pan spring) = low Cl hot springs and fumaroles (September samples from 3 and 4 belong to another subgroup); 5, 6 = area of the new fumaroles; line is clearly visible by the dead trees; site symbols correspond to subgroup symbols used in the previous figures

The 3 sites sampled at Frying Pan Spring (YNPNL02, 03, 04; Figure 35 and Figure 55) belong to the subgroup 1 of hot springs and fumaroles with the lowest Cl concentrations (on average 5 mg/L; Figure 51). This subgroup also shows the lowest As concentrations with an average of 80 $\mu\text{g}/\text{L}$. Methylated Hg concentrations determined in June at NL02 (9.04 ng/L), and NL04 (6.3 ng/L) are

the highest found throughout the sampling campaigns. Total Hg concentrations of 72 ng/L at NL04 are lower compared to other sampling sites. Volatile As concentrations with an average of 11.5 mg/m³ are the second lowest of all areas sampled after the Nymph Lake fumaroles described before (subgroup B; Figure 54).

During the third sampling campaign in September, YNPNL03 and 04 showed significantly increased conductivities, caused mainly by increased concentrations of H⁺ and S(VI). Some trace elements like Al, Mn, Fe (at NL04 only), Sr, and Zn were increased, too. Arsenic concentrations decreased with decreasing pH. A trend could already be observed during the first two sampling campaigns with conductivities increasing from June to July (Figure 56). The relative distance in cluster analysis between the samples YNPNL03-3W and 04-3W and the samples from subgroup 1 required their separation in an own subgroup 2 (Appendix 11; Appendix 12). Volatile As concentrations increased from 4.3 mg/m³ in June and 3.8 mg/m³ in July to 90 mg/m³ in September (NL04). Such differences in gas and water chemistry between sampling from early summer to late autumn, detected also at other sampling sites (see below), are assumed to be no artifacts but an expression of the seasonal “disturbances” discussed in section 4.1.2.3 for Norris Geyser Basin. Interestingly, YNPNL02 (all sampling campaigns in subgroup 1), shows an inverse trend with decreasing conductivities, decreasing S(VI) concentrations, and an increasing pH from June through July to September (Figure 56). The number of samples is unfortunately too low to confirm a seasonal shift in activity between the northeastern and the southwestern part of the Frying Pan Spring area.



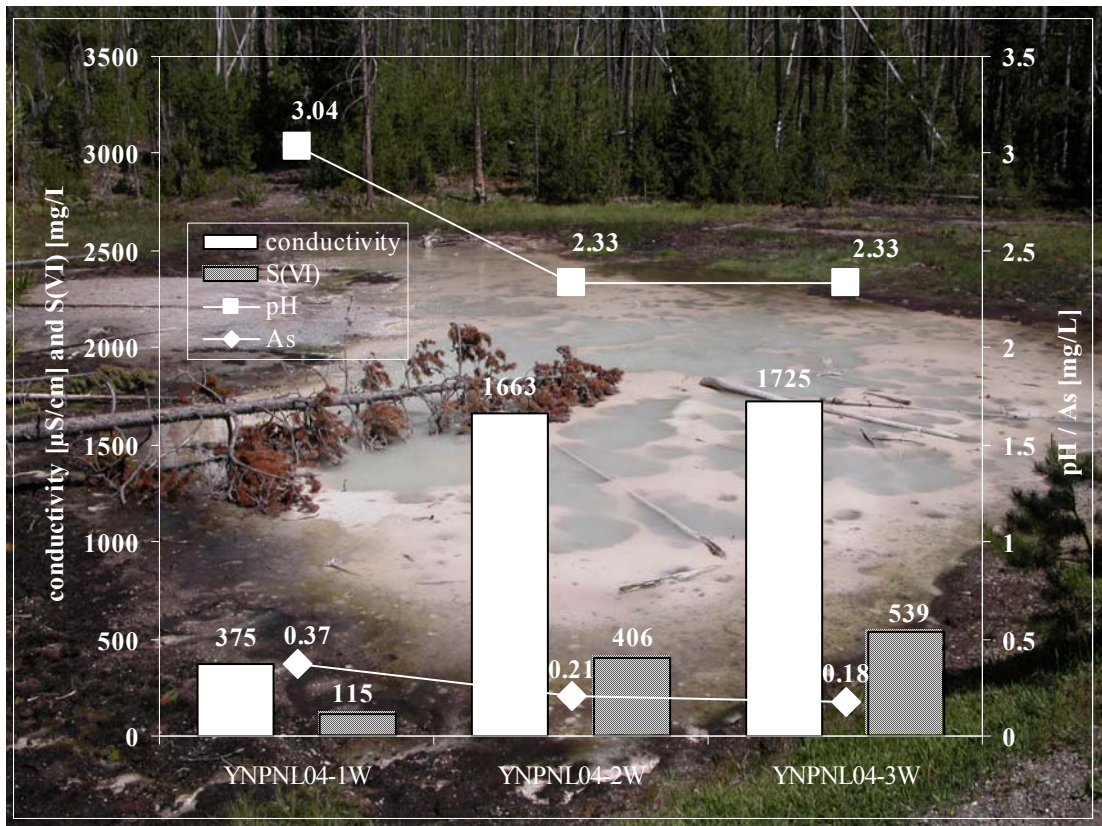
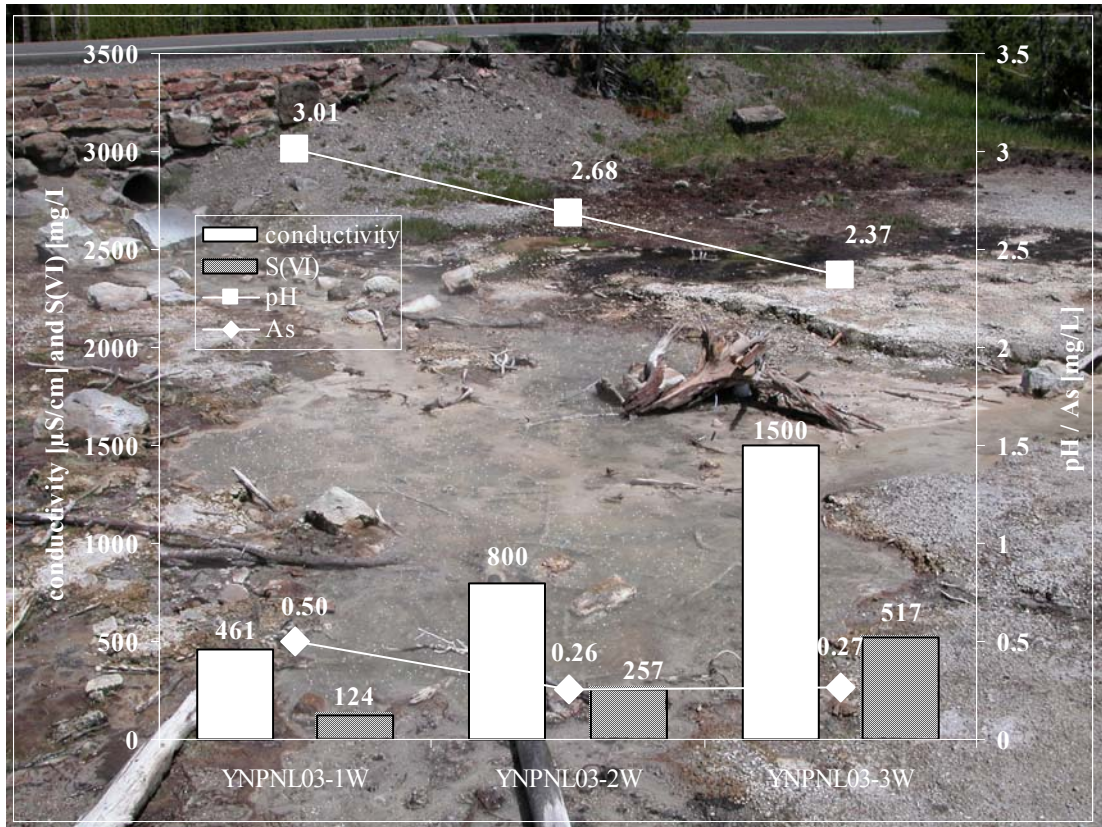


Figure 56 Seasonal trends at Frying Pan Spring from June through July to September with increasing conductivity and S(VI) concentrations, and decreasing pH and As concentrations at YNP NL03 and YNP NL04 and vice versa at YNP NL02

The only sample taken at Nymph Lake (YNPNL01) belongs to subgroup 4 of the lake samples and will be discussed with the samples from Hazle Lake.

Hazle Lake

Two samples from the Hazle Lake shores (YNPHL01 and 02) constitute the subgroup 4 “lake samples” together with YNPNL01. Characteristic are the low temperatures (average 24°C; Figure 53), the highest pH in their group of sulfate-dominated waters (on average 3.6, up to 6.0 at HL02) and a higher than average concentration of Ca (13 mg/L) and TIC (13 mg/L). At YNPHL01 1.6 ng/L methylated Hg were detected. Total As concentrations were higher than in the Nymph Lake / Frying Pan Spring area with an average of 280 µg/L and - in contrast to all other sampling sites - significant amounts of DMAA (Figure 57). Volatile As concentrations (subgroup C; Figure 54) are also higher. However, no significant correlation with volatile As was found neither for dissolved total As nor DMAA. Bivariate correlation analysis revealed that only dissolved As(III) correlates with volatile As (Appendix 23). Lower volatile Si concentrations for the lake samples compared to the hot springs from Frying Pan Spring correlate with lower temperatures (Figure 53; Figure 54; Appendix 23). For the lower volatile S concentrations no explanation could be found, because volatile S does not correlate with any other gaseous or aqueous parameter (Appendix 22; Appendix 23).

Comparing the three sampling campaigns from June, July, and September at HL01, increasing conductivities (1030 - 1456 - 1890 µS/cm) reflect increasing concentrations of Cl, S(VI), Ca, K, Mg, and Na as well as F, Br, B, Li, and Sr. Total As concentrations increase from 197 to 414 and 536 µg/L. Dimethylated As predominates in June and September, As (III) in July (Figure 57). The Fe(II) increases from 88 to 94 and 96% and TOC from 1.8 to 3.3 and 6.4 mg/L.

The small hot spring at the northern side of the lake about 3 m above lake level (YNPHL03) belongs to the subgroup of low Cl hot springs and shows a clear predominance of As(III) like the hot springs at Frying Pan Spring (Figure 57).

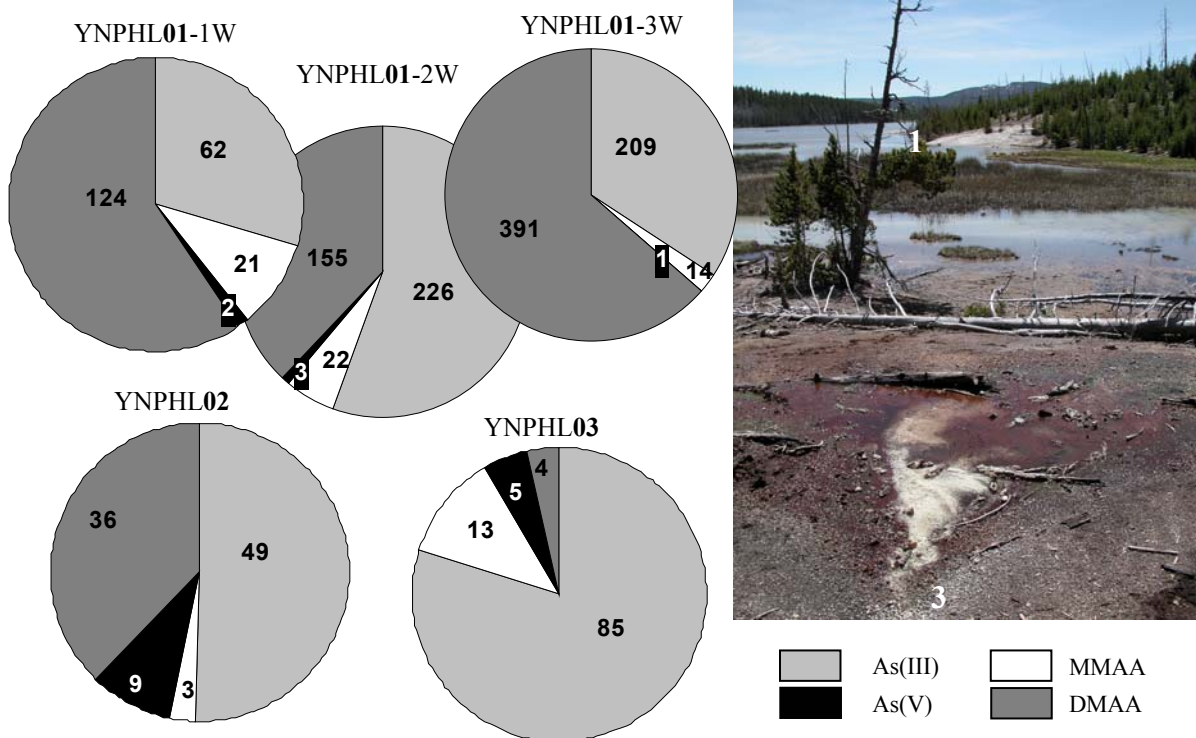


Figure 57 Aerial overview of Hazle Lake with the lake samples YNPHL01 and YNPHL02 and the low Cl hot spring YNPHL03; pie charts show that significant amounts of dimethylated As are found in the lake samples only, while As(III) clearly predominates in the hot spring sample YNPHL03 (concentrations in µg/L); numbers in photos correspond to bold numbers in sampling code

Norris Geyser Basin (Ragged Hills)

The only sites in the Ragged Hills area that belong to type I steam-heated waters are “Verde Pool” (Figure 38) and the “Milky Way” - “Kaolin Spring” complex that is connected by a discharge breakthrough from “Kaolin Spring” since the winter 2002/ 2003 (Figure 39).

The highest As concentrations (1500 µg/L) in steam-heated waters with a predominance of As(III) (76%) are found in the “Verde Pool” subgroup (Figure 50; Figure 52). Conductivities of about 2500 µS/cm are second only to samples from the 2003 fumaroles at Nymph Lake (Figure 53). Average concentrations of Cl are 200 mg/L, S(VI) 500 mg/L, and SiO₂ 306 mg/L. The pH is low with an average of 2.3. Temperatures of 45°C are the second lowest apart from the lake samples. Accordingly, the gas chemistry is similar to that of the lake samples described before with high volatile As and low volatile Si and S concentrations (Figure 54). Methylated Hg concentrations of 0.03 and 0.04 ng/L for YNPRH03-1W and 04-1W respectively are the lowest sampled during this field trip. From June through July to September pH decreased while conductivity and S(VI) concentrations increased at YNPRH04 as observed for YNPHL01, NL03, 04, and 05. Total As concentrations peaked in July with 1968 µg/L compared to 1895 µg/L in June and 1778 µg/L in September. The As(III) fraction increased from 70 to 77 and 83% throughout September.

With concentrations of 200 mg/L for both Cl and S(VI) (Figure 51), samples from the “Milky Way” - “Kaolin Spring” complex (subgroup 7) plot between the fields for deep thermal waters and steam-heated waters in Figure 48. Average As concentrations are 660 µg/L with a clear predominance of As(III) (81%). With 490 ng/L (YNPRH18-4W) and 600 ng/L (YNPRH01-1W) total Hg concentrations are among the highest found in the Park. Methylated Hg concentrations are lower, being 0.22 and 0.47 ng/L respectively. The sampling site YNPRH01 showed a slight decrease in conductivity from June through July to September (1608 - 1512 - 1440 µS/cm) mainly from decreasing Cl concentrations (245 to 209 mg/L). Sulfate concentrations stayed constant at 205 mg/L.

Upon close observation a linear structure seems to connect those two zones in the aerial photograph of the Ragged Hills area in Figure 58. The most prominent features along that “lineament” are a red alteration zone at the southern side of “Verde Pool”, linear clearings through the sparsely wooded hill side east of “Verde Pool” and a small hot spring west of the “Milky Way” - “Kaolin Spring” complex. Unfortunately no information exist about the mineral composition or genesis of the red alteration zone nor about the hydrogeochemistry of the small hot spring that could support the hypothesis that the similar hydrogeochemistry between “Verde Pool” and the “Milky Way” - “Kaolin Spring” complex might be explicable by their location on one fracture zone providing ascent paths for geothermal gases.

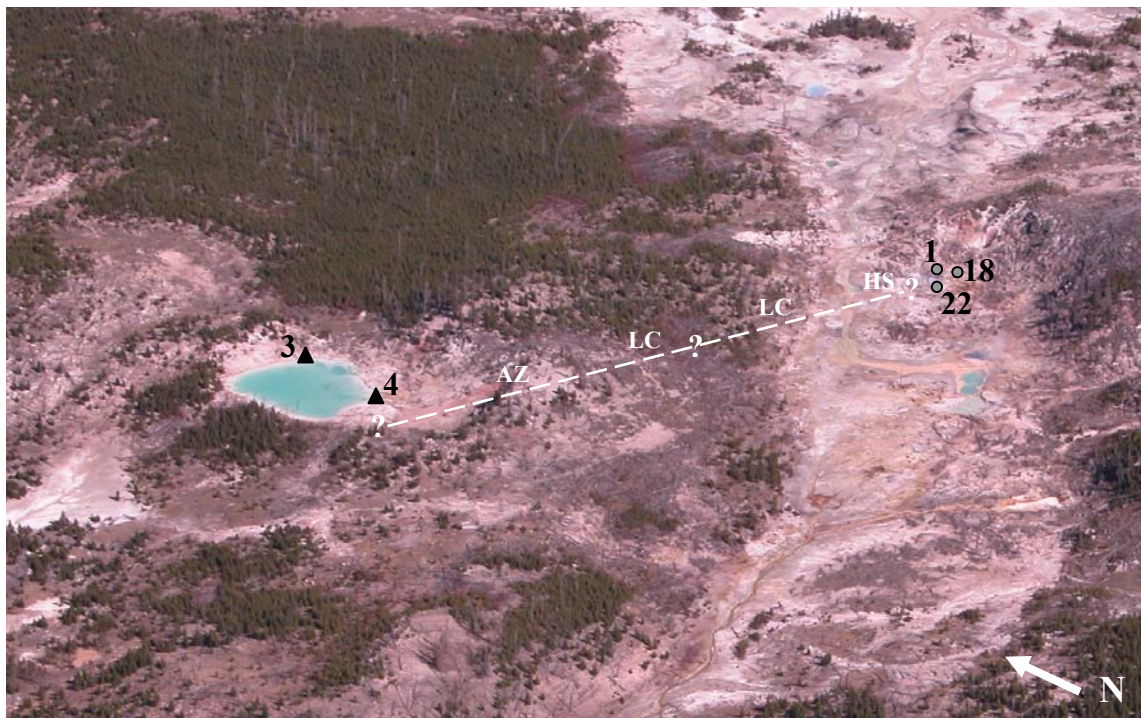


Figure 58 Aerial photograph of the Ragged Hills area with “Verde Pool” (YNPRH03, 04) and the “Milky Way” - “Kaolin Spring” complex (YNPRH01, 18, 22); a linear structure seems to connect both areas (dashed white line arbitrarily drawn a few millimeter below the structure shows its heading; AZ = alteration zone, LC = linear clearings; HS = hot spring); numbers in photo correspond to bold numbers in sampling code

Gibbon Geyser Basin (Geysers Springs group)

The samples from subgroup 5 (Gibbon Geyser Basin GG04 and GG08; Figure 40) are closest to equilibrium with respect to the mineral system albite-potassium feldspar-muscovite (Figure 49). They have the highest pH apart from the lake samples with an average pH of 3.4, Cl concentrations of 150 mg/L and S(VI) concentrations of 320 mg/L (Figure 51). Distinctive are their high temperatures of 83°C (Figure 53), the high Na concentrations of 190 mg/L, and the high F concentrations of 4.5 mg/L (average each). Arsenic concentrations are on average 630 µg/L with a clear predominance of As(III) (82% on average). No significant differences were observed for the three sampling campaigns at GG04, except for As that shows higher concentrations during the second sampling campaign (823 µg/L) compared to the first and forth (580 and 528 µg/L) and an increasing As(III) fraction of 74 to 79 to 84% from June through July to October.

4.3.2.2 Type II deep thermal waters

Type II waters only include samples from Norris Geyser Basin, Gibbon Geyser Basin and Lower Geyser Basin, no samples from the Nymph Lake and Hazle Lake area along the Norris-Mammoth corridor. Seven subgroups can be distinguished within the deep thermal type II waters that are mostly in partial to full equilibrium with regard to the mineral system albite-potassium feldspar-muscovite (Figure 59; Figure 60). The assignment of individual water samples to the 7 subgroups is given in Appendix 21.

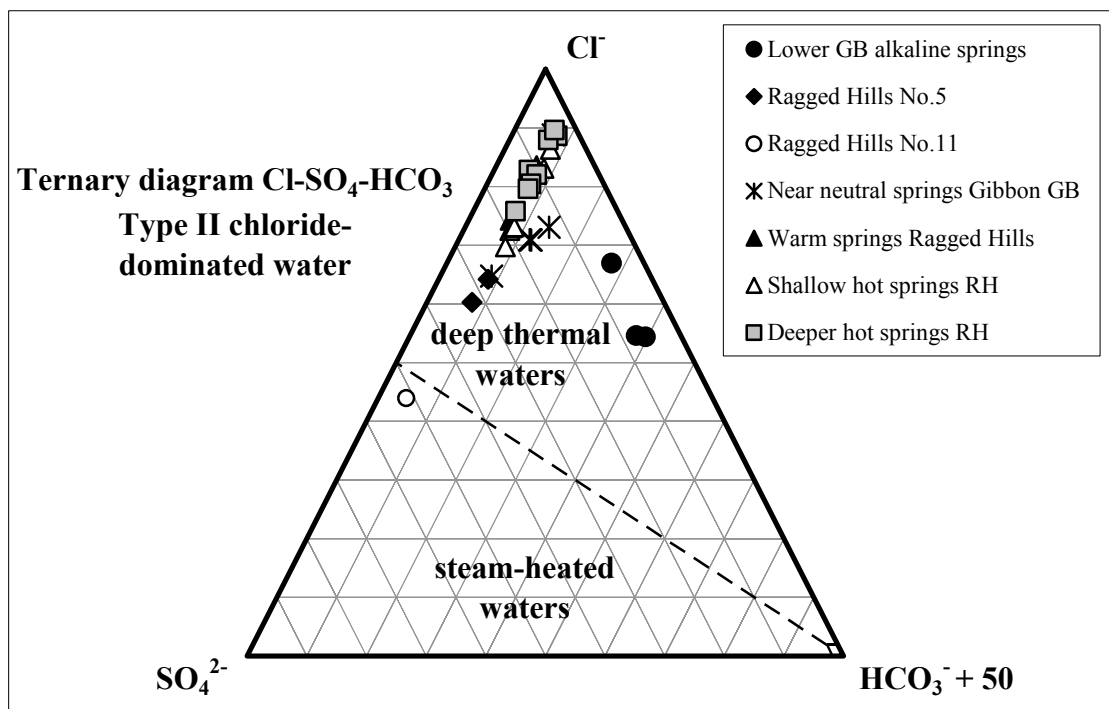


Figure 59 Ternary diagram Cl-SO₄-HCO₃ showing the origin of the subgroups 8-14 of type II deep thermal waters (modified after the classification scheme of Giggenbach and Goguel 1989, HCO₃⁻ + 50 instead of HCO₃⁻; for subgroup affiliation see Appendix 21)

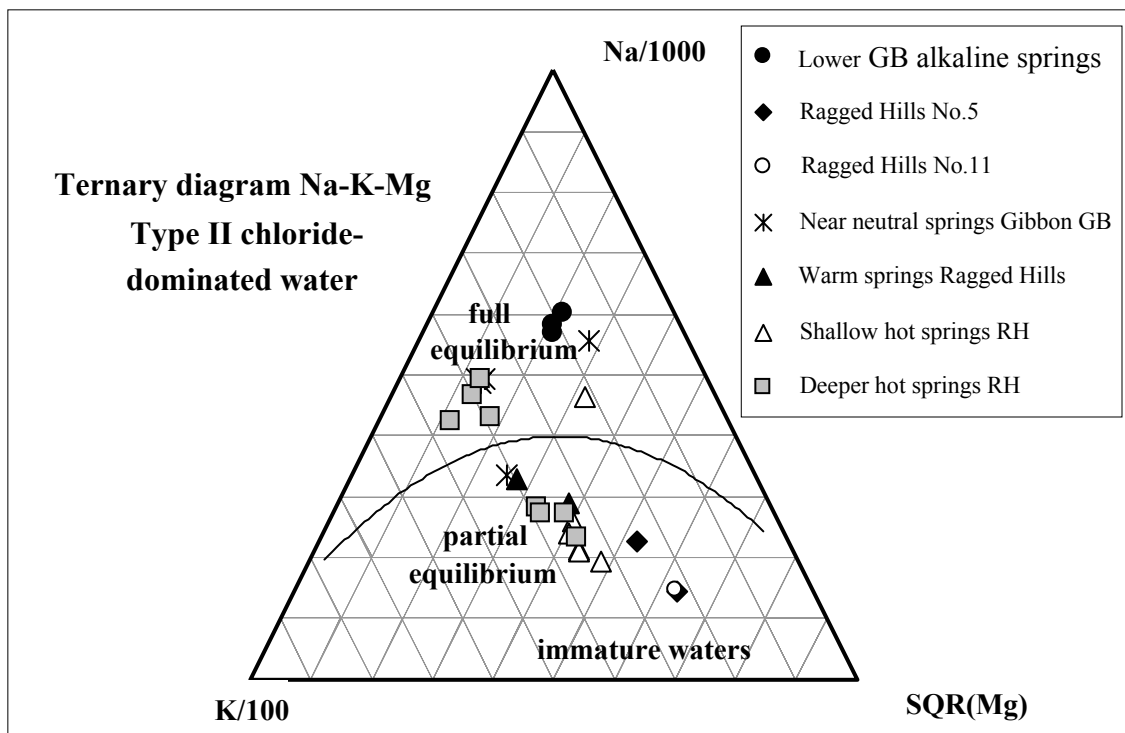


Figure 60 Ternary diagram Na-K-Mg showing the subgroups of type II chloride dominated waters mostly in partial or full equilibrium with the mineral system albite-potassium feldspar-muscovite-clinocllore-silica (equilibrium line calculated for 75 to 350 °C in intervals of 25°C according to the equation for Na/K geothermometer by Arnórsson et al. (1998, cited in Arnórsson 2000) and for K/Mg geothermometer by Giggenbach (1988); for subgroup affiliation see Appendix 21)

Figure 61 to Figure 64 show the main differences in mean values of pH, conductivity, temperature, S(VI), Cl, dissolved total As and As species concentrations for the 7 water subgroups.

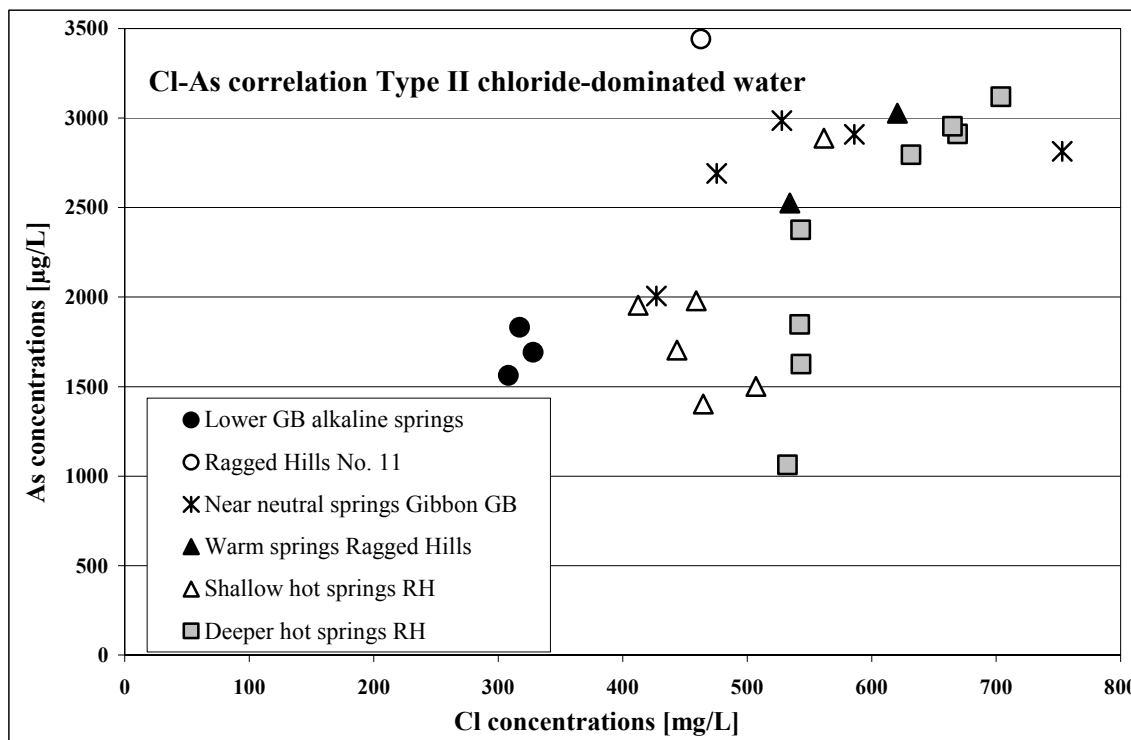


Figure 61 Positive correlation of As and Cl concentrations in deep thermal type II waters (the two samples of subgroup 9 (YNPRH05-1W, 3W with Cl: 399 and 385 mg/L, As: 6940 and 11085 µg/L) are excluded from the graph (outlier); for subgroup affiliation see Appendix 21)

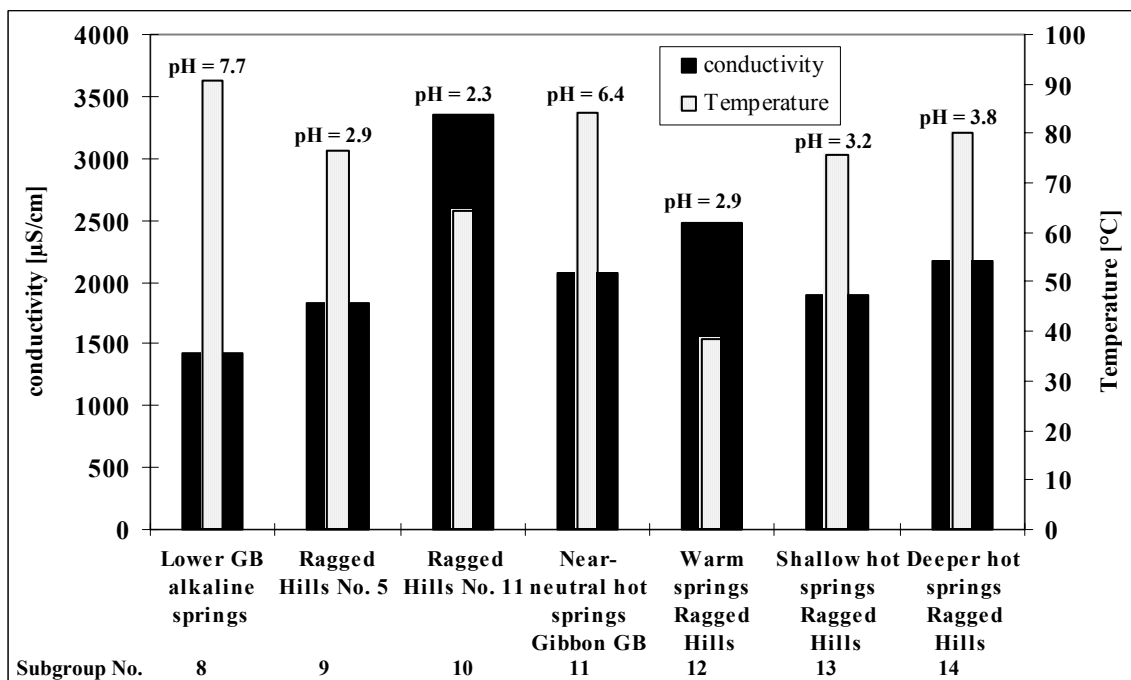


Figure 62 Differences in temperature, conductivity, and pH for the 7 subgroups of type II waters (for subgroup affiliation see Appendix 21)

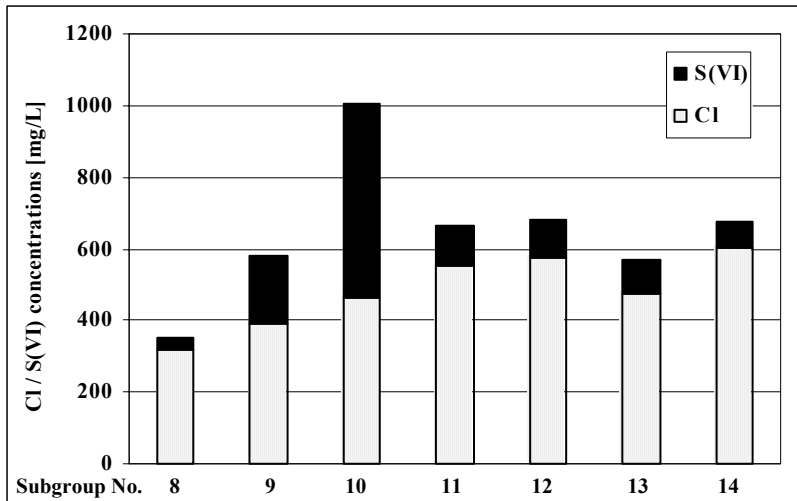


Figure 63 Differences in S(VI) and Cl concentrations for the 7 subgroups of deep thermal type II waters with a clear predominance of Cl

Figure 64 Differences in dissolved As species for the 7 subgroups of type II waters with an overall clear predominance of As(III)

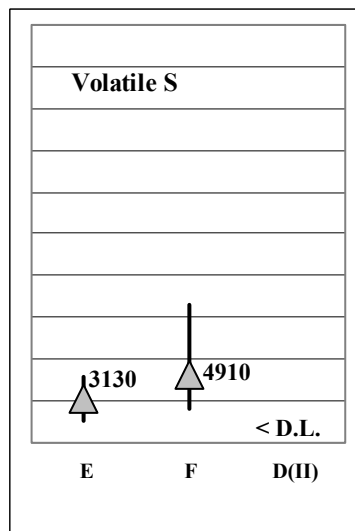
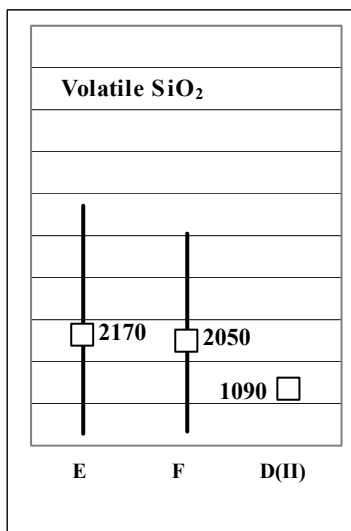
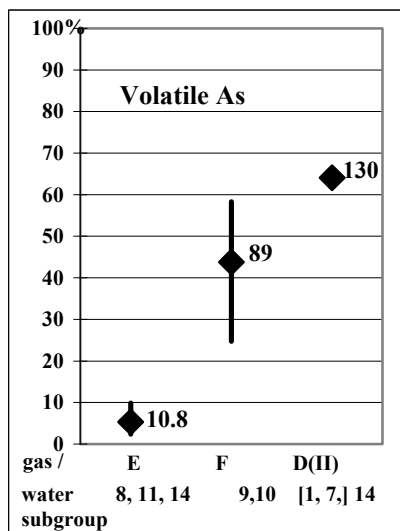
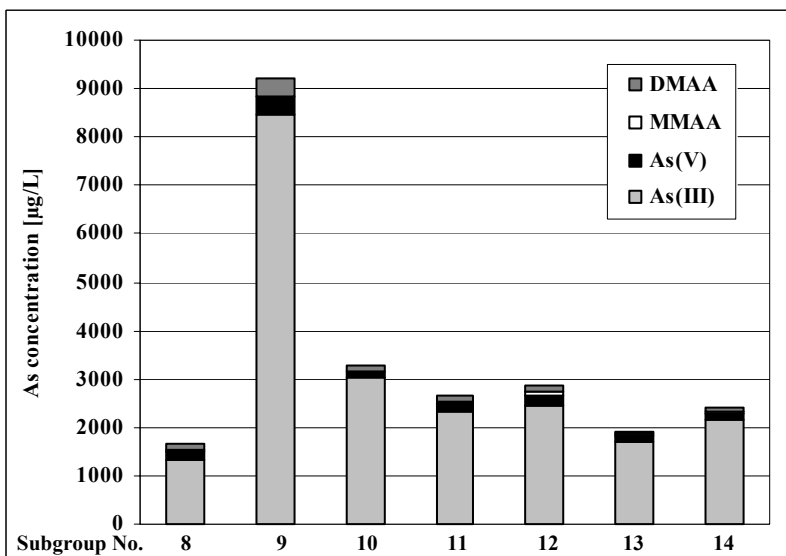


Figure 65 Volatile As, SiO₂, and S concentrations for the 2 gas subgroups E and F of type II waters; subgroup D contains only one sample of type II waters: D(II); type I waters are not considered (Figure 54); values are standardized to a range of 0 to 100 % (= highest concentration for each volatile species); mean value marked by symbol and number for mean concentration in mg/m³; bars represent maximum and minimum concentrations; <D.L. = below detection limit

Considering their gas chemistry, the samples of the 7 water subgroups can be subdivided into the gas subgroups E (Lower Geyser Basin alkaline hot springs; near neutral pH hot springs at Gibbon Geyser Basin and deeper hot springs Ragged Hills) and F (Ragged Hills No. 5 and No. 11) (Appendix 21). Figure 65 shows the differences of the mean values of volatile As, SiO₂, and S concentrations for these 3 subgroups. Subgroup D with the highest volatile As concentrations contains only one type II water sample (YNPRH20), all others are type I as shown in Figure 54.

Norris Geyser Basin (Ragged Hills)

Five different subgroups of type II waters could be distinguished at Ragged Hills (Figure 66).

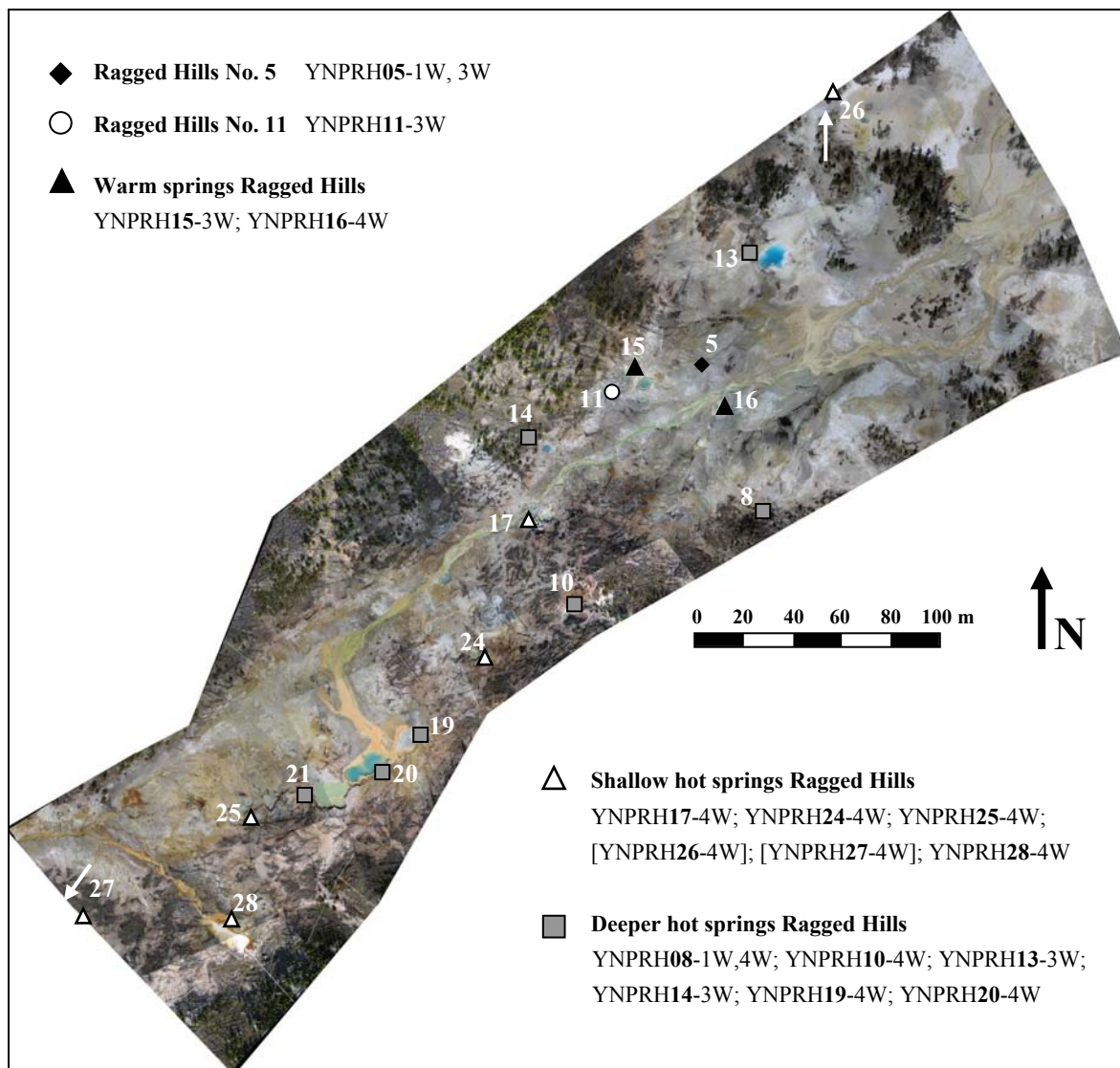


Figure 66 Ragged Hills (aerial photograph from Becker 2004) with sampling locations of the type II waters; numbers in photo correspond to bold numbers in sampling code

The majority of type II waters at Ragged Hills belongs to two subgroups (subgroup 13 with 6 cases and subgroup 14 with 8 cases) with the highest Cl concentrations sampled (Figure 61). Subgroup 13 contains mainly smaller features of only a few centimeters water depths like “Milky Way II” or “Dragon Spring”, subgroup 14 mainly the larger structures like the “Persnickety” - “Titanic” -

“Life Boat” complex, “Elk Geysler”, “Rainbow Growler” and Crystal Springs. The bottom of these larger structures is often not visible, thus exact water depths can not be defined. Comparing the smaller, shallower structures with the larger, deeper structures, average conductivities (2038 and 2168 $\mu\text{S}/\text{cm}$), pH (3.2 and 3.8), average concentrations of Si (268 and 382 mg/L), Cl (505 and 603 mg/L), Na (278 and 335 mg/L), Ba (0.16 and 0.05 mg/L), and Sb (75 and 130 $\mu\text{g}/\text{L}$) are generally lower (Figure 62; Figure 63; Figure 67). Average S(VI) concentrations are higher in the shallower structures compared to the larger ones (94 and 69 mg/L; Figure 63). From the two samples taken for Hg YNPRH08 had 0.35 ng/L methylated Hg and 170 ng/L total Hg, YNPRH20-4W only 0.04 ng/L methylated Hg and 28 ng/L total Hg. The gas chemistry of the deeper hot springs is similar to that of hot springs at Gibbon Geysler Basin and Lower Geysler Basin (see below).

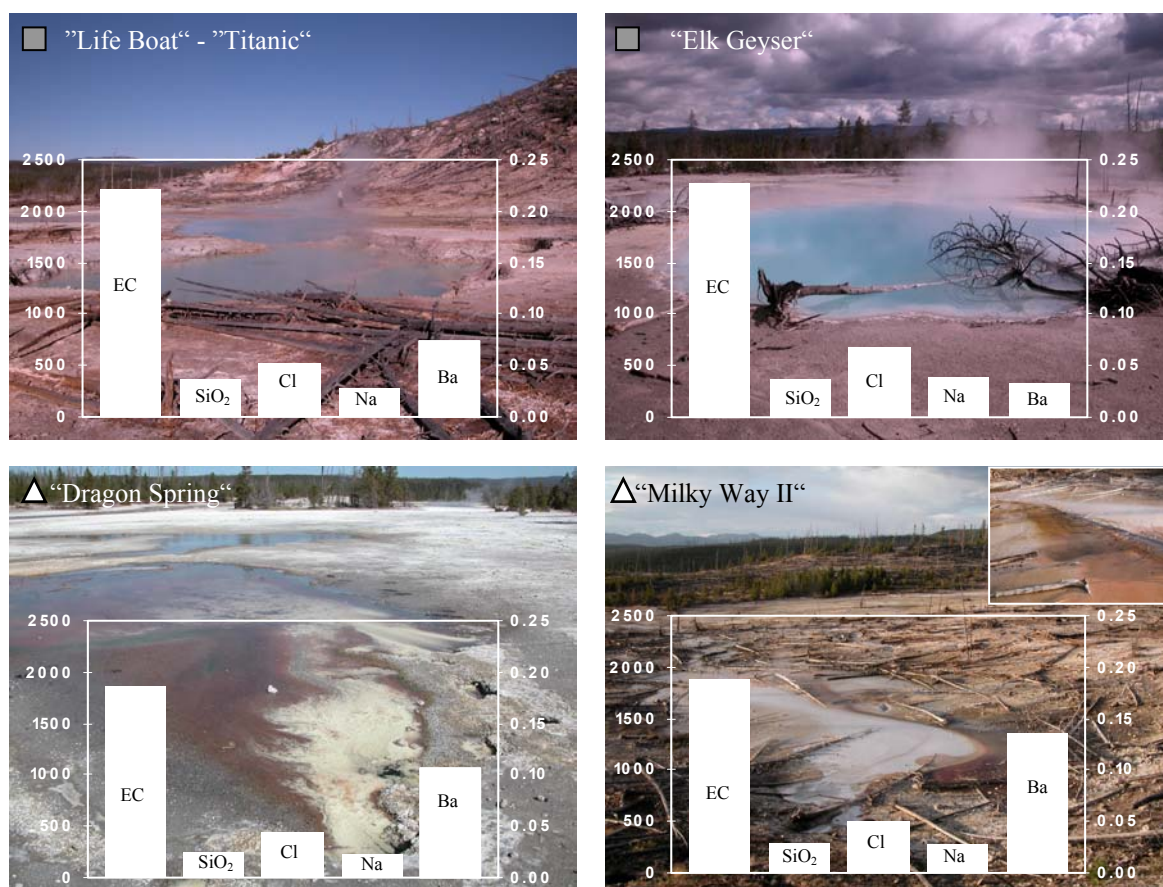


Figure 67 Larger deeper geothermal features like the “Life Boat” – “Titanic” – “Persnickety complex” and “Elk Geysler” show higher electrical conductivities (EC), SiO₂, Cl, and Na concentrations (units on primary y-axis in $\mu\text{S}/\text{cm}$ and mg/L) and lower Ba concentrations (units on secondary y-axis in mg/L) compared to the smaller and shallower structures like “Dragon Spring” and “Milky Way II”

The two samples from the subgroup of “warm springs” in the western part of the Ragged Hills area are characterized by lower than average temperatures (37.8 and 38.9 °C for YNPRH15-3W and 16-4W respectively; Figure 62). Remarkable are their high average Ba concentrations of 0.24 mg/L. In mid September, the hot spring YNPRH15 showed a smeary bio-film on its surface with single flakes of foam floating on top (Figure 68). After 2 weeks this bio-film disappeared and the hot spring’s water was clear again.

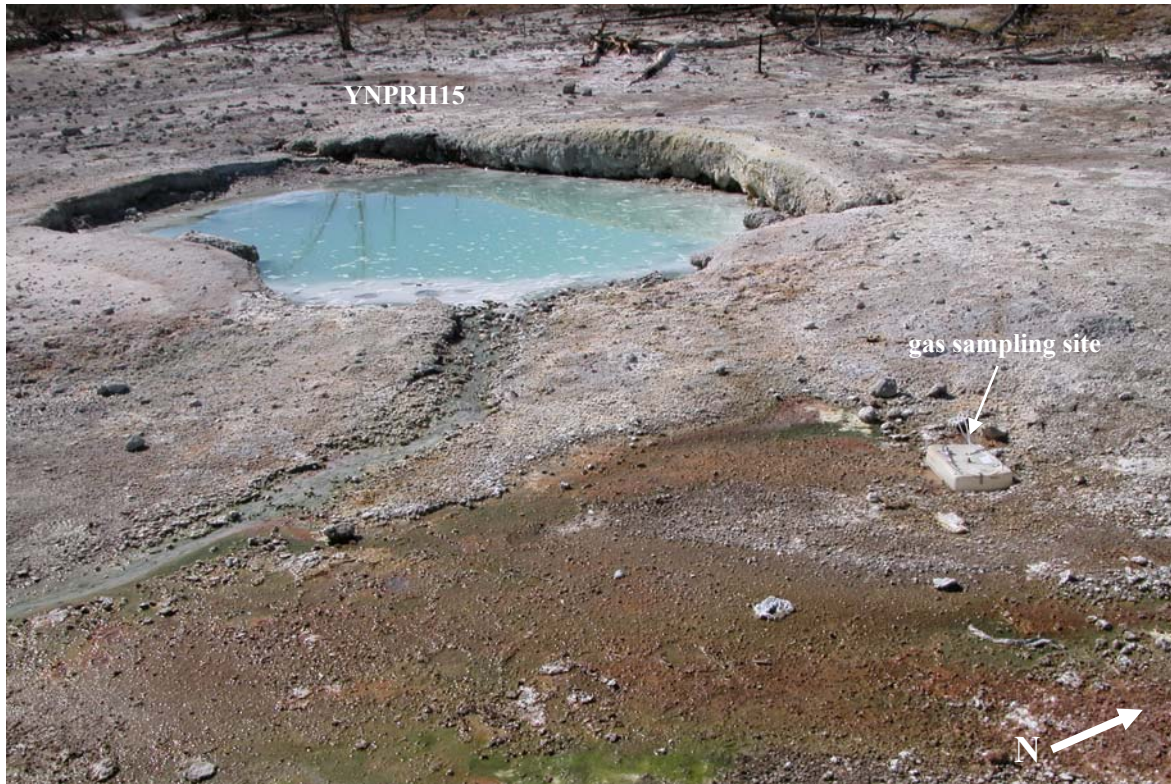


Figure 68 Warm spring YNPRH15 mid of September with white foam flakes on its surface

The highest As concentrations (6.9 and 11 mg/L; Figure 64) were found at a small hot spring of approximately 1 m diameter (YNPRH05; Figure 69). Arsenite predominates at this site with 89 and 94% for the June and September sampling respectively. In Figure 60 the sampling site plots in the field between immature waters and waters in partial equilibrium with respect to the mineral system albite-potassium feldspar-muscovite. It shows low pH (2.9) and relatively high S(VI) concentrations (190 mg/L) within its group of chloride-dominated waters (Figure 62; Figure 63).



Figure 69
Sampling YNPRH05,
with 6.9 and 11 mg/L
the hot spring with the
highest dissolved As
concentrations

The lowest pH (2.3) and the highest conductivity (3350 $\mu\text{S}/\text{cm}$) within the group of type II waters, shows YNPRH11, an ellipse shaped (1 to 2 m) hot spring that changed to mud pot activity during October 2003 (Figure 62). With 541 mg/L it contains a significant amount of S(VI) besides 463 mg/L Cl (Figure 63) and plots between deep thermal and steam-heated waters (Figure 59). It is also the most immature water within its group (Figure 60). Arsenic concentrations of 3.4 mg/L are the second highest after YNPRH05 (Figure 61; Figure 64).

The two sampling sites with the highest total As concentrations, YNPRH05 and 11, belong to the gas subgroup F, characterized by the second highest volatile As concentrations with a mean of 89 mg/m^3 (Figure 65). The fact that these samples also show the highest dissolved As(III) fraction of all samples (Figure 64) corresponds well with the observed correlation of dissolved As(III) and volatile As (Appendix 23). The sites YNPRH05 and 11 are also the only ones, besides those of gas subgroup D, with significant concentrations of volatile Li (42 mg/m^3) and B (138 mg/m^3).

Gibbon Geyser Basin (Geyser Springs group)

Subgroup 11 contains the sites GG02, 06, and 07 at Gibbon Geyser Basin and RH09 at Ragged Hills. Their pH is near neutral (6-7). While all the samples from Gibbon Geyser Basin within this subgroup are in full equilibrium, YNPRH09 is only in partial equilibrium with respect to the mineral system albite-potassium feldspar-muscovite (Figure 60). Low concentrations of methyl Hg were detected in YNPRH09 (0.04 ng/L).

Like the deeper hot springs at Ragged Hills and Lower Geyser Basin, chloride-dominated hot springs at Gibbon Geyser Basin show the lowest volatile As concentrations of all samples with an average of 10.8 mg/m^3 (gas subgroup E; Figure 65). A negative correlation with the highest dissolved TIC concentrations (average 17 mg/L) was found to be significant on a level of 3.2% (Appendix 23). Remarkable are also the low concentrations of volatile Al (200 mg/m^3), Fe (14.5 mg/m^3), and Ba (43 mg/m^3) compared to other subgroups. They correlate with low volatile As concentrations and dissolved Fe(III) concentrations close to detection limit (0.03 mg/L) or below (for correlation analysis replaced by $0.3 \cdot \text{detection limit}$).

Lower Geyser Basin (Pocket Basin)

All 3 samples taken from within the Yellowstone caldera, at Pocket Basin in the Lower Geyser Basin area (Figure 41), form their own subgroup. They are the only samples with alkaline pH from 7.3 to 8.7 (Figure 62). At 91°C they have the highest temperatures of all samples (Figure 62), the highest F concentrations (25 mg/L), and the lowest S(VI) concentrations (34 mg/L) (Figure 63). Within their group of type II waters, they have the lowest Cl concentrations (318 mg/L) and the lowest conductivities (1400 $\mu\text{S}/\text{cm}$). The water at all three sampling sites is in full equilibrium with respect to the mineral system albite-potassium feldspar-muscovite (Figure 60). Total inorganic carbon concentrations of 32 mg/L indicate an influence of peripheral waters on the deep thermal waters (Figure 59). Remarkable are the W concentrations (390 to 430 $\mu\text{g}/\text{L}$) being 1 to 2 orders of magnitude higher than in all other samples. Cluster analysis confirms the differences of this sub-

group from all other type II subgroups, containing only samples from Gibbon Geyser Basin and Ragged Hills. The gas chemistry is similar to deeper hot springs at Ragged Hills and chloride-dominated hot springs at Gibbon Geyser Basin as described above.

4.3.3 Modeling As species and mineral phases

Speciation calculations show that in accordance with other reports on geothermal As (Cleverley et al. 2003; Spycher and Reed 1989; Webster and Nordstrom 2003) $\text{H}_3\text{AsO}_3(\text{aq})$ is the predominant As species in almost all samples (Appendix 24). A predominance of As(V) species is only found for samples from Hazle and Nymph Lake, identified in the speciation modeling as H_2AsO_4^- . Species separation showed that those pentavalent species are probably rather methylated than inorganic species (Figure 57; Figure 70 left) but the organic species could not be considered in the speciation modeling because of a lack of thermodynamic data. Modeling confirms that the non-charged pentavalent complex H_3AsO_4^0 would make up only 20% on average of all As(V) species. Its concentration is more or less equal to that of H_2AsO_4^- in 7 of 60 cases and it becomes the predominant As(V) species with 70 and 75 % only in the two samples from the Nymph Lake fumaroles (YNPNL05). The total share of inorganic As(V) in these two samples is, however, <1% (Figure 70 right). This minimal occurrence of the non-charged As(V) complex is important to justify the application of the ion exchanger method with the problem of non-charged As(V) being determined erroneously as As(III) as discussed in section 4.2.3.1.

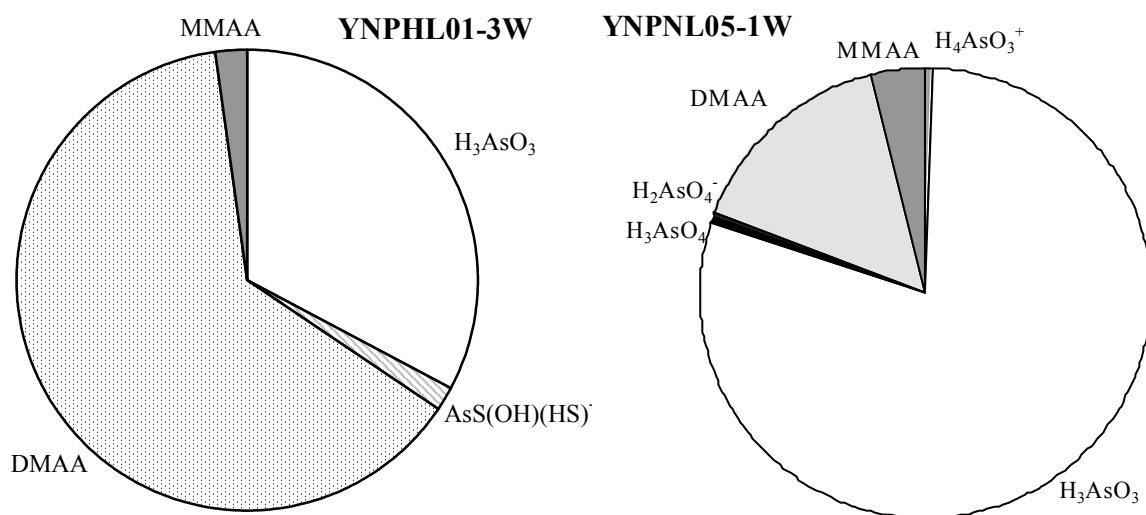


Figure 70 Left: Predominance of methylated species* in Hazle Lake, the share of non-charged H_3AsO_4 is significantly lower than in other geothermal samples; Right: Only in samples from the new fumarole area at Nymph Lake did the non-charged H_3AsO_4 predominate over H_2AsO_4^- but both As(V) species make up less than 1% of all As species, the non-charged As(III) species H_3AsO_3 predominates like in most geothermal waters

* Share of methylated species derived from on-site separation as explained in the sections 2.7.2 and 4.2.1.2; individual inorganic As(III), As(III)-S, and As(V) complexes modeled with PhreeqC, for modeling methylated species were added to the As(V) species as explained in section 4.2.3.5

In all samples with near neutral to alkaline pH and S(-II) concentrations above detection limit (YNPLG01-2W, 03-2W, YNPGG02-2W, 06-2W, 07-2W, 4W, YNPRH08-4W) AsS(OH)(HS)^- was calculated in concentrations of several tens to hundreds $\mu\text{g As/L}$ (Figure 71 top left). At YNPLG02 with a pH of 8.7, the S(-II) concentrations are so high (3.75 mg/L) that polysulfides (S_5^{2-} , S_4^{2-} , and S_6^{2-}) form according to the speciation modeling, and the concentration of AsS(OH)(HS)^- (20 $\mu\text{g/L}$) is negligible (Figure 71 top right). At Hazle Lake, low pH values of 3.0 to 3.1 inhibit the formation of AsS(OH)(HS)^- at As concentrations of 200-540 $\mu\text{g/L}$, even though S(-II) concentrations are high (0.9-1.7 mg/L). The concentrations of AsS(OH)(HS)^- are 1 to 10 $\mu\text{g/L}$ only, H_2S is the predominant S(-II) species. For three sites at Ragged Hills (YNPRH05-1W, 3W, YNPRH11 and 26) modeling showed AsS(OH)(HS)^- (30 to 90 $\mu\text{g/L}$) at pH values as low as at Hazle Lake (2.3 to 3.0). Still, H_2S is the predominant S(-II) species, but higher As concentrations (1.7 to 11 mg/L) lead to higher AsS(OH)(HS)^- concentrations. The predominant As-S species is $\text{As}_3\text{S}_4(\text{HS})_2^-$ (130 to 240 $\mu\text{g/L}$) that only occurs in these four samples (Figure 71 left).

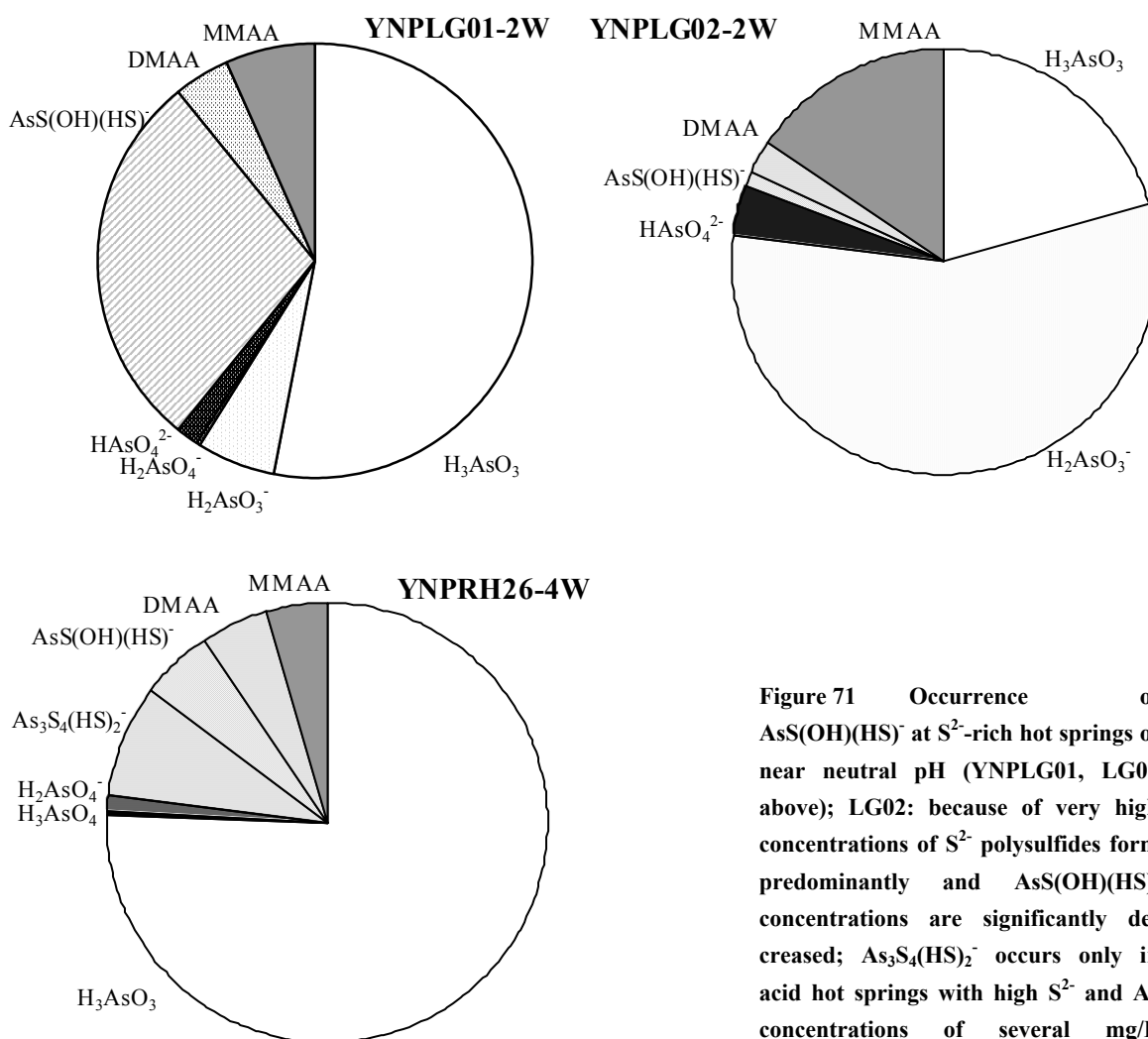


Figure 71 Occurrence of AsS(OH)(HS)^- at S^{2-} -rich hot springs of near neutral pH (YNPLG01, LG02 above); LG02: because of very high concentrations of S^{2-} polysulfides form predominantly and AsS(OH)(HS)^- concentrations are significantly decreased; $\text{As}_3\text{S}_4(\text{HS})_2^-$ occurs only in acid hot springs with high S^{2-} and As concentrations of several mg/L (YNPRH26 left)

Supersaturation with regard to the As minerals listed in the WATEQ4F database was found only for 5 samples at 3 sites (Appendix 25). At Hazle Lake the saturation index for orpiment is +0.4,

+0.6 and +1.6 for the June, July, and September sampling respectively. In September, additionally amorphous As_2S_3 was slightly supersaturated ($\text{SI} = 0.2$). According to Cleverley et al. (2003) amorphous As_2S_3 can be observed in meta-stable equilibrium with orpiment in natural settings. A possible precipitation of orpiment at Hazle Lake is not as striking bright yellow as at “Orpiment Puddle” and “Orpiment Puddle Son” but the sides of the small geothermal feature are covered with a yellowish precipitation the color of which is mainly obscured by the color of the algae rich lake water (Figure 72). No microprobe analysis have been conducted yet to confirm whether the precipitate is orpiment. The temperatures and S(-II) concentrations observed at Hazle Lake are lower (20-26°C and 0.9-1.7 mg/L) compared to “Orpiment Puddle” (43-53°C and 3.5-4.25 mg/L; Nordstrom et al. 2003), pH, conductivity, redox potential, and As concentrations are comparable. Like “Orpiment Puddle” the samples from Hazle Lake show an anomalously low As/Cl ratio compared to all other samples indicating As removal by precipitation (Figure 50).



Figure 72 Left: Geothermal feature at the south side of Hazle Lake (YNPHL01); yellowish precipitations at the sides could indicate the occurrence of orpiment that is supersaturated according to PHREEQC modeling (Appendix 25); right: for comparison: the bright yellow “Orpiment Puddle Son” USGS sampling September, 4th, 2003 from left to right: Beate Böhme, Jim Ball, JoAnn Holloway, and Kirk Nordstrom

The other two samples that show supersaturation for an As mineral phase are YNPRH15 and 16, the warm springs at Ragged Hills (Figure 62). Saturation indices for realgar are +2.4 and +1.8 respectively. The precipitation of realgar directly from solution at temperatures less than 100°C is not very commonly found (Nordstrom and Archer 2003). Also the samples do not show a depletion of As compared to Cl that could indicate mineral precipitation (Figure 61). However, the precipitation of an As rich-phase was actually observed when taking a gas sample by passive sampling from the 4th of October until the 7th of October 2003 close to YNPRH15 (Figure 68). During the 3 days of sampling a metallic precipitation formed under the gas hood (Figure 73). Upon removal of the gas hood the precipitation vanished within half an hour. The experiment was repeated from 24th to 27th of October and the results were confirmed. Microprobe analysis indicated a material rich in Fe, S, and As that is amorphous to electron microscope diffraction (HRTEM and SEM).



Figure 73 Precipitation of amorphous Fe, S, and As rich material at YNPRH15 underneath a gas hood (33 x 24 x 8 cm) installed for 3 days to sample volatile metallics on SPME

Unfortunately this site was not sampled for total volatile metallics but only species-selective with a SPME fiber. No As species were identified on the SPME fiber. This result could indicate a scavenging effect by the mineral precipitation, but the reliability of reproducible As sorption on the SPME fibers is still questionable as discussed in the next section (4.3.4).

4.3.4 Volatile As speciation

No volatile As species were detected neither on the 20 Tenax nor on the 20 Carboxen 564 solid sorbents. This result might be attributed to the lower sensitivity of solid sorbents compared to SPME fibers, but also to longer storage times. Analyses were not performed until 9 to 15 days later since the solid sorbents had to be sent back to Germany for a GC-MS with a thermal desorption port.

From the 57 gas samples taken by SPME fibers (12 PDMS 100, 31 PDMS-CAR, 14 PDMS-CAR-DVB) 34 showed no volatile As. Four different volatile As species were identified in the remaining 23 samples. Chromatograms and mass spectra are presented in the digital database (Appendix 9). Peak areas are indicated for internal comparison only, a quantification was not attempted as explained in section 3.2.3.2. Three fibers not exposed to the geothermal gases but stored in the same way as the gas samples were used as blank values and did not show any volatile As peaks. One PDMS and 2 PDMS-CAR fibers broke in the field and no samples could be obtained. The volatile As species detected on SPME fibers did not show apparent differences between the 6 gas sub-groups.

The most predominant volatile As species identified in 22 samples is $(\text{CH}_3)_2\text{AsCl}$. It has only been reported from laboratory experiments (section 2.5.3.6). Far less common is $(\text{CH}_3)\text{AsCl}_2$ detected in 3 samples with a peak area about 20-40% smaller than that of $(\text{CH}_3)_2\text{AsCl}$ (Figure 74). Its detection in a natural aquatic environment is also a novelty. Retention times for $(\text{CH}_3)_2\text{AsCl}$ and $(\text{CH}_3)\text{AsCl}_2$

are about 3.2 and 5.6 minutes respectively. The fully chlorinated AsCl_3 with a boiling point of 130°C did not occur in any sample. The fully methylated $(\text{CH}_3)_3\text{As}$ with a boiling point of 52°C (section 2.5.3.4) and short retention times of about 1.9 minutes was detected in 8 chromatograms. The fourth species positively identified in 7 samples is $(\text{CH}_3)_2\text{AsS}(\text{CH}_3)$ (Figure 75; Kösters et al. 2003). It has the highest boiling point of the four As species. Its retention time is about 6.1 minutes and it always occurred together with large peak areas of $(\text{CH}_3)_2\text{AsCl}$ and with one exception also of $(\text{CH}_3)_3\text{As}$. Its discovery is especially interesting because it has only been synthesized in the laboratory and nothing is known about its abundance in the environment (section 2.5.3.5). No correlation between the occurrence of volatile chloroarsines and dissolved or gaseous Cl and between the occurrence of volatile sulfurarsine and dissolved or gaseous S was found. Trimethylarsine was preferably detected at low total volatile As and S concentrations and low As(III) ratios in water. Because of the lack of calibration standards neither peak heights nor peak areas were calibrated. Therefore a meaningful correlation analysis could not be performed.

In respect to the choice of SPME fiber material no significant sorption preference was found in contrast to the different sorption behavior observed in the laboratory (section 3.2.3.2; Figure 26). The only generalization that can be made is that volatile $(\text{CH}_3)_2\text{AsS}(\text{CH}_3)$ was exclusively detected on PDMS-CAR and PDMS-CAR-DVB, not on PDMS 100. The preferable sorption of $(\text{CH}_3)_2\text{AsCl}$ and $(\text{CH}_3)\text{AsCl}_2$ on PDMS 100 and of $(\text{CH}_3)_3\text{As}$ and $(\text{CH}_3)_2\text{AsS}(\text{CH}_3)$ on PDMS-CAR was only observed for the sampling site YNPLG02. At all other sites larger peak areas for chloroarsines were detected on PDMS-CAR or PDMS-CAR-DVB compared to PDMS 100. At most sites the volatile As species showed different sorption behavior on individual fibers during different sampling campaigns. For YNPHL01, $(\text{CH}_3)_2\text{AsS}(\text{CH}_3)$ was observed on PDMS-CAR during the first sampling campaign in June, but only on PDMS-CAR-DVB, not on PDMS-CAR, during the second sampling campaign in July. Another example is YNPNL04, where three volatile As species, $(\text{CH}_3)_3\text{As}$, $(\text{CH}_3)_2\text{AsCl}$ and $(\text{CH}_3)_2\text{AsS}(\text{CH}_3)$, were found on PDMS 100 and PDMS-CAR-DVB in June. The PDMS-CAR fiber did not show any volatile As peaks. In September, only PDMS-CAR yielded one volatile As species, $(\text{CH}_3)_2\text{AsCl}$, while none was desorbed from the other two fibers.

Sampling duration reached from 18 to 98 hours with an average of 70 hours. In the laboratory, equilibrium in the ternary phase system sample solution – headspace – SPME fiber is achieved within minutes. Thus, shorter sampling times should be possible. Figure 76 shows a comparison of chromatograms sampling YNPRH05 for 94 hours and 2.3 hours (140 minutes) only. Most peaks are identical but the peak areas are smaller for the shorter sampling duration. The volatile As peak of $(\text{CH}_3)_2\text{AsCl}$ at 3.8 minutes is missing in the chromatogram of the short-term sampling. Obviously, equilibrium on the fiber takes longer in the field compared to laboratory experiments. On the other hand, a sampling duration of 70 hours might not be necessary considering that the two largest peaks for $(\text{CH}_3)_2\text{AsCl}$ were detected at YNPRH05 and 06 after 23 hours of sampling. Another explanation could of course be that distinct species occur only sporadically, but as long as the sampling techniques are not optimized a natural variation cannot be verified.

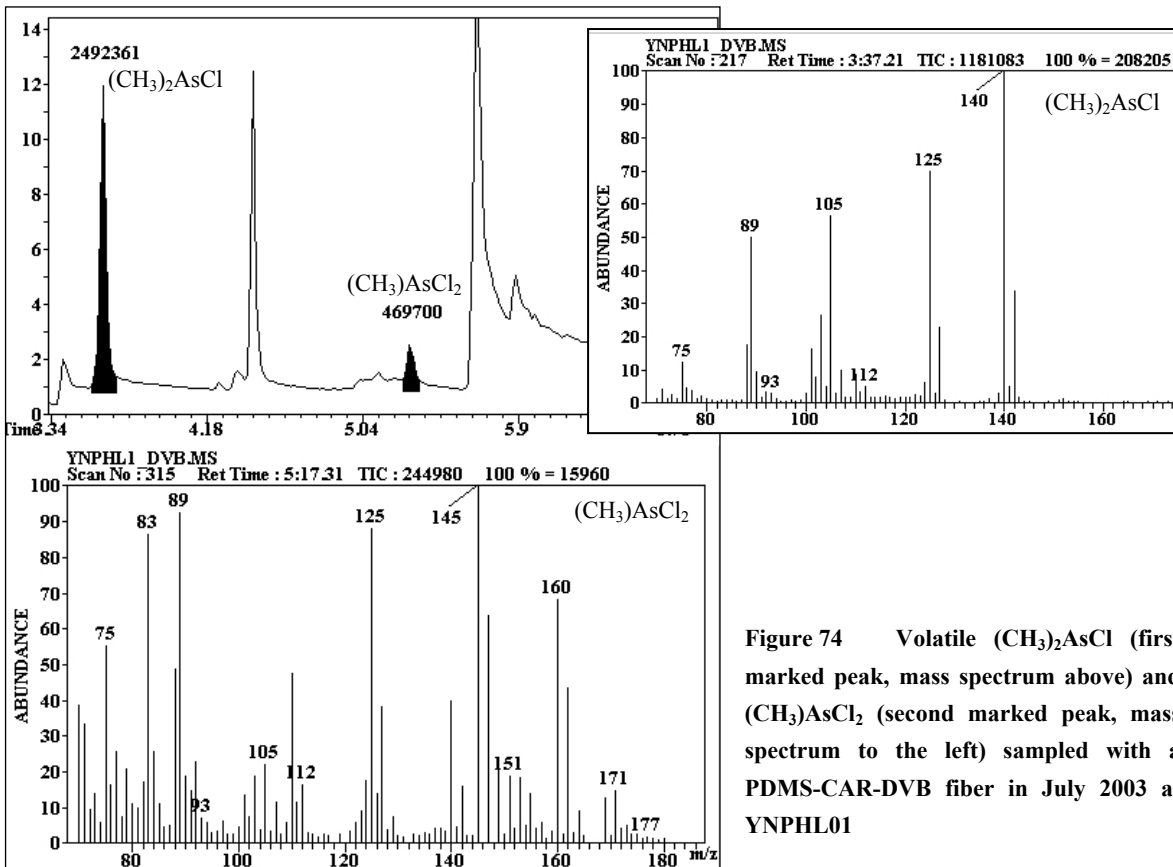


Figure 74 Volatile $(\text{CH}_3)_2\text{AsCl}$ (first marked peak, mass spectrum above) and $(\text{CH}_3)\text{AsCl}_2$ (second marked peak, mass spectrum to the left) sampled with a PDMS-CAR-DVB fiber in July 2003 at YNPHL01

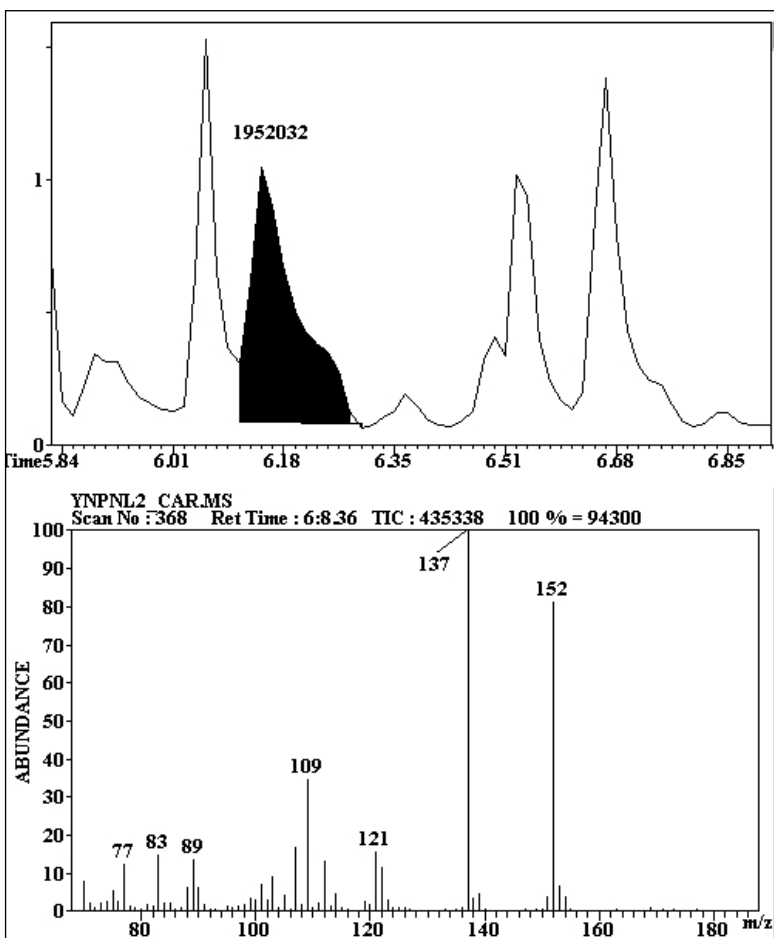


Figure 75 First discovery of volatile $(\text{CH}_3)_2\text{AsS}(\text{CH}_3)$ in a natural aquatic environment sampled with a PDMS-CAR fiber in June 2003 at YNPNL02

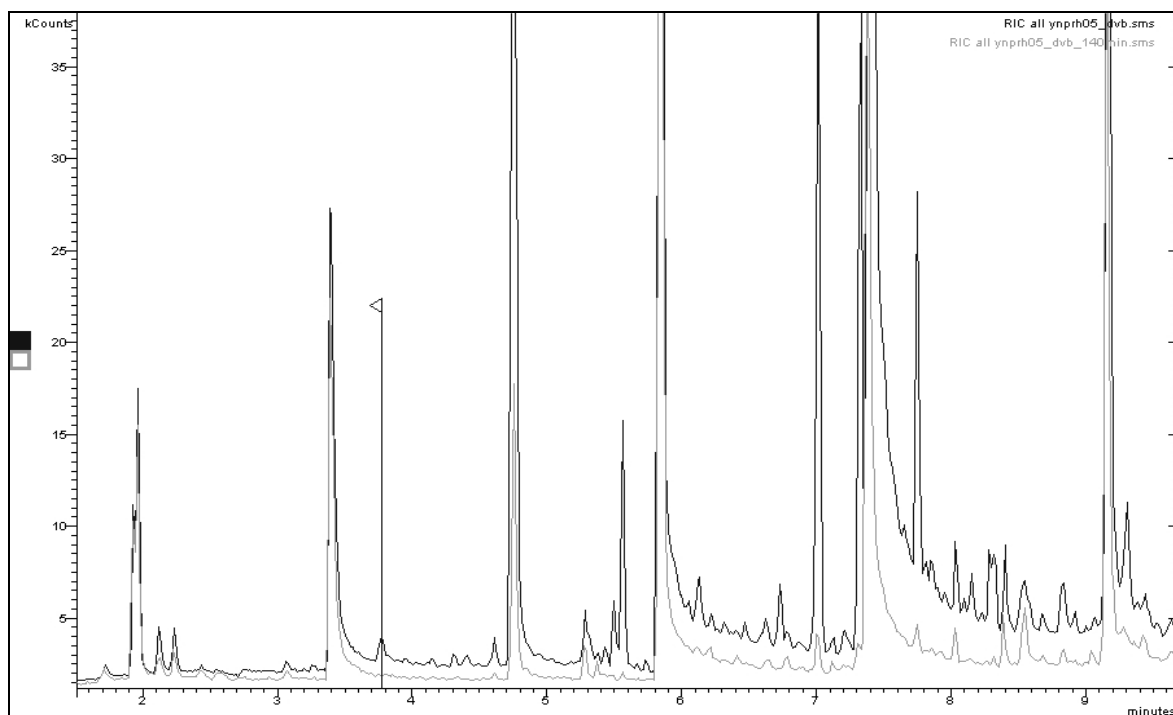


Figure 76 Chromatograms from gas sampling with PDMS-CAR-DVB SPME fibers at YNPRH05 for 94 hours (black line) and 2.3 hours (gray line); while most peaks are identical, the $(\text{CH}_3)_2\text{AsCl}$ peak (flagged in the chromatogram) clearly only appears when longer sampling times are applied

The biggest challenge for a reliable interpretation is a reproducible sorption of all occurring volatile As species. As mentioned before, different sorption behavior was observed on individual fibers during different sampling campaigns. There seems to be a trend of fewer occurrence of $(\text{CH}_3)_3\text{As}$, $(\text{CH}_3)_2\text{AsCl}$, and $(\text{CH}_3)_2\text{AsS}(\text{CH}_3)$ from June and July to September and October. If this observed difference is not arbitrary it must be attributed to competing sorption reactions with other gases, maybe of seasonally changing composition. It is also striking that volatile As species were only detected in 23 of 57 gas samples even though the results of total volatile As from oxidation solutions confirm their presence in all samples. This contradiction might be explained by the presence of other volatile As species oxidized in NaOCl but not effectively sorbed on SPME fibers, such as $(\text{CH}_3)_2\text{AsH}$, $(\text{CH}_3)\text{AsH}_2$, or AsH_3 . Because of their low boiling points these compounds are not trapped on SPME fibers at ambient temperatures.

One more drawback is that under the GC-MS conditions described in Table 6 retention times still varied significantly between the different runs (Table 12) requiring a MS-detector for unambiguous peak identification. Some of the chromatograms also showed a poor peak resolution from background noise or a significant peak tailing over up to 2 minutes.

Table 12 Minimum, average and maximum retention times for the four volatile As species detected by GC-MS

retention time	$(\text{CH}_3)_3\text{As}$	$(\text{CH}_3)_2\text{AsCl}$	$(\text{CH}_3)\text{AsCl}_2$	$(\text{CH}_3)_2\text{AsSCH}_3$
min	1.42	1.88	5.32	4.72
mean	1.90	3.22	5.61	6.09
max	2.21	4.89	6.11	6.64

Species-selective interpretation of other volatile elements detected besides volatile As was not an objective of this thesis. Thus, only speculations about the nature of these volatile elements can be made. The elements Li, Ba, B, Al, Si, S, and Cl can form simple volatile hydrides. For Cu, Fe, K, Sr, and Zn a transition to the gaseous phase is rather likely bonded to volatile organic substance, e.g., to carbonyls as reported for Mo and W (chapter 1). The chromatograms obtained were scanned for known mass spectra of any of these compounds, however, none could be identified. Detection of very low-molecular compounds such as BH_3 ($m = 13.8$ g/mol) or H_2S ($m = 43$ g/mol) as well as high-molecular compounds was excluded a priori by the selection of the mass scan range from 70-180 for an optimum resolution of the target compounds of volatile As.

4.3.5 Modeling volatile As speciation

In the WATEQ4F database no thermodynamic data for volatile As species were available. Thus, data for As(g) , $\text{As}_2(\text{g})$, $\text{As}_3(\text{g})$, $\text{As}_4(\text{g})$, $\text{AsCl}_3(\text{g})$, $\text{AsF}_3(\text{g})$, $\text{AsF}_5(\text{g})$, $\text{AsH}_3(\text{g})$, $\text{As}_4\text{O}_6(\text{g})$, AsS(g) , and $\text{As}_4\text{S}_4(\text{g})$ compiled by Spycher and Reed (1989) were added to the PHREEQC input file (Appendix 26). Partial pressures for all volatile As species considered were negligibly low (Appendix 27). The highest partial pressure was found for As_4S_4 with 10^{-11} to 10^{-30} Vol%. The species AsH_3 is third in abundance of gaseous As species with partial pressures as low as 10^{-23} to 10^{-34} Vol%. This insignificance of fractionation of the considered As species into the gas phase is in accordance with results from Spycher and Reed (1989) for geothermal fluids. The authors give various explanations for the discrepancy between detection of volatile As species in geothermal gases and the inability of modeling it. Possible reasons could be excess enthalpy boiling, leaching of previously deposited As minerals by dry steam or inaccurate stability constants for aqueous or gaseous species. The omission of volatile organometallic species in thermodynamic databases is acknowledged but considered negligible. This conclusion was withdrawn from modeling $\text{Sb}(\text{CH}_3)_3$, one of the few volatile organometallics for which thermodynamic data were available and which yielded very low fugacities. Based on the results from As species-selective sampling described in the previous section (4.3.4), the insignificance of volatile organoarsines has to be questioned: Four different species were positively identified at various sites. Modeling of the results remained impossible since no thermodynamic data could be found for any of the species.

Still, the question remains about the nature of the volatile As species that were trapped in NaOCl solution but not sorbed on SPME fibers as discussed in the previous section (4.3.4). The explanation of Spycher and Reed (1989) that As is only carried in water droplets entrained in steam can be excluded from the use of water traps mounted before the oxidizing traps. Pokrovski et al. (2002) showed in their experimental study on As speciation in the vapor phase that with increasing temperature $\text{As}(\text{OH})_3(\text{g})$ becomes the predominant gaseous As species. Including $\text{As}(\text{OH})_3(\text{g})$ in the modeling by considering its Henry constant ($\log k = 11.2$ at 25°C ; Pokrovski et al. 2002) yielded partial pressures of $6.8 \cdot 10^{-14}$ to $8.0 \cdot 10^{-17}$ Vol%. Thus, $\text{As}(\text{OH})_3(\text{g})$ was the predominant species in 52 of 60 cases, but its partial pressures are still insignificantly low. Because of the lack of thermodynamic data for other volatile As species no further information could be obtained. A second

shortcoming is that microbial reactions are not considered in thermodynamic equilibrium modeling. The effect of this simplification is not known because there is so far no information about the importance of purely chemical volatilization compared to microbially catalyzed volatilization in geothermal waters.

4.3.6 Quantification of volatile metallics

In section 4.3.2 concentrations of volatile metallics were just given without further discussion. Because quantification is not trivial, it shall be discussed in greater detail in the following. Table 13 and Table 14 show concentrations for volatile metallics from 55 gas samples in NaOCl trapping solutions and for volatile Cl from 38 gas samples in NaOH trapping solutions taken with the standard setups 1 and 2 (Figure 42). As explained in section 4.2.3.2, setup 1 and 2 integrate concentrations from underneath the gas hood directly above the sampled feature that enter the oxidizing bottle via one inlet and concentrations from ambient air approximately 25 cm above the sampled feature that enter the oxidizing bottle via a second inlet. The comparisons made for the sampling sites YNPRH01, 04, and 22 between the setups 1 and 2 generally showed higher concentrations of volatile metallics, thus a more effective dissolution, when the tube was immersed in the oxidizing solution (setup 1) compared to when it was left in the headspace above (setup 2). For both setups, gaseous concentrations can only be estimated as upper limits for both compartments from two end-member models. Assuming that volatile metallics entered the oxidizing bottle exclusively via the short tube open to the atmosphere gives an upper limit for concentrations approximately 25 cm above the sampling site (Table 13). If the concentrations of metallics in the oxidizing solution are exclusively attributed to diffusion via the long tube connected to the gas hood the data in Table 14 present an upper limit for the gaseous concentrations directly above the sampling site.

Table 13 Ambient concentrations [mg/m^3] of volatile metallics for 55 NaOCl samples and of volatile Cl for 38 NaOH samples (setup 1 and 2, Figure 42) assuming that the volatile metallics all come from ambient air as explained in section 4.2.3.2

mg/m^3	As	Al	B	Ba	Cu	Fe	K	Li	SiO ₂	Sr	Zn	S	Cl
min	0.07	<12	<1.2	<0.09	<0.4	<0.8	<20	<0.12	<10	<0.03	<0.5	<155	78
mean	5.1	39	5.6	0.8	1.6	3.9	190	1.0	150	0.48	3.7	520	850
max	29	130	56	5.5	5.5	32	740	11	1200	1.4	42	4,300	4190

Table 14 Source concentrations [mg/m^3] of volatile metallics for 55 NaOCl samples and of volatile Cl for 38 NaOH samples (setup 1 and 2, Figure 42) assuming that the volatile metallics all come from underneath the gas hood (section 4.2.3.2)

mg/m^3	As	Al	B	Ba	Cu	Fe	K	Li	SiO ₂	Sr	Zn	S	Cl
min	0.9	<140	<14	<1.1	-4.2	<9.8	<240	<1.4	<123	<0.4	<5.6	<1,900	940
mean	62	460	67	9.5	19	46	2300	12.5	1850	5.8	45	6,230	10,240
max	350	1,580	670	66	66	390	8900	130	14300	16	510	52,000	50,300

The assumption of exclusive diffusion of volatile metallics from ambient air seems unlikely because the distribution of volatile metallics is limited by diffusion, turbulent convection (eddy flux), dilution, hydrolysis, and oxidation in the atmosphere. To evaluate whether there is any significant

amount of volatile metallics approximately 25 cm above hot springs at all, the results from setup 3 (Figure 42) were used. Setup 3 was not connected to a gas hood and both valves were left open to the atmosphere. Volatile metallics were found in all of the 20 NaOCl samples and volatile Cl was found in all of the 10 NaOH samples. Accidental contamination was excluded by repeated laboratory and field blank values. For 16 NaOCl and 8 NaOH samples setups 1 and 3 were run parallel. The results from setup 3 were used to determine the share of volatile metallics from ambient air in setup 1 and a corrected concentration of volatile metallics underneath the gas hood could be determined as explained in section 4.2.3.2 (Table 15). Only the 6 elements with the highest concentrations (As, Al, K, SiO₂, Si and Cl) were considered. The average concentrations of all volatile metallics decrease rapidly after degassing from a geothermal feature (assumed as 100%) to only about 6% in ambient air above the sampled feature. Table 15 shows that this decrease varies between 2% and 11% for the different sampling sites and between 3% and 10% for the elements considered.

Table 15 Concentrations of volatile metallics in ambient air (AA) approximately 25 cm above the sampling site compared to concentrations underneath a gas hood (GH) directly above the sampling site in mg/m³ (calculations from setup 1 and 3 (Figure 42) as explained in section 4.2.3.2) and as percentage (AA:GH-100)

	As (AA)	As (GH)	Al (AA)	Al (GH)	K (AA)	K (GH)	SiO ₂ (AA)	SiO ₂ (GH)	S (AA)	S (GH)	Cl (AA)	Cl (GH)	average % in AA per site
YNPGG02-4G	1.5*	1.3*	1.1	269	30	1185	109	5031	24	2342	96	1789	
% in AA	118*		0.4		2.5		2.2		1.0		5.4		2.3
YNPGG03-4G	0.4	20	7.3	474	30	809	128	4063	24	3724	128	1565	
% in AA	2.1		1.6		3.7		3.2		0.7		8.2		3.2
YNPGG04-4G	0.7	22	13	150	30	622	79	4664	23	280	112	1716	
% in AA	3.3		8.5		4.8		1.7		8.3		6.5		5.5
YNPGG05-4G	0.5	4.5	8.7	155	70	552	1.1	339	25	304	94	1360	
% in AA	10		5.6		13		0.3		8.3		6.9		7.3
YNPHL01-3G	0.01	1.9	4.5	54	3.0	18	121*	54*	101	1207			
% in AA	0.4		8.3		17		222*		8.3				8.4
YNPNL02-2G	0.9	46	16	430	185	2432	2.4	2858	211	3315			
% in AA	1.9		3.7		7.6		0.1		6.4				3.9
YNPRH01-3G	0.07	8.1	17	307	26	929	303	4367	811	10413			
% in AA	0.8		5.4		2.8		6.9		7.8				4.7
YNPRH01-3G-tni	0.07*	0.07*	17	437	26	815	303	4918	811	10072			
% in AA	94*		3.8		3.2		6.2		8.1				5.3
YNPRH04-3G	11.5*	-38*	45	405	180	1268	482*	438*	100	15305			
% in AA	-30*		11		14		110*		0.7				8.6
YNPRH05-3G	9.2	76	2.7	262	54	1913	642	7068	431	11859			
% in AA	12.1		1.1		2.8		9.1		3.6				5.7
YNPRH05-4G	10.6*	6.0*	24	543	217	3933	118	3068	161	5568			
% in AA	177*		4.5		5.5		3.9		2.9				4.2
YNPRH05-4G-tni	10.6	77	24	396	217	3753	118	3450	161	2233			
% in AA	14		6.2		5.8		3.4		7.2				7.3
YNPRH06-2G	7.0*	2.7*	22	341	115	2710	3.6	426	428	6103			
% in AA	258*		6.6		4.3		0.8		7.0				4.7
YNPRH22-4G	4.5	147	45	1543	133	5220	3.1	2897	68	4638	205	1823	
% in AA	3.1		2.9		2.5		0.1		1.5		11		3.6

Continuation of Table 15

	As (AA)	As (GH)	Al (AA)	Al (GH)	K (AA)	K (GH)	SiO ₂ (AA)	SiO ₂ (GH)	S (AA)	S (GH)	Cl (AA)	Cl (GH)	average % in AA per site
YNPRH22-4G-tni	4.5	50	45	549	133	2501	3.1	37	68	818	205	786	
% in AA	9.0		8.2		5.3		8.3		8.3		26		10.9
YNPRH23-4G	3.7	61	36	719	88	3538	2.9	1735	33	391	136	1989	
% in AA	6.1		4.9		2.5		0.2		8.3		6.8		4.8
YNPRH23-4G-tni											136	1892	
% in AA											7.2		7.2
average % in AA per element	5.7		5.2		6.1		3.3		5.5		9.8		5.8

* 7 samples for which the concentrations underneath the gas hood were lower than in ambient air; the reason for this uncommon distribution can either be natural caused by local turbulences leading to higher concentrations in ambient air than underneath the gas hood or (more likely) artificial caused by analytical errors at low gaseous concentrations; those values were not considered for the calculation of average percentage per site or per element in ambient air

If this decrease of 6% on average is also assumed for the other sites sampled with setup 1 corrected values can be calculated instead of the upper limits given in Table 13 and Table 14 according to the following equation:

$$\frac{\Delta c_1}{\Delta x_1} + \frac{\Delta c_2}{\Delta x_2} = \frac{m}{t \cdot A \cdot D} \quad \text{with } \Delta c_1 = 0.06 \cdot \Delta c_2$$

$$\frac{0.06 \cdot \Delta c_2 \cdot \Delta x_2 + \Delta c_2 \cdot \Delta x_1}{\Delta x_1 \cdot \Delta x_2} = \frac{m}{t \cdot A \cdot D}$$

$$\Delta c_2 \cdot (0.06 \cdot \Delta x_2 + \Delta x_1) = \frac{m \cdot \Delta x_2}{t \cdot A \cdot D} \cdot \Delta x_1$$

$$\Delta c_2 = \frac{m \cdot \Delta x_2}{t \cdot A \cdot D} \cdot \frac{\Delta x_1}{(0.06 \cdot \Delta x_2 + \Delta x_1)} \quad \text{with } \Delta x_1 = 5 \text{ cm, } \Delta x_2 = 60 \text{ cm}$$

$$\Delta c_2 = \frac{m \cdot \Delta x_2}{t \cdot A \cdot D} \cdot 0.58 \quad (\text{compare calculation for setup 1 with } \Delta c_2 = 0 \text{ in section 4.2.3.2})$$

From this assumption, the upper limits given in Table 14 were corrected by a factor of 0.58 to get an approximation for the concentrations underneath the gas hood. Concentrations given in section 4.3.2 are all concentrations underneath a gas hood corrected by this factor 0.58.

The results from the diffusion bowls (DBs) confirm the rapid decrease of volatile As with increasing distance from a geothermal feature. The DBs were set up about 1-2 m from the geothermal feature at the shores of Hazle Lake (YNPHL01, 03), around the hot springs at Frying Pan Spring (YNPNL02, 04), along “Milky Way” (YNPRH01), and around “Rainbow Growler” (YNPRH10). Concentrations of volatile metallics ranging from <0.1 to 36 µg/m³ are 2 to 3 orders of magnitude lower than in ambient air 25 cm above the feature (see digital database; Appendix 9). Figure 77 shows an example of decreasing concentrations of volatile As with increasing distance from the hot spring at “Rainbow Growler”.

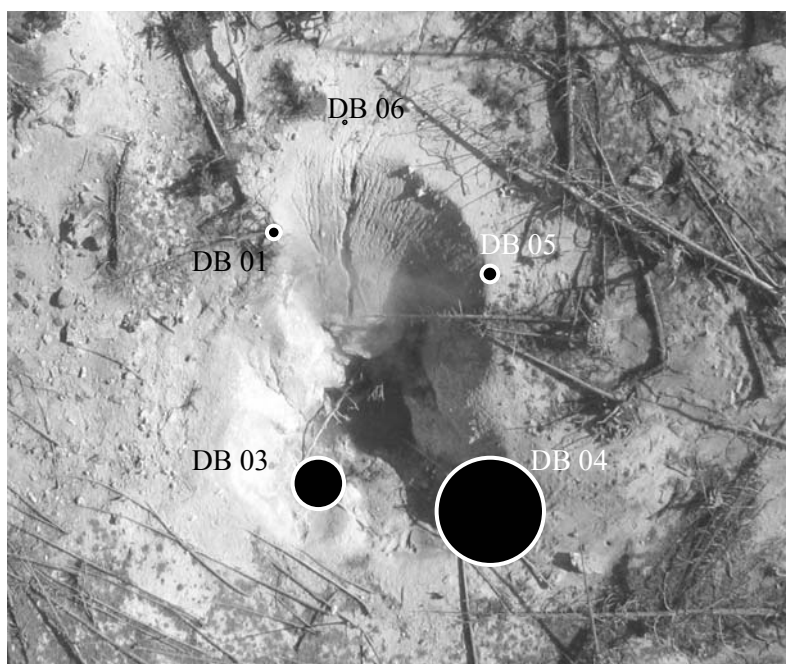


Figure 77 Setup of diffusion bowls around YNPRH10 (“Rain-bow Growler”); concentrations of volatile As decrease from 7.1 and 3.4 $\mu\text{g}/\text{m}^3$ at DB04 and DB03 to 1.1 and 0.9 $\mu\text{g}/\text{m}^3$ at DB05 and DB01; at DB06, the sampling site furthest away from the hot spring, concentrations dropped below 0.1 $\mu\text{g}/\text{m}^3$

The concentrations of volatile As discussed in the previous paragraphs with a minimum of about 500 $\mu\text{g}/\text{m}^3$, an average of 36 mg/m^3 , and a maximum of 200 mg/m^3 (Table 14, corrected by the factor 0.58) directly above geothermal features are high compared to other values cited in literature. However, it also has to be seen that only few data exist for quantifying volatile As. A global balance of Chilvers and Peterson (1987) estimates an average volatile As concentration over land of 2.8 ng/m^3 in the northern hemisphere, and 1 ng/m^3 in the southern hemisphere. Increased concentrations of volatile As were quantified by Feldmann (1995) for waste heaps (up to 50 $\mu\text{g}/\text{m}^3$) and digester gas (up to 25 $\mu\text{g}/\text{m}^3$ for mesophilic digestion and up to 30 $\mu\text{g}/\text{m}^3$ for thermophilic digestion). Wongsanoon et al. (1997) used NaOCl-trapping of volatile As from soils in a mining district in a similar way as it was done for the geothermal gases of Yellowstone within this research (section 2.7.5.1). Their concentrations in the NaOCl solution (13 μg As/L maximum, 1.5 μg As/L on average) are very similar to the ones found for Yellowstone gases (14 μg As/L maximum, 2 μg As/L on average) but Wongsanoon et al. (1997) did not try to convert the concentrations in trapping solution to concentrations in the gas phase and no data are given for exposure duration.

The concentrations derived from active pumping for 1 to 4.5 hours at four sampling sites are shown in Table 16. Compared to concentrations from passive sampling they are 1 to 2 orders of magnitude lower for volatile S, and 2 to 3 order of magnitude lower for all other volatile elements. With several tens to hundreds of $\mu\text{g}/\text{m}^3$ they are similar to the concentrations determined by Feldmann (1995) for waste heaps and digester gas.

Table 16 Concentrations of volatile metallics [$\mu\text{g}/\text{m}^3$] from active pumping for 1 to 4.5 hours

$\mu\text{g}/\text{m}^3$	As	Al	B	Ba	Cu	Fe	K	Li	SiO ₂	Sr	Zn	S
YNPGG04-2G-wGH-P	60	<600	<100	42	36	950	7,006	<10	<600	36	69	210,000
YNPHL01-2G-wGH-P	18	476	<50	19	37	516	4,014	<5	<300	17	<20	87,000
YNPRH01-2G-wGH-P	30	717	<100	26	183	146	7,834	<10	<600	29	<40	132,000
YNPRH06-2G-wGH-P	102	1,250	319	33	189	1,348	<800	<20	<1,200	17	281	351,000

Two processes may be responsible for the significant differences between active and passive gas sampling. Dilution with ambient air during pumping can not be excluded for active gas sampling because, with the simple Dräger hand pump, the gas flow rate could not be adjusted to a sampling volume equivalent to the amount of gas available at a specific site. Furthermore, active gas sampling was done in the afternoon, the time of lowest gas activity, whereas passive sampling over several days yielded an integrated signal of average gas concentrations. Concentrations from active sampling are thus likely to be too low. The high results from passive gas sampling on the other hand seem to conflict with the odor threshold of 1.6 mg/m^3 for AsH_3 at 25°C (NJ Hazardous Substance Fact Sheets 1993). However, this odor threshold does not necessarily present an upper limit for volatile As concentrations. The absence of the typical garlic-like odor at all sampled features could also be explained by other volatile As species predominating, or masking by other gases such as H_2S . Also, concentrations decrease rapidly already at 25 cm above the sampling site as shown before, and no olfactometric testing was done so close to the ground.

The preceding discussion shows how difficult it is to quantify volatile metallics. Nevertheless this study provides the first data on volatile metallics for the Yellowstone National Park and one of the largest database for quantification of volatile metallics in natural aquatic systems at all. The quantitative information is especially valuable in the light of toxicity. As described in section 2.5.3.1, a concentration of $160 \text{ } \mu\text{g/m}^3$ can result in acute toxicity for exposure times over 1 hour (Office of Environmental Health Hazard Assessment 1999). However, the available data also showed that the significantly increased concentrations directly above a geothermal feature decrease rapidly to levels below detection limit within several decimeters to 1 m at maximum. While humans rarely approach geothermal features that close for longer exposure times, animals might be endangered because of the fact that they breathe air from lower distances above ground and that, especially in winter times, they assemble around the warm geothermal features (Figure 78).



Figure 78 Bison herd grazing at a hot spring – a potential health hazard considering increased concentrations of volatile metallics, especially As, in the vicinity of geothermal features

The observed decrease in life expectancy of elk populations in areas with a large number of geothermal features compared to control populations is so far attributed to high As concentrations in

forage species found in aquatic and riparian habitats and to accelerated dental aging caused by high F concentrations (Garrott et al. 2003; Kocar et al. 2004). A chronic effect of high volatile As concentrations was not considered so far. An acute toxic effect of volatile As species seems even less likely. However, several deaths of animals were reported in the park's history attributed to accumulation of toxic gases denser than air in topographically low areas especially during inverted atmospheric conditions (Fournier 1959; Frisbee 1960; Jagger 1899; Love and Good 1970; Weed 1889). The most recent death of 5 bisons occurred around March, 1st, 2004 just north of the Norris Geyser Basin along the Gibbon River downstream of multiple gas vents. Current expert opinion is that high concentrations of H₂S (up to > 200 ppm) and CO₂ asphyxiated the bisons (Heasler and Jaworowski 2004). Again, volatile As - also more dense than air and with an even higher toxicity potential than CO₂ or H₂S - is so far no object of research.

4.4 Summary of chapter 4

As an example for an aqueous environment predestined for the release of volatile metallics Yellowstone National Park was investigated. It is located over the largest continental hot spot world wide and contains more than 10,000 geothermal features. After the first detection of volatile As during a reconnaissance study in 2002, 5 study areas (Nymph Lake, Hazle Lake, Ragged Hills, Gibbon Geyser Basin, and Lower Geyser Basin) were sampled for their water and gas chemistry. Steam-heated sulfate-dominated waters with low pH and As concentrations between 20 and 2,000 µg/L were differentiated from deep thermal chloride-dominated waters with near neutral pH and As concentrations between 1,050 and 11,000 µg/L. The precipitation of As minerals was thermodynamically calculated for Hazle Lake (orpiment supersaturation) and actually observed for a low temperature hot spring at Ragged Hills (precipitation of an amorphous Fe, S, and As rich material).

Volatile As was found in all samples together with volatile Al, B, Ba, Cu, Fe, K, Li, Si, Sr, Zn, and S. By species-selective sampling on SPME fibers, four volatile As species were detected: (CH₃)₃As, (CH₃)AsCl₂, (CH₃)₂AsCl, and (CH₃)₂AsSCH₃. The latter three were all found for the first time in a natural environment. Modeling of the gaseous As species proved impossible because of a lack of thermodynamic constants for the species detected. The volatile inorganic As, As-S, As-F, and As-Cl species for which thermodynamic data were available showed negligible partial pressures of <10⁻¹¹ Vol%. Total concentrations in the trapping solution from passive, diffusion based sampling were converted to concentrations in gas phase using Fick's first law. Medium concentrations were 8 and 28 mg/m³ for the two clusters within steam-heated waters and 11 and 89 mg/m³ for the two clusters within deep thermal waters. Concentrations from active gas sampling by pumping were lower (20-100 µg/m³) but are supposed to be subject to significant dilution by withdrawing ambient air from over-pumping. The detected concentrations are significantly increased compared to the acute toxicity limit for 1 hour exposure (160 µg/m³) with respect to AsH₃ that, however, is probably not the predominant volatile species. Even though concentrations decrease rapidly with increasing distance from a geothermal feature (to about 6% the original value in 25 cm above

the sampled structures and 0.06-0.006% in 1 to 2 m horizontal distance) animals grazing and warming up at hot springs especially during winter times might be exposed to significant amounts of volatile metallics, including As. Both chronic effects such as the observed decrease in life expectancy of elk populations in areas with a large number of geothermal features compared to control populations as well as acute poisoning such as the asphyxiation of bisons north of Norris Geyser Basin in March 2004 could be attributed to high volatile As concentrations but have so far never been investigated.

5 RECOMMENDATIONS

During the present research, a robust method was developed for in-situ collection of volatile metallics from aqueous environments. Volatile As was detected in significant concentrations in geothermal waters of Yellowstone National Park and species-selective sampling showed three new species never detected in natural waters or gases before. Yet, this is a mere drop in the ocean.

Sampling and quantification of total volatile metallic concentrations must be optimized. An alternative to passive diffusion based sampling could be active gas sampling by low-flow pumping avoiding the withdrawal of ambient air by over-pumping and the dilution of target concentrations. Quantification of individual As species would be most desirable, but before that basic information must be obtained about preferential sorption of As species on different sorption material and about possible competitive sorption with gases that could typically occur in environments where volatile metallics are found, such as CO₂, CH₄, H₂S, and SO₂. For an economic screening, sampling duration must be minimized. A mobile GC-MS equipment set up directly in the field would help to avoid storage losses or species conversions. Cryotrapping could be applied to detect lower concentrations and provide sample stability, yet the problem of transporting and handling liquid N₂ in the field has to be considered. For analysis, the GC program must be further optimized to achieve exactly reproducible retention times. Mass spectra of other volatile metallics so far missing in standard databases must be gathered from recent publications or obtained by own experiments.

Yellowstone National Park provides a wide variety of hydrogeochemical conditions and further correlation between hydrogeochemical parameters and volatile metallics, especially As, will surely be found in more detailed studies. One of the most interesting questions is about the origin of the volatile As. Is its formation purely chemical and if so does it correlate with geothermal activity? Do microbes contribute significantly to volatilization and which of the various microorganisms living under extreme conditions of pH and heat control the volatilization of each species? Are there seasonal variations in volatilization rates? Another interesting question is about the stability and distribution of the volatile metallics. Samples must be taken in vertical and horizontal sections from the source to determine the rate of hydrolysis and oxidation of the volatile species. Site-specific meteorological data will be needed. Laboratory experiments can help to obtain hydrolysis and oxidation rates, but they are mostly limited to one-metal-standard solutions not taking into account the presence and effects of other gases. The stability and distribution of volatile metallics will directly affect studies about chronic and acute poisoning of humans and animals by volatile metallics. Further interdisciplinary collaboration of geologists, hydrogeologists, chemists, microbiologists, biologists, and toxicologists is required to achieve more detailed knowledge.

6 REFERENCES

- Abedin JMD, Cresser MS, Meharg A, Feldmann J, Cotter-Howells J (2002) Arsenic Accumulation and Metabolism in Rice (*Oryza sativa* L.). *Environ Sci Technol* 36, 962-968.
- Ackely KL, Hymer CB, Sutton JA, Caruso J (1999) Speciation of arsenic in fish tissue using microwave-assisted extraction followed by HPLC-ICP-MS. *J Anal Atom Spectrom* 14, 845-850.
- Agterdenbos J, Bax D (1986) Mechanisms in hydride generation AAS. *Fresen Z Anal Chem* 323 (7), 783-787.
- Ahmann D, Krumholz LR, Hemond HF, Lovley DR, Morel FMM (1997) Microbial mobilization of arsenic from sediments of the Aberjona watershed. *Environ Sci Technol* 31 (10), 2923-2930.
- Allen ET, Day AL (1935) Hot springs of the Yellowstone National Park. *Carnegie Inst Wash Publ* 466, 525.
- Amouroux D, Donard OFX (1996) Maritime emission of selenium to the atmosphere in eastern Mediterranean seas. *Geophys Res Lett* 23 (14), 1777-1780.
- Amouroux D, Tessier E, Péchéryran C, Donard OFX (1998) Sampling and probing volatile metal(loid) species in natural waters by in-situ purge and cryogenic trapping followed by gas chromatography and inductively coupled plasma mass spectrometry (P-CT-GC-ICP/MS). *Anal Chim Acta* 377 (2-3), 214-254.
- Anderson LCD, Bruland KW (1991) Biogeochemistry of arsenic in natural waters: the importance of methylated species. *Environ Sci Technol* 25 (3), 420-427.
- Andino JM, Butler JW (1991) A study of the stability of methanol-fueled vehicle emissions in Tedlar bags. *Environ Sci Technol* 25, 1644-1646.
- Andreae MO (1978) Distribution and speciation of arsenic in natural waters and some marine algae. *Deep Sea Res* 25, 391-402.
- Andreae MO (1979) Arsenic speciation in seawater and industrial waters. *Limnol Oceanogr* 24, 440-452.
- Andreae MO, Asmodé JF, Foster P, Van't Dack L (1981) Determination of antimony(III), antimony(V), and methylantimony species in natural waters by atomic absorption spectrometry with hydride generation. *Anal Chem* 53, 1766-1771.
- Andreae MO, Froehlich PN (1984) Arsenic, antimony, and germanium biogeochemistry in the Baltic Sea. *Tellus* 36, 101-117.
- Andrewes P, Cullen WR, Polishchuk E (2000) Arsenic and antimony biomethylation by *Scopulariopsis brevicaulis*: Interaction of arsenic and antimony compounds. *Environ Sci Technol* 34 (11), 2249-2253.
- Aposhian HV (1997) Enzymatic methylation of arsenic compounds: II. An overview. In Abernathy C, Calderon R, Chappell W (eds) *Human Health II*, Chapman and Hall, London, 296-321.
- Aposhian HV, Zakharyan RA, Wildfang EK, Healy SM, Gailer J, Radabaugh TR, Bogdan GM, Powell LA, Aposhian MM (1999) How is inorganic arsenic detoxified?. in Chappell WR, Abernathy CO, Calderon RL (eds) *Arsenic exposure and health effects*. Elsevier, 289-297.
- Aposhian HV, Gurzau ES, Le XC, Gurzau A, Healy SM, Lu X, Ma M, Yip L, Zakharyan RA, Maiorino RM, Dart RC, Tircus MG, Gonzalez-Ramirez D, Morgan DL, Avram D, Aposhian MM (2000) Occurrence of monomethylarsonous acid in urine of humans exposed to inorganic arsenic. *Chem Res Toxicol* 13 (8), 693-697.
- Arcand GM (1957) Distribution of tripositive arsenic between hydrochloric acid solutions and β - β' -dichlorodiethyl ether. *J Am Chem Soc* 79 (8), 1865-1870.
- Armienta MA, Rodríguez R, Aguayo A, Cenicerros N, Villasenor G, Cruz O (1997) Arsenic contamination of groundwater at Zimapán, Mexico. *Hydrogeol J* 5, 39-46.
- Armienta MA, Villasenor G, Rodríguez R, Ongley LK, Mango H (2001) The role of arsenic-bearing rocks in groundwater pollution at Zimapán Valley, México. *Environ Geol* 40 (4-5), 571-581.
- Arnórsson S, Andrésdóttir A, Gunnarsson I, Stefánsson A (1998) New calibration for the quartz and Na/K geothermometers – valid in the range 0-350°C (in Icelandic). *Proc Geoscience Society of Iceland Annual Meeting*, April 1994, 42-43.
- Arnórsson S (ed) (2000) *Isotopic and chemical techniques in geothermal exploration, development and use – Sampling methods, data handling, interpretation*. International Atomic Energy Agency, Austria.
- Arthur CL, Pawliszyn J (1990) Solid phase microextraction with thermal desorption using fused silica optical fibers. *Anal Chem* 62 (19), 2145-2148.
- Ashe AJ, Ludwig EG (1986) The exchange reaction of tetramethyldipnictogens with dimethyldichalcogenides. *Organomet Chem* 308, 289-296.
- Aström O (1982) Flow injection analysis for the determination of bismuth by atomic absorption spectrometry with hydride generation. *Anal Chem* 54, 190-193.
- Azcue JM, Nriagu JO (1994) Arsenic: historical perspectives. In Nriagu JO (ed) *Arsenic in the environment – Part I: Cycling and characterization*. *Adv Environ Sci* 26, 1-15.
- Azcue JM, Murdoch A, Rosa F, Hall GEM (1994) Effects of abandoned gold mine tailings on the arsenic concentrations in water and sediments of Jack of Clubs Lake, BC. *Environ Technol* 15, 669-678.
- Baes CF, Mesmer RE (1976) *The hydrolysis of cations*. John Wiley, New York.
- Ball JW, Nordstrom DK (1991) User's manual for WATEQ4F, with revised thermodynamic data base and test cases for calculating speciation of major, trace, and redox elements in natural waters. *US Geol Survey Open-File Report* 91-183.

- Ball JW, Nordstrom DK, Jenne EA, Vivit DV (1998a) Chemical analyses of hot springs, pools, geysers, and surface waters from Yellowstone National Park, Wyoming, and vicinity, 1974-1975. US Geol Survey Open-File Report 98-182.
- Ball JW, Nordstrom DK, Cunningham KM, Schoonen MAA, Xu Y, DeMonge JM (1998b) Water-chemistry and on-site sulfur-speciation data for selected springs in Yellowstone National Park, Wyoming, 1994-1995. US Geol Survey Open-File Report 98-574.
- Ball JW, Nordstrom DK (2001) Application of D/H and $^{18}\text{O}/^{16}\text{O}$ values to the interpretation of subsurface fluid mixing at Yellowstone National Park, USA. Applied Isotope Geochemistry IV, June 25-29 2001, Pacific Grove, California.
- Ball JW, Nordstrom DK, McCleskey RB, Schoonen MAA, Xu Y (2001) Water-chemistry and on-site sulfur-speciation data for selected springs in Yellowstone National Park, Wyoming, 1996-1998. US Geol Survey Open-File Report 01-49.
- Ball JW, McCleskey RB, Nordstrom DK, Holloway JM, Verplanck PL (2002) Water-chemistry data for selected springs, geysers, and streams in Yellowstone National Park, Wyoming, 1999-2000. US Geol Survey Open-File Report 02-382.
- Ballantyne JM, Moore JN (1988) Arsenic geochemistry in geothermal systems. *Geochim Cosmochim Acta* 52, 475-483.
- Baltussen E, Sandra P, David F, Cramers J (1999) Stir bar sorptive extraction (SBSE), a novel extraction technique for aqueous samples: theory and principles. *J Microcol Sep* 11 (10), 737-747.
- Bargar KE, Fournier RO (1988) Effects of glacial ice on subsurface temperatures of hydrothermal systems in Yellowstone National Park, Wyoming; Fluid inclusion evidence. *Geology* 16, 1077-1080.
- Becker J (2004) High resolution aerial and ground mapping of geothermal features in Ragged Hills, Yellowstone National Park. Unpublished master thesis, Technische Universität Bergakademie Freiberg, Department of Geology.
- Bednar AJ, Garbarino JR, Ranville JF, Wildeman TR (2002) Preserving the distribution of inorganic arsenic species in groundwater and acid mine drainage samples. *Environ Sci Technol* 36, 2213-2218.
- Bednar AJ, Garbarino JR, Burkhardt MR, Ranville JF, Wildeman TR (2004) Field and laboratory arsenic speciation methods and their application to natural-water analysis. *Water Res* 38, 355-364.
- Bentley R, Chasteen TG (2002a) Arsenic curiosa and humanity. *Chem Educator* 7 (2), 51-60.
- Bentley R, Chasteen TG (2002b) Microbial methylation of metalloids: arsenic, antimony, and bismuth. *Microbiol Mol Biol R* 66 (2), 250-271.
- Berg M, Tran HC, Nguyen TC, Pham HV, Schertenleib R, Giger W (2001) Arsenic contamination of groundwater and drinking water in Vietnam: a human health threat. *Environ Sci Technol* 35, 2621-2626.
- Bergmann A, Glindemann D (1997) Analytik flüchtiger Metalloid- und Metall-Verbindungen für die Untersuchung ihrer Wurzelraum-Atmosphäre-Austauschprozesse. Wissenschaftlicher Sachbericht, Förderkennzeichen UFZ-21/97; Umweltforschungszentrum Leipzig-Halle GmbH.
- Bermejo-Barrera P, Moreda-Pineiro J, Moreda-Pineiro A, Bermejo-Barrera A (1998) Selective medium reactions for the arsenic(III), arsenic (V), dimethylarsonic acid and monomethylarsonic acid determination in waters by hydride generation on-line electrothermal atomic absorption spectrometry with in situ preconcentration on Zr-coated graphite tubes. *Anal Chim Acta* 374, 231-240.
- Biggar JW, Jayaweera GR (1993) Measurement of selenium volatilization in the field. *Soil Sci* 155 (1), 31-36.
- Biginelli P (1900a) Composizione e costituzione chimica del gas arsenical delle tappezzerie. Nota I Atti Reala Accad Lincei 9, 210-214.
- Biginelli P (1900b) Composizione e costituzione chimica del gas arsenical delle tappezzerie. Nota II Atti Reala Accad Lincei 9, 242-249.
- Bissen M, Frimmel FH (2000) Speciation of As(III), As(V), MMA and DMA in contaminated soil extracts by HPLC-ICP/MS. *Fresen J Anal Chem* 367, 51-55.
- Blasco F, Jeanjean R, Gaudin C (1972) Absorption of arsenate ions by *Chlorellas* - Partial reduction of arsenate to arsenite. Characteristics Comptes Rendus des Seances de l'Academie des Sciences, Serie D: Sciences Naturelles, 275 (12), 1223-1226.
- Bothe JV, Brown PW (1999) Arsenic immobilization by calcium arsenate formation. *Environ Sci Technol* 33 (21), 3806-3811.
- Borho M, Wilderer P (1997) A reliable method for preservation and determination of arsenate(III) concentrations in groundwater and water works samples. *J Water SRT Aqua* 46, 138-143.
- Braman RS, Foreback CC (1973) Methylated forms of arsenic in the environment. *Science* 182, 1247-1249.
- Branfireun BA, Heyes A, Roulet NT (1996) The hydrology and methylmercury dynamics of a Precambrian Shield headwater peatland. *Water Resour Res* 32 (6), 1785-1794.
- Bright DA, Dodd M, Reimer KJ (1996) Arsenic in subarctic lakes influenced by gold mine effluent: the occurrence of organoarsenicals and 'hidden' arsenic. *Sci Total Environ* 180 (2), 165-182.
- British Geological Survey Department of Public Health Engineering (2001) Arsenic contamination of groundwater in Bangladesh. In: Kinniburgh DG, Smedley PL (eds) British Geological Survey (Technical Report, WC/00/19. 4 Volumes). British Geological Survey, Keyworth.
- Brookins DG (1988) EH-pH diagrams for geochemistry. Springer, Berlin.
- Brooks WE (2004) Arsenic statistics and information. US Geol Survey, Mineral Commodity Summaries, <http://minerals.usgs.gov/minerals/pubs/commodity/arsenic/> (27.03.2003), 24-25.
- Brünnich JC (1909) *Rep Aust Ass Adv Sci* 12, 129.

- Brumbaugh WG, Ingersoll CG, Kemble NE, May TW, Zajicek JL (1994) Chemical characterization of sediments and pore water from the upper Clark Fork river and Milltown Reservoir, Montana. *Environ Toxicol Chem* 13 (12), 1971-1983.
- Buchet JP, Lauwerys R, Roels H (1981) Comparison of the urinary excretion of arsenic metabolites after a single oral dose of sodium arsenite, monomethylarsonate, or dimethylarsinate in man. *Int Arch Occup Environ Health* 48, 71-79.
- Bundesminister für Ernährung, Landwirtschaft und Forsten (1974) Verordnung zur Neufassung der Verordnung über Anwendungsverbote und -beschränkungen für Pflanzenschutzmittel vom 31. Mai 1974. *Bundesgesetzbl* 1974/I:1204-1210, Bonn.
- Bzezinska A, Loon van J, Williams D, Oguma K, Fuwa K, Haraguchi IH (1983) A study of the determination of dimethylmercury and methylmercury chloride in air. *Spectrochim Acta* 38B (10), 1339-1346.
- Cabon JY, Cabon N (2000) Speciation of major arsenic species in seawater by flow injection hydride generation atomic absorption spectrometry. *Fresen J Anal Chem* 368, 484-489.
- Cai Y, Jaffe R, Jones R (1997) Ethylmercury in the soils and sediments of the Florida Everglades. *Environ Sci Technol* 31, 302-305.
- Cai Y, Jaffe R, Jones R (1999) Interactions between dissolved organic carbon and mercury species in surface waters of the Florida Everglades. *Appl Geochem* 14, 395-407.
- Calogirou A, Richter Larsen B, Brussol C, Duane M, Kotzias D (1996) Decomposition of terpenes by ozone during sampling on Tenax. *Anal Chem* 68(9), 1499-1506.
- Cantoni GL (1953) S-Adenosylmethionine; A new intermediate formed enzymatically from L-methionine and adenosinetriphosphate. *J Biol Chem* 204, 403-416.
- Cao XL, Hewitt CN (1994) Build-up of artifacts on adsorbents during storage and its effect on passive sampling and gas chromatography - flame ionization detection of low concentrations of volatile organic compounds in air. *J Chromatogr A* 688, 368-374.
- Carrero P, Malave A, Burguera JL, Burguera M, Rondon C (2001) Determination of various arsenic species by flow injection hydride generation atomic absorption spectrometry: investigation of the effects of the acid concentration of different reaction media on the generation of arsines. *Anal Chim Acta* 438, 195-204.
- Carson BL, Ellis HV, McCann JL (1986) Toxicology and biological monitoring of metals in humans - including feasibility and need. Lewis Publishers. Inc Chelsea.
- Challenger F, Higginbottom C, Ellis L (1933) Formation of organometalloid compounds by microorganisms. I. Trimethylarsine and dimethylarsine. *Chem Soc* 95-101.
- Challenger F (1945) Biological methylation. *Chem Rev* 36, 315-361.
- Challenger F (1951) Biological methylation. *Adv Enzymol* 12, 429-491.
- Challenger F, Lisle DB, Dransfield PB (1954) Studies in biological methylation. Part XIV. The formation of trimethylarsine and dimethyl selenide in mould cultures from methyl sources containing ^{14}C . *J Chem Soc*, 1760-1771.
- Chausseau M, Roussel C, Gilon N, Mermet JM (2000) Optimization of HPLC-ICP-AES for the determination of arsenic species. *Fresen J Anal Chem* 366, 476-480.
- Chen SL, Dzen SR, Yang MH, Chlu KH, Shieh GM, Wal CM (1994) Arsenic species in groundwaters of the Blackfoot disease areas, Taiwan. *Environ Sci Technol* 28, 877-881.
- Cheng CN, Focht DD (1979) Production of arsine and methylarsine in soil and in culture. *Appl Environ Microbiol* 38, 494-498.
- Cherry JA, Shaikh AU, Tallmann DE, Nicholson RV (1979) Arsenic species as an indicator of redox conditions in groundwater. *J Hydrol* 43 (1-4), 373-392.
- Chilvers DC, Peterson PJ (1987) Global cycling of arsenic. In: Hutchinson TC, Meema KM (eds) Lead, mercury, cadmium, and arsenic in the environment. *SCOPE* 31, 279-301, John Wiley and Sons.
- Chiu VQ, Hering JG (2000) Arsenic adsorption and oxidation at manganite surfaces. 1- Method for simultaneous determination of adsorbed and dissolved arsenic species. *Environ Sci Technol* 34 (10), 2029-2034.
- Chou S, Odin M, Sage GW, Little S (2000) Toxicological profile for arsenic. US Department of Health and Human Services, Public Health Service, Agency for Toxic Substances and Disease Registry.
- Christiansen RL (2001) The Quaternary and Pliocene Yellowstone Plateau Volcanic Field of Wyoming, Idaho, and Montana. *US Geol Survey Professional Paper* 729-G.
- Christiansen RL, Foulger GR, Evans JR (2002) Upper-mantle origin of the Yellowstone hotspot. *Geol Soc Am Bull* 114 (10), 1245-1256.
- Chukhlantsev VG (1956) Solubility products of arsenates. *J Inorg Chem (USSR)* 1, 1975-1982.
- Church PE, Vroblecky DA, Lyford FP, Willey RE (2002) Guidance on the use of passive-vapor-diffusion samplers to detect volatile organic compounds in ground-water-discharge areas, and example applications in New England. *US Geol Survey Water-Resour Invest Rept* 02-4186.
- Cicerone RJ, Oremland RS (1988) Biogeochemical aspects of atmospheric methane. *Global Biogeochem Cy* 2, 299-327.
- Clayton GD, Clayton FE (eds) (1981) Patty's industrial hygiene and toxicology. Vol 2 A-C: Toxicology. 3rd ed, John Wiley.
- Clemens JB, Lewis RG (1988) In: Keith LH (ed) Principles of Environmental Sampling, ACS Professional Reference Book, 287.

- Cleverley JS, Benning LG, Mountain BW (2003) Reaction path modelling in the As-S system: a case study for geothermal As transport. *Appl Geochem* 18, 1325-1345.
- Col M, Col C, Soran A, Sayli BS, Ozturk S (1999) Arsenic related Bowen's disease, Palmar keratosis, and skin cancer. *Environ Health Persp* 107, 687-689.
- Conrad R (1996) Soil Microorganisms as Controllers of Atmospheric Trace Gases (H₂, CO, CH₄, OCS, N₂O, and NO). *Microbiol Rev* 60(4), 609-640.
- Coury L (1999) Conductance measurements, Part 1: Theory. *Current Separations.com*, 18:3 <http://www.currentseparations.com/issues/18-3/cs18-3c.pdf>.
- Cox DP, Alexander M (1973) The production of trimethylarsine gas from various arsenic compounds by three sewage fungi. *Bull Environ Contam Toxicol* 9, 84-88.
- Craig H, Boato G, White DE (1956) Isotope geochemistry of thermal waters. National Research Council Publication 400, 29-38.
- Craig PJ (1986) Organometallic compounds in the environment. Longman, Harlow, 368.
- Craig PJ (1989) In: Hartley FR (ed) Chemistry of metal-carbon bond. Vol.5, Wiley, Chichester, 437.
- Crecelius EA, Robertson DE, Fruchter JS, Ludwick JD (1976) Chemical forms of mercury and arsenic emitted by a geothermal power plant. In: Hemphil DD (ed) Trace Substances in Environmental Health, University of Missouri, Columbia, 287-293.
- Crecelius EA (1977a) Arsenite and arsenate levels in wine. *Bull Environ Contam Toxicol* 1, 227-230.
- Crecelius EA (1977b) Changes in the chemical speciation of arsenic following ingestion by man. *Environ Health Persp* 19, 147-150.
- Crecelius EA, Bloom NS, Cowan CE, Jenne EA (1986) Speciation of selenium and arsenic in natural waters and sediments: arsenic speciation. Electric Power Research Institute Vol.2, EA-4641, Project 2020-2.
- Creed JT, Magnuson ML, Brockhoff CA (1996) Arsenic determination in saline waters utilizing a tubular membrane as a gas-liquid separator for hydride generation inductively coupled plasma mass spectrometry. *J Anal Atom Spectrom* 11, 505-509.
- Crompton TR (1998) Occurrence and analysis of organometallic compounds in the environment. Wiley, New York, 237.
- Cullen WR, McBride BC, Reglinski J (1984) The reduction of trimethylarsine oxide to trimethylarsine by thiols: a mechanistic model for the biological reduction of arsenical. *J Inorg Biochem* 21, 45-60.
- Cullen WR and Dodd (1989) Arsenic speciation in clams of British Columbia. *Appl Organomet Chem* 3(1), 79-88.
- Cullen WR, McBride BC, Manji H, Pickett AW, Reglinski J (1989) The metabolism of methylarsine oxide and sulfide. *Appl Organomet Chem* 3, 71-78.
- Cullen WR, Reimer KJ (1989) Arsenic speciation in the environment. *Chem Rev* 89, 713-764.
- Cullen WR, Li H, Pergantis SA, Eigendorf GK, Mosi AA (1995) Arsenic biomethylation by the microorganism *Apiotrichum humicola* in the presence of L-methionine-methyl-d₃. *Appl Organomet Chem* 9 (7), 507-515.
- Daus B, Mattusch J, Wennrich R, Weiss H (2002) Investigation on stability and preservation of arsenic species in iron rich water samples. *Talanta* 58, 57-65.
- Davidson PJ, Lappert MF, Pearce R (1976) Metal σ -hydrocarbyls, MR_n, stoichiometry, structures, stabilities, and thermal decomposition pathways. *Chem Rev* 76, 219-242.
- De Bettencourt AMM, Andraea MO (1991) Refractory arsenic species in estuarine waters. *Appl Organomet Chem* 5, 111-116.
- De Bettencourt AMM, Florencio MH, Duarte MFN, Gomes MLR, Vilas Boas LFC (1994) Refractory methylated arsenic compounds in estuarine waters: Tracing back elusive species. *Appl Organomet Chem* 8, 43-56.
- Delnomdedieu M, Basti MM, Otvos JD, Thomas DJ (1994) Reduction and binding of arsenate and dimethylarsinate by glutathione: a magnetic resonance study. *Chem Biol Interact* 90, 139-155.
- Del Razo LM, Arellano MA, Cebrián ME (1990) The oxidation states of arsenic in well-water from a chronic arsenicosis area of northern Mexico. *Environ Pollut* 64, 143-153.
- Del Razo LM, García-Vargas GG, Hernández MC, Gómez-Munoz A, Cebrián ME (1999) Profile of urinary arsenic metabolites in children chronically exposed to inorganic arsenic in Mexico. In: Chappell WR, Abernathy CO, Calderon RL (eds) Arsenic exposure and health effects, Elsevier, 281-287.
- Department of Energy (2003) News Release October 21, 2003, <http://newsdesk.inel.gov/contextnews.cfm?ID=472>.
- Devesa V, Martínez A, Suárez MA, Benito V, Vélez D, Montoro R (2001) Kinetic study of transformations of arsenic species during heat treatment. *J Agric Food Chem* 49, 2267-2271.
- Doak GO, Freedman LD (1970) Organometallic compounds of arsenic, antimony, and bismuth John Wiley, New York.
- Dobson PF, Kneafsey TJ, Hulen J, Simmons A (2003) Porosity, permeability, and fluid flow in the Yellowstone geothermal system, Wyoming. *J Volcanol Geotherm Res* 123, 313-324.
- Donahoe-Christiansen J, D'Imperio S, Jackson CR, Inskeep WP, McDermott TR (2004) Arsenite-oxidizing hydrogenobaculum strain isolated from an acid-sulfate-chloride geothermal spring in Yellowstone National Park. *Appl Environ Microbiol* 70, 1865-1868.
- Donard OFX and Weber JH (1988) Volatilization of tin as stannane in anoxic environment. *Nature* 332, 339-341.
- Duncan RA (1982) A captured island chain in the Coast Range of Oregon and Washington. *J Geophys Res* 87, 10827-10837.
- Dzurisin D, Yamashita KM (1987) Vertical surface displacements at Yellowstone caldera, Wyoming, 1976-1986. *J Geophys Res* 92, 13753-13766.

- Dzurisin D, Savage JC, Fournier RO (1990) Recent crustal subsidence at Yellowstone caldera. *B Volcanol* 52, 247-270.
- Dzurisin D, Yamashita K, Kleinmann JW (1994) Mechanisms of crustal uplift and subsidence at the Yellowstone caldera. *B Volcanol* 56, 261-270.
- Dzurisin D, Wicks C, Thatcher W (1999) Renewed uplift at the Yellowstone Caldera measure by leveling surveys and satellite radar interferometry. *B Volcanol* 61, 349-355.
- Ebdon L, Hill S, Ward RW (1987) Directly coupled chromatography-atomic spectroscopy. Part 1. Directly coupled gas chromatography-atomic spectroscopy. A review. *Analyst* 111, 1113-1138.
- Edmonds JS, Francesconi KA, Cannon JR, Raston CL, Skelton BW, White AH (1977) Isolation, crystal structure and synthesis of arsenobetaine, the arsenical constituent of the western rock lobster *Panulirus longipes cygnus* George. *Tetrahedron Lett* 18, 1543-1546.
- Edmonds JS, Francesconi KA (1981) Arseno-sugars from brown kelp (*Ecklonia radiata*) as intermediates in cycling of arsenic in a marine ecosystem. *Nature* 289, 602-604.
- Edmonds JS, Francesconi KA, Healy PC, White AH (1982) Isolation and crystal structure of an arsenic-containing sugar sulphate from the kidney of the giant clam, *Tridacna maxima*. X-ray crystal structure of (2S)-3- [5-deoxy-5-(dimethylarsinoyl)- B-D-ribofuranosyloxy] -2-hydroxypropyl hydrogen sulphate. *Journal of the Chemical Society, Perkin Transactions I*, 2989-2993.
- Edmonds JS, Shibata Y, Francesconi KA, Rippingale RJ, Morita M (1997) Arsenic transformations in short marine food chains studied by HPLC-ICPMS. *Appl Organomet Chem* 11, 281-287.
- Edwards M, Patel S, McNeill L, Chim H, Frey M, Eaton AD, Antweiler RC, Taylor HE (1998) Considerations in As analysis and speciation. *J Am Water Works Assoc* 90, 103-113.
- Ehrlich HL (2002) *Geomicrobiology*, 4th ed., Marcel Dekker Inc, New York.
- Ellenhorn MJ (1997) *Medical toxicology, diagnosis and treatment of human poisoning* 2nd ed. Williams and Wilkins Co.
- Ellis A, Mahon W (1964) Natural hydrothermal system and experimental hot-water/rock interactions. *Geochim Cosmochim Acta* 28, 1323-1357.
- Elsenbroich C, Salzer A (1992) *Organometallics – A concise introduction*, VCH, Weinheim.
- Environmental Protection Agency (2001) 40 CFR Parts 9, 141, and 142 National Primary Drinking Water Regulations; Arsenic and Clarifications to Compliance and New Source Contaminants Monitoring; Final Rule. Part VIII. Federal Register 66 (14), 6976-7066.
- Essington ME (1988) Division S-2 - soil chemistry: solubility of barium arsenate. *Soil Sci Soc Amer J* 52, 1566-1570.
- Ewers GR, Keays RR (1977) Volatile and precious metal zoning in the Broadlands geothermal field, New Zealand. *Econ Geol* 72, 1337-1354.
- Fahlquist L, Janik CJ (1992) Procedures for collecting and analyzing gas samples from geothermal systems. US Geol Survey Open-File Report 92-211.
- Falter R, Hintelmann H, Quevauviller P (1999) Conclusion of the workshop on sources of error in methylmercury determination during sample preparation, derivatisation and detection. *Chemosphere* 39, 1039-1049.
- Fanning JC (2000) The chemical reduction of nitrate in aqueous solution. *Coord Chem Rev* 199, 159-179.
- Farago ME, Kavanagh P (1999) Proportions of arsenic species in human urine. In: Chappell W.R., Abernathy C.O., Calderon R.L. (eds): *Arsenic exposure and health effects* 325-334 Elsevier.
- Feeney R, Kounaves SP (2000) On-site analysis of arsenic in groundwater using a microfabricated gold ultramicroelectrode array. *Anal Chem* 72, 2222-2228.
- Feldmann J, Grümping R, Hirner AV (1994) Determination of volatile metal and metalloid compounds in gases from domestic waste deposits with GC/ ICP-MS. *Fresen J Anal Chem* 350, 228-234.
- Feldmann J (1995) Erfassung flüchtiger Metall- und Metalloidverbindungen in der Umwelt mittels GC/ICP-MS. Unpublished PhD thesis Department of Chemistry, University Essen.
- Feldmann J, Hirner AV (1995) Occurrence of volatile metal and metalloid species in landfill and sewage gases. *Intern J Environ Anal Chem* 60, 339-359.
- Feldmann J, Riechmann T, Hirner AV (1996) Determination of organometallics in intra-oral air by LT-GC/ICP-MS. *Fresen J Anal Chem* 354, 620-623.
- Feldmann J (1997) Summary of a calibration method for the determination of volatile metal(loids) compounds in environmental gas samples by using gas chromatography - inductively coupled plasma mass spectrometry. *J Anal Atom Spectrom* 12 (9), 1069-1076.
- Feldmann J, Cullen WR (1997) Occurrence of volatile transition metal compounds in landfill gas: synthesis of molybdenum and tungsten carbonyls in the environment. *Environ Sci Technol* 31 (7), 2125-2129.
- Feldmann J, Kleinmann J (1997) Flüchtige Metallverbindungen im Faulgas. *Korrespondenz Abwasser* 44 (1), 99-104.
- Feldmann J, Krupp EM, Glindemann D, Hirner AV, Cullen WR (1999a) Methylated bismuth in the environment. *Appl Organomet Chem*, 13 (10), 739-748.
- Feldmann J, Lai VWM, Cullen WR, Ma M, Lu X, Le XC (1999b) Sample preparation and storage can change arsenic speciation in human urine. *Clinical Chemistry* 45 (11), 1988-1997.
- Feldmann J, Naels L, Haas K (2001) Cryotrapping of CO₂-rich atmospheres for the analysis of volatile metal compounds using capillary GC-ICP-MS. *J Anal Atom Spectrom* 16, 1040-1043.
- Feldmann J, Devalla S, Raab A, Hansen HR (2004) Analytical strategies for arsenic speciation in environmental and biological samples. in Hirner AV, Emons H (eds) *Organic Metal and Metalloid Species in the Environment - Analysis, Distribution, Processes and Toxicological Evaluation*, 41-70.

- Ferris MJ, Magnuson TS, Fagg JA, Thar R, Kühl M, Sheehan KB, Henson JM (2003) Microbially mediated sulphide production in a thermal, acidic algal mat community in Yellowstone National Park. *Environ Microbiol* 5 (10), 954-960.
- Ficklin WH (1983) Separation of arsenic(III) and arsenic(V) in ground waters by ion exchange. *Talanta* 30, 371-373.
- Finn CA, Morgan LA (2002) High-resolution aeromagnetic mapping of volcanic terrain, Yellowstone National Park. *J Volcan Geotherm Res* 115, 207-231.
- Fleck HZ (1872) *Biol* 8, 444.
- Florea AM, Dopp E, Obe G, Rettenmeier AW (2004) Genotoxicity of organometallic species. in Hirner AV, Emons H (eds) *Organic Metal and Metalloid Species in the Environment - Analysis, Distribution, Processes and Toxicological Evaluation*, 205-219.
- Fournier RO (1959) Death Gulch gas analysis. Yellowstone National Park, Yellowstone Research Library, vertical file.
- Fournier RO, Truesdell AH (1973) An empirical Na-K-Ca geothermometer for natural waters. *Geochim Cosmochim Acta* 37, 1255-1275.
- Fournier RO, White DE, Truesdell AH (1976) Convective heat flow in Yellowstone National Park. *Proceedings of the 2nd U.N. Symposium Development and Use of Geothermal Resources*, San Francisco 1975, Washington, 731-739.
- Fournier RO, Potter RW (1982) A revised and expanded silica (quartz) geothermometer. *Geotherm Res Council Bull* 11, 3-9.
- Fournier RO, Thompson JM, Hutchinson RA (1986) Fluctuations in composition of Cistern Spring, Norris Geyser Basin, Yellowstone National Park, Wyoming – variable boiling and mixing 1962-1985. *Extended Abstract, Fifth International Symposium Water-Rock Interaction*, Reykjavik, Iceland, 206-209.
- Fournier RO (1989) Geochemistry and dynamics of the Yellowstone National Park hydrothermal system. *Annu Rev Earth Pl Sc* 17, 13-53.
- Fournier RO, Thompson JM, Hutchinson RA (1992) The geochemistry of hot spring waters at Norris Geyser Basin, Yellowstone National Park, USA. In: Kharaka YK, Maest AS (eds) *Proc. 7th Internat. Symp. Water-Rock Interaction, WRI-7*, Park City, Utah, USA, July 13-18, 1289-1292.
- Fournier RO, Thompson JM, Hutchinson RA (1994a) The geochemistry of hot spring waters at Norris Geyser Basin, Yellowstone National Park. *Geothermal Resources Council Transactions* 18, 177-179.
- Fournier RO, Christiansen RL, Hutchinson RA, Pierce KL (1994b) A field-trip guide to Yellowstone National Park, Wyoming, Montana and Idaho - Volcanic, hydrothermal, and glacial activity in the region. *US Geol Survey Bull* 2099.
- Fournier RO, Weltman U, Counce D, White LD, Janik CJ (2002) Results of weekly chemical and isotopic monitoring of selected springs in Norris Geyser Basin, Yellowstone National Park During June-September, 1995. *US Geol Survey Open-File Report* 02-344.
- Fournier RO (2004) Yellowstone caldera inflation-deflation and hydrothermal Cl flux revisited. In: Wanty RB, Seal RR (eds) *Water-Rock Interaction Proc of the 11th Int Symp Water-Rock Interaction, II*, Balkema, 53-58.
- Fowler BA (ed) (1983) *Biological and environmental effects of arsenic*. *Topics in environmental health* 6, 281. Elsevier.
- Francesconi KA, Edmonds JS, Hatcher BG (1988) Examination of the arsenic constituents of the herbivorous marine gastropod *Tectus pyramis*: isolation of tetramethylarsonium ion. *Comp Biochem Physiol* 90C, 313-316.
- Francesconi KA, Edmonds JS (1997) Arsenic and marine organisms. *Adv Inorg Chem* 44, 147-189.
- Frankenberger WT, Karlson U (1989) Environmental factors affecting microbial production of dimethyl selenide in a selenium-contaminated sediment. *Soil Sci Soc Am J* 53, 1435-1442.
- Freeman MC (1985) The reduction of arsenate to arsenite by an *Anabaena* assemblage isolated from the Waikato River. *N Z J Mar Freshwater Res* 19, 277-282.
- Frisbee R (1960) Report on Death Gulch. Yellowstone National Park, Yellowstone Research Library, vertical file, 3.
- Froehlich PN, Kaul LW, Byrd JT, Andreae MO, Roe KK (1985) Arsenic, barium, germanium, tin, dimethylsulfide and nutrient biogeochemistry in Charlotte Harbor, Florida, a phosphorus-enriched estuary. *Estuar Coast Shelf S* 20, 239-264.
- Fujii R, Swain WC (1995) Areal distribution of selected trace elements, salinity, and major ions in shallow ground water, Tulare basin, southern San Joaquin Valley, California. *US Geol Survey Water-Resour Invest Rept* 95-4048.
- Fuller EN, Schettler PD, Giddings JC (1966) A new method for prediction of binary gas-phase diffusion coefficients. *Ind Eng Chem* 58(5), 19-27.
- Gailer J, George GN, Pickering IJ, Prince RC, Ringwald SC, Pemberton JE, Glass RS, Younis HS, DeYoung DW, Aposhian HV (2000) A metabolic link between arsenic and selenite: The seleno-bis(S-gluthathionyl) arsinium ion. *J Am Chem Soc* 122 (19), 4637-4639.
- Gallagher PA, Shoemaker JA, Wei X, Brockhoff-Schwegel CA, Creed JT (2001a) Extraction and detection of arsenicals in seaweed via accelerated solvent extraction with ion chromatographic separation and ICP-MS detection. *Fresen J Anal Chem* 369, 71-80.
- Gallagher PA, Schwegel CA, Wei X, Creed JT (2001b) Speciation and preservation of inorganic arsenic in drinking water sources using EDTA with IC separation and ICP-MS detection. *J Environ Monit* 3, 371-376.
- Gardiner JA, Collat JW (1965) Kinetics of the stepwise hydrolysis of tetrahydroborate ion. *J Am Chem Soc* 87 (8), 1692-1700.
- Garrott RA, Eberhardt LL, Otton JK, White PJ, Chaffee MA (2003) A geochemical trophic cascade in Yellowstone's geothermal environments. *Ecosystems* 5, 659-666.

- Geislinger AE, Goessler W, Francesconi KA (2002) Biotransformation of arsenate to the tetramethylarsonium ion in the marine Polychaetes *Nereis diversicolor* and *Nereis virens*. *Environ Sci Technol* 36, 2905-2910.
- Gettar RT, Garavaglia RN, Gautier EA, Batistoni DA (2000) Determination of inorganic and organic anionic arsenic species in water by ion chromatography coupled to hydride generation-inductively coupled plasma atomic emission spectrometry. *J Chromatogr A* 884, 211-221.
- Giggenbach WF (1975) A simple method for the collection and analysis of volcanic gas samples. *B Volcanol* 39, 132-145.
- Giggenbach WF (1988) Geothermal solute equilibria - derivation of Na-K-Ca geothermometers. *Geochim Cosmochim Acta* 52, 2749-2765.
- Giggenbach WF, Goguel RL (1989) Collection and analysis of geothermal and volcanic water and gas discharges. Peatone, New Zealand, Department of Science and Industrial Research, Chemistry Division, Report CD 3401.
- Gihring TM, Druschel GK, McCleskey RB, Hamers RJ, Banfield JF (2001) Rapid arsenite oxidation by *Thermus aquaticus* and *Thermus thermophilus*: Field and laboratory investigations. *Environ Sci Technol* 35 (19), 3857-3862.
- Gilmour CC, Riedel GS, Ederington MC, Bell JT, Benoit JM, Gill GA, Stordal MC (1998) Methylmercury concentrations and production rates across a trophic gradient in the northern Everglades. *Biogeochem* 40, 327-345.
- Gmelin L (1839) Warnung vor gewissen grünen Tapeten und Anstrichen. *Karlsruher Zeit*, November 24, suppl. 326.
- Göhler S (2003) Untersuchungen zu Wärmeentwicklung und Gasaustritten der Deutschlandschachtal. Unpublished master thesis, Technische Universität Bergakademie Freiberg, Department of Geology.
- Goff F, Janik CJ (2002) Gas geochemistry of the Valles caldera region, New Mexico and comparisons with gases at Yellowstone, Long Valley and other geothermal systems. *J Volcanol Geotherm Res* 116, 299-323.
- Goldhahn C (2003) Behavior of arsenic in a constructed wetland facility. Unpublished master thesis, Technische Universität Bergakademie Freiberg, Department of Geology.
- Gómez M, Cámara C, Palacios MA, López-González A (1997) Anionic cartridge preconcentrators for inorganic arsenic, monomethylarsonate and dimethylarsinate determination by on-line HPLC-HG-AAS. *Fresen J Anal Chem* 357, 844-849.
- Gong Z, Lu X, Cullen WR, Le XC (2001) Unstable trivalent arsenic metabolites, monomethylarsonous acid and dimethylarsonous acid. *J Anal Atom Spectrom* 16, 1409-1413.
- Gong Z, Lu X, Ma M, Watt C, Le XC (2002) Arsenic speciation analysis. *Talanta* 58, 77-96.
- Gooch FA, Whitfield JE (1888) Analyses of waters of the Yellowstone National Park, with an account of the methods of analysis employed. *US Geol Survey Bull* 47, 84.
- Gorby M (1994) Arsenic in Human Medicine. In: Nriagu JO (ed) *Arsenic in the environment - Part II: Human Health and Ecosystem Effects*. *Adv Environ Sci* 26, 1-8.
- Gosio B (1893) Action de quelques moisissures sur les composés fixes d'arsenic. *Arch Ital Biol* 18, 253-265.
- Gosio B (1901) Recherches ultérieures sur la biologie et sur le chimisme des arsenio-moisissures. *Arch Ital Biol* 35, 201-211.
- Gottschalk S (1997) Hydrogeologische Untersuchungen am Uran-Tailing Schneckenstein. Unpublished master thesis, Technische Universität Bergakademie Freiberg, Department of Geology.
- Green HH (1918) Description of a bacterium which oxidizes arsenite to arsenate, and of one which reduces arsenate to arsenite, isolated from a cattle-dipping tank. *S Afr J Sci* 14, 465-467.
- Greschonig H, Schmid MG, Gübitz G (1998) Capillary electrophoretic separation of inorganic and organic arsenic compounds. *Fresen J Anal Chem* 362, 218-223.
- Grümping R, Mikolajczak D, Hirner AV (1998) Determination of trimethylsilanol in the environment by LT-GC/ICP-OES and GC-MS. *Fresen J Anal Chem* 361, 133-139.
- Grüter UM, Kresimon J, Hirner AV (2000) A new HG/LT-GC/ICP-MS multi-element speciation technique for real samples in different matrices. *Fresen J Anal Chem* 368, 67-72.
- Guerin T, Molénat N, Astruc A, Pinel R (2000) Arsenic speciation in some environmental samples: a comparative study of HG-GC-QFAAS and HPLC-ICP-MS methods. *Appl Organomet Chem* 14, 401-410.
- Gulens J, Champ DR, Jackson RE (1979) Influence of redox environments on the mobility of arsenic in ground water. In: Jenne EA (ed) *Chemical Modelling in Aqueous Systems*. *Am Chem Soc*, 81-95.
- Gurzau ES, Gurzau AE (2001) Arsenic in drinking water from groundwater in Transylvania, Romania. In: Chapell WR, Abernathy CO, Calderon RL (eds) *Arsenic exposure and health effects IV*. Elsevier, Amsterdam, 181-184.
- Haas K, Feldmann J (2000) Sampling of trace volatile metal(loid) compounds in ambient air using polymer bags: a convenient method. *Anal Chem* 72 (17), 4205-4211.
- Hall GEM, Pelchat JC, Gauthier G (1999) Stability of inorganic arsenic (III) and arsenic (V) in water samples. *J Anal Atom Spectrom* 14, 205-214.
- Hamsch B, Raue B, Brauch HJ (1995) Determination of arsenic (III) for the investigation of the microbial oxidation of arsenic (III) to arsenic (V). *Acta Hydroch Hydrob* 23 (4), 166-172.
- Hansen SH, Larsen EH, Pritzl G, Cornett C (1992) Separation of seven arsenic compounds by high-performance liquid chromatography with on-line detection by hydrogen-argon flame atomic absorption spectrometry and inductively coupled plasma mass spectrometry. *J Anal Atom Spectrom* 7, 629-634.
- Hansen HR, Pickford R, Thomas-Oates J, Jaspars M, Feldmann J (2004) 2-Dimethylarsinothioyl acetic acid identified in a biological sample: the first occurrence of a mammalian arsiniothio(y)l metabolite. *Angewandte Chemie (Int. Ed.)* 43, 337-340.

- Harrington JM, Fendorf SE, Rosenzweig RF (1998) Biotic generation of arsenic (III) in metal(loid) contaminated freshwater lake sediments. *Environ Sci Technol* 32 (16), 2425-2430.
- Hasegawa H, Sohrin Y, Matsui M, Hojo M, Kawashima M (1994) Speciation of arsenic in natural waters by solvent extraction and hydride generation atomic absorption spectrometry. *Anal Chem* 66, 3247-3252.
- Hasegawa H, Sohrin Y, Matsui M, Takeda N, Ueda K (2002) Chemical speciation of inorganic and methylarsenic(III) compounds in aqueous solutions. *Appl Organomet Chem* 16, 446-450.
- Healy SM, Zakharyan RA, Aposhian HV (1997) Enzymatic methylation of arsenic compounds. IV. In vitro and in vivo deficiency of the methylation of arsenite and monomethylarsonic acid in the guinea pig. *Mutation Res* 386, 229-239.
- Heasler H, Jaworowski C (2004) Geologic overview of a bison-carcass site at Norris Geyser Basin, March 2004. Yellowstone National Park Geology Report, 23.03.2004, 6 pages; <http://www.nps.gov/yell/nature/geology/reports/norrisbison.pdf>
- Heinrichs G, Udluft P (1999) Natural arsenic in Triassic rocks: a source of drinking-water contamination in Bavaria, Germany. *Hydrogeol J* 7, 468-476.
- Henson JM, Ferris MJ (2003) Analysis of a eukaryotic microbial mat community across environmental gradients in a thermal, acidic stream. NSF Award Abstract #9977922.
- Hirner AV, Feldmann J, Krupp E, Grümping R, Goguel R, Cullen WR (1998) Metal(loid)organic compounds in geothermal gases and waters. *Org Geochem* 29 (5-7), 1765-1778.
- Hirner AV, Grüter UM, Kresimon J (2000) Metal(loid)organic compounds in contaminated soil. *Fresen J Anal Chem* 368, 263-267.
- Hirner AV, Emons H (eds) (2004) Organic metal and metalloid species in the environment - analysis, distribution, processes and toxicological evaluation. Springer, 328.
- Hofmeister F (1894) Ueber methylierung im Thierkörper. *Arch Exp Pathol Pharmacol* 22, 253-260.
- Hopenhayn-Rich C, Smith AH, Goeden HM (1993) Human studies do not support the methylation threshold hypothesis for the toxicity of inorganic arsenic. *Environ Res* 60, 161-177.
- Hopenhayn-Rich C, Biggs ML, Fuchs A, Bergoglio R, Tello E, Nicolli H, Smith AH (1996a) Arsenic and bladder cancer mortality. *Epidemiology* 7, 557-558.
- Hopenhayn-Rich C, Biggs ML, Smith AH, Kalman DA, Moore LE (1996b) Methylation study of population environmentally exposed to arsenic in drinking water. *Environ Health Persp* 104, 620-628.
- Horiguchi H (1970) Pollution and Poisonous Dangerous Compounds. Sankyosyuppan, Tokyo, 229.
- Howard AG, Arbab-Zavar MH, Apte S (1982) Seasonal variability of biological arsenic methylation in the River Beaulieu. *Mar Chem* 11, 493-498.
- Howard AG, Arbab-Zavar MH, Apte S (1984) The behaviour of dissolved arsenic in the estuary of the River Beaulieu. *Estuar Coast Shelf S* 19, 493-504.
- Howard AG, Hunt LE (1993) Coupled photooxidation-hydride AAS detector for the HPLC of arsenic compounds. *Anal Chem* 65, 2995-2998.
- Howard AG, Comber SDW, Kifle D, Anatai EE, Purdie DA (1995) Arsenic speciation and seasonal changes in nutrient availability and micro-plankton abundance in Southampton Water, U.K. *Estuar Coast Shelf S* 40, 435-450.
- Howard AG (1997) (Boro)Hydride techniques in trace element speciation. *J Anal Atom Spectrom* 12, 267-272.
- Hug SJ, Canonica L, Wegelin M, Gechter D, von Gunten U (2001) Solar oxidation and removal of arsenic at circumneutral pH in iron containing waters. *Environ Sci Technol* 35, 2114-2121.
- Humphreys ED, Dueker KG, Schutt DL, Smith RB (2000) Beneath Yellowstone: evaluating plume and nonplume models using teleseismic images of the upper mantle. *GSA Today* 10 (12), 1-7.
- Hurley JP, Krabbenhoft DP, Cleckner LB, Olson ML, Aiken GR, Rawlik PS (1998) System controls on the aqueous distribution of mercury in the northern Florida Everglades. *Biogeochemistry* 40, 293-310.
- Intergovernmental Panel on Climate Change (1992) Climate change. In: Houghton JT, Callender BA, Varney SK (eds) The supplementary report to the IPCC scientific assessment, Cambridge University Press, UK.
- Ishiguro S (1992) Industries using arsenic and arsenic compounds. *Appl Organomet Chem* 6, 323-331.
- Iyer HM, Evans JR, Zandt G, Stewart RM, Coakley JM, Roloff JN (1981) A deep low-velocity body under the Yellowstone caldera, Wyoming: Delineation using teleseismic P-wave residuals and tectonic interpretation. *Geol Soc Am Bull*, Part II, 92, 1471-1646.
- Jackson CR, Langner HW, Donahoe-Christiansen J, Inskeep WP, McDermott TR (2001) Molecular analysis of microbial community structure in an arsenite-oxidizing acidic thermal spring. *Environ Microbiol* 3, 532-542.
- Jagger TA (1899) Death Gulch - A natural bear-trap. *Appelton's popular science monthly*, 54 (4), 475-481.
- Jamoussi B, Zafzouf M, Ben Hassine B (1996) Interferences by transition metals and their elimination by cyanide as a complexing agent in the determination of arsenic using continuous flow HG-ICP-AES. *Fresen J Anal Chem* 355, 331-334.
- Jantzen E (1992) Analytische Untersuchungen zur Beurteilung der Bindungsformen (Speciation) des Zinns in Elbesedimenten unter Zuhilfenahme von GC-AAS, GC-MS, TRFA, GFAAS. Unpublished PhD thesis, University Hamburg.
- Jenkins RO, Craig PJ, Goessler W, Miller D, Ostah N, Irgolic KJ (1998) Biomethylation of inorganic antimony compounds by an aerobic fungus: *Scopulariopsis brevicaulis*. *Environ Sci Technol* 32 (7), 882-885.
- Jenkins RO, Morris TA, Craig PJ, Goessler W, Ostah N, Wills KM (2000) Evaluation of cot mattress inner foam as a potential site for microbial generation of toxic gases. *Hum Exp Toxicol* 19, 693-702.

- Jewett KL, Brinckmann FE, Bellama JM (1975) Chemical factors influencing metal alkylation in water. in Church TM (ed) *Marine Chemistry in the Coastal Environment*. ACS Symp Ser 18, 304-318.
- Johnson DL, Pilson MEQ (1975) The oxidation of arsenite in seawater. *Environ Lett* 8, 157-171.
- Jokai Z, Hegoczki J, Fodor P (1998) Stability and optimization of extraction of four arsenic species. *Microchem J* 59, 117-124.
- Kaise T, Ogura M, Nozaki T, Saitoh K, Sakurai T, Matsubara C, Watanabe C, Hanaoka K (1997) Biomethylation of arsenic in an arsenic-rich freshwater environment. *Appl Organomet Chem* 11, 297-304.
- Kennedy BM, Lynch MA, Reynolds JH, Smith SP (1985) Intensive sampling of noble gases in fluids at Yellowstone: I. Early overview of the data: Regional patterns. *Geochim Cosmochim Acta* 49, 1251-1261.
- Kennedy BM, Reynolds JH, Smith SP, Truesdell AH (1987) Helium isotopes: Lower Geyser Basin, Yellowstone National Park. *J Geophys Res* 92, 12477-12489.
- Kharaka YK, Mariner RH, Bullen TD, Kennedy BM, Sturchio NC (1991) Geochemical investigations of hydraulic connections between the Corwin Springs Known Geothermal Resources Area and adjacent parts of Yellowstone National Park. in Sorey ML (ed) *Effects of potential geothermal development in the Corwin Springs Known Geothermal Resources Area, Montana, on the thermal features of Yellowstone National Park*. US Geol Survey Water-Resour Invest Rept 91-4052, FI-F38.
- Kharaka YK, Sorey ML, Thordsen JJ (2000) Large-scale hydrothermal fluid discharges in the Norris-Mammoth corridor, Yellowstone National Park, USA. *J Geochem Expl* 69-70, 201-205.
- Kharaka YK, Thordsen JJ, White LD (2002) Isotope and chemical compositions of meteoric and thermal waters and snow from the Greater Yellowstone National Park Region. US Geol Survey Open-File Report 02-194.
- Killelea DR, Aldstadt JH (2002) Identification of dimethylchloroarsine near a former herbicide factory by headspace solid-phase microextraction gas chromatography-mass spectrometry. *Chemosphere* 48 (9), 1003-1008.
- Kim MJ, Nriagu J, Haack S (2000) Carbonate ions and arsenic dissolution by groundwater. *Environ Sci Technol* 34 (15), 3094-3100.
- Kim MJ (2001) Separation of inorganic arsenic species in groundwater using ion exchange method. *Bull Environ Contam Toxicol* 67 (1), 46-51.
- Kiver EP, Harris DV (1999) *Geology of U.S. Parklands*. 5th edition, John Wiley, New York.
- Kleno JG, Wolkoff P, Clausen PA, Wilkins CK, Pedersen T (2002) Degradation of the adsorbent Tenax TA by nitrogen oxides, ozone, hydrogen peroxide, OH radical, and limonene oxidation products. *Environ Sci Technol* 36, 4121-4126.
- Klumpp DW, Peterson PJ (1981) Chemical characteristics of arsenic in a marine food chain. *Mar Biol* 62 (4), 297-305.
- Klusman R (1991) Method and apparatus for the collection of reduced gases. United States Patent, No. 4,993,874.
- Knobloch T, Engewald W (1995) Sampling and gas chromatographic analysis of volatile organic compounds in hot and extremely humid emissions. *J High Resol Chromatogr* 18, 635-642.
- Kocar BD, Garrott RA, Inskeep WP (2004) Elk exposure to arsenic in geothermal watersheds of Yellowstone National Park, USA. *Environ Toxicol Chem* 23 (4), 982-989.
- Koch I, Feldmann J, Wang L, Andrewes P, Reimer KJ, Cullen WR (1999) Arsenic in the Meager Creek hot springs environment, British Columbia. *Sci Tot Environ* 236, 101-117.
- Kösters J, Diaz-Bone RA, Planer-Friedrich B, Rothweiler B, Hirner AV (2003) Identification of organic arsenic, tin, antimony and tellurium compounds in environmental samples by GC-MS. *J Mol Struct*, 661-662, 347-356.
- Korte NE, Fernando Q (1991) A review of arsenic (III) in groundwater. *Crit Rev Env Contr* 21 (1), 1-39.
- Krabbenhoft DP, Hurley JP, Olson ML, Cleckner LB (1998) Diel variability of mercury phase and species distributions in the Florida Everglades. *Biogeochemistry* 40, 311-325.
- Krabbenhoft DP, Olson ML, Dewild JF, Clow DW, Striegl RS, Dornblaser MM, VanMetre P (2002) Mercury loading and methylmercury production and cycling in high-altitude lakes from the western United States. *Water Air Soil Poll Focus* 2, 233-249.
- Krupp EM, Grümping R, Furchtbar URR, Hirner AV (1996) Speciation of metals and metalloids in sediments with LTGC/ICP-MS. *Fresen J Anal Chem* 354, 546-549.
- Kumaraswamy S, Rath AK, Ramakrishnan B, Sethunathan N (2000) Wetland rice soils as sources and sinks of methane: a review and prospects for research. *Biol Fertil Soils* 31, 449-461.
- Kuo TL (1968) Arsenic content of artesian well water in endemic area of chronic arsenic poisoning. *Rep Inst Pathol National Taiwan Univ* 20, 7-13.
- Kutschke S (1998) Weiterführende hydrogeologische Untersuchungen an der Industriellen Absetzanlage Schneckenstein. Unpublished master thesis, Technische Universität Bergakademie Freiberg, Department of Geology.
- Lai VWM, Cullen WR, Harrington CE, Reimer KJ (1997) The characterization of arsenosugars in commercially available algal products including a Nostoc species of terrestrial origin. *Appl Organomet Chem* 11, 797-803.
- Landgraf A (2002) Bestimmung des Schadstoff-Rückhaltevermögens eines natürlichen Feuchtgebietes (Schneckenstein, Vogtland). Unpublished master thesis, Technische Universität Bergakademie Freiberg, Department of Geology.
- Landgraf A, Planer-Friedrich B, Merkel B (2002) Natural attenuation in a wetland under unfavorable conditions - Uranium tailing Schneckenstein / Germany. In: Merkel B, Planer-Friedrich B, Wolkersdorfer C (eds) *Uranium in the aquatic environment*. Springer, 853-860.
- Landner L (1989) *Chemicals in the aquatic environment - Advanced Hazard Assessment*. Springer, Berlin.

- Langner HW, Jackson CR, McDermott TR, Inskip WP (2001) Rapid oxidation of arsenite in a hot spring ecosystem, Yellowstone National Park. *Environ Sci Technol* 35, 3302-3309.
- Lantzy RJ, MacKenzie FT (1979) Atmospheric trace metals: global cycles and assessment of man's impact. *Geochim Cosmochim Acta* 43, 511-525.
- Larsen EH, Pritzl G, Hansen SH (1993) Speciation of eight arsenic compounds in human urine by high-performance liquid chromatography with inductively coupled plasma mass spectrometric detection using antimonate for internal chromatographic standardization. *J Anal Atom Spectrom* 8, 557-564.
- Le XC, Cullen WR, Reimer KJ (1993) Determination of urinary arsenic and impact of dietary arsenic intake. *Talanta* 40 (2), 185-193.
- Le XC, Ma M (1997) Speciation of arsenic compounds by using ion-pair chromatography with atomic spectrometry and mass spectrometry detection. *J Chromatogr A* 764, 55-64.
- Le XC, Ma M (1998) Short-column liquid chromatography with hydride generation atomic fluorescence detection for the speciation of arsenic. *Anal Chem* 70, 1926-1933.
- Le XC, Lu X, Ma M, Cullen WR, Aposhian HV, Zheng B (2000a) Speciation of key arsenic metabolic intermediates in human urine. *Anal Chem* 72 (21), 5172-5177.
- Le XC, Ma M, Lu X, Cullen WR, Aposhian HV, Zheng B (2000b) Determination of monomethylarsonous acid, a key arsenic methylation intermediate in human urine. *Environ Health Persp* 108 (11), 1015-1018.
- Le XC, Yalcin S, Ma M (2000c) Speciation of submicrogram per liter levels of arsenic in water: on-site species separation integrated with sample collection. *Environ Sci Technol* 34 (11), 2342-2347.
- Lehmann JA, Smith RB, Schilly MM (1982) Upper crustal structure of the Yellowstone caldera from seismic delay time analyses and gravity correlations. *J Geophys Res* 87, 2713-2730.
- Léonard A (1991) Arsenic. In: Merian E (ed) *Metals and their compounds in the environment*, VCH, 751-774.
- Lewis AJ, Palmer MR, Sturchio NC, Kemp AJ (1997) The rare earth element geochemistry of acid-sulphate and acid-sulphate-chloride geothermal systems from Yellowstone National Park, Wyoming, USA. *Geochim Cosmochim Acta* 61 (4), 695-706.
- Lido DR (ed) (2003) *CRC Handbook of Chemistry and Physics*. 84th ed. CRC Press.
- Lin S, Cullen WR, Thomas DJ (1999) Methylarsenicals and arsinothiols are potent inhibitors of mouse liver thioredoxin reductase. *Chem Res Toxicol* 12, 924-930.
- Lindemann T, Prange A, Dannecker W, Neidhart B (1999) Simultaneous determination of arsenic, selenium and antimony species using HPLC/ICP-MS. *Fresen J Anal Chem* 364, 462-466.
- Lindemann T, Prange A, Dannecker W, Neidhart B (2000) Stability studies of arsenic, selenium, antimony and tellurium species in water, urine, fish and soil extracts using HPLC/ICP-MS. *Fresen J Anal Chem* 368, 214-220.
- Locke WM, Meyer GA (1994) A 12,000-year record of vertical deformation across the Yellowstone caldera margin: The shorelines of Yellowstone Lake. *J Geophys Res* 99, 20079-20094.
- Londesborough S, Mattusch J, Wennrich R (1999) Separation of organic and inorganic arsenic species by HPLC-ICP-MS. *Fresen J Anal Chem* 363, 577-581.
- Love JD, Good JM (1970) Hydrocarbons in thermal areas, Northwestern Wyoming. *US Geol Survey Professional Paper* 644-B, 23.
- Lowenthal DH, Pilson MEQ, Byrne RH (1977) The determination of the apparent dissociation constants of arsenic acid in seawater. *J Mar Res* 35, 653-669.
- Luna AS, Sturgeon RE, de Campos RC (2000) Chemical vapor generation: atomic absorption by Ag, Au, Cu, and Zn following reduction of aquo ions with sodium tetrahydroborate(III). *Anal Chem* 72, 3523-3531.
- Ma M, Le XC (1998) Effect of arsenosugar ingestion on urinary arsenic speciation. *Clin Chem* 44 (3), 539-550.
- MacKenzie FT, Lantzy RJ, Paterson V (1979) Global trace metal cycles and predictions. *Math Geol* 11, 99-142.
- Maeda S (1994) Safety and environmental effects. In: Patai S (ed) *The chemistry of organic arsenic, antimony, and bismuth compounds*, John Wiley, New York, 725-759.
- Maillefer S, Lehr CR, Cullen WR (2003) The analysis of volatile trace compounds in landfill gases, compost heaps and forest air. *Appl Organomet Chem* 17, 154-160.
- Mandal BK, Suzuki KT (2002) Arsenic round the world: a review. *Talanta* 58, 201-235.
- Mannigel S (2002) Hydrogeochemische Charakterisierung der Selbstreinigungsprozesse im bergbaulich beeinflussten wetland Lengenfeld / Vogtland. Unpublished master thesis, Technische Universität Bergakademie Freiberg, Department of Geology.
- Marafante E, Vather M, Norin H, Envall J, Sandström M, Christakopoulos A, Ryhage R (1987) Biotransformation of dimethylarsinic acid in mouse, hamster and man. *J Appl Toxicol* 7, 111-117.
- Marler GD (1964) Effects of the Hebgen Lake earthquake of August 17, 1959, on the hot springs of the Firehole Geysir Basins, Yellowstone National Park. In: *The Hebgen Lake, Montana earthquake of August 17, 1959*. *US Geol Survey Professional Paper* 435, 185-198.
- Marsh J (1836) Marsh arsenic test. *Edinburgh New Phil J* 23, 207.
- Mass MJ, Tennant A, Roop BC, Cullen WR, Styblo M, Thomas DJ, Kligerman AD (2001) Methylated trivalent arsenic species are genotoxic. *Chem Res Toxicol* 14, 355-361.
- Matschullat J (2000) Arsenic in the geosphere - a review. *Sci Total Environ* 249, 297-312.
- McBride BC, Wolfe RS (1971) Biosynthesis of dimethylarsine by methanobacterium. *Biochemistry* 10, 4312-4317.

- McCleskey RB, Nordstrom DK, Ball JW (2001) Cation-exchange separation of interfering metals from acid mine waters for accurate determination of total arsenic and arsenic(III) by hydride generation-atomic absorption spectrometry. USGS Workshop on Arsenic in the Environment, February 21-22, 2001, Denver, CO.
- McCleskey RB, Nordstrom DK (2002) Water sample preservation for dissolved arsenic (III/V). 2002 Denver Annual Meeting (October 27-30, 2002), Paper No.131-6.
- McCleskey RB, Nordstrom DK, Ball JW (2003) Metal interferences and their removal prior to the determination of As(T) and As(III) in acid mine waters by hydride generation atomic absorption spectrometry. US Geol Survey Water-Resour Invest Rept 03-4117.
- McCleskey RB, Nordstrom DK, Maest AS (2004) Preservation of water samples for arsenic(III/V) determinations: an evaluation of the literature and new analytical results. *Appl Geochem* 19, 995-1009.
- McSheehy S, Marcinek M, Chassaing H, Szpunar J (2000) Identification of dimethylarsinoyl-riboside derivatives in seaweed by pneumatically assisted electrospray tandem mass spectrometry. *Anal Chim Acta* 410, 71-84.
- Meharg AA, Hartley-Whitaker J (2002) Arsenic uptake and metabolism in arsenic resistant and nonresistant plant species. *New Phytol* 154, 29-43.
- Merck (1983) An encyclopedia of chemicals, drugs, and biologicals. 10th ed., Rahway NJ, Merck Inc.
- Merkel B, Preußer R, Namoun T, Gottschalk S, Kutschke S (1998) Natural Leaching of uranium from the Schneckenstein uranium mine tailing. In: Merkel B, Helling C (eds) Uranium Mining and Hydrogeology II. Proc Int Conf, Sven von Loga, Köln, 68-76.
- Merkel B, Sperling B (1998) Hydrogeochemische Stoffsysteme, Teil II. DVWK-Schriften 117 Kommissionsvertrieb Wirtschafts- und Verlagsgesellschaft Gas und Wasser mbH, Bonn.
- Mester Z, Sturgeon RE, Lam JW (2000) Sampling and determination of metal hydrides by solid phase microextraction thermal desorption inductively coupled plasma mass spectrometry. *J Anal Atom Spectrom* 15 (11), 1461-1465.
- Mester Z, Sturgeon R (2001) Detection of volatile arsenic chloride species during hydride generation: a new prospectus. *J Anal Atom Spectrom* 16 (5), 470-474.
- Mester Z, Sturgeon R (2002) Detection of volatile organometal chloride species in model atmosphere above seawater and sediment. *Environ Sci Technol* 36 (6), 1198-1201.
- Michalke K, Schramel P (1997) Coupling of capillary electrophoresis with ICP-MS for speciation investigation. *Fresen J Anal Chem* 357, 594-599.
- Michalke K, Wickenheiser EB, Mehring M, Hirner AV, Hensel R (2000) Production of volatile derivatives of metal(loid)s by microflora involved in anaerobic digestion of sewage sludge. *Appl Environ Microbiol* 66 (7), 2791-2796.
- Moore JN, Ficklin WH, Johns C (1988) Partitioning of arsenic and metals in reducing sulfidic sediments. *Environ Sci Technol* 22 (4), 432-437.
- Moore JN, Luoma SN (1990) Hazardous wastes from large-scale metal extraction. *Environ Sci Technol* 24 (9), 1279-1285.
- Moore JN, Landrigan EM (1999) Mobilization of metal-contaminated sediment by ice-jam floods. *Environ Geol* 37 (1-2), 96-101.
- Moore JN, Woessner WW (2003) Arsenic contamination in the water supply of Milltown, Montana. In: Welch AH, Stollenwerk KG (eds) Arsenic in ground water: geochemistry and occurrence. Norwell, Massachusetts, Kluwer Academic Publishers, 329-350.
- Morrison GMP, Batley GE, Florence TM (1989) Metal speciation and toxicity. *Chem Br* 25, 791.
- Mortimer CE (1987) Chemie, 5.Aufl. Georg Thieme Verlag Stuttgart.
- Mosier AR, Delgado JA, Cochran VL, Valentine DW, Parton WJ (1997) Impact of agriculture on soil consumption of atmospheric CH₄ and a comparison of CH₄ and N₂O flux in subarctic, temperate and tropical grasslands. *Nutr Cycl Agroecosys* 49, 71-83.
- Mosier AR (1998) Soil processes and global change. *Biol Fertil Soils* 27, 221-229.
- Moxon AL (1938) The effect of arsenic on the toxicity of seleniferous grains. *Science* 88, 81.
- Muffler LJP, White DE, Truesdell AH (1971) Hydrothermal explosion craters in Yellowstone National Park. *Bull Geol Soc Amer* 82, 723-740.
- Mukai H, Ambe Y, Muku T, Takeshita K, Fukuma T (1986) Seasonal variations in methylarsenic compounds in airborne particulate matter. *Nature* 324, 239-241.
- Mukhopadhyay R, Rosen BP, Phung LT, Silver S (2002) Microbial arsenic: from geocycles to genes and enzymes. *FEMS Microbiol Rev* 26, 311-325.
- Murphy JB, Opliger GL, Brimhall GH (1998) Plume-modified orogeny: An example from the western United States. *Geology* 26, 731-734.
- Myers DJ, Heimbrook ME, Osteryoung J, Morrison SM (1973) Arsenic oxidation state in the presence of microorganisms. Examination by differential pulse polarography. *Environ Lett* 5, 53-61.
- Naumov GB, Ryzhenko BN, Khodakovskiy IL (1974) Handbook of thermodynamic data. Moskau.
- Neue H (1993) Methane emission from rice fields: Wetland rice fields may make a major contribution to global warming. *BioScience* 43 (7), 466-73.
- New Jersey Hazardous Substances Fact Sheets (1993) Right to know program, New Jersey Department of Public Health, Trenton, New Jersey, Denver (CO) Micromedex Inc.
- Newman DK, Kennedy EK, Coates JD, Ahmann D, Ellis DJ, Lovley DR, Morel FMM (1997) Dissimilatory arsenate and sulfate reduction in *Desulfotomaculum auripigmentum*, sp. nov. *Arch Microbiol* 165, 380-388.

- Niggemyer A, Spring S, Stackebrandt E, Rosenzweig RF (2001) Isolation and characterization of a novel As(V)-reducing bacterium: Implications for arsenic mobilization and the genus *Desulfitobacterium*. *Appl Environ Microbiol* 67 (12), 5568-5580.
- Nordstrom DK (2000) Thermodynamic properties of environmental arsenic species: Limitations and needs. in Young C (ed) *Minor elements 2000, processing and environmental aspects of As, Sb, Se, Te, and Bi*. Society for Mining, Metallurgy, and Exploration, 325-331.
- Nordstrom DK, McCleskey RB, Ball JW (2001) Processes governing arsenic geochemistry in the thermal waters of Yellowstone National Park. USGS Workshop on Arsenic in the Environment, February 21-22, 2001, Denver, CO.
- Nordstrom DK (2002) Worldwide occurrences of arsenic in ground water. *Science* 296 (5576), 2143-2145.
- Nordstrom DK (2003) Effects of microbiological and geochemical interactions in mine drainage. in Jambor JL, Blowes DW, Ritchie AIM (eds) *Environmental Aspects of Mine Wastes*. Mineralogical Association of Canada 31, 227-238.
- Nordstrom DK, Archer DG (2003) Arsenic thermodynamic data and environmental geochemistry. in Welch AH, Stollenwerk KG (eds) *Arsenic in ground water: geochemistry and occurrence*. Boston, Kluwer Academic Publishers, 1-26.
- Nordstrom DK, McCleskey RB, Ball JW (2003) Orpiment solubility equilibrium and arsenic speciation for a hot spring at Yellowstone National Park using revised thermodynamic data. *Geol Soc Am Abstracts with Programs* 35 (6), 47.
- Norin H, Ryhage R, Christakopoulos A, Sandström M (1983) New evidence for the presence of arsenocholine in shrimps (*Pandalus borealis*) by use of pyrolysis gas chromatography — atomic absorption spectrometry/mass spectrometry. *Chemosphere* 12, 299-315.
- Nriagu JO (ed) (1994a) *Arsenic in the environment - Part I: cycling and characterization*. Adv Environ Sci 26. John Wiley and Sons Inc. New York.
- Nriagu JO (ed) (1994b) *Arsenic in the environment - Part II: human health and ecosystem effects*. Adv Environ Sci 27. John Wiley and Sons Inc. New York.
- Obradovich JD (1992) Geochronology of the late Cenozoic volcanics of Yellowstone National Park and adjoining areas, Wyoming and Idaho. US Geol Survey Open-File Report 92-048.
- Office of Environmental Health Hazard Assessment (1999) Acute reference exposure levels (RELs), averaging times, and toxicologic endpoints. http://www.oehha.ca.gov/air/acute_rels/pdf/7784421A.pdf.
- Onishi H (1969) Arsenic. In: Wedepohl KH (ed) *Handbook of geochemistry*. Berlin. Springer, II(3).33.
- Oremland RS, Stolz JF (2003) The ecology of arsenic. *Science* 300, 939-944.
- Oscarson DW, Huang PM, Defosse C, Herbillon A (1981) Oxidative power of Mn(IV) and Fe(III) oxides with respect to As(III) in terrestrial and aquatic environments. *Nature* 291, 50-51.
- Palacios MA, Gomez M, Camara C, Lopez MA (1997) Stability studies of arsenate, monomethylarsenate, dimethylarsinate, arsenobetaine and arsenocholine in deionized water, urine and clean-up dry residue from urine samples and determination by liquid chromatography with microwave-assisted oxidation-hydride generation atomic absorption spectrometric detection. *Anal Chim Acta* 340, 209-220.
- Pantsar-Kallio M, Korpela A (2000) Analysis of gaseous arsenic species and stability studies of arsine and trimethylarsine by gas chromatography-mass spectrometry. *Anal Chim Acta* 410, 71-84.
- Parkhurst DL, Appelo CAJ (1999) User's guide to PHREEQC (version 2) - a computer program for speciation, batch-reaction, one-dimensional transport, and inverse geochemical calculations. US Geol Survey Water-Resour Invest Rept 99-4259.
- Parris GE, Brinckman FE (1976) Reactions which relate to environmental mobility of arsenic and antimony. II. Oxidation of trimethylarsine and trimethylstibine. *Environ Sci Technol* 10, 1128-1134.
- Péchevran C, Quétel CR, Martin Lecuyer FM, Donard OFX (1998) Simultaneous determination of volatile metal (Pb, Hg, Sn, In, Ga) and nonmetal species (Se, P, As) in different atmospheres by cryofocusing and detection by ICP-MS. *Anal Chem* 70 (13), 2639-2645.
- Péchevran C, Lalère B, Donard OFX (2000) Volatile metal and metalloid species (Pb, Hg, Se) in a European urban atmosphere (Bordeaux, France). *Environ Sci Technol* 34 (1), 27-32.
- Pellizzari ED, Krost KJ (1984) Chemical transformations during ambient air sampling for organic vapors. *J Anal Chem* 56, 1813-1819.
- Pelton JR, Smith RB (1982) Contemporary vertical surface displacements in Yellowstone National Park. *J Geophys Res* 87, 2745-2761.
- Penrose WR (1974) Arsenic in the marine and aquatic environments: analysis, occurrence and significance. *CRC Crit Rev Environ Control* 4, 465-482.
- Pergantis SA, Winnik W, Heithmar EM, Cullen WR (1997) Investigations of arsine-generating reactions using deuterium-labeled reagents and mass spectrometry. *Talanta* 44, 1941-1947.
- Pergantis SA, Wangkarn S, Francesconi KA, Thomas-Oates JE (2000) Identification of arsenosugars at the picogram level using nano-electrospray quadrupole time-of-flight mass spectrometry. *Anal Chem* 72, 357-366.
- Petänen T, Virta M, Karp M, Romantschuk M (2001) Construction and use of broad host range mercury and arsenite sensor plasmids in the soil bacterium *Pseudomonas fluorescens* OS8. *Microbial Ecol* 40, 360-368.
- Peters RL, Renesse v. Duivenbode JAD, Duyzer JH, Verhagen H (1994) The determination of terpenes in forest air. *L Atmos Environ* 28A, 2413-2419.
- Peterson PJ, Benson LM, Zieve R (1981) Metalloids. In: Lepp NW (ed) *Effect of heavy metal pollution on plants, 1: Effects of trace metals on plant function*. 279-342 Applied Science Publishers.

- Petito CT, Beck BD (1990) Evaluation of evidence for nonlinearities in the dose-response curve for arsenic carcinogenesis. in Hemphill DD, Cothorn CR (eds) Trace substances in environmental health XXIV. Science Reviews Limited, Northwood, 143-176.
- Patrick JS, Ayala-Fierro F, Cullen WR, Carter DE, Aposhian HV (2000) Monomethylarsonous acid (MMAIII) is more toxic than arsenite in Chang human hepatocytes. *Toxicol Appl Pharmacol* 163, 203-207.
- Phillips SE, Taylor ML (1976) Oxidation of arsenite to arsenate by *Alcaligenes faecalis*. *Appl Environ Microbiol* 32, 392-399.
- Pickett AW, McBride BC, Cullen WR (1988) Metabolism of trimethylarsine oxide. *Appl Organomet Chem* 2, 479-482.
- Pierce KL (1979) History and dynamics of glaciation in the northern Yellowstone National Park area. US Geol Survey Professional Paper 729F.
- Pierce KL, Morgan LA (1990) The track of the Yellowstone hotspot: Volcanism, faulting, and uplift. US Geol Survey Open-File Report 90-415.
- Pierce KL, Morgan LA (1992) The track of the Yellowstone hotspot: Volcanism, faulting, and uplift. in Link PK, Kuntz MA, Platt LB (eds) Regional Geology of Eastern Idaho and Western Wyoming. *Geol Soc Am Memoir* 179, 1-53.
- Pierce KL, Cannon KP, Meyer GA (1997) Yellowstone caldera "heavy breathing" based on Yellowstone Lake and river changes in post-glacial time. *Eos* 78, 802.
- Pierce KL, Morgan LA, Saltus RW (2000) Yellowstone plume head: postulated tectonic relations to the Vancouver slab, continental boundaries, and climate. US Geol Survey Open-File Report 00-498.
- Pierce KL, Cannon KP, Meyer GA, Trebesch MJ, Watts RD (2002) Post-glacial inflation-deflation cycles, tilting, and faulting in the Yellowstone caldera based on Yellowstone Lake shorelines. US Geol Survey Open-File Report 02-0142.
- Pilson MEQ (1974) Arsenate uptake and reduction by *Pocillopora verrucosa*. *Limnol Oceanogr* 19, 339-341.
- Planer-Friedrich B, Matschullat J, Merkel B, Roewer G, Volke P (2002) Development of a robust technique for sampling volatile metal(loid)s in wetlands. *Anal Bioanal Chem* 374 (7-8), 1191-1198.
- Pokrovski GS, Zakirov IV, Roux J, Testemale D, Hazemann JL, Bychkov AY, Golikova GV (2002) Experimental study of arsenic speciation in vapor phase to 500°C: Implications for As transport and fractionation in low-density crustal fluids and volcanic gases. *Geochim Cosmochim Acta* 66 (19), 3453-3480.
- Prohaska T, Pfeffer M, Tulipan M, Stinger G, Mentler A, Wenzel WW (1999) Speciation of arsenic of liquid and gaseous emissions from soil in a microcosmos experiment by liquid and gas chromatograph with inductively coupled plasma mass spectrometry (ICP-MS) detection. *Fresen J Anal Chem* 364, 467-470.
- Pyle DG, Hanan BB, Graham DW, Duncan RA (1997) Siletzia-geochemistry and geochronology of Yellowstone hot spot volcanism in a suboceanic setting. *Geol Soc Am Abstracts with Programs* 29 (6), A-298.
- Rauret G, Rubio R, Padro A (1991) Arsenic speciation using HPLC-hydride generation (HG)-inductively coupled plasma (ICP)-atomic emission spectrometry (AES) with gas-liquid separator. *Fresen J Anal Chem* 340(3), 157-160.
- Ravenscroft P, McArthur JM, Hoque BA (2001) Geochemical and palaeohydrological controls on pollution of groundwater by arsenic. In: Chappell WR, Abernathy CO, Calderon R (eds) Arsenic Exposure and Health Effects IV, 53-78.
- Reamer DC, Zoller WH (1980) Selenium biomethylation products from soil and sewage sludge. *Science* 208, 500-502.
- Reay PF, Asher CJ (1977) Preparation and purification of ⁷⁴As-labeled arsenate and arsenite for use in biological experiments. *Anal Biochem* 78, 557-560.
- Richardson BA (1994) Sudden infant death syndrome: a possible primary cause. *J Forensic Sci Soc* 34, 199-204.
- Ritchie JA (1961) Arsenic and antimony in New Zealand thermal waters. *New Zealand Journal of Science* 4, 218-229.
- Roberto FF, Barnes JM, Bruhn DF (2002) Evaluation of a GFP reporter gene construct for environmental arsenic detection. *Talanta* 58, 181-188.
- Robertson FN (1989) Arsenic in groundwater under oxidizing conditions, south-west United States. *Environ Geochem Health* 11, 171-185.
- Robins RG (1985) The solubility of barium arsenate: Sherritt's barium arsenate process. *Metallurgical Transactions B*, 16B, 404-406.
- Roscoe HE, Schorlemmer CA (1911) A treatise on chemistry. Macmillan and Co. Ltd., London, 697.
- Rosen BP (2002) Biochemistry of arsenic detoxification. *FEBS Lett* 529, 86-92.
- Rossum JR (1975) Checking the accuracy of water analysis through the use of conductivity. *J Americ Water Works Assoc* 67, 204-205.
- Rowe JJ, Fournier RO, Morey GW (1973) Chemical analysis of thermal waters in Yellowstone National Park, Wyoming, 1960-65. US Geol Survey Bull 1303.
- Rüde TR (1996) Beiträge zur Geochemie des Arsens. *Karlsruher Geochemische Hefte* 19, 206.
- Sadiq M, Zaidi TH, Mian AA (1983) Environmental behavior of arsenic in soils: theoretical. *Water Air Soil Poll* 20, 369-377.
- Saeki K, Sakakibara H, Sakai H, Kunito T, Tanabe S (2000) Arsenic accumulation in three species of sea turtles. *Bio-metals* 13, 241-250.
- Sakurai T, Kaise T, Matsubara C (1998) Inorganic and methylated arsenic compounds induce cell death in murine macrophages via different mechanisms. *Chem Res Toxicol* 11 (4), 273-283.
- Salmassi TM, Venkateswaren K, Satomi M, Neilson KH, Newman DK, Hering JG (2002) Oxidation of arsenite by *Agrobacterium albertimagni*, AOL15, sp. nov., isolated from Hot Creek, California. *Geomicrobiol J* 19, 53-66.

- Sampayo-Reyes A, Zakharyan RA, Healy SM, Aposhian HV (2000) Monomethylarsonic acid reductase and monomethylarsonous acid in hamster tissue. *Chem Res Toxicol* 13 (11), 1181-1186.
- Sancha AM, Castro ML (2001) Arsenic in Latin America: occurrence, exposure, health effects and remediation. In: Chapell WR, Abernathy CO, Calderon RL (eds) *Arsenic Exposure and Health Effects IV*. Elsevier, Amsterdam, 87-96.
- Sanders (1979) Microbial role in the demethylation and oxidation of methylated arsenicals in seawater. *Chemosphere* 8, 135-137.
- Sanders JG (1985) Arsenic geochemistry in Chesapeake Bay: dependence upon anthropogenic inputs and phytoplankton species composition. *Mar Chem* 17, 329-340.
- Santini JM, Sly LI, Schnagl RD, Macy JM (2000) A new chemolithoautotrophic arsenite-oxidizing bacterium isolated from a gold mine: phylogenetic, physiological, and preliminary biochemical studies. *Appl Environ Microbiol* 66 (1), 92-97.
- Santosa SJ (2001) Arsenic and selenium species behavior during microwave-assisted conversion to their volatile hydride forming species. *Anal Sci* 17, i25-i28.
- Sass RL (1994) Summary chapter for methane, In: Minami K, Mosier A, Sass RL (eds) *CH₄ and N₂O global emissions and controls from rice fields and other agricultural and industrial sources*. National Institute of Agro-Environmental Sciences, Yokendo, 1-7.
- Savage KS, Tingle TN, O'Day PA, Wayhunas GA, Bird DK (2000) Arsenic speciation in pyrite and secondary weathering phases, Mother Lode Gold District, Tuolumne County, California. *Appl Geochem* 15, 1219-1244.
- Sax NI (ed) (1986) *Rapid guide to hazardous chemicals in the workplace*. Van Nostrand Reinhold Co.
- Schall I (1995) *Hydrogeologische und hydrochemische Untersuchungen im Bereich der ehemaligen Uranerzaufbereitungsanlage Lengenfeld (Vogtland)*. Unpublished master thesis Rheinisch-Westfälische Technische Hochschule Aachen.
- Schedlbauer OF, Heumann KG (1999) Development of an isotope dilution mass spectrometric method for dimethylthallium speciation and first evidence of its existence in the ocean. *Anal Chem* 71 (24), 5459-5464.
- Schlegel D, Mattusch J, Wennrich R (1996) Speciation analysis of arsenic and selenium compounds by capillary electrophoresis. *Fresen J Anal Chem* 354, 535-539.
- Schroeder WH (1982) Sampling and analysis of mercury and its compounds in the atmosphere. *Environ Sci Technol* 16, 394-400.
- Schweigkofler M, Niessner R (1999) Determination of siloxanes and VOC in landfill gas and sewage gas by canister sampling and GC-MS/AES analysis. *Environ Sci Technol* 33 (20), 3680-3685.
- Scudlark JR, Johnson DL (1982) Biological oxidation of arsenite in sea water. *Estuar Coast Shelf S* 14, 693-706.
- Seidel M (2002) Sorption von Metallen und Halbmetallen an Sedimenten im bergbaulich beeinflussten wetland Lengenfeld / Vogtland. *Freiberg Online Geosciences FOG 8*; http://www.geo.tu-freiberg.de/fog/FOG_Vol_8.pdf.
- Seidel M, Mannigel S, Planer-Friedrich B, Merkel B (2002) Hydrogeochemical characterisation of surface water, sorption of metal(loid)s on sediments and exchange processes within the wetland Lengenfeld / Germany. In: Merkel B, Planer-Friedrich B, Wolkersdorfer C (eds) *Uranium in the aquatic environment*. Springer, 871-880.
- Seyler P, Martin JM (1989) Biogeochemical processes affecting arsenic species distribution in a permanently stratified lake. *Environ Sci Technol* 23, 1258.
- Shariatpanahi M, Anderson AC, Abdelghani AA, Englande AJ, Hughes J, Wilkinson RF (1981) Biotransformation of the pesticide sodium arsenate. *J Environ Sci Health, Part B* 16 (1), 35-47.
- Shariatpanahi M, Anderson AC, Abdelghani AA, Englande AJ (1983) Microbial metabolism of an organic arsenical herbicide. In: Oxley TA, Barry S (eds) *Biodeterioration 5* Wiley, New York, 268-277.
- Shibata Y, Morita M, Fuwa K (1992) Selenium and arsenic in biology: their chemical forms and biological functions. *Adv Biophys* 28, 31-80.
- Shimizu N, Inoue Y, Daishima S, Yamaguchi K (1999) Liquid chromatography-mass spectrometry of arsenic compounds using the electrospray ionization with postcolumn addition of methanol. *Anal Sci* 15, 685-687.
- Shiomi K, Kakehashi Y, Yamanaka H, Kikuchi T (1987) Identification of arsenobetaine and a tetramethylarsonium salt in the clam *Meretrix lusoria*. *Organomet Chem* 1, 177-183
- Shiomi K (1994) Arsenic in marine organisms: Chemical forms and toxicological aspects. In: Nriagu JO (ed) *Arsenic in the environment – Part II: Human Health and Ecosystem Effects*. *Adv Environ Sci* 27, 261-282.
- Shraim A, Chiswell B, Olszowy H (1999) Speciation of arsenic by hydride generation - atomic absorption spectrometry (HG-AAS) in hydrochloric acid reaction medium. *Talanta* 50, 1109-1127.
- Shraim A, Chiswell B, Olszowy H (2000) Use of perchloric acid as a reaction medium for speciation of arsenic by hydride generation-atomic absorption spectrometry. *Analyst* 125, 949-954.
- Smedley PL, Zhang M, Zhang G, Luo Z (2001) Arsenic and other redox-sensitive elements in groundwater from the Huhhot Basin, Inner Mongolia. In: Cidu R (ed) *Water-Rock Interaction 2001 Vol. 1*. Swets and Zeitlinger, Lisse, 581-584.
- Smedley PL, Kinniburgh DG (2002) A review of the source, behaviour and distribution of arsenic in natural waters. *Appl Geochem* 17, 517-568.
- Smedley PL, Nicolli HB, MacDonald DMJ, Barros AJ, Tullio JO (2002) Hydrogeochemistry of arsenic and other inorganic constituents in groundwaters from La Pampa, Argentina. *Appl Geochem* 17, 259-284.

- Smith AH, Lingas EO, Rahman M (2000) Contamination of drinking-water by arsenic in Bangladesh: a public health emergency. *B World Health Organ* 78 (9), 1093-1103.
- Smith RB, Braile LW (1994) The Yellowstone hotspot. *J Volcan Geotherm Res* 61, 121-188.
- Smith RB, Siegel LJ (2000) *Windows into the earth – The geological story of Yellowstone and Grand Teton National Parks*. Oxford United Press.
- Sohrin Y, Matsui M, Kawashima M, Hojo M, Hasegawa H (1997) Arsenic biogeochemistry affected by eutrophication in Lake Biwa, Japan. *Environ Sci Technol* 31 (10), 2712-2720.
- Splithoff HM, Mason RP, Hemond HF (1995) Interannual variability in the speciation and mobility of arsenic in a dimictic lake. *Environ Sci Technol* 29, 2157-2161.
- Spycher NF, Reed MH (1989) Evolution of a broadlands-type epithermal ore fluid along alternative p-T-paths: implications for the transport and deposition of base, precious, and volatile metals. *Econ Geol* 84, 328-359.
- Squibb KS, Fowler BA (1983) The toxicity of arsenic and its compounds. In Fowler BA (ed) *Biological and environmental effects of arsenic*, 233-269 Amsterdam, Elsevier.
- Stanley WD, Hoover DB, Sorey ML, Rodriguez BD, Heran WD (1991) Electrical geophysical investigations in the Norris-Mammoth corridor, Yellowstone National Park, and the adjacent Corwin Springs known geothermal resources area. In: Sorey ML (Ed) *Effects of potential geothermal development in the Corwin Springs known geothermal resources area, Montana, on the thermal features of Yellowstone National Park*. US Geol Survey Water-Resour Invest Rept 91-4052, D1-D8.
- Stauffer RE, Jenne EA, Ball JW (1980) Chemical studies of selected trace elements in hot-spring drainages of Yellowstone National Park. US Geol Survey Professional Paper 1044-F.
- Stauffer RE, Thompson JM (1984) Arsenic and antimony in geothermal waters of Yellowstone National Park, Wyoming, USA. *Geochim Cosmochim Acta* 48 (2), 2547-2561.
- Stein S, Levitsky A, Fateev O, Mallard G (1998) NIST mass spectral search program, Vers. 1.6d (24/08/98).
- Stolz JF, Ellis DJ, Blum JS, Ahmann D, Lovley DR, Oremland RS (1999) *Sulfurospirillum barnesii* sp. nov. and *Sulfurospirillum arsenophilum* sp. nov., new members of the Sulfurospirillum clade of the Proteobacteria. *Internat J Sys Bacteriol* 49, 1177-1180.
- Stummeyer J, Harazim B, Wippermann T (1996) Speciation of arsenic in water samples by high-performance liquid chromatography-hydride generation-atomic absorption spectrometry at trace levels using a post-column reaction system. *Fresen J Anal Chem* 354, 344-351.
- Styblo M, Serves SV, Cullen WR, Thomas DJ (1997) Comparative inhibition of yeast glutathione reductase by arsenicals and arsenothiols. *Chem Res Toxicol* 10, 27-33.
- Styblo M, Vega L, Germolec DR, Luster MI, Del Razo LM, Wang C, Cullen WR, Thomas DJ (1999a) Metabolism and toxicity of arsenicals in cultured cells. In: Chappell WR, Abernathy CO, Calderon RL (eds) *Arsenic exposure and health effects*, Elsevier, 311-323.
- Styblo M, Del Razo L, LeCluyse EL, Hamilton GE, Wang C, Cullen WR, Thomas DJ (1999b) Metabolism of arsenic in primary cultures of human and rat hepatocytes. *Chem Res Toxicol* 12, 560-565.
- Styblo M, Del Razo LM, Vega L, Germolec DR, LeCluyse EL, Hamilton GA, Reed W, Wang C, Cullen WR, Thomas DJ (2000) Comparative toxicity of trivalent and pentavalent inorganic and methylated arsenicals in human cells. *Arch Toxicol* 74, 289-299.
- Sun GF, Pi JB, Li B, Guo XY, Yamauchi H, Yoshida T (2001) Progresses on researches of endemic arsenism in China: population at risk, intervention actions, and related scientific issues. In: Chappell WR, Abernathy CO, Calderon RL (eds) *Arsenic Exposure and Health Effects IV*. Elsevier, Amsterdam, 79-85.
- Sur R (1999) Kopplung von gas- und flüssigkeitschromatographischen Methoden mit atom- und massenspektrometrischen Detektoren zur Elementspeziesanalytik in biologischen Matrices am Beispiel von Arsen, Platin und Palladium. Verlag Mainz, Wissenschaftsverlag, Aachen.
- Takizawa Y (1979) Epidemiology of mercury poisoning. In Nriagu JO (ed) *The Biogeochemistry of Mercury in the Environment*, Elsevier, 325-365.
- Talmi Y, Bostick DT (1975) Determination of alkylarsenic acids in pesticide and environmental samples by gas chromatography with a microwave emission spectrometric detection system. *Anal Chem* 47 (13), 2145-2150.
- Taniguchi T, Tao H, Tominaga M, Miyazaki J (1999) Sensitive determination of three arsenic species in water by ion exclusion chromatography-hydride generation-inductively coupled plasma mass spectrometry. *J Anal Atom Spectrom* 14, 651-656.
- Tesfalidet S, Irgum K (1988) Volatilization of arsenic as the trichloride for sample introduction in atomic spectroscopy. *Anal Chem* 60, 2031-2035.
- Thayer JS (1995) *Environmental chemistry of the heavy elements: hydrido and organo compounds*. VCH Publ, Weinheim, 145.
- Thomas JE, Rhue RD (1997) Volatilization of arsenic in contaminated cattle dipping. *Bull Environ Contam Toxicol* 59, 882-887.
- Thomas P, Sniatecki K (1995) Determination of trace amounts of arsenic species in natural waters by high-performance liquid chromatography-inductively coupled plasma mass spectrometry. *J Anal Atom Spectrom* 10, 615-618.
- Thompson JM, Presser TS, Barnes RB, Bird DB (1975) Chemical analysis of the waters of Yellowstone National Park, Wyoming from 1965 to 1973. US Geol Survey Open-File Report 75-25.

- Thompson JM, Yadav S (1979) Chemical analysis of waters from geysers, hot springs and pools in Yellowstone National Park, Wyoming from 1974 to 1978. US Geol Survey Open-File Report 79-704.
- Thompson JM, Keith TEC, Consul JJ (1985) Water chemistry and mineralogy of Morgan and Growler hot springs, Lassen KGRA, California. Transactions of the Geothermal Research Council 9, 357-362.
- Thompson JM, DeMonge JM (1996) Chemical analyses of hot springs, pools, and geysers from Yellowstone National Park, Wyoming, and vicinity, 1980-1993. US Geol Survey Open-File Report 96-68.
- Thornton I, Farago M (1997) The geochemistry of arsenic. in Abernathy CO, Calderon RI, Chappell WR (eds) Arsenic Exposure and Health Effects. Chapman Hall, London, 1-16.
- Tingle JB (1911) Oxidation of arsenious and antimonius oxides. J Am Chem Soc 33, 1762-1763.
- TrinkwV (1990) Verordnung über Trinkwasser und Wasser für Lebensmittelbetriebe (Trinkwasserverordnung vom 5.Dezember 1990). BGBI.I, Bonn, 2612-2629.
- Truesdell AH, Fournier RO (1976) Conditions in the deeper parts of the hot spring systems of Yellowstone National Park, Wyoming. US Geol Survey Open-file report 76-428.
- Truesdell AH, Nathenson M, Rye RO (1977) The effects of subsurface boiling and dilution on the isotopic compositions of Yellowstone thermal waters. J Geophys Res 82, 3694-3704.
- Truesdell AH, Thompson JM (1982) The geochemistry of Shoshone Geyser Basin, Yellowstone National Park. In Guidebook Wyoming Geol Assoc Annu Field Conf 33rd, 153-159.
- Tseng WP, Chu HM, How SW, Fong JM, Lin CS, Yeh S (1968) Prevalence of skin cancer in an endemic area of chronic arsenicism in Taiwan. J Nat Cancer Inst 40, 453-463.
- Tsuruta D, Hamada T, Mochida K, Nakagawa K, Kobayashi H, Ishii M (1998) Merkel cell carcinoma, Bowen's disease and chronic occupational arsenic poisoning. Br.J. Dermatol 139, 241-244.
- Tucker WA, Nelken LH (1990) Diffusion coefficients in air and water. In: Lyman WJ, Reehl WF, Rosenblatt DH: Handbook of Chemical Property Estimation Methods. 1st ed, Am Chem Soc.
- Turner AW (1949) Bacterial oxidation of arsenite. Nature 164, 76-77.
- Ünlü MY, Fowler SW (1979) Factors affecting the flux of arsenic through the mussel *Mytilus galloprovincialis*. Mar Biol 51, 209-219.
- Vaithyanathan P, Richardson CJ, Kavanaugh RG, Craft CB, Barkay T (1996) Relationships of eutrophication to the distribution of mercury and to the potential for methylmercury production in the peat soils of the Everglades. Environ Sci Technol 30, 2591-2597.
- Van Elteren JT, Das HA, Deligny CL, Agterdenbos J, Bax D (1994) Arsenic speciation in aqueous samples using a selective As(III)/As(V) preconcentration in combination with an automatable cryotrapping hydride generation procedure for monomethylarsonic acid and dimethylarsinic acid. J Radioanal Nucl Chem 179 (2), 211-219.
- Van Elteren JT, Slejkovec Z (1997) Ion-exchange separation of eight arsenic compounds by high-performance liquid chromatography - UV decomposition - hydride generation - atomic fluorescence spectrometry and stability tests for food treatment procedures. J Chromatogr A 789, 339-348.
- Vanifatova NG, Spivakov BY, Mattusch J, Wennrich R (1999) Separation of arsenic and selenium species by capillary zone electrophoresis in a coated capillary. J AOAC Internat 82 (6), 1587-1593.
- Vather M (1999) Variation of human metabolism of arsenic. In: Chappell W.R., Abernathy C.O., Calderon R.L. (eds): Arsenic exposure and health effects 267-279.
- Wagemann R (1978) Some theoretical aspects of stability and solubility of inorganic arsenic in the freshwater environment. Water Res 12, 139-145.
- Walsh PR, Duce RA, Fasching JL (1979) Consideration of enrichment, sources, and flux of arsenic in the troposphere. Geophys Res 84, 1719-1726.
- Wang L, Huang J (1994) Chronic arsenism from drinking water in some areas of Xinjiang, China. in Nriagu JO (ed) Arsenic in the Environment, Part II: Human Health and Ecosystem Effects. John Wiley, New York, 159-172.
- Wang Y, Raihala TS, Jackman AP, John RS (1996) Use of tedlar bags in VOC testing and storage: evidence of significant VOC losses. Environ Sci Technol 30 (10), 3115-3117.
- Wanklyn JA (1901) Arsenic. Kegan Paul, Trench, Trübner and Co. Ltd, London, 3-4.
- Wassmann R, Aulakh MS (2000) The role of rice plants in regulating mechanisms of methane emissions. Biol Fertil Soils 31, 20-29.
- Watanabe I, Hashimoto T, Shimoyama A (1997) Methane-oxidizing activities and methanotrophic populations associated with wetland rice plants. Biol Fertil Soils 24, 261-265.
- Webster JG (1999) The source of arsenic (and other elements) in the Marble-Matingao River Catchment, Mindanao-Philippines. Geothermics 28 (1), 95-111.
- Webster JG, Nordstrom DK (2003) Geothermal arsenic - The source, transport and fate of arsenic in geothermal systems. In: Welch AH, Stollwerk KG (eds) Arsenic in ground water. Kluwer Academic Publishers, Boston, 101-125.
- Wedepohl KH (1995) The composition of the continental crust. Geochim Cosmochim Acta 59 (7), 1217-1232.
- Weed WH (1889) A deadly gas-spring in the Yellowstone Park. Science 13 (315), 130-132.
- Weeger W, Lievreumont D, Perret M, Lagarde F, Hubert JC, Leroy M, Lett MC (1999) Oxidation of arsenite to arsenate by a bacterium isolated from an aquatic environment. Biometals 12, 141-149.
- Welch AH, Lico MS, Hughes JL (1988) Arsenic in ground water of the western United States. Ground Water 26 (3), 333-347.

- Welch AH, Lico MS (1998) Factors controlling As and U in shallow ground water, southern Carson Desert, Nevada. *Appl Geochem* 13, 521-539.
- Wester RC, Maibach HI, Sedik L, Melendres J, Wade M (1993) In vivo and in vitro percutaneous absorption and skin decontamination of arsenic from water and soil. *Fundam Appl Toxicol* 20, 336-340.
- White DE, Muffler LJP, Truesdell AH (1971) Vapor-dominated hydrothermal systems compared with hot-water systems. *Econ Geol* 66, 75-97.
- White DE, Hutchinson RA, Keith TEC (1988) The geology and remarkable thermal activity of Norris Geyser Basin, Yellowstone National Park, Wyoming. US Geol Survey Professional Paper 1456, Washington.
- Whitfield FB, Freeman DJ, Shaw KJ (1983) Trimethylarsine: an important off-flavor component in some prawn species. *Chem Ind* 20, 786-787.
- Wickenheiser EB, Michalke K, Drescher C, Hirner AV, Hensel R (1998) Development and application of liquid and gas-chromatographic speciation techniques with element specific (ICP-MS) detection to the study of anaerobic arsenic metabolism. *Fresen J Anal Chem* 362, 498-501.
- Wicks C, Thatcher W, Dzurisin D (1998) Migration of fluids beneath Yellowstone Caldera inferred from satellite radar interferometry. *Science* 282 (5388), 458-462.
- Wicks CW, Thatcher W, Dzurisin D (2002) Satellite InSAR reveals a new style of deformation at Yellowstone caldera. *Eos Trans AGU*, 83(47), Fall Meet Suppl Abstract T12A-1291.
- Wicks CW, Thatcher W, Dzurisin D (2003) Stress transfer, thermal unrest, and implications for seismic hazards associated with the Norris Uplift Anomaly in Yellowstone National Park. *Eos Trans AGU*, 84(46), Fall Meet Suppl Abstract G31B-0714.
- Wildfang EK, Zakharyan RA, Aposhian HV (1997) Lack of in vitro arsenite and monomethylarsonic acid methyltransferase activity in the chimpanzee and squirrel monkey. *The Toxicologist* 36 (1,2), 34-35.
- Wildfang E, Zakharyan RA, Aposhian HV (1998) Enzymatic methylation of arsenic compounds, VI. Characterization of hamster liver arsenite and methylarsonic acid methyltransferase activities in vitro. *Toxicol Appl Pharmacol* 152, 366-375.
- Wilhelm E, Battino R, Wilcock RJ (1977) Low-pressure solubility of gases in liquid water. *Chem Rev* 77, 219-262.
- Wilkie JA, Hering JG (1998) Rapid oxidation of geothermal arsenic(III) in streamwaters of the eastern Sierra Nevada. *Environ Sci Technol* 32, 657-662.
- Wilkin RT, Wallschläger D, Forda RG (2003) Speciation of arsenic in sulfidic waters. *Geochem Trans* 4(1), 1-7.
- Williams M (2001) Arsenic in mine waters: an international study. *Environ Geol* 40 (3), 267-278.
- Witekowa S, Farbotko W (1972) Chemical effects of ultrasonic waves. XVII. Oxidation of arsenous acid under ultrasonic irradiation. *Acta Chim* 17, 91-95.
- Woessner WW, Moore JN, Johns C, Popoff MA, Sartor LC, Sullivan ML (1984) Arsenic Source and Water Supply Remedial Action Study - Milltown, Montana. Final Report, prepared for Solid Waste Bureau Montana Department of Health and Environmental Sciences, Helena, Montana.
- Wongsanon J, Boonchalermit S, Srilachai S, Fukuda M, Nakamura S, Klusman R (1997) A novel soil gas technique applied to an arsenic contaminated area of Ron Phibun, Southern Thailand. Conference: Toxic metal studies of Pak Panang and Pattani river basins October 17, 1997, Research and Development office, Prince of Songkla University, pp. 17.
- Wood JM (1974) Biological cycles for toxic elements in the environment. *Science* 183, 1049.
- Woolson EA (1983) Emissions, cycling, and effects of arsenic in soil ecosystems. In: Fowler B.A. (ed) *Biological and environmental effects of arsenic*. 51-139 Elsevier.
- World Health Organization (1993) *Guidelines for Drinking-Water Quality*, 2nd ed, WHO, Geneva.
- Xu Y, Schoonen MAA (1995) The stability of thiosulfate in the presence of pyrite in low-temperature aqueous solutions. *Geochim Cosmochim Acta* 59, 4605-4622.
- Xu Y, Schoonen MAA, Nordstrom DK, Cunningham KM, Ball JW (1998) Sulfur geochemistry of hydrothermal waters in Yellowstone National Park: I. The origin of thiosulfate in hot spring waters. *Geochim Cosmochim Acta* 62 (23/24), 3729-3743.
- Yalcin S, Le CX (2001) Speciation of arsenic using solid phase extraction cartridges. *J Environ Monit* 3, 81-85.
- Yamamoto M, Yasuda M, Yamamoto Y (1985) Hydride-generation atomic absorption spectrometry coupled with flow injection analysis. *Anal Chem* 57, 1382-1385.
- Yamanaka K, Hayashi H, Tachikawa W, Kato K, Hasegawa A, Oku N, Okada S (1997) Metabolic methylation is a possible genotoxicity-enhancing process of inorganic arsenic. *Mut Res* 394, 95-101.
- Yamauchi H, Yamamura Y (1984a) Metabolism and excretion of orally administered dimethylarsinic acid in the hamsters. *Toxicol Appl Pharmacol* 74, 134-140.
- Yamauchi H, Yamamura Y (1984b) Metabolism and excretion of orally ingested trimethylarsenic in man. *Bull Environ Contam Toxicol* 32(6), 682-7.
- Yamauchi H, Fowler BA (1994) Toxicity and metabolism of inorganic and methylated arsenicals. In Nriagu JO (ed) *Arsenic in the environment - Part II: Human Health and Ecosystem Effects*. *Adv Environ Sci* 27, 35-43.
- Yang SS, Chang HL (2001) Methane emission from paddy fields in Taiwan. *Biol Fertil Soils* 33, 157-165.
- Yano Y, Miyama T, Ito Y, Yasuda T (2000) Convenient measurements and speciation of arsenic in water by use of simple pretreatments for atomic absorption spectrometry in combination with hydride generation. *Anal Sci* 16, 939-943.

- Yin X, Hoffmann E, Lüdke C (1996) Differential determination of arsenic(III) and total arsenic with L-cysteine as prereductant using flow injection non-dispersive atomic absorption device. *Fresen J Anal Chem* 355, 324-326.
- Yoshida K, Chen H, Inoue Y, Wanibuchi H, Fukushima S, Kuroda K, Endo G (1997) The urinary excretion of arsenic metabolites after a single oral administration of dimethylarsinic acid to rats. *Arch Environ Contam Toxicol* 32, 1-6.
- Zakharyan RA, Aposhian HV (1999) Enzymatic reduction of arsenic compounds in mammalian systems: The rate-limiting enzyme of rabbit liver arsenic biotransformation is MMA(V) reductase. *Chem Res Toxicol* 12, 1278-1283.
- Zakharyan RA, Ayala-Fierro F, Cullen WR, Carter DM, Aposhian HV (1999) Enzymatic methylation of arsenic compounds, VII. Monomethylarsonous acid (MMAIII) is the substrate for MMA methyltransferase of rabbit liver and human hepatocytes. *Toxicol Appl Pharmacol* 158, 9-15.
- Zhang Z, Pawliszyn J (1993) Headspace solid-phase microextraction. *Anal Chem* 65, 1843-1852.
- Zoback ML, Thompson GA (1978) Basin and Range rifting in northern Nevada: Clues from a mid-Miocene rift and its subsequent offsets. *Geology* 6, 111-116.

7 APPENDIX

Appendix 1 Brief description of various sites sampled for volatile metallics in a first reconnaissance study

Abandoned Uranium tailings Lengenfeld und Schneckenstein / Germany

Investigations started in June 2001 in wetlands at two abandoned German uranium tailings, Lengenfeld (Schall 1995) and Schneckenstein (Gottschalk 1997; Kutschke 1998; Merkel et al. 1998). The wetlands developed at the tailing dam foots and were found to have a natural attenuation effect by decreasing the metal load from tailing drainage and seepage waters. Natural attenuation is an ecologically, economically, and politically favorable alternative to continuous active waste water treatment. Wetlands are, however, also predestined for volatilization processes because of their reducing conditions. Volatilization would interfere with the positive effects of natural attenuation because of the transformation of dissolved metals in their more toxic volatile species and possible transfer through the atmosphere in the - non-monitored - vicinity of the contamination site. In Lengenfeld, aqueous As concentrations of up to several mg/L were observed to decrease rapidly to background values while passing the wetland (Mannigel 2002). Sorption to iron oxides and the residual fraction was shown to be the main attenuation process (Seidel 2002; Seidel et al. 2002). During a first survey volatile As concentrations dissolved in water were found to be between about 10-20 ng/L. Compared to values reported from literature (e.g. 0.1 to 1.8 µg/L in cattle dipping vat sites by Thomas and Rhue 1997) these values for gaseous As were low. Due to low gas sampling volumes (0.2 - 0.7 L) concentrations in the trapping solution were only 2-3 times above the detection limit and, thus, uncertainties large. Further investigations with longer accumulation times could not be conducted at this site because the wetland was drained in the course of rehabilitation measures. The wetland at Schneckenstein showed only 20% removal capacity of the original dissolved As load (Landgraf 2002; Landgraf et al. 2002). Volatile As concentrations were lower than in Lengenfeld (<1 to about 14 ng/L), probably caused by unfavorable climatic conditions with low average annual temperatures of about 5°C combined with a short growing season, low bioactivity and a reduced organic layer of only 1-3 cm thickness.

US superfund site Milltown Reservoir / USA

Another mine-waste influenced wetland was investigated in June 2002: The U.S. Superfund site Milltown Reservoir 10 km east of Missoula, Montana / USA. Since the construction of the reservoir's dam in 1907, the Clark Fork river had delivered contaminated water and sediments from Au, Cu, Pb, and Zn mining at Butte 150 km upstream and from smelter facilities at Anaconda 240 km upstream. The amount of contaminated sediment that accumulated in the Milltown Reservoir is 6.5 million tons. Four public water wells adjacent to the reservoir had to be closed in 1981 containing As concentrations of 220 to 550 µg/L (Brumbaugh et al. 1994; Moore et al. 1988; Moore and Luoma 1990; Moore and Landrigan 1999; Moore and Woessner 2003; Woessner et al. 1984). Volatile As concentrations sampled from the water saturated mud along the partly flooded reservoir in June 2002 were between <5 and about 250 ng/L.

Geothermal waters Yellowstone National Park / USA

During the same sampling campaign in June 2002 hot springs and a geothermally influenced wetland in the Yellowstone National Park were sampled. Yellowstone National Park is located over the world's largest continental hot spot and contains more than 10,000 geothermal features. Increased dissolved As concentrations up to several mg/L, partly reducing, acid conditions and a large variety of microorganisms are favorable conditions for methylation and volatilization of As. Increased concentrations of methylated mercury were detected in a previous project by the U.S. Geological Survey for the geothermally influenced wetland. Volatile As concentrations sampled from the aqueous phase were between less than 10 and about 260 ng/L. Problems were encountered with the PTFE collector cells at all hot springs with temperatures $>40^{\circ}\text{C}$ because the PTFE material deformed and water breakthrough contaminated the gas trapping solution. An easier gas collection method was applied, sampling the volatile As directly from the gas phase by gas hoods over the hot spring discharges. Concentrations of volatile As in the gas phase directly above the hot springs ranged from less than 0.4 up to about 50 mg/m³. Compared to the few values on volatile As concentrations reported so far (e.g. 50 µg/m³ for gases from waste heaps; Feldmann 1995) these values were significantly higher.

Mine water irrigated rice fields / China

In August 2002, three rice field sites near Luoqiaqiao town / China with 1.5 and 3 month-old rice were sampled. Rice fields like natural wetlands are known to be significant CH₄ emitters (Conrad 1996; Mosier et al. 1997; Mosier 1998; Neue 1993; Wassmann and Aulakh 2000; Watanabe et al. 1997; Yang and Chang 2001) making up between 20 Tg/year (Intergovernmental Panel on Climate Change 1992; Sass 1994) to 170 Tg/year (Cicerone and Oremland 1988) of a global total CH₄ emission of 600 Tg/year (Kumaraswamy et al. 2000). Sediments of the Chinese rice field at Luoqiaqiao showed increased As concentration from contaminated sediments deposited during floods from the Jangtse river as well as through irrigation with As-rich waste water from a Cu-Zn refinery. Irrigation with As-rich water is not unusual in other Asian countries neither and concentrations of soil As can reach up to 83 mg/kg (Abedin et al. 2002). The reducing conditions of the flooded rice fields were thought to be prone for release of volatile As similar to the release of CH₄. Unfortunately sampling could be only conducted for 3 hours and no volatile As was detected in the small gas volume sampled.

Constructed wetland Jülich and coal heap Oelsnitz / Germany

Investigations on a constructed reed wetland at the research center Jülich / Germany in autumn 2002 (Goldhahn 2003) as well as gas sampling on a smouldering heap of As rich coal in Oelsnitz / Erzgebirge / Germany in winter 2002/2003 (Göhler 2003) yielded no detectable volatile As concentrations, in both cases probably also owed to the inability of sampling sufficient amounts of gas.

Natural wetland Florida Everglades / USA

In March 2003, 3 samples were taken from the Water Conservation Area 1 at the Loxahatchee National Wildlife Refuge in the subtropical Florida Everglades. With 600,000 ha the Everglades are one of the biggest natural wetlands. In the late 1980's, elevated methylmercury concentrations of

more than 1.5 $\mu\text{g/g}$ were detected in fish and other wildlife from the Everglades. Sediments show up to 5 ng/g MeHg (Gilmour et al. 1998). Cai et al. (1997) report the occurrence of ethylmercury up to 5 ng/g in soils and sediments. Total dissolved Hg concentrations in the marshes are < 5 ng/L, MeHg up to 1 ng/L (Hurley et al. 1998). Dissolved gaseous Hg concentrations are 0.02 to 0.04 ng/L (Krabbenhoft et al. 1998). Input from increased global atmospheric Hg deposition or photolytic desorption and in situ methylation of Hg from peat deposits are discussed as possible Hg sources. Krabbenhoft et al. (1998) calculated an annual massflux of mercury leaving the Everglades of 2.2 $\mu\text{g/m}^2/\text{year}$ equal to only 10% of the annual input from atmospheric deposition. Eutrophication by nutrient-enriched agricultural runoffs does not contribute significantly to total Hg built up (Gilmour et al. 1998; Vaithyanathan et al. 1996). Similar microbial transformations as for methylated and ethylated mercury were also suspected to increase methylated and volatile As concentrations. A previous screening by the research group of Prof. Hirner (Department for Environmental Analytics and Applied Geochemistry, University Essen / Germany), showed 5-630 ng/L volatile inorganic and organic As (unpublished results). The 3 samples taken in March 2003 yielded similar concentrations of about 90, 120, and 5700 ng/L total volatile As.

The database for the individual sampling sites ranges from a 1-year hydrogeochemical study including sampling of the gas phase and sequential extractions of the sediments at Lengenfeld to a 1-day sampling of only total volatile As and dissolved As speciation without the determination of further water parameters in the Chinese rice fields. In most cases, gas samples were only taken once without replicates or quality control. The results of these reconnaissance studies are thus not included in the present research work.

On the following pages:

Appendix 2 Optimization of abiotic arsine generation by hydride generation from large volume solutions in a reaction vessel

Note: For experimental setup see Figure 19; RV = reaction vessel, SS = stainless steel, SS-T = stainless steel Teflon (PTFE) coated, Vial = 300 mL Vial with 200 mL solution and 100 mL Headspace, HS = headspace, CC = collector cell (description of prototypes 1-3 see section 3.1), c_C , V_C = concentration and volume of initial solution before reaction C (control), c_R , V_R = concentration and volume of solution after reaction R (remaining), concentrations below detection limit (1.5 $\mu\text{g/L}$) presented as 0.3·DL = 0.5 $\mu\text{g/L}$; for data interpretation and calculation of % As not volatilized see section 3.2.1

Appendix 3 Optimization of trapping volatile As in liquid sorbents

Note: For experimental setup see Figure 19; for conditions of arsine generation, concentrations and volumes of C- and R-samples see Appendix 2, same experiment numbers, experiments No. 52, 53, 85-105, 111, 112, 129-136, 0A-0E used solid sorbents, results shown in Appendix 5 and discussed in section 3.2.3.1; c_O , V_O = concentration and volume of oxidizing solution; SS = stainless steel, PFA = perfluoroalkoxy, PTFE = polytetrafluorethylene; T2x4 = teflon rings 2 mm inner diameter, 4 mm outer diameter, T4x6 and T6x8 analogue; for data interpretation and calculation of %As trapped see section 3.2.2

Appendix 2		equipment setup						course of the experiment								solutions / reagents								results					
Experiment No.	Date	RV	CC prototype No.	CC porosity [μm]	CC side thickness [mm]	porous ceramic disk used	gas transport mode	pre-HG-flush N_2 [min]	first injection NaBH_4 [min]	post- NaBH_4 -flush N_2 [min]	second injection HCl [min]	second injection NaBH_4 [min]	post-HG flush N_2 [min]	Pressure [mbar]	duration of experiment [min]	c_c [$\mu\text{g/L}$]	V_c [mL]	1 N HCl [ml] in 1 L C solution	pH of C solution	first injection NaBH_4 [mL] in NaOH	NaBH_4 %	NaOH %	second injection HCl [mL]	second injection NaBH_4 [mL]	pH after reaction	c_R [$\mu\text{g/L}$]	V_R mL]	%As not volatilized	% As volatilized
1	31.03.01	SS	1	5	3	yes	pump	---	121	---	---	---	---	61	640	1000	950	140	1.0	30	6	2	---	---	1.3	270	980	28	72
2	01.04.01	SS	1	5	3	yes	pump	---	93	---	---	---	---	60	320	1100	950	200	0.9	30	6	2	---	---	1.3	530	980	50	50
3	01.04.01	SS	1	5	3	yes	pump	---	87	---	---	---	---	60	1080	1210	950	200	0.9	30	6	2	---	---	1.5	280	980	24	76
4	02.04.01	SS	1	5	3	yes	pump	---	97	---	---	---	---	60	185	1030	950	200	0.9	30	6	2	---	---	1.2	570	980	57	43
5	03.04.01	SS	1	5	3	yes	pump	---	94	---	---	---	---	60	915	1030	950	200	0.9	30	6	2	---	---	1.7	290	980	29	71
6	03.04.01	SS	1	5	3	yes	pump	---	151	---	---	---	---	60	507	1060	950	200	1.0	30	6	2	---	---	1.4	290	980	28	72
7	04.04.01	SS	1	5	3	yes	pump	---	69	---	---	---	---	60	790	1130	950	200	0.8	30	6	2	---	---	1.6	240	980	22	78
8	04.04.01	SS	1	5	3	yes	pump	---	82	---	---	---	---	60	435	1100	950	200	0.8	30	6	2	---	---	1.3	360	980	34	66
9	05.04.01	SS	1	5	3	yes	pump	---	111	---	---	---	---	60	864	1040	950	200	0.8	30	6	2	---	---	1.5	230	980	23	77
10	05.04.01	SS	1	5	3	yes	pump	---	38	---	---	---	---	60	371	1090	950	100	1.1	10	15	5	---	---	1.6	360	960	33	67
11	06.04.01	SS	1	5	3	yes	pump	---	62	---	---	---	---	60	1122	950	950	100	1.1	20	15	5	---	---	8.4	40	970	4	96
12	06.04.01	SS	1	5	6	yes	pump	---	185	---	---	---	---	60	378	1020	950	100	1.1	20	15	5	---	---	8.2	45	970	5	95
13	07.04.01	SS	1	5	6	yes	pump	---	96	---	---	---	---	60	1126	970	950	100	1.1	15	15	5	---	---	2.9	260	965	27	73
14	08.04.01	SS	1	5	6	yes	pump	---	144	---	---	---	---	60	438	960	950	200	0.8	15	15	5	---	---	1.8	110	965	12	88
15	09.04.01	SS	1	5	6	yes	pump	---	286	---	---	---	---	50	1091	970	950	100	1.2	17	15	5	---	---	3.2	318	967	33	67
16	10.04.01	SS	1	5	6	yes	pump	---	15	---	---	---	---	60	1452	980	950	100	1.1	17	15	5	---	---	2.8	110	967	11	89
17	11.04.01	SS	1	10	3	yes	pump	---	19	---	---	---	---	60	1452	970	950	100	1.1	17	15	5	---	---	2.7	176	967	18	82
18	12.04.01	SS	1	10	3	yes	pump	---	180	---	---	---	---	60	1109	1030	950	50	1.4	17	15	5	---	---	9.2	21	967	2	98
19	14.04.01	SS	1	10	3	yes	pump	---	105	---	---	---	---	60	1315	107	950	60	1.4	17	15	5	---	---	9.0	19	967	18	82
20	15.04.01	SS	1	10	3	yes	pump	---	105	---	---	---	---	60	506	97	950	70	1.3	17	15	5	---	---	8.8	15	967	16	84

Appendix 2		equipment setup						course of the experiment								solutions / reagents								results					
Experiment No.	Date	RV	CC prototype No.	CC porosity [μm]	CC side thickness [mm]	porous ceramic disk used	gas transport mode	pre-HG-flush N_2 [min]	first injection NaBH_4 [min]	post- NaBH_4 -flush N_2 [min]	second injection HCl [min]	second injection NaBH_4 [min]	post-HG flush N_2 [min]	Pressure [mbar]	duration of experiment [min]	c_c [$\mu\text{g/L}$]	V_c [mL]	1 N HCl [ml] in 1 L C solution	pH of C solution	first injection NaBH_4 [mL] in NaOH	NaBH_4 %	NaOH %	second injection HCl [mL]	second injection NaBH_4 [mL]	pH after reaction	c_R [$\mu\text{g/L}$]	V_R mL	%As not volatilized	% As volatilized
21	16.04.01	SS	1	5	6	yes	pump	---	105	---	---	---	---	60	1310	95	950	70	1.3	17	15	5	---	---	8.8	11	967	12	88
22	17.04.01	SS	1	10	3	yes	pump	---	105	---	---	---	---	60	1250	99	950	70	1.3	18	15	5	---	---	8.8	14	968	14	86
23	18.04.01	SS	1	10	3	yes	pump	---	36	---	---	---	---	Var.	1190	100	950	70	1.2	20	15	5	---	---	9.0	27	970	28	72
24	04.05.01	SS	1	10	3	yes	N2	5	30	35	---	---	---	n.d.	70	77	950	100	1.2	20	15	5	---	---	---	16	970	21	79
25	04.05.01	SS	1	10	3	no	N2	10	30	20	---	---	---	n.d.	60	72	480	100	1.2	20	15	5	---	---	---	19	500	27	73
26	05.05.01	SS	1	10	3	no	N2	20	15	35	---	---	---	n.d.	70	72	480	100	1.2	20	15	5	---	---	---	12	500	17	83
27	13.05.01	SS	2	10	6.4	no	N2	10	20	60	---	---	---	500	90	78	950	100	1.2	20	15	5	---	---	---	5	970	7	93
28	13.05.01	SS	2	10	6.4	no	N2	10	20	60	---	---	---	800	90	59	475	100	1.2	20	15	5	---	---	---	4	495	7	93
29	15.05.01	SS	2	10	6.4	no	N2	10	20	5	20	15	20	700	90	59	475	100	1.2	20	15	5	40	20	---	1	555	1	99
30	16.05.01	SS	2	10	6.4	no	N2	10	20	60	---	---	---	500	90	82	475	100	1.2	20	15	5	---	---	---	10	495	13	87
31	17.05.01	SS	2	10	6.4	no	N2	10	20	0	---	20	40	500	90	82	475	100	1.2	20	15	5	---	20	---	8	515	11	89
32	17.05.01	SS	2	10	6.4	no	N2	10	10	0	20	10	40	500	90	82	475	100	1.2	10	15	5	20	10	---	9	515	12	88
33	18.05.01	SS	2	10	6.4	no	N2	10	20	5	20	5	20	500	80	82	475	100	1.2	20	15	5	40	6	---	7	541	10	90
34	18.05.01	SS	2	10	6.4	no	N2	5	10	0	10	10	5	200	40	77	475	50	---	20	15	5	40	20	---	8	555	12	88
35	20.05.01	SS	2	10	6.4	no	N2	5	5	0	5	5	5	200	25	77	475	50	---	10	15	5	20	10	---	11	515	15	85
36	21.05.01	SS	2	10	6.4	no	N2	5	10	0	10	10	10	200	45	72	475	100	1.2	20	15	5	40	20	---	5	555	8	92
37	21.05.01	SS	2	10	6.4	no	N2	5	10	0	10	10	10	200	45	72	475	100	1.2	20	15	5	40	20	---	6	555	10	90
38	22.05.01	SS	2	10	6.4	no	N2	10	20	5	20	15	20	200	90	78	475	100	1.2	20	15	5	40	20	---	1	555	1	99
39	23.05.01	SS	2	10	6.4	no	N2	5	10	0	10	10	10	200	45	78	475	100	1.2	20	15	5	40	20	---	n.d.	555	n.d.	n.d.
40	23.05.01	SS	2	10	6.4	no	N2	5	10	0	0	0	20	200	35	1	450	100	1.2	10	15	5	0	0	---	1	460	n.d.	n.d.

Appendix 2		equipment setup						course of the experiment								solutions / reagents								results					
Experiment No.	Date	RV	CC prototype No.	CC porosity [μm]	CC side thickness [mm]	porous ceramic disk used	gas transport mode	pre-HG-flush N_2 [min]	first injection NaBH_4 [min]	post- NaBH_4 -flush N_2 [min]	second injection HCl [min]	second injection NaBH_4 [min]	post-HG flush N_2 [min]	Pressure [mbar]	duration of experiment [min]	c_C [$\mu\text{g/L}$]	V_C [mL]	1 N HCl [ml] in 1 L C solution	pH of C solution	first injection NaBH_4 [mL] in NaOH	NaBH_4 %	NaOH %	second injection HCl [mL]	second injection NaBH_4 [mL]	pH after reaction	c_R [$\mu\text{g/L}$]	V_R [mL]	%As not volatilized	% As volatilized
41	11.06.01	SS-T	2	10	6.4	no	N2	10	20	5	20	15	20	200	90	73	475	100	1.2	20	15	5	40	20	---	1	555	1	99
42	11.06.01	SS-T	2	10	6.4	no	N2	10	20	5	20	15	20	200	90	76	475	100	1.2	20	15	5	40	20	---	5	555	8	92
43	12.06.01	SS-T	2	10	6.4	no	N2	10	20	5	20	15	20	200	90	76	475	100	1.2	20	15	5	40	20	---	7	555	11	89
44	12.06.01	SS-T	2	10	6.4	no	N2	10	20	5	20	15	20	200	90	73	475	100	1.2	20	15	5	40	20	---	3	555	5	95
45	13.06.01	SS-T	2	10	6.4	no	N2	10	20	5	20	15	20	200	90	73	475	100	1.2	20	15	5	40	20	---	1	555	1	99
46	13.06.01	SS-T	2	10	6.4	no	N2	10	20	5	20	15	20	200	90	74	475	100	1.2	20	15	5	40	20	---	2	555	3	97
47	13.06.01	SS-T	2	10	6.4	no	N2	10	20	5	20	15	20	200	90	74	475	100	1.2	20	15	5	40	20	---	2	555	3	97
48	15.06.01	SS-T	1	5	3	no	N2	10	20	5	20	15	20	200	90	76	475	100	1.2	20	15	5	40	20	---	2	555	3	97
49	15.06.01	SS-T	1	10	3	no	N2	10	20	5	20	15	20	200	90	76	475	100	1.2	20	15	5	40	20	---	1	555	1	99
50	16.06.01	SS-T	1	5	6	no	N2	10	20	5	20	15	20	200	90	69	475	100	1.2	20	15	5	40	20	---	1	555	1	99
51	18.06.01	SS-T	1	10	6	no	N2	10	20	5	20	15	20	200	90	69	475	100	1.2	20	15	5	40	20	---	1	555	1	99
52	18.06.01	SS-T	2	10	6.4	no	N2	10	20	5	20	15	20	200	90	75	475	100	1.2	20	15	5	40	20	---	4	555	6	94
53	19.06.01	SS-T	2	10	6.4	no	N2	10	20	5	20	15	20	200	90	57	475	50	1.2	20	15	5	40	20	---	2	555	4	96
54	18.06.01	SS-T	2	10	6.4	no	N2	10	20	5	20	15	20	200	90	38	475	50	1.2	20	15	5	40	20	---	1	555	2	98
55	19.06.01	SS-T	2	10	6.4	no	N2	10	20	5	20	15	20	200	90	38	475	50	1.2	20	15	5	40	20	---	1	555	3	97
56	28.07.01	SS-T	3	0.1	M	no	N2	10	20	5	20	15	20	25	90	77	470	100	1.2	20	15	5	40	20	---	13	550	20	80
57	29.07.01	SS-T	3	0.1	M	no	N2	10	40	15	5	0	0	var.	70	77	475	100	1.2	20	15	5	2	0	---	n.d.	497	n.d.	n.d.
58	17.08.01	SS-T	3	0.1	M	no	N2	10	20	5	20	15	0	55	70	65	475	100	1.2	20	15	5	40	20	---	3	555	5	95
59	20.08.01	SS-T	3	0.1	M	no	N2	10	20	5	20	15	45	30	115	65	475	100	1.2	20	15	5	40	20	---	3	555	5	95
60	20.08.01	SS-T	3	0.1	M	no	N2	30	30	5	20	15	20	30	120	34	475	100	1.2	20	15	5	40	20	---	3	555	10	90

Appendix 2		equipment setup						course of the experiment									solutions / reagents								results				
Experiment No.	Date	RV	CC prototype No.	CC porosity [μm]	CC side thickness [mm]	porous ceramic disk used	gas transport mode	pre-HG-flush N_2 [min]	first injection NaBH_4 [min]	post- NaBH_4 -flush N_2 [min]	second injection HCl [min]	second injection NaBH_4 [min]	post-HG flush N_2 [min]	Pressure [mbar]	duration of experiment [min]	c_c [$\mu\text{g/L}$]	V_c [mL]	1 N HCl [ml] in 1 L C solution	pH of C solution	first injection NaBH_4 [mL] in NaOH	NaBH_4 %	NaOH %	second injection HCl [mL]	second injection NaBH_4 [mL]	pH after reaction	c_R [$\mu\text{g/L}$]	V_R [mL]	%As not volatilized	% As volatilized
61	09.10.01	SS-T	3	0.1	M	no	N2	10	20	5	20	15	20	30	90	71	475	100	1.2	20	15	5	40	20	---	1	555	1	99
62	09.10.01	SS-T	3	0.1	M	no	N2	10	20	5	20	15	20	30	90	71	475	100	1.2	20	15	5	40	20	---	6	555	10	90
63	09.10.01	SS-T	3	0.1	M	no	N2	10	20	5	20	15	20	30	90	73	475	100	1.2	20	15	5	40	20	---	4	555	6	94
64	09.10.01	SS-T	3	0.1	M	no	N2	10	20	5	20	15	20	30	90	73	475	100	1.2	20	15	5	40	20	---	1	555	2	98
65	10.10.01	SS-T	3	0.1	M	no	N2	10	20	5	20	15	20	30	90	50	475	50	1.2	20	15	5	40	20	---	1	555	1	99
66	10.10.01	SS-T	3	0.1	M	no	N2	10	20	5	20	15	20	30	90	50	475	50	1.2	20	15	5	40	20	---	1	555	1	99
67	25.10.01	SS-T	3	0.1	M	no	N2	10	20	5	20	15	20	30	90	72	475	100	1.2	20	15	5	40	20	---	1	555	2	98
68	27.10.01	SS-T	3	0.1	M	no	N2	10	20	5	20	15	25	30	95	72	475	100	1.2	20	15	5	40	20	---	3	555	5	95
69	27.10.01	SS-T	3	0.1	M	no	N2	10	20	5	20	15	20	30	90	72	455	100	1.2	20	15	5	40	20	---	3	535	4	96
70	28.10.01	SS-T	3	0.1	M	no	N2	10	20	5	20	15	20	30	90	77	475	100	1.2	20	15	5	40	20	---	2	555	4	96
71	28.10.01	SS-T	3	0.1	M	no	N2	10	20	5	20	15	20	30	90	77	475	100	1.2	20	15	5	40	20	---	1	555	2	98
72	29.10.01	SS-T	3	0.1	M	no	N2	10	20	5	20	15	20	30	90	101	488	100	1.2	20	15	5	40	20	---	4	568	5	95
73	29.10.01	SS-T	3	0.1	M	no	N2	10	20	5	20	15	20	30	90	101	488	100	1.2	20	15	5	40	20	---	3	568	3	97
74	30.10.01	SS-T	3	0.1	M	no	N2	10	20	5	20	15	20	30	90	99	475	100	1.2	20	15	5	40	20	---	3	555	4	96
75	05.11.01	SS-T	3	0.1	M	no	N2	10	20	5	20	15	20	30	90	73	475	100	1.2	20	15	5	40	20	---	3	555	5	95
76	05.11.01	SS-T	3	0.1	M	no	N2	10	20	5	20	15	20	30	90	73	475	100	1.2	20	15	5	40	20	---	3	555	5	95
77	05.11.01	SS-T	3	0.1	M	no	N2	10	20	5	20	15	20	30	90	34	475	50	1.2	20	15	5	40	20	---	2	555	8	92
78	05.11.01	SS-T	3	0.1	M	no	N2	10	20	5	20	15	20	30	90	82	475	100	1.2	20	15	5	40	20	---	2	555	3	97
79	06.11.01	SS-T	3	0.1	M	no	N2	10	20	5	20	15	20	30	90	6	475	10	1.2	20	15	5	40	20	---	2	555	36	64
80	06.11.01	SS-T	3	0.1	M	no	N2	10	20	5	20	15	20	30	90	6	475	10	1.2	20	15	5	40	20	---	1	555	16	84

Appendix 2		equipment setup						course of the experiment									solutions / reagents								results				
Experiment No.	Date	RV	CC prototype No.	CC porosity [μm]	CC side thickness [mm]	porous ceramic disk used	gas transport mode	pre-HG-flush N_2 [min]	first injection NaBH_4 [min]	post- NaBH_4 -flush N_2 [min]	second injection HCl [min]	second injection NaBH_4 [min]	post-HG flush N_2 [min]	Pressure [mbar]	duration of experiment [min]	c_c [$\mu\text{g/L}$]	V_c [mL]	1 N HCl [ml] in 1 L C solution	pH of C solution	first injection NaBH_4 [mL] in NaOH	NaBH_4 %	NaOH %	second injection HCl [mL]	second injection NaBH_4 [mL]	pH after reaction	c_R [$\mu\text{g/L}$]	V_R [mL]	%As not volatilized	% As volatilized
81	06.11.01	SS-T	3	0.1	M	no	N2	10	20	5	20	15	20	30	90	15	475	25	1.2	20	15	5	40	20	---	1	555	5	95
82	02.12.01	SS-T	3	0.1	M	no	N2	10	20	5	20	15	20	30	90	96	475	100	1.2	20	15	5	40	20	---	2	555	2	98
82 a	02.12.01	SS-T	3	0.1	M	no	N2	10	20	5	20	15	20	30	90	72	475	100	1.2	20	15	5	40	20	---	0.5	555	1	99
82 b	02.12.01	SS-T	3	0.1	M	no	N2	10	20	5	20	15	20	30	90	72	475	100	1.2	20	15	5	40	20	---	2	555	3	97
82 c	03.12.01	SS-T	3	0.1	M	no	N2	10	20	5	20	15	20	30	90	72	475	100	1.2	20	15	5	40	20	---	2	555	3	97
82 d	03.12.01	SS-T	3	0.1	M	no	N2	10	20	5	20	15	20	30	90	72	475	100	1.2	20	15	5	40	20	---	1	555	2	98
82 e	03.12.01	SS-T	3	0.1	M	no	N2	10	20	5	20	15	20	30	90	72	475	100	1.2	20	15	5	40	20	---	0.5	555	1	99
82 f	04.12.01	SS-T	3	0.1	M	no	N2	10	20	5	20	15	20	30	90	72	475	100	1.2	20	15	5	40	20	---	0.5	555	1	99
83	04.12.01	SS-T	3	0.1	M	no	N2	10	20	5	20	15	20	30	90	96	475	100	1.2	20	15	5	40	20	---	1	555	1	99
84	04.12.01	SS-T	3	0.1	M	no	N2	10	20	5	20	15	20	30	90	152	475	0	1.2	20	15	5	40	20	---	77	555	59	41
85	06.12.01	SS-T	3	0.1	M	no	N2	10	20	5	20	15	20	30	90	31	475	100	1.2	20	15	5	40	20	---	1	555	2	98
86	06.12.01	SS-T	3	0.1	M	no	N2	10	20	5	20	15	20	30	90	31	475	100	1.2	20	15	5	40	20	---	1	555	2	98
87	06.12.01	SS-T	3	0.1	M	no	N2	10	20	5	20	15	20	30	90	31	475	100	1.2	20	15	5	40	20	---	1	555	3	97
88	06.12.01	SS-T	3	0.1	M	no	N2	10	20	5	20	15	20	30	90	31	475	100	1.2	20	15	5	40	20	---	1	555	3	97
89	10.12.01	SS-T	3	0.1	M	no	N2	10	20	5	20	15	20	30	90	31	475	100	1.2	20	15	5	40	20	---	1	555	2	98
90	10.12.01	SS-T	3	0.1	M	no	N2	10	20	5	20	15	20	30	90	31	475	100	1.2	20	15	5	40	20	---	1	555	2	98
91	11.12.01	SS-T	3	0.1	M	no	N2	10	20	5	20	15	20	30	90	36	475	100	1.2	20	15	5	40	20	---	1	555	2	98
92	11.12.01	SS-T	3	0.1	M	no	N2	10	20	5	20	15	20	30	90	36	475	100	1.2	20	15	5	40	20	---	1	555	2	98
93	11.12.01	SS-T	3	0.1	M	no	N2	10	20	5	20	15	20	30	90	45	475	100	1.2	20	15	5	40	20	---	1	555	1	99
94	12.12.01	SS-T	3	0.1	M	no	N2	10	20	5	20	15	20	30	90	45	475	100	1.2	20	15	5	40	20	---	4	555	12	88

Appendix 2		equipment setup						course of the experiment								solutions / reagents								results					
Experiment No.	Date	RV	CC prototype No.	CC porosity [μm]	CC side thickness [mm]	porous ceramic disk used	gas transport mode	pre-HG-flush N_2 [min]	first injection NaBH_4 [min]	post- NaBH_4 -flush N_2 [min]	second injection HCl [min]	second injection NaBH_4 [min]	post-HG flush N_2 [min]	Pressure [mbar]	duration of experiment [min]	c_c $\mu\text{g/L}$	V_c [mL]	1 N HCl [ml] in 1 L C solution	pH of C solution	first injection NaBH_4 [mL] in NaOH	NaBH_4 %	NaOH %	second injection HCl [mL]	second injection NaBH_4 [mL]	pH after reaction	c_R [$\mu\text{g/L}$]	V_R [mL]	%As not volatilized	% As volatilized
95	13.12.01	SS-T	3	0.1	M	no	N_2	10	20	5	20	15	20	30	90	44	475	100	1.2	20	15	5	40	20	---	2	555	6	94
96	13.12.01	SS-T	3	0.1	M	no	N_2	10	20	5	20	15	20	30	90	44	475	100	1.2	20	15	5	40	20	---	1	555	3	97
97	13.12.01	SS-T	3	0.1	M	no	N_2	10	20	5	20	15	20	30	90	41	475	100	1.2	20	15	5	40	20	---	1	555	3	97
98	13.12.01	SS-T	3	0.1	M	no	N_2	10	20	5	20	15	20	30	90	41	475	100	1.2	20	15	5	40	20	---	1	555	2	98
99	14.12.01	SS-T	3	0.1	M	no	N_2	10	20	5	20	15	20	30	90	43	475	100	1.2	20	15	5	40	20	---	2	555	6	94
100	14.12.01	SS-T	3	0.1	M	no	N_2	10	20	5	20	15	20	30	90	43	475	100	1.2	20	15	5	40	20	---	2	555	5	95
101	19.02.02	SS-T	3	0.1	M	no	N_2	10	20	5	20	15	20	30	90	33	475	100	1.2	20	15	5	40	20	---	2	555	5	95
102	19.02.02	SS-T	3	0.1	M	no	N_2	10	20	5	20	15	20	30	90	33	475	100	1.2	20	15	5	40	20	---	1	555	4	96
103	24.02.02	SS-T	3	0.1	M	no	N_2	10	20	5	20	15	20	30	90	66	475	100	1.2	20	15	5	40	20	---	1	555	1	99
104	16.04.02	SS-T	3	0.1	M	no	N_2	10	20	5	20	15	20	30	90	68	475	100	1.2	20	15	5	40	20	---	2	555	3	97
105	17.04.02	SS-T	3	0.1	M	no	N_2	10	20	5	20	15	20	30	90	62	475	100	1.2	20	15	5	40	20	---	2	555	3	97
111	04.05.03	Vial	3	0.1	M	no	HS	---	---	---	---	---	---	---	40	500	200	100	---	20	15	5	---	---	---	---	220	---	---
112	06.05.03	SS-T	3	0.1	M	no	N_2	10	20	5	20	15	20	30	90	250	475	100	---	20	15	5	40	20	---	---	555	---	---
129	18.05.03	SS-T	3	0.1	M	no	N_2	10	20	5	20	15	20	30	90	500	475	100	---	20	15	5	40	20	---	---	555	---	---
130	19.05.03	SS-T	3	0.1	M	no	N_2	10	20	5	20	15	20	30	90	500	475	100	---	20	15	5	40	20	---	---	555	---	---
131	19.05.03	SS-T	3	0.1	M	no	N_2	10	20	5	20	15	20	30	90	500	475	100	---	20	15	5	40	20	---	---	555	---	---
132	20.05.03	SS-T	3	0.1	M	no	N_2	10	20	5	20	15	20	30	90	500	475	100	---	20	15	5	40	20	---	---	555	---	---
133	20.05.03	SS-T	3	0.1	M	no	N_2	10	20	5	20	15	20	30	90	500	475	100	---	20	15	5	40	20	---	---	555	---	---
134	21.05.03	SS-T	3	0.1	M	no	N_2	10	20	5	20	15	20	30	90	500	475	100	---	20	15	5	40	20	---	---	555	---	---
135	21.05.03	SS-T	3	0.1	M	no	N_2	10	20	5	20	15	20	30	90	500	475	100	---	20	15	5	40	20	---	---	555	---	---
136	29.05.03	SS-T	3	0.1	M	no	N_2	10	20	5	20	15	20	30	90	500	475	100	---	20	15	5	40	20	---	---	555	---	---

Appendix 2		equipment setup						course of the experiment								solutions / reagents								results					
Experiment No.	Date	RV	CC prototype No.	CC porosity [μm]	CC side thickness [mm]	porous ceramic disk used	gas transport mode	pre-HG-flush N_2 [min]	first injection NaBH_4 [min]	post- NaBH_4 -flush N_2 [min]	second injection HCl [min]	second injection NaBH_4 [min]	post-HG flush N_2 [min]	Pressure [mbar]	duration of experiment [min]	c_c [$\mu\text{g/L}$]	V_c [mL]	1 N HCl [ml] in 1 L C solution	pH of C solution	first injection NaBH_4 [mL] in NaOH	NaBH_4 %	NaOH %	second injection HCl [mL]	second injection NaBH_4 [mL]	pH after reaction	c_R [$\mu\text{g/L}$]	V_R [mL]	%As not volatilized	% As volatilized
0A	18.02.01	SS	1	10	3	yes	pump	---	27	---	---	---	---	40	40	1000	950	100	1.1	45	3	1	---	---	1.4	---	995	---	---
0B	26.02.01	SS	1	5	3	yes	pump	---	100	---	---	---	---	65	774	1000	950	100	1.3	30	6	2	---	---	---	---	980	---	---
0C	27.02.01	SS	1	5	3	yes	pump	---	122	---	---	---	---	60	623	1000	950	100	1.2	30	6	2	---	---	1.8	---	980	---	---
0D	19.04.01	SS	1	10	3	yes	pump	---	7	---	---	---	---	-76	1275	100	950	65	1.3	20	15	5	---	---	9.0	---	970	---	---
0E	23.04.01	SS	1	10	3	yes	pump	---	18	---	---	---	---	-20	1667	100	950	70	1.3	20	15	5	---	---	9.0	---	970	---	---

Appendix 3

Experiment No.	equipment		oxidation first trap							oxidation second trap					results						
	kind of oxidation trap	oxidizing surface increased by	oxidizing agent	amount of oxidizing agent [mL]	strength of oxidizing agent	additive to oxidizing agent	amount of additive [mL]	strength of additive	pH oxidizing solution	oxidizing agent	amount oxidizing agent [mL]	additive to oxidizing agent	amount of additive [mL]	pH oxidizing solution	c ₀ [µg/L] (first ox trap)	c ₀ [µg/L] (second ox trap)	V ₀ [µg/L] (first ox trap)	V ₀ [µg/L] (second ox trap)	% As trapped (first ox trap)	% As trapped (second ox trap)	% As not trapped (first trap)
1	glass	glass beads	H ₂ O ₂	30	10%	NaOH	30	0.1 N	10.5	---	---	---	---	---	1840	---	60	0	16	---	84
2	glass	glass beads	H ₂ O ₂	30	10%	NaOH	30	0.1 N	10.1	---	---	---	---	---	490	---	60	0	6	---	94
3	glass	glass beads	H ₂ O ₂	30	10%	NaOH	30	0.1 N	10.3	---	---	---	---	---	490	---	60	0	3	---	97
4	glass	glass beads	H ₂ O ₂	30	10%	NaOH	30	0.1 N	9.8	---	---	---	---	---	640	---	60	0	9	---	91
5	glass	glass beads	H ₂ O ₂	30	10%	NaOH	30	1N	12.5	---	---	---	---	---	530	---	60	0	5	---	95
6	glass	glass beads	H ₂ O ₂	30	20%	NaOH	30	1N	12.2	---	---	---	---	---	530	---	60	0	4	---	96
7	glass	glass beads	H ₂ O ₂	30	30%	NaOH	30	1N	12.5	---	---	---	---	---	2010	---	60	0	14	---	86
8	glass	glass beads	H ₂ O ₂	60	30%	---	---	---	5.3	---	---	---	---	---	1300	---	60	0	11	---	89
9	glass	glass beads	H ₂ O ₂	60	10%	---	---	---	4.7	---	---	---	---	---	1100	---	60	0	9	---	91
10	glass	glass beads	H ₂ O ₂	60	20%	---	---	---	4.1	---	---	---	---	---	1020	---	60	0	9	---	91
11	glass	glass beads	H ₂ O ₂	60	20%	---	---	---	4.4	---	---	---	---	---	1220	---	60	0	8	---	92
12	glass	glass beads	H ₂ O ₂	60	20%	---	---	---	4.1	---	---	---	---	---	620	---	60	0	4	---	96
13	glass	glass beads	H ₂ O ₂	60	20%	---	---	---	4.2	---	---	---	---	---	810	---	60	0	7	---	93
14	glass	glass beads	H ₂ O ₂	60	20%	---	---	---	4.0	---	---	---	---	---	1200	---	60	0	9	---	91
15	glass	glass beads	H ₂ O ₂	30	30%	NaOH	20	1N	12.6	H ₂ O ₂	30	NaOH	20	11.45	690	270	50	50	6	2	94
16	glass	glass beads	H ₂ O ₂	30	30%	NaOH	20	1N	12.3	H ₂ O ₂	30	NaOH	20	11.55	980	580	50	50	6	4	94
17	glass	glass beads	H ₂ O ₂	30	30%	NaOH	20	1N	12.4	H ₂ O ₂	30	NaOH	20	12.23	1050	790	50	50	7	5	93
18	glass	glass beads	H ₂ O ₂	30	30%	NaOH	20	1N	12.4	H ₂ O ₂	30	NaOH	20	12.32	640	370	50	50	3	2	97
19	glass	glass beads	H ₂ O ₂	30	30%	NaOH	20	1N	12.4	---	---	---	---	---	200	---	50	0	12	---	88
20	glass	glass beads	H ₂ O ₂	40	30%	NaOH	10	1N	10.2	---	---	---	---	---	260	---	50	0	17	---	83
21	glass	glass beads	H ₂ O ₂	40	30%	NaOH	10	1N	9.2	---	---	---	---	---	120	---	50	0	8	---	92
22	glass	glass beads	H ₂ O ₂	20	30%	NaOH	30	1N	12.5	---	---	---	---	---	150	---	50	0	9	---	91

App.3																					
equipment			oxidation first trap							oxidation second trap						results					
Experiment No.	kind of oxidation trap	oxidizing surface increased by	oxidizing agent	amount of oxidizing agent [mL]	strength of oxidizing agent	additive to oxidizing agent	amount of additive [mL]	strength of additive	pH oxidizing solution	oxidizing agent	amount oxidizing agent [mL]	additive to oxidizing agent	amount of additive [mL]	pH oxidizing solution	c _o [µg/L] (first ox trap)	c _o [µg/L] (second ox trap)	V _o [µg/L] (first ox trap)	V _o [µg/L] (second ox trap)	% As trapped (first ox trap)	% As trapped (second ox trap)	% As not trapped (first trap)
23	glass	glass beads	H ₂ O ₂	30	30%	NaOH	20	1N	11.9	---	---	---	---	---	150	---	50	0	11	---	89
24	SS	glass beads	H ₂ O ₂	95	30%	---	---	---	---	---	---	---	---	---	134	---	95	0	22	---	78
25	SS	glass beads	H ₂ O ₂	96	30%	---	---	---	---	---	---	---	---	---	26	---	96	0	10	---	90
26	SS	glass beads	Na ₂ S ₂ O ₈	96	1.5 M	---	---	---	---	---	---	---	---	---	---	---	96	0	n.d.	---	n.d.
27	SS	glass beads	NaOCl	95	6-14% Cl	---	---	---	---	---	---	---	---	---	490	---	95	0	67	---	33
28	SS	glass beads	NaOCl	95	6-14% Cl	---	---	---	---	---	---	---	---	---	160	---	95	0	58	---	42
29	SS	glass beads	NaOCl	95	6-14% Cl	---	---	---	---	---	---	---	---	---	250	---	95	0	86	---	14
30	SS	none	NaOCl	475	6-14% Cl	---	---	---	---	---	---	---	---	---	38	---	475	0	53	---	47
31	SS	none	NaOCl	190	6-14% Cl	---	---	---	---	---	---	---	---	---	100	---	190	0	55	---	45
32	SS	none	NaOCl	95	6-14% Cl	---	---	---	---	---	---	---	---	---	272	---	95	0	75	---	25
33	SS	glass beads	NaOCl	47.5	6-14% Cl	deion.H ₂ O	95	0	---	---	---	---	---	---	189	---	143	0	77	---	23
34	SS	glass beads	NaOCl	95	6-14% Cl	---	---	---	---	---	---	---	---	---	195	---	95	0	58	---	42
35	SS	glass beads	NaOCl	95	6-14% Cl	---	---	---	---	---	---	---	---	---	230	---	95	0	71	---	29
36	SS	glass beads	NaOCl	47.5	6-14% Cl	deion.H ₂ O	47.5	0	---	---	---	---	---	---	232	---	95	0	70	---	30
37	SS	glass beads	NaOCl	47.5	6-14% Cl	HCl	47.5	1N	---	---	---	---	---	---	2.5	---	95	0	1	---	99
38	SS	glass beads	NaOCl	95	6-14% Cl	---	---	---	---	---	---	---	---	---	305	---	95	0	79	---	21
39	SS	glass beads	NaOCl	47.5	6-14% Cl	NaOH	47.5	1N	---	---	---	---	---	---	222	---	95	0	57	---	43
40	SS	glass beads	NaOCl	90	6-14% Cl	---	---	---	---	---	---	---	---	---	28	---	90	0	n.d.	---	n.d.
41	PFA	none	NaOCl	95	6-14 % Cl	---	---	---	11.5	---	---	---	---	---	162	---	95	0	45	---	55
42	PFA	T6x8	NaOCl	95	6-14 % Cl	---	---	---	11.6	---	---	---	---	---	270	---	95	0	77	---	23
43	PFA	T6x8, T2x4	NaOCl	95	6-14 % Cl	---	---	---	---	---	---	---	---	---	158	---	95	0	47	---	53
44	PFA	T6x8, T2x4	NaOCl	140	6-14 % Cl	---	---	---	---	---	---	---	---	---	117	---	140	0	50	---	50

App.3																					
Experiment No.	equipment		oxidation first trap							oxidation second trap				results							
	kind of oxidation trap	oxidizing surface increased by	oxidizing agent	amount of oxidizing agent [mL]	strength of oxidizing agent	additive to oxidizing agent	amount of additive [mL]	strength of additive	pH oxidizing solution	oxidizing agent	amount oxidizing agent [mL]	additive to oxidizing agent	amount of additive [mL]	pH oxidizing solution	c ₀ [µg/L] (first ox trap)	c ₀ [µg/L] (second ox trap)	V ₀ [µg/L] (first ox trap)	V ₀ [µg/L] (second ox trap)	% As trapped (first ox trap)	% As trapped (second ox trap)	% As not trapped (first trap)
45	PFA	none	NaOCl	260	6-14 % Cl	---	---	---	---	---	---	---	---	56	---	260	0	42	---	58	
46	PFA	T6x8, T2x4	NaOCl	95	6-14 % Cl	---	---	---	---	---	---	---	---	153	---	95	0	43	---	57	
47	PFA	T6x8, T2x4	NaOCl	95	6-14 % Cl	---	---	---	---	---	---	---	---	150	---	95	0	42	---	58	
48	PFA	T6x8, T2x4	NaOCl	95	6-14 % Cl	---	---	---	---	---	---	---	---	228	---	95	0	62	---	38	
49	PFA	T6x8, T2x4	NaOCl	95	6-14 % Cl	---	---	---	---	---	---	---	---	166	---	95	0	44	---	56	
50	PFA	T6x8, T2x4	NaOCl	95	6-14 % Cl	---	---	---	---	---	---	---	---	163	---	95	0	48	---	52	
51	PFA	T6x8, T2x4	NaOCl	95	6-14 % Cl	---	---	---	---	---	---	---	---	146	---	95	0	43	---	57	
54	PFA	T6x8, T2x4	NaOCl	95	6-14 % Cl	---	---	---	---	---	---	---	---	43	---	95	0	23	---	77	
55	PFA	T6x8, T2x4	NaOCl	95	6-14 % Cl	---	---	---	---	---	---	---	---	47	---	95	0	26	---	74	
56	PTFE	T4x6	NaOCl	142.5	6-14 % Cl	---	---	---	---	---	---	---	---	120	---	143	0	59	---	41	
57	PTFE	T4x6	NaOCl	95	6-14 % Cl	---	---	---	---	NaOCl	95	---	---	---	170	17	95	95	n.d.	n.d.	n.d.
58	PTFE	T4x6	NaOCl	95	6-14 % Cl	---	---	---	---	---	---	---	---	248	---	95	0	81	---	19	
59	PTFE	T4x6	NaOCl	95	6-14 % Cl	---	---	---	---	NaOCl	95	---	---	---	163	39	95	95	53	13	47
60	PTFE	T4x6	NaOCl	95	6-14 % Cl	---	---	---	---	NaOCl	95	---	---	---	88	3	95	95	58	2	42
61	PTFE	T4x6	NaOCl	95	6-14 % Cl	---	---	---	---	NaOCl	95	---	---	---	262	31	95	95	74	9	26
62	PTFE	T4x6	NaOCl	9.5	6-14 % Cl	deion.H ₂ O	85.5	0	---	NaOCl	95	---	---	---	197	4	95	95	62	1	38
63	PTFE	T4x6	NaOCl	1.9	6-14 % Cl	deion.H ₂ O	93.1	0	---	NaOCl	95	---	---	---	293	10	95	95	86	3	14
64	PTFE	T4x6	NaOCl	0.95	6-14 % Cl	deion.H ₂ O	94.05	0	---	NaOCl	95	---	---	---	276	21	95	95	77	6	23
65	PTFE	T4x6	NaOCl	95	6-14 % Cl	deion.H ₂ O	0	0	---	NaOCl	95	---	---	---	162	31	95	95	66	13	34
66	PTFE	T4x6	NaOCl	1.9	6-14 % Cl	deion.H ₂ O	93.1	0	---	NaOCl	95	---	---	---	191	17	95	95	77	7	23
67	PTFE	T4x6	deion.H ₂ O	95	0	---	---	---	---	NaOCl	95	---	---	---	3	307	95	95	1	86	99
68	PTFE	T4x6	NaOCl	95	6-14 % Cl	---	---	---	---	NaOCl	95	---	---	---	302	4	95	95	89	1	11

App.3																					
equipment			oxidation first trap							oxidation second trap					results						
Experiment No.	kind of oxidation trap	oxidizing surface increased by	oxidizing agent	amount of oxidizing agent [mL]	strength of oxidizing agent	additive to oxidizing agent	amount of additive [mL]	strength of additive	pH oxidizing solution	oxidizing agent	amount oxidizing agent [mL]	additive to oxidizing agent	amount of additive [mL]	pH oxidizing solution	c _o [µg/L] (first ox trap)	c _o [µg/L] (second ox trap)	V _o [µg/L] (first ox trap)	V _o [µg/L] (second ox trap)	% As trapped (first ox trap)	% As trapped (second ox trap)	% As not trapped (first trap)
69	PTFE	T4x6	NaOCl	50	6-14 % Cl	deion.H ₂ O	50	0	---	NaOCl	100	---	---	---	223	1	100	100	71	1	29
70	PTFE	T4x6	NaOCl	9.5	6-14 % Cl	deion.H ₂ O	85.5	0	---	NaOCl	95	---	---	---	290	4	95	95	78	1	22
71	PTFE	T4x6	NaOCl	0.95	6-14 % Cl	deion.H ₂ O	94.05	0	---	NaOCl	95	---	---	---	304	11	95	95	81	3	19
72	PTFE	T4x6	NaOCl	1.9	6-14 % Cl	deion.H ₂ O	93.1	0	---	NaOCl	95	---	---	---	455	2	95	95	92	1	8
73	PTFE	T4x6	NaOCl	0.475	6-14 % Cl	deion.H ₂ O	94.53	0	---	NaOCl	95	---	---	---	228	86	95	95	45	17	55
74	PTFE	T4x6	NaOCl	0.19	6-14 % Cl	deion.H ₂ O	94.81	0	---	NaOCl	95	---	---	---	180	62	95	95	38	13	62
75	PTFE	T4x6	NaOCl	0.19	6-14 % Cl	deion.H ₂ O	94.81	0	---	NaOCl	9.5	deion.H ₂ O	85.5	---	166	63	95	95	48	18	52
76	PTFE	T4x6	NaOCl	1.9	6-14 % Cl	deion.H ₂ O	93.1	0	---	NaOCl	9.5	deion.H ₂ O	85.5	---	278	5	95	95	81	1	19
77	PTFE	T4x6	NaOCl	0.95	6-14 % Cl	deion.H ₂ O	94.05	0	---	NaOCl	0.95	deion.H ₂ O	94.05	---	132	1	95	95	85	1	15
78	PTFE	T4x6	NaOCl	0.95	6-14 % Cl	deion.H ₂ O	94.05	0	---	NaOCl	0.95	deion.H ₂ O	94.05	---	373	1	95	95	94	1	6
79	PTFE	T4x6	NaOCl	0.95	6-14 % Cl	deion.H ₂ O	94.05	0	---	NaOCl	0.95	deion.H ₂ O	94.05	---	17	1	95	95	83	2	17
80	PTFE	T4x6	NaOCl	0.95	6-14 % Cl	deion.H ₂ O	94.05	0	---	NaOCl	0.95	deion.H ₂ O	94.05	---	26	1	95	95	96	2	4
81	PTFE	T4x6	NaOCl	0.95	6-14 % Cl	deion.H ₂ O	94.05	0	---	NaOCl	0.95	deion.H ₂ O	94.05	---	72	1	95	95	100	1	0
82	PTFE	T4x6	NaOCl	0.95	6-14 % Cl	deion.H ₂ O	94.05	0	---	---	---	---	---	---	364	---	95	0	78	---	22
82 a	PTFE	T4x6	NaOCl	0.95	6-14 % Cl	deion.H ₂ O	94.05	0	---	---	---	---	---	---	283	---	95	0	79	---	21
82 b	PTFE	T4x6	NaOCl	0.95	6-14 % Cl	deion.H ₂ O	94.05	0	---	---	---	---	---	---	278	---	95	0	80	---	20
82 c	PTFE	T4x6	NaOCl	0.95	6-14 % Cl	deion.H ₂ O	94.05	0	---	---	---	---	---	---	285	---	95	0	82	---	18
82 d	PTFE	T4x6	NaOCl	0.95	6-14 % Cl	deion.H ₂ O	94.05	0	---	---	---	---	---	---	312	---	95	0	88	---	12
82 e	PTFE	T4x6	NaOCl	0.95	6-14 % Cl	deion.H ₂ O	94.05	0	---	---	---	---	---	---	296	---	95	0	83	---	17
82 f	PTFE	T4x6	NaOCl	0.95	6-14 % Cl	deion.H ₂ O	94.05	0	---	---	---	---	---	---	289	---	95	0	81	---	19
83	PTFE	T4x6	NaOCl	0.95	6-14 % Cl	deion.H ₂ O	94.05	0	---	---	---	---	---	---	398	---	95	0	83	---	17
84	PTFE	T4x6	NaOCl	0.95	6-14 % Cl	deion.H ₂ O	94.05	0	---	---	---	---	---	---	101	---	95	0	32	---	68

Appendix 4 Custom-made and commercial sorption tubes used for species-selective sampling of volatile As

sorption tube No.	description	first bed			second bed			third bed			total		
		amount of silanized glass wool [mg]	kind of sorption material	amount of sorption material [mg]	amount of silanized glass wool [mg]	kind of sorption material	amount of sorption material [mg]	amount of silanized glass wool [mg]	kind of sorption material	amount of sorption material [mg]	silanized glass wool	total amount sorption material [mg]	total amount silanized glass wool [mg]
1	double layer with Tenax	26	Tenax TA	50	13	Chromosorb 106	100	---	---	---	15	150	54
2		26	Tenax TA	50	13	Chromosorb 105	100	---	---	---	15	150	54
3		26	Tenax TA	50	13	Carboxen	100	---	---	---	15	150	54
4		26	Tenax TA	50	13	Carboxen	140	---	---	---	15	190	54
5		26	Tenax TA	50	13	Carbosieve III	150	---	---	---	15	200	54
6		26	Tenax TA	50	13	Carbotrap	100	---	---	---	15	150	54
7		26	Tenax TA	30	13	Chromosorb 106	120	---	---	---	15	150	54
8		26	Tenax TA	30	13	Chromosorb 105	120	---	---	---	15	150	54
9		26	Tenax TA	30	13	Carbosieve S III	170	---	---	---	15	200	54
10	triple layer with Tenax	26	Tenax TA	30	13	Chromosorb 106	70	13	Carbosieve S III	150	15	250	67
11		26	Tenax TA	30	13	Chromosorb 105	70	13	Carbosieve S III	150	15	250	67
12		26	Tenax TA	30	13	Carbotrap	70	13	Carbosieve S III	150	15	250	67
13		26	Tenax TA	30	13	Chromosorb 105	70	13	Carbosieve S III	150	15	250	67
14	double layer without Tenax	26	Chromosorb 105	100	13	Carbosieve S III	150	---	---	---	15	250	54
15		26	Chromosorb 106	100	13	Carbosieve S III	150	---	---	---	15	250	54
16		26	Carbotrap	100	13	Carbosieve S III	150	---	---	---	15	250	54
17	single layer	26	Chromosorb 105	200	---	---	---	---	---	15	200	41	
18		26	Chromosorb 106	200	---	---	---	---	---	15	200	41	
19		26	Carbosieve S III	200	---	---	---	---	---	15	200	41	
20		26	Carbotrap	200	---	---	---	---	---	15	200	41	
21	commercial tubes from SKC Tenax double layer	27	Tenax TA	45	13	Tenax TA	90	---	---	---	15	135	55
22		?	Tenax TA, fine mesh size	?	?	unknown material, probably Carbotrap	?	---	---	---	?	?	?
23		?	Tenax TA, fine mesh size	?	?	unknown material, probably Carbosieve S III	?	---	---	---	?	?	?
24		27	Tenax TA	45	13	Tenax TA	90	---	---	---	15	135	55
25		27	Tenax TA	45	13	Tenax TA	90	---	---	---	15	135	55
26		27	Tenax TA	45	13	Tenax TA	90	---	---	---	15	135	55
27		27	Tenax TA	45	13	Tenax TA	90	---	---	---	15	135	55
28	double layer glass wool	26	---	---	13	---	---	---	---	---	16	---	55
29		26	---	---	13	---	---	---	---	---	16	---	55
30	commercial tubes from SKC Tenax double layer	27	Tenax TA	45	13	Tenax TA	90	---	---	---	15	135	55
31	27	Tenax TA	45	13	Tenax TA	90	---	---	---	15	135	55	
32	27	Tenax TA	45	13	Tenax TA	90	---	---	---	15	135	55	

Appendix 5 Experiments with sorption tubes and GC-MS analysis

Note: For arsine generation conditions see Appendix 2; Exp.103 tube No. 29 mounted behind tube No. 28, Exp. 104 tube 26 mounted behind 24, parallel 27 mounted behind 25; Exp. 105 tube 31 mounted behind 21, parallel 32 mounted behind 30; sorption tube numbers as explained in Appendix 4; column properties: DB-624 (L=30m, ID=0.25mm, fd=0.25µm), DB-5 (L=12m, ID=0.32mm, fd=1 µm), MDN-12 (L=30m, (from Exp. 111 on only 25 m) ID=0.25mm, fd=0.25µm)

Experiment No.	Date of experiment	sorption tube No.	Date of analysis	gas pressure [bar]	GC column	Desorption [min / at °C]	Temperature-Time-program [°C / min hold / °C/min heating rate]	Total time [min]	TMA retention time [min]	TMA peak area	(CH ₃) ₂ AsCl retention time [min]	(CH ₃) ₂ AsCl peak area
0A	18.02.01		18.02.	0.75	MDN12	3 / 240	40/1/4;70/2/8;1 40/3/15;240/1	30	7.4	6011800	11	1044700
0B	26.02.01		26.02.	0.75	DB-5	3 / 220	30/2/3;45/2/7;8 0/3/15;180/2	26	0.9	2470400	---	---
0C	27.02.01		27.02.	0.75	DB-5	3 / 220	20/4/2;40/2/5;7 0/2/15;180/2	33	2.7	5622600	---	---
0D	19.04.01	30	19.04.	0.75	DB-5	3 / 240	30/4/3;50/2/6;7 0/1/15;180/1.7	26	0.6	822510	---	---
0E	23.04.01	30	23.04.	0.75	DB-5	3 / 240	25/4/2;40/3/3;6 0/2/4;80/2.8	31	0.7	286890	---	---
52	18.06.01	26-4	18.06.	0.5	DB-5	3 / 240	20/4/2;40/3/3;6 0/2/4;80/2.8	34	---	---	---	---
53	19.06.01	26-4	19.06.	0.5	DB-5	3 / 240	20/4/2;40/3/3;6 0/2/4;80/2.8	34	---	---	---	---
85	06.12.01	21	12.12.	0.5	DB-624	3 / 210	40/2/4;70/2/3;1 30/1/5;180/2.5	45	---	---	---	---
86	06.12.01	9	12.12.	0.5	DB-624	3 / 210	40/2/4;70/2/3;1 30/1/5;180/2.5	45	---	---	---	---
87	06.12.01	4	11.12.	0.5	DB-624	3 / 210	20/4/2;40/3/3;6 0/2/4;80/2.8	34	---	---	---	---
88	06.12.01	5	13.12.	0.5	DB-624	3 / 210	40/2/4;70/2/3;1 30/1/5;180/2.5	45	---	---	---	---
89	10.12.01	6	13.12.	0.5	DB-624	3 / 210	40/2/4;70/2/3;1 30/1/5;180/2.5	45	---	---	---	---
90	10.12.01	12	11.12.	0.5	DB-624	3 / 210	20/4/2;40/3/3;6 0/2/3;100/3	42	---	---	---	---
91	11.12.01	3	11.12.	0.5	DB-624	3 / 210	20/4/2;40/3/3;6 0/2/3;150/4.3	60	---	---	---	---
92	11.12.01	19	11.12.	0.5	DB-5	3 / 210	20/4/2;40/3/3;6 0/2/4;80/2.8	34	---	---	---	---
93	11.12.01	20	12.12.	0.5	DB-624	3 / 210	40/2/4;70/2/3;1 30/1/5;180/2.5	45	---	---	---	---
94	12.12.01	23	13.12.	0.5	DB-624	3 / 210	40/2/4;70/2/3;1 30/1/5;180/2.5	45	---	---	---	---
95	13.12.01	4	13.12.	0.5	DB-624	3 / 210	40/2/4;70/2/3;1 30/1/5;180/2.5	45	---	---	---	---
96	13.12.01	16	13.12.	0.5	DB-624	3 / 210	40/2/4;70/2/3;1 30/1/5;180/2.5	45	---	---	---	---
97	13.12.01	22	13.12.	0.5	DB-624	3 / 210	40/2/4;70/2/3;1 30/1/5;180/2.5	45	---	---	---	---
98	13.12.01	3	13.12.	0.5	DB-624	3 / 210	40/2/4;70/2/3;1 30/1/5;180/2.5	45	---	---	---	---
99	14.12.01	12	14.12.	0.5	DB-624	3 / 210	40/2/4;70/2/3;1 30/1/5;180/2.5	45	---	---	---	---

Appendix 5

Experiment No.	Date of experiment	sorption tube No.	Date of analysis	gas pressure [bar]	GC column	Desorption [min / at °C]	Temperature-Time-program [°C / min hold / °C/min heating rate]	Total time [min]	TMA retention time [min]	TMA peak area	(CH ₃) ₂ AsCl retention time [min]	(CH ₃) ₂ AsCl peak area
100	14.12.01	19	15.12.	0.5	DB-624	3 / 210	40/2/4;70/2/3;1 30/1/5;180/2.5	45	---	---	---	---
101	19.02.02	4	19.02.	0.5	DB-624	10 / 210	40/0/6;100/2/2; 140/0/5;220/2	50	---	---	---	---
102	19.02.02	12	19.02.	0.5	DB-624	3 / 210	40/2/4;70/2/3;1 30/1/5;180/2.5	45	---	---	---	---
103	24.02.02	28-29	25.02.	0.5	DB-624	3 / 240	25/4/2;40/3/3;6 0/2/4;180/1.8	55	---	---	---	---
104	16.04.02	24-26 25-27	21.04.	0.5	DB624	3 / 210	60/0/8;100/0/2; 140/0/3;200/0	45	---	---	---	---
105	17.04.02	21-31 30-32	19.04.	0.5	DB-624	3 / 240	20/4/2;40/3/3;6 0/2/4;100/1.8	39	---	---	---	---
111	04.05.03	3	04.05.	0.3	MDN12	3 / 250	30/3/10;250/10	35	---	---	---	---
112	06.05.03	3	06.05.	0.3	MDN12	3 / 250	40/3/10;250/10	34	---	---	---	---
	second desorption		18.05.	0.15	MDN12	3 / 250	40/3/10;250/10	34	3.0	4223300	6.0	3077300
129	18.05.03	3	18.05.	0.15	DB-5	3 / 250	40/3/10;250/10	34	3.0	3018600	---	---
	second desorption		18.05.	0.15	DB-5	3 / 300	40/3/10;250/10	34	3.2	55891000	6.0	867180
	third desorption		18.05.	0.15	DB-5	3 / 300	40/3/10;250/10	34	3.1	4267400	---	---
130	19.05.03	21	19.05.	0.15	DB-5	3 / 300	40/3/10;250/10	34	---	---	---	---
	second desorption		19.05.	0.15	DB-5	3 / 300	40/3/10;250/10	34	---	---	---	---
131	19.05.03	3	19.05.	0.15	DB-5	3 / 300	40/3/10;250/10	34	3.0	329290000	---	---
	second desorption		20.05.	0.15	DB-5	3 / 300	40/3/10;250/10	34	3.0	595700	---	---
132	20.05.03	18	20.05.	0.15	DB-5	3 / 220	40/3/10;220/10	31	2.8	492910	---	---
133	20.05.03	17	20.05.	0.15	DB-5	3 / 220	40/3/10;220/10	31	---	---	---	---
134	21.05.03	19	21.05.	0.15	DB-5	3 / 300	40/3/10;250/10	34	3.2	796720	---	---
135	21.05.03	20	21.05.	0.15	DB-5	3 / 300	40/3/10;250/10	34	---	---	---	---
136	29.05.03	Car- boxen (new)	29.05.	0.15	DB-5	3 / 300	40/3/10;300/10	34	3.1	28189000	---	---

Appendix 6 Arsenic concentrations in oxidizing solutions mounted behind the sorption tubes during the experiments described in Appendix 5 to control As breakthrough

Note: sorption tube No. as explained in Appendix 4; c_C , V_C = concentration and volume of initial solution before reaction C (control), c_R , V_R = concentration and volume of solution after reaction R (remaining), c_O , V_O = concentration and volume of oxidizing solution; concentrations below detection limit ($1.5 \mu\text{g/L}$) presented as $0.3 \cdot \text{DL} = 0.5 \mu\text{g/L}$;

Experiment No.	sorption tube No. (kind of sorption material)	c_C [$\mu\text{g/L}$]	V_C [mL]	c_R [$\mu\text{g/L}$]	V_R [mL]	c_O [$\mu\text{g/L}$] first tube	c_O [$\mu\text{g/L}$] second tube	V_O [mL]	As % trapped behind 1. sorption tube	As % trapped behind 2. sorption tube	total As % trapped
85	21 (Tenax TA)	31	475	1	555	132	---	95	84	---	
86	9 (Tenax TA / Carbosieve III)	31	475	1	555	1	---	95	0	---	
87	4 (50 mg/L Tenax TA und 140 mg/L Carboxen)	31	475	1	555	1	---	95	0	---	
88	5 (Tenax TA / Carbosieve S III)	31	475	1	555	1	---	95	0	---	
89	6 (Tenax TA / Carbotrap)	31	475	1	555	127	---	95	82	---	
90	12 (Tenax TA / Carbotrap / Carbosieve S III)	31	475	1	555	1	---	95	0	---	
91	3 (Tenax TA / Carboxen)	36	475	1	555	1	---	95	0	---	
92	19 (Carbosieve S III)	36	475	1	555	72	---	95	41	---	
93	20 (Carbotrap)	45	475	1	555	124	---	95	53	---	
94	23 (Tenax TA / Carbosieve S III)	45	475	4	555	1	---	95	0	---	
95	4 (Tenax TA / Carboxen)	44	475	2	555	1	---	95	0	---	
96	16 (Carbotrap / Carbosieve S III)	44	475	1	555	1	---	95	0	---	
97	22 (Tenax TA / Carbotrap)	41	475	1	555	1	---	95	0	---	
98	3 (Tenax TA / Carboxen)	41	475	1	555	1	---	95	0	---	
99	12 (Tenax TA / Carbotrap / Carbosieve S III)	43	475	2	555	1	---	95	0	---	
100	19 (Carbosieve S III)	43	475	2	555	73	---	95	36	---	
101	4 (Tenax TA / Carboxen)	33	475	2	555	5	---	95	3	---	
102	12 (Tenax TA / Carbotrap / Carbosieve S III)	33	475	1	555	115	---	95	73	---	
103	28-29 (double layer glass wool)	66	475	1	555	66	220	95	20	67	88
104	24-26 and 30-32 (Tenax TA)	68	475	2	555	110	162	95	33	49	82
105	21-31 and 30-32 (Tenax TA)	75	475	2	555	183	152	95	50	42	92

Appendix 7 Experiments with SPME (solid-phase micro extraction) technique and GC-MS analysis

Note: SPME type: 1 = PDMS 100, 2 = PDMS-CAR, 3 = PDMS-CAR-DVB; column properties: DB-624 (L=30m, ID=0.25mm, fd=0.25 μm), DB-5 (L=12m, ID=0.32mm, fd=1 μm), MDN-12 (L=25m, ID=0.25mm, fd=0.25 μm), HP5-ms (L=30m, ID=0.25mm, fd=0.25 μm ; low bleed); Exp. 107-109 desorption in injection port 2 min before program start, Exp. 110 desorption in injection port 3 min before program start, all other experiments immediate program start upon injection; n.q. = not quantifiable

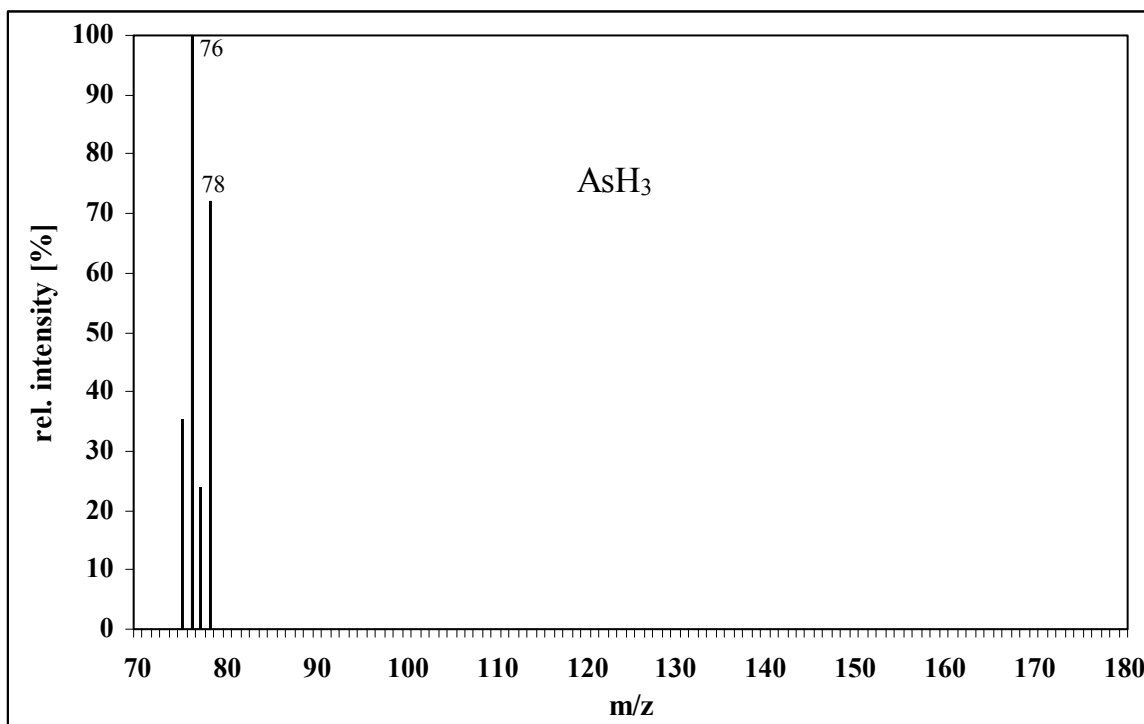
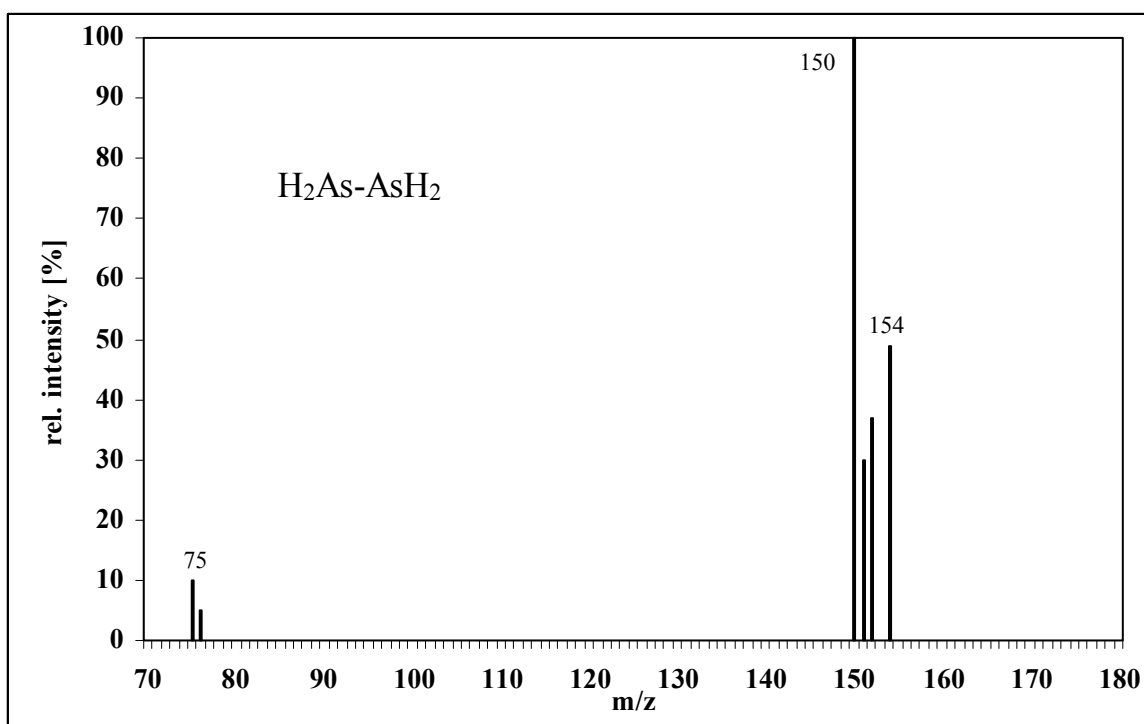
Appendix 7

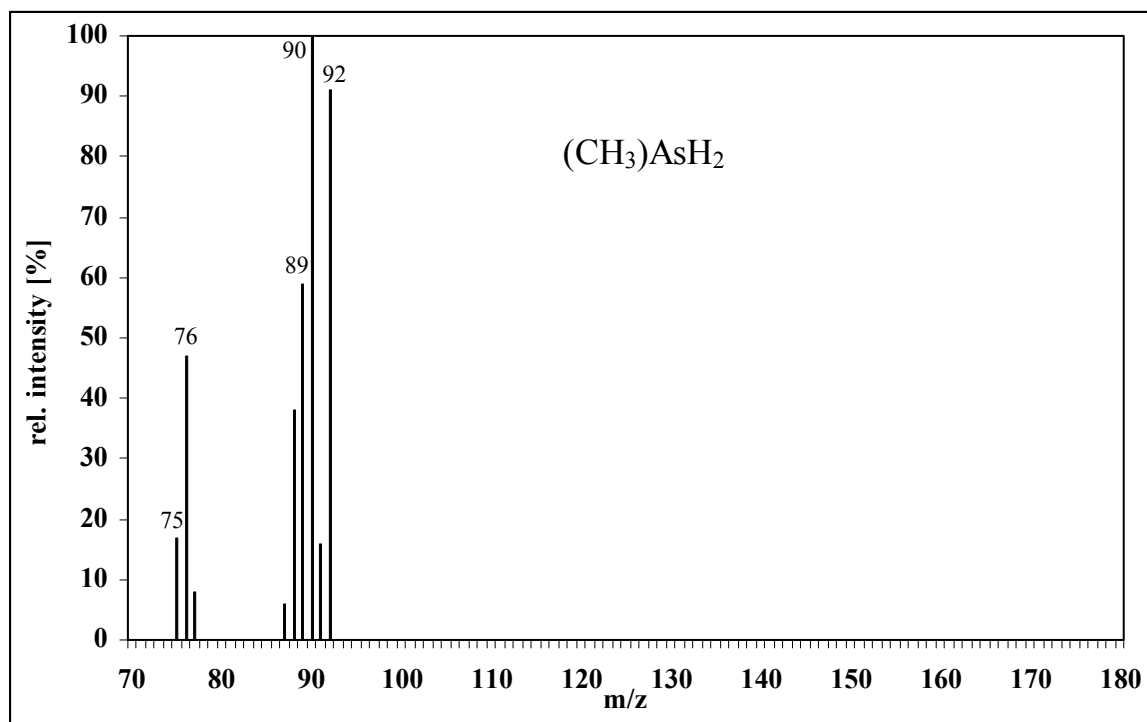
Experiment No.	Date of Experiment	solution / reaction vial volume [mL]	amount of As [μ g]	reducing agent (NaBH ₄ in NaOH) [mL]	NaBH ₄ %	NaOH %	Total time of exposition [min]	SPME type	Date of Analysis	GC-MS carrier gas	GC column	Injection Temperature [°C]	Temperature-Time-Program [°C / min hold / °C/min heating rate]	Total time [min]	MMA retention time	MMA peak area	DMA retention time	DMA peak area	TMA retention time	TMA peak area	(CH ₃)AsCl ₂ retention time	(CH ₃)AsCl ₂ peak area	(CH ₃) ₂ AsCl retention time	(CH ₃) ₂ AsCl peak area
106a	15.04.03	475/ 1100	47.5	20+20	15	5	90	1	15.04.03	N2	DB-624	200	30/2/10;200/5	24	---	---	---	---	---	---	---	---	---	---
106b	15.04.03	475/ 1100	47.5	20+20	15	5	90	2	15.04.03	N2	DB-624	200	30/2/10;200/5	24	---	---	---	---	---	---	---	---	---	---
107	18.04.03	4/50	1	1	2	0.7	20	1	18.04.03	N2	DB-5	200	30/2/10;200/5	24	---	---	---	---	---	---	---	---	---	---
108	19.04.03	2/50	0.5	8.5	2	0.7	20	3	19.04.03	N2	DB-5	200	30/2/10;200/5	24	---	---	---	---	---	---	---	---	---	---
109	19.04.03	2/50	0.5	2	15	5	20	2	19.04.03	N2	DB-5	200	30/2/10;200/5	24	---	---	---	---	---	---	---	---	---	---
110	01.05.03	12.5/26	6.25	1	2	0.7	5	2	01.05.03	N2	MDN12	250	30/3/10;250/10	30	---	---	---	---	---	---	---	---	---	---
113	02.05.03	10/26	5	1	2	0.7	15	1	02.05.03	He	HP-5ms	250	40/3/10;250/10	34	---	---	---	---	---	---	---	---	---	---
114	02.05.03	10/26	5	1	2	0.7	15	2	02.05.03	He	HP-5ms	250	40/3/10;250/10	34	---	---	1.32	12094	1.60- 2.30	2455180	---	---	---	---
115	02.05.03	10/26	5	1	2	0.7	15	3	02.05.03	He	HP-5ms	250	40/3/10;250/10	34	1.21	n.q.	1.38	272189	1.52 1.59	132618 102566	---	---	---	---
116	05.05.03	200/300	100	1	15	5	20	1	05.05.03	He	HP-5ms	250	40/3/10;250/10	34	---	---	---	---	---	---	2.68 2.74	51759 125697	4.12	1002335
117	05.05.03	200/300	100	1	15	5	20	2	05.05.03	He	HP-5ms	250	40/3/10;250/10	34	---	---	1.41	1975	1.56 1.68	17121 212715	---	---	2.97 3.55 3.96	78523654 15478354 6124721
118	05.05.03	200/300	100	1	15	5	20	3	05.05.03	He	HP-5ms	250	40/3/10;250/10	34	1.24	788	1.41	145451	1.55 1.62	377284 254414	---	---	---	---

Appendix 7

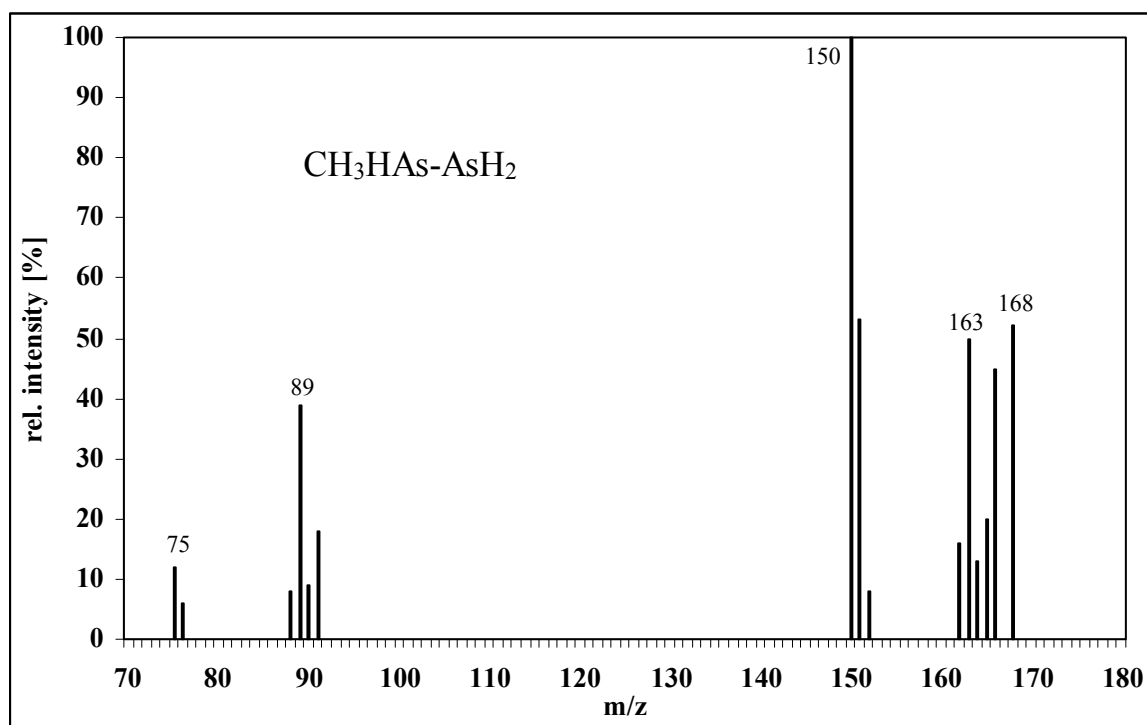
Experiment No.	Date of Experiment	solution / reaction vial volume [mL]	amount of As [μ g]	reducing agent (NaBH ₄ in NaOH) [mL]	NaBH ₄ %	NaOH %	Total time of exposition [min]	SPME type	Date of Analysis	GC-MS carrier gas	GC column	Injection Temperature [°C]	Temperature-Time-Program [°C / min hold / °C/min heating rate]	Total time [min]	MMA retention time	MMA peak area	DMA retention time	DMA peak area	TMA retention time	TMA peak area	(CH ₃) ₂ AsCl ₂ retention time	(CH ₃) ₂ AsCl ₂ peak area	(CH ₃) ₂ AsCl retention time	(CH ₃) ₂ AsCl peak area
119	09.05.03	200/300	100	1	15	5	40	1	09.05.03	N2	MDN12	250	40/3/10;250/10	34	---	---	---	---	---	---	---	---	---	---
120	09.05.03	200/300	100	1	15	5	40	2	09.05.03	N2	MDN12	250	40/3/10;250/10	34	---	---	---	---	---	---	---	---	7.15	65464
121	13.05.03	200/300	100	1	15	5	40	2	14.05.03	N2	DB-5	250	40/3/10;250/10	34	---	---	---	---	2.69	n.q	---	---	5.74	683710
122	14.05.03	200/300	100	1	15	5	40	2	14.05.03	N2	DB-5	250	40/3/10;250/10	34	---	---	---	---	2.72	n.q	---	---	5.81	2050800
123	14.05.03	200/300	100	1	15	5	40	2	14.05.03	N2	DB-5	250	40/3/10;250/10	34	---	---	---	---	2.71	n.q	---	---	5.85	882660
124	14.05.03	10/26	5	1	2	0.7	40	2	14.05.03	N2	DB-5	250	40/3/10;250/10	34	---	---	---	---	---	---	---	---	5.81	473210
127a	17.05.03	200/300	100	1	7.5	2.5	40	2 old	17.05.03	N2	DB-5	250	40/3/10;250/10	34	---	---	---	---	2.61	n.q.	---	---	5.79	1962900
								2 (1 st use)	17.05.03	N2	DB-5	250	40/3/10;250/10	34	---	---	---	---	2.78	851420	---	---	5.85	5297000
127b	17.05.03	200/300	100	1	7.5	2.5	40	2 old	20.05.03	N2	DB-5	250	40/3/10;250/10	34	---	---	---	---	---	---	---	---	6.04	2590500
								2 (2 nd use)	20.05.03	N2	DB-5	250	40/3/10;250/10	34	---	---	---	---	2.7	n.q	---	---	5.84	2704600
128	17.05.03	200/300	100	1	7.5	2.5	40	1	17.05.03	N2	DB-5	250	40/3/10;250/10	34	---	---	---	---	---	---	---	---	---	---
								3	17.05.03	N2	DB-5	250	40/3/10;250/10	34	---	---	---	---	---	---	---	---	---	---

Appendix 8 Mass spectra of different volatile arsine species from literature

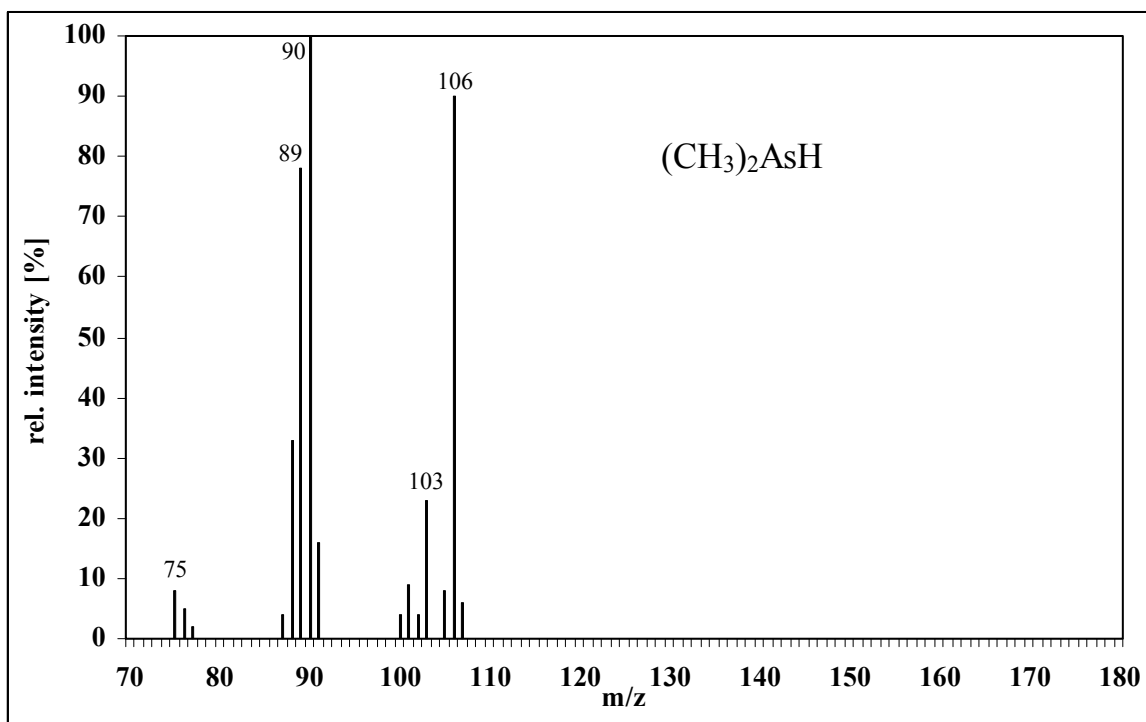
Appendix 8-1 Mass spectrum for AsH_3 (as published with minor variations e.g., in Stein et al. 1998 Cullen et al. 1995 Sur 1999 Pantsar-Kallio and Korpela 2000 Mester and Sturgeon 2001)Appendix 8-2 Mass spectrum for As_2H_4 (as identified by Kösters et al. 2003)



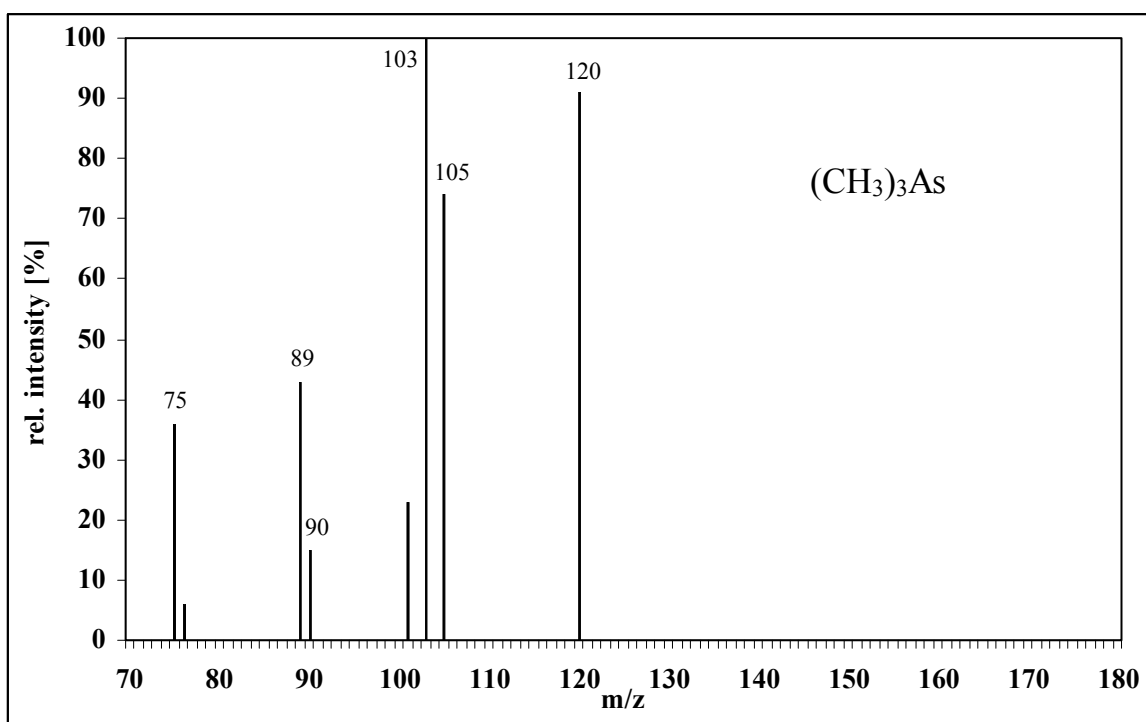
Appendix 8-3 Mass spectrum for $(\text{CH}_3)\text{AsH}_2$ (as published with minor variations e.g., in Pergantis et al. 1997 Cullen et al. 1995 Sur 1999 Pantsar-Kallio and Korpela 2000 Mester and Sturgeon 2001)



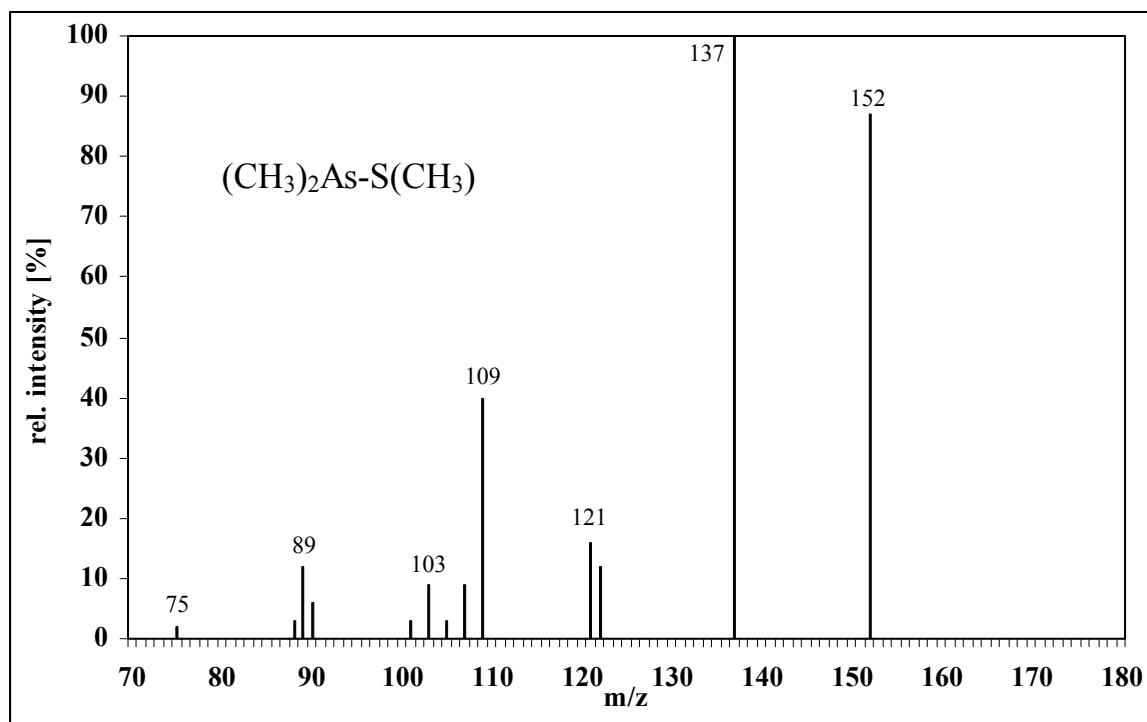
Appendix 8-4 Mass spectrum for $\text{CH}_3\text{As}_2\text{H}_3$ (as identified by Kösters et al. 2003)



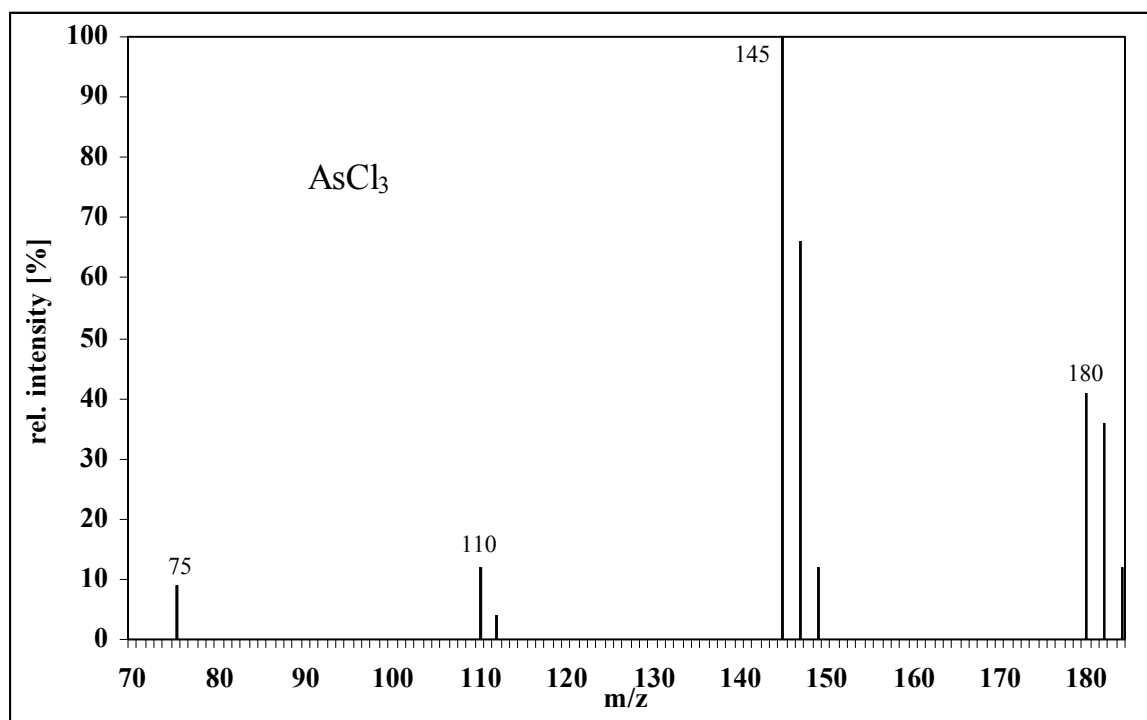
Appendix 8-5 Mass spectrum for $(\text{CH}_3)_2\text{AsH}$ (as published with minor variations e.g., in Pergantis et al. 1997 Cullen et al. 1995 Sur 1999 Pantsar-Kallio and Korpela 2000 Mester and Sturgeon 2001)



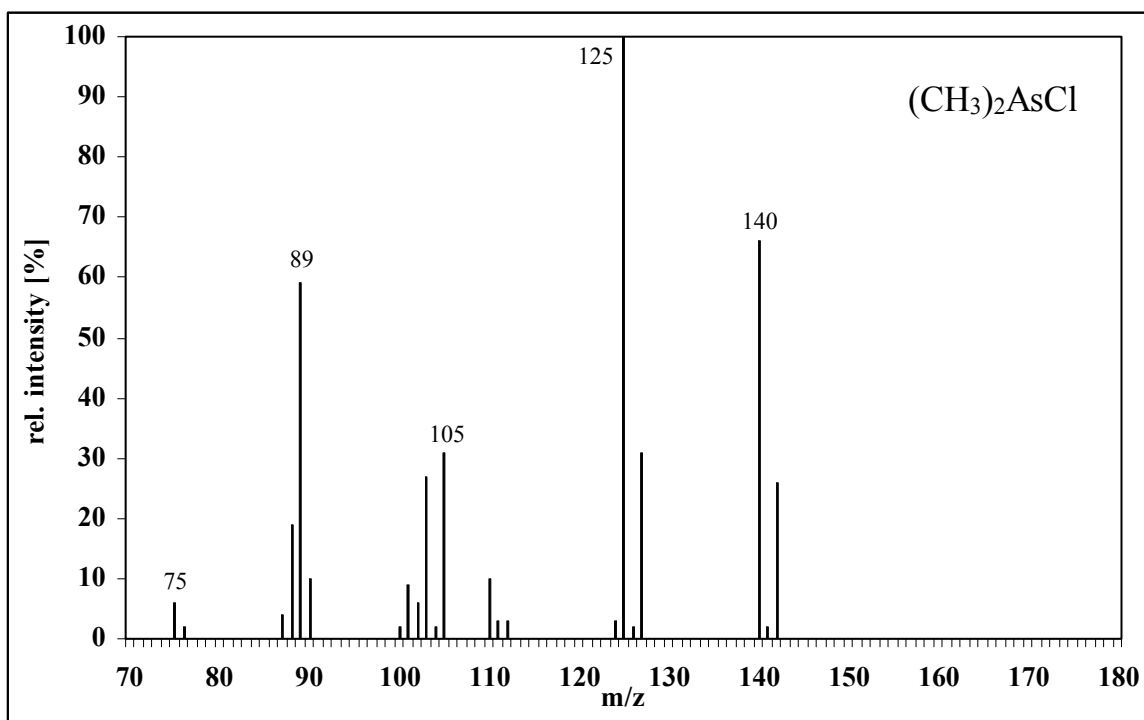
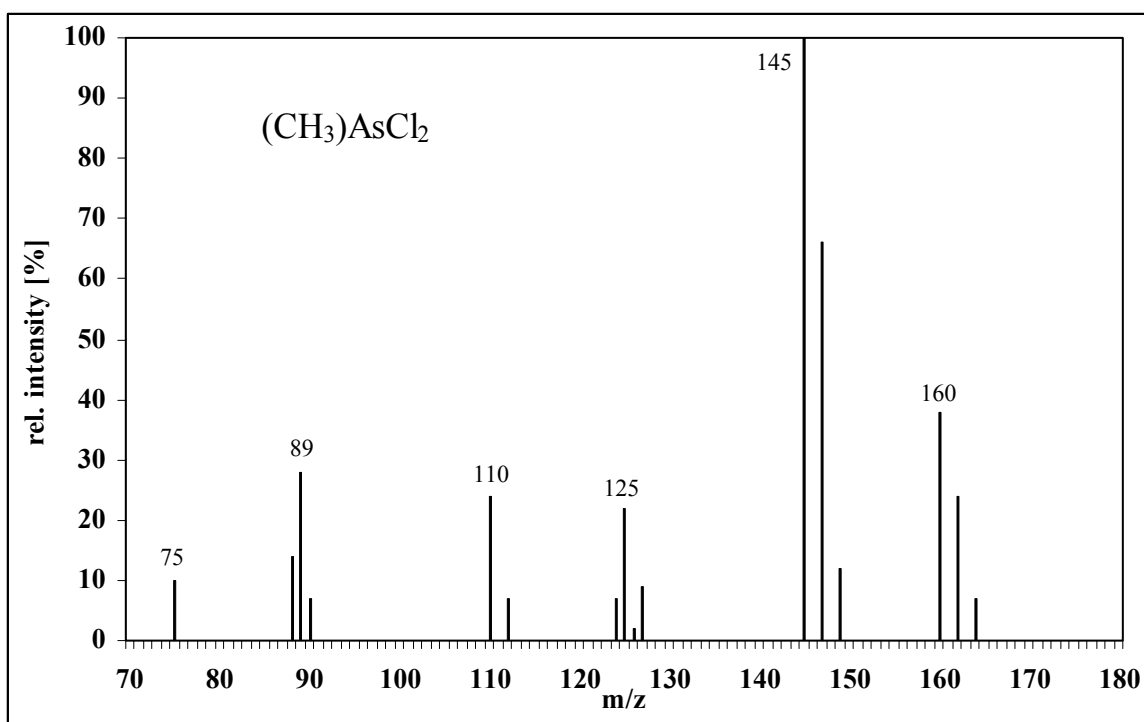
Appendix 8-6 Mass spectrum for $(\text{CH}_3)_3\text{AsH}$ (as published with minor variations e.g., in Stein et al. 1998 Cullen et al. 1995 Sur 1999 Pantsar-Kallio and Korpela 2000)



Appendix 8-7 Mass spectrum for $(\text{CH}_3)_2\text{AsS}(\text{CH}_3)$ (as identified by Kösters et al. 2003)

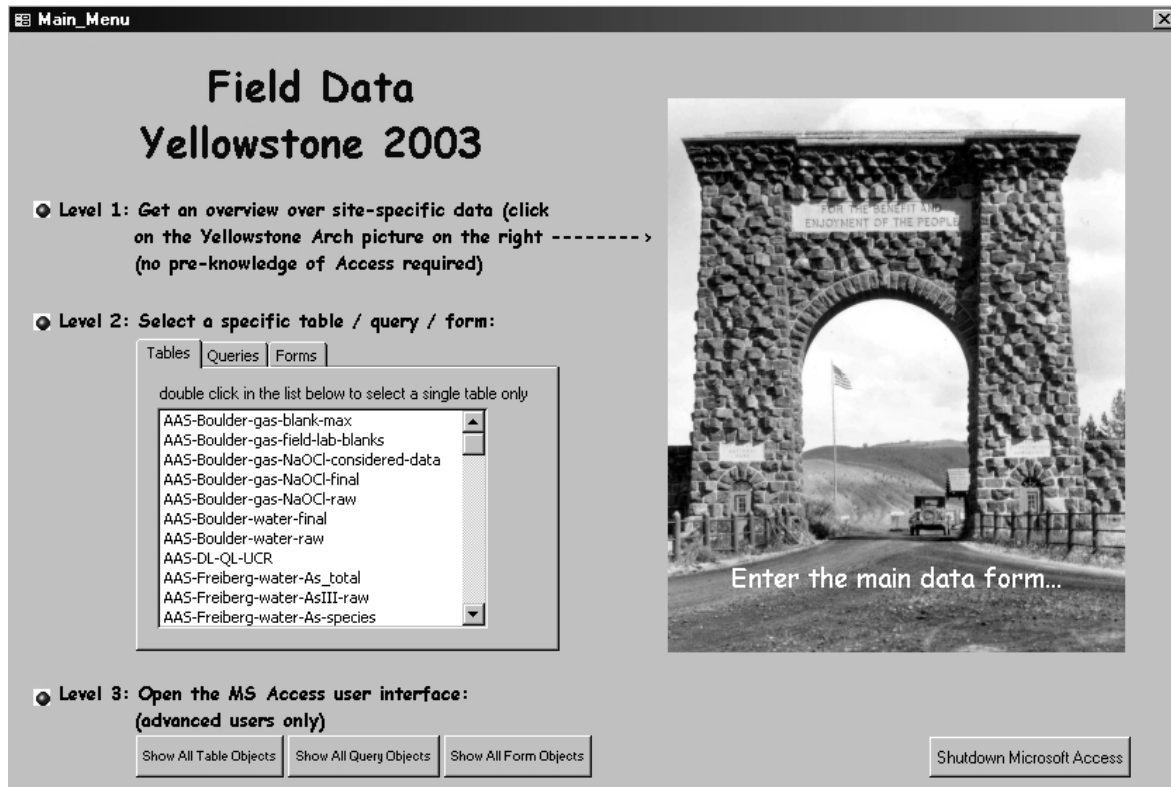


Appendix 8-8 Mass spectrum for AsCl_3 (as published with minor variations e.g., in Stein et al. 1998 Mester and Sturgeon 2001)

Appendix 8-9 Mass spectrum for $(\text{CH}_3)_2\text{AsCl}$ (as published e.g., in Mester and Sturgeon 2001)Appendix 8-10 Mass spectrum for $(\text{CH}_3)\text{AsCl}_2$ (as published e.g., in Mester and Sturgeon 2001)

Appendix 9 Explanation to the digital database for Yellowstone sampling 2003

Site information, pictures, and all data gathered from the sampling of Yellowstone geothermal areas in 2003 are presented in an Access database (**Yellowstone2003.mdb**) on the enclosed CD. Opening the Access file, you see a welcome screen that you can confirm with OK to get to the main menu:



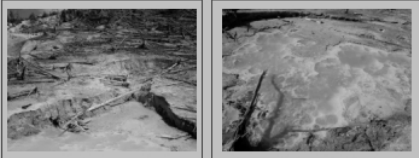
Here you have 3 options:

- **Level 1** (if you are not familiar with Access): click on the Yellowstone Arch picture to enter the **Main_Data_Form** and get a site-specific overview over the gathered data that does not require any pre-knowledge in Access. This main data form will be explained in detail in the following and contains a combination of all available data).
- **Level 2:** If you are familiar with Access, and are looking for a special information you can directly proceed to a table, query, or form object by double click on the scroll list below
- **Level 3** (advanced users only): open the usual MS Access user interface with the display of all tables, queries, and forms, where you can edit or create new tables, queries, or forms.

The **Main Data Form** opens with 6 pages: “general information”, “water”, “Gas - total conc.”, “Gas comparison wGH-nGH”, “Gas - total conc. (P, DB)”, and “Gas - As speciation”. The record bar on the bottom shows 48 records in alphabetical order for the 48 sites sampled (8 sites at Geyser Spring Group, Gibbon Geyser Basin; 3 sites at Hazle Lake; 3 sites in the Pocket Basin, Lower Geyser Basin; 6 sites in the Nymph Lake / Frying Pan Spring area; 28 sites at Ragged Hills, Norris Geyser Basin). The information listed for each record is linked to different columns of different tables under Objects / Tables in the Access Menu. These source information are explained in the following. Throughout the database mouseover provides additional information.

First page: General Information:

The **primary key** (the unique link, under which all information can be defined unambiguously) for all information on this page is the **Site_Code**. The bold area name on top stems from the column "Area" in the table "Names_Descriptions" ([table!]column = [Names_Descriptions]!Area).

Main_Data_Form					
General Information	Water	Gas - total conc.	Gas comparison wGH-nGH	Gas - total conc. (P, DB)	Gas - As speciation
Ragged Hills, Norris Geyser Basin					
Site Code:	YNPRH01			Available information for this site (with sampling date 2003):	
Site Name:	"Milky Way"	double click enlarges the picture		Water:	
Longitude:	-110.71342			Standard parameters: 11.06 / 04.07 / 14.09	
Latitude:	44.728175			ICP-MS: 11.06 / 14.09	
Altitude:	2286 m			Mercury: 17.06	
Site Description:	hot pool downstream of YNPRH18, approximately 30 m long, 20 m wide, discharging to the main drainage of the area west of the Gap; water milky, depth 3-10 cm max., muddy underground			Gas-total concentrations:	
				AAS, ICP-AES: 17.06 (S1) / 04.07 (S1) / 15.09 (S1,2,3)	
				ICP-MS: 17.06 (S1) / 15.09 (S1)	
				Cl in NaOH: 30.06 (S1) / 11.07 (S1)	
				Gas-comparison with and without gas hood:	
				Cl in NaOH:	
				As in NaOCl: 15.09 (S1-S3, S2-S3)	
				Gas-total concentrations (P, DB):	
				NaOCl pumping: 11.07	
				NaOCl diffusion bowls: 08.09	
				Gas-As speciation	
				Solid sorbent: 30.06	
				SPME fibers: 21.06 CAR, PDMS / 09.09 CAR, PDMS	
Datensatz: 21 von 48					

Site Code [Names_Descriptions]!Site_Code; Code abbreviation: YNP = Yellowstone National Park; Area (GG = Gibbon Geyser Basin, HL = Hazle Lake, LG = Lower Geyser Basin, NL = Nymph Lake, RH = Ragged Hills); No. Sampling Site

Site Name [Names_Descriptions]!Site_Name; names in quotation marks are unofficial

Longitude [Coordinates_Altitudes_calc]!Longitude; value is a calculated value, according to the following query [Query: calc- Coordinates_Altitudes]:

```
If([Coordinates-Altitudes-DiffGPS]!Site_Code=[Coordinates-Altitudes]!Site_Code;[Coordinates-Altitudes-DiffGPS]!Longitude_calcTNTmips;if([Coordinates-Altitudes]!Longitude2nd=-999;[Coordinates-Altitudes]!Longitude1st;if([Coordinates-Altitudes]!Longitude1st=-999;[Coordinates-Altitudes]!Longitude2nd;([Coordinates-Altitudes]!Longitude1st+[Coordinates-Altitudes]!Longitude2nd)/2)))
```

In the Ragged Hills area several sites were surveyed by Differential GPS. Since this information is more accurate than normal GPS measurements, it was taken whenever available. The horizontal precision of the differential GPS is given in [Coordinates-Altitudes-DiffGPS]!horizontal_precision_m. [Coordinates-Altitudes-DiffGPS]!Easting contains the original UTM values (Zone 12 North, spheroid GRS80, datum NAD83). The longitude (datum WGS 72) was calculated from the UTM coordinates with the GIS program TNTmips 6.8 from Mi-

croImages ([Coordinates-Altitudes-DiffGPS]!Longitude_calcTNTmips). When no information from differential GPS was available, data obtained from a GPS GARMIN-12 were taken ([Coordinates-Altitudes]!Longitude1st and [Coordinates-Altitudes]!Longitude2nd). In the case of two measurements the mean value was calculated.

- Latitude** [Coordinates_Altitudes_calc]!Latitude (calculated analogous to the longitude)
- Altitude** [Coordinates_Altitudes_calc]!Altitude_m; similar calculation like for longitude and latitude; vertical precision indicated in [Coordinates-Altitudes-DiffGPS]!vertical_precision_m; mean altitude in feet is given in [Coordinates_Altitudes_calc]!Altitude_feet (feet · 0.3048 = meter)
- Site Description** [Names_Descriptions]!Site_Description
- Left picture** [Pictures]!Picture1 contains the file name of each picture that is linked via a Visual Basic Script to and will be displayed together with each record; physically the pictures are saved in the folder Figures / Database-Yellowstone2003; double-click on the thumbnail picture opens an enlarged version of the same picture ([Pictures]! Picture1G)
- Right picture** [Pictures]!Picture2 (thumbnail); [Pictures]!Picture2G (enlarged version)
- Available information for this site (with sampling date 2003)**

The fields herein are clustered in 5 sections corresponding to the 5 pages on top. The list gives an overview where information can be expected for each sampling site. The fields contain sampling dates, whenever samples were taken, otherwise the field (and also the corresponding page) is blank. Mouseover gives further information, e.g., on what “standard parameters” are (field information from table [Summary-available-site-information]!)

Second page: Water

Data on this page are linked to the subform “Water-subform”. This subform contains 62 records for 41 sites, 7 of the sampling sites had mainly fumarole activity and could not be sampled for water. Some of the sites were sampled not only once, but 2 or 3 times.

- primary key** **Analysis-code-water** ([Analysis-code-water]!Analysis-code-water); the analysis code water consists of the site code, the No. of the sampling campaign (1 = June, 5th, to June, 21st, 2003; 2 = June, 30th, to July, 12th, 2003; 3 = September, 3rd, to September, 15th, 2003; 4 = September 21st, to October, 9th, 2003), and W for water (e.g., YNPGG04-1W is the first water sampling campaign for site YNPGG04, YNPGG04-2W the second, etc.)

- Note:** The record bar within the subform “water” shows 1 of 3 records, indicating that sampling site YNPRH04 was sampled 3 times. Arrows to the left and right can be used to scroll within the subform water. To go to the next sampling site, the lower record bar (of the Main Data Form) has to be used. The page “water” is blank when there are no water data. Missing values are administered as -999

(e.g., Mercury - Hg); values below detection limit as negative values (e.g., <0.06 N(V) = -0.06). Mouseover on values shows sample preparation, analytical methods and devices.

Main_Data_Form

General Information | Water | Gas

1. sampling campaign | 19.06.2003 | 10:15:00 | Analysis-code: YNPRH04-1W

On-site physicochemical parameters

pH: 2.37 | conductivity: 2440 $\mu\text{S}/\text{cm}$ | Temperature: 44.9 $^{\circ}\text{C}$
 EH: 726 WTW MultiLine P4 with SenTix 97/T pH electrode %

On-site photometry [mg/L]

SiO2: 285 | Fe(II): 1.82 | 21%
 S-2: 0.05 | Fe(tot): 8.85 | Fe(III): 7.03 | 79%

Arsenic speciation [$\mu\text{g}/\text{L}$]

As(tot): 1895 | As(III): 1459 | 69.70%
 As(V): 5 | 0.24%
 MMAA: 124 | 5.91%
 DMAA: 506 | 24.14%

Ion chromatography [mg/L]

Cl-: 195 | F-: 2.3 | Br-: 0.6
 SO4-2: 476 | NO3-: -0.06

Carbon [mg/L]

TIC_mean_mg/L: 10.34 | TOC_mean_mg/L: 0.91

ICP-AES [mg/L]

As: 1.87 | Cd: 0.001 | Li: 1.42 | Pb: -0.008

Datensatz: 1 von 3

Datensatz: 24 von 48

Quality Control:
 Arsenic QC? Mean: 1994 +/- 5%
 AAS: 1895 | ICP-AES: 1870 | Sum-As-species: 2094
 Mean: 1882 +/- 1% | Mean: 1982 +/- 6%
 QC? analytical error: -1.88
 measured conductivity: 2440 $\mu\text{S}/\text{cm}$ | mean conductivity [$\mu\text{S}/\text{cm}$]: 2473 +/- 1.35%
 calculated conductivity: 2507 $\mu\text{S}/\text{cm}$
 Comment: too many anions

number of sampling campaign [Analysis-code-water]!Sampling_No

Sampling date [Analysis-code-water]!Sampling_Date

Sampling time [Analysis-code-water]!Sampling_Time

On-site physicochemical parameters:

pH [On-site-pH]!pH_corrected (= field pH; field pH was not accepted when the analytical error exceeded 5%, then either the laboratory pH was taken or pH was adapted to best fit from speciation modeling within a range of ± 0.1 pH units)

conductivity [On-site-conductivity]!conductivity_uS/cm

Temperature [On-site-Temperatures-calc]!Temperature_Mean_ $^{\circ}\text{C}$; the value was calculated as the mean of temperature read from pH ([On-site-Temperature]!Temperature_pH_ $^{\circ}\text{C}$) and conductivity meter ([On-site-Temperature]!Temperature_conductivity_ $^{\circ}\text{C}$), except when one of the values was not accepted, e.g., due to device failure [Query: calc-Temperatures]:

```
If([On-site-Temperatures-calc]!Accept_temp_cond=false;[On-site-Temperature]!Temperature_pH_°C;If([On-site-Temperatures-calc]!Accept_temp_pH=False;[On-site-Temperature]!Temperature_conductivity_°C;([On-site-Temperature]!Temperature_conductivity_°C+[On-site-Temperature]!Temperature_pH_°C)/2))
```

Redox potential [On-site-Redoxpotential-calc]!EH_corrected_mV; redox potential was measured in the field against the Ag/AgCl-electrode; [On-site-Redoxpotential-

calc]!EH_AgAgCl-Potential_mV) and corrected for standard hydrogen potential and temperature [Query: calc-Redoxpotential]:

```
If([On-site-Redoxpotential]!EH_AgAgCl-Potential_mV]=-999;-999;([On-site-Redoxpotential]!EH_AgAgCl-Potential_mV)+(-0.7443*[On-site-Temperatures-calc]!Temperature_Mean_°C+224.98)))
```

pe value was calculated from the corrected E_H value ([On-site-Redoxpotential-calc]!pe) according to the following query [Query: calc-Redoxpotential]:

```
If([On-site-Redoxpotential]!EH_AgAgCl-Potential_mV]=-999;-999;16.9*[On-site-Redoxpotential-calc]!EH_corrected_mV/1000)
```

Oxygen

[On-site-Oxygen]!O2_%, and [On-site-Oxygen]!O2_mg/L

Due to problems with the device (especially at temperatures > 50°C), Oxygen was measured only in 22 samples; these data had to be attached via a sub-subform [Form On-site-Oxygen]; in the water subform data fields will be empty when no data exist

On-site photometry:

SiO₂ [On-site-photometry-SiO2]!SiO2_mgL,
SiO2 QC photometry / ICP-AES, default: invisible, click on the option displays mean value and range of analysis (ROA) of values from on-site photometry compared to those from ICP-AES for a quality check (table [Comparison-Si-determination]! based on the Query calc-Comparison-Si)

S(-II) [On-site-photometry-S2-]!S2-_mgL

Fe [On-site-photometry-Fe]!Fe_tot_mgL and [On-site-photometry-Fe]!Fe_II_mgL:
[On-site-photometry-Fe-calc]!Fe_III_mgL, [On-site-photometry-Fe-calc]!Fe_II_%, and [On-site-photometry-Fe-calc]!Fe_III_%; values calculated as difference and percentage [Query: calc-Photometry-Fe]

Fe QC photometry / ICP-AES, default: invisible, click on the option displays mean value and range of analysis (ROA) of values from on-site photometry compared to those from ICP-AES for a quality check (table [Comparison-Fe-determination]! based on the Query: calc-Comparison-Fe)

Arsenic speciation:

Total As (AAS) [Comparison-As-determination]!Total-As-AAS (essentially the same as [AAS-Freiberg-water-As_total]!As_final_concentration_ugL, but rounded down to 2 decimals); raw data in the same table: extinction_1st_determination, extinction_2nd_determination, extinction_mean; concentrations derived via Excel calibration curves (not shown in the Access database) are in the column As_concentration_ugL; column As_final_concentration_ugL considers dilution ratios

As(III) [AAS-Freiberg-water-As-species]!AsIII_ugL and [AAS-Freiberg-water-As-species]!AsIII_% [Query: calc-Arsenic-species]

As(V)	<p>(raw data as explained for total As in table AAS-Freiberg-water-AsIII-raw)</p> <p>[AAS-Freiberg-water-As-species]!AsV_ugL and [AAS-Freiberg-water-As-species]!AsV_% [Query: calc-Arsenic-species]</p> <p>(raw data as explained for total As in table AAS-Freiberg-water-AsV-raw; ion exchangers were eluted at least 2 times for As(V) species: the code YNPGG02-AsV1-2W and YNPGG02-AsV2-2W indicates the first and second elution of As(V) with 1 N HCl for the site YNPGG02 during the second sampling campaign; second, third and fourth elution of the anion exchanger with acetic acid (“MMAA” fraction; YNPGG02-MMA2-2W, YNPGG02-MMA3-2W, YNPGG02-MMA4-2W) were added to the As(V) fraction, since continuing high concentrations after the first elution peak were thought to result from desorption of As(V) already; the column AsV_final_concentration_ugL considers dilution factors during analysis; the real “final” value [AAS-Freiberg-water-As-species]!AsV_ugL is a sum of all elutions (YNPGG02-AsV1-2W + YNPGG02-AsV2-2W + YNPGG02-MMA2-2W + YNPGG02-MMA3-2W + YNPGG02-MMA4-2W) divided by 2 to correct for the enrichment factor 2 resulting from the application of 20 mL sample in the field and the elution with 10 mL extractant in the laboratory)</p>
MMAA	<p>[AAS-Freiberg-water-As-species]!MMAA_ugL and [AAS-Freiberg-water-As-species]!MMAA_% [Query: calc-Arsenic-species]</p> <p>(raw data as explained for As(V) in table AAS-Freiberg-water-MMAA-raw, only one elution per sample, second, third, fourth elutions were attributed to the As(V) fraction)</p>
DMAA	<p>[AAS-Freiberg-water-As-species]!DMAA_ugL and [AAS-Freiberg-water-As-species]!DMAA_% [Query: calc-Arsenic-species]</p> <p>(raw data as explained for As(V) in table AAS-Freiberg-water-DMAA-raw; two elutions per sample)</p>
Arsenic QC?	<p>default: invisible, only total As concentrations determined by GF-AAS are displayed; click on the Option “Arsenic QC?” displays As additionally as determined by ICP-AES and as the sum of As species from GF-AAS; the latter suffers from analytical errors of four single determinations (As(III), As(V), MMAA, DMAA;) and is thus regarded as less precise; mean, range and ROA are calculated as explained in the following [Query: calc-Comparison-As]:</p> <p>[Comparison-As-determination]!Sum-As-species-AAS from [AAS-Freiberg-water-As-species]!</p> <p>[AAS-Freiberg-water-As-species]!AsIII_ugL+[AAS-Freiberg-water-As-species]![MMAA_ugL]+[AAS-Freiberg-water-As-species]!AsV_ugL+[AAS-Freiberg-water-As-species]![DMAA_ugL]</p> <p>[Comparison-As-determination]!Total-As-AAS</p> <p>[AAS-Freiberg-water-As_total]!As_final_concentration_ugL</p>

[Comparison-As-determination]!Total-As-ICP-AES

[ICP-AES-water-final-data]!As_mgL·1000

[Comparison-As-determination]!Mean-Sum-species-AAS (analogous for Sum-species-ICP-AES, and AAS-ICP-AES)

([Comparison-As-determination]![Sum-As-species-AAS]+[Comparison-As-determination]![Total-As-AAS])/2

[Comparison-As-determination]!Range-Sum-species-AAS (analogous for Sum-species-ICP-AES, and AAS-ICP-AES), range is not displayed in the water sub-form

If(Abs([Comparison-As-determination]![Mean-Sum-species-AAS]-[Comparison-As-determination]![Sum-As-species-AAS])>Abs([Comparison-As-determination]![Mean-Sum-species-AAS]-[Comparison-As-determination]![Total-As-AAS]);Abs([Comparison-As-determination]![Mean-Sum-species-AAS]-[Comparison-As-determination]![Sum-As-species-AAS]);Abs([Comparison-As-determination]![Mean-Sum-species-AAS]-[Comparison-As-determination]![Total-As-AAS]))

[Comparison-As-determination]!ROA-Sum-species-AAS (analogous for Sum-species-ICP-AES, and AAS-ICP-AES)

[Comparison-As-determination]![Range-Sum-species-AAS]/[Comparison-As-determination]![Mean-Sum-species-AAS]·100

Ion chromatography: Cl, S(VI), F, Br, N(V)

[IC-water-final-data]!Cl_corrected_mgL, [IC-water-final-data]!SO4_corrected_mgL, [IC-water-final-data]!F_corrected_mgL, [IC-water-final-data]!Br_mgL, [IC-water-final-data]!NO3_mgL;

Raw data including standard calibration from the IC are listed in table [IC-water-raw-data-area-heights]!; concentrations derived via Excel calibration curves (not shown in the Access database) are in table [IC-water-raw-data-conc]!; all samples were measured in three different dilutions: undiluted, diluted 1:10, diluted 1:100, the best fit within quantification limit ([IC-QuantLimit]!) and upper calibration range ([IC-UpperCalibRange]!) was determined according to the following query, e.g., for F⁻ [Query: calc-IC-water-final-values]:

If([IC-water-raw-data-conc]!F_mgL_dil100>[IC-QuantLimit]!F_mgL;If([IC-water-raw-data-conc]!F_mgL_dil100<[IC-UpperCalibRange]!F_mgL;[IC-water-raw-data-conc]!F_mgL_dil100·100;999);If([IC-water-raw-data-conc]!F_mgL_dil10>[IC-QuantLimit]!F_mgL;If([IC-water-raw-data-conc]!F_mgL_dil10<[IC-UpperCalibRange]!F_mgL;[IC-water-raw-data-conc]!F_mgL_dil10·10;999);If([IC-water-raw-data-conc]!F_mgL_dil1>[IC-QuantLimit]!F_mgL;If([IC-water-raw-data-conc]!F_mgL_dil1<[IC-UpperCalibRange]!F_mgL;[IC-water-raw-data-conc]!F_mgL_dil1·1;999);If([IC-water-raw-data-conc]!F_mgL_dil1>[IC-DetectionLimit]!F_mgL;[IC-water-raw-data-conc]!F_mgL_dil1·1;If([IC-water-raw-data-conc]!F_mgL_dil1=-999;-999;-[IC-DetectionLimit]!F_mgL))))))

Concentrations below the detection limit ([IC-DetectionLimit]!) are indicated as negative values; final data from the automated calculation are listed in the table [IC-water-final-data]!, e.g., [IC-water-final-data]!F_mgL; all values were checked manually afterwards, and some were corrected (e.g., [IC-water-final-data]!F_corrected_mgL), based on better fit of other dilutions or re-analyses with another IC ([IC-Freiberg-water]!), comments on each record manually adapted are given e.g., in [IC-water-final-data]!F_corrected_comment

Analysis QC?

[Data-check-summary-QC]!; default: invisible, click on the Option “QC?” displays the analytical error, and a comparison between measured and calculated conductivity as well as an evaluation of the analysis based on the criteria discussed in section 4.2.3.1 and shown in Table 11. A general evaluation was based on a 5% criteria; whenever analytical error or range of analysis of measured and calculated conductivities were more than 5% a warning is displayed.

To determine analytical error and calculate conductivity the speciation modeling program PHREEQC was used. The query to combine data from different tables to import into PHREEQC is [PhreeqC-data-combination]. The results from PHREEQC modeling (database WATEQ4F; folder PHREEQC/ YNP03-data-check on the CD) are export via Selected_Output and imported into Access as the table [Data-check-PhreeqC-raw-data]!

To compare measured conductivity with calculated conductivities (Rossum 1975), the following is needed:

- concentrations of the cations / anions (query [calc-data-check-PhreeqC-mmolL] to convert concentrations in mol/L to mmol/L: [Data-check-PhreeqC-mmolL]!)
- the charge of the cations / anions ([Data-check-parameter-charge]!), and
- their contribution to conductivity at 25°C ([Data-check-parameter-ioncond-25]!)

The following calculations are conducted:

Query [calc-data-check-cond-equiv] yields table [Data-check-cond-equiv]!

[Data-check-PhreeqC-mmolL]![H_mmolL] · [Data-check-parameter-ioncond-25]![H]

(analogous for the other cations / anions)

Query [calc-data-check-cZ] yields [Data-check-cZ]!

[Data-check-PhreeqC-mmolL]![H_mmolL] · ([Data-check-parameter-charge]![H])

(analogous for the other cations / anions)

Query [calc-data-check-cZ2] yields table [Data-check-cZ2]!

[Data-check-PhreeqC-mmolL]![H_mmolL] · ([Data-check-parameter-charge]![H]^2)

(analogous for the other cations / anions)

And finally Query [calc-data-check-final] yields table [Data-check-final-calc]!

c- Sum of anion concentrations

[Data-check-PhreeqC-mmolL]!OH_mmolL+[Data-check-PhreeqC-mmolL]!CO3_mmolL+[Data-check-PhreeqC-mmolL]!HCO3_mmolL+[Data-check-PhreeqC-mmolL]!SO4_mmolL+[Data-check-PhreeqC-mmolL]!Cl_mmolL+[Data-check-PhreeqC-mmolL]!NO3_mmolL+[Data-check-PhreeqC-mmolL]!F_mmolL+[Data-check-PhreeqC-mmolL]!Br_mmolL+[Data-check-PhreeqC-mmolL]!HSO4_mmolL

c+ Sum of cation concentrations

[Data-check-PhreeqC-mmolL]!H_mmolL+[Data-check-PhreeqC-mmolL]!Ca_mmolL+[Data-check-PhreeqC-mmolL]!Mg_mmolL+[Data-check-PhreeqC-mmolL]!Na_mmolL+[Data-check-PhreeqC-mmolL]!K_mmolL+[Data-check-PhreeqC-mmolL]!Li_mmolL+[Data-check-PhreeqC-mmolL]!Fe2_mmolL+[Data-check-PhreeqC-mmolL]!Al_mmolL+[Data-check-PhreeqC-mmolL]!Ba_mmolL+[Data-check-PhreeqC-mmolL]!Fe3_mmolL+[Data-check-PhreeqC-mmolL]!Sr_mmolL

err analytical error

$([\text{Data-check-final-calc}]![\text{c+}] - [\text{Data-check-final-calc}]![\text{c-}]) / (0.5 \cdot ([\text{Data-check-final-calc}]![\text{c+}] + [\text{Data-check-final-calc}]![\text{c-}]))$

G0- sum of concentration · equivalent conductance for anions

[Data-check-cond-equiv]!OH_mmolL+[Data-check-cond-equiv]!CO3_mmolL+[Data-check-cond-equiv]!HCO3_mmolL+[Data-check-cond-equiv]!SO4_mmolL+[Data-check-cond-equiv]!Cl_mmolL+[Data-check-cond-equiv]!NO3_mmolL+[Data-check-cond-equiv]!F_mmolL+[Data-check-cond-equiv]!Br_mmolL+[Data-check-cond-equiv]!HSO4_mmolL

G0+ sum of concentration · equivalent conductance for cations

[Data-check-cond-equiv]!H_mmolL+[Data-check-cond-equiv]!Ca_mmolL+[Data-check-cond-equiv]!Mg_mmolL+[Data-check-cond-equiv]!Na_mmolL+[Data-check-cond-equiv]!K_mmolL+[Data-check-cond-equiv]!Li_mmolL+[Data-check-cond-equiv]!Fe2_mmolL+[Data-check-cond-equiv]!Al_mmolL+[Data-check-cond-equiv]!Ba_mmolL+[Data-check-cond-equiv]!Fe3_mmolL+[Data-check-cond-equiv]!Sr_mmolL

cZ2- sum of concentrations · square of charge for anions

[Data-check-cZ2]!OH_mmolL+[Data-check-cZ2]!CO3_mmolL+[Data-check-cZ2]!HCO3_mmolL+[Data-check-cZ2]!SO4_mmolL+[Data-check-cZ2]!Cl_mmolL+[Data-check-cZ2]!NO3_mmolL+[Data-check-cZ2]!F_mmolL+[Data-check-cZ2]!Br_mmolL+[Data-check-cZ2]!HSO4_mmol

cZ2+ sum of concentrations · square of charge for cations

[Data-check-cZ2]!H_mmolL+[Data-check-cZ2]!Ca_mmolL+[Data-check-cZ2]!Mg_mmolL+[Data-check-cZ2]!Na_mmolL+[Data-check-cZ2]!K_mmolL+[Data-check-cZ2]!Li_mmolL+[Data-check-cZ2]!Fe2_mmolL+[Data-check-cZ2]!Al_mmolL+[Data-check-cZ2]!Ba_mmolL+[Data-check-cZ2]!Fe3_mmolL+[Data-check-cZ2]!Sr_mmolL

cZ- sum of products concentrations · charge for anions

```

[Data-check-cZ]!OH_mmolL+[Data-check-cZ]!CO3_mmolL+[Data-check-
cZ]!HCO3_mmolL+[Data-check-cZ]!SO4_mmolL+[Data-check-cZ]!Cl_mmolL+[Data-check-
cZ]!NO3_mmolL+[Data-check-cZ]!F_mmolL+[Data-check-cZ]!Br_mmolL+[Data-check-
cZ]!HSO4_mmolL
cZ+    sum of products concentrations · charge for cations
[Data-check-cZ]!H_mmolL+[Data-check-cZ]!Ca_mmolL+[Data-check-cZ]!Mg_mmolL+[Data-
check-cZ]!Na_mmolL+[Data-check-cZ]!K_mmolL+[Data-check-cZ]!Li_mmolL+[Data-check-
cZ]!Fe2_mmolL+[Data-check-cZ]!Al_mmolL+[Data-check-cZ]!Ba_mmolL+[Data-check-
cZ]!Fe3_mmolL+[Data-check-cZ]!Sr_mmolL
Z-    effective ion charge anions
[Data-check-final-calc]![cZ2-]/[Data-check-final-calc]![cZ-]
Z+    effective ion charge cations
[Data-check-final-calc]![cZ2+]/[Data-check-final-calc]![cZ+]
Lambda-    average value for ionic conductance of the anions
[Data-check-final-calc]![G0-]/[Data-check-final-calc]![c-]
Lambda+    average value for ionic conductance of the cations
[Data-check-final-calc]![G0+]/[Data-check-final-calc]![c+]
Lambda 0    total ionic conductance
[Data-check-final-calc]![lambda-]+[Data-check-final-calc]![lambda+]
Q
([Data-check-final-calc]![Z+]·[Data-check-final-calc]![Z-]·[Data-check-final-
calc]!lambda0)/((([Data-check-final-calc]![Z+] + [Data-check-final-calc]![Z-])·([Data-check-final-
calc]![Z+]·[Data-check-final-calc]![lambda-] + [Data-check-final-calc]![Z-]·[Data-check-final-
calc]![lambda+]))
C
([Data-check-final-calc]![c-] + [Data-check-final-calc]![c+])/2
G    calculated conductivity
[Data-check-final-calc]![G0+] + [Data-check-final-calc]![G0-] - ((([Data-check-final-calc]!lambda0·
[Data-check-final-calc]![Z+]·[Data-check-final-calc]![Z-])/(115.2·([Data-check-final-
calc]![Z+] + [Data-check-final-calc]![Z-]))·((2·[Data-check-final-calc]!Q)/(1 + [Data-check-final-
calc]!Q^0.5)))) + 0.668·([Data-check-final-calc]![Z+] + [Data-check-final-calc]![Z-])·[Data-check-
final-calc]!C)^1.5

```

Finally, [Data-check-summary-QC]! lists the percentage error, mean and ROA of measured and calculated conductivity, as well as a comment on the reason for deviations ([Data-check-summary-QC]!Comment) and an evaluation of the analysis ([Data-check-summary-QC]!Comment2) according to the following query [calc-data-check-Summary-QC]:

Comment:

```

If([Data-check-summary-QC]!percent_error<0          and          [Data-check-summary-
QC]!conductivity_calculated>[Data-check-summary-QC]!conductivity_measured;"too many ani-

```

ons";If([Data-check-summary-QC]!percent_error<0 and [Data-check-summary-QC]!conductivity_calculated<[Data-check-summary-QC]!conductivity_measured;"not enough cations";If([Data-check-summary-QC]!percent_error>0 and [Data-check-summary-QC]!conductivity_calculated>[Data-check-summary-QC]!conductivity_measured;"too many cations";"not enough anions"))

Evaluation:

If([Data-check-summary-QC]!percent_error>5 and [Data-check-summary-QC]![ROA%]>5; "Attention! Analysis off by more than 5%!"); If([Data-check-summary-QC]!percent_error>5 and [Data-check-summary-QC]![ROA%]<5; "Attention! Analytical error too high, even though conductivity seems ok"); If([Data-check-summary-QC]!percent_error<-5 and [Data-check-summary-QC]![ROA%]>5; "Attention! Analysis off by more than 5%!"); If([Data-check-summary-QC]!percent_error<-5 and [Data-check-summary-QC]![ROA%]<5; "Attention! Analytical error too high, even though conductivity seems ok"); If([Data-check-summary-QC]!percent_error<5 and [Data-check-summary-QC]![ROA%]>5; "Attention! Range of analysis for conductivities >5%, even though analytical error seems ok"; "analysis ok"))))

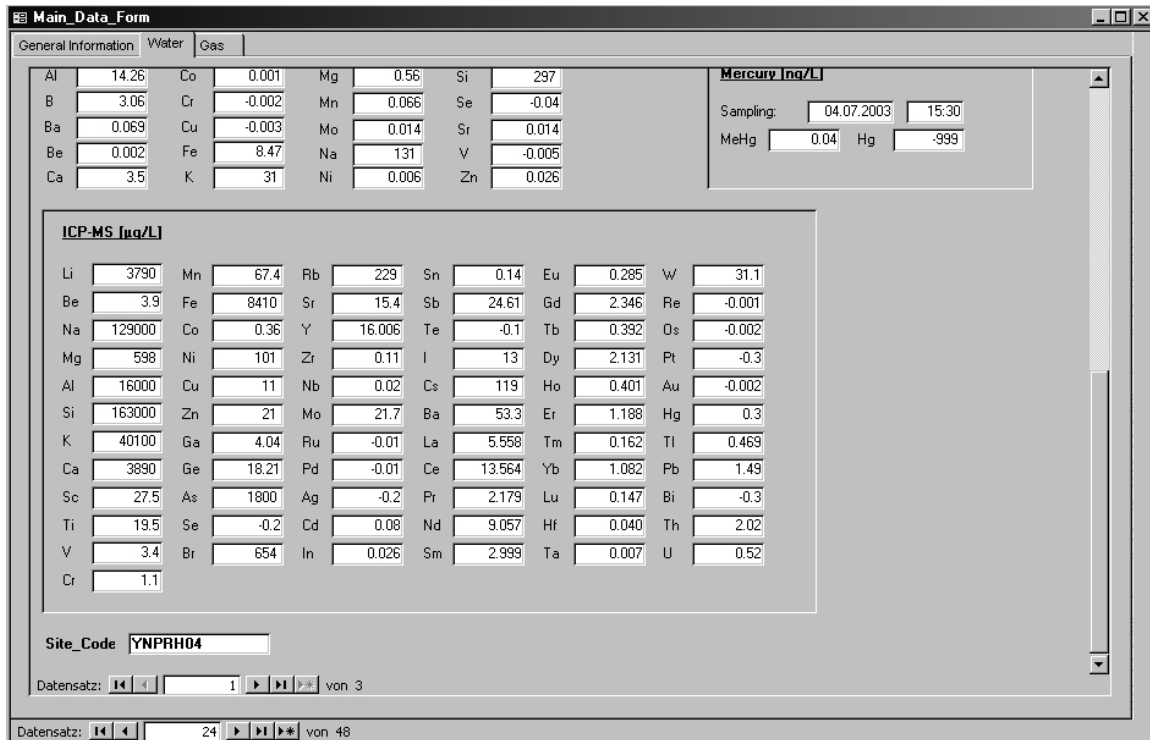
Carbon:

TOC

[TOC-water-mean]!TOC_mean_mgL; value is calculated as the mean of double determinations ([TOC-water-raw-data]!TOC_1st-determ_mgL, and [TOC-water-raw-data]!TOC_2nd-determ_mgL) [Query: calc-TOC-mean]

TIC

[TIC-water-mean]!TIC_mean_mgL; value is calculated as the mean of double determinations ([TIC-water-raw-data]!TIC_1st-determ_mgL, and [TIC-water-raw-data]!TIC_2nd-determ_mgL) [Query: calc-TIC-mean]



Mercury:

[Mercury]!Hg_ngL, [Mercury]!MeHg_ngL [Mercury]!Sampling_date, [Mercury]!Sampling_time

Mercury data only exist for 12 samples, thus these data had to be attached via a subform [Form Mercury]; in the main form data fields will be empty where no data exist

ICP-AES: **As, Al, B, Ba, Be, Ca, Cd, Co, Cr, Cu, Fe, K, Li, Mg, Mn, Mo, Na, Ni, Pb, Si, Se, Sr, V, Zn**

[ICP-AES-water-final-data]!

Raw data from the ICP-AES are listed in table [ICP-AES-water-raw-data]!; information on Wavelength, Scan Mode, and ControlMaterial given in the tables [ICP-AES-Wavelength]!, [ICP-AES-ScanMode]!, [ICP-MS-ControlMaterial]!); all samples were measured in three different dilutions: undiluted, diluted 1:10, diluted 1:100, the best fit within quantification limit ([ICP-AES-QuantLimit]!) and upper calibration range ([ICP-AES-UpperCalibRange]!) was determined via a query [Query: calc-ICP-AES-water-final-values] analogous to shown before for IC. Concentrations below the detection limit ([ICP-AES-DetectionLimit]!) are indicated as negative values; like for IC all values were checked manually afterwards, and some were corrected

ICP-MS: **Li, Be, Na, Mg, Al, Si, K, Ca, Sc, Ti, V, Cr, Mn, Fe, Co, Ni, Cu, Zn, Ga, Ge, As, Se, Br, Rb, Sr, Y, Zr, Nb, Mo, Ru, Pd, Ag, Cd, In, Sn, Sb, Te, I, Cs, Ba, La, Ce, Pr, Nd, Sm, Eu, Gd, Tb, Dy, Ho, Er, Tm, Yb, Lu, Hf, Ta, W, Re, Os, Pt, Au, Hg, Tl, Pb, Bi, Th, U**

[ICP-MS-water]!

ICP-MS data only exist for 27 samples, thus these data had to be attached via a subform [Form ICP-MS-water]; in the main form data fields will be empty where no data exist

Site Code at the bottom of the water subform page is only displayed for better orientation (it also essentially connects the water subform to the main data form, so that not all 62 records are displayed for all sites, but only the records with matching site codes)

Third page: Gas - total concentrations

The page “Gas - total conc.” contains data from the subforms “Gas-NaOCl-subform” (75 records), and “Gas-NaOH-subform” (48 records).

Gas-NaOCl subform (NaOCl samples):

primary key **Analysis-code-gas-NaOCl** ([Analysis-code-gas-NaOCl]!Analysis-code-gas-NaOCl); the analysis code gas NaOCl consists of the site code, the No. of the sampling campaign (1 = June, 5th, to June, 21st, 2003; 2 = June, 30th, to July, 12th, 2003; 3 = September, 3rd, to September, 15th, 2003; 4 = September 21st, to October, 9th, 2003), and G for gas, NaOCl for the oxidizing reagent, and an abbrevia-

tion for gas hood – oxidizing bottle –setup (according to Figure 42: wGH = with gas hood, wGH-tni = with gas hood, tube not immersed, nGH = no gas hood, nGH-cv = no gas hood, closed valves)

Sampling from... to [Analysis-code-gas-NaOCl]!Date_start, Time_start
[Analysis-code-gas-NaOCl]!Date_end, Time_end

Duration [NaOCl-time-calc]!Duration_exposed_days,
[NaOCl-time-calc]!Duration_exposed_hours [Query: calc-NaOCl-time]

The table [Analysis-code-gas-NaOCl]! as well as the other [analysis-code-gas]! tables also contain information about type of gas hood and oxidizing bottle used in each experiment that is not displayed in the respective subforms ([Analysis-code-gas-NaOCl]!Gashood_type from table: [Gashood_Type]! and ([Analysis-code-gas-NaOCl]!Oxidation_bottle_type from table [Oxidation_bottle_type!] with information on material, and size).

Figure in the center shows the setup type according to Figure 42 (link in [Pictures-Gashood-Setup]!Picture1; pictures in folder Figures / Database-Yellowstone2003)

Concentrations given on the left side are underneath the GH “wGH” (fields are empty, when sampling was done without gas hood), concentrations on the right side are in ambient air (“nGH”). Calculation from dissolved concentrations in the oxidizing solution to concentrations in the gas phase are done according to the following equation (details explained in section 4.2.3.2):

$$c = \frac{m \cdot \Delta x}{t \cdot A \cdot D}$$

The origin of the single parameters is explained in the following for the case with gas hood, the non gas hood case goes analogous. Note: As described in section 4.2.3.2 concentrations for setups with gas hoods are upper limits for the two end-member models of zero concentration in ambient air and underneath the gas hood (a similar warning is displayed at the end of the page “Gas - total conc.”).

AAS (As) **m** conc. [μg] = [AAS-Boulder-gas-NaOCl-considered-data]! [$\mu\text{g/L}$] · 0.1 [L] oxidizing solution

* raw data from up to 3 triple determinations in [AAS-Boulder-gas-NaOCl-raw]!

* converted to final data calculating means of the triple determinations and considering dilution factor ([AAS-Boulder-water-final]! via Query: calc-AAS-Boulder-gas-NaOCl)

* final data are corrected for the max value of three blank determinations (2 lab blanks 1:100 diluted NaOCl (YNPBW02-1G-NaOCl, YNPBW04-2G-NaOCl), and 1 field blank YNPHL01-3G-NaOCl-nGH-cv in table [AAS-Boulder-gas-field-lab-blanks]!), [AAS-Boulder-gas-blank-max]! contains the maximum As blank; Query [calc-AAS-Boulder-gas-NaOCl-considered-data] corrects every As value for this blank and writes it back to table [AAS-Boulder-gas-NaOCl-considered-data]! considering values below detection limit ([AAS-DL-QL-UCR]!) as negative values

Δx [Gas-Difflength-area-NaOCl-NaOH]!wGH_Diffusion_length_cm

A [Gas-Difflength-area-NaOCl-NaOH]!wGH_Area_cm2

t [NaOCl-time-calc]!Duration_exposed_hours · 60 · 60

D [Gas-Diffcoeff-NaOCl-As]! Diffusion_coefficient_mean_cm2s-1 (Query [calc-Gas-Diffcoeff-NaOCl-As] calculated as explained in section 4.2.3.2 according to the following equation:

$$D = 0.001 \frac{T^{1.75} \cdot M_r^{0.5}}{P \cdot (V_A^{1/3} - V_B^{1/3})^2}$$

Option “show range” (default invisible; click displays minimum and maximum values considering uncertainties for m, Δx , and D; uncertainties of A and t were considered to be negligible)

m max. concentration: m · 1.01; min. concentration: m = 0.99

Δx [Gas-Difflength-area-NaOCl-NaOH]!wGH_max_Diffusion_length_cm considering wGH_Diffusion_length_uncertainty_cm via Query [calc-Gas-Difflength-area-NaOCl-NaOH], analogous for minimum length

D maximum diffusion coefficient considers uncertainty in temperature, and dominant species in gas, maximum value is for Temperature +10°C and an assumed predominance of AsH₃ (with the lowest molecular weight for any volatile species), minimum values is for Temperature -10°C and an assumed predomi-

nance of AsCl_3 (with the highest molecular weight) according to the following formulas in Query [calc-Gas-Diffcoeff-NaOCl-As]:

$$0.001 \cdot [\text{Gas-Diffcoeff-NaOCl-As}]! [\text{Temperature_at_30cm_K}+10]^{1.75} \cdot [\text{Gas-Diffcoeff-NaOCl-As}]! \text{Mr_AsH}_3^{0.5} / [\text{Gas-Diffcoeff-NaOCl-As}]! p_bar / ([\text{Gas-Diffcoeff-NaOCl-As}]! [\text{VA_cm}^3\text{mol}^{-1}]^{1/3} + [\text{Gas-Diffcoeff-NaOCl-As}]! [\text{VB_AsH}_3\text{_cm}^3\text{mol}^{-1}]^{1/3})^2$$

$$0.001 \cdot [\text{Gas-Diffcoeff-NaOCl-As}]! [\text{Temperature_at_30cm_K}-10]^{1.75} \cdot [\text{Gas-Diffcoeff-NaOCl-As}]! \text{Mr_AsCl}_3^{0.5} / [\text{Gas-Diffcoeff-NaOCl-As}]! p_bar / ([\text{Gas-Diffcoeff-NaOCl-As}]! [\text{VA_cm}^3\text{mol}^{-1}]^{1/3} + [\text{Gas-Diffcoeff-NaOCl-As}]! [\text{VB_AsCl}_3\text{_cm}^3\text{mol}^{-1}]^{1/3})^2$$

Since the diffusion coefficient shows an inverse correlation with concentration in the gas phase, minimum diffusion coefficients had to be taken for maximum concentrations and vice versa-

ICP-AES (analogous to HG-AAS explained before)

m [ICP-AES-gas-NaOCl-raw-data]!; [ICP-AES-gas-NaOCl-final-data]!

Query: calc-ICP-AES-gas-NaOCl-final-values considers the different dilutions as explained for ICP-AES water before; values in [ICP-AES-gas-NaOCl-considered-data]! are corrected for the maximum blank values ([ICP-AES-gas-field-lab-blanks]! and [ICP-AES-gas-blank-max]!); only elements with concentrations significantly above detection limit and blank value were considered: As, Al, B, Ba, Cu, Fe, K, Li, SiO_2 , Sr, Zn

Δx , A, t, and D are the same values as for As determination described before

Range for m, uncertainties of $\pm 2\%$ were considered, expect for As ($\pm 1\%$) and K ($\pm 3\%$)

IC (S(VI)) (analogous to HG-AAS explained before)

m [IC-Freiberg-gas-NaOCl-SO4-2]!SO4_mgL; uncertainty $\pm 5\%$

ICP-MS (analogous to HG-AAS and ICP-AES explained before)

m [ICP-MS-gas-NaOCl-raw-data]!; [ICP-MS-gas-NaOCl-final-data]!

Query: calc-ICP-MS-gas-NaOCl-final-values considers dilution of NaOCl samples before sending them to Actlab (1:1); [ICP-MS-gas-NaOCl-considered-data]! corrected for blank value ([ICP-MS-gas-blank]!), and only elements significantly above detection limit ([ICP-MS-Detection-Limit]!) and blank: Li, Mg, Al, Si, K, Ti, V, Cr, Mn, Fe, Co, Ni, Cu, Zn, Ga, Ge, As, Rb, Sr, Y, Zr, Nb, Mo, Cd, Sb, Cs, Ba, La, Ce, Pr, Nd, Sm, Gd, Dy, Er, Yb, Hf, W, Pb, Th.

Range is not displayed for ICP-MS due to the large amount of data disturbing the form's clarity. If required it can easily be calculated the same way as described for ICP-AES.

Analysis code at the end of the page displayed again just for orientation

Main_Data_Form

General Information | Water | Gas - total conc. | Gas comparison wGH-nGH | Gas - total conc. (P. DB) | Gas - As speciation

NaOCl samples
ICP-MS [$\mu\text{g}/\text{m}^3$]

Mean upper conc. [$\mu\text{g}/\text{m}^3$] underneath gas hood*				Mean upper conc. [$\mu\text{g}/\text{m}^3$] in ambient air*					
Li	16957	Ga	279	La	mean upper limit (see *explanation at the end of this page!)			La	20
Mg	150862	Ge	-52	Ce	275	Mg	12572	Ge	-4
Al	361925	As	163003	Pr	22	Al	30160	As	13584
Si	8308317	Fb	2273	Nd	53	Si	692360	Fb	189
K	16625315	Sr	8216	Sm	13	K	1385443	Sr	685
Ti	12346	Y	41	Gd	16	Ti	1029	Y	3
V	4519	Zr	888	Dy	7	V	377	Zr	74
Cr	32357	Nb	318	Er	7	Cr	2696	Nb	27
Mn	2155	Mo	22389	Yb	7	Mn	180	Mo	1866
Fe	54745	Cd	-52	Hf	22	Fe	4562	Cd	-4
Co	114	Sb	26644	W	10474	Co	10	Sb	2220
Ni	2691253	Cs	-5	Pb	773	Ni	224271	Cs	0
Cu	196835	Ba	79105	Th	39	Cu	16403	Ba	6592
Zn	210767					Zn	17564		

Datensatz: 1 von 1

***Attention!**
For setups with gas hoods (GH), concentrations given are upper limits. Their calculation is based on the assumption of two end member models. In the first case it is assumed that there is no concentration gradient between oxidising solution and gashood ($c(\text{GH}) = 0$). The total amount of volatile compounds then results from diffusion between ambient air and oxidising solution ($c(\text{ambient air}) = \text{max}$). In the other end member calculation there is no concentration gradient between ambient air and oxidising solution ($c(\text{ambient air}) = 0$) and all volatile compounds diffuse via the gashood ($c(\text{GH}) = \text{max}$).

Analysis code: YNPRH01-1G-NaOCl-wGH

Datensatz: 1 von 5

Datensatz: 21 von 48

NaOH samples

Analysis code: YNPRH01-1G-NaOH-wGH

Sampling from: 21.06.2003 12:15:00
to: 30.06.2003 10:30:00

Duration: 8.92 days 214 hours

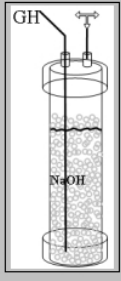
Photometry [mg/m^3]:

Ambient air:
(for setups with gas hood conc. given are upper limits)

Cl: 131
(71 to 204)

Gas hood:
(conc. given are upper limits)

Cl: 1573
(943 to 2332)



Datensatz: 1 von 2

Gas-NaOH-subform (NaOH samples)

primary key Analysis-code-gas-NaOH [Analysis-code-gas-NaOH]!Analysis-code-gas-NaOH; analysis code analogous to analysis code NaOCl described before

Sampling from... to, Duration analogous to fields described before for NaOCl

Figure in the center shows the setup type according to Figure 42 (link in [Pictures-Gashood-Setup]!Picture2; pictures in folder Figures / Database-Yellowstone2003)

Photometry (Cl)

m [Photometry-gas-NaOH-Cl]!Cl_mgL Gas-Diffcoeff-NaOH-Cl; uncertainty $\pm 5\%$

D [Gas-Diffcoeff-NaOH-Cl]!Diffusion_coefficient_mean_cm2s-1 (for range only temperature uncertainty was considered with $\pm 10^\circ\text{C}$) (Query: [calc-Gas-Diffcoeff-NaOH-Cl])

Fourth page: Gas comparison wGH-nGH

The page "Gas comparison wGH-nGH" contains data from the subforms "Comparison-wGH-nGH-NaOCl-As" (17 records), and "Comparison-wGH-nGH-NaOH" (8 records). While the concentrations for gas hood setups (wGH) on page "Gas- total conc." are only upper limits for either ambient air or gas hood, this page takes concentrations in ambient air from nGH setups as representative for wGH setups, too, and considering this concentration, calculates the mean concentration underneath the gas hood as described in section 4.2.3.2. Since this was only possible at sites, where nGH and wGH were done parallel the dataset is smaller.

Subform “Comparison-wGH-nGH-NaOCl-As”

Site codes of setup with (wGH on top) and without gas hood (nGH below); primary key is nGH for calculations in ambient air, for all others it is wGH

AAS **ambient air:** [Gas-ugm-3-corrected-NaOCl-wGH-nGH-mean]!nGH_As_ugm-3 ([essentially the same as Gas-ugm-3-NaOCl-mean]!nGH_As_ugm-3, only negative values (below detection limit) were replaced by -0.3 · detection limit, since this value (c₁) is needed for the following calculation of c₂ according to equation:

$$\Delta c_2 = \Delta x_2 \cdot \left(\frac{m}{t \cdot A \cdot D} - \frac{\Delta c_1}{\Delta x_1} \right)$$

under gas hood [Gas-ugm-3-corrected-NaOCl-wGH-nGH-mean]!wGH_As_ugm-3 (calculated via the Query [calc-Gas-ugm-3-corrected-NaOCl-wGH-nGH-mean])

decrease to... [%] ambient air : gas hood · 100 in table [Gas-ugm-3-corrected-NaOCl-wGH-nGH-gradientsAs]!mean-gradient-wGH-nGH from Query [calc-Gas-ugm-3-corrected-NaOCl-gradientsAs]

Range calculations done as explained before. For a maximum value of c₂, maximum x₂, maximum m, and minimum D, c₁, and x₁ were taken, vice versa for minimum c₂.

Only As concentrations from HG-AAS are displayed in this main data form. The tables [calc-Gas-ugm-3-corrected-NaOCl-wGH-nGH-mean]!, max and min also contain the data for all other elements determined by ICP-AES and for S(VI) determined by IC.

Subform “Comparison-wGH-nGH-NaOH”

Analogous to As explained before.

Table [Gas-mgm-3-corrected-NaOH]! Contains mean, maximum, and minimum concentrations for ambient air and gas hood derived from Query [calc-Gas-mgm-3-corrected-NaOH]

Fifth page: Gas - total conc. (P, DB)

The page “Gas – total conc. (P, DB)” contains data from the subforms “Gas-NaOCl-P-subform” (4 records), and “Gas-NaOCl-DB-subform” (21 records).

Gas-NaOCl-P-subform

primary key **Analysis-code-gas-NaOCl-P** [Analysis-code-gas-NaOCl-P]! Analysis-code-gas-NaOCl-P; analysis code analogous to analysis code NaOCl described before

Sampling from... to, Duration analogous to fields described before for NaOCl

Sampled gas volume [NaOCl-P-time-amount-calc]! sampled_gas_volume_L calculated from pump_hubs · 0.1 L per hub via Query [calc-NaOCl-P-time-amount]

AAS, ICP-AES Concentration is calculated as $c = \frac{m}{V}$ as described in section 4.2.3.2

For **m** the tables [AAS-Boulder-gas-NaOCl-considered-data]! and [ICP-AES-gas-NaOCl-considered-data]! were used; results in [Gas-ugm-3-NaOCl-P] (Query [calc-Gas-ugm-3-NaOCl-P])

The screenshot shows a software interface with two main data entry panels. The left panel, titled 'NaOCl sample from active gas pumping', contains fields for 'Analysis code' (YNPHL01-2G-NaOCl-wGH-P), 'Sampling from' (09.07.2003 11:15:00 to 09.07.2003 12:25:00), 'Duration' (0.04 days, 0.9 hours), 'sampled gas volume' (20 L), 'AAS [µg/m3]' (As: 18), and a table for 'ICP-AES [µg/m3]' with values for As, Ba, K, Sr, Al, Cu, Li, Zn, B, Fe, SiO2, and SO4. The right panel, titled 'NaOCl sample from diffusion bowls', contains fields for 'Analysis code' (YNPHL01-3G-NaOCl-DB31), 'Sampling from' (09.09.2003 14:00:00 to 12.09.2003 11:00:00), 'Duration' (2.88 days, 69 hours), and 'AAS [µg/m3]' (As: -0.1, range -0.1 to -0.2). At the bottom right, there is a 'Datensatz:' section showing '1' of '5' records.

Gas-NaOCl-DB-subform

primary key **Analysis-code-gas-NaOCl-DB** [Analysis-code-gas-NaOCl-DB]! Analysis-code-gas-NaOCl-DB; analysis code analogous to analysis codes described before

Sampling from... to, Duration analogous to fields described before for NaOCl

AAS Only As was determined for DB setups [AAS-Boulder-gas-NaOCl-considered-data]!; results in [Gas-ugm-3-NaOCl-DB]!As_ugm-3_mean, max, and min from Query [calc-Gas-ugm3-NaOCl-DB] as described before on page “gas – total conc.”

Sixth page: Gas - As speciation

The page “Gas - As speciation” contains records from the “SPME-subform” (60 records) in the center as well as a link to the “SS-subform” (40 records) in the lower right corner.

Main_Data_Form

General Information | Water | Gas - total conc. | Gas comparison wGH-nGH | Gas - total conc. (P, DB) | Gas - As speciation

SPME (solid phase micro extraction)

Analysis code:

Sampling from: to

Duration: days hours

SPME type:

Identified volatile As species:

[CH3]3As: @ min

[CH3]2AsCl: @ min

[CH3]AsCl2: @ min

[CH3]2AsSCH3: @ min

* Note: No standard calibration was done. Integrated peak areas are for semiquantitative comparison only. Occasional poor peak resolution from the background or double peaks can be seen in the respective figures (black area = integrated area).

Datensatz: von 4

Open Subform Solid Sorbents

only general information on solid sorbents setup (NO volatile As species found)

Datensatz: von 48

SPME-subform (solid-phase micro extraction)

primary key [Analysis-code-gas-SPME]!Analysis-code-gas-SPME; analysis code analogous to analysis code NaOCl described before, instead of NaOCl type of fiber (PDMS, CAR, DVB) and No. of GC-MS analysis campaign (1, 2, 4 analyzed in Denver, 3 and 5 in Bozeman); respective GC-MS equipment, columns, and operating conditions are in table [GC-MS-conditions]!

Sampling from... to, Duration analogous to fields described before

SPME type [Analysis-code-gas-SPME]!SPME_type, detailed description of types, application range, max. temperatures, pH conditions, etc. in table [SPME-Type]!

Picture1 Chromatogram; link in [Pictures-Chromatograms]!Picture1, pictures saved in Folder Figures / Database-Yellowstone2003; double-click on the small picture opens an enlarged version of the same picture ([Pictures-Chromatograms]!Picture1B)

Picture2 detected (CH₃)₃As; [Pictures-Chromatograms]!Picture2 and Picture2B. If there is no volatile (CH₃)₃As detected in the chromatogram, a picture with the text “No volatile As species found in chromatogram” is displayed.

Picture3 (CH₃)₂AsCl

Picture4 (CH₃)AsCl₂

Picture5 (CH₃)₂AsS(CH₃)

Area [SPME-peak-area]!

Retention time [SPME-retention-time]!

The **subform** for **solid sorbents** (SS-subform) is not included in the main data form, since no volatile As species were found on solid sorbents at all. Via the command “Open Subform Solid Sorbents” in the lower right corner it is possible to get general information on solid sorbent setup for each site. The sub-window is blank if no solid sorbent was used for the site. Information on sampling date and time origin from the respective tables as explained before. Primary key is [Analysis-code-gas-SS]!Analysis-code-gas-SS. The table [SS-Type]! contains detailed description of SS types, surface area, sampling range, max. temperatures, etc.

Appendix 10 Overview of sampling sites with parameters determined in the field campaigns from June, 5th to July, 16th, 2003 and from September, 2nd to October, 12th 2003

Area	Site	Standard water sample ¹	Water sample ICP-MS ²	Mercury ³	Gas sample NaOCl ⁴	Gas sample NaOCl ICP-MS ⁵	Gas sample P / DB ⁶	Gas sample NaOH ⁷	Gas sample SS ⁸	Gas sample SPME ⁹
Gibbon Geyser Basin	YNPGG01				05.07. ^{S1}			08.07. ^{S1}	12.07.	
	YNPGG02	03.07.			05.07. ^{S1} 02.10. ^{S1,3}			10.07. ^{S1} 07.10. ^{S1,3}		12.07. CAR
	YNPGG03				05.07. ^{S1} 02.10. ^{S1,3}			10.07. ^{S1} 07.10. ^{S1,3}		12.07. CAR
	YNPGG04	03.07. 11.07. 22.09.	22.09.		05.07. ^{S1} 02.10. ^{S1,3}	02.10. ^{S1}	10.07. P	08.07. ^{S1} 07.10. ^{S1,3}	12.07.	
	YNPGG05	10.07. 07.10.			05.07. ^{S1} 02.10. ^{S1,3}			08.07. ^{S1} 07.10. ^{S1,3}	12.07.	
	YNPGG06	05.07.								
	YNPGG07	10.07. 07.10.			02.10. ^{S1}			07.10. ^{S1}		
	YNPGG08	07.10.			02.10. ^{S3}			07.10. ^{S3}		
Hazle Lake	YNPHL01	18.06. 09.07. 09.09.	18.06. 09.09.	07.06.	18.06. ^{S1} 04.07. ^{S1} 12.09. ^{S1,3,4}	18.06. ^{S1} 12.09. ^{S1}	09.07. P 09.09. DB	09.07. ^{S1} 15.09. ^{S1}	30.06.	21.06. CAR 12.07. CAR, DVB 15.09. CAR
	YNPHL02	16.06.		07.06.	18.06. ^{S1}				30.06.	
	YNPHL03	14.09.			15.09. ^{S3}		09.09. DB	15.09. ^{S3}		15.09. CAR
Lower Geyser B.	YNPLG01	01.07.	01.07.		17.06. ^{S1} 09.07. ^{S1}	09.07. ^{S1}		12.07. ^{S1}		
	YNPLG02	02.07.	02.07.		05.07. ^{S1}	05.07. ^{S1}		09.07. ^{S1}	12.07.	12.07. CAR, PDMS
	YNPLG03	02.07.	02.07.		06.07. ^{S1}	06.07. ^{S1}		09.07. ^{S1}	12.07.	
Nymph Lake / Frying Pan Spring	YNPNL01	12.06.			18.06. ^{S1}					
	YNPNL02	12.06. 06.07. 14.09.	12.06.	18.06. MeHg	**18.06. ^{S1} 12.07. ^{S3} 04.07. ^{S1} *12.09. ^{S1}	18.06. ^{S1}	09.09. DB	08.07. ^{S1} 12.09. ^{S1}	12.07.	21.06. CAR 12.07. CAR 09.09. CAR, DVB
	YNPNL03	18.06. 06.07. 14.09.	18.06.		18.06. ^{S1} 06.07. ^{S1} **12.09. ^{S1}	18.06. ^{S1}		08.07. ^{S1} 12.09. ^{S1}	12.07.	09.09. CAR, DVB
	YNPNL04	12.06. 07.07. 13.09.	12.06.	18.06.	18.06. ^{S1} 07.07. ^{S1} *12.09. ^{S1}	18.06. ^{S1}	09.09. DB	30.06. ^{S1} 12.09. ^{S1}	30.06.	21.06. CAR, DVB, PDMS 09.09. CAR, DVB, PDMS
	YNPNL05	16.06. 07.07.	16.06.	18.06.	20.06. ^{S1} 07.07. ^{S1}	20.06. ^{S1}		30.06. ^{S1}	30.06.	
	YNPNL06				20.06. ^{S1}					
Ragged Hills	YNPRH01	11.06. 04.07. 14.09.	11.06. 14.09.	17.06.	17.06. ^{S1} 04.07. ^{S1} 15.09. ^{S1,2,3}	17.06. ^{S1} 15.09. ^{S1}	11.07. P 08.09. DB	30.06. ^{S1} 11.07. ^{S1}	30.06.	21.06. CAR, PDMS 09.09. CAR, PDMS
	YNPRH02				17.06. ^{S1}			30.06. ^{S1}	30.06.	21.06. CAR
	YNPRH03	11.06.		17.06.	17.06. ^{S1}			04.07. ^{S1}	30.06.	21.06. CAR
	YNPRH04	19.06. 04.07. 14.09.	19.06. 14.09.	04.07. MeHg	20.06. ^{S1} 04.07. ^{S1} 15.09. ^{S1,3}	20.06. ^{S1} 15.09. ^{S1}		30.06. ^{S1} 08.07. ^{S1} 15.09. ^{S3}	11.07.	09.09. CAR, PDMS 15.09. DVB
	YNPRH05	14.06. 13.09.	14.06. 13.09.		17.06. ^{S1} 15.09. ^{S1,3} 30.09. ^{S1,2,3}	17.06. ^{S1} 15.09. ^{S1}		30.06. ^{S1} 15.09. ^{S1}	30.06.	21.06. CAR 09.09. CAR, DVB 15.09. DVB (2x), PDMS 07.10. CAR, PDMS

Appendix 10

Area	Site	Standard water sample ¹	Water sample ICP-MS ²	Mercury ³	Gas sample NaOCl ⁴	Gas sample NaOCl ICP-MS ⁵	Gas sample P / DB ⁶	Gas sample NaOH ⁷	Gas sample SS ⁸	Gas sample SPME ⁹
Ragged Hills, Norris Geyser Basin	YNPRH06				20.06. ^{S1} 11.07. ^{S3} 04.07. ^{S1} 15.09. ^{S3}	20.06. ^{S1} 15.09. ^{S3}	11.07. P	08.07. ^{S1}	30.06.	11.07. CAR 09.09. CAR 15.09. CAR, DVB, PDMS 07.10. CAR, DVB
	YNPRH07	11.07.	11.07.		20.06. ^{S1} 04.07. ^{S1}	04.07. ^{S1}		30.06. ^{S1} 08.07. ^{S1}	30.06.	11.07. CAR, PDMS
	YNPRH08	15.06. 29.09.	29.09.	17.06.	20.06. ^{S1} 08.07. ^{S1}			30.06. ^{S1}	30.06.	
	YNPRH09	15.06.		17.06. MeHg	20.06. ^{S1}				30.06.	
	YNPRH10	29.09.	29.09.		15.09. ^{S3}	15.09. ^{S3}	08.09. DB			15.09. CAR
	YNPRH11	12.09.			15.09. ^{S3} 30.09. ^{S1,3} **30.09. ^{S2}			15.09. ^{S3}		15.09. CAR, PDMS
	YNPRH12				15.09. ^{S3} 30.09. ^{S1}					15.09. CAR
	YNPRH13	13.09.	13.09.							
	YNPRH14	13.09.								
	YNPRH15	13.09.								07.10. CAR
	YNPRH16	29.09.								
	YNPRH17	29.09.	29.09.							
	YNPRH18	30.09.	30.09.	01.06.						
	YNPRH19	30.09.	30.09.							
	YNPRH20	30.09.	30.09.	30.05.	05.10. ^{S1}	05.10. ^{S1}		09.10. ^{S1}		
	YNPRH21	02.10.	02.10.							
	YNPRH22	02.10.			05.10. ^{S1,2,3}			09.10. ^{S1,2,3}		
	YNPRH23				05.10. ^{S1,2} **05.10. ^{S3}			09.10. ^{S1,2,3}		
	YNPRH24	02.10.								
	YNPRH25	02.10.								
YNPRH26	05.10.	05.10.							07.10. DVB (3x), CAR (3x), PDMS (2x)	
YNPRH27	05.10.	05.10.								
YNPRH28	05.10.									
Σ	48	60	27	12	80	21		49	20	60

¹ Standard water sample includes measurement of temperature, pH, conductivity, on-site photometry on Fe(II)/Fe(tot), S(-II), SiO₂, total As, As species (As(III) / As(V) / MMAA / DMAA), IC (Cl, S(VI), F, Br, N(V)), TOC, TIC, ICP-AES (As, Al, B, Ba, Be, Ca, Cd, Co, Cr, Cu, Fe, K, Li, Mg, Mn, Mo, Na, Ni, Pb, Si, Se, Sr, V, Zn); redox potential and oxygen were not determined at all sites and all times due to unstable values and problems with the devices due

² Water sample ICP-MS was analyzed for Li, Be, Na, Mg, Al, Si, K, Ca, Sc, Ti, V, Cr, Mn, Fe, Co, Ni, Cu, Zn, Ga, Ge, As, Se, Br, Rb, Sr, Y, Zr, Nb, Mo, Ru, Pd, Ag, Cd, In, Sn, Sb, Te, I, Cs, Ba, La, Ce, Pr, Nd, Sm, Eu, Gd, Tb, Dy, Ho, Er, Tm, Yb, Lu, Hf, Ta, W, Re, Os, Pt, Au, Hg, Tl, Pb, Bi, Th, U

³ Mercury sampling includes inorganic Hg and Methyl-Hg unless otherwise stated

⁴ Gas sample NaOCl was analyzed for the sum of volatile metallics by ICP-AES, for As by HG-AAS; and for dissolved S(VI) from volatile H₂S by IC; ^{S1-4} = Setup No. according to Figure 42; * not enough sample left for ICP-AES analysis, ** samples analyzed, but results dismissed due to possible contaminations in the field (bottles not tight)

⁵ Gas sample NaOCl ICP-MS was analyzed for the sum of volatile metallics by ICP-MS

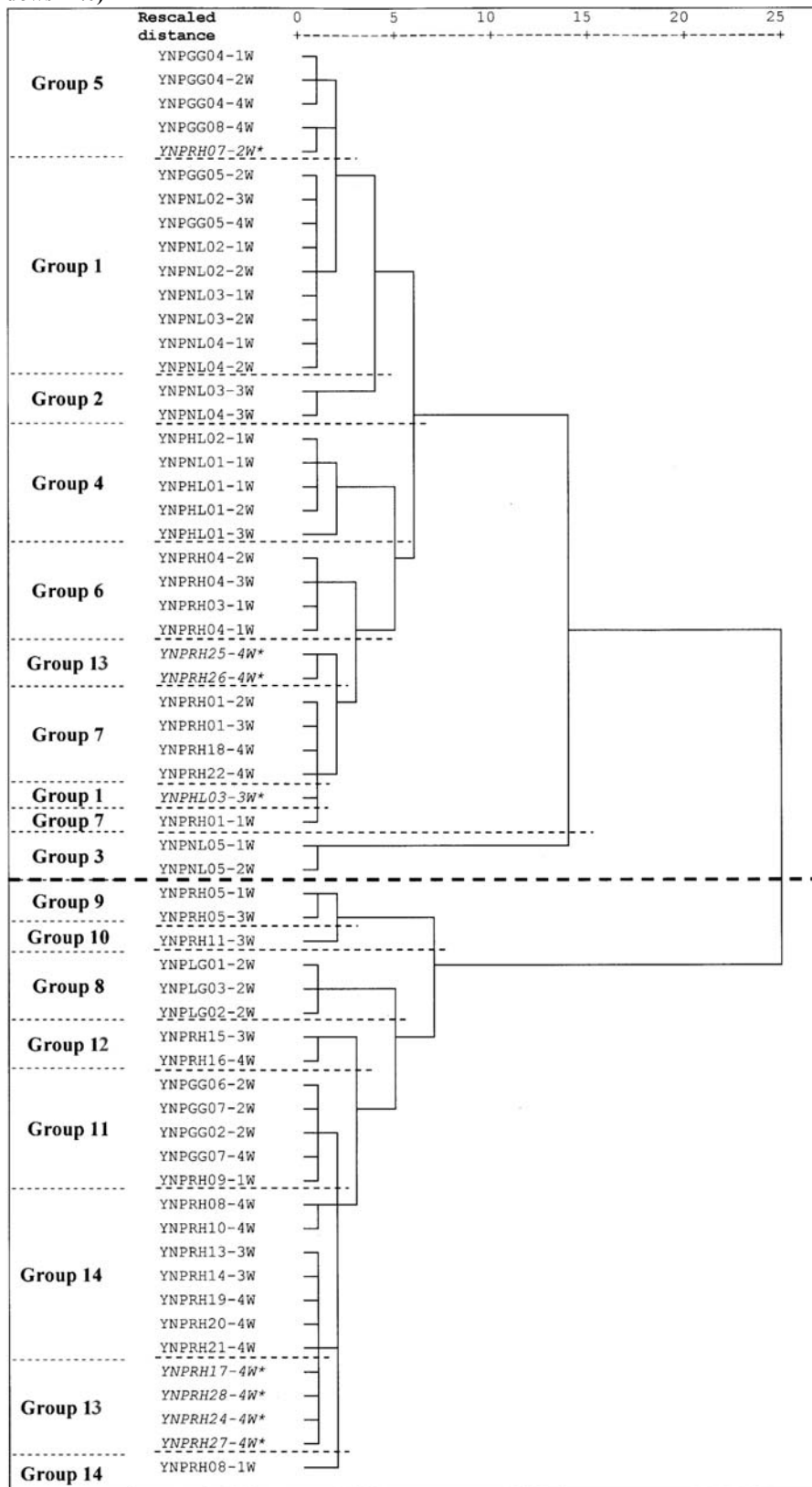
⁶ Gas sample NaOCl collected by active pumping (P) and by diffusion bowls (DB)

⁷ Gas sample NaOH was analyzed for dissolved Cl from volatile HCl

⁸ Gas sample SS = solid sorbent (Tenax TA and Carboxen 564)

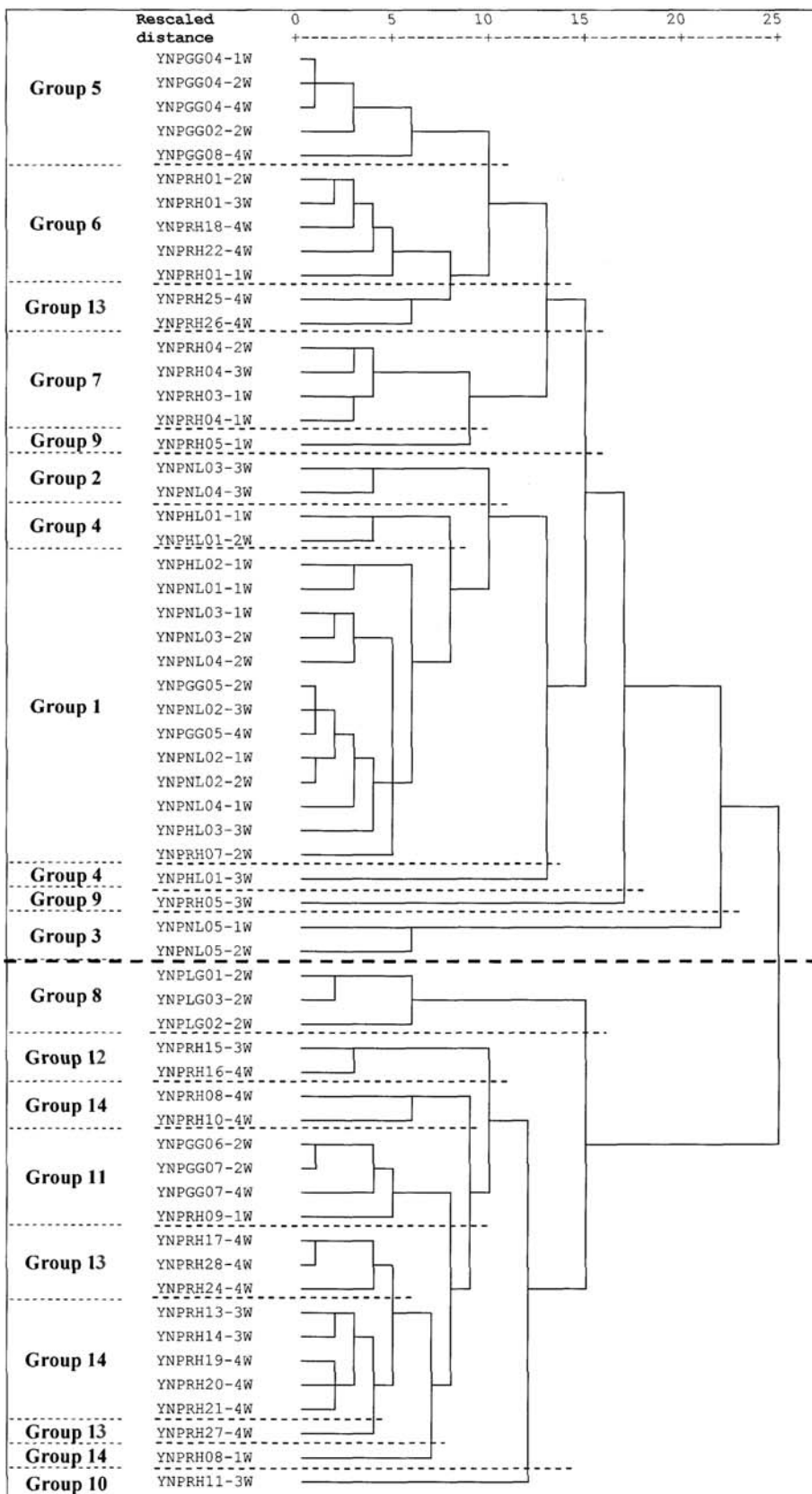
⁹ Gas sample SPME = Solid-phase micro-extraction fibers (PDMS = polydimethylsiloxane, PDMS-CAR = polydimethylsiloxane Carboxen, PDMS-CAR-DVB = polydimethylsiloxane Carboxen divinylbenzene)

Appendix 11 Dendrogram of cluster analysis of 60 water samples by Ward's method (program: SPSS for Windows 11.0)



* Manual adaptations made to the membership in this dendrogram for the final cluster membership are: YNPRH07-2W shifted from subgroup 5 to subgroup 1 (as it is in Average Linkage), YNPHL03-3W shifted from subgroup 7 to subgroup 1 (as it is in Average Linkage), YNPRH25-4W, YNPRH26-4W joined to subgroup 13, subgroup 14 separated from subgroup 13

Appendix 12 Dendrogram of cluster analysis of 60 water samples by the Average Linkage Within Groups method (program: SPSS for Windows 11.0)



Appendix 13 Kruskal-Wallis test for overall difference between the 14 subgroups derived from cluster analysis for water samples after Ward's method, Average Linkage Within Groups method and an optimized cluster analysis based on Ward's method with manual adaptation as explained in Appendix 11; df = degree of freedom; significance levels > 1% (not accepted as significant) are marked in bold

	Ward's method			Average Linkage Within Group method			Optimized cluster analysis (Ward and manually adapted)		
	Chi-Square	df	significance level	Chi-Square	df	significance level	Chi-Square	df	significance level
{H⁺}	46	13	0.00%	40	13	0.01%	48	13	0.00%
temperature	41	13	0.01%	36	13	0.07%	40	13	0.01%
conductivity	49	13	0.00%	51	13	0.00%	49	13	0.00%
F	50	13	0.00%	48	13	0.00%	52	13	0.00%
Cl	54	13	0.00%	53	13	0.00%	55	13	0.00%
Br	54	13	0.00%	53	13	0.00%	56	13	0.00%
N(V)	25	13	2.40%	21	13	7.70%	23	13	4.20%
S(VI)	50	13	0.00%	50	13	0.00%	50	13	0.00%
As(III)	53	13	0.00%	51	13	0.00%	54	13	0.00%
As(V)	51	13	0.00%	50	13	0.00%	50	13	0.00%
MMAA	46	13	0.00%	43	13	0.00%	44	13	0.00%
DMAA	49	13	0.00%	39	13	0.02%	50	13	0.00%
Al	44	13	0.00%	42	13	0.01%	44	13	0.00%
B	53	13	0.00%	52	13	0.00%	54	13	0.00%
Ba	40	13	0.01%	30	13	0.51%	49	13	0.00%
Be	44	13	0.00%	36	13	0.07%	41	13	0.01%
Ca	39	13	0.02%	27	13	1.20%	42	13	0.01%
Cd	28	13	0.93%	31	13	0.35%	29	13	0.66%
Co	30	13	0.52%	29	13	0.71%	29	13	0.61%
Cr	46	13	0.00%	50	13	0.00%	46	13	0.00%
Cu	22	13	5.00%	19	13	11.00%	14	13	38.00%
K	43	13	0.01%	36	13	0.05%	40	13	0.01%
Li	53	13	0.00%	51	13	0.00%	56	13	0.00%
Mg	45	13	0.00%	39	13	0.02%	43	13	0.00%
Mn	46	13	0.00%	39	13	0.02%	44	13	0.00%
Mo	52	13	0.00%	50	13	0.00%	51	13	0.00%
Na	52	13	0.00%	51	13	0.00%	55	13	0.00%
Ni	40	13	0.01%	38	13	0.03%	41	13	0.01%
Pb	28	13	1.00%	38	13	0.03%	25	13	2.10%
Sr	41	13	0.01%	29	13	0.69%	40	13	0.02%
V	59	13	0.00%	59	13	0.00%	59	13	0.00%
Zn	48	13	0.00%	42	13	0.01%	45	13	0.00%
SiO₂	51	13	0.00%	48	13	0.00%	51	13	0.00%
S(-II)	40	13	0.02%	32	13	0.21%	35	13	0.10%
Fe(II)	47	13	0.00%	45	13	0.00%	46	13	0.00%
Fe(III)	42	13	0.01%	36	13	0.06%	42	13	0.01%
TIC	41	13	0.01%	30	13	0.49%	38	13	0.03%
TOC	40	13	0.01%	40	13	0.01%	43	13	0.00%

	{H ⁺ }	temp	cond	F	Cl	Br	N(V)	S(VI)	As	As(III)	As(V)	MMAA	DMAA
Mn	0.51	-0.43	-0.06	-0.58	-0.38	-0.39	0.23	0.55	-0.38	-0.40	-0.48	-0.49	-0.05
	0.0%	0.1%	66.0%	0.0%	0.2%	0.2%	8.2%	0.0%	0.2%	0.2%	0.0%	0.0%	68.0%
Mo	-0.55	0.43	0.44	0.74	0.73	0.71	-0.17	-0.64	0.58	0.59	0.60	0.59	0.34
	0.0%	0.1%	0.1%	0.0%	0.0%	0.0%	19.8%	0.0%	0.0%	0.0%	0.0%	0.0%	0.8%
Na	-0.71	0.38	0.57	0.89	0.95	0.93	-0.08	-0.66	0.88	0.87	0.83	0.76	0.66
	0.0%	0.3%	0.0%	0.0%	0.0%	0.0%	56.6%	0.0%	0.0%	0.0%	0.0%	0.0%	0.0%
Ni	0.59	-0.29	0.27	-0.32	-0.21	-0.23	0.24	0.56	-0.05	-0.10	-0.11	-0.23	0.15
	0.0%	2.4%	3.9%	1.2%	10.5%	7.3%	6.4%	0.0%	72.3%	45.2%	41.0%	8.1%	25.5%
Pb	0.19	0.20	0.28	0.05	0.04	0.04	-0.02	0.17	0.08	0.11	-0.08	-0.19	-0.06
	14.8%	13.1%	3.2%	69.7%	75.4%	76.5%	88.5%	20.1%	52.2%	41.8%	56.5%	15.0%	66.5%
Sr	0.18	-0.38	0.21	-0.21	0.02	0.02	0.13	0.10	-0.11	-0.12	-0.24	-0.16	0.16
	18.1%	0.3%	10.3%	11.2%	87.7%	87.5%	30.7%	43.7%	40.1%	35.8%	6.9%	21.9%	23.2%
V	0.44	0.02	0.27	-0.23	-0.22	-0.25	0.16	0.47	-0.21	-0.19	-0.31	-0.36	-0.21
	0.0%	89.3%	3.9%	7.7%	8.8%	5.8%	23.3%	0.0%	10.2%	14.2%	1.5%	0.4%	11.1%
Zn	0.52	-0.26	0.19	-0.34	-0.12	-0.14	0.36	0.38	-0.04	-0.03	-0.10	-0.15	0.08
	0.0%	4.7%	14.6%	0.8%	37.0%	28.8%	0.5%	0.3%	78.6%	79.5%	45.1%	25.4%	54.0%
SiO₂	-0.18	0.25	0.65	0.52	0.64	0.60	-0.29	-0.32	0.48	0.51	0.43	0.37	0.34
	17.5%	5.7%	0.0%	0.0%	0.0%	0.0%	2.2%	1.2%	0.0%	0.0%	0.1%	0.4%	0.9%
S(-II)	-0.04	-0.02	-0.30	-0.15	-0.30	-0.30	0.16	0.14	-0.18	-0.18	-0.24	-0.28	0.03
	75.0%	88.2%	2.0%	26.3%	1.9%	1.8%	21.3%	28.8%	17.0%	16.0%	6.2%	3.2%	79.6%
Fe(II)	0.67	-0.34	-0.02	-0.64	-0.43	-0.42	0.18	0.62	-0.33	-0.31	-0.41	-0.49	-0.10
	0.0%	0.9%	85.8%	0.0%	0.1%	0.1%	15.9%	0.0%	1.0%	1.4%	0.1%	0.0%	43.9%
Fe(III)	0.63	-0.38	0.22	-0.40	-0.21	-0.21	0.23	0.51	-0.10	-0.11	-0.11	-0.23	0.06
	0.0%	0.3%	9.3%	0.1%	11.1%	10.3%	7.8%	0.0%	45.2%	38.2%	41.2%	8.1%	62.6%
TIC	0.02	-0.23	-0.24	-0.18	-0.36	-0.36	-0.01	0.12	-0.22	-0.25	-0.24	-0.26	0.03
	88.9%	7.2%	6.0%	16.9%	0.5%	0.5%	93.5%	34.2%	9.8%	5.3%	6.4%	4.9%	82.6%
TOC	0.57	-0.31	-0.29	-0.65	-0.60	-0.58	0.41	0.60	-0.48	-0.48	-0.53	-0.51	-0.30
	0.0%	1.7%	2.3%	0.0%	0.0%	0.0%	0.1%	0.0%	0.0%	0.0%	0.0%	0.0%	2.0%

	Al	B	Ba	Be	Ca	Cd	Co	Cr	Cu	K	Li	Mg	Mn
Al	1.00	---	---	---	---	---	---	---	---	---	---	---	---
	.	---	---	---	---	---	---	---	---	---	---	---	---
B	-0.50	1.00	---	---	---	---	---	---	---	---	---	---	---
	0.0%	.	---	---	---	---	---	---	---	---	---	---	---
Ba	0.39	0.19	1.00	---	---	---	---	---	---	---	---	---	---
	0.2%	15.2%	.	---	---	---	---	---	---	---	---	---	---
Be	0.54	0.02	0.45	1.00	---	---	---	---	---	---	---	---	---
	0.0%	90.1%	0.0%	.	---	---	---	---	---	---	---	---	---
Ca	-0.03	0.28	0.12	0.22	1.00	---	---	---	---	---	---	---	---
	84.1%	3.2%	37.7%	8.8%	.	---	---	---	---	---	---	---	---
Cd	0.32	-0.01	0.15	0.39	-0.02	1.00	---	---	---	---	---	---	---
	1.2%	91.2%	24.4%	0.2%	86.7%	.	---	---	---	---	---	---	---
Co	0.25	0.17	0.35	0.40	0.21	0.36	1.00	---	---	---	---	---	---
	5.6%	19.0%	0.6%	0.1%	10.0%	0.4%	.	---	---	---	---	---	---
Cr	0.46	-0.14	0.30	0.25	0.22	0.21	0.43	1.00	---	---	---	---	---
	0.0%	27.5%	1.9%	5.2%	9.3%	10.9%	0.1%	.	---	---	---	---	---
Cu	0.15	-0.04	0.18	0.32	0.04	0.02	0.21	0.07	1.00	---	---	---	---
	24.7%	77.3%	17.6%	1.3%	78.9%	89.5%	10.0%	61.1%	.	---	---	---	---
K	-0.04	0.69	0.47	0.51	0.53	0.17	0.33	0.08	0.06	1.00	---	---	---
	74.6%	0.0%	0.0%	0.0%	0.0%	19.8%	1.1%	56.8%	62.3%	.	---	---	---
Li	-0.55	0.89	-0.01	-0.15	0.23	-0.14	0.07	-0.16	-0.11	0.58	1.00	---	---
	0.0%	0.0%	96.1%	23.8%	8.3%	27.2%	61.4%	23.7%	40.4%	0.0%	.	---	---

	Al	B	Ba	Be	Ca	Cd	Co	Cr	Cu	K	Li	Mg	Mn
Mg	0.63	-0.52	0.38	0.56	0.39	0.16	0.12	0.34	0.23	0.08	-0.61	1.00	---
	0.0%	0.0%	0.3%	0.0%	0.2%	22.9%	36.5%	0.8%	8.3%	53.8%	0.0%	.	---
Mn	0.61	-0.36	0.42	0.68	0.48	0.24	0.29	0.46	0.30	0.25	-0.46	0.94	1.00
	0.0%	0.4%	0.1%	0.0%	0.0%	6.4%	2.3%	0.0%	1.9%	5.3%	0.0%	0.0%	.
Mo	-0.58	0.73	-0.13	-0.13	0.05	0.03	0.16	-0.28	-0.05	0.30	0.72	-0.63	-0.56
	0.0%	0.0%	30.7%	31.8%	68.0%	84.8%	23.0%	3.0%	68.8%	2.0%	0.0%	0.0%	0.0%
Na	-0.62	0.91	-0.06	-0.22	0.20	-0.14	0.01	-0.17	-0.15	0.54	0.96	-0.63	-0.50
	0.0%	0.0%	65.7%	9.4%	11.7%	27.3%	93.1%	19.0%	24.2%	0.0%	0.0%	0.0%	0.0%
Ni	0.61	-0.22	0.31	0.47	0.28	0.31	0.20	0.53	0.29	0.10	-0.26	0.56	0.62
	0.0%	9.5%	1.7%	0.0%	3.3%	1.7%	12.8%	0.0%	2.2%	46.5%	4.6%	0.0%	0.0%
Pb	0.12	0.05	0.04	0.09	0.08	0.46	0.44	0.29	-0.13	0.09	0.03	-0.09	0.03
	34.6%	70.5%	73.7%	49.0%	56.1%	0.0%	0.0%	2.5%	30.7%	50.6%	83.0%	48.8%	81.3%
Sr	0.25	0.05	0.46	0.32	0.78	0.02	0.26	0.37	0.13	0.44	-0.11	0.65	0.67
	5.4%	71.6%	0.0%	1.3%	0.0%	88.3%	4.5%	0.3%	30.9%	0.0%	41.8%	0.0%	0.0%
V	0.44	-0.21	0.17	0.27	0.30	0.30	0.41	0.81	-0.05	0.01	-0.24	0.33	0.45
	0.0%	10.1%	20.1%	3.6%	1.9%	2.1%	0.1%	0.0%	72.5%	94.6%	6.8%	1.0%	0.0%
Zn	0.53	-0.12	0.53	0.76	0.17	0.32	0.50	0.49	0.46	0.33	-0.21	0.61	0.71
	0.0%	35.1%	0.0%	0.0%	18.2%	1.3%	0.0%	0.0%	0.0%	0.9%	11.0%	0.0%	0.0%
SiO₂	-0.15	0.72	0.18	0.37	0.17	0.30	0.30	-0.05	0.14	0.60	0.56	-0.30	-0.17
	24.2%	0.0%	17.4%	0.4%	20.4%	2.1%	2.2%	69.5%	28.2%	0.0%	0.0%	1.9%	20.0%
S(-II)	0.07	-0.32	-0.26	-0.12	0.02	-0.19	-0.32	0.14	-0.09	-0.27	-0.24	0.14	0.10
	59.3%	1.1%	4.6%	35.3%	86.1%	14.0%	1.4%	30.2%	48.2%	4.0%	6.0%	29.0%	44.5%
Fe(II)	0.72	-0.41	0.52	0.67	0.16	0.26	0.24	0.45	0.30	0.12	-0.49	0.78	0.83
	0.0%	0.1%	0.0%	0.0%	21.7%	4.4%	6.5%	0.0%	2.2%	36.4%	0.0%	0.0%	0.0%
Fe(III)	0.61	-0.19	0.64	0.66	0.16	0.44	0.41	0.42	0.34	0.24	-0.32	0.62	0.68
	0.0%	15.2%	0.0%	0.0%	21.8%	0.0%	0.1%	0.1%	0.8%	6.0%	1.4%	0.0%	0.0%
TIC	0.01	-0.36	-0.32	-0.28	-0.03	-0.09	-0.43	0.00	-0.15	-0.36	-0.30	0.10	-0.05
	94.4%	0.5%	1.3%	3.0%	83.2%	48.6%	0.1%	98.5%	24.3%	0.5%	1.9%	46.6%	72.9%
TOC	0.50	-0.65	0.23	0.18	0.11	0.08	0.04	0.38	0.06	-0.26	-0.61	0.66	0.58
	0.0%	0.0%	8.1%	16.1%	39.4%	54.9%	79.0%	0.3%	63.6%	4.2%	0.0%	0.0%	0.0%

	Mo	Na	Ni	Pb	Sr	V	Zn	SiO ₂	S(-II)	Fe(II)	Fe(III)	TIC	TOC
Mo	1.00	---	---	---	---	---	---	---	---	---	---	---	---
	.	---	---	---	---	---	---	---	---	---	---	---	---
Na	0.72	1.00	---	---	---	---	---	---	---	---	---	---	---
	0.0%	.	---	---	---	---	---	---	---	---	---	---	---
Ni	-0.32	-0.31	1.00	---	---	---	---	---	---	---	---	---	---
	1.4%	1.6%	.	---	---	---	---	---	---	---	---	---	---
Pb	0.04	0.02	0.05	1.00	---	---	---	---	---	---	---	---	---
	78.1%	87.4%	70.7%	.	---	---	---	---	---	---	---	---	---
Sr	-0.20	-0.10	0.39	-0.03	1.00	---	---	---	---	---	---	---	---
	12.1%	45.4%	0.2%	83.9%	.	---	---	---	---	---	---	---	---
V	-0.26	-0.24	0.50	0.40	0.38	1.00	---	---	---	---	---	---	---
	4.1%	6.1%	0.0%	0.2%	0.3%	.	---	---	---	---	---	---	---
Zn	-0.27	-0.29	0.69	0.07	0.34	0.42	1.00	---	---	---	---	---	---
	3.7%	2.5%	0.0%	60.4%	0.7%	0.1%	.	---	---	---	---	---	---
SiO₂	0.68	0.53	-0.02	0.09	0.00	-0.05	0.11	1.00	---	---	---	---	---
	0.0%	0.0%	87.4%	51.6%	97.7%	71.6%	39.3%	.	---	---	---	---	---
S(-II)	-0.37	-0.18	0.21	-0.02	0.05	0.18	-0.04	-0.50	1.00	---	---	---	---
	0.3%	16.5%	11.5%	87.3%	70.4%	16.2%	78.9%	0.0%	.	---	---	---	---
Fe(II)	-0.57	-0.57	0.61	0.08	0.39	0.42	0.77	-0.12	0.10	1.00	---	---	---
	0.0%	0.0%	0.0%	54.5%	0.2%	0.1%	0.0%	37.4%	44.2%	.	---	---	---

	Mo	Na	Ni	Pb	Sr	V	Zn	SiO ₂	S(-II)	Fe(II)	Fe(III)	TIC	TOC
Fe(III)	-0.29	-0.39	0.65	0.14	0.36	0.31	0.81	0.08	-0.18	0.77	1.00	---	---
	2.7%	0.2%	0.0%	27.5%	0.4%	1.4%	0.0%	54.1%	16.2%	0.0%	.	---	---
TIC	-0.36	-0.21	0.02	-0.08	0.02	0.03	-0.24	-0.45	0.68	-0.10	-0.24	1.00	---
	0.5%	10.5%	88.4%	53.8%	85.9%	84.5%	6.9%	0.0%	0.0%	43.4%	6.9%	.	---
TOC	-0.64	-0.63	0.48	0.15	0.31	0.35	0.37	-0.55	0.30	0.60	0.44	0.15	1.00
	0.0%	0.0%	0.0%	25.6%	1.6%	0.6%	0.3%	0.0%	1.8%	0.0%	0.0%	26.3%	.

Appendix 15 Saturation indices for albite, potassium feldspar (adularia), muscovite (Kmica), Mg-clinochlore (chlorite 14A), and silica (quartz, and SiO₂(a)); these minerals determine the partial or full equilibrium of waters according to the simplified ternary diagram after Giggenbach (1988); site names in black are in full equilibrium according to the ternary diagrams in Figure 46, Figure 49, and Figure 60 , site names in italic are in partial equilibrium

Site name	Albite	Adularia	Kmica	Chlorite14A	Quartz	SiO ₂ (a)
YNPGG02-2W	-0.20	0.05	7.36	-20.07	0.84	-0.13
<i>YNPGG04-1W</i>	-4.38	-3.92	0.20	-42.24	0.71	-0.23
<i>YNPGG04-2W</i>	-5.49	-5.13	-3.27	-44.45	0.72	-0.22
<i>YNPGG04-4W</i>	-5.35	-4.98	-2.37	-43.31	0.66	-0.27
YNPGG05-2W	-9.18	-7.56	-7.82	-60.07	0.79	-0.23
YNPGG05-4W	-9.54	-7.56	-8.30	-61.19	0.81	-0.25
YNPGG06-2W	0.69	1.28	7.33	-9.60	0.89	-0.04
YNPGG07-2W	-0.43	0.16	6.29	-18.28	0.79	-0.14
YNPGG07-4W	-0.70	-0.12	5.63	-19.16	0.78	-0.15
YNPGG08-4W	-8.97	-8.27	-11.22	-62.44	0.90	-0.10
YNPHL01-1W	-7.33	-5.40	-6.87	-59.41	1.40	0.09
YNPHL01-2W	-6.37	-4.70	-5.65	-55.85	1.48	0.22
YNPHL01-3W	-6.92	-5.10	-6.94	-57.91	1.45	0.18
YNPHL02-1W	<i>0.92</i>	<i>2.72</i>	<i>12.09</i>	-17.07	<i>1.28</i>	<i>0.04</i>
YNPHL03-3W	-6.70	-4.81	-4.50	-51.15	1.22	0.13
YNPLG01-2W	0.07	0.32	5.30	-6.81	0.78	-0.14
YNPLG02-2W	-0.25	-0.07	2.49	3.91	0.61	-0.30
YNPLG03-2W	-0.09	0.18	5.01	-6.95	0.75	-0.16
YNPNL01-1W	-9.77	-7.74	-12.40	-65.90	1.34	0.04
YNPNL02-1W	-8.31	-7.09	-8.03	-58.33	0.97	-0.08
YNPNL02-2W	-7.98	-6.94	-7.48	-56.18	0.89	-0.10
YNPNL02-3W	-12.17	-10.12	-12.96	-65.65	0.49	-0.58
YNPNL03-1W	-8.11	-6.49	-4.74	-45.54	0.56	-0.43
YNPNL03-2W	-7.99	-6.52	-4.77	-46.31	0.62	-0.33
YNPNL03-3W	-8.82	-7.25	-6.36	-50.81	0.64	-0.32
YNPNL04-1W	-8.89	-6.88	-8.00	-54.57	0.94	-0.23
YNPNL04-2W	-10.22	-8.56	-11.46	-59.03	0.91	-0.16
YNPNL04-3W	-9.53	-7.84	-8.90	-57.18	0.81	-0.22
YNPNL05-1W	-8.59	-7.04	-8.84	-60.17	1.10	0.09
YNPNL05-2W	-8.28	-6.72	-7.78	-57.88	1.06	0.11
YNPRH01-1W	-6.75	-5.44	-5.72	-53.47	1.13	0.09
YNPRH01-2W	-6.43	-5.19	-4.68	-51.57	1.06	0.04
YNPRH01-3W	-6.70	-5.43	-4.98	-51.96	1.04	0.03
YNPRH03-1W	-8.47	-6.91	-10.92	-66.80	1.48	0.30
YNPRH04-1W	-8.13	-6.64	-9.75	-64.39	1.40	0.25

Site name	Albite	Adularia	Kmica	Chlorite14A	Quartz	SiO ₂ (a)
YNPRH04-2W	-8.11	-6.64	-9.87	-64.72	1.42	0.27
YNPRH04-3W	-8.31	-6.87	-10.10	-64.65	1.38	0.26
YNPRH05-1W	-7.43	-6.49	-6.91	-54.35	0.79	-0.25
YNPRH05-3W	-8.38	-7.48	-8.95	-49.00	0.56	-0.37
YNPRH07-2W	-10.67	-9.06	-9.62	-61.65	0.40	-0.55
YNPRH08-1W	-8.29	-7.48	-13.13	-59.98	1.21	0.20
YNPRH08-4W	-0.18	0.50	6.31	-22.66	1.10	0.15
YNPRH09-1W	0.67	1.56	7.37	-6.61	0.97	-0.01
YNPRH10-4W	-5.32	-4.47	-4.06	-39.83	0.95	0.03
YNPRH11-3W	-8.85	-7.76	-9.83	-59.06	0.77	-0.27
YNPRH13-3W	-6.22	-5.39	-8.39	-48.49	1.11	0.13
YNPRH14-3W	-5.35	-4.72	-6.47	-41.59	1.00	0.05
YNPRH15-3W	-9.72	-8.47	-15.73	-68.60	1.35	0.16
YNPRH16-4W	-9.30	-8.05	-15.00	-67.36	1.34	0.16
YNPRH17-4W	-7.28	-6.21	-8.26	-54.56	1.10	0.09
YNPRH18-4W	-6.64	-5.43	-3.56	-47.13	0.82	-0.11
YNPRH19-4W	-6.82	-6.01	-8.52	-47.02	1.02	0.10
YNPRH20-4W	-7.45	-6.41	-11.01	-53.91	1.30	0.28
YNPRH21-4W	-8.81	-7.90	-13.28	-58.61	1.12	0.14
YNPRH22-4W	-7.12	-5.89	-5.88	-55.78	1.07	-0.01
YNPRH24-4W	-8.16	-7.03	-11.46	-61.66	1.31	0.21
YNPRH25-4W	-6.83	-5.92	-7.10	-46.34	0.91	-0.01
YNPRH26-4W	-6.06	-5.01	-4.24	-50.43	0.99	0.00
YNPRH27-4W	-6.52	-6.14	-8.48	-42.33	0.84	-0.09
YNPRH28-4W	-7.55	-6.56	-10.62	-47.69	1.03	0.04

Appendix 16 Reservoir temperatures calculated from the following geothermometers: Si (Fournier and Potter 1982), K-Mg (Giggenbach 1988), Na-K (Arnórsson et al. 1998), Na-K-Ca (Fournier and Truesdell 1973)*

Analysis-code-water	Cluster No.	Temp [°C] from Si geotherm.	Temp [°] from K-Mg geotherm.	Temp [°C] from Na-K geotherm.	Temp [°C] from Na-K-Ca geotherm.
YNPGG04-2W	5	165	136	140	228
YNPLG01-2W	8	181	168	128	235
YNPLG02-2W	8	175	163	119	226
YNPLG03-2W	8	177	168	131	238
YNPGG02-2W	11	171	148	117	210
YNPGG06-2W	11	193	215	178	273
YNPGG07-2W	11	178	211	178	271
YNPGG07-4W	11	175	209	175	266
YNPRH27-4W	13	183	154	143	239
YNPRH08-1W	14	212	199	191	281
YNPRH08-4W	14	216	215	187	276
YNPRH13-3W	14	207	226	206	294
YNPRH14-3W	14	200	211	177	270

* Si-geothermometer: $T = -53.5 + 0.11236 \cdot S - 0.5559 \cdot 10^{-4} \cdot S^2 + 0.1772 \cdot 10^{-7} \cdot S^3 + 88.390 \log S$ ($S = \text{SiO}_2$ [mg/L])

K-Mg-geotherm.: $T = 4410 : (14.0 - \log X) - 273.15$ ($X = \log (\text{K}[\text{mg/L}]^2 / \text{Mg}[\text{mg/L}])$)

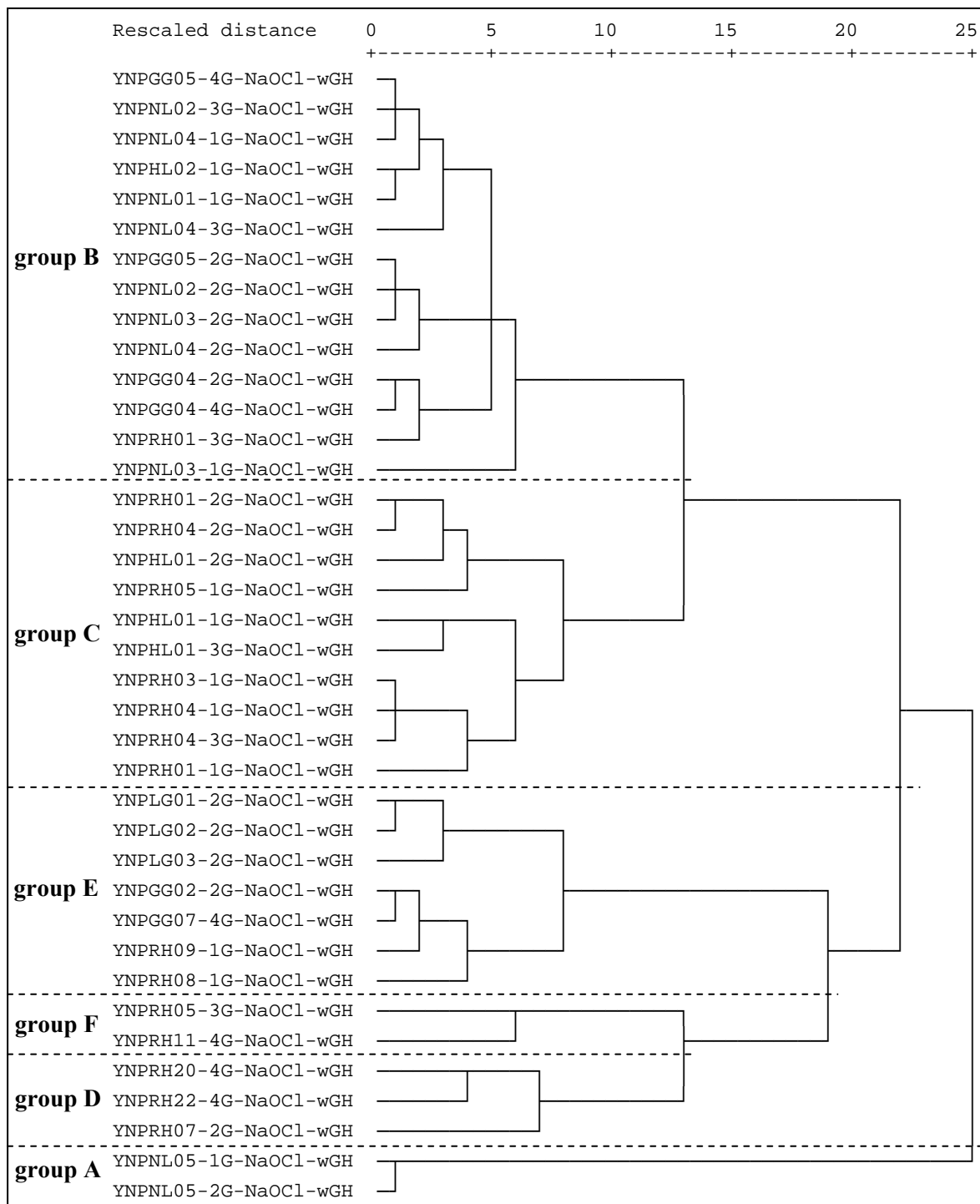
Na-K-geotherm.: $T = 733.6 - 770.551 \cdot Y + 378.189 \cdot Y^2 - 95.753 \cdot Y^3 + 9.544 \cdot Y^4$ ($Y = \log \text{Na} [\text{mol/L}] / \text{K} [\text{mol/L}]$)

Na-K-Ca-geotherm.: $T = 1647 : (\log (\text{Na}/\text{K}) + 1/3 \cdot \log (\text{Ca}^{0.5}/\text{Na}) + 2.24) - 273.15$ (concentrations in mol/L)

Appendix 17 Mann-Whitney Test for the difference between the two major groups for 60 water samples derived from cluster analysis; significance levels > 1% (not accepted as significant) are marked in bold

	Mann-Whitney U	Wilcoxon W	Z	significance level (2-tailed)
{H ⁺ }	130.5	508.5	-4.7	0.00%
temperature	220	781	-3.4	0.08%
conductivity	193.5	754.5	-3.7	0.02%
F	36	597	-6.1	0.00%
Cl	0	561	-6.6	0.00%
Br	0	561	-6.6	0.00%
N(V)	433	811	-0.2	82.00%
S(VI)	59	437	-5.7	0.00%
As(III)	22	583	-6.3	0.00%
As(V)	60	621	-5.7	0.00%
MMAA	64.5	625.5	-5.7	0.00%
DMAA	178.5	739.5	-4.0	0.01%
Al	115.5	493.5	-4.9	0.00%
B	19	580	-6.3	0.00%
Ba	382	943	-0.9	35.00%
Be	324	702	-1.9	5.40%
Ca	376	937	-1.0	30.00%
Cd	378	756	-1.8	7.20%
Co	392.5	953.5	-0.8	41.00%
Cr	421	799	-0.6	54.00%
Cu	412	790	-0.6	53.00%
K	209	770	-3.5	0.04%
Li	5	566	-6.5	0.00%
Mg	143	521	-4.5	0.00%
Mn	194	572	-3.7	0.02%
Mo	121	682	-5.2	0.00%
Na	1	562	-6.6	0.00%
Ni	293	671	-2.5	1.30%
Pb	430.5	991.5	-0.4	71.00%
Sr	439	817	-0.1	92.00%
V	406	784	-1.2	22.00%
Zn	356	734	-1.4	17.00%
SiO ₂	226	787	-3.3	0.11%
S(-II)	375	753	-1.1	29.00%
Fe(II)	197.5	575.5	-3.7	0.02%
Fe(III)	281.5	659.5	-2.4	1.50%
TIC	364	742	-1.2	23.00%
TOC	173.5	551.5	-4.0	0.01%

Appendix 18 Dendrogram of cluster analysis for 38 samples with combined data from gas analysis (As (from HG-AAS), Al, B, Ba, Cu, Fe, K, Li, Si, Sr, Zn, S) and water analysis (pH, temperature, conductivity, F, Cl, Br, N(V), S(VI), As, As(III), As(V), MMAA, DMAA, Al, B, Ba, Be, Ca, Cd, Co, Cr, Cu, K, Li, Mg, Mn, Mo, Na, Ni, Pb, Sr, V, Zn, SiO₂, S(-II), Fe(II), Fe(III), TIC, TOC) (all variables standardized to a range of 0 to 1 and rescaled before cluster analysis; Ward's method, program: SPSS for Windows 11.0)*



* for gas samples where no contemporaneous water samples existed the following cases were assigned to the respective subgroups: **A:** YNPNL06-1G; **B:** YNPGG03-2G, 4G; YNPRH01-3G setup 2; YNPRH02-1G; **D:** YNPRH07-1G; YNPRH12-4G; YNPRH22-4G setup 2; YNPRH23-4G; **F:** YNPRH05-4G setup 1 and 2; YNPRH06-1G, 2G; **E:** YNPGG01-2G; YNPGG02-4G; YNPLG01-1G; YNPRH08-2G

Appendix 19 Kruskal-Wallis test for overall difference between the 6 subgroups derived from cluster analysis of 38 samples with both gas and water data after Ward's method; df = degree of freedom = 5; significance levels > 5% (not accepted as significant) are marked in bold

Parameters from gas samples	Chi-Square	significance level	Parameters from gas and water samples	Chi-Square	significance level	Parameters from water samples	Chi-Square	significance level
As (AAS) nGH*	15	0.9%	Zn wGH	5	46.9%	Cd	21	0.1%
As (AAS) wGH*	15	0.9%	S(VI) nGH	3	76.4%	Co	11	4.3%
Al nGH	17	0.4%	S(VI) wGH	3	74.6%	Cr	24	0.0%
Al wGH	17	0.4%	{H ⁺ }	19	0.2%	Cu	2	80.9%
B nGH	11	5.2%	temperature	18	0.3%	K	20	0.1%
B wGH	11	5.2%	conductivity	22	0.1%	Li	23	0.0%
Ba nGH	8	13.6%	F	21	0.1%	Mg	18	0.3%
Ba wGH	9	11.8%	Cl	27	0.0%	Mn	21	0.1%
Cu nGH	6	30.6%	Br	27	0.0%	Mo	24	0.0%
Cu wGH	7	24.7%	N(V)	9	9.6%	Na	26	0.0%
Fe nGH	12	3.4%	S(VI)	21	0.1%	Ni	20	0.1%
Fe wGH	12	3.4%	As	26	0.0%	Pb	20	0.1%
K nGH	11	5.7%	As(III)	25	0.0%	Sr	8	18.1%
K wGH	11	5.7%	As(V)	25	0.0%	V	21	0.1%
Li nGH	14	1.4%	MMAA	17	0.4%	Zn	21	0.1%
Li wGH	18	0.3%	DMAA	26	0.0%	SiO ₂	16	0.6%
SiO ₂ nGH	8	16.8%	Al	23	0.0%	S(-II)	6	32.1%
SiO ₂ wGH	8	16.8%	B	27	0.0%	Fe(II)	26	0.0%
Sr nGH	7	23.3%	Ba	29	0.0%	Fe(III)	27	0.0%
Sr wGH	8	14.2%	Be	24	0.0%	TIC	8	16.7%
Zn nGH	4	50.2%	Ca	4	51.9%	TOC	19	0.2%

* all parameters for setups with gas hood (setup 1 or 2 in Figure 42); "nGH" behind an element indicates that the concentration in air was calculated from the first end-member model "all As from ambient air" (assuming a "no gas hood" case); "wGH" indicates the second end-member model "all As from underneath the gas hood" (further explanation see section 4.2.3.2.)

Appendix 20 Kruskal-Wallis test for overall difference between the 6 subgroups derived from cluster analysis considering only the data of 55 gas samples (no water data) after Ward's method; df = degree of freedom = 5; significance levels > 5% (not accepted as significant) are marked in bold

Parameters from gas samples	Chi-Square	significance level	Parameters from gas samples	Chi-Square	significance level	Parameters from gas samples	Chi-Square	significance level
As (AAS) nGH	29	0.00%	Cu nGH	6	26.52%	SiO ₂ nGH	9	10.42%
As (AAS) wGH	29	0.00%	Cu wGH	7	18.83%	SiO ₂ wGH	9	10.42%
Al nGH	21	0.07%	Fe nGH	16	0.72%	Sr nGH	12	3.85%
Al wGH	21	0.07%	Fe wGH	16	0.72%	Sr wGH	13	2.48%
B nGH	20	0.12%	K nGH	19	0.16%	Zn nGH	7	19.55%
B wGH	20	0.12%	K wGH	19	0.16%	Zn wGH	8	18.04%
Ba nGH	19	0.20%	Li nGH	22	0.06%	S(VI) nGH	3	67.29%
Ba wGH	19	0.16%	Li wGH	25	0.01%	S(VI) wGH	3	66.55%

* all parameters for setups with gas hood (setup 1 or 2 in Figure 42); “nGH” behind an element indicates that the concentration in air was calculated from the first end-member model “all As from ambient air” (assuming a “no gas hood” case); “wGH” stands for calculations from the second end-member model “all As from underneath the gas hood” (further explanation see section 4.2.3.2.)

Appendix 21 Assignment of individual water samples to the water and gas subgroups derived by cluster analysis (Appendix 11; Appendix 18)

Individual water samples	Water type	Water subgroup ¹	Gas subgroup ²
YNPGG01-2G			E
YNPGG02-2W, 2G	2	11	E
YNPGG02-4G			E
YNPGG03-2G			B
YNPGG03-4G			B
YNPGG04-1W	1	5	
YNPGG04-2W, 2G	1	5	B
YNPGG04-4W, 4G	1	5	B
YNPGG05-2W	1	1	B
YNPGG05-4W, 4G	1	1	B
YNPGG06-2W	2	11	
YNPGG07-2W	2	11	
YNPGG07-4W, 4G	2	11	E
YNPGG08-4W	1	5	
YNPHL01-1W, 1G	1	4	C
YNPHL01-2W, 2G	1	4	C

Individual water samples	Water type	Water subgroup ¹	Gas subgroup ²
YNPNL02-2W, 2G	1	1	B
YNPNL02-3W, 3G	1	1	B
YNPNL03-1W, 1G	1	1	B
YNPNL03-2W, 2G	1	1	B
YNPNL03-3W	1	2	
YNPNL04-1W, 1G	1	1	B
YNPNL04-2W, 2G	1	1	B
YNPNL04-3W, 3G	1	2	B
YNPNL05-1W, 1G	1	3	A
YNPNL05-2W, 2G	1	3	A
YNPNL06-1G			A
YNPRH01-1W, 1G	1	7	C
YNPRH01-2W, 2G	1	7	C
YNPRH01-3W, 3G	1	7	B
YNPRH02-1G			B
YNPRH03-1W, 1G	1	6	C

Individual water samples	Water type	Water subgroup ¹	Gas subgroup ²
YNPRH07-2W, 2G	1	1	D
YNPRH08-1W, 1G	2	14	E
YNPRH08-2G			E
YNPRH08-4W	2	14	
YNPRH09-1W, 1G	2	11	E
YNPRH10-4W	2	14	
YNPRH11-3W, 4G	2	10	F
YNPRH12-4G			D
YNPRH13-3W	2	14	
YNPRH14-3W	2	14	
YNPRH15-3W	2	12	
YNPRH16-4W	2	12	
YNPRH17-4W	2	13	
YNPRH18-4W	1	7	
YNPRH19-4W	2	14	
YNPRH20-4W, 4G	2	14	D

Individual water samples	Water type	Water subgroup ¹	Gas subgroup ²	Individual water samples	Water type	Water subgroup ¹	Gas subgroup ²	Individual water samples	Water type	Water subgroup ¹	Gas subgroup ²
YNPHL01-3W, 3G	1	4	C	YNPRH04-1W, 1G	1	6	C	YNPRH21-4W	2	14	
YNPHL02-1W, 1G	1	4	B	YNPRH04-2W, 2G	1	6	C	YNPRH22-4W, 4G	1	7	D
YNPHL03-3W	1	1		YNPRH04-3W, 3G	1	6	C	YNPRH23-4G			D
YNPLG01-1G			E	YNPRH05-1W, 1G	2	9	C	YNPRH24-4W	2	13	
YNPLG01-2W, 2G	2	8	E	YNPRH05-3W, 3G	2	9	F	YNPRH25-4W	2	13	
YNPLG02-2W, 2G	2	8	E	YNPRH05-4G			F	YNPRH26-4W	2	13	
YNPLG03-2W, 2G	2	8	E	YNPRH06-1G			F	YNPRH27-4W	2	13	
YNPNL01-1W, 1G	1	4	B	YNPRH06-2G			F	YNPRH28-4W	2	13	
YNPNL02-1W	1	1		YNPRH07-1G			D				

1) Water subgroup

Subgroup	Subgroup Name	No. of cases
Type I steam-heated waters		
1	Low Cl hot springs and fumaroles at Hazle Lake, Nymph Lake, Gibbon Geyser Basin and Ragged Hills	11
2	Frying Pan Spring during September sampling	2
3	Fumaroles at Nymph Lake from 2003	2
4	Lake samples	5
5	Hot springs at Gibbon Geyser Basin	4
6	“Verde Pool”	4
7	“Milky Way” - “Kaolin Spring” complex	5
Type II deep geothermal waters		
8	Lower Geyser Basin alkaline hot springs	3
9	Ragged Hills No. 5	2
10	Ragged Hills No. 11	1
11	Near neutral pH hot springs at Gibbon Geyser Basin	5
12	Warm springs Ragged Hills	2
13	Shallow hot springs Ragged Hills	6
14	Deeper hot springs Ragged Hills	8

2) Gas subgroup

Subgroup	Subgroup Name	No. of cases
A	lowest total volatile concentrations (Fumaroles at Nymph Lake from 2003)	3
B	low to medium volatile As, high volatile Si, S concentrations due to high water temperatures (low Cl hot springs, fumaroles; hot springs at Gibbon GB, “Verde Pool”)	18
C	medium to high volatile As, low volatile Si, S concentrations due to low water temperatures (Lakes and “Milky Way” - “Kaolin Spring” complex)	10
D	highest volatile As concentrations of all samples taken	7
E	low volatile As and S concentrations (Lower Geyser Basin alkaline hot springs; near neutral pH hot springs at Gibbon Geyser Basin and deeper hot springs Ragged Hills)	11
F	high volatile As, medium Si and S concentrations (Ragged Hills No. 5 and No. 11)	6

Appendix 22 Bivariate correlation of volatile metallics considering 55 gas samples (values below detection limit were dismissed, thus for some parameter combination (e.g., Li-Fe) as little as 9 cases were considered; c = Spearman correlation coefficient, N = number of cases, sig = two tailed level of significance in %)

		As	Al	B	Ba	Cu	Fe	K	Li	SiO ₂	Sr	Zn	S(VI)
As	c	1.00	0.55	0.09	0.41	-0.30	0.46	0.54	0.81	0.27	0.35	-0.34	0.20
	N	55	47	18	45	36	31	52	20	29	42	20	43
	sig	.	0.0%	72.3%	0.6%	7.5%	0.9%	0.0%	0.0%	15.4%	2.1%	14.8%	19.7%
Al	c	0.55	1.00	-0.26	0.17	-0.21	0.57	0.59	0.19	0.07	0.14	-0.42	0.09
	N	47	47	16	40	34	30	47	18	29	37	14	38
	sig	0.0%	.	32.7%	30.3%	24.3%	0.1%	0.0%	44.8%	70.9%	39.3%	13.1%	59.5%
B	c	0.09	-0.26	1.00	0.63	-0.17	-0.25	-0.11	-0.02	0.32	0.20	-0.13	0.39
	N	18	16	18	18	15	14	18	11	14	17	14	16
	sig	72.3%	32.7%	.	0.5%	53.3%	39.2%	65.1%	95.8%	26.0%	44.5%	64.8%	13.4%
Ba	c	0.41	0.17	0.63	1.00	-0.33	0.38	0.03	0.05	0.46	-0.13	0.00	0.11
	N	45	40	18	45	36	28	45	18	22	42	19	38
	sig	0.6%	30.3%	0.5%	.	5.3%	4.6%	85.8%	83.6%	3.1%	40.5%	99.4%	51.4%
Cu	c	-0.30	-0.21	-0.17	-0.33	1.00	-0.33	0.02	-0.76	-0.10	0.42	0.46	0.27
	N	36	34	15	36	36	26	36	12	18	36	13	29
	sig	7.5%	24.3%	53.3%	5.3%	.	10.0%	91.8%	0.5%	68.1%	1.2%	11.7%	15.7%
Fe	c	0.46	0.57	-0.25	0.38	-0.33	1.00	0.38	0.57	0.28	-0.02	-0.22	0.39
	N	31	30	14	28	26	31	31	9	21	27	10	24
	sig	0.9%	0.1%	39.2%	4.6%	10.0%	.	3.3%	11.2%	21.8%	91.3%	53.3%	5.9%
K	c	0.54	0.59	-0.11	0.03	0.02	0.38	1.00	0.44	0.13	0.45	-0.35	0.19
	N	52	47	18	45	36	31	52	20	29	42	19	43
	sig	0.0%	0.0%	65.1%	85.8%	91.8%	3.3%	.	5.0%	50.8%	0.3%	14.7%	23.2%
Li	c	0.81	0.19	-0.02	0.05	-0.76	0.57	0.44	1.00	0.41	0.48	-0.42	0.38
	N	20	18	11	18	12	9	20	20	13	16	11	18
	sig	0.0%	44.8%	95.8%	83.6%	0.5%	11.2%	5.0%	.	16.2%	5.8%	20.1%	11.5%
SiO₂	c	0.27	0.07	0.32	0.46	-0.10	0.28	0.13	0.41	1.00	-0.08	0.09	0.19
	N	29	29	14	22	18	21	29	13	29	19	10	23
	sig	15.4%	70.9%	26.0%	3.1%	68.1%	21.8%	50.8%	16.2%	.	73.7%	80.3%	38.1%
Sr	c	0.35	0.14	0.20	-0.13	0.42	-0.02	0.45	0.48	-0.08	1.00	-0.35	0.32
	N	42	37	17	42	36	27	42	16	19	42	18	35
	sig	2.1%	39.3%	44.5%	40.5%	1.2%	91.3%	0.3%	5.8%	73.7%	.	15.2%	5.7%
Zn	c	-0.34	-0.42	-0.13	0.00	0.46	-0.22	-0.35	-0.42	0.09	-0.35	1.00	0.10
	N	20	14	14	19	13	10	19	11	10	18	20	18
	sig	14.8%	13.1%	64.8%	99.4%	11.7%	53.3%	14.7%	20.1%	80.3%	15.2%	.	70.5%
S(VI)	c	0.20	0.09	0.39	0.11	0.27	0.39	0.19	0.38	0.19	0.32	0.10	1.00
	N	43	38	16	38	29	24	43	18	23	35	18	43
	sig	19.7%	59.5%	13.4%	51.4%	15.7%	5.9%	23.2%	11.5%	38.1%	5.7%	70.5%	.

Appendix 23 Bivariate correlation of volatile metallics with water parameters considering 38 samples with gas and water data (values below detection limit were dismissed; c = Spearman correlation coefficient, N = number of cases, sig = two tailed level of significance in %)

		As (g)	Al (g)	B (g)	Ba (g)	Cu (g)	Fe (g)	K (g)	Li (g)	SiO ₂ (g)	Sr (g)	Zn (g)	S(VI) (g)
Al	c	0.30	0.43	0.56	0.16	-0.01	0.11	0.13	-0.33	-0.14	0.03	-0.27	0.09
	N	38	30	11	31	24	18	35	12	18	29	14	28
	sig	6.3%	1.9%	7.1%	39.2%	95.5%	67.5%	44.0%	29.7%	57.3%	89.1%	34.2%	66.6%
As	c	0.26	0.03	-0.25	0.07	-0.12	0.02	0.07	0.41	0.28	0.04	-0.26	-0.09
	N	38	30	11	31	24	18	35	12	18	29	14	28
	sig	11.7%	88.4%	46.7%	70.1%	56.5%	94.5%	70.0%	19.1%	25.7%	83.9%	36.6%	66.6%
As(III)	c	0.33	0.03	-0.15	0.04	-0.06	0.02	0.08	0.50	0.27	0.12	-0.26	-0.01
	N	38	30	11	31	24	18	35	12	18	29	14	28
	sig	4.6%	87.3%	66.9%	83.4%	77.6%	92.6%	64.3%	10.1%	28.0%	52.4%	37.9%	95.0%
As(V)	c	0.29	0.10	-0.35	0.09	0.05	0.17	0.16	0.40	0.41	0.13	-0.26	0.01
	N	38	30	11	31	24	18	35	12	18	29	14	28
	sig	7.3%	58.5%	29.8%	61.9%	82.6%	49.9%	36.6%	19.9%	9.4%	48.8%	36.6%	95.9%
MMAA	c	0.16	0.08	-0.82	0.16	0.06	0.26	0.18	0.56	0.44	0.23	-0.01	-0.17
	N	38	30	11	31	24	18	35	12	18	29	14	28
	sig	34.3%	67.7%	0.2%	39.8%	78.6%	28.8%	29.2%	5.8%	6.6%	22.4%	98.2%	38.5%
DMAA	c	0.07	0.20	-0.34	0.09	-0.10	-0.15	0.06	-0.06	0.26	-0.09	-0.28	-0.20
	N	38	30	11	31	24	18	35	12	18	29	14	28
	sig	68.1%	28.5%	31.2%	64.2%	64.9%	55.3%	73.6%	84.6%	30.3%	62.6%	32.6%	31.0%
B	c	0.09	0.15	-0.65	-0.19	0.09	-0.07	0.18	0.16	0.14	0.14	-0.33	-0.20
	N	38	30	11	31	24	18	35	12	18	29	14	28
	sig	59.9%	42.1%	2.9%	29.7%	68.9%	77.3%	30.6%	61.8%	58.1%	46.0%	24.6%	31.1%
Ba	c	0.31	0.38	0.42	0.39	-0.10	0.37	0.19	0.13	0.01	0.05	-0.23	0.01
	N	38	30	11	31	24	18	35	12	18	29	14	28
	sig	5.8%	4.1%	20.1%	2.9%	64.1%	13.5%	26.4%	68.1%	96.4%	78.4%	42.7%	96.7%
Be	c	0.22	0.51	-0.12	0.15	-0.08	0.34	0.05	-0.26	-0.16	-0.02	-0.22	-0.01
	N	38	30	11	31	24	18	35	12	18	29	14	28
	sig	17.8%	0.4%	73.3%	43.2%	69.5%	16.7%	79.4%	41.3%	52.1%	90.8%	44.1%	94.9%
Br	c	0.17	0.00	-0.41	0.05	-0.09	-0.10	0.10	0.44	0.32	0.11	-0.31	-0.11
	N	38	30	11	31	24	18	35	12	18	29	14	28
	sig	29.8%	98.6%	21.6%	79.4%	66.0%	70.0%	56.9%	15.2%	20.1%	56.3%	27.7%	58.7%
Ca	c	-0.22	0.03	-0.15	0.04	-0.32	-0.11	-0.13	-0.24	-0.37	-0.37	0.20	-0.33
	N	38	30	11	31	24	18	35	12	18	29	14	28
	sig	17.6%	89.0%	65.0%	81.4%	12.6%	66.3%	44.4%	44.3%	12.6%	5.2%	48.3%	8.8%
Cd	c	0.05	0.32	0.20	0.20	-0.21	0.12	-0.17	-0.57	-0.12	-0.42	-0.07	-0.25
	N	38	30	11	31	24	18	35	12	18	29	14	28
	sig	77.7%	8.4%	55.5%	29.1%	31.3%	64.4%	33.1%	5.3%	64.3%	2.5%	81.6%	19.5%
Cl	c	0.18	-0.02	-0.41	0.03	-0.11	-0.04	0.08	0.38	0.29	0.08	-0.31	-0.16
	N	38	30	11	31	24	18	35	12	18	29	14	28
	sig	27.9%	92.1%	21.2%	87.2%	59.3%	88.0%	65.2%	21.7%	23.6%	69.2%	27.4%	40.5%
Co	c	0.07	0.06	-0.02	0.37	-0.61	0.50	-0.29	0.35	-0.25	-0.43	-0.42	-0.14
	N	38	30	11	31	24	18	35	12	18	29	14	28
	sig	68.3%	75.8%	94.5%	4.1%	0.2%	3.3%	9.3%	27.0%	31.2%	2.1%	13.9%	47.9%
Cond.	c	0.26	0.29	0.03	0.06	-0.16	-0.02	0.07	-0.17	-0.15	-0.09	-0.43	-0.10
	N	38	30	11	31	24	18	35	12	18	29	14	28
	sig	11.8%	11.7%	93.7%	72.9%	45.0%	93.8%	67.7%	58.7%	54.8%	64.6%	12.4%	62.3%

Appendix 23

		As (g)	Al (g)	B (g)	Ba (g)	Cu (g)	Fe (g)	K (g)	Li (g)	SiO ₂ (g)	Sr (g)	Zn (g)	S(VI) (g)
Cr	c	0.24	0.12	0.40	0.04	-0.20	0.13	0.03	0.02	-0.14	-0.15	0.10	0.04
	N	38	30	11	31	24	18	35	12	18	29	14	28
	sig	14.5%	53.4%	21.7%	81.6%	35.3%	62.0%	87.5%	94.9%	57.5%	43.3%	72.6%	84.9%
Cu	c	-0.14	0.08	-0.46	0.35	-0.14	0.62	-0.24	0.20	0.13	-0.38	0.40	0.25
	N	38	30	11	31	24	18	35	12	18	29	14	28
	sig	40.7%	67.8%	15.4%	5.4%	51.9%	0.6%	17.4%	53.0%	61.4%	4.0%	16.0%	20.8%
F	c	0.19	-0.04	-0.45	-0.17	0.08	-0.17	0.16	0.45	0.35	0.13	-0.39	0.03
	N	38	30	11	31	24	18	35	12	18	29	14	28
	sig	24.6%	82.4%	17.0%	35.7%	72.5%	51.0%	35.9%	14.5%	15.7%	49.2%	16.9%	87.3%
Fe(II)	c	0.19	0.32	0.43	0.26	-0.12	0.35	0.01	-0.31	-0.13	-0.02	0.43	-0.03
	N	38	30	11	31	24	18	35	12	18	29	14	28
	sig	25.3%	8.1%	19.0%	16.5%	58.7%	15.1%	95.5%	33.1%	61.8%	91.6%	12.2%	86.5%
Fe(III)	c	0.23	0.42	0.10	0.38	-0.29	0.55	-0.04	-0.49	-0.20	-0.17	0.15	-0.08
	N	38	30	11	31	24	18	35	12	18	29	14	28
	sig	16.1%	2.0%	75.9%	3.4%	16.8%	1.7%	80.6%	10.6%	41.8%	37.4%	60.4%	69.3%
K	c	0.09	0.34	-0.31	0.04	-0.17	0.03	0.08	0.17	-0.14	-0.12	-0.24	-0.33
	N	38	30	11	31	24	18	35	12	18	29	14	28
	sig	57.2%	6.7%	35.5%	84.0%	44.0%	90.0%	64.6%	58.7%	57.0%	54.5%	40.1%	9.0%
Li	c	0.20	-0.09	-0.40	0.00	-0.14	-0.17	0.09	0.47	0.37	0.10	-0.31	-0.15
	N	38	30	11	31	24	18	35	12	18	29	14	28
	sig	21.7%	62.4%	22.3%	98.1%	51.4%	51.0%	62.2%	12.4%	13.5%	60.6%	28.1%	43.6%
Mg	c	-0.19	0.10	0.51	0.09	-0.15	-0.06	-0.14	-0.22	-0.36	-0.16	0.28	0.00
	N	38	30	11	31	24	18	35	12	18	29	14	28
	sig	25.0%	61.6%	11.0%	63.7%	48.5%	81.7%	41.8%	48.4%	14.2%	39.5%	33.4%	99.1%
Mn	c	-0.07	0.19	0.34	0.12	-0.30	0.10	-0.12	-0.21	-0.20	-0.24	0.36	-0.09
	N	38	30	11	31	24	18	35	12	18	29	14	28
	sig	69.4%	31.7%	31.2%	50.5%	15.5%	68.7%	51.0%	51.3%	42.8%	20.5%	20.8%	65.3%
Mo	c	0.20	-0.03	-0.53	-0.02	-0.05	-0.01	-0.05	0.24	0.08	-0.02	-0.35	-0.01
	N	38	30	11	31	24	18	35	12	18	29	14	28
	sig	21.7%	88.2%	9.6%	92.0%	82.0%	96.4%	79.2%	45.4%	76.3%	90.1%	22.6%	96.5%
Na	c	0.11	-0.12	-0.47	-0.16	0.01	-0.30	0.08	0.38	0.33	0.15	-0.29	-0.16
	N	38	30	11	31	24	18	35	12	18	29	14	28
	sig	50.8%	51.9%	14.2%	38.7%	97.1%	23.3%	66.2%	21.7%	18.2%	42.9%	31.1%	42.3%
Ni	c	0.10	0.26	-0.13	0.22	-0.16	0.37	0.04	-0.13	-0.05	-0.32	0.25	-0.16
	N	38	30	11	31	24	18	35	12	18	29	14	28
	sig	54.3%	16.8%	70.7%	23.0%	46.9%	13.1%	83.8%	68.1%	84.5%	8.7%	39.1%	42.0%
N(V)	c	0.03	-0.16	0.31	0.49	-0.54	0.23	-0.35	0.53	0.03	-0.20	0.14	-0.13
	N	38	30	11	31	24	18	35	12	18	29	14	28
	sig	83.6%	39.3%	35.8%	0.5%	0.6%	35.0%	4.2%	7.9%	90.4%	30.1%	64.2%	51.6%
Pb	c	0.18	0.07	0.61	0.14	-0.28	0.12	0.09	-0.15	0.04	-0.14	-0.10	-0.09
	N	38	30	11	31	24	18	35	12	18	29	14	28
	sig	27.6%	70.4%	4.8%	46.1%	18.8%	63.0%	60.7%	64.1%	87.6%	48.2%	72.6%	63.6%
pH	c	0.22	0.31	0.73	0.27	-0.11	0.24	0.03	-0.19	-0.29	-0.08	-0.12	0.12
	N	38	30	11	31	24	18	35	12	18	29	14	28
	sig	18.3%	9.2%	1.1%	14.1%	61.5%	33.4%	84.5%	55.6%	24.5%	68.6%	67.5%	56.0%
S(-II)	c	-0.17	-0.34	0.44	-0.10	0.40	-0.29	-0.07	-0.13	0.10	0.07	0.51	0.07
	N	38	30	11	31	24	18	35	12	18	29	14	28
	sig	30.6%	6.7%	17.4%	59.7%	5.0%	24.4%	70.7%	68.1%	68.3%	72.6%	6.4%	74.0%

Appendix 23

		As (g)	Al (g)	B (g)	Ba (g)	Cu (g)	Fe (g)	K (g)	Li (g)	SiO ₂ (g)	Sr (g)	Zn (g)	S(VI) (g)
SiO₂	c	0.19	0.48	-0.55	-0.19	0.19	-0.01	0.12	0.01	-0.16	0.05	-0.35	-0.04
	N	38	30	11	31	24	18	35	12	18	29	14	28
	sig	25.7%	0.8%	7.7%	29.9%	37.9%	95.8%	50.7%	96.6%	51.5%	81.5%	21.5%	85.1%
S(VI)	c	0.22	0.27	0.69	0.18	-0.18	-0.10	0.04	-0.48	-0.07	-0.07	-0.12	-0.05
	N	38	30	11	31	24	18	35	12	18	29	14	28
	sig	19.0%	15.1%	1.9%	34.1%	39.3%	69.3%	82.2%	11.8%	77.9%	72.4%	69.2%	79.9%
Sr	c	-0.23	0.16	0.25	0.04	-0.10	-0.10	0.01	-0.22	-0.36	-0.35	0.14	-0.18
	N	38	30	11	31	24	18	35	12	18	29	14	28
	sig	17.3%	40.6%	46.7%	84.3%	64.8%	69.3%	94.3%	49.9%	14.5%	6.7%	63.7%	35.0%
temp	c	0.18	-0.24	-0.05	-0.33	0.28	-0.09	0.20	0.30	0.68	0.28	-0.02	0.25
	N	38	30	11	31	24	18	35	12	18	29	14	28
	sig	28.2%	19.9%	87.3%	6.7%	18.9%	71.7%	25.3%	34.7%	0.2%	13.9%	95.8%	19.5%
TIC	c	-0.35	-0.36	0.61	-0.24	0.29	-0.71	-0.16	-0.59	-0.21	-0.12	0.37	0.07
	N	38	30	11	31	24	18	35	12	18	29	14	28
	sig	3.2%	5.4%	4.7%	19.5%	16.5%	0.1%	35.5%	4.2%	39.5%	52.3%	19.1%	73.6%
TOC	c	-0.05	-0.04	0.78	0.39	-0.17	0.15	-0.07	0.11	0.13	-0.04	0.30	0.07
	N	38	30	11	31	24	18	35	12	18	29	14	28
	sig	78.1%	83.5%	0.4%	3.2%	43.2%	54.8%	67.2%	73.7%	61.6%	82.5%	29.1%	71.5%
V	c	0.11	0.11	0.50	0.02	-0.20	0.04	0.09	-0.24	-0.15	-0.15	.	-0.22
	N	38	30	11	31	24	18	35	12	18	29	14	28
	sig	50.7%	55.4%	11.7%	93.5%	35.3%	87.0%	61.4%	45.9%	55.4%	43.3%	.	26.5%
Zn	c	0.12	0.25	0.01	0.40	-0.33	0.58	-0.06	0.24	-0.14	-0.16	-0.01	-0.13
	N	38	30	11	31	24	18	35	12	18	29	14	28
	sig	48.0%	18.2%	96.8%	2.7%	11.7%	1.1%	71.1%	45.7%	59.3%	42.1%	97.0%	51.2%

Appendix 24 Arsenic species distribution modeled with PHREEQC 2.8.03 (Parkhurst and Appelo 1999) using database WATEQ4F (V.2.4 with revised data from Nordstrom and Archer 2003); parameters and species considered were pH, Temp, pe, F, Cl, Br, N(V), S(VI), As(III), As(V), Al, B, Ba, Ca, Cd, Cu, K, Li, Mg, Mn, Na, Ni, Pb, Se, Sr, Zn, Si, S(-II), Fe(II), Fe(III), and C(IV); MMAA and DMAA were added to inorganic As(V) for calculations, concentrations given for As(V) complexes refer to the inorganic As(V) fraction actually determined by on-site species separation; only concentrations $> 10^{-08}$ mol/L are printed in black

Sampling site	H ₄ AsO ₃ ⁺	H ₃ AsO ₃	H ₂ AsO ₃ ⁻	HAsO ₃ ²⁻	AsO ₃ ³⁻	H ₃ AsO ₄	H ₂ AsO ₄ ⁻	HAsO ₄ ²⁻	AsO ₄ ³⁻	As ₃ S ₄ (HS) ₂ ⁻	AsS(OH)(HS) ⁻
YNPGG02-2W	1.9E-11	1.9E-05	5.3E-08	7.1E-16	8.6E-25	1.5E-10	3.5E-07	2.8E-08	2.4E-13	3.3E-12	1.0E-06
YNPGG04-1W	6.6E-10	5.8E-06	1.6E-10	2.1E-20	2.2E-31	1.3E-08	2.3E-07	1.5E-10	1.1E-17	6.4E-14	1.1E-08
YNPGG04-2W	8.7E-10	7.7E-06	2.1E-10	2.7E-20	2.9E-31	1.4E-08	2.5E-07	1.6E-10	1.2E-17	1.4E-13	1.4E-08
YNPGG04-4W	7.7E-10	5.5E-06	1.3E-10	1.4E-20	1.3E-31	1.3E-08	1.8E-07	9.7E-11	6.1E-18	1.2E-13	1.2E-08
YNPGG05-2W	3.5E-10	2.3E-07	2.4E-13	1.1E-24	4.0E-37	6.1E-09	8.1E-09	2.9E-13	8.7E-22	3.4E-15	6.7E-10
YNPGG05-4W	2.8E-10	2.0E-07	1.9E-13	7.1E-25	2.4E-37	1.6E-09	2.5E-09	9.6E-14	2.7E-22	1.0E-15	4.9E-10
YNPGG06-2W	2.0E-12	2.8E-05	1.4E-06	3.7E-13	8.5E-21	5.6E-12	1.7E-07	2.0E-07	3.0E-11	2.1E-12	5.0E-06
YNPGG07-2W	1.3E-11	2.9E-05	2.1E-07	8.1E-15	2.7E-23	6.6E-11	3.0E-07	5.2E-08	1.2E-12	9.8E-11	5.1E-06
YNPGG07-4W	1.4E-11	3.0E-05	2.2E-07	7.9E-15	2.5E-23	3.8E-11	1.7E-07	3.0E-08	6.3E-13	1.6E-11	2.8E-06
YNPGG08-4W	1.8E-08	8.3E-06	8.0E-12	3.6E-23	1.5E-35	3.3E-10	3.3E-10	1.0E-14	3.3E-23	1.0E-22	1.8E-12
YNPHL01-1W	3.6E-10	8.2E-07	6.6E-13	1.8E-24	6.1E-37	3.1E-09	2.3E-08	2.7E-12	1.1E-20	1.2E-12	1.1E-08
YNPHL01-2W	1.3E-09	3.0E-06	3.2E-12	1.2E-23	5.9E-36	5.7E-09	4.0E-08	5.2E-12	2.9E-20	1.1E-10	5.2E-08
YNPHL01-3W	1.4E-09	2.7E-06	2.3E-12	7.1E-24	2.9E-36	9.8E-10	6.1E-09	6.7E-13	3.1E-21	2.2E-09	1.3E-07
YNPHL02-1W	1.5E-13	2.8E-07	2.6E-10	8.5E-19	3.1E-28	2.0E-11	1.1E-07	9.9E-09	3.8E-14	7.0E-14	3.8E-07
YNPHL03-3W	7.8E-10	1.1E-06	2.0E-12	1.3E-23	8.6E-36	1.5E-08	5.0E-08	4.1E-12	2.2E-20	2.3E-25	4.8E-13
YNPLG01-2W	3.9E-13	1.3E-05	1.4E-06	8.2E-13	3.8E-20	1.8E-12	1.1E-07	2.7E-07	8.5E-11	1.2E-12	7.0E-06
YNPLG02-2W	5.5E-15	4.4E-06	1.2E-05	1.7E-10	2.0E-16	8.4E-15	1.3E-08	8.1E-07	6.1E-09	1.0E-19	2.6E-07
YNPLG03-2W	6.5E-14	2.2E-06	2.6E-07	1.5E-13	7.2E-21	1.2E-12	7.9E-08	2.1E-07	6.7E-11	7.2E-12	1.3E-05
YNPNL01-1W	1.5E-10	1.6E-07	6.2E-14	7.8E-26	1.2E-38	9.5E-08	3.3E-07	1.7E-11	3.1E-20	8.8E-21	1.3E-11
YNPNL02-1W	3.8E-09	1.9E-06	1.6E-12	5.5E-24	1.8E-36	1.4E-08	1.7E-08	5.3E-13	1.4E-21	9.1E-12	8.3E-09
YNPNL02-2W	5.9E-09	3.3E-06	4.2E-12	2.4E-23	1.2E-35	1.2E-08	1.4E-08	5.3E-13	1.9E-21	2.8E-09	6.1E-08
YNPNL02-3W	5.3E-10	3.6E-07	3.0E-13	9.7E-25	2.8E-37	7.9E-09	1.2E-08	4.2E-13	1.0E-21	9.5E-14	2.1E-09
YNPNL03-1W	2.4E-10	4.5E-07	1.7E-12	2.6E-23	3.1E-35	1.4E-08	5.0E-08	5.4E-12	4.9E-20	4.1E-16	6.8E-10
YNPNL03-2W	2.1E-10	1.9E-07	4.4E-13	4.6E-24	3.7E-36	4.4E-09	7.3E-09	3.8E-13	2.2E-21	4.7E-16	4.3E-10
YNPNL03-3W	6.3E-10	2.7E-07	3.1E-13	1.7E-24	7.4E-37	2.1E-09	1.8E-09	5.2E-14	1.6E-22	1.5E-15	4.0E-10
YNPNL04-1W	1.3E-10	2.6E-07	3.9E-13	2.0E-24	1.1E-36	7.2E-09	3.6E-08	3.6E-12	1.8E-20	5.2E-13	7.7E-09
YNPNL04-2W	4.1E-10	1.6E-07	8.6E-14	1.9E-25	4.0E-38	2.3E-09	2.0E-09	4.7E-14	8.2E-23	3.4E-25	2.3E-13
YNPNL04-3W	5.2E-10	2.0E-07	1.4E-13	4.0E-25	1.1E-37	3.6E-10	3.0E-10	7.7E-15	1.5E-23	3.5E-15	5.0E-10
YNPNL05-1W	1.0E-08	1.9E-06	7.6E-13	1.5E-24	2.8E-37	9.3E-09	4.0E-09	5.7E-14	8.5E-23	1.0E-13	1.0E-09
YNPNL05-2W	1.2E-08	1.7E-06	7.7E-13	1.9E-24	4.2E-37	5.0E-10	1.7E-10	2.1E-15	3.4E-24	1.1E-15	2.0E-10
YNPRH01-1W	1.1E-08	1.1E-05	1.7E-11	1.1E-22	7.4E-35	7.2E-08	1.6E-07	9.8E-12	5.1E-20	8.4E-12	1.2E-08
YNPRH01-2W	8.4E-09	8.4E-06	1.6E-11	1.4E-22	1.1E-34	9.6E-08	2.1E-07	1.4E-11	8.7E-20	7.8E-13	5.8E-09
YNPRH01-3W	7.6E-09	6.8E-06	1.2E-11	9.9E-23	7.0E-35	4.3E-08	8.3E-08	4.9E-12	2.7E-20	9.7E-11	2.7E-08
YNPRH03-1W	4.7E-08	2.0E-05	6.3E-12	7.9E-24	1.1E-36	7.1E-08	8.7E-08	2.2E-12	3.1E-21	8.3E-20	1.6E-11
YNPRH04-1W	4.7E-08	1.9E-05	7.4E-12	1.2E-23	2.0E-36	3.2E-08	3.6E-08	9.6E-13	1.5E-21	2.6E-15	4.9E-10
YNPRH04-2W	5.2E-08	2.0E-05	7.6E-12	1.2E-23	2.0E-36	9.3E-08	9.9E-08	2.5E-12	4.0E-21	1.3E-17	8.1E-11
YNPRH04-3W	6.4E-08	2.0E-05	6.7E-12	9.6E-24	1.5E-36	1.8E-08	1.5E-08	3.1E-13	4.2E-22	4.0E-13	2.2E-09
YNPRH05-1W	5.4E-08	7.4E-05	1.7E-10	1.9E-21	2.0E-33	1.0E-07	3.3E-07	3.2E-11	2.6E-19	3.2E-06	1.2E-06
YNPRH05-3W	9.7E-08	1.4E-04	6.1E-10	1.4E-20	2.6E-32	9.8E-08	2.8E-07	2.9E-11	3.7E-19	1.7E-06	9.7E-07
YNPRH07-2W	2.9E-09	1.1E-06	1.1E-12	5.2E-24	1.9E-36	7.2E-08	5.2E-08	1.3E-12	3.4E-21	4.2E-15	5.2E-10

Appendix 24

Sampling site	H_4AsO_3^+	H_3AsO_3	H_2AsO_3^-	HAsO_3^{2-}	AsO_3^{3-}	H_3AsO_4	H_2AsO_4^-	HAsO_4^{2-}	AsO_4^{3-}	$\text{As}_3\text{S}_4(\text{HS})_2^-$	$\text{AsS}(\text{OH})(\text{HS})^-$
YNPRH08-1W	1.6E ⁻⁰⁸	3.4E ⁻⁰⁵	1.6E ⁻¹⁰	3.7E ⁻²¹	8.1E ⁻³³	1.2E ⁻⁰⁷	6.0E ⁻⁰⁷	1.0E ⁻¹⁰	1.7E ⁻¹⁸	1.2E ⁻¹⁰	5.5E ⁻⁰⁸
YNPRH08-4W	3.9E ⁻¹¹	3.2E ⁻⁰⁵	7.8E ⁻⁰⁸	9.6E ⁻¹⁶	1.0E ⁻²⁴	2.3E ⁻¹⁰	4.1E ⁻⁰⁷	2.6E ⁻⁰⁸	2.0E ⁻¹³	5.8E ⁻¹¹	2.2E ⁻⁰⁶
YNPRH09-1W	2.0E ⁻¹²	3.2E ⁻⁰⁵	1.3E ⁻⁰⁶	2.6E ⁻¹³	4.8E ⁻²¹	2.8E ⁻¹²	1.0E ⁻⁰⁷	1.2E ⁻⁰⁷	1.7E ⁻¹¹	3.5E ⁻¹⁷	1.4E ⁻⁰⁷
YNPRH10-4W	3.7E ⁻⁰⁹	3.2E ⁻⁰⁵	1.0E ⁻⁰⁹	1.6E ⁻¹⁹	2.2E ⁻³⁰	9.7E ⁻⁰⁹	1.7E ⁻⁰⁷	1.1E ⁻¹⁰	1.0E ⁻¹⁷	1.9E ⁻¹⁹	1.6E ⁻¹⁰
YNPRH11-3W	8.9E ⁻⁰⁸	3.3E ⁻⁰⁵	2.2E ⁻¹¹	7.2E ⁻²³	2.3E ⁻³⁵	1.0E ⁻⁰⁷	9.8E ⁻⁰⁸	2.8E ⁻¹²	7.5E ⁻²¹	2.1E ⁻⁰⁶	4.5E ⁻⁰⁷
YNPRH13-3W	1.8E ⁻⁰⁹	3.6E ⁻⁰⁵	1.8E ⁻⁰⁹	4.7E ⁻¹⁹	1.1E ⁻²⁹	1.5E ⁻⁰⁸	7.0E ⁻⁰⁷	1.1E ⁻⁰⁹	1.9E ⁻¹⁶	4.4E ⁻¹⁹	3.7E ⁻¹⁰
YNPRH14-3W	6.3E ⁻¹⁰	3.8E ⁻⁰⁵	6.9E ⁻⁰⁹	6.3E ⁻¹⁸	5.1E ⁻²⁸	5.0E ⁻⁰⁹	6.5E ⁻⁰⁷	3.2E ⁻⁰⁹	1.8E ⁻¹⁵	1.7E ⁻¹⁵	1.2E ⁻⁰⁸
YNPRH15-3W	2.7E ⁻⁰⁸	2.8E ⁻⁰⁵	2.1E ⁻¹¹	6.4E ⁻²³	2.3E ⁻³⁵	2.5E ⁻⁰⁷	7.8E ⁻⁰⁷	5.1E ⁻¹¹	1.9E ⁻¹⁹	4.7E ⁻²²	5.0E ⁻¹²
YNPRH16-4W	2.0E ⁻⁰⁸	3.8E ⁻⁰⁵	5.4E ⁻¹¹	3.1E ⁻²²	2.1E ⁻³⁴	1.1E ⁻⁰⁷	5.8E ⁻⁰⁷	6.9E ⁻¹¹	4.6E ⁻¹⁹	2.0E ⁻²¹	1.2E ⁻¹¹
YNPRH17-4W	1.4E ⁻⁰⁸	1.6E ⁻⁰⁵	3.7E ⁻¹¹	4.1E ⁻²²	4.3E ⁻³⁴	1.1E ⁻⁰⁷	2.8E ⁻⁰⁷	2.3E ⁻¹¹	1.8E ⁻¹⁹	1.7E ⁻²¹	8.4E ⁻¹²
YNPRH18-4W	5.0E ⁻⁰⁹	4.3E ⁻⁰⁶	1.1E ⁻¹¹	1.4E ⁻²²	1.4E ⁻³⁴	6.9E ⁻⁰⁸	1.1E ⁻⁰⁷	6.5E ⁻¹²	4.2E ⁻²⁰	4.3E ⁻²³	2.0E ⁻¹²
YNPRH19-4W	5.1E ⁻⁰⁹	2.3E ⁻⁰⁵	3.8E ⁻¹⁰	3.3E ⁻²⁰	2.3E ⁻³¹	2.8E ⁻⁰⁸	2.6E ⁻⁰⁷	9.2E ⁻¹¹	4.4E ⁻¹⁸	2.0E ⁻¹³	1.1E ⁻⁰⁸
YNPRH20-4W	5.4E ⁻⁰⁹	2.0E ⁻⁰⁵	1.4E ⁻¹⁰	4.6E ⁻²¹	1.4E ⁻³²	4.4E ⁻⁰⁸	3.8E ⁻⁰⁷	1.0E ⁻¹⁰	2.5E ⁻¹⁸	9.3E ⁻²¹	3.3E ⁻¹¹
YNPRH21-4W	1.0E ⁻⁰⁸	1.1E ⁻⁰⁵	3.0E ⁻¹¹	3.7E ⁻²²	4.3E ⁻³⁴	1.7E ⁻⁰⁷	4.2E ⁻⁰⁷	3.2E ⁻¹¹	2.8E ⁻¹⁹	7.5E ⁻²²	6.3E ⁻¹²
YNPRH22-4W	5.3E ⁻⁰⁹	4.9E ⁻⁰⁶	5.8E ⁻¹²	2.9E ⁻²³	1.3E ⁻³⁵	1.4E ⁻⁰⁷	2.9E ⁻⁰⁷	1.5E ⁻¹¹	6.1E ⁻²⁰	9.1E ⁻¹⁶	5.6E ⁻¹⁰
YNPRH24-4W	1.9E ⁻⁰⁸	2.2E ⁻⁰⁵	3.3E ⁻¹¹	2.1E ⁻²²	1.3E ⁻³⁴	2.2E ⁻⁰⁷	6.5E ⁻⁰⁷	5.2E ⁻¹¹	2.9E ⁻¹⁹	1.9E ⁻¹⁸	8.9E ⁻¹¹
YNPRH25-4W	8.7E ⁻⁰⁹	2.4E ⁻⁰⁵	2.3E ⁻¹⁰	1.1E ⁻²⁰	4.6E ⁻³²	2.2E ⁻⁰⁸	1.2E ⁻⁰⁷	2.5E ⁻¹¹	7.0E ⁻¹⁹	5.3E ⁻¹³	1.0E ⁻⁰⁸
YNPRH26-4W	1.0E ⁻⁰⁸	1.5E ⁻⁰⁵	5.3E ⁻¹¹	8.6E ⁻²²	1.3E ⁻³³	4.5E ⁻⁰⁸	1.5E ⁻⁰⁷	1.7E ⁻¹¹	1.8E ⁻¹⁹	1.7E ⁻⁰⁶	1.0E ⁻⁰⁶
YNPRH27-4W	1.3E ⁻⁰⁹	3.3E ⁻⁰⁵	2.8E ⁻⁰⁹	1.2E ⁻¹⁸	4.5E ⁻²⁹	1.2E ⁻⁰⁸	6.4E ⁻⁰⁷	1.3E ⁻⁰⁹	3.3E ⁻¹⁶	6.9E ⁻¹⁶	5.1E ⁻⁰⁹
YNPRH28-4W	2.1E ⁻⁰⁹	1.8E ⁻⁰⁵	3.6E ⁻¹⁰	3.3E ⁻²⁰	2.8E ⁻³¹	1.7E ⁻⁰⁸	3.3E ⁻⁰⁷	2.1E ⁻¹⁰	1.2E ⁻¹⁷	2.9E ⁻¹⁷	8.4E ⁻¹⁰

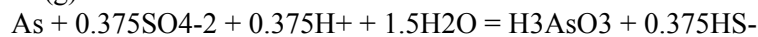
Appendix 25 Saturation indices for As minerals modeled with PHREEQC 2.8.03 (Parkhurst and Appelo 1999) using database WATEQ4F (V.2.4 with revised data from Nordstrom and Archer 2003); for parameters and species considered see Appendix 24; supersaturated phases marked in bold; other As minerals listed in the WATEQ4F database and not displayed in the table below (As_2O_5 ; $\text{AlAsO}_4 \cdot 2\text{H}_2\text{O}$; $\text{Ca}_3(\text{AsO}_4)_2 \cdot 4\text{H}_2\text{O}$; $\text{Cu}_3(\text{AsO}_4)_2 \cdot 6\text{H}_2\text{O}$; $\text{Mn}_3(\text{AsO}_4)_2 \cdot 8\text{H}_2\text{O}$; $\text{Ni}_3(\text{AsO}_4)_2 \cdot 8\text{H}_2\text{O}$; $\text{Pb}_3(\text{AsO}_4)_2$; $\text{Zn}_3(\text{AsO}_4)_2 \cdot 2.5\text{H}_2\text{O}$) are all undersaturated

Sampling site	Scorodite	Arsenolite	Claudetite	Orpiment	$\text{As}_2\text{S}_3(\text{am})$	Realgar	Sampling site	Scorodite	Arsenolite	Claudetite	Orpiment	$\text{As}_2\text{S}_3(\text{am})$	Realgar
YNPGG02-2W	-6.3	-8.8	-8.8	-7.9	-8.8	-6.0	YNPRH01-1W	-4.9	-9.2	-9.2	-4.6	-5.7	-6.8
YNPGG04-1W	-7.0	-10.0	-10.0	-8.8	-9.6	-6.4	YNPRH01-2W	-5.1	-9.5	-9.5	-5.9	-6.8	-9.4
YNPGG04-2W	-7.0	-9.7	-9.7	-8.6	-9.4	-6.3	YNPRH01-3W	-5.9	-9.7	-9.7	-5.1	-6.0	-7.9
YNPGG04-4W	-6.7	-10.0	-10.0	-8.8	-9.7	-10.0	YNPRH03-1W	-4.8	-8.3	-8.3	-5.0	-6.3	-13.7
YNPGG05-2W	-8.8	-12.6	-12.6	-7.4	-8.4	-8.7	YNPRH04-1W	-4.6	-8.4	-8.4	-3.6	-4.8	-13.3
YNPGG05-4W	-8.0	-12.6	-12.6	-6.8	-7.9	-7.3	YNPRH04-2W	-5.1	-8.3	-8.4	-4.8	-6.0	-12.3
YNPGG06-2W	-8.1	-8.6	-8.6	-9.6	-10.4	-6.5	YNPRH04-3W	-5.4	-8.4	-8.4	-3.1	-4.2	-6.4
YNPGG07-2W	-7.2	-8.6	-8.6	-8.3	-9.1	-7.1	YNPRH05-1W	-3.9	-7.5	-7.5	-1.6	-2.6	-5.7
YNPGG07-4W	-7.3	-8.6	-8.6	-8.6	-9.4	-7.2	YNPRH05-3W	-4.5	-7.3	-7.3	-4.2	-5.0	-7.4
YNPGG08-4W	-6.9	-9.5	-9.5	-11.0	-12.0	-8.3	YNPRH07-2W	-6.9	-11.4	-11.4	-8.8	-9.6	-7.3
YNPHL01-1W	-4.5	-10.7	-10.7	0.4	-1.0	-7.7	YNPRH08-1W	-6.5	-8.2	-8.2	-4.8	-5.8	-5.4
YNPHL01-2W	-5.0	-9.7	-9.7	0.6	-0.8	-7.9	YNPRH08-4W	-6.2	-8.5	-8.5	-7.6	-8.5	-8.3
YNPHL01-3W	-5.1	-9.8	-9.8	1.6	0.2	-3.1	YNPRH09-1W	-7.6	-8.4	-8.4	-10.7	-11.6	-9.6
YNPHL02-1W	-4.8	-11.8	-11.9	-3.5	-4.9	-7.8	YNPRH10-4W	-5.5	-8.6	-8.6	-11.8	-12.6	-4.2
YNPHL03-3W	-5.9	-11.0	-11.0	-10.9	-12.0	-6.5	YNPRH11-3W	-6.1	-8.2	-8.2	-1.5	-2.5	-3.9
YNPLG01-2W	-8.9	-9.4	-9.3	-10.3	-11.1	-6.6	YNPRH13-3W	-5.8	-8.3	-8.3	-10.2	-11.1	-12.7
YNPLG02-2W	-12.0	-10.3	-10.3	-14.7	-15.5	-8.5	YNPRH14-3W	-5.8	-8.3	-8.3	-9.2	-10.1	-10.7
YNPLG03-2W	-8.7	-10.9	-10.9	-10.2	-11.0	-5.8	YNPRH15-3W	-5.4	-7.9	-7.9	-6.1	-7.4	2.4
YNPNL01-1W	-5.6	-12.1	-12.2	-4.0	-5.4	-7.4	YNPRH16-4W	-5.9	-7.7	-7.7	-6.0	-7.3	1.8
YNPNL02-1W	-7.2	-10.7	-10.7	-4.8	-5.8	-9.0	YNPRH17-4W	-5.2	-8.9	-8.9	-10.3	-11.2	-9.9
YNPNL02-2W	-8.6	-10.3	-10.3	-4.8	-5.7	-5.0	YNPRH18-4W	-6.4	-10.3	-10.2	-13.1	-13.9	-8.9
YNPNL02-3W	-7.9	-12.0	-12.0	-5.5	-6.5	-6.1	YNPRH19-4W	-6.6	-8.8	-8.8	-8.7	-9.5	-7.5
YNPNL03-1W	-5.8	-12.0	-12.0	-8.7	-9.6	-13.1	YNPRH20-4W	-5.8	-8.7	-8.7	-9.7	-10.6	-14.1
YNPNL03-2W	-6.9	-12.9	-12.9	-9.9	-10.7	-8.8	YNPRH21-4W	-5.9	-9.3	-9.3	-11.0	-12.0	-8.7
YNPNL03-3W	-7.2	-12.6	-12.6	-9.3	-10.2	-7.4	YNPRH22-4W	-5.2	-9.8	-9.8	-6.0	-7.1	-5.2
YNPNL04-1W	-6.7	-12.1	-12.1	-3.3	-4.5	-4.7	YNPRH24-4W	-5.8	-8.4	-8.4	-6.6	-7.7	-8.6
YNPNL04-2W	-8.4	-12.8	-12.8	-11.5	-12.5	-8.7	YNPRH25-4W	-5.3	-8.8	-8.8	-8.3	-9.1	-6.9
YNPNL04-3W	-7.8	-12.7	-12.7	-7.4	-8.3	-8.8	YNPRH26-4W	-5.9	-9.0	-9.0	-3.2	-4.1	-2.4
YNPNL05-1W	-6.8	-10.8	-10.8	-6.5	-7.4	-11.9	YNPRH27-4W	-5.8	-8.5	-8.5	-9.8	-10.6	-9.7
YNPNL05-2W	-7.2	-11.0	-11.0	-8.7	-9.6	-12.2	YNPRH28-4W	-5.6	-8.9	-8.9	-9.0	-9.9	-8.8

Appendix 26 Thermodynamic data for gaseous As species from Spycher and Reed (1989) and Pokrovski et al. (2002)

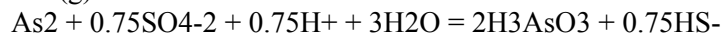
Spycher and Reed (1989):

As(g)



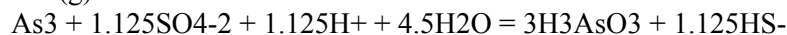
log_k 45.78

As₂(g)



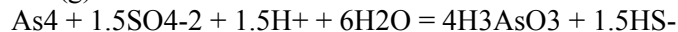
log_k 24.89

As₃(g)



log_k 35.61

As₄(g)



log_k 18.22

AsCl₃(g)



log_k 12.97

AsF₃(g)



log_k 0.58

AsF₅(g)



log_k 20.97

AsH₃(g)



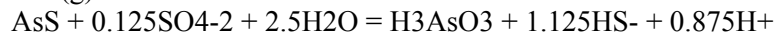
log_k 24.86

As₄O₆(g)



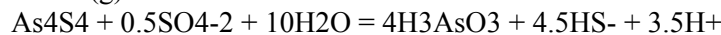
log_k 8.01

AsS(g)



log_k 13.65

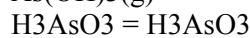
As₄S₄(g)



log_k -51.05

Pokrovski et al. (2002):

As(OH)₃(g)



log_k 11.3

Appendix 27 Partial pressure of gaseous As species considering the thermodynamic data from Spycher and Reed (1989) and Pokrovski et al. (2002; Appendix 26) in PHREEQC; for parameters and dissolved species considered see Appendix 24

Sampling site	As(g)	As ₂ (g)	As ₃ (g)	As ₄ (g)	AsCl ₃ (g)	AsF ₃ (g)	AsF ₅ (g)	AsH ₃ (g)	AsS(g)	As ₄ S ₄ (g)	As ₂ O ₆ (g)	As(OH) ₃ (g)
YNPGG02-2W	1.8E ⁻⁴⁸	1.5E ⁻³¹	3.2E ⁻⁴⁶	8.4E ⁻³³	1.1E ⁻³⁹	6.2E ⁻³²	1.9E ⁻⁷¹	8.4E ⁻²⁷	2.0E ⁻²⁹	7.3E ⁻¹⁶	1.4E ⁻²⁵	9.8E ⁻¹⁵
YNPGG04-1W	1.6E ⁻⁵⁰	1.3E ⁻³⁵	2.4E ⁻⁵²	5.8E ⁻⁴¹	2.7E ⁻³⁵	3.2E ⁻³¹	6.8E ⁻⁶⁹	2.3E ⁻³⁰	4.0E ⁻³⁰	1.1E ⁻¹⁸	1.2E ⁻²⁷	2.9E ⁻¹⁵
YNPGG04-2W	2.2E ⁻⁵⁰	2.2E ⁻³⁵	5.6E ⁻⁵²	1.8E ⁻⁴⁰	4.2E ⁻³⁵	1.4E ⁻²⁹	3.3E ⁻⁶⁶	3.1E ⁻³⁰	5.2E ⁻³⁰	3.4E ⁻¹⁸	3.5E ⁻²⁷	3.9E ⁻¹⁵
YNPGG04-4W	1.5E ⁻⁵⁰	1.0E ⁻³⁵	1.7E ⁻⁵²	3.8E ⁻⁴¹	6.2E ⁻³⁵	6.3E ⁻³⁰	1.1E ⁻⁶⁶	2.0E ⁻³⁰	4.4E ⁻³⁰	1.6E ⁻¹⁸	9.4E ⁻²⁸	2.8E ⁻¹⁵
YNPGG05-2W	1.8E ⁻⁵²	1.6E ⁻³⁹	3.4E ⁻⁵⁸	9.3E ⁻⁴⁹	3.0E ⁻³⁹	5.3E ⁻³⁷	3.2E ⁻⁷⁷	7.6E ⁻³³	5.0E ⁻³¹	2.8E ⁻²²	2.6E ⁻³³	1.1E ⁻¹⁶
YNPGG05-4W	1.7E ⁻⁵²	1.3E ⁻³⁹	2.6E ⁻⁵⁸	6.5E ⁻⁴⁹	3.2E ⁻³⁹	1.5E ⁻³⁶	2.0E ⁻⁷⁶	7.2E ⁻³³	3.8E ⁻³¹	9.5E ⁻²³	1.6E ⁻³³	1.0E ⁻¹⁶
YNPGG06-2W	1.8E ⁻⁴⁷	1.6E ⁻²⁹	3.3E ⁻⁴³	8.9E ⁻²⁹	1.5E ⁻⁴²	2.3E ⁻³⁴	3.8E ⁻⁷⁶	5.8E ⁻²⁵	2.8E ⁻²⁹	2.6E ⁻¹⁵	6.6E ⁻²⁵	1.4E ⁻¹⁴
YNPGG07-2W	6.0E ⁻⁴⁸	1.7E ⁻³⁰	1.1E ⁻⁴⁴	1.0E ⁻³⁰	3.2E ⁻⁴⁰	5.5E ⁻³²	7.3E ⁻⁷²	6.1E ⁻²⁶	5.0E ⁻²⁹	2.7E ⁻¹⁴	7.2E ⁻²⁵	1.5E ⁻¹⁴
YNPGG07-4W	5.6E ⁻⁴⁸	1.5E ⁻³⁰	9.5E ⁻⁴⁵	7.9E ⁻³¹	2.5E ⁻⁴⁰	1.1E ⁻³¹	2.5E ⁻⁷¹	5.2E ⁻²⁶	3.6E ⁻²⁹	7.9E ⁻¹⁵	8.3E ⁻²⁵	1.5E ⁻¹⁴
YNPGG08-4W	8.1E ⁻⁵²	3.1E ⁻³⁸	2.8E ⁻⁵⁶	3.4E ⁻⁴⁶	2.0E ⁻³¹	1.9E ⁻²⁸	2.1E ⁻⁶³	3.9E ⁻³³	8.6E ⁻³²	2.5E ⁻²⁵	4.7E ⁻²⁷	4.2E ⁻¹⁵
YNPHL01-1W	1.6E ⁻⁵¹	1.3E ⁻³⁷	2.4E ⁻⁵⁵	5.8E ⁻⁴⁵	1.1E ⁻³⁴	3.7E ⁻³⁶	1.9E ⁻⁷⁶	1.7E ⁻³¹	2.7E ⁻³⁰	2.5E ⁻¹⁹	4.4E ⁻³¹	4.1E ⁻¹⁶
YNPHL01-2W	5.5E ⁻⁵¹	1.4E ⁻³⁶	9.1E ⁻⁵⁴	7.5E ⁻⁴³	1.8E ⁻³³	1.7E ⁻³⁴	4.9E ⁻⁷⁴	5.2E ⁻³¹	1.1E ⁻²⁹	5.9E ⁻¹⁷	7.7E ⁻²⁹	1.5E ⁻¹⁵
YNPHL01-3W	5.5E ⁻⁵¹	1.4E ⁻³⁶	8.8E ⁻⁵⁴	7.1E ⁻⁴³	6.7E ⁻³³	1.6E ⁻³³	2.1E ⁻⁷²	5.6E ⁻³¹	1.8E ⁻²⁹	4.5E ⁻¹⁶	5.0E ⁻²⁹	1.3E ⁻¹⁵
YNPHL02-1W	6.2E ⁻⁵⁰	1.8E ⁻³⁴	1.3E ⁻⁵⁰	1.2E ⁻³⁸	1.6E ⁻⁴⁴	6.7E ⁻³⁸	2.1E ⁻⁸⁰	6.9E ⁻²⁸	1.6E ⁻³⁰	2.7E ⁻²⁰	5.9E ⁻³³	1.4E ⁻¹⁶
YNPHL03-3W	2.6E ⁻⁵²	3.1E ⁻³⁹	9.2E ⁻⁵⁸	3.5E ⁻⁴⁸	1.3E ⁻³⁷	1.4E ⁻³⁵	6.1E ⁻⁷⁵	2.9E ⁻³³	1.3E ⁻³²	1.2E ⁻²⁸	1.6E ⁻³⁰	5.7E ⁻¹⁶
YNPLG01-2W	2.3E ⁻⁴⁷	2.4E ⁻²⁹	6.4E ⁻⁴³	2.2E ⁻²⁸	1.0E ⁻⁴⁴	7.4E ⁻³⁵	4.8E ⁻⁷⁷	2.0E ⁻²⁴	2.1E ⁻²⁹	8.6E ⁻¹⁶	2.6E ⁻²⁶	6.4E ⁻¹⁵
YNPLG02-2W	3.5E ⁻⁴⁷	5.7E ⁻²⁹	2.3E ⁻⁴²	1.2E ⁻²⁷	2.6E ⁻⁴⁹	2.1E ⁻³⁹	1.0E ⁻⁸⁴	1.4E ⁻²³	7.8E ⁻³¹	1.7E ⁻²¹	3.7E ⁻²⁸	2.2E ⁻¹⁵
YNPLG03-2W	5.9E ⁻⁴⁸	1.6E ⁻³⁰	1.1E ⁻⁴⁴	9.8E ⁻³¹	1.4E ⁻⁴⁵	1.0E ⁻³⁵	4.6E ⁻⁷⁸	7.9E ⁻²⁵	1.3E ⁻²⁹	1.4E ⁻¹⁶	2.4E ⁻²⁹	1.1E ⁻¹⁵
YNPNL01-1W	8.0E ⁻⁵³	3.0E ⁻⁴⁰	2.7E ⁻⁵⁹	3.2E ⁻⁵⁰	1.0E ⁻³⁶	1.0E ⁻³³	1.7E ⁻⁷¹	2.0E ⁻³³	3.8E ⁻³²	9.5E ⁻²⁷	6.5E ⁻³⁴	8.0E ⁻¹⁷
YNPNL02-1W	1.2E ⁻⁵¹	7.1E ⁻³⁸	1.0E ⁻⁵⁵	1.8E ⁻⁴⁵	3.1E ⁻³⁵	6.5E ⁻³³	6.0E ⁻⁷¹	3.9E ⁻³²	5.2E ⁻³⁰	3.2E ⁻¹⁸	1.4E ⁻²⁹	9.7E ⁻¹⁶
YNPNL02-2W	3.1E ⁻⁵¹	4.4E ⁻³⁷	1.5E ⁻⁵⁴	6.9E ⁻⁴⁴	9.2E ⁻³⁵	4.9E ⁻³¹	4.4E ⁻⁶⁸	1.4E ⁻³¹	2.0E ⁻²⁹	6.5E ⁻¹⁶	1.2E ⁻²⁸	1.7E ⁻¹⁵
YNPNL02-3W	3.5E ⁻⁵²	5.8E ⁻³⁹	2.4E ⁻⁵⁷	1.2E ⁻⁴⁷	4.1E ⁻⁴⁰	1.8E ⁻³³	1.6E ⁻⁷¹	1.7E ⁻³²	1.2E ⁻³⁰	8.0E ⁻²¹	1.6E ⁻³²	1.8E ⁻¹⁶
YNPNL03-1W	6.8E ⁻⁵²	2.1E ⁻³⁸	1.7E ⁻⁵⁶	1.7E ⁻⁴⁶	2.7E ⁻⁴⁰	2.3E ⁻³⁵	7.3E ⁻⁷⁵	5.1E ⁻³²	5.1E ⁻³¹	3.0E ⁻²²	4.1E ⁻³²	2.3E ⁻¹⁶
YNPNL03-2W	1.7E ⁻⁵²	1.4E ⁻³⁹	2.8E ⁻⁵⁸	7.2E ⁻⁴⁹	2.4E ⁻³⁹	3.1E ⁻³⁶	6.4E ⁻⁷⁶	8.1E ⁻³³	3.2E ⁻³¹	4.8E ⁻²³	1.2E ⁻³³	9.3E ⁻¹⁷
YNPNL03-3W	1.4E ⁻⁵²	8.9E ⁻⁴⁰	1.4E ⁻⁵⁸	2.9E ⁻⁴⁹	5.6E ⁻³⁸	6.8E ⁻³⁷	5.9E ⁻⁷⁷	3.6E ⁻³³	4.3E ⁻³¹	1.5E ⁻²²	5.0E ⁻³³	1.3E ⁻¹⁶
YNPNL04-1W	6.8E ⁻⁵²	2.2E ⁻³⁸	1.7E ⁻⁵⁶	1.7E ⁻⁴⁶	2.1E ⁻⁴⁰	6.2E ⁻³⁶	8.0E ⁻⁷⁶	8.9E ⁻³²	1.5E ⁻³⁰	2.3E ⁻²⁰	4.4E ⁻³³	1.3E ⁻¹⁶
YNPNL04-2W	2.0E ⁻⁵³	1.9E ⁻⁴¹	4.5E ⁻⁶¹	1.3E ⁻⁵²	3.4E ⁻³⁸	6.0E ⁻³⁵	3.7E ⁻⁷³	1.3E ⁻³⁴	5.3E ⁻³³	3.4E ⁻³⁰	6.4E ⁻³⁴	8.0E ⁻¹⁷
YNPNL04-3W	9.8E ⁻⁵³	4.5E ⁻⁴⁰	5.1E ⁻⁵⁹	7.5E ⁻⁵⁰	8.3E ⁻³⁸	2.5E ⁻³⁶	6.7E ⁻⁷⁶	2.4E ⁻³³	4.3E ⁻³¹	1.5E ⁻²²	1.6E ⁻³³	1.0E ⁻¹⁶
YNPNL05-1W	4.2E ⁻⁵²	8.2E ⁻³⁹	3.9E ⁻⁵⁷	2.4E ⁻⁴⁷	6.5E ⁻³³	5.6E ⁻³³	9.6E ⁻⁷¹	4.6E ⁻³³	2.0E ⁻³⁰	6.8E ⁻²⁰	1.3E ⁻²⁹	9.6E ⁻¹⁶
YNPNL05-2W	2.5E ⁻⁵²	3.0E ⁻³⁹	8.8E ⁻⁵⁸	3.3E ⁻⁴⁸	5.8E ⁻³³	2.5E ⁻³³	3.3E ⁻⁷¹	1.9E ⁻³³	8.0E ⁻³¹	1.8E ⁻²¹	8.2E ⁻³⁰	8.5E ⁻¹⁶
YNPRH01-1W	9.5E ⁻⁵¹	4.2E ⁻³⁶	4.6E ⁻⁵³	6.5E ⁻⁴²	1.7E ⁻³¹	1.3E ⁻³²	4.7E ⁻⁷¹	4.3E ⁻³¹	1.2E ⁻²⁹	9.1E ⁻¹⁷	1.2E ⁻²⁶	5.3E ⁻¹⁵
YNPRH01-2W	7.1E ⁻⁵¹	2.4E ⁻³⁶	1.9E ⁻⁵³	2.0E ⁻⁴²	1.2E ⁻³¹	2.9E ⁻³³	4.8E ⁻⁷²	3.0E ⁻³¹	7.0E ⁻³⁰	1.1E ⁻¹⁷	4.9E ⁻²⁷	4.2E ⁻¹⁵
YNPRH01-3W	7.5E ⁻⁵¹	2.6E ⁻³⁶	2.3E ⁻⁵³	2.5E ⁻⁴²	8.4E ⁻³²	1.1E ⁻³²	4.0E ⁻⁷¹	4.2E ⁻³¹	1.6E ⁻²⁹	2.7E ⁻¹⁶	2.1E ⁻²⁷	3.4E ⁻¹⁵
YNPRH03-1W	2.2E ⁻⁵¹	2.3E ⁻³⁷	5.8E ⁻⁵⁵	1.9E ⁻⁴⁴	1.8E ⁻³⁰	5.9E ⁻³¹	7.3E ⁻⁶⁸	1.2E ⁻³²	4.3E ⁻³¹	1.6E ⁻²²	1.5E ⁻²⁵	9.9E ⁻¹⁵
YNPRH04-1W	4.1E ⁻⁵¹	8.0E ⁻³⁷	3.8E ⁻⁵⁴	2.3E ⁻⁴³	1.8E ⁻³⁰	1.7E ⁻³¹	6.1E ⁻⁶⁹	4.4E ⁻³²	3.0E ⁻³⁰	3.6E ⁻¹⁹	1.4E ⁻²⁵	9.8E ⁻¹⁵
YNPRH04-2W	3.0E ⁻⁵¹	4.1E ⁻³⁷	1.4E ⁻⁵⁴	6.2E ⁻⁴⁴	3.3E ⁻³⁰	3.3E ⁻³¹	2.3E ⁻⁶⁸	2.2E ⁻³²	1.1E ⁻³⁰	7.0E ⁻²¹	1.7E ⁻²⁵	1.0E ⁻¹⁴
YNPRH04-3W	4.7E ⁻⁵¹	1.0E ⁻³⁶	5.5E ⁻⁵⁴	3.8E ⁻⁴³	3.4E ⁻³⁰	2.8E ⁻³⁰	6.1E ⁻⁶⁷	5.5E ⁻³²	7.6E ⁻³⁰	1.5E ⁻¹⁷	1.5E ⁻²⁵	1.0E ⁻¹⁴
YNPRH05-1W	1.3E ⁻⁴⁹	7.9E ⁻³⁴	1.2E ⁻⁴⁹	2.2E ⁻³⁷	1.6E ⁻³⁰	7.7E ⁻³⁰	3.5E ⁻⁶⁷	1.1E ⁻²⁹	3.2E ⁻²⁸	4.5E ⁻¹¹	3.0E ⁻²³	3.7E ⁻¹⁴
YNPRH05-3W	2.4E ⁻⁴⁹	2.7E ⁻³³	7.4E ⁻⁴⁹	2.6E ⁻³⁶	2.4E ⁻³⁰	1.5E ⁻²⁶	6.8E ⁻⁶²	2.1E ⁻²⁹	3.8E ⁻²⁸	9.8E ⁻¹¹	3.3E ⁻²²	6.8E ⁻¹⁴
YNPRH07-2W	4.6E ⁻⁵²	1.0E ⁻³⁸	5.3E ⁻⁵⁷	3.6E ⁻⁴⁷	5.8E ⁻³⁶	1.2E ⁻³³	7.1E ⁻⁷²	9.8E ⁻³³	9.9E ⁻³¹	4.3E ⁻²¹	1.4E ⁻³⁰	5.5E ⁻¹⁶
YNPRH08-1W	7.0E ⁻⁵⁰	2.3E ⁻³⁴	1.8E ⁻⁵⁰	1.9E ⁻³⁸	9.0E ⁻³¹	1.0E ⁻²⁵	3.8E ⁻⁶⁰	7.0E ⁻³⁰	3.8E ⁻²⁹	9.3E ⁻¹⁵	1.4E ⁻²⁴	1.7E ⁻¹⁴
YNPRH08-4W	5.7E ⁻⁴⁸	1.5E ⁻³⁰	1.0E ⁻⁴⁴	8.5E ⁻³¹	1.1E ⁻³⁸	2.4E ⁻³¹	8.6E ⁻⁷¹	5.1E ⁻²⁶	5.4E ⁻²⁹	3.8E ⁻¹⁴	1.0E ⁻²⁴	1.6E ⁻¹⁴
YNPRH09-1W	1.6E ⁻⁴⁷	1.2E ⁻²⁹	2.1E ⁻⁴³	4.9E ⁻²⁹	2.6E ⁻⁴²	3.2E ⁻³⁵	1.5E ⁻⁷⁷	3.9E ⁻²⁵	4.2E ⁻³⁰	1.4E ⁻¹⁸	1.0E ⁻²⁴	1.6E ⁻¹⁴

Sampling site	As(g)	As ₂ (g)	As ₃ (g)	As ₄ (g)	AsCl ₃ (g)	AsF ₃ (g)	AsF ₅ (g)	AsH ₃ (g)	AsS(g)	As ₄ S ₄ (g)	As ₄ O ₆ (g)	As(OH) ₃ (g)
YNPRH10-4W	5.2E ⁻⁵⁰	1.3E ⁻³⁴	7.4E ⁻⁵¹	5.7E ⁻³⁹	6.3E ⁻³³	6.9E ⁻²⁸	1.2E ⁻⁶³	4.2E ⁻³⁰	9.3E ⁻³¹	3.3E ⁻²¹	1.0E ⁻²⁴	1.6E ⁻¹⁴
YNPRH11-3W	2.3E ⁻⁵⁰	2.5E ⁻³⁵	6.6E ⁻⁵²	2.3E ⁻⁴⁰	4.7E ⁻²⁹	3.5E ⁻³⁰	3.0E ⁻⁶⁷	7.9E ⁻³¹	1.8E ⁻²⁸	4.6E ⁻¹²	1.2E ⁻²⁴	1.7E ⁻¹⁴
YNPRH13-3W	1.3E ⁻⁴⁹	7.8E ⁻³⁴	1.1E ⁻⁴⁹	2.2E ⁻³⁷	1.0E ⁻³³	8.6E ⁻²⁷	4.3E ⁻⁶²	2.3E ⁻²⁹	1.3E ⁻³⁰	1.2E ⁻²⁰	1.6E ⁻²⁴	1.8E ⁻¹⁴
YNPRH14-3W	5.8E ⁻⁴⁹	1.6E ⁻³²	1.0E ⁻⁴⁷	8.7E ⁻³⁵	3.8E ⁻³⁵	9.7E ⁻²⁸	4.1E ⁻⁶⁴	4.3E ⁻²⁸	7.0E ⁻³⁰	1.1E ⁻¹⁷	2.2E ⁻²⁴	1.9E ⁻¹⁴
YNPRH15-3W	5.9E ⁻⁵¹	1.6E ⁻³⁶	1.1E ⁻⁵³	9.5E ⁻⁴³	3.6E ⁻³⁰	1.7E ⁻²⁶	1.0E ⁻⁶⁰	5.7E ⁻³²	2.3E ⁻³¹	1.3E ⁻²³	7.1E ⁻²⁵	1.4E ⁻¹⁴
YNPRH16-4W	1.5E ⁻⁵⁰	1.1E ⁻³⁵	1.8E ⁻⁵²	4.0E ⁻⁴¹	1.2E ⁻³⁰	3.5E ⁻²⁶	1.9E ⁻⁶⁰	2.9E ⁻³¹	3.8E ⁻³¹	9.3E ⁻²³	2.1E ⁻²⁴	1.9E ⁻¹⁴
YNPRH17-4W	4.5E ⁻⁵¹	9.6E ⁻³⁷	5.0E ⁻⁵⁴	3.4E ⁻⁴³	9.4E ⁻³¹	8.1E ⁻²⁹	1.7E ⁻⁶⁴	6.5E ⁻³²	2.3E ⁻³¹	1.4E ⁻²³	6.4E ⁻²⁶	8.0E ⁻¹⁵
YNPRH18-4W	9.1E ⁻⁵²	3.8E ⁻³⁸	4.0E ⁻⁵⁶	5.3E ⁻⁴⁶	2.2E ⁻³²	2.0E ⁻³³	9.9E ⁻⁷²	9.4E ⁻³³	6.3E ⁻³²	7.1E ⁻²⁶	3.5E ⁻²⁸	2.2E ⁻¹⁵
YNPRH19-4W	5.9E ⁻⁵⁰	1.6E ⁻³⁴	1.1E ⁻⁵⁰	9.3E ⁻³⁹	3.1E ⁻³²	1.5E ⁻²⁶	1.8E ⁻⁶¹	7.4E ⁻³⁰	1.0E ⁻²⁹	5.0E ⁻¹⁷	2.9E ⁻²⁵	1.2E ⁻¹⁴
YNPRH20-4W	1.5E ⁻⁵⁰	1.0E ⁻³⁵	1.8E ⁻⁵²	3.9E ⁻⁴¹	5.3E ⁻³²	2.4E ⁻²⁶	1.0E ⁻⁶⁰	5.4E ⁻³¹	3.9E ⁻³¹	1.1E ⁻²²	1.7E ⁻²⁵	1.0E ⁻¹⁴
YNPRH21-4W	3.3E ⁻⁵¹	5.2E ⁻³⁷	2.0E ⁻⁵⁴	1.0E ⁻⁴³	1.1E ⁻³⁰	3.7E ⁻²⁶	5.6E ⁻⁶⁰	4.9E ⁻³²	1.8E ⁻³¹	4.2E ⁻²⁴	1.7E ⁻²⁶	5.7E ⁻¹⁵
YNPRH22-4W	2.9E ⁻⁵¹	4.0E ⁻³⁷	1.3E ⁻⁵⁴	5.7E ⁻⁴⁴	2.5E ⁻³²	9.1E ⁻³⁴	1.3E ⁻⁷²	8.7E ⁻³²	1.6E ⁻³⁰	2.7E ⁻²⁰	5.5E ⁻²⁸	2.4E ⁻¹⁵
YNPRH24-4W	9.3E ⁻⁵¹	4.0E ⁻³⁶	4.3E ⁻⁵³	5.8E ⁻⁴²	1.1E ⁻³⁰	2.3E ⁻²⁷	2.7E ⁻⁶²	1.9E ⁻³¹	1.0E ⁻³⁰	4.6E ⁻²¹	2.5E ⁻²⁵	1.1E ⁻¹⁴
YNPRH25-4W	3.9E ⁻⁵⁰	7.1E ⁻³⁵	3.2E ⁻⁵¹	1.8E ⁻³⁹	6.7E ⁻³²	3.7E ⁻²⁷	2.3E ⁻⁶²	3.1E ⁻³⁰	1.2E ⁻²⁹	7.9E ⁻¹⁷	3.4E ⁻²⁵	1.2E ⁻¹⁴
YNPRH26-4W	4.8E ⁻⁵⁰	1.1E ⁻³⁴	5.8E ⁻⁵¹	4.1E ⁻³⁹	3.2E ⁻³¹	2.0E ⁻³⁰	7.2E ⁻⁶⁸	7.4E ⁻³⁰	1.5E ⁻²⁸	2.5E ⁻¹²	5.4E ⁻²⁶	7.7E ⁻¹⁵
YNPRH27-4W	2.3E ⁻⁴⁹	2.5E ⁻³³	6.5E ⁻⁴⁹	2.2E ⁻³⁶	2.6E ⁻³⁴	1.4E ⁻²⁶	6.5E ⁻⁶²	8.0E ⁻²⁹	5.0E ⁻³⁰	2.7E ⁻¹⁸	1.2E ⁻²⁴	1.7E ⁻¹⁴
YNPRH28-4W	4.7E ⁻⁵⁰	1.0E ⁻³⁴	5.7E ⁻⁵¹	4.0E ⁻³⁹	3.2E ⁻³³	1.8E ⁻²⁶	2.9E ⁻⁶¹	6.2E ⁻³⁰	1.9E ⁻³⁰	5.8E ⁻²⁰	1.1E ⁻²⁵	9.1E ⁻¹⁵